Forschungszentrum Karlsruhe
Technik und Umwelt

Wissenschaftliche Berichte
FZKA 5633

Proceedings of the IEA-Technical Workshop on the Test Cell System for an International Fusion Materials Irradiation Facility Karlsruhe, Germany July 3 – 6, 1995

IEA-Implementing Agreement for a Programme of Research and Development on Fusion Materials

A. Möslang, R. Lindau (Editors)
Institut für Materialforschung
Projekt Kernfusion
Association Forschungszentrum Karlsruhe/Euratom

September 1995

Forschungszentrum Karlsruhe
Technik und Umwelt
Wissenschaftliche Berichte
FZKA 5633

Proceedings of the IEA-Technical Workshop on the Test Cell System for an International Fusion Materials Irradiation Facility Karlsruhe, Germany July 3 - 6, 1995

IEA-Implementing Agreement for a Programme of Research and Development on Fusion Materials

A. Möslang, R. Lindau (Editors)

Institut für Materialforschung
Projekt Kernfusion
Association Forschungszentrum Karlsruhe / Euratom

Forschungszentrum Karlsruhe GmbH, Karlsruhe

1995

Forschungszentrum Karlsruhe GmbH
Postfach 3640, 76021 Karlsruhe

ISSN 0947-8620

Contents

IFMIF-CDA Technical Workshop on Test Cell System
Karlsruhe, July 3-6, 1995

Summary

After a Conceptual Design Activity (CDA) study on an International Fusion Materials Irradiation Facility (IFMIF) has been launched under the auspices of the IEA, working groups and relevant tasks have been defined and agreed in an IEA-workshop that was held September 26-29 1994 at Karlsruhe. For the Test Cell System 11 tasks were identified which can be grouped into the three major fields neutronics, test matrix/ users and test cell engineering. In order to discuss recently achieved results and to coordinate necessary activities for an effective design integration, a technical workshop on the Test Cell System was initiated. This workshop was organized on July 3-6 1995 by the Institute for Materials Research I at the Forschungszentrum Karlsruhe and attended by 20 specialists working in the fields neutronics, fusion materials R&D and test cell engineering in the European Union, Japan, and the United States of America.

The presentations and discussions during this workshop have shown together with the elaborated lists of action items, that on the basis of already existing concepts and computer codes significant progress has been achieved in all three fields, and that from the future IFMIF experimental program for a number of materials a database covering widespread loading conditions up to DEMO-reactor relevant end-of-life damage levels can be expected.

Neutronics:

On the basis of available neutron source functions, initial neutronic analyses for deuteron beam energies between 30 and 40 MeV have been performed for standard loading concentrations of the high flux test cell region. The calculations also confirmed earlier recommendations that a beam spot size of 5x20 cm^2 is a good compromise between maximum test volume, small flux gradients and flexibility of the test cell configuration. Although an increase of beam energy from 30 to 40 MeV roughly doubles the high flux test volume, serious reservations with respect to the correlated increased high energy tail in the neutron spectra could not be dissipated. Therefore, uncertainty analysis mainly on gas production and transmutation rates taking into account neutron energies from 20-50 MeV are urgently needed. These calculations imply ongoing

efforts in establishing processed nuclear data for key nuclides in this energy range in order to ensure that IFMIF adequately simulates the nuclear environment in fusion reactors.

Test Matrix / Users:

For the high flux region, equivalent to a >2 MW/m^2 first wall neutron loading, detailed specimen loading matrices have been elaborated. Assuming a beam-on-target availability of 70% in this high flux test volume of approximately 0.5 liter, damage levels of 15 to 40 dpa/year can be achieved. The present loading matrix is based on 7 miniaturized specimen geometries, it allows within a ten to twenty year program the irradiation up to DEMO-relevant lifetime doses in a wide temperature range, and different heats from all three reference structural materials (ferritic/martensitic steels, vanadium alloys and SiC/SiC composites) will be included. In contrast to former concepts the specimens are encapsulated to avoid a direct interaction with the coolant.

While the high flux region has to provide materials data based on postirradiation examinations, the medium and low regions are important for selected in-situ tests for a design data base on structural materials and allow instrumented tests on special purpose materials (e.g. Rf windows, diagnostic materials, ceramic breeding materials). Although such experiments often require sophisticated techniques, significant progress has been achieved the last few months. Even for in-situ tests with controlled mechanical loadings design concepts are available in the meantime. However, a comprehensive matrix of reference in-situ and instrumented tests including out-of-cell equipment requirements, has still to be established.

Initial listings of the equipment necessary to perform the various postirradiation tests on miniaturized specimens at the IFMIF facility show, that beside standard hot cells for structural materials with an estimated area requirements of nearly 500 m^2 additional space will be necessary for tritium handling hot cells. An advanced hot cell facility designed for post-irradiation examination of various kinds of miniaturized specimens ("modular type hot cell") was also proposed.

Test Cell Engineering:

An advanced design concept based on NaK as coolant is available for the high flux test chamber. It can also be applied to conventional instrumented tests in lower flux test regions. NaK is suitable within the temperature regime of interest for metallic structural materials, and it's heat capacity guarantees sufficiently good temperature control during beam-on and beam-off periods. On the other hand, experiences with various helium gas cooled reactor and accelerator devices together with recent calculations have shown, that helium gas as a coolant allows similar package densities in the high flux region, but might have advantages e.g. with respect to the allowable temperature window, safety considerations and overall test cell flexibility. However, additional investigations for the helium cooling option are urgently needed to guarantee temperature stability for "loss of beam" conditions and to establish an integrated test assembly design. Therefore, a competing assessment of both concepts necessary for a design integration was postponed a few months.

Finally, design concepts for the entire set of test assemblies were discussed and preliminary shielding analyses, including estimations of the thickness of the test cell walls, were performed. A more realistic analysis can be done only after a reference test cell configuration is established.

AM

IFMIF Test Cell Activities

(July - October, 1995)

Neutronics

Nuclear data library
Establish a suitable IFMIF library for neutron transport calculations with data format consistent with ENDF6 - Reffo, Oyama

Neutron source term
Perform a comparison of available data and establish an improved neutron source term - Gomes/Oyama

Uncertainty analysis
Perform a preliminary examination of the effect of high energy neutron tail on dpa, gas production, transmutation (energies from 20 - 50 MeV) - Gomes
Take into account the possibility of increasing the D energy from 30 to 40 MeV

Analyze the impact of uncertainty of neutron source function on the neutron spectrum and nuclear responses- Gomes/Oyama

Estimate the fraction of He/H transmutation products by neutrons greater than 20 MeV - Gomes

Check mesh size effects - Oyama

Check whether the uncertainty fits into the range expected for DT fusion reactors - Fischer

Estimate nuclear heating rates versus location in test cell - Oyama

Determine dpa contours for the test cell down to at least 0.1 dpa to establish test cell size - Gomes

Establish neutron shielding requirements based on reference IFMIF configuration and established methodology - Monti

IFMIF Test Cell Activities

(July - October, 1995)

Test Cell Engineering

Further develop the helium cooled test module design concept - Viola

Perform transient thermal analyses for "loss of beam" conditions to establish whether required response time is feasible - Viola, Jitsukawa
Develop concept that meets requirements for the standard high flux loading - Haines, Jitsukawa
Integrate design with test cell/establish a test assembly design concept - Haines
Establish an installation and removal approach - Haines, Hoshiya

Develop test assembly handling design - Antonucci, Haines
Select approach and define equipment requirements for test assembly handling
Define hot cell requirements for test assembly maintenance

Develop layout for PIE and hot cells dedicated to test cell operations - Martone, Noda

Develop Test Cell Design Parameters List - Haines

IFMIF Test Cell Activities

(July - October, 1995)

Materials/Users Group

Provide guidance on acceptable ranges of H/dpa, He/dpa and transmutaion/dpa for ferritic steels, vanadium, and SiC-SiC - August 15 - Zinkle

Prepare a comprehensive table of reference in-situ experiments includng type of measurement (dpa/yr), irradiation volume requirements, and out-of-cell equipment requirements - October 1 - Moeslang/Noda

Create a list of materials of highest priority for neutronics analysis - August 1 - Zinkle

Establish requirements, including space and equiment lists, for the PIE and hot cells dedicated to test cell aperations - August 1 - Moeslang/Noda

Agenda

IEA Technical Workshop on the Test Cell System for an International Fusion Materials Irradiation Facility

Karlsruhe, Germany
July 3-6, 1995

Monday, July 3

12:00	Bus pick-up from hotel	
12:30	Lunch	
		Chairman: K. Noda
14:00	Welcome address	*K. Ehrlich*
	Status of CDA-Activities	*T. Shannon*
	Short review of task descriptions	*A. Möslang*
14:30	Session on specimen geometries, P.I.E. test matrix and cell configuration (CDA-D-3):	
	- Activities of JP	*K. Noda*
	- Activities of USA	*S. Zinkle*
	- Preliminary agreement on references (specimen geometries, test matrix, specimen package), interaction with existing irrad. sources	
	Session on in-situ tests (CDA-D-5):	
	- Activities of JP	*K. Noda*
	- Activities of USA	*S. Zinkle*
	- Activities of EU	*A. Möslang*
	- First discussion of proposed experiments incl. feasibility	
18:00	Departure to hotel	

Tuesday, July 4

8:00	Bus pick-up from hotel

9:00	Session on CDA-D-5 (Continuation)	*Chairman: J. Haines*
	Session on neutron source function (CDA-D-1):	
	- Neutron Source Term	*I.Gomes*
	- Comments to distributed data	*Y. Oyama*
	- Discussion, further needs	
	Session on neutronics analyses of high flux standard test module (CDA-D-2):	
	- Activities of JP	*Y. Oyama*
	- Activities of USA	*I. Gomes*
	- Activities of EU	*U. Fischer*
	- Discussion, consequences on cell configuration and design	
12:30	Lunch	
14:00	Session on processed nuclear data (CDA-D-7):	*Chairman: M. Martone*
	- Activities of JP	*Y. Oyama*
	- Activities of USA	*I. Gomes*
	- Activities of EU	*U. von Möllendorff*
		G. Reffo
	- Discussion of progress and problems	
15:30	Departure to Monastery of Maulbronn and dinner in the castle Ravensburg	
22:00	Departure to hotel	

Wednesday, July 5

8:30	Bus pick-up from hotel	
9:00	Session on design concepts for specimen loading (CDA-D-4)	*Chairman: Y. Oyama*
	- Activities of JP	*K. Noda*
	- Activities of USA	*J. Haines*
	- Activities of EU	*R. Conrad, R. Viola*
	- Discussion of different design concepts	
	Session on design concepts for typical test modules (CDA-D-6):	
	- Activities of JP	*K. Noda*
	- Activities of USA	*J. Haines*

- Activities of EU — *R. Conrad, R. Viola*
- Agreement on initial reference design concepts

12:45 Lunch

Chairman: (S. Zinkle)

14:00 Session on materials testing equipment (CDA-D-8):
- Activities of JP — *K. Noda*
- Activities of EU — *A. Möslang*
- Initial agreement on main hot cell equipment

Session on reference test matrixes (CDA-D-9):
- Discussion of strategy and next step activities

Session on dosimetry design concepts (CDA-D-10):
- Activities of EU — *B. Esposito, M. Martone*
- Activities of JP — *Y. Oyama*
- General discussion incl.agreement on urgent activities

Session on assembling and Test Cell shielding (CDA-D-11):
- Activities JP — *K. Noda*
- Activities USA — *J. Haines, I. Gomes*
- Activities of EU — *M. Martone*
- Preliminary agreement on reference test assemblies configuration

17:30 Departure to hotel

Thursday, July 6

8:30 Bus pick-up from hotel

9:00 Preparation of a summary including — *Chairman: K. Ehrlich*
- short conclusions of each task

12:30 - Lunch:

14:00 - Elaboration of IFMIF Test Cell Activities with regard to the Design Meeting (Oct. 1995, USA)
- recommendations from the present meeting to Li-Target and Accelerator workshops

- Closing remarks

17:30 - Departure to hotel

Participants IFMIF-CDA Technical Workshop on Test Cell System

Name	Organisation
Dr. C. Antonucci	ENEA, V.M. di Monte Sole, 4 40129 Bologna, Italy
Dr. F. Cozzani	European Commission Rue de la Loi - 200 B-1049 Brussels
Dr. F. Filotto	ENEA, C.R. Brasimone Camugnano (BO) 40032 Italy
Dr. I. C. Gomes	Fusion Power Program TD/207 Argonne National Laboratory 9700 South Cass Ave. Argonne, IL 60439-4841
Dr. J. Haines	ORNL Post Office Box 2009 Oak Ridge, TN 37831-8071 USA
Dr. M. Martone	ENEA - Centro dei Frascati Via E. Fermi, 27 - C.P. 65 Frascati (RM) 00044 Italy
Dr. K. Noda	JAERI Tokai-mura, Naka-gun, Ibaraki-ken Japan 319-11
Dr. Y. Oyama	JAERI Tokai-mura, Naka-gun, Ibaraki-ken Japan 319-11
Dr. G. Reffo	ENEA
Dr. T.F. Shannon	University of Tennessee Dept. of Nuclear Engineering Knoxville, TN 379962300 USA
Dr. R. Viola	CEC-JRC-IAM NL-1755 ZG Petten
Dr. St. Zinkle	ORNL P.O. Box 2008 Oak Ridge, TN 37831-6376 USA
Fr. Dr. I. Broeders	Forschungszentrum Karlsruhe INR Postfach 3640 D-76021 Karlsruhe
Dr. U. Fischer	Forschungszentrum Karlsruhe INR Postfach 3640 D-76021 Karlsruhe

Participants IFMIF-CDA Technical Workshop on Test Cell System

Name	Organisation
Dr. U. v. Möllendorff	Forschungszentrum Karlsruhe INR Postfach 3640 D-76021 Karlsruhe
Dr. H.D. Röhrig	Forschungszentrum Karlsruhe PKF/PL Postfach 3640 D-76021 Karlsruhe
Prof. Dr. K. Ehrlich	Forschungszentrum Karlsruhe IMF I Postfach 3640 D-76021 Karlsruhe
Dr. A. Möslang	Forschungszentrum Karlsruhe IMF I Postfach 3640 D-76021 Karlsruhe
R. Lindau	Forschungszentrum Karlsruhe IMF I Postfach 3640 D-76021 Karlsruhe
E. Daum	Forschungszentrum Karlsruhe IMF I Postfach 3640 D-76021 Karlsruhe

IFMIF-CDA : Test Cell Tasks and Responsible Persons*

		D-1	D-2	D-3	D-4	D-5	D-6	D-7	D-8	D-9	D-10	D-11
S. Jitsukawa	J			✳	✳	○	○		○	✳		
K. Noda	J			●	●	●	●		●	○		●
Y. Oyama	J	●	●					●			○	
J. Haines	US				●		●					●
I. Gomes	US	●	●					●				
S. Zinkle	US			●		●			○	○		
R. Conrad, R. Viola	EU				●		●				○	
B. Esposito, M. Martone	EU										●	
U. Fischer, E. Daum	EU		●									
U. v. Möllendorff	EU							●				
S. Monti	EU											✳
A. Möslang	EU			○		●			●	○		
G. Reffo	EU							●				

* as specified at the IFMIF-CDA Workshop at Karlsruhe, Sept. 1994

Status: June 29 1995

● Presentation } Technical Test Cell Workshop Karlsruhe, July 3-6 1995
✳ Prepared hand-outs }
○ Not yet available (July 1995)

T. E. Shannon
The University of Tennessee

Status of CDA Activities

IFMIF-CDA Technical Workshop
Test Cell System
Karlsruhe, Germany
July 4, 1995

BASELINE DESIGN STRATEGY

1. Major System Workshops

• Test Cell	July 3-6	FZK-Germany
• Lithium Target	July 18-21	JAERI/Tokai-Japan
• Accelerator	September 11-13	Santa Fe, NM-USA
• Design Integration	October 16-27	ORNL-USA

2. Workshop Objectives

- Technical Review of Tasks Defined at KfK

- Define Concept for Baseline Design
  - Review WBS
  - List Requirements
  - List Design Parameters
  - Define Configuration

- Document Meeting

BASELINE DESIGN STRATEGY
(Continued)

3. Define Tasks for remainder of 1995

- Provide Information for Design Integration Workshop in October
  - Equipment Layout
  - Facility and Utility Requirements
  - Interface Requirements

- Document Baseline Design Description by 12/95

4. Design Integration Meeting on July 4

- Additional Guidance Following Meeting

IFMIF Test Cell/Users Task CDA-D-1:

Neutron Source Function for given Target-, Beam-, and Energy Parameters

Task Responsible: Y. Oyama
IFMIF Test Cell/Users Group of JAERI

1. Introduction

To evaluate neutron irradiation field obtained from d-Li neutron source of IFMIF (International Fusion Material Irradiation Facility), neutron source functions were prepared for the proposed acceleration energies of 30, 35 and 40 MeV. The source functions are used for neutronics calculations of damage parameters of standard samples located in front of the Li target. The standard loading samples were specified for the CDA-D-2 that includes evaluations of the irradiation characteristics when the test matrix is taken place.

The source function was calculated based on the method developed in the previous work for ESNIT at JAERI.[1)] For the present work, the two beam geometry and three dimensional capability was added. Finally the source function was provided as the homogenized distributed source by simplification and suitable for successive neutron transport calculations. The neutron transport codes to be used are assumed for groupwise cross section codes such as Monte Carlo codes MORSE-CG because only the HILO86 groupwise cross section set is currently available for such high energy neutron transport calculation.

2. Nuclear Reaction Model

2.1 Deuteron Slowing Down

Assuming that the attenuation of deuteron flux through the range is negligible, the integration through the trajectory can be transformed to the integration by deuteron energy using stopping power. Here we replace the integration with respect to z' by the deuteron energy which can be related to the depth z' by using the stopping power.

We calculate the d-Li reaction rate at deuteron depth z in the Li layer as follows:

$$S(z,E_n,\Omega)dz d\Omega_{Lab} dE_{n,Lab} = \frac{N\cdot J}{e}\left[\left(\frac{d^2\sigma}{d\Omega dE_n}\right)_{CM}\left|\frac{\partial(\Omega_{CM},E_{n,CM})}{\partial(\Omega_{Lab},E_{n,Lab})}\right|\frac{1}{(dE_d/dz)}dz\right]d\Omega_{Lab}dE_{n,Lab}\ ,$$

[n/s/sr/MeV/cm] (2.1)

where (dE_d/dX) is the stopping power of deuterons in Li, J the deuteron current density, N the Li density, $(d^2\sigma/d\Omega dE)$ the d-Li cross section, and Jacobian term. The stopping power is represented for the incident energy range of 1-100 MeV as the following formula given in Ref. 2.

$$\left(\frac{dE_d}{dX}\right) = \left(A_6/\beta^2\right)\left[\ln\left(\frac{A_7\beta^2}{1-\beta^2}\right)-\beta^2-\sum_{i=0}^{4} A_{i+8}(\ln E_d)^i\right]$$

$[\mathrm{eV}/(10^{15}\mathrm{atoms/cm^2})]$ (2.2)

where E_d = deuteron energy/deuteron mass [keV/amu], β = v/c and A_i is given for lithium in the table of Ref. 2 as A_6=0.00153, A_7=21470, A_8=-0.5831, A_9=0.562, A_{10}=-0.1183, A_{11}=0.009298 and A_{12}=-0.000166, respectively.

2.2 Cross Section Model

The differential cross section is calculated by the same assumption as that of Johnson et al.,[3] except some modifications. The neutron production reaction of ^{7}Li(d,n)^{8}Be is only considered for the main reaction among the possible reactions, and in the calculation of cross sections the Serber's stripping reaction model[4] and the evaporation process are taken into account by the following linear combination.

$$\left(\frac{d^2\sigma}{d\Omega dE_n}\right) = A_S \cdot \left(\frac{d^2\sigma}{d\Omega dE_n}\right)_{Serber} + A_C \cdot \left(\frac{d^2\sigma}{d\Omega dE_n}\right)_{Evapolation}, \quad (2.3)$$

The first term by the Serber's theory is written as follows:

$$\left(\frac{d^2\sigma}{d\Omega dE_n}\right)_{Serber} = \frac{1}{2} \cdot \frac{(E_d-E_b)\cdot E_b}{\left[(E_n-E_d/2)^2 + E_b\cdot E_d\right]^{3/2}} \cdot \frac{\Theta_0}{\left(\Theta_0^2+\Theta^2\right)^{3/2}} \quad \text{for } |E_n-E_d/2| < 2(\Delta E)_{1/2}$$

$$= 0 \quad \text{for } |E_n-E_d/2| \geq 2(\Delta E)_{1/2} \quad (2.4)$$

where E_d : Incident deuteron energy,
E_b : Binding energy of deuteron,
Θ_0 : $\sqrt{E_b/E_d}$.

And the second term of evaporation process is due to compound reaction:

$$\left(\frac{d^2\sigma}{d\Omega dE_n}\right)_{Evapolation} = E_n \cdot e^{(-E_n/T)}, \quad (2.5)$$

where T : $3.2\sqrt{E_d/A}$ (A:mass number).

Here we modified the Serber's cross section by adding the energy cut-off ($E_c = E_d/2 \pm$ FWHM , full-width-half-maximum) for the neutron spectrum tail by Eq. (2.4), because the high energy tail of Serber's spectrum breaks an energy conservation law and that model may be valid only for a gross structure. This energy cut-off, however, can not eliminate producing the negative energy neutrons in lower energy tail by this model. This may provide the unreasonable increase of the lower energy neutrons below ~2 MeV, and also the break-up reactions to two or three bodies should be taken into account for low energy range. Hence this modification is not valid for such low energy region. The other type of reaction is also necessary to be considered for the higher energy neutrons above E_d; Q-value of 15 MeV means there is a possibility for generating the high energetic neutrons of E_d+15 MeV to the ground state of residual nuclei. Since this is not considered here, higher energy neutrons are produced only as an evaporation tail.

The A_S and A_C are energy dependent mixing parameters of two spectral shapes. The energy cut-off of 6 MeV for A_S comes from the low energy limit of stripping reaction for ^{7}Li. The shoulder of 10 MeV was introduced as an energy-weighting parameter but it was insensitive. The parameter A_C was weighted for lower energy deuterons shown in Fig.2.1. The energy cut-off of 2 MeV for the energy of coulomb barrier and the high energy cut-off of 15 MeV for energy weighting parameter were introduced for A_C. The values of parameters in A_S and A_C were determined by the trial and error method to reproduce the measured spectrum and angular distribution. The evaporation part is essential for representing the angular dependence of neutron spectrum.

2.3 Normalization and Validation

The source term of $S(z, E_n, \Omega) dz d\Omega_{Lab} dE_{n,Lab}$ was normalized by comparison with the experiment. The experiments were always measured at the position far from the target. This measured flux corresponds to the followings:

The source term of $S(z, E_n, \Omega) dz d\Omega_{Lab} dE_{n,Lab}$ was normalized by comparison with the experiment. The experiments were always measured at the position far from the target. This measured flux corresponds to the followings:

$$\Phi(E_n, \Omega) d\Omega_{Lab} dE_{n,Lab} = [\int_{surface}^{range} S(z, E_n, \Omega) dz] d\Omega_{Lab} dE_{n,Lab}$$

$$[\ \mathrm{n/s/sr/MeV}\ ] \quad . \qquad (2.6)$$

The integration is performed from the Li target surface to deuteron stopping range, i.e., 13, 17 and 22 mm for 30, 35 and 40 MeV, respectively. The normalization was done at 32 MeV deuteron energy using Lone and Sugimoto experiments(5,6), taking average of both experimental value of flux integration above 2 MeV for emission at 0 degree direction. The comparison with Sugimoto experiment is shown in Fig. 2.2. A good agreement can be seen as a whole, though the peak shape is a little broad. The detailed comparison is given in Table 2.1 in percentage difference. The agreement is generally within 15%.

The angular distributions of the present calculations are shown in Fig. 2.3 for 250 mA with a point approximation. Figs. 2.4 - 2.6 show the neutron spectra of 30, 35 and 40 MeV deuteron energies at the forward direction for different polar angles.

3. Two Beam-on Target Geometry

At the KfK meeting on September, 1994, two separated beam injection is recommended to reduce the risk for development of high current accelerator. To check the effect of two beam geometry on the flux distribution in the irradiation field, the program was modified to calculate the flux superposed by two beams with a fixed angle. This calculation was done for 100 x 100 mm square target configuration as shown in Fig. 3.1. The beam angles of 0, 5 and 15 degrees from the center were examined in terms of volume-flux and flux gradient relation.

The contour flux distributions are shown in Figs. 3.2-3.4 for the beam angles of 0, 5 and 10 degrees, respectively. The width of equal flux region increases with increase of incident angle but decreases the depth. Thus, the flux gradient increases on the z axis. Figs. 3.5 and 3.6 show dpa rate and He production rate as a function of the distance from the target surface and Table 3.1 summarizes the gradient of dpa and He production rates. The results show that the beam angle within 10 degree could be within 10%/cm gradient, though the gradient becomes steeper with increase of beam angle. As for the flux-volume relation, the beam angle does not affect significantly as summarized in Table 3.2.

Thus it is recommended that the beam angle should be 10 degree from the center axis to keep the gradient requirement.

4. Simplified Source Function for Providing Homogeneous Distributed Source (CDA-D-1 Deliverable)

To calculate the flux distribution inside the standard loading test matrix that specified at the KfK meeting on September 1994, a neutron source function is requested as an input for such calculations. This is the objective of CDA-D-1. However, the source term described above is rather complicated. When we use the deuteron energy dependent source term, i.e., depth dependent source term, the source file is very large and complicated for inputting to successive neutron transport code. Therefore we made the simplified distributed source function that can be used for the volumetric source input option.

In this source function, the distributed source is given by averaged source over the volume that defined by deuteron stopping range and the target area, and normalized by the total neutron emission yield produced by total beam current. Hence the source function is given by $S(E_n, \Omega)$ [n/s/sr/cm^3/MeV], i.e., three dimension data with energy, polar and azmuthal angles. The number of energy bin was given by 17, 19 and 22 for 30, 35 and 40 MeV, respectively. The numbers of polar and azmuthal angle bins were 30 and 26, respectively. The intensity of source function was obtained by dividing the normalized total emission yield by the source volume. The source volumes were defined by the target areas of 100x100, 50 x 200 and 25 x 400 mm^2 and the stopping ranges of 13, 17, and 22 mm for 30, 35 and 40 MeV, respectively. The data format of the present source function is given in Appendix 1.

5. Summary

To providing neutron source function, a detailed model is developed taking account of deuteron deceleration and incident angle of two beam configuration. The present model was compared with the recent experiments and confirmed within 15% accuracy in spectrum. The analysis also found that the beam angle should be less than 10 degree.

To provide neutron source function suitable for analysis of neutron irradiation characteristics for standard loading test matrix that specified for the task CDA-D-2, the simplified source function was provided for 30, 35 and 40 MeV deuteron energies.

References

(1) Y. Oyama, S. Yamaguchi, K. Kosako, H. Maekawa, " Calculation of Neutron Field Generated at Thick Li Target bombarded with 10-40 MeV Deuterons for Energy Selective Neutron Irradiation Test facility," JAERI-M 92-191 (1992)
(2) H. M.Anderson and J. F. Ziegler, "Hydrogen Stopping Power and Ranges in All Elements," Pergamon (1977)
(3) D. L. Johnson, F. M. Mann , J.W. Watson , J. Ullmann and W. G.Wyckoff, J. Nucl. Materials, 85 & 86, 467 (1979)
(4) R.Serber, Phys. Rev., 72, 1008 (1947)
(5) M. A. Lone and C. B.Bigham," Neutron Source for Basic Physics and Application," Chapter VI, OECD/NEA report, p.140 (1983)
(6) M. Sugimoto, et al., private communication, JAERI (1994)

Table 2.1 Comparison of the caluculated forward flux to the measured ones

(Measurement by M. Sugimoto, et.al. [Angle=0 degree, Ed=32MeV])

Energy range for integration	Experiment [n/sr/s/A]	Fraction to total flux of 1-50 MeV	Calculation	C/E
1- 2 MeV	1.2745+10	0.051	1.2048+10	0.945
2-10 MeV	7.6628+10	0.304	8.4601+10	1.104
10-15 MeV	8.4000+10	0.333	7.1235+10	0.848
15-30 MeV	7.7576+10	0.308	7.0637+10	0.911
30-40 MeV	1.0979+ 9	0.004	1.3057+ 8	0.119
40-50 MeV	1.6340+ 8	0.00065	---	---

Table 3.1 Spatial gradient of DPA and He production distributions

(Ed=35MeV, 100 mm x 100 mm Target)

DPA on Z-axis

Beam angle (degree)	Z= 2 cm	Z= 10 cm	Z= 15 cm	Z= 20 cm
0, 5	13%	9.3%	7.5%	6.7%
15	13%	11%	11%	9.7%

He production on Z-axis

Beam angle (degree)	Z= 2 cm	Z= 10 cm	Z= 15 cm	Z= 20 cm
0, 5	9.2%	7.5%	6.8%	6.4%
15	9.9%	9.4%	10%	9.6%

Table 3.2 Irradiation volume of neutron flux by three incident angles of deuteron beam.

Lower limit of neutron flux [n/cm^2/sec]	DPA [/yr]	Irradiation Volume [cm^3]		
		0 deg.	5 deg.	15 deg.
5 x 10^{14}	38	90.0	86.0	86.0
3 x 10^{14}	23	417	413	372
1.5 x 10^{14}	12	1330	1320	1220
1 x 10^{14}	8	2400	2360	2230
5 x 10^{13}	4	489	4950	5380

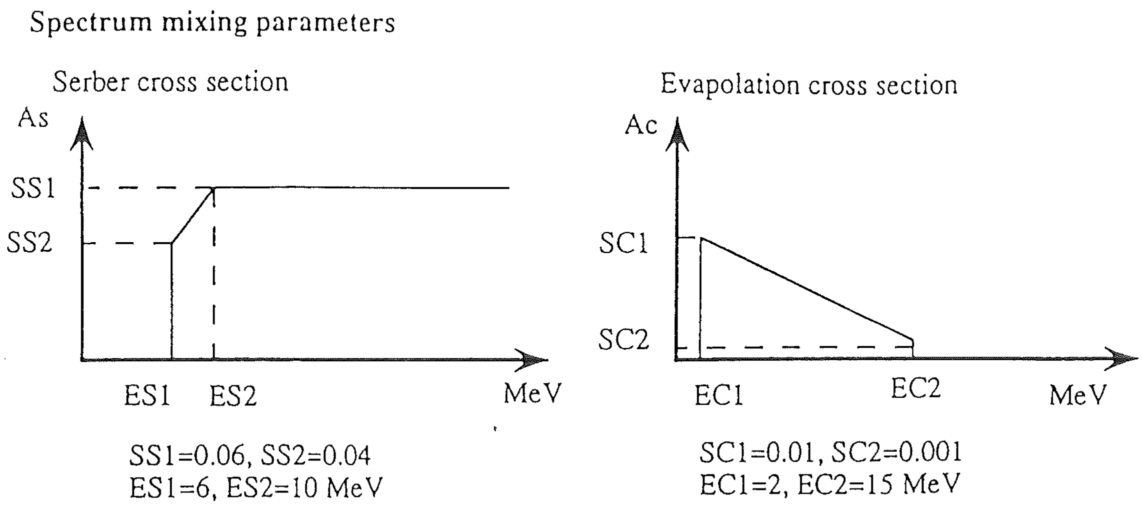

Fig. 2.1 Energy dependance adopted for mixing parameters of two spectra

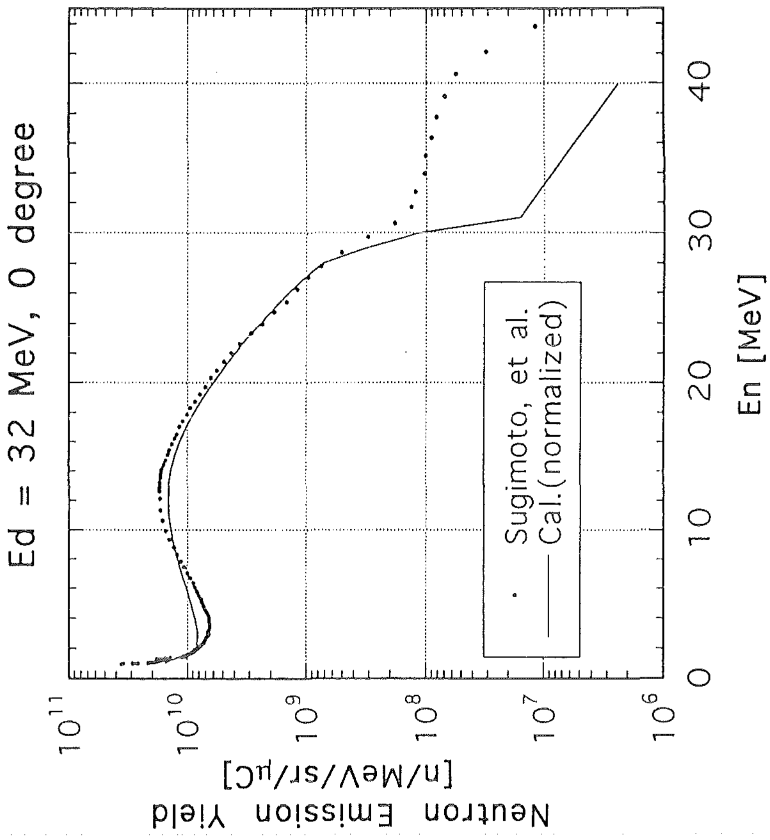

Fig. 2.2

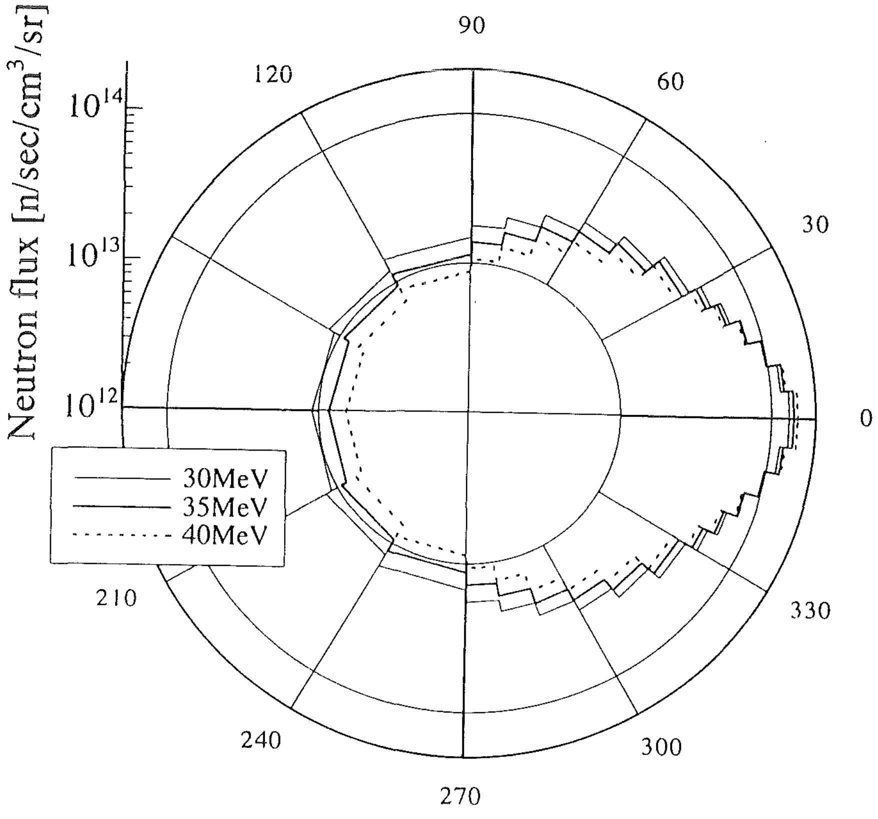

Fig. 2.3 IFMIF : Horizontal angular distribution of d+Li neutron source

Fig. 2.4 IFMIF : Source neutron spectra with 30 MeV deuteron on horizontal directions; (θ=0-5 degrees)

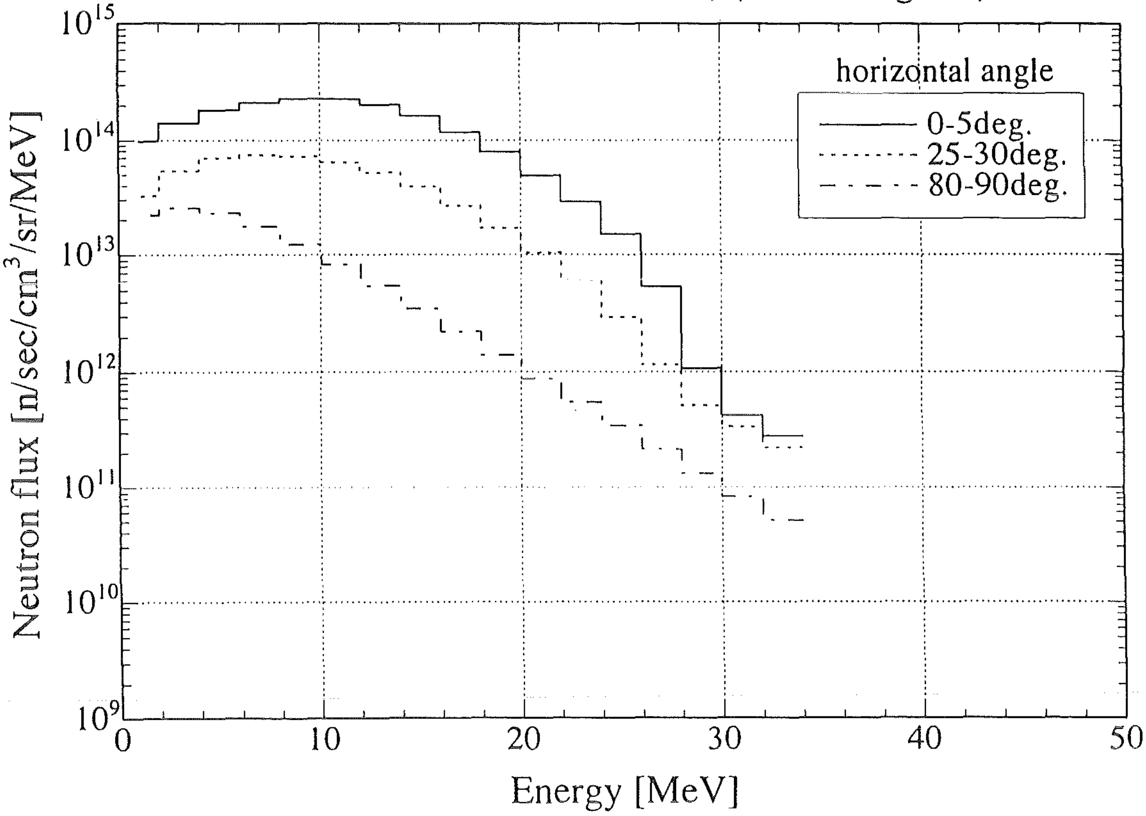

Fig. 2.5 IFMIF : Source neutron spectra with 35 MeV deuteron on horizontal directions; (θ=0-5 degrees)

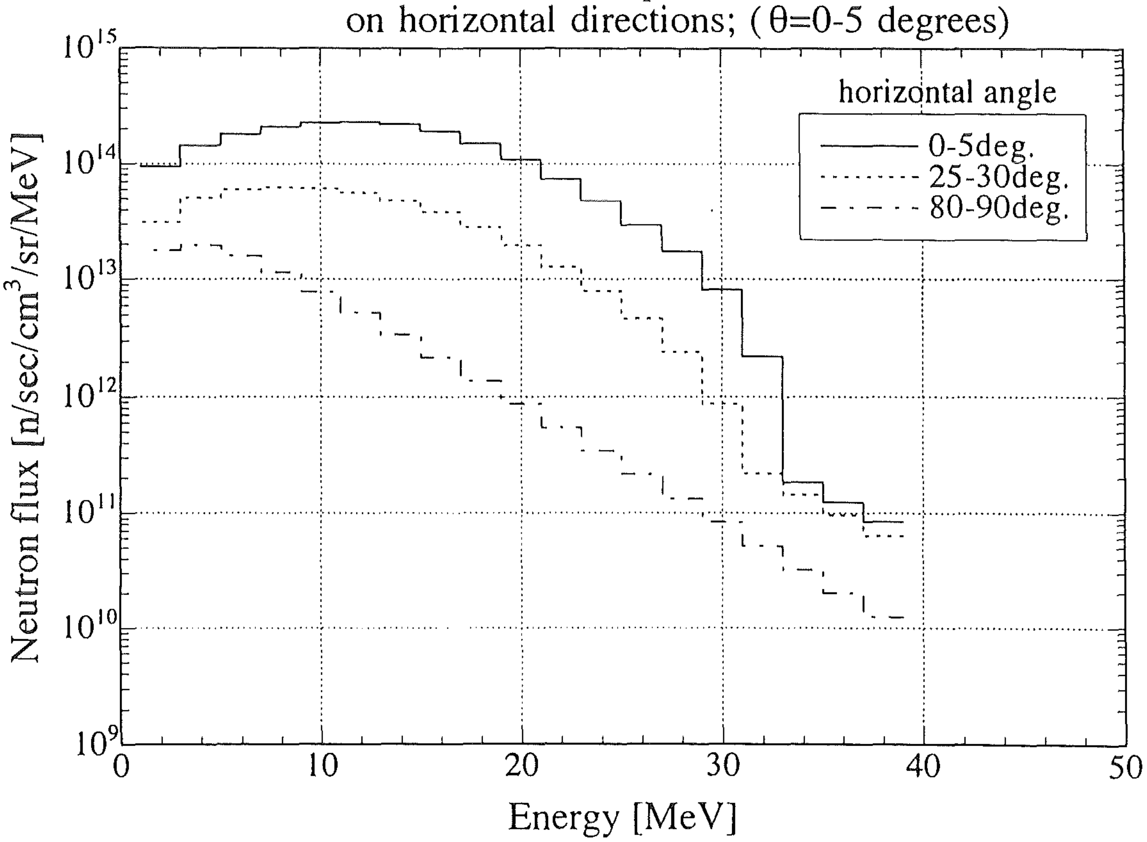

Fig. 2.6 IFMIF : Source neutron spectra with 40 MeV deuteron on horizontal directions; (θ=0-5 degrees)

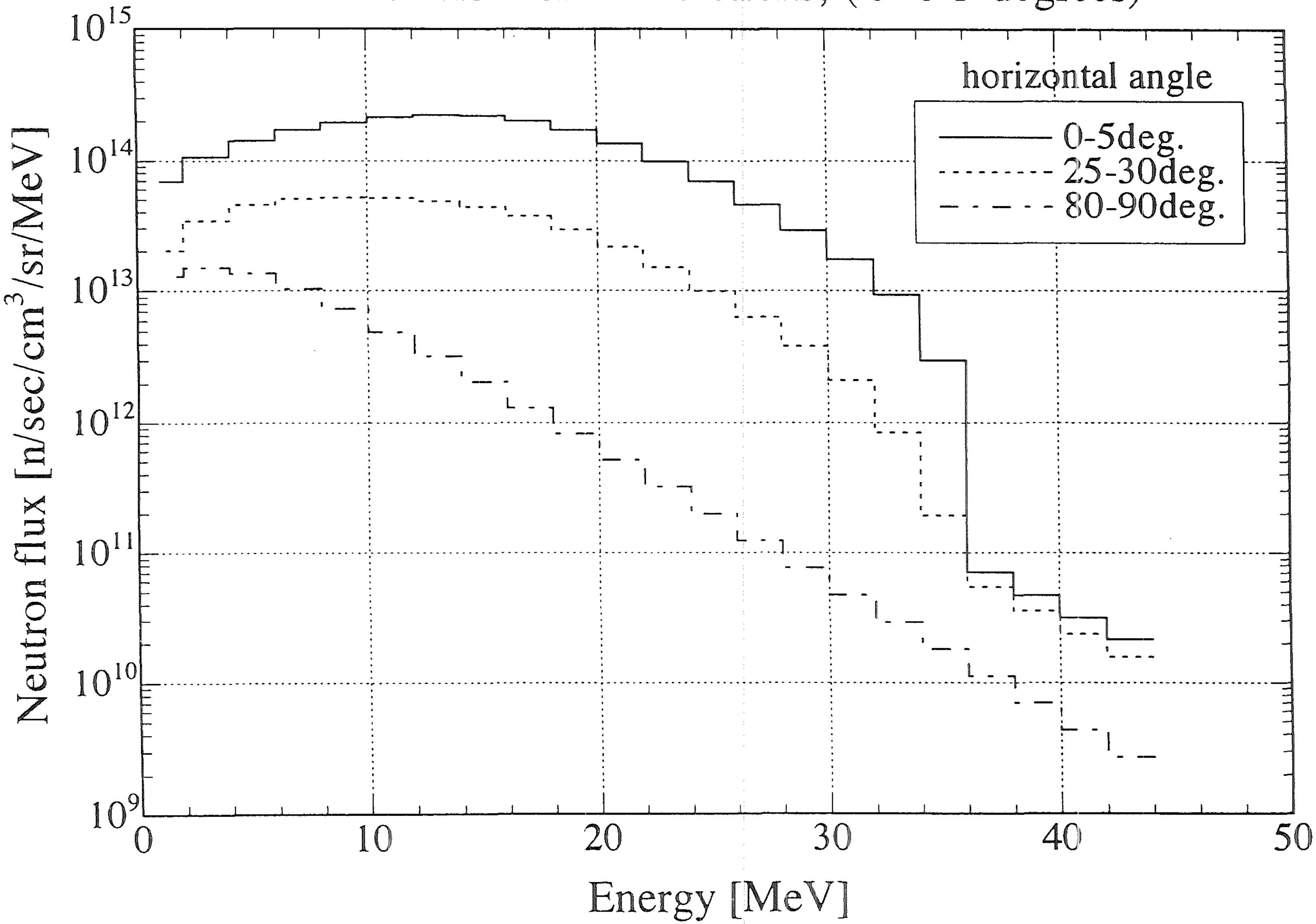

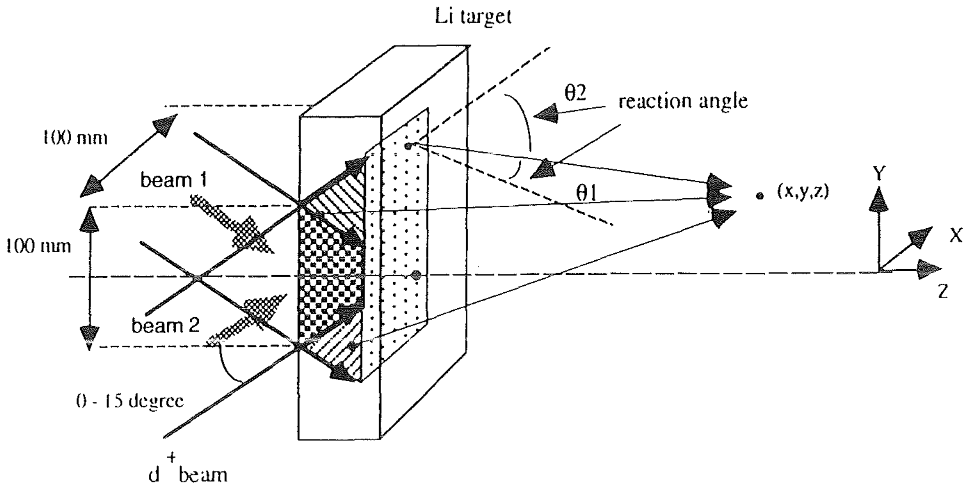

deuteron incident angle

Fig. 3.1 Neutron Flux and Spectrum Calculation Model at Positions in Irradiation Field

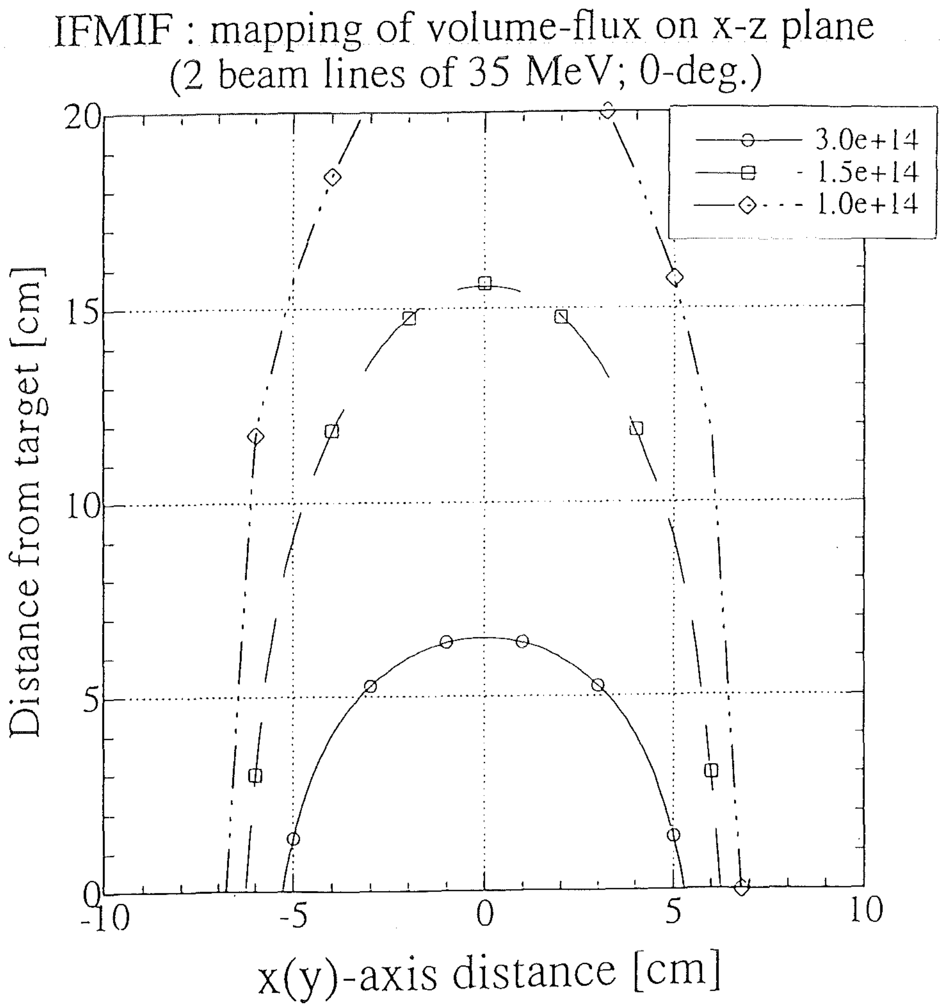

Fig. 3.2

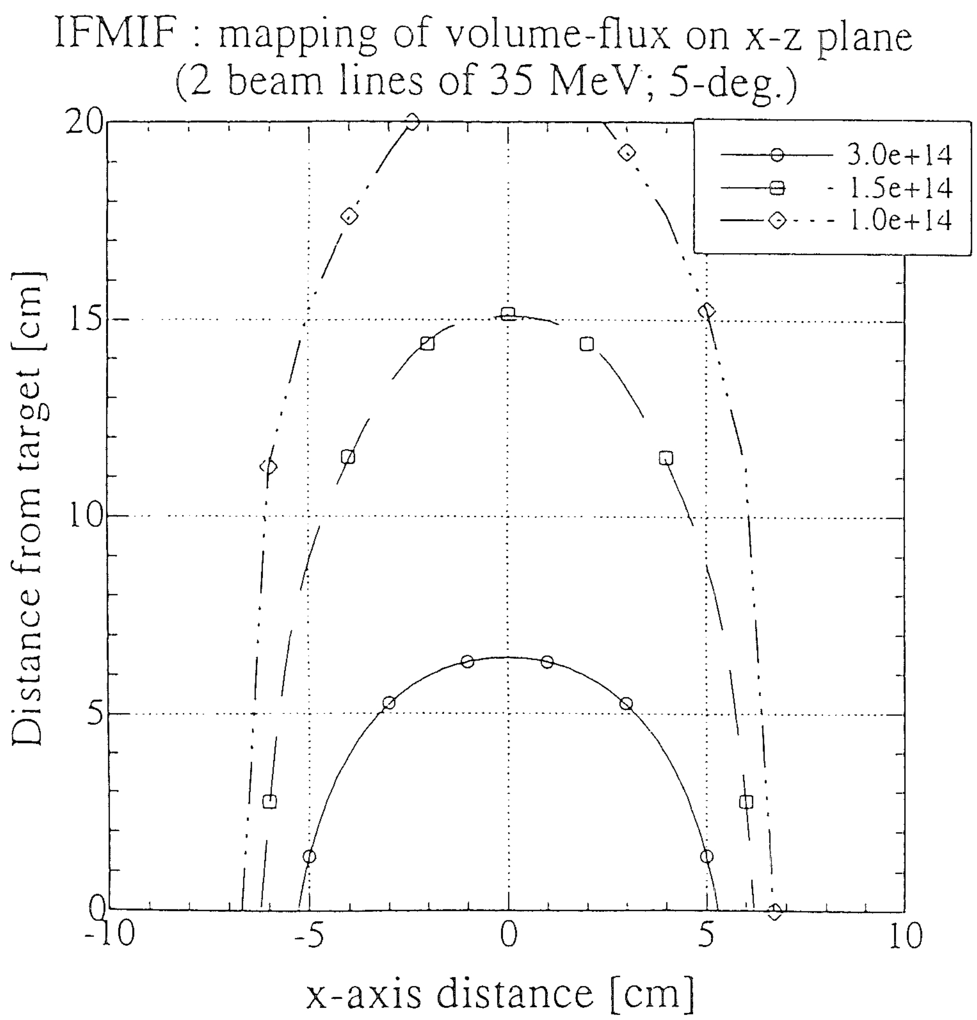

IFMIF : mapping of volume-flux on x-z plane
(2 beam lines of 35 MeV; 5-deg.)
3.0e+14
1.5e+14
1.0e+14
Distance from target [cm]
x-axis distance [cm]

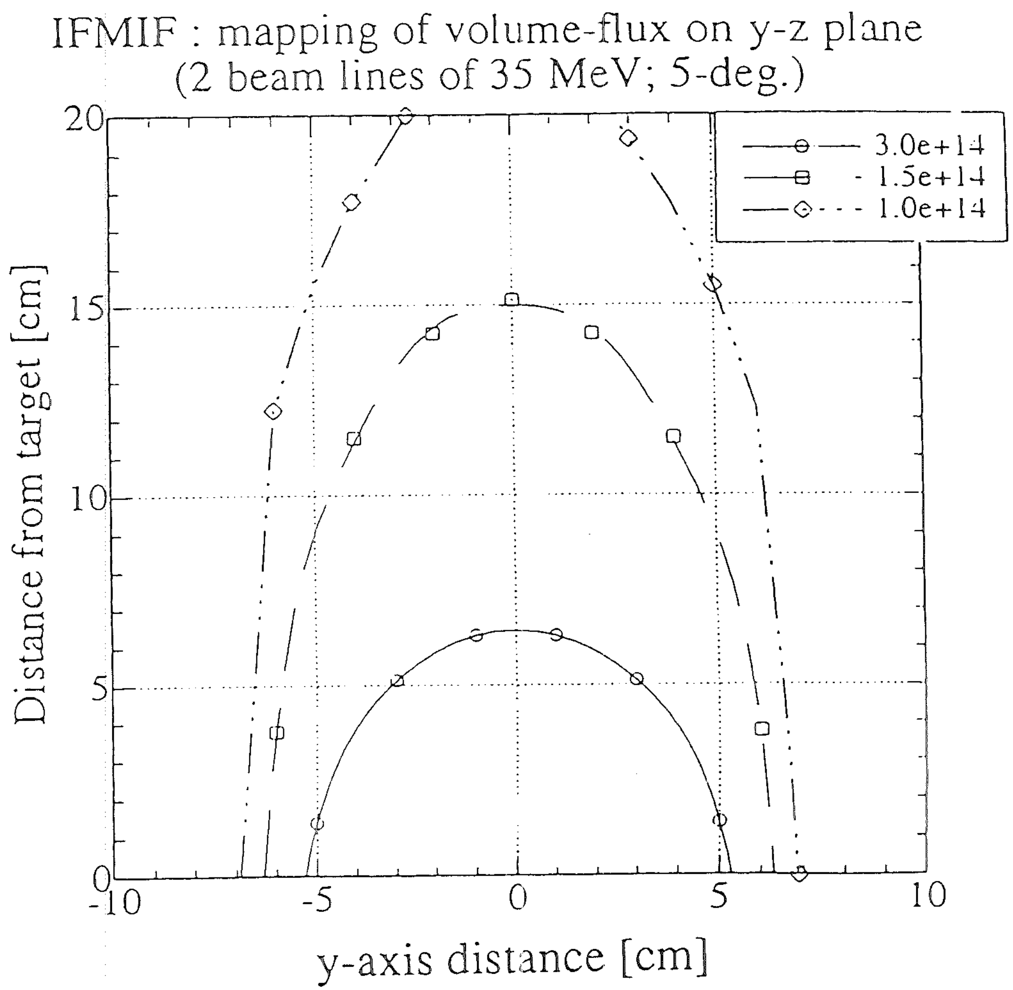

IFMIF : mapping of volume-flux on y-z plane
(2 beam lines of 35 MeV; 5-deg.)
3.0e+14
1.5e+14
1.0e+14
Distance from target [cm]
y-axis distance [cm]

Fig. 3.3

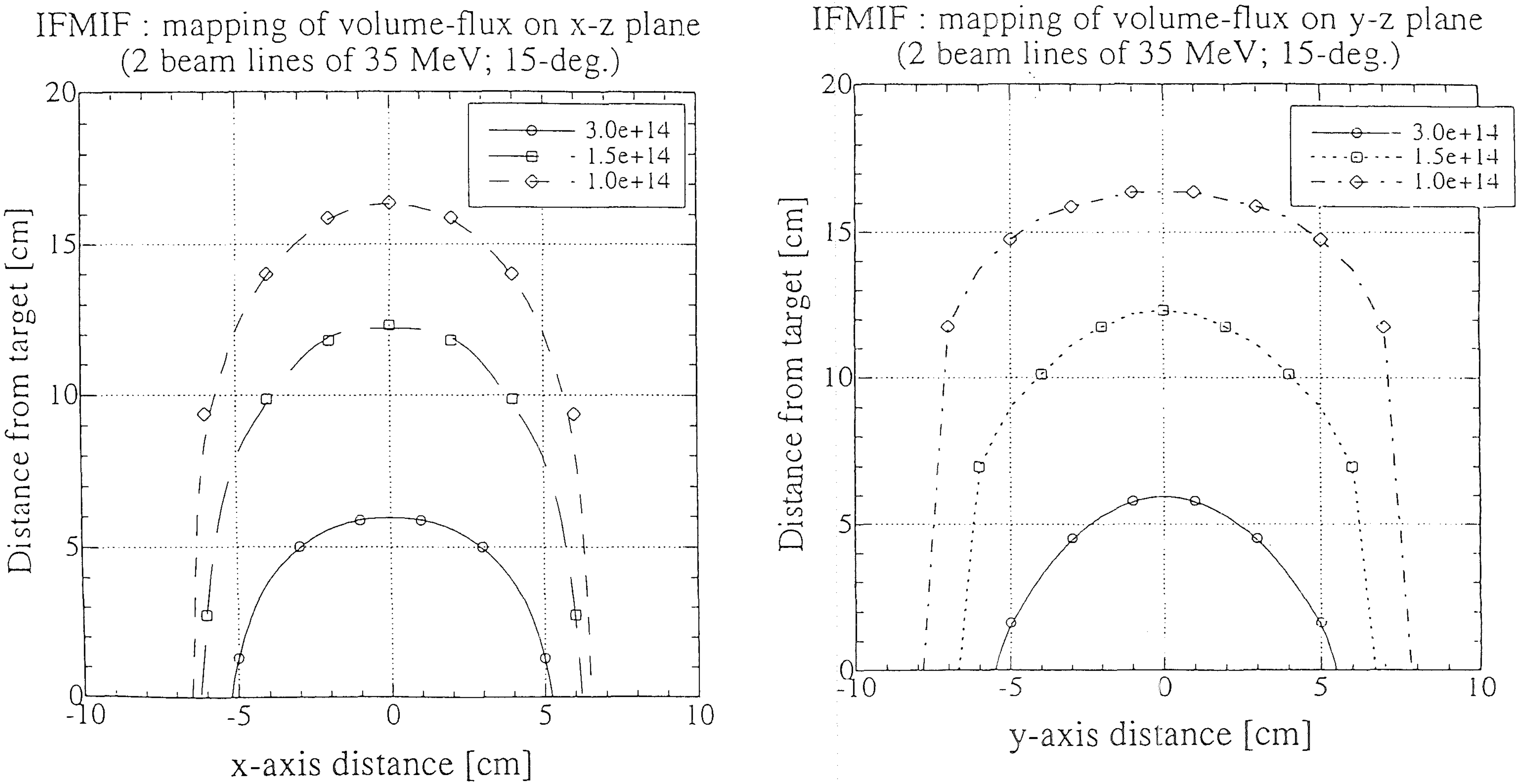
IFMIF : mapping of volume-flux on x-z plane
(2 beam lines of 35 MeV; 15-deg.)
3.0e+14
1.5e+14
1.0e+14
Distance from target [cm]
x-axis distance [cm]
20
15
10
5
0
-10
-5
0
5
10
IFMIF : mapping of volume-flux on y-z plane
(2 beam lines of 35 MeV; 15-deg.)
3.0e+14
1.5e+14
1.0e+14
Distance from target [cm]
y-axis distance [cm]

Fig. 3.4

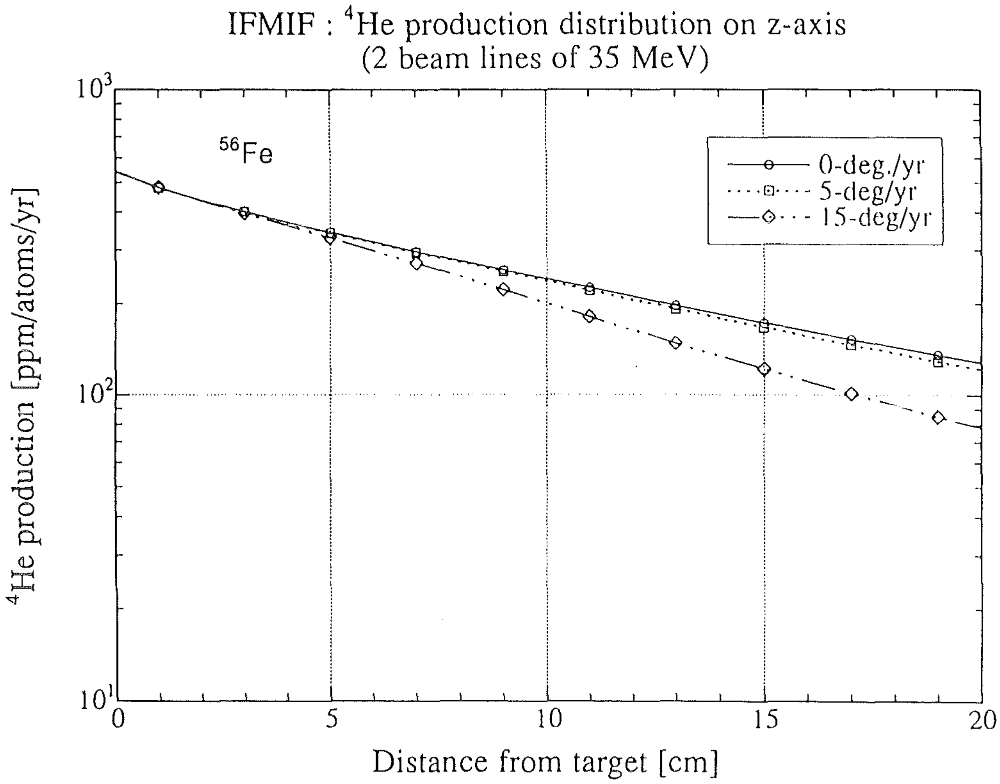
IFMIF : ⁴He production distribution on z-axis
(2 beam lines of 35 MeV)
^{56}Fe
0-deg./yr
5-deg/yr
15-deg/yr
^{4}He production [ppm/atoms/yr]
Distance from target [cm]

Fig. 3.5

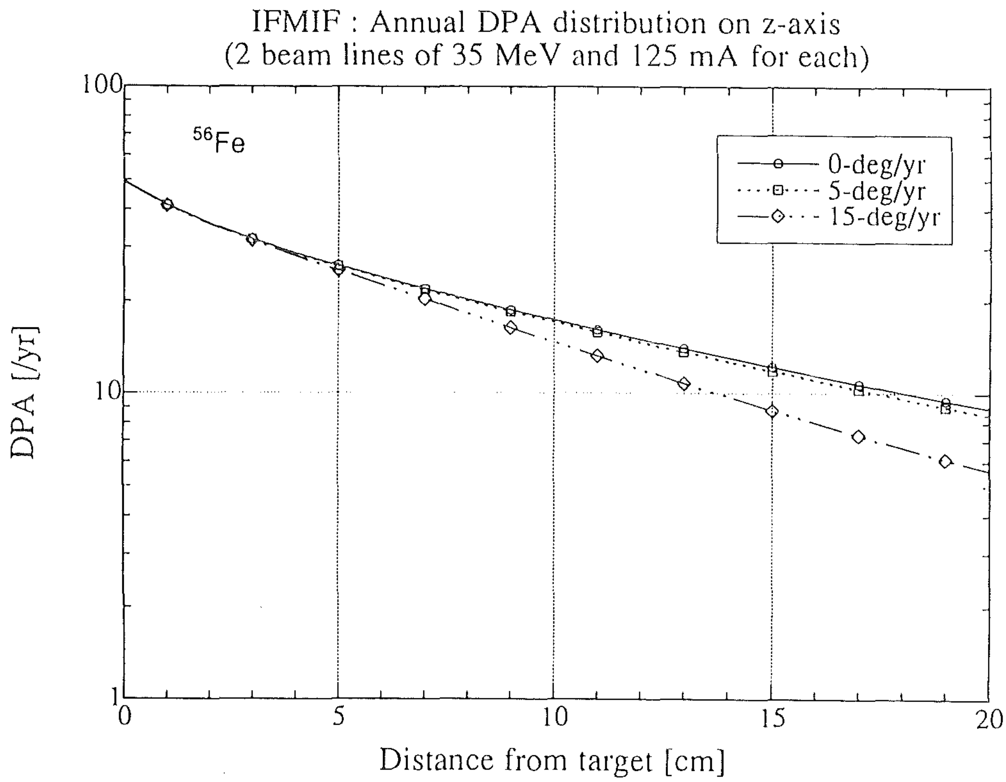
IFMIF : Annual DPA distribution on z-axis
(2 beam lines of 35 MeV and 125 mA for each)
^{56}Fe
0-deg/yr
5-deg/yr
15-deg/yr
DPA [/yr]
Distance from target [cm]

Fig. 3.6

Appendix 1. Data Format of Provided Source Function

readme.txt Novembr 15, 1995

Data are written in the following format

No.1-record (a80)	title card
No.2-record (a80)	comment on source condition
No.3-record (3i8) idlt, iah, iav	energy group, azmuthal angular bins, polar angular bins
No.4-record (10f8.2) (en(i),i=1,idlt+1)	energy boundary (downward)
No.5-record (10f8.2) (ah(i),i=1,iah+1)	azmuthal angular boundary (degrees)
No.6-record (10f8.2) (av(i),i=1,iav+1)	polar angular boundary (degrees)
do j=1,iah	
do i=1,iav	
n=n+1	
No.(6+n)-record (6d13.5) (S(j,i,k),k=1,idlt)	source intensity (n/sec/cm3 /4p)
enddo	
enddo	

Calculational Model for Surveying Neutronics Characteristics in Irradiation Test Matrix

Source Condition

Source is provided as follows:

1) 2 beam with 10 degrees is assumed
2) neutron emission probability function is averaged along with deuteron track
3) volumetric source is assumed to homogeneously distributed over the source region which is defined as area of target multiplied by the deuteron range
4) source is provided as a function of energy, and polar and azmuthal angles ie., $S=S(En,\theta,\Phi)$, in unit volume

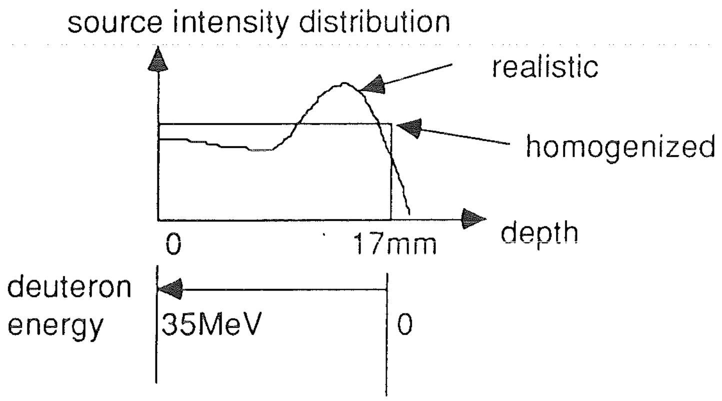

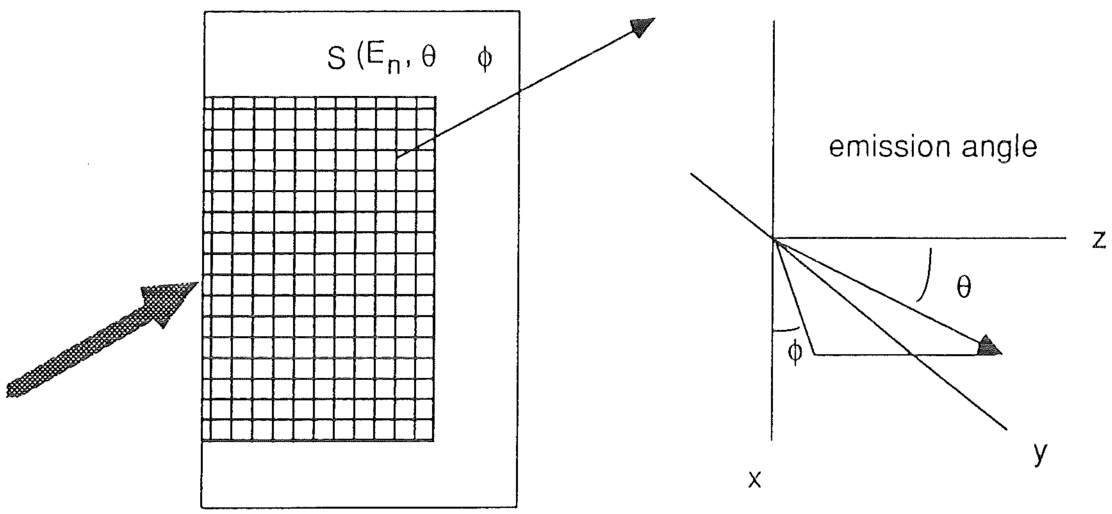

incident beam angle
$(\theta, \phi)=$ (10,0) and (10,180)

Neutron Source Term
Task CDA - D1

Test Cell Design Team Meeting

Karlsruhe - Germany

Itacil C. Gomes

Argonne National Laboratory

July 3-6, 1995

- Neutrons are produced from the interaction of Deuterons with the Lithium Flowing Target.

- The general source term can be expressed by:

$$S(\bar{r}, E_n, \bar{\Omega}) = N \frac{d^2\Sigma(E_d, E_n, \bar{\Omega})}{dE_n d\Omega} \delta\Omega \delta E_n \delta x$$

where:

$N = I(y,z) N_0 \, dy \, dz$ = number of deuterons at the differential volume dxdydz around r.

$\frac{d^2\Sigma(E_d, E_n, \Omega)}{dE_n d\Omega} =$ Double differential macroscopic cross section for the D-Li reaction.

- The number of neutrons produced depend on the number/flux of deuterons.

- The number of deuterons depends on the total current:
$N = 6.242 \times 10^{18} \times \text{current}$

- The cross section for the D-Li reaction is based on fitting of experimental data and on nuclear models.

- Four possible ways to model D + Li reactions:

1. Stripping of the deuteron's proton
2. Formation of a compound nucleus followed by evaporation of neutrons.
3. Breaking up of the deuteron by long range Coulomb potential.
4. Interaction of the deuteron with only neutron from the lithium nucleus.

- 3 and 4 are less likely than 1 and 2 due to low atomic number of the lithium and relatively low energy of the deuterons.

- Serber stripping model and Evaporation model are used and their parameters are adjusted to agree with experiments.

- The weight of each model is a function of the deuteron energy (serber high, evaporation low)

- For $0 \langle E_n \langle E_d$ the Serber model gives:

$$\frac{d^2\sigma}{d\Omega dE_n} = \left.\frac{d\sigma(Ed,\theta)}{d\Omega}\right|_{\theta} (Ed, En)$$

where

$$S(E_d, E_n) = K \, f(E_n, E_d) \frac{E_b E_d}{\left[(E_n - E_d/2)^2 + E_b E_d^{3/2}\right]}$$

$$f(E_n, E_d) = \min\left\{\left[\frac{E_n^{\,2}}{(0.35 E_d)^2}\right], 1\right\}$$

E_b = deuteron's binding energy (~ 2 MeV)

- For $E_n \rangle E_d$ the Serber model breaks down for D-Li. Dominant reaction is the ground and first excited states of ^8Be. Experimental data is used in this region.

- Evaporation model - For $E_n \langle E_d$ classical model is used.

- Evaporation model - For $E_n \rangle E_d$

$$\frac{d^2\sigma}{d\Omega dE_n} = \frac{d^2\sigma(Ed,\theta)}{d\Omega}\bigg|_\theta R(E_d,E_n)$$

$$R(E_d,E_n) = \frac{1}{T}\exp\left(\frac{-E_n}{T}\right) + g(E_d,E_n)$$

$$T = 0.55 E_d^{1/2}$$

$$g(E_d,E_n) = .01\,E_d - 0.2\min\{E_n, .05\,E_d\}$$

- The energy of the generated neutrons is dependent on the instantaneous deuteron energy.

Implementation of the Source Term to the Monte Carlo Code MCNP

- **Process the cross section to generate probability tables.**

1. Make deuteron energy the independent variable. Calculate the total D-Li cross section for deuteron energy (40 deuteron energy groups with a width of 1 MeV each). Multiply the cross section by the lithium atom density and by the distance traveled by a deuteron (with the energy of the energy group considered) until it loses 1 MeV of its energy.

2. Produced a table for each deuteron energy for the polar angle.

3. Produce other tables for each deuteron energy and each polar angle for the neutron energy.

- **The selection process is set as following:**

1. Select a spatial interval and the deuteron energy for the collision from the above defined probability distribution.

2. Select the outcoming polar angle and energy for the neutron from the appropriate probability distributions.

3. Select the azimuthal angle from a uniform probability distribution.

4. Use the nuclear model to better define the neutron energy within each energy group.

5. Select the "y" and "z" coordinates (plane perpendicular to the beam direction) of the collision point from uniform probability distributions (or any other suitable distribution).

6. Select the "x" position inside the spatial interval (selected in item 1) from a uniform probability distribution.

Notes:

1. The cross section data generated for the FMIT project by Fred Mann is given in milibarns per steradian per MeV. Then, in creating the probability tables, one has to integrate the cross section along the azimuthal angle.

2. Straggling effects are not considered in this formulation.

3. The loss of the deuteron beam intensity (less than 5%) is not considered in this model.

Neutrons from the D-Li Reaction

- Higher deuteron energy means:
  1. Higher neutron production rate.
  2. Higher average neutron energy
  3. Higher number of neutrons above 20MeV
  4. Thicker lithium jet.

Neutrons from the D-Li Reaction

- The higher the deuteron energy the higher the lower the dE/dx value => penetrates more until it loses a unit of energy.
- The higher the neutron energy the more forward peaked is the angular distribution at the generation point.

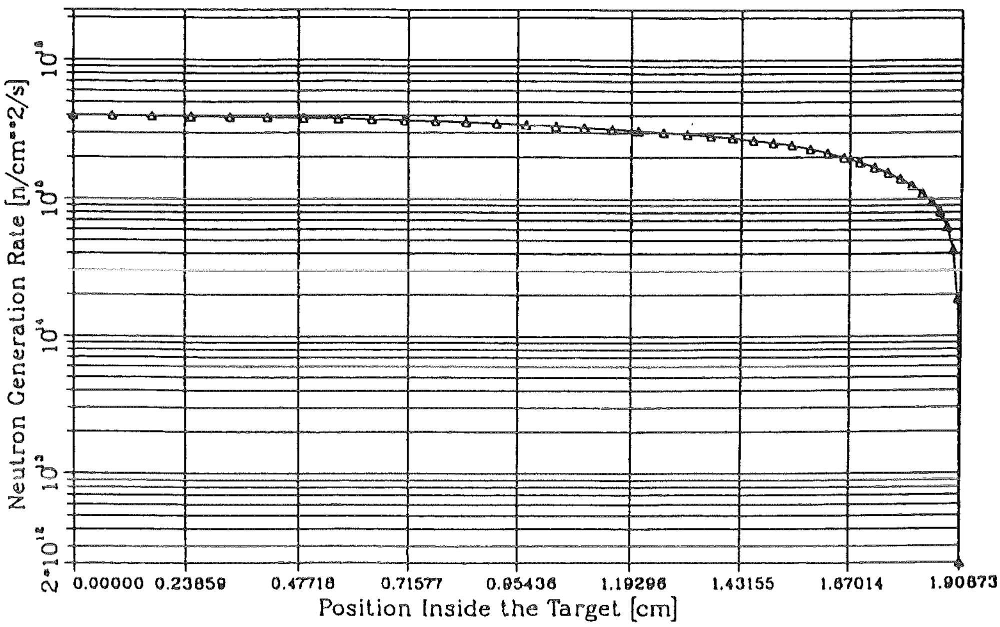

Figure 6. Neutron generation rate per 1 MeV deuteron energy loss as a function of the position inside the lithium target for a 40 MeV incident deuteron energy.

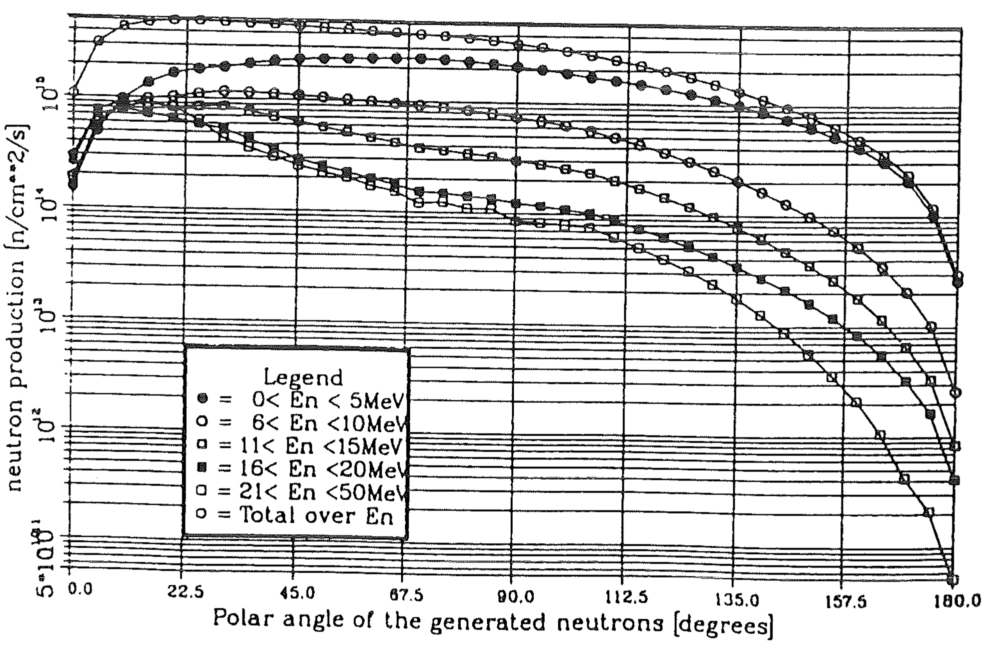

Figure 12. Neutron generation rate as a function of the polar angle of the generated neutrons for an incident deuteron energy of 40 MeV.

Table 1
Comparison of Neutron Generation Rate, Average Energy, and Energy Distribution for Three Incident Deuteron Energies

	Deuteron Incident Energy		
	30 Mev	35 MeV	40 MeV
Percentage of Neutrons Born in Each Energy (MeV) Interval (%)			
from 0 to 15	91.94	88.12	84.33
from 15 to 21	5.51	7.63	9.28
from 21 to 32	2.12	3.54	5.39
from 32 to 43	0.42	0.66	0.90
from 43 to 50	0.0022	0.059	0.10
Total Neutron Generation rate for a 250 mA D-beam (neutrons/sec)	6.460e+16	8.364e+16	1.035e+17
Average Neutron Energy (MeV)	5.36	6.06	6.71

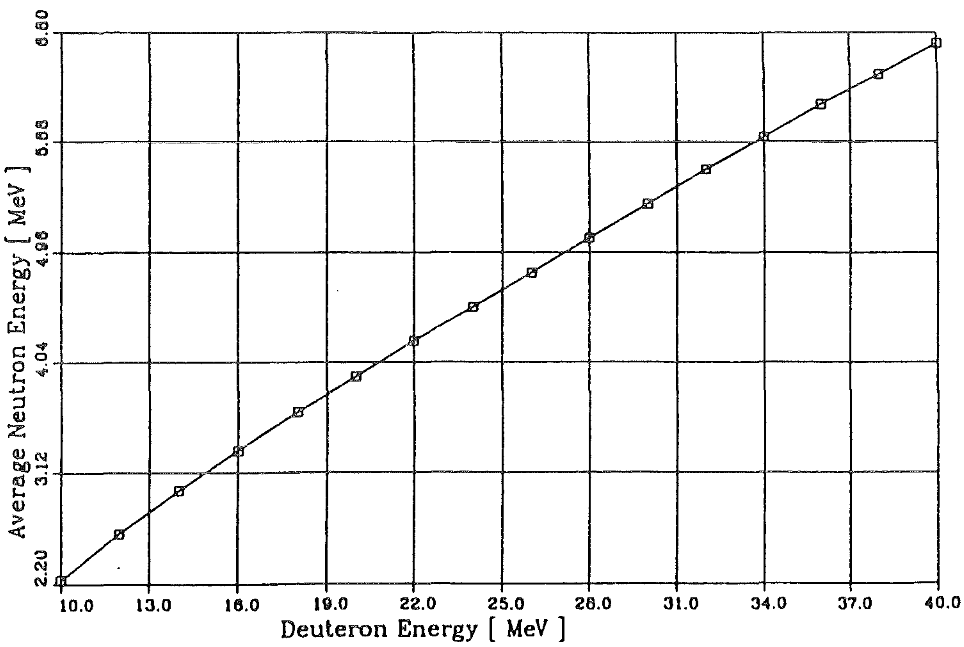

Figure 1. Average energy of the neutrons as a function of the deuteron incident energy.

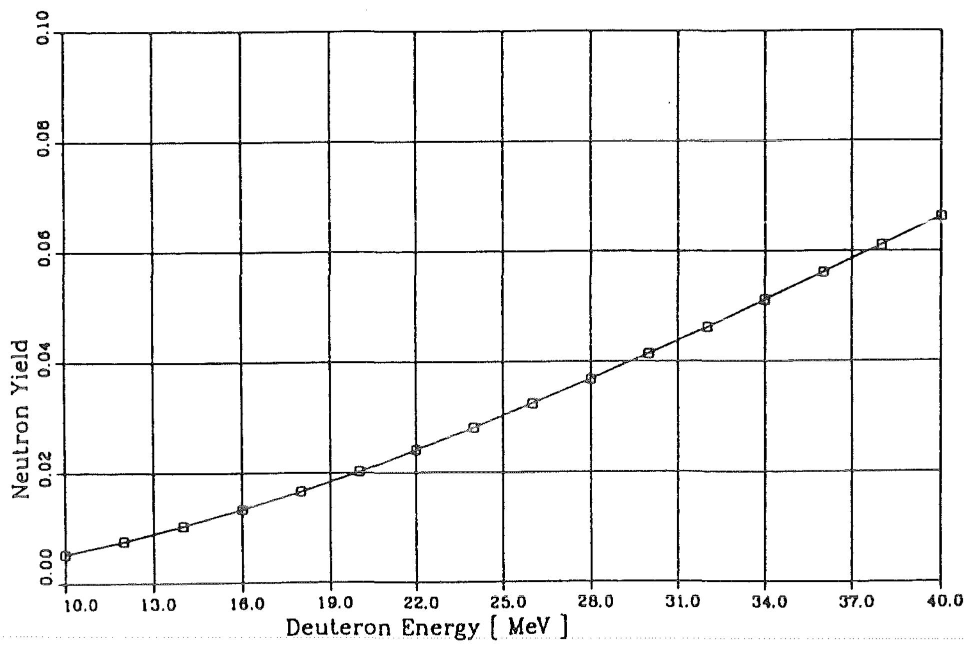

Figure 2. Neutron yield as a function of the incident deuteron energy.

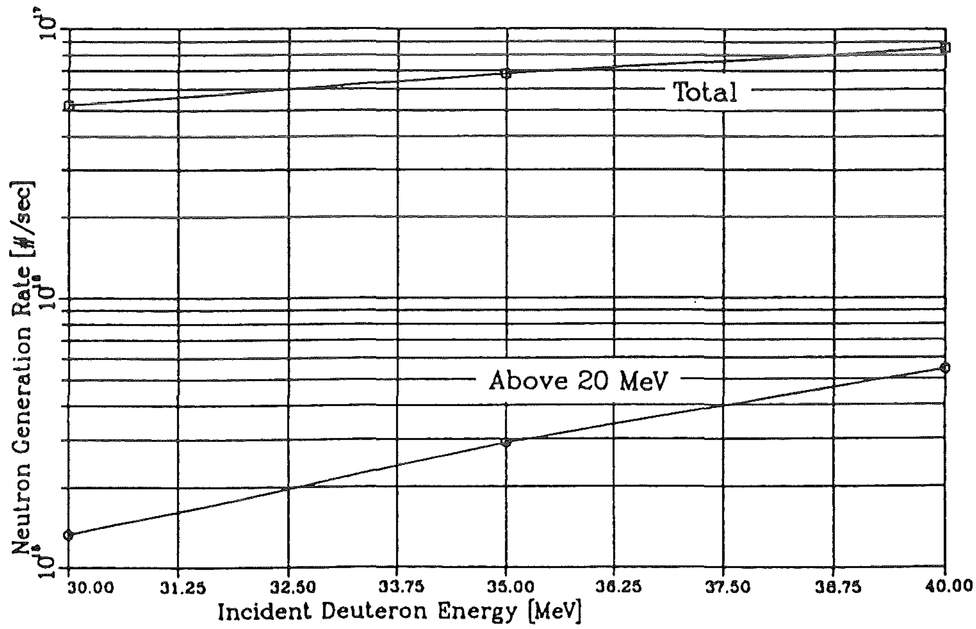

Figure 3. Generation rate of neutrons with energy above 20 MeV compared with the total neutron generation rate as a function of the incident deuteron energy.

Conclusion

- There are important advantages, in terms of neutron generation, in increasing the deuteron energy.
- The increase in deuteron energy do not create an unacceptable number of neutrons out of the range of a fusion reactor.
- The neutron energy spectrum of a fusion reactor is fully covered by the D-Li neutrons.

I.C.Gomes - Argonne National Laboratory

IFMIF Test Cell/Users Task CDA-D-2:

Detailed Neutronics Analysis and Other Parameters for a Test Cell with Standard Loading Configuration

Task Responsible: Y. Oyama
IFMIF Test Cell/Users Group of JAERI

1. Introduction

The task CDA-D-2 aims at performing quantative estimation of useful spatial volume in the IFMIF irradiation field for the four standard loading samples with different cooling materials. The reference conditions of the IFMIF deuteron beam-Li target configuration are 250 mA and 35 MeV for deuteron beam current and energy, and the target size is 50 mm x 200 mm square, respectively. The two beams of 125 mA are injected to the target with angle of 20 degrees (10 deg from the center axis).

The calculation was performed to obtain the relationship between the IFMIF irradaition and the reactor equivalent irradiation. The parameters to be compare are followings:

1) Volume available for the desired dpa rate inside standard loading
2) Neutron flux distribution inside the loaded samples
3) Nuclear heating for the loaded samples
4) The dpa distribution
5) Gas production, transmutation

For the typical reactor irradiation conditions, the SSTR and DREAM design were adopted, which are using ferritic stainless steel and SiC for first wall and structural materials, and water and helium for coolant materials, respectively. The reference wall load was 5 MW/m^2.

2. Source Function

The source function providing energy spectrum, angular distribution and intensity of neutrons emitted from Li target was given by the task CDA-D-1 that was reported seperately. The source function was expressed as uniform distribution over the 35 MeV deuteron stopping range, and then the distributed source is defined to that region. This approximation to homogenize the source function inside the Li layer, neglecting the change of deuteron reaction energy, is good approximation except for the positions very close to the deuteron reaction region. The further approximation was adopted to reduce the sampling time of source position, i.e., the source was placed at the 6 mm depth from the Li surface as a plane, where the neutron production rate is highest as shown in Fig. 2.1. This approximation was checked for flux distribution without sample and the results of comparison with volumetric source showed a good agreement with 8%. This means the calculation error of the same order.

3. Standard Loading Model

Four standard loading configurations were specified at the KfK meeting as follows: for iron sample,

1) Fe 50%, He (and Void) 50%,
2) Fe 50%, NaK 30%, Void 20%,

and for SiC sample,

3) SiC 50%, He (and Void) 50%,
4) SiC 50%, NaK 30%, Void 20%.

The test matrices with the standard loadings were averaged by the volume fraction and homogenized. The estimated parameters are calculated for the element of 100% density. The configuration model for calculations is shown in Appendix 1. The test matrix was placed at 2 mm from the target surface that was 1 mm backwall and 2 mm Li margin for the deuteron range, i.e., for 35 MeV deuteron 19 mm thick Li target was assumed. The matrix region was 20 % bigger than the target area and 200 mm in thickness. For example, for the 50 mm x 200 mm target, the 60 mm x 240 mm x 200 mm matrix was placed.

Neutronics calculation was performed using the Monte Carlo neutron transport code, GMVP, that was vectorized from MORSE-CG. The nuclear data library used is HILO86/J3 that was modified from HILO86 by replacing the data below 20 MeV by JENDL-3.1 with self shielding factor. The test matrix was devided into 20mm cubics, which corresponds 360 cubics for the 60 mm x 240 mm x 200 mm matrix, and each cubic was assigned to tarck length cell detetor, as shown in Fig.3.1. The mass and atomic number deneisties are listed in Table 3.1. The irradaition volume above the desired flux or dpa rate was estimated by counting these cubics. The displacement energies used here are given in Table 3.2 for Fe, Si and C. The dpa cross section and KERMA factors were extrapolated from 20 to 50 MeV.

4. Results

4.1 Volume-Flux Relation

The volumes to be obtained the flux over the desired flux are sumarized in Table 4.1. In the table, the four cases of standard loading configuration for the reference target shape, and the two other target shapes are compared. The cases without the matrix are also compared for three target shapes. The maximum volume to be able to caluculate is 2880 cm^3. Table 4.2 also gives the volumes to be obtained the dpa rate over the desired limit for Fe and SiC, respectively.

Figures 4.1-4.13 show the contour graphs of the desired limit of dpa rate. The effect of the Fe samples can be seen from Figs. 4.1-4 and 4.5-7, respectively. The effect is very remarkable in the region below 10 dpa/yr. Figs 4-8-4.13 show the cases of SiC seperately for dpa rates of Si and C.

Beam current dependence of the irradiation flux can be seen from Fig.4.14. The figure plots the relation of volume to the obtained dpa rate for both cases of 250 and 300 mA . From the dpa rate of 20 ppm/yr, the volume increases from 0.3 to 0.4 litter.

Flux gradients in front of the target are shown for two caases with and without test matrix in Fig. 4.15. The requirement of 10%/cm for flux gradient (in dpa rate) is satisfied only by 100 x 100 mm square target and by the uncollided flux as seen in the figures. The thinner rectangle targets increse the gradient. For the case with standard sample loaded test matrix, the gradient can not be reached to 10%/cm, and the gradients for four standard loading cases are 15%/cm. The gradient of the direction parallel to the target surface is worse with the distance from the target and worse with thinning the target area.

4.2 Gas production and dpa

Table 4.3 shows dpa rate, He production rate and He/dpa ratios for Fe. The ratio of He production to dpa rate is around 14, so that the ratio is very close to the fusion condition.

4.3 Demo Reactor and Transmutation

For the reference case, two designs of the DEMO reactors were chosen from the Japanese DEMO designs, i.e., SSTR and DREAM. The SSTR reactor uses F82-H steel for structural material and water for coolant, and the DREAM uses SiC and He, respectively. The conceptual view of the reactor is shown in Fig. 4.16 and the calculation models for both reactors is shown in Fig. 4.17 and 4.18. Figs 4.19 and 4.20 compare the neutron spectra of both the averaged flux of IFMIF and the first wall flux of SSTR, and the first wall flux of DREAM, respectively.

Fig 4.21 presents the production rates of major transmuted nuclides from Fe by the IFMIF neutrons of 5x 10^{14} n/cm^{2}s and from F82H steel by the SSTR neutrons of 5MW/m^2 wall load (about 2.4 x10^{14} n/cm^{2}s) after 1000 days irradiation. The averaged spectrum in the whole sample volume was used to calculate the transmuation, so that the 25 x400 mm^2 target case is lower than the others. The transmurtaions of IFMIF are higher than the SSTR even considering the flux intensity. Fig. 4.22 shows ratio of transmutation to the ^{55}Mn production. The productions of ^{54}Cr and ^{53}Cr are slightly different, where the ^{51}V is a product from ^{52}Cr of F82H.

Fig. 4.23 also shows the production rates for the SIC sample and the DREAM reactor. It is seen from this figure that the production of ^{27}Al and ^{24}Mg in the IFMIF is larger than the DREAM. The ^{21}Ne production comes from high energy reaction. The ratios to ^{25}Mg show that the production are two time higher for ^{27}Al and four times higher for ^{24}Mg.

4.4 Nuclear Heat

Nuclear heating in the standard loading samples was calculated and the results are summarized in Table 4.6. For iron sample, the gamma-ray heating is 50% larger than neutron heating, and for SiC sample, the gamm-ray heating is one tenth of neutron heating. However, total heating is alomost the same for both samples and that is around 20-23 W/cm^3 at maximum. The avearge heating is about half of the maximum.

5. Summary

From the present calculations, it can be concluded for Fe and SiC irradaition that:

Volume-Flux:

1) The reference target shape, 50 mm x 200 mm , provides 0.3 litter and 0.75 litter irradiation volumes for NaK and He coolant cases, for 20 and 10 dpa/yr, respectively. If the 100 mm x 100 mm target is used, the 0.4 and 1 litter volumes for 20 and 10 dpa/yr can be obtained. To increase the irradiation volume for the reference target by 0.4 litter, the beam current should be increased by 300 mA.
2) The effect of sample loading, i.e., perturbation due to matrix, is about 20-40% reduction of irradiation volume and the lower flux region has higher reduction.
3) For SiC, the 0.5 and 1 litter volumes can be obtained in the reference target for 20 and 10 dpa/yr of Si, respectively.
4) Flux gradient inside matrix exceeds 10%/cm and close to 15%/cm, though the flux gradient without matrix is within 10%/cm.

Gas production, dpa and Transmutation:

1) The He/dpa ratio ranges 13.6 to 14.5, and the ratio increases for the thinner target of 25 mm x 400 mm.
2) For transmutation production from Fe, the production ratios of ^{54}Cr is larger but that of ^{53}Cr is smaller than those of ferritic steel in the SSTR, i.e., the ferritic steel and water cooling reactor.

3) For transmutation production from SiC, the production ratios of ^{27}Al and ^{24}Mg are larger than that of DREAM, i.e., SiC/He reactor.

Nuclear Heating:

1) Nuclear heating by neutrons in the Fe matrix is alomost equal to the gamma-ray heating, but neutron heating in the SiC matrix is ten times larger.
2) The total heating is about 20 W/cm^3 at front region of the matrix.

6. Concluding Remarks

1) The target size should be thicker than 50 x 200 mm square. For 50 x 200 mm target, a 300 mA of deuteron beam current is required for Fe loading matrix to exceed 0.4 litter for a region over 20 dpa .

2) The flux gradient inside the matrix is steeper than 10%/cm and close to 15%/cm.

References

1) Y. Oyama, et al., CDA-D-1 report
2) M.B. Emmett, " The MORSE Monte Carlo Radiation Transport Code System," ORNL-4972, Oak Ridge National Laboratory (1975).
3) K. Kosako and Y. Oyama, HILO86/J3
4) R. G. Jr. Alsmiller and J. Barish, " Neutron-Photon Multigroup Cross Sections for Neutron Energies ≤ 400MeV," ORNL/TM-7818, Oak Ridge National Laboratory (1981).
5) T. Mori, et al., GMVP
6) N. Yamano, et al., TRANSM
7) Y. Seki, et al., SSTR and DREAM

Table 3.1 The density and atomic number density of irradiated materials for IFMIF.

material	density [g/cm^3]	nuclide	atomic number density [1×10^{24}/cm^3]
Iron	7.86	Fe	8.4760×10^{-2}
NaK	0.762	^{23}Na	4.4312×10^{-3}
		K	9.1312×10^{-3}
SiC	3.12	Si	4.6860×10^{-2}
		^{12}C	4.6860×10^{-2}

Table 3.2 Displacement energy, E_D, of the irradiation samples.

Sample material	Displacement energy [eV]
C-12	25
Si	25
Fe	40

Table 4.1 The cumulative volume of total flux by the sample materials and sizes in GMVP calculations.

	Cumulative volume [cm^3]								
Area [cm^2]	24x6				12x12	48x3	24x6	12x12	48x3
Lower flux [/cm^2/sec]	Fe-50% NaK-30%	Fe-50%	SiC-50% NaK-30%	SiC-50%	Fe-50% NaK-30%	Fe-50% NaK-30%	Without material		
5.0×10^{14}	112	80	64	64	160	0	64	128	0
3.0×10^{14}	416	440	400	400	480	240	368	480	240
1.5×10^{14}	896	944	880	896	1216	480	1088	1408	672
1.0×10^{14}	1296	1328	1264	1312	1600	696	1656	2192	1032
5.0×10^{13}	1968	2000	2048	2096	2336	1224	2736	2880	2040
0.0	2880	2880	2880	2880	2880	2880	2880	2880	2880

* Neutron flux is integrated over the whole energy region below 50 MeV

Table 4.2 The cumulative volume of DPA by the sample materials and sizes in GMVP calculations.

	DPA cumulative volume of Fe [cm^3]						
Area [cm^2]	24 x 6		12 x 12	48 x 3	24 x 6	12 x 12	48 x 3
Lower DPA [/yr]	Fe 50% NaK 30%	Fe 50%	Fe 50% NaK 30%		Without material		
20	304	304	416	<240*	416	512	240
15	496	496	576	240	688	832	456
10	736	752	960	480	1120	1504	696
5	1360	1392	1648	912	2432	2792	1368
2	2240	2288	2528	1488	2880	2880	2568
0	2880	2880	2880	2880	2880	2880	2880

* The volume should be less than this value but can not be specified because of spatial resolution of flux estimator

Table 4.2 (continued)

	DPA cumulative volume of Si [cm^3]			DPA cumulative volume of ^{12}C [cm^3]		
Area [cm^2]	24 x 6					
Lower DPA [/yr]	SiC 50% NaK 30%	SiC 50%	Without material	SiC 50% NaK 30%	SiC 50%	Without material
20	496	496	512	0	0	0
15	720	736	864	0	0	0
10	976	1008	1360	176	176	80
5	1728	1840	2576	608	608	576
2	2736	2752	2880	1440	1440	1864
0	2880	2880	2880	2880	2880	2880

Table 4.3 The ratio of ^{4}He and DPA of Fe for the sample materials and sizes.

Area [cm^2]	24 x 6		12 x 12	48 x 3
Sample	Fe 50% NaK 30%	Fe 50%	Fe 50% NaK 30%	
Averaged DPA of Fe [/yr]	8.04	8.20	9.54	5.38
Averaged ^{4}He of Fe [ppm/yr]	111.8	114.6	130.2	78.2
^{4}He / DPA	13.9	14.0	13.6	14.5

Table 4.4 Nuclear heating at front region (2 cm-thickness) of sample.

		Nuclear heating by Fe [W/cm^3]				Nuclear heating by SiC [W/cm^3]	
Area [cm^2]		24 x 6		12 x 12	48 x 3	24 x 6	
Sample		Fe 50% NaK 30%	Fe 50%	Fe 50% NaK 30%		SiC 50% NaK 30%	SiC 50%
Gamma-ray	Average	9.593	9.473	11.76	5.726	1.303	1.208
	Maximum	14.12	13.93	17.71	6.952	1.874	1.740
Neutron	Maximum	9.483	9.498	10.29	6.464	17.61	17.63

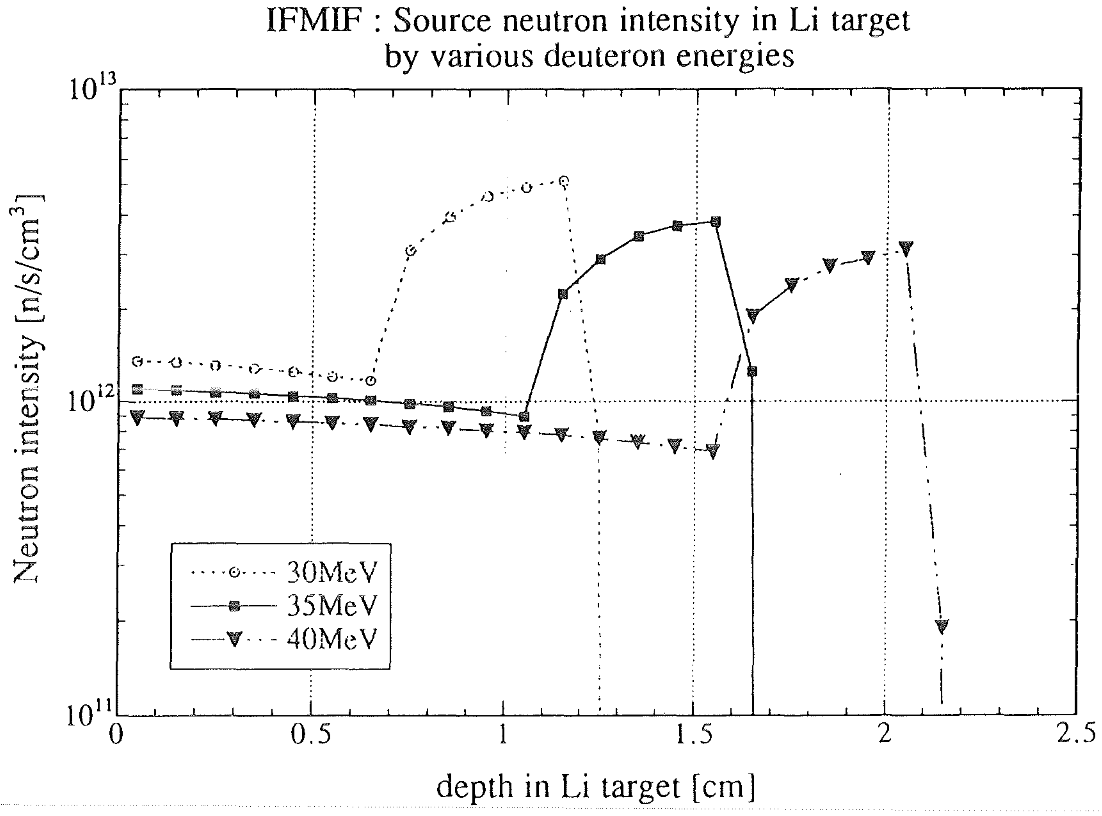

Fig. 2.1

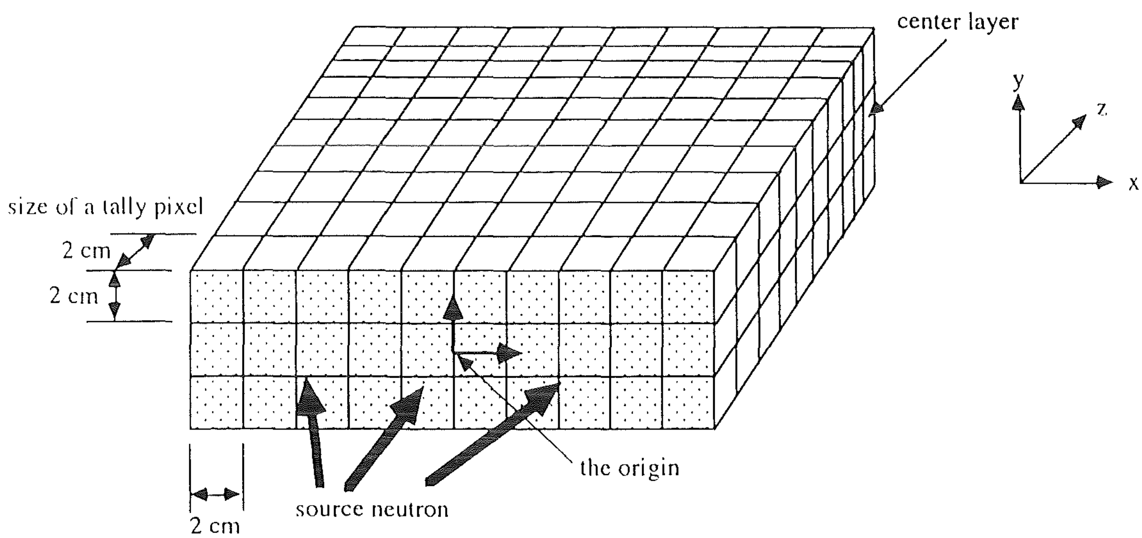

Fig. 3.1 Arrangement of tally-pixels in a irradiation sample used by GMVP calculation (for 24x6x20 cm size).

Fig. 4.1

IFMIF : mapping of Fe volume-dpa [/yr] on x-z plane
(Fe-50%, NaK-30% ; 24*6*20 cm^3)

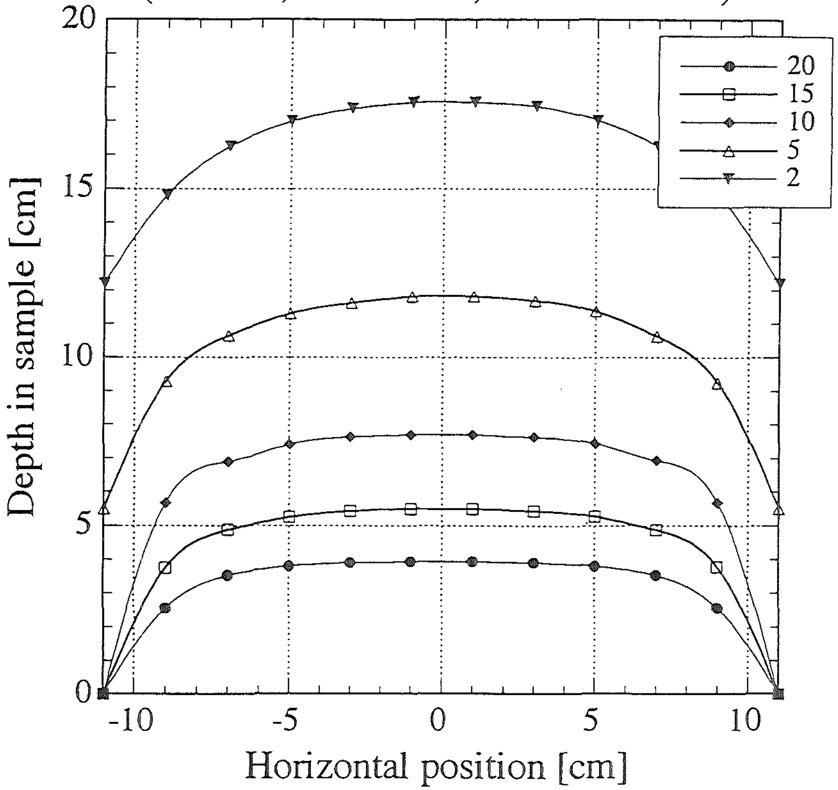

Fig. 4.2

IFMIF : mapping of Fe volume-dpa [/yr] on x-z plane
(Fe-50% ; 24*6*20 cm^3)

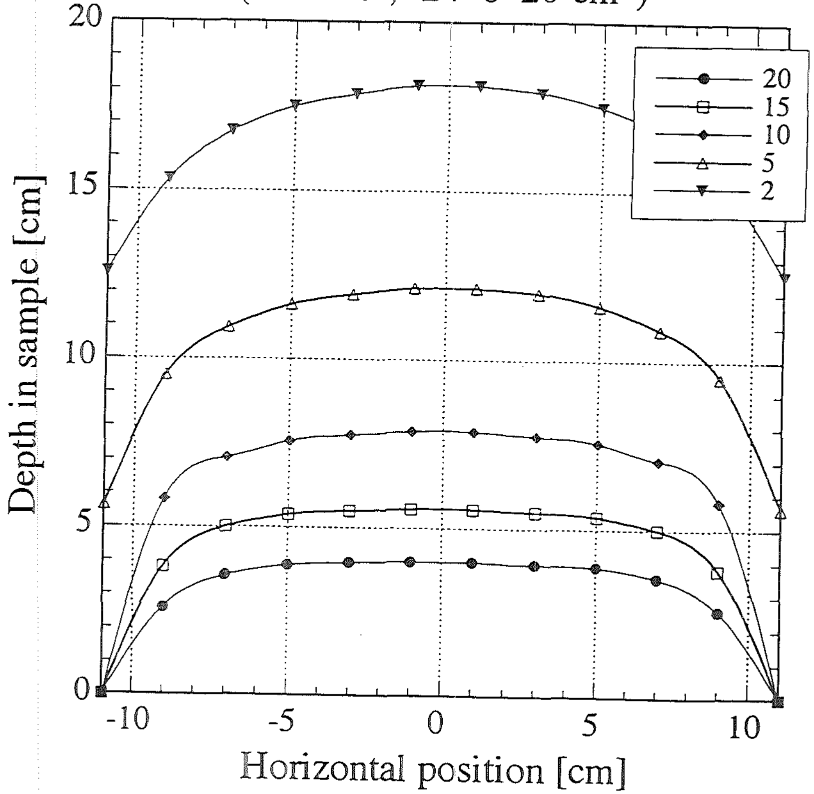

Fig. 4.3

IFMIF : mapping of Fe volume-dpa [/yr] on x-z plane (Fe-50%, NaK-30% ; 12*12*20 cm^3)

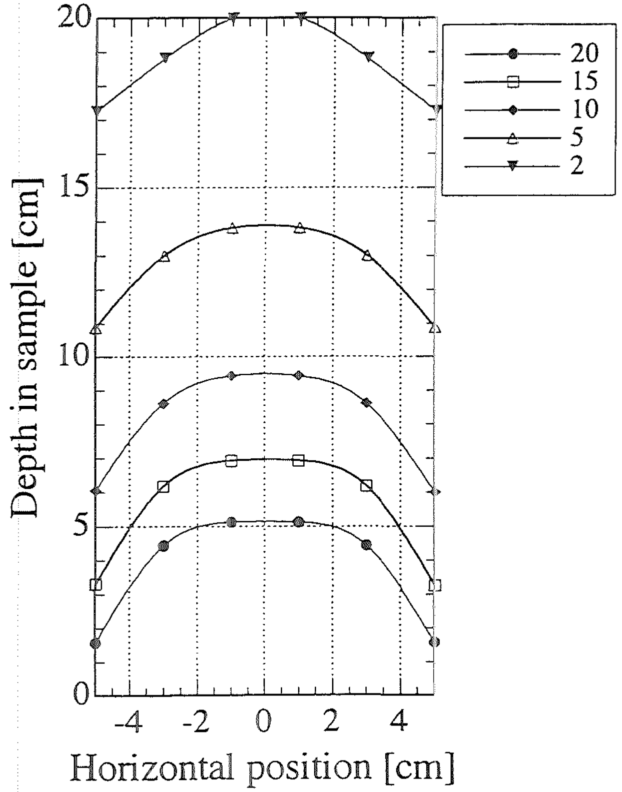

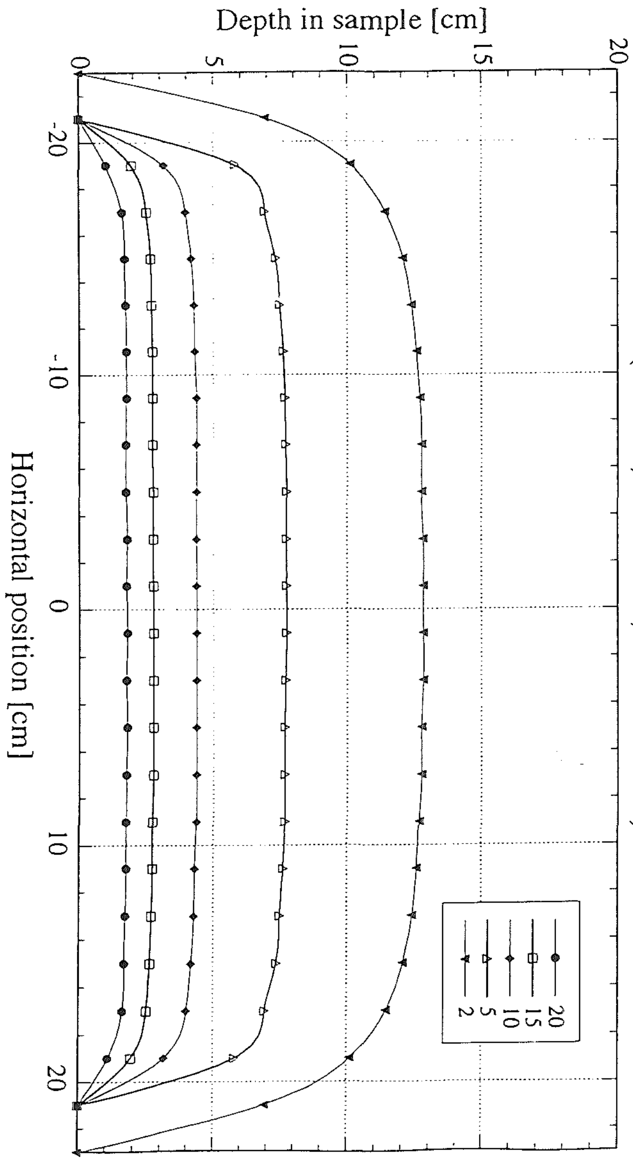

Fig. 4.4 IFMIF : mapping of Fe volume-dpa [/yr] on x-z plane (Fe-50%, NaK-30% ; 48*3*20 cm^3)

Fig. 4.5

IFMIF : mapping of Fe volume-dpa [/yr] on x-z plane (nothing ; 24*6*20 cm^3)

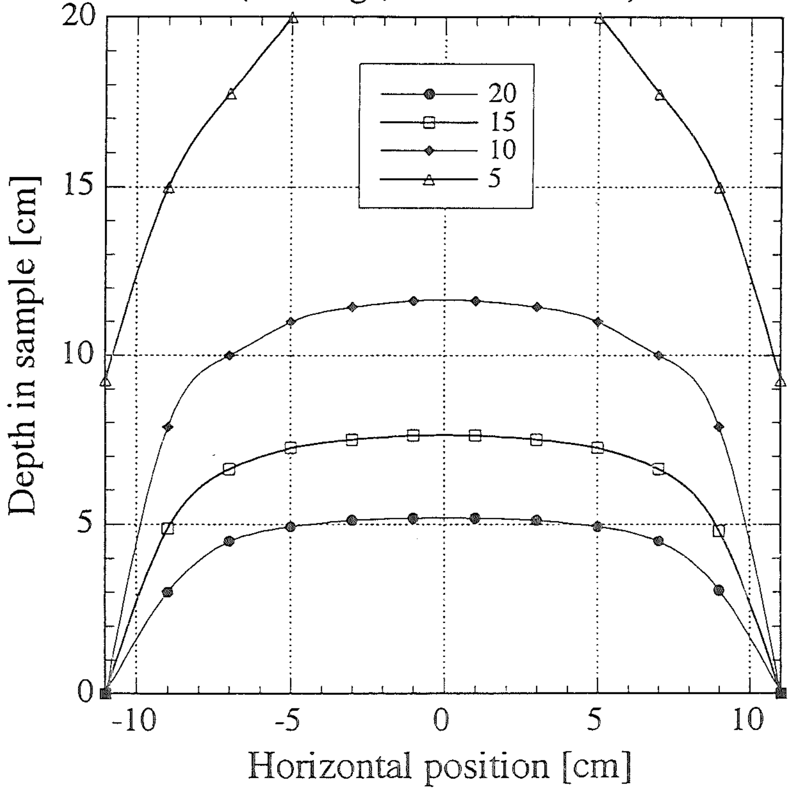

Fig. 4.6

IFMIF : mapping of Fe volume-dpa [/yr] on x-z plane (nothing ; 12*12*20 cm^3)

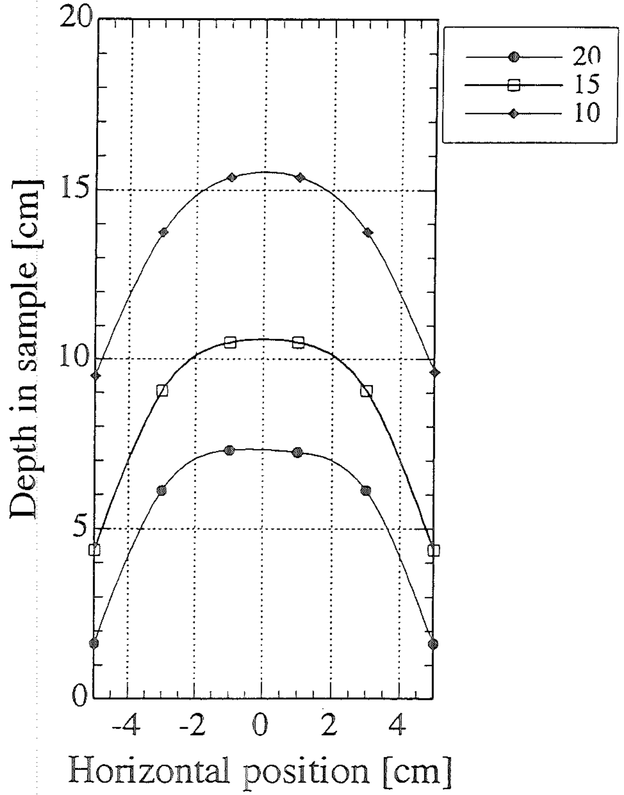

Fig. 4.8

IFMIF : mapping of Si volume-dpa [/yr] on x-z plane
(SiC-50%, NaK-30% ; 24*6*20 cm^3)

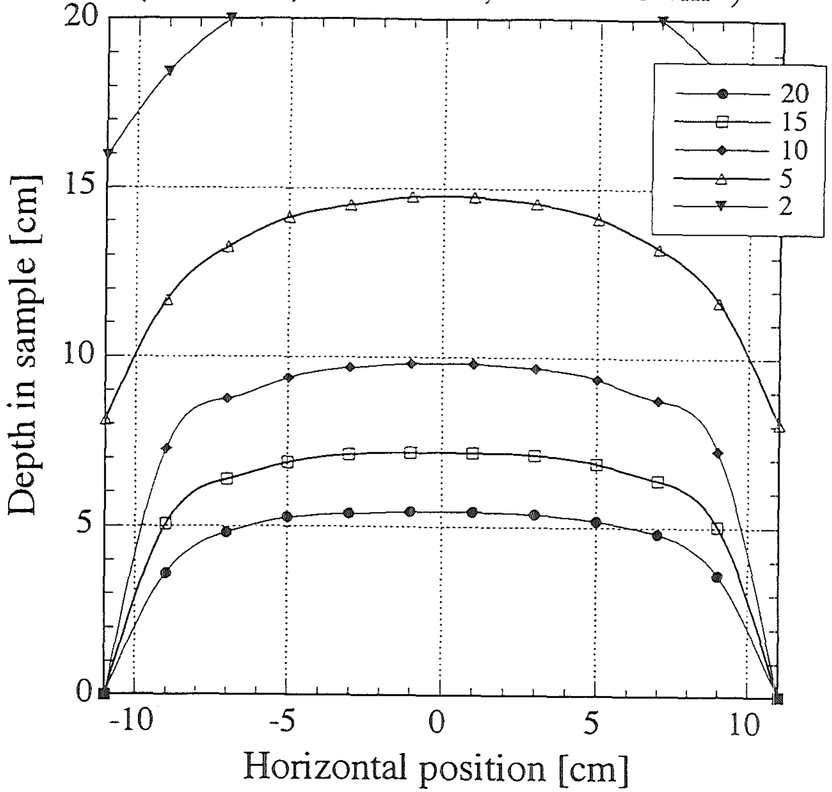

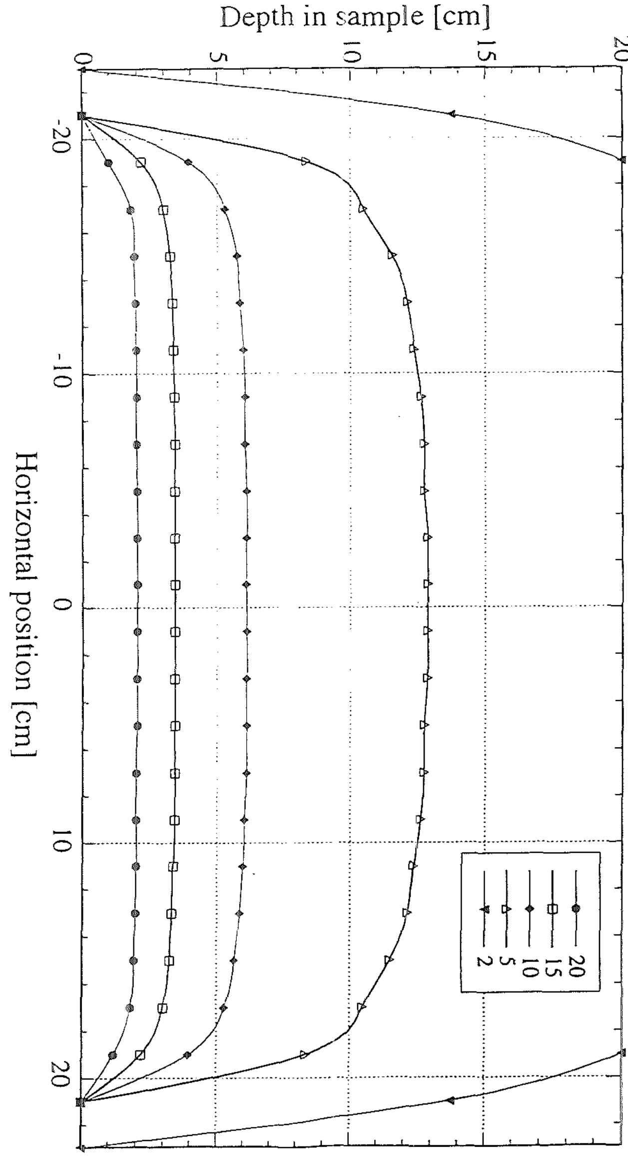

Fig. 4.7 IFMIF : mapping of Fe volume-dpa [/yr] on x-z plane
(nothing ; 48*3*20 cm^3)

Fig. 4.9

IFMIF : mapping of Si volume-dpa [/yr] on x-z plane

(SiC-50% ; 24*6*20 cm^3)

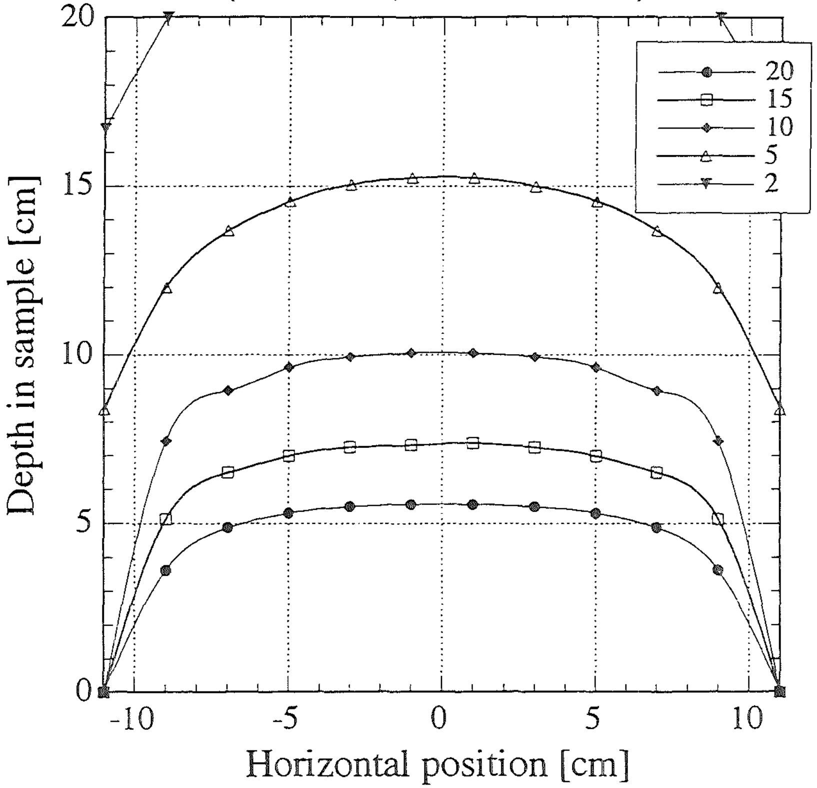

Fig. 4.10

IFMIF : mapping of Si volume-dpa [/yr] on x-z plane

(nothing ; 24*6*20 cm^3)

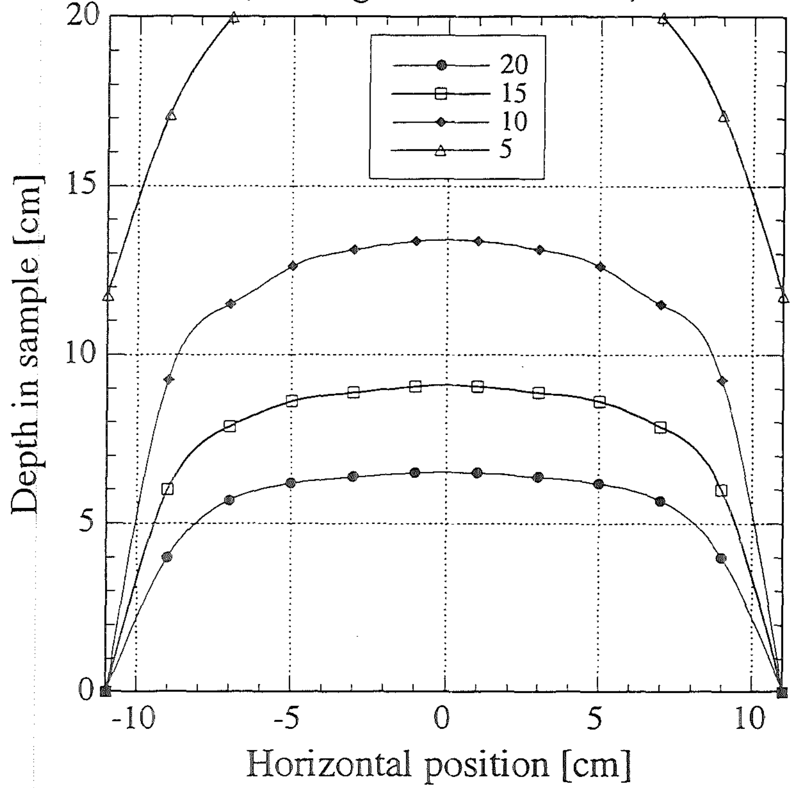

Fig. 4.11

IFMIF : mapping of C volume-dpa [/yr] on x-z plane
(SiC-50%, NaK-30% ; 24*6*20 cm^3)

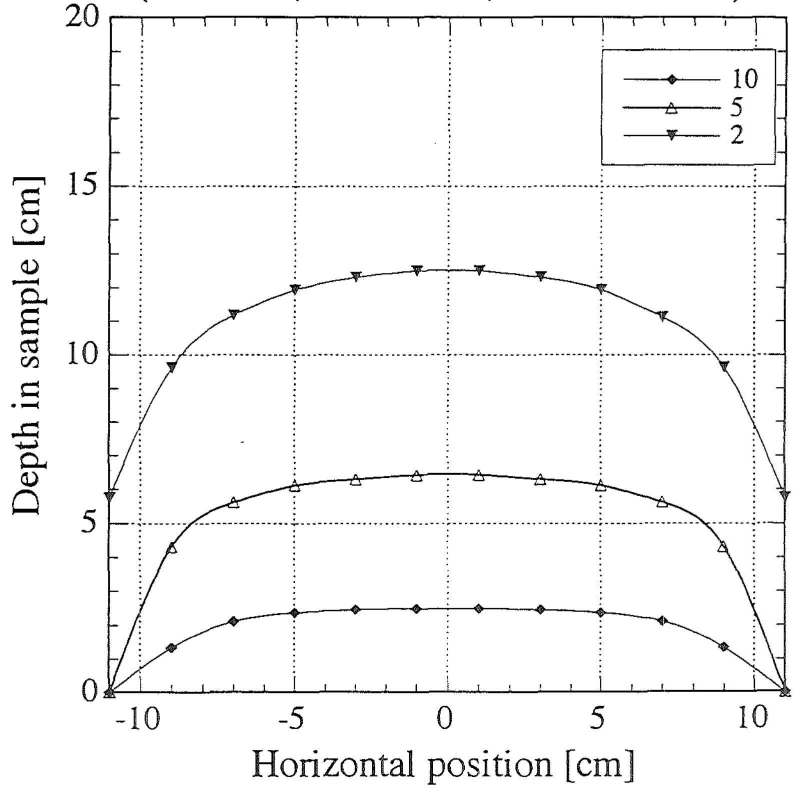

Fig. 4.12

IFMIF : mapping of C volume-dpa [/yr] on x-z plane
(SiC-50% ; 24*6*20 cm^3)

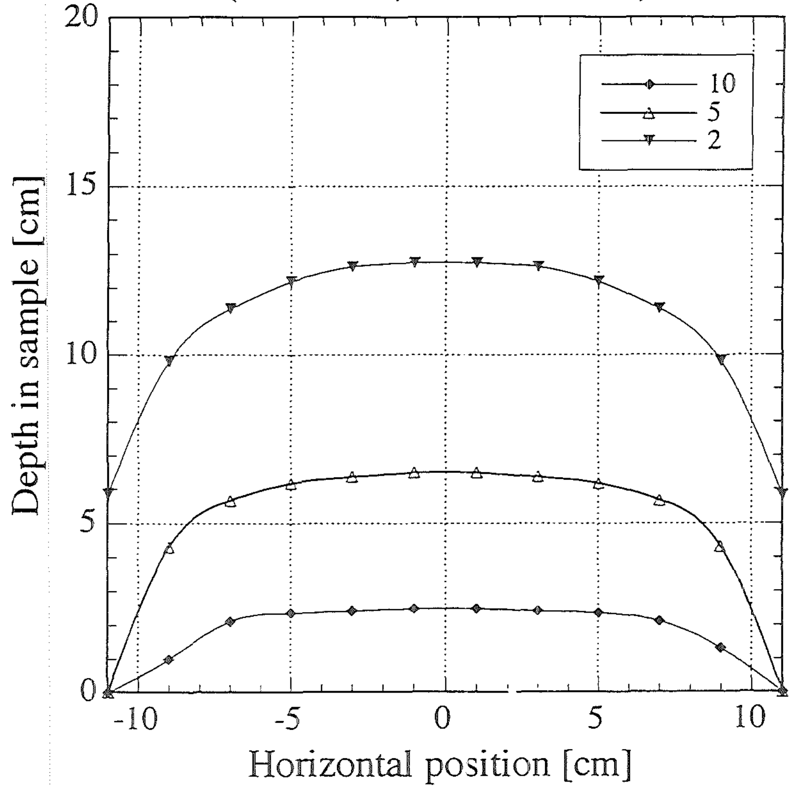

Fig. 4.13

IFMIF : mapping of C volume-dpa [/yr] on x-z plane

(nothing ; 24*6*20 cm^3)

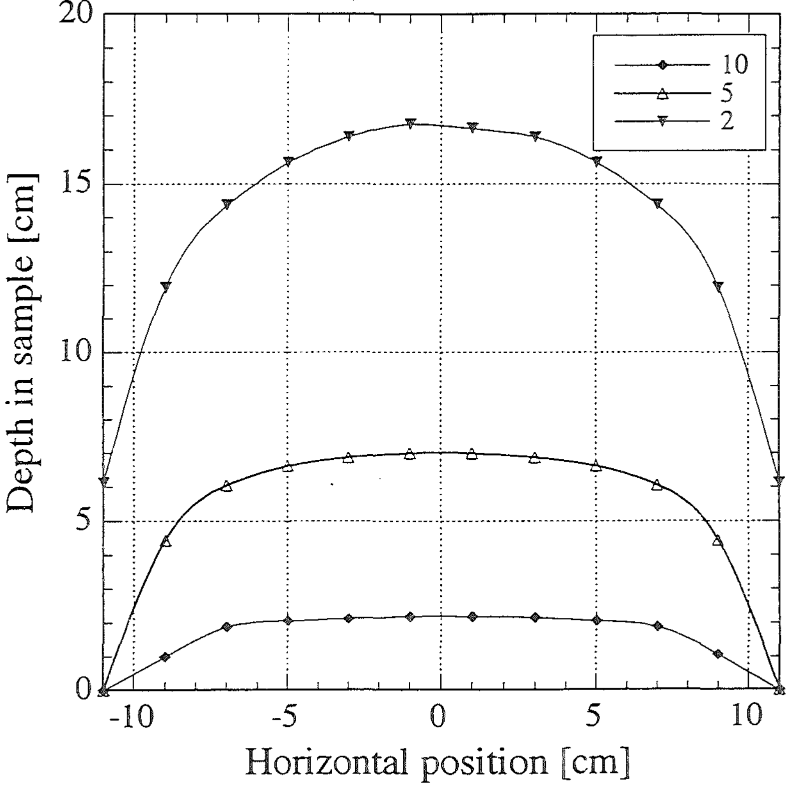

Dpa-Volume with beam current

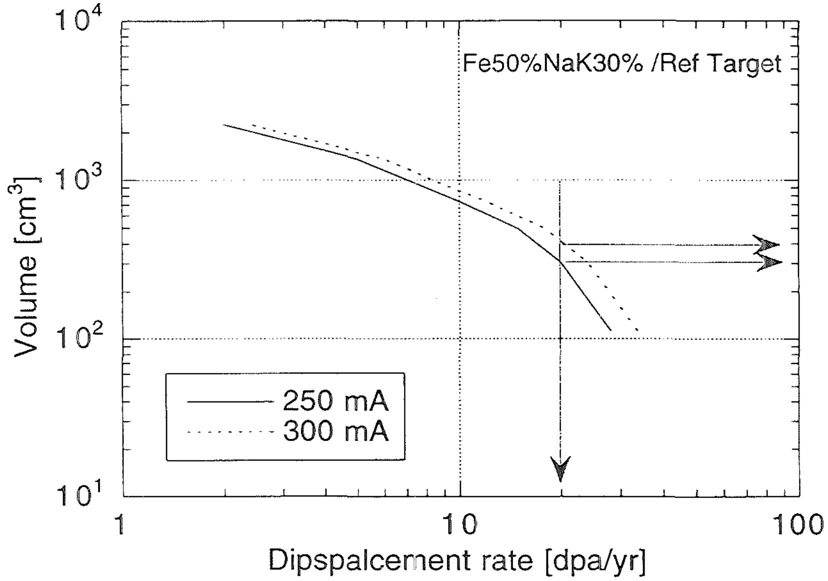

Fig. 4.14

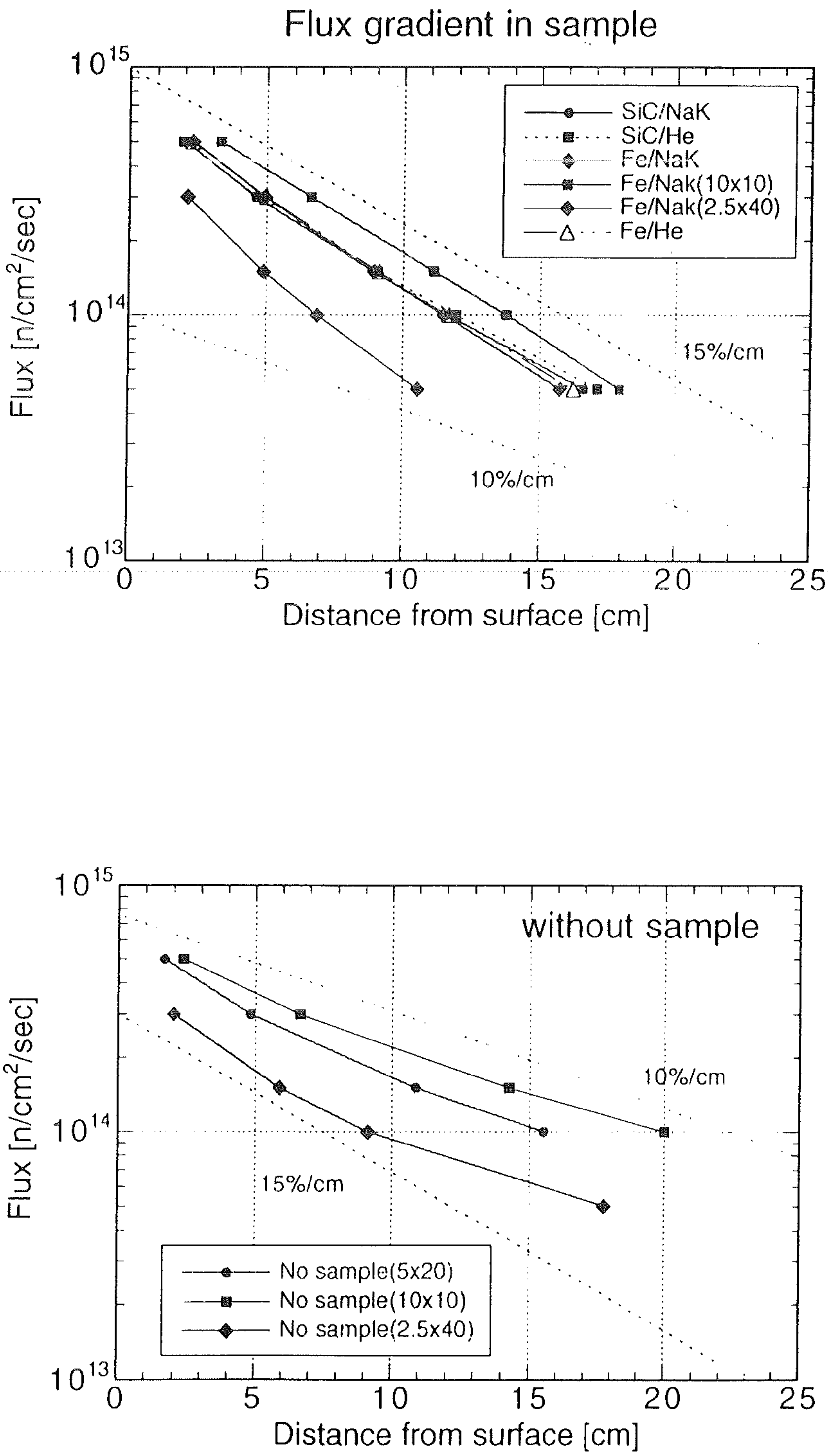

Flux gradient in sample
10^{15}
10^{14}
10^{13}
0
5
10
15
20
25
Flux [n/cm²/sec]
Distance from surface [cm]
SiC/NaK
SiC/He
Fe/NaK
Fe/Nak(10x10)
Fe/Nak(2.5x40)
Fe/He
15%/cm
10%/cm
without sample
No sample(5x20)
No sample(10x10)
No sample(2.5x40)

Fig. 4.15

Major parameters of SSTR

Major Radius	R_p	7.0m	Bootstrap Current	$I_{bootstrap}$	9 MA
Minor Radius	a_p	1.75m	Beam Driven Current	I_{beam}	3 MA
Elongation	κ	1.8	NBI Power	P_{NBI}	60 MW
Triangularity	δ	0.3	Beam Energy	E_{beam}	2MeV
Aspect Ratio	A	4.0	Fusion Power	P_{fusion}	3000MW
Plasma Volume	V	760m^3	Power Gain	Q	50
Plasma Current	I_p	12MA	Total Thermal Output	P_{th}	3710MW
Toroidal Field	B_t	9T	Max. Neutron Wall Load	P_n	5MW/m^2
Safety Factor	q(95%)	5.0	Gross Electric Power	P_{eG}	1280MWe
Safety Factor	q(0)		Net Electric Power	P_{enet}	1080MWe
Toroidal Beta	β_t	2.52%			
Poloidal Beta	β_p	2.0			
Troyon Factor	g	3.3			
Average Density	$\langle n_e \rangle$	1.45×10^{20} m^{-3}			
Average Temperature	$\frac{\langle nT \rangle}{\langle n \rangle}$	17keV			
Effective Charge	Z_{eff}	1.8			
He Concentration	f(He)	0.05			

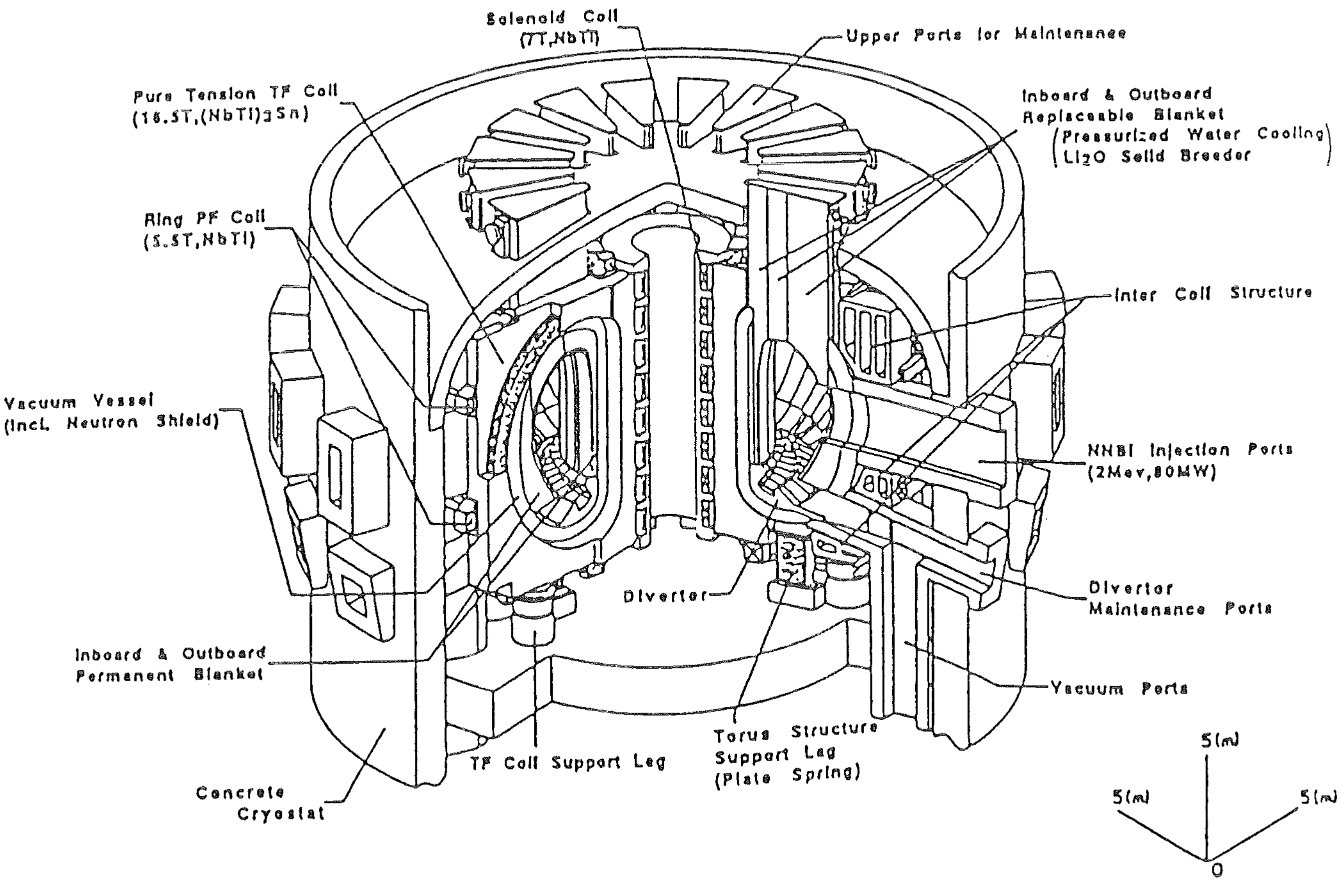

Fig. 4.16 Bird's-eye view of SSTR

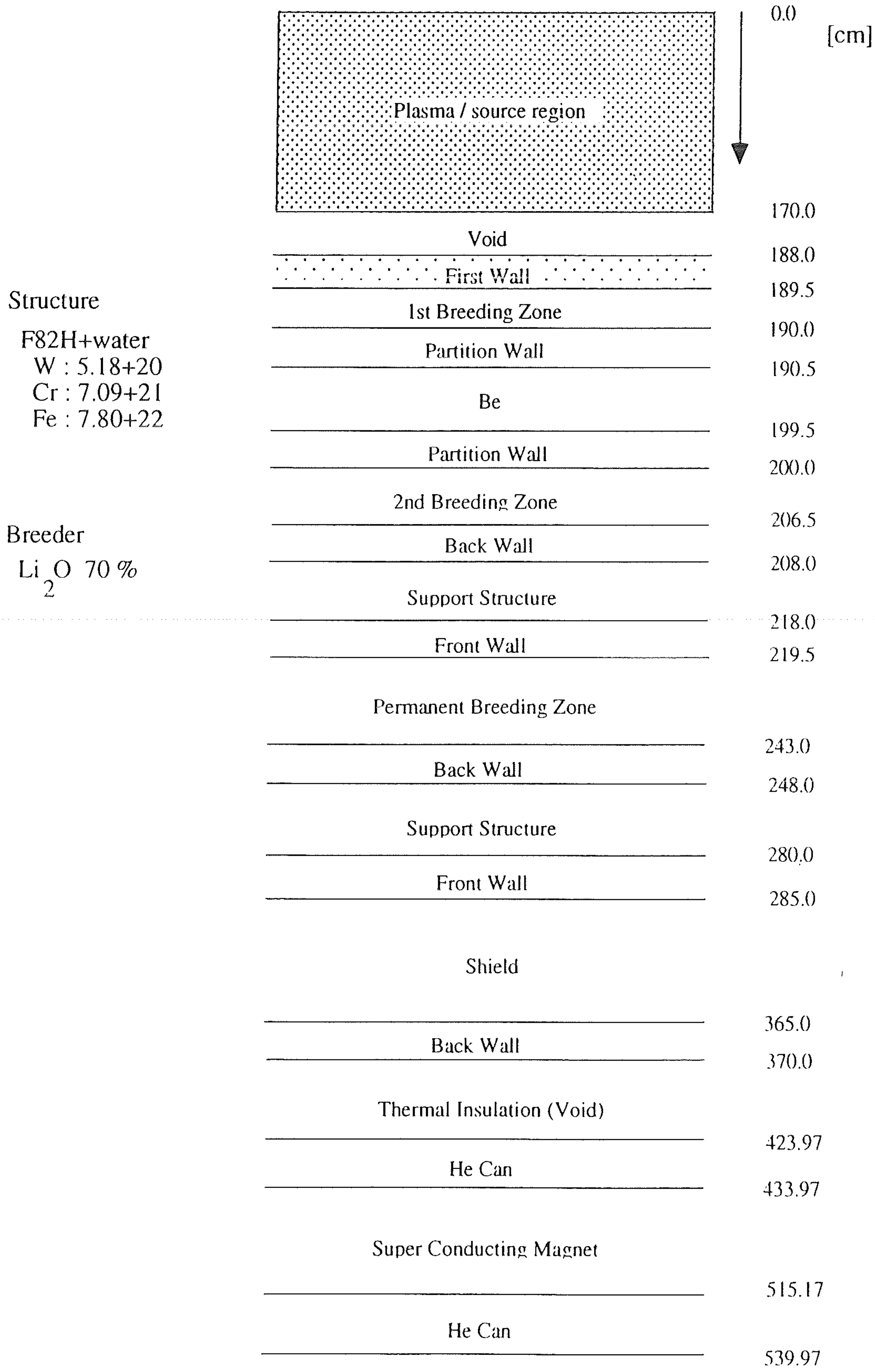

Fig. 4.17 One-dimension Cylinder Model for ANISN of the SSTR.

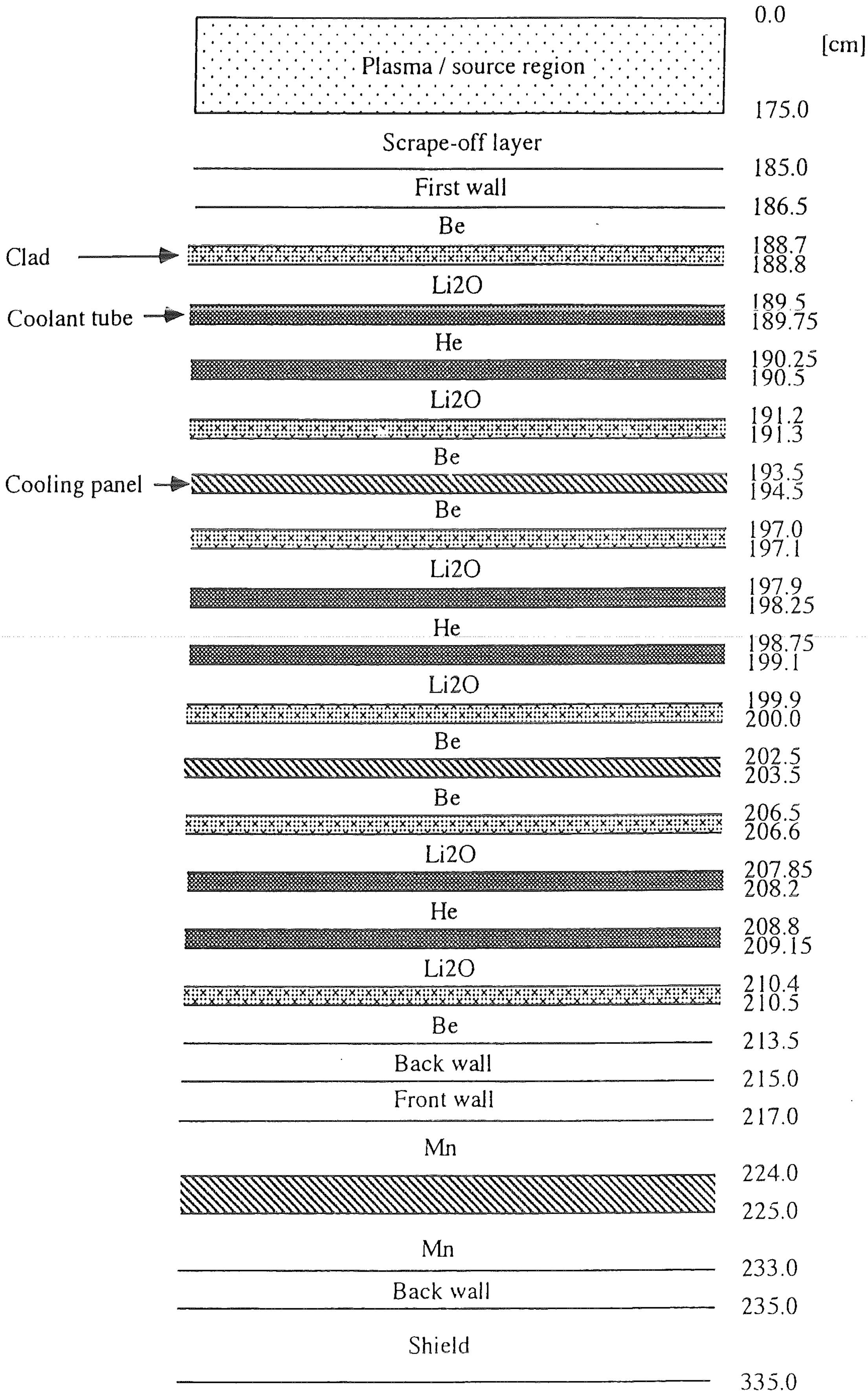

Fig. 4.18 One-dimension cylinder model for ANISN of the DREAM.

Fig. 4.19 Comparison of neutron flux

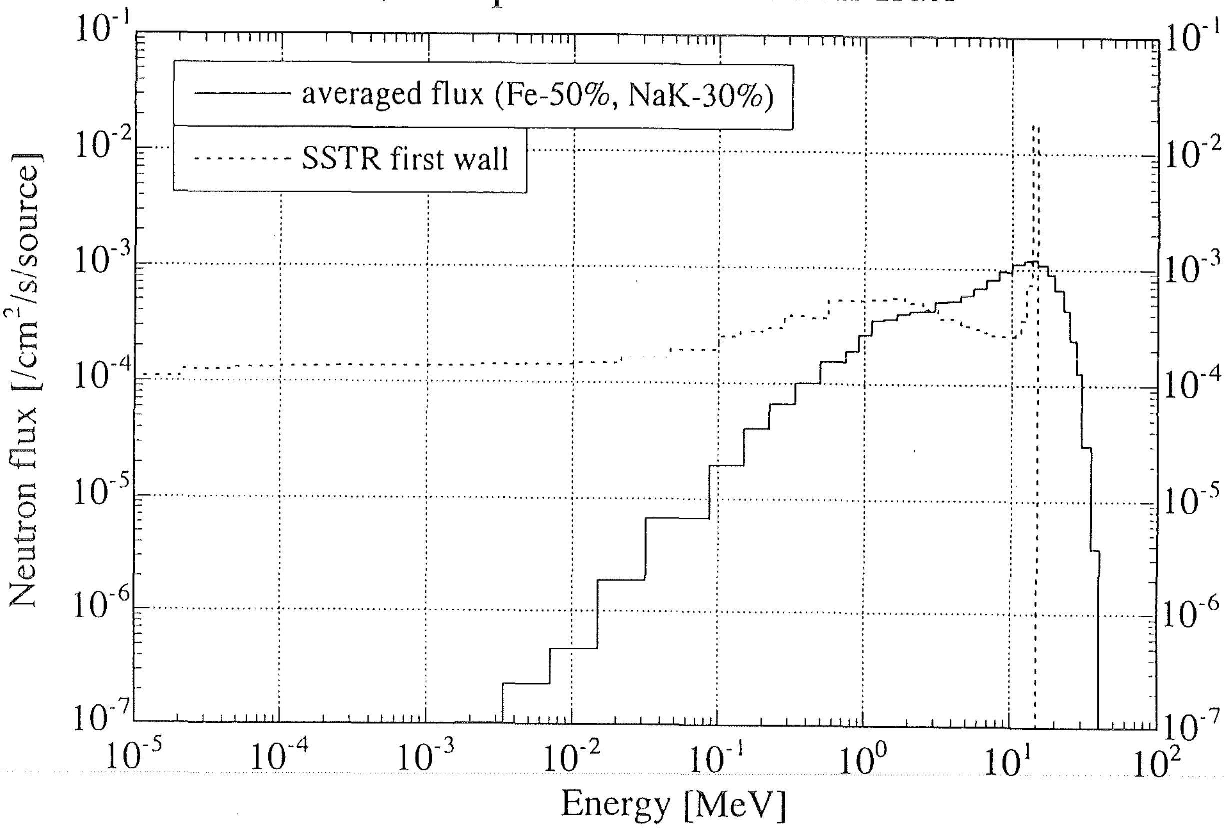

Fig. 4.20 Comparison of neutron flux

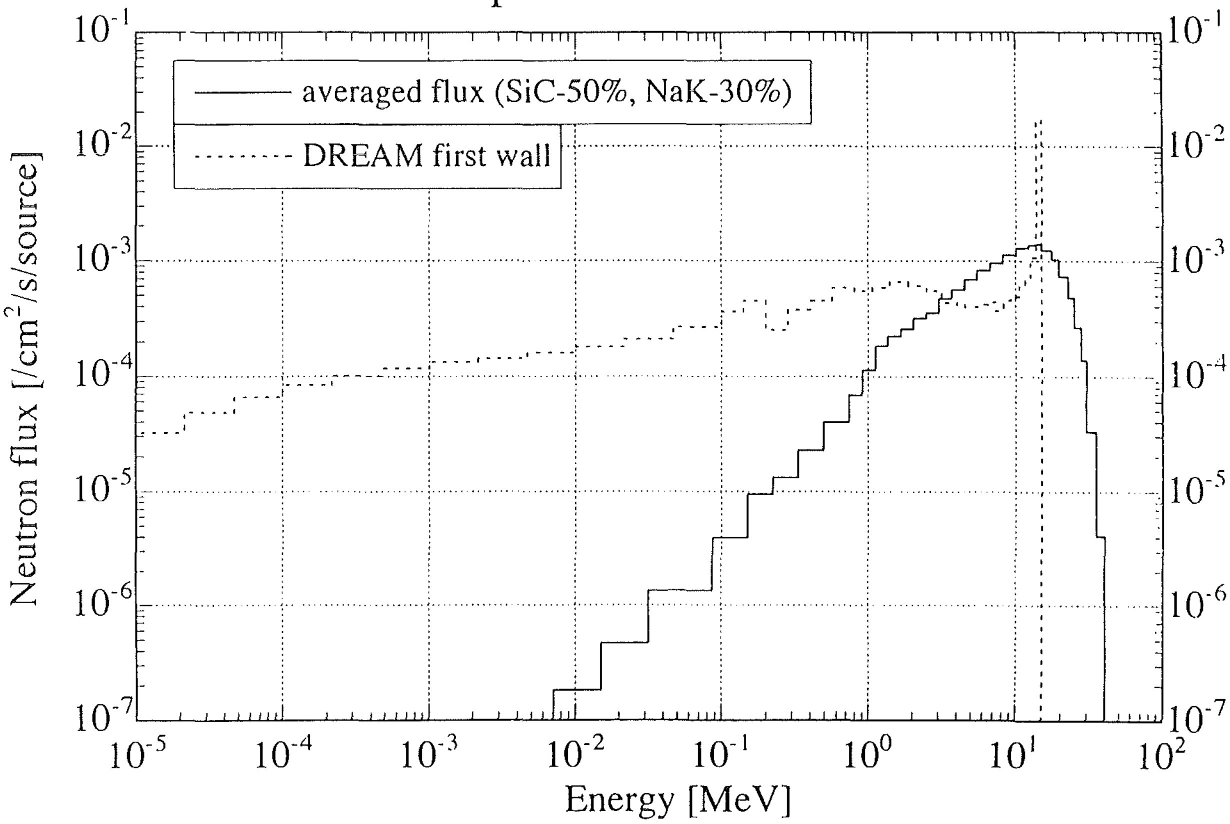

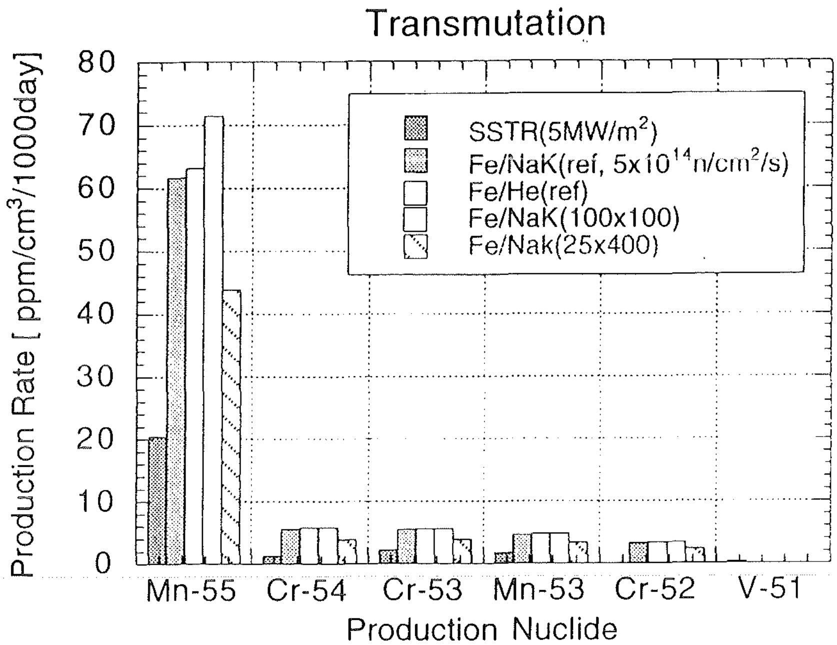

Fig. 4.21

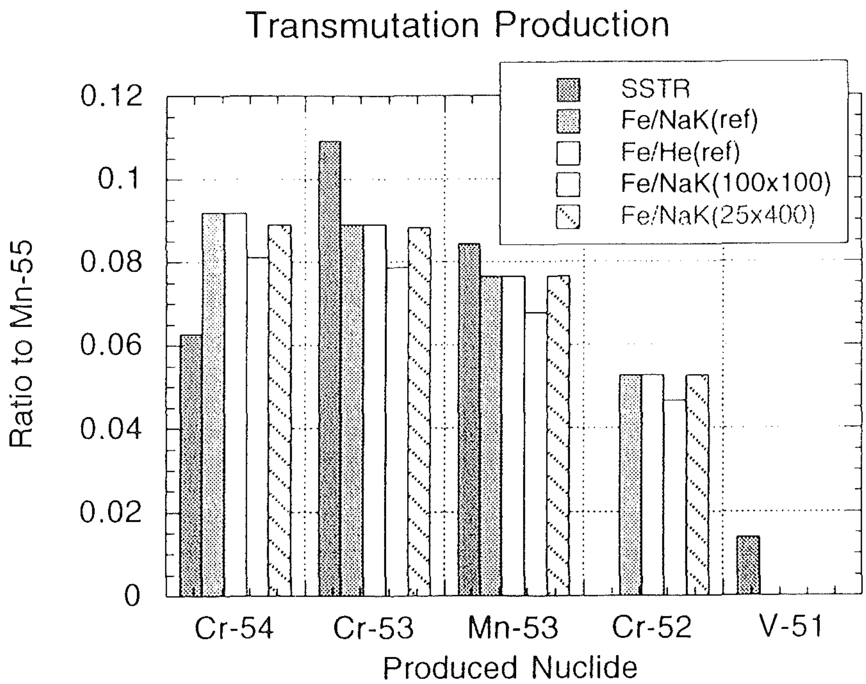

Fig. 4.22

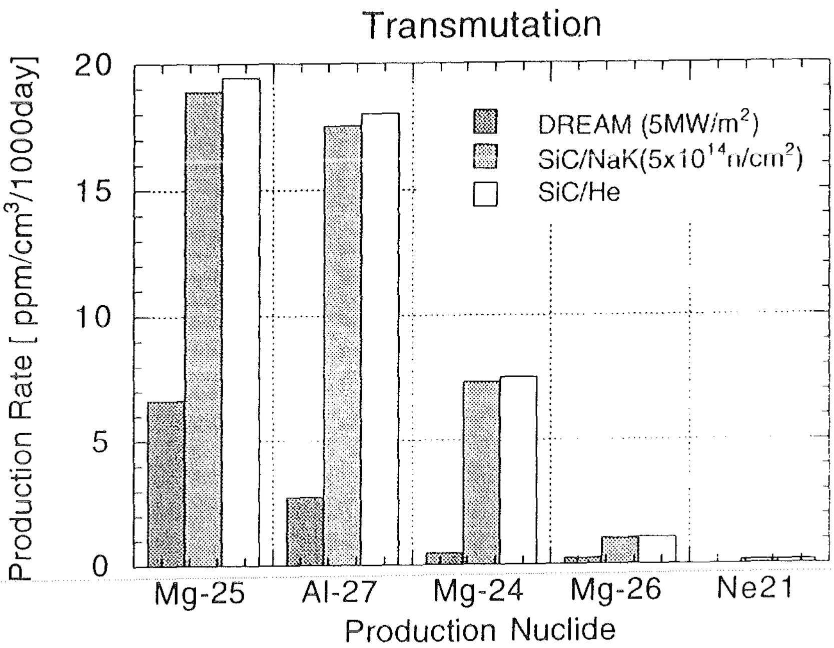

Fig. 4.23

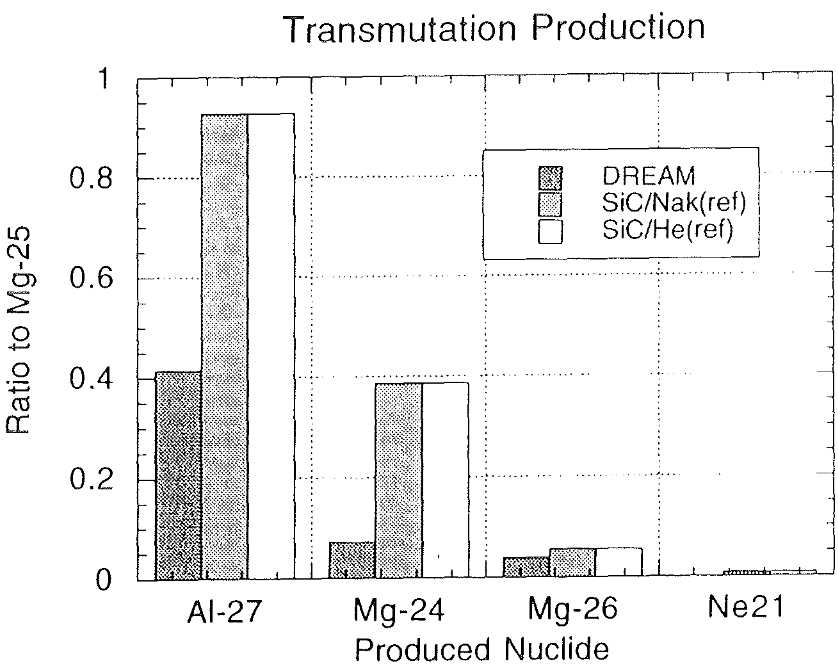

Fig. 4.24

Appendix 1 Geometry model for Analysis

standard sample loading for test matrix region

1) Fe 50%, NaK 30%, Void 20%
2) Fe 50%, Void 50%
3) SiC 50%, NaK 30%, Vois 20%
4) SiC 50%, Void 50%

reference reactor condition

SSTR (Steady State Tokamak Reactor) proposed for DEMO by JAERI
Li_2O/He cooling

parameters to be evaluated

1) neutron flux-volume relation
2) dpa
3) transmutation
4) activation
5) gamma-ray dose, gamma-ray heating

Code and Library

MORSE-CG + HILO86 or HILO86J (JAERI version)

Model configuration

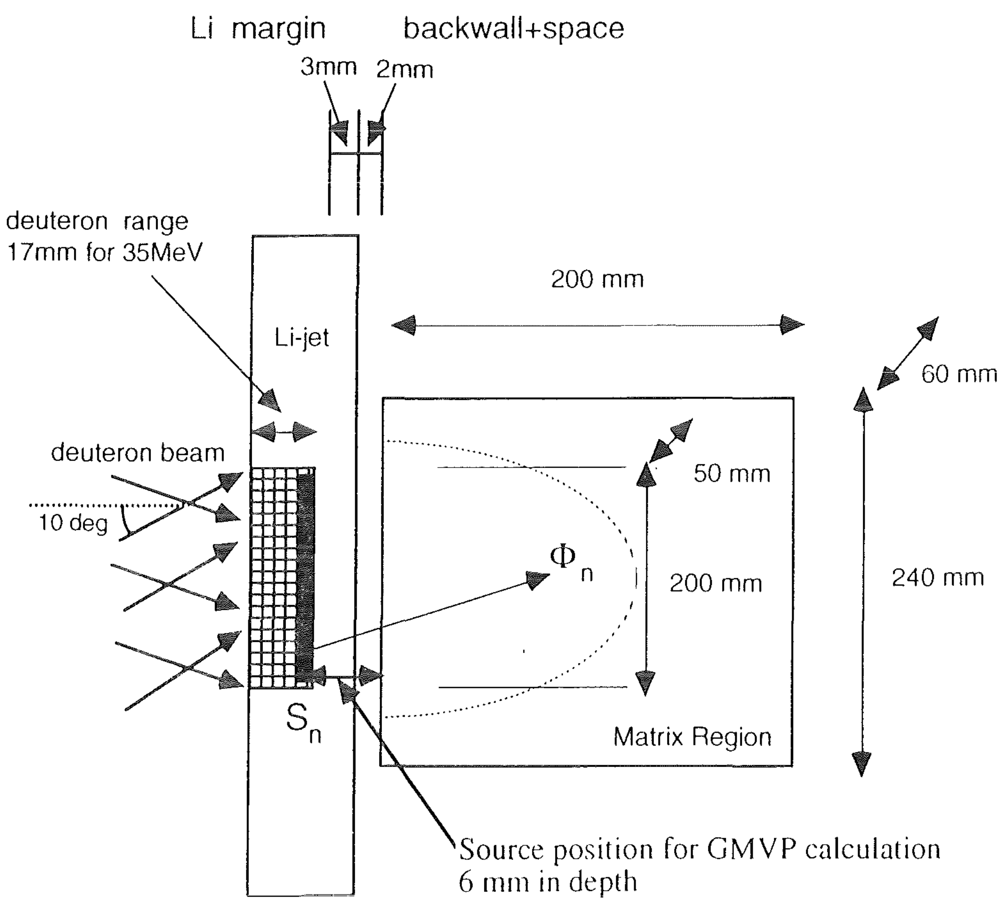

Testing Volume as a Function of the Material Loading

IFMIF Test Cell Design Meeting

Karlsruhe - Germany

Itacil C. Gomes

July 3-6, 1995

I.C.Gomes - Argonne National Laboratory

Variation of the Testing Volume for Fe, SiC, and NaK

Cases analyzed :

1. Influence of the beam shape (2.5x40, 5x20, and 10x10)
2. Influence of the deuterons energy (30, 35, and 40 MeV)
3. Influence of the material loading

I.C.Gomes - Argonne National Laboratory

Variation of the Testing Volume with DPA Rate Above 20 dpa/fpy for 30MeV Deuterons - 250mA

- case #1 = 50% Fe, 30% NaK, 20% vacuum
- case #2 = 50% Fe, 50% vacuum
- case #3 = 50% SiC, 50% vacuum
- case #4 = 50% SiC, 30% NaK, 20% vacuum

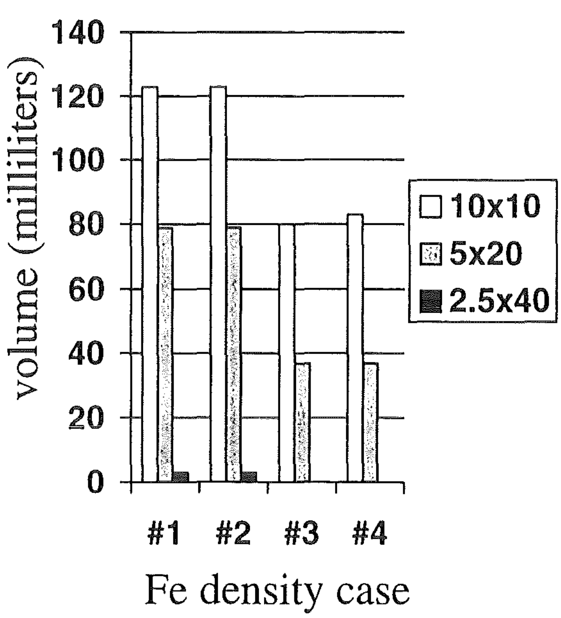

I.C.Gomes - Argonne National Laboratory

Variation of the Testing Volume with DPA Rate Above 20 dpa/fpy for 35 MeV Deuterons - 250mA

- case #1 = 50% Fe, 30% NaK, 20% vacuum
- case #2 = 50% Fe, 50% vacuum
- case #3 = 50% SiC, 50% vacuum
- case #4 = 50% SiC, 30% NaK, 20% vacuum

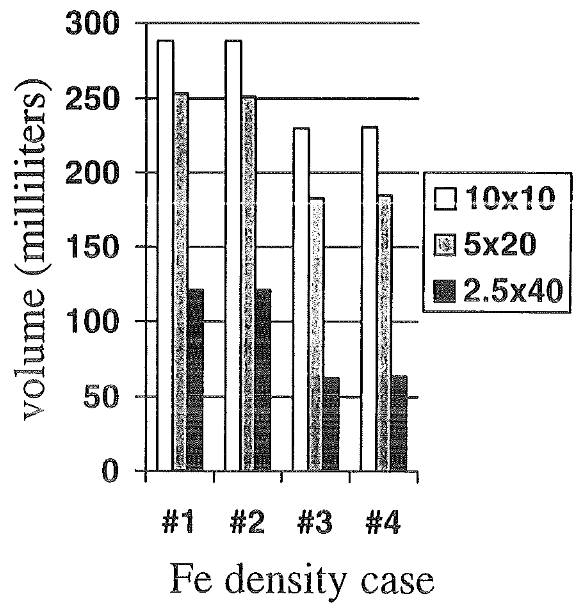

I.C.Gomes - Argonne National Laboratory

Variation of the Testing Volume with DPA Rate Above 20 dpa/fpy for 40 MeV Deuterons - 250mA

- case #1 = 50% Fe, 30% NaK, 20% vacuum
- case #2 = 50% Fe, 50% vacuum
- case #3 = 50% SiC, 50% vacuum
- case #4 = 50% SiC, 30% NaK, 20% vacuum

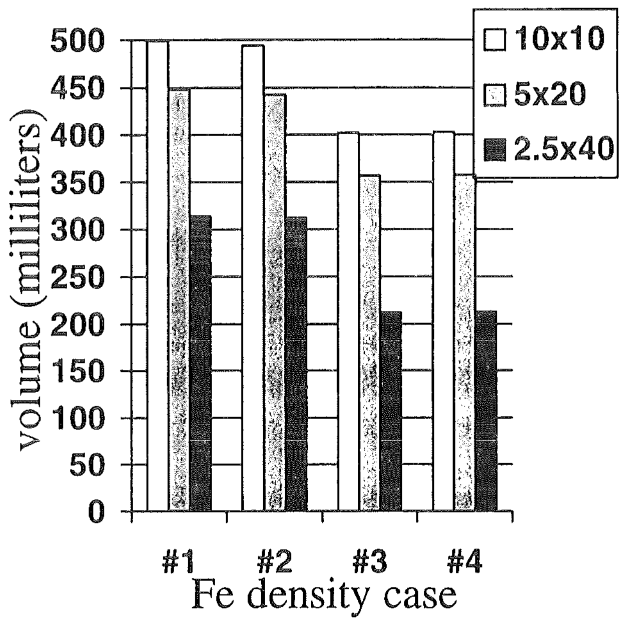

I.C.Gomes - Argonne National Laboratory

Variation of the Testing Volume with DPA Rate Above 10 dpa/fpy for 30 MeV deuterons - 250mA

- case #1 = 50% Fe, 30% Nak, 20% vacuum
- case #2 = 50% Fe, 50% vacuum
- case #3 = 50% SiC, 50% vacuum
- case #4 = 50% SiC, 30% Nak, 20% vacuum

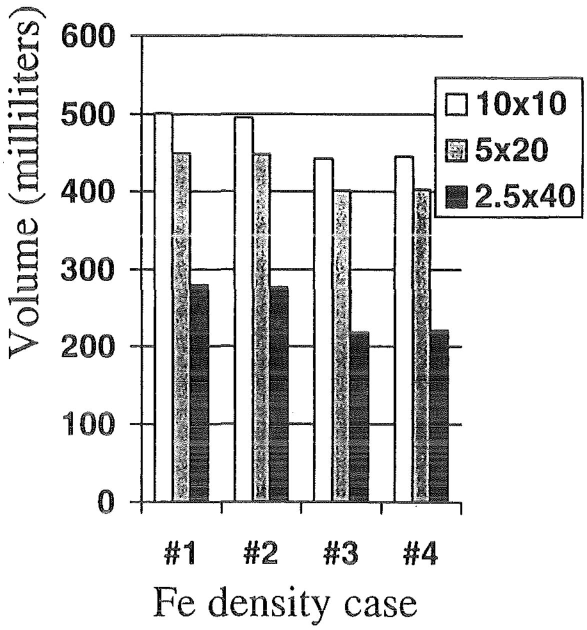

I.C.Gomes - Argonne National Laboratory

Variation of the Testing Volume with DPA Rate Above 10 dpa/fpy for 35 MeV Deuterons - 250mA

- case #1 = 50% Fe, 30% NaK, 20% vacuum
- case #2 = 50% Fe, 50% vacuum
- case #3 = 50% SiC, 50% vacuum
- case #4 = 50% SiC, 30% NaK, 20% vacuum

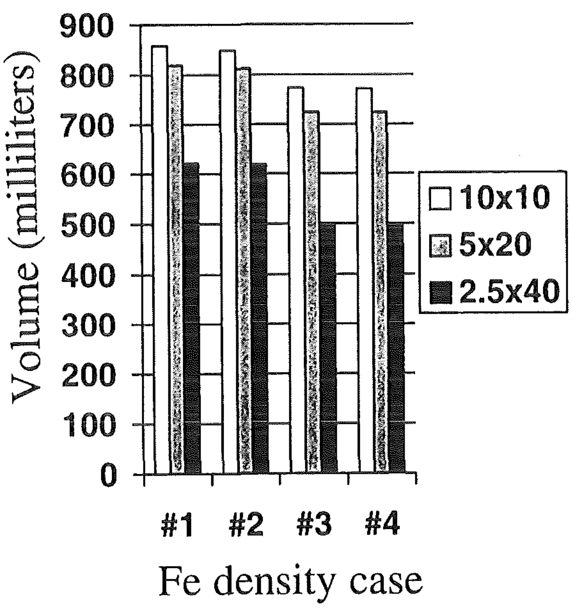

I.C.Gomes - Argonne National Laboratory

Variation of the Testing Volume with DPA Rate Above 10 dpa/fpy for 40 MeV Deuterons - 250mA

- c#1 = 50% Fe, 30% Nak, 20% vacuum
- c#2 = 50% Fe, 50% vacuum
- c#3 = 50% SiC, 50% vacuum
- c#4 = 50% SiC, 30% NaK, 20% vacuum

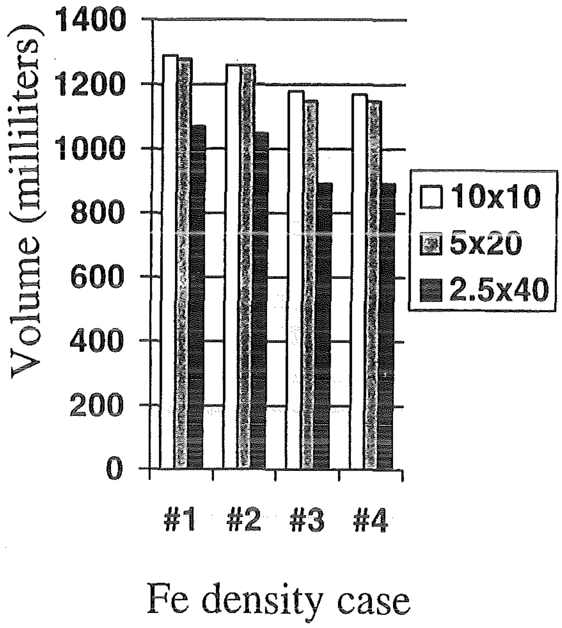

I.C.Gomes - Argonne National Laboratory

Variation of the Testing Volume with the Beam Cross-Sectional Shape - 35MeV Deuterons - 250mA Current

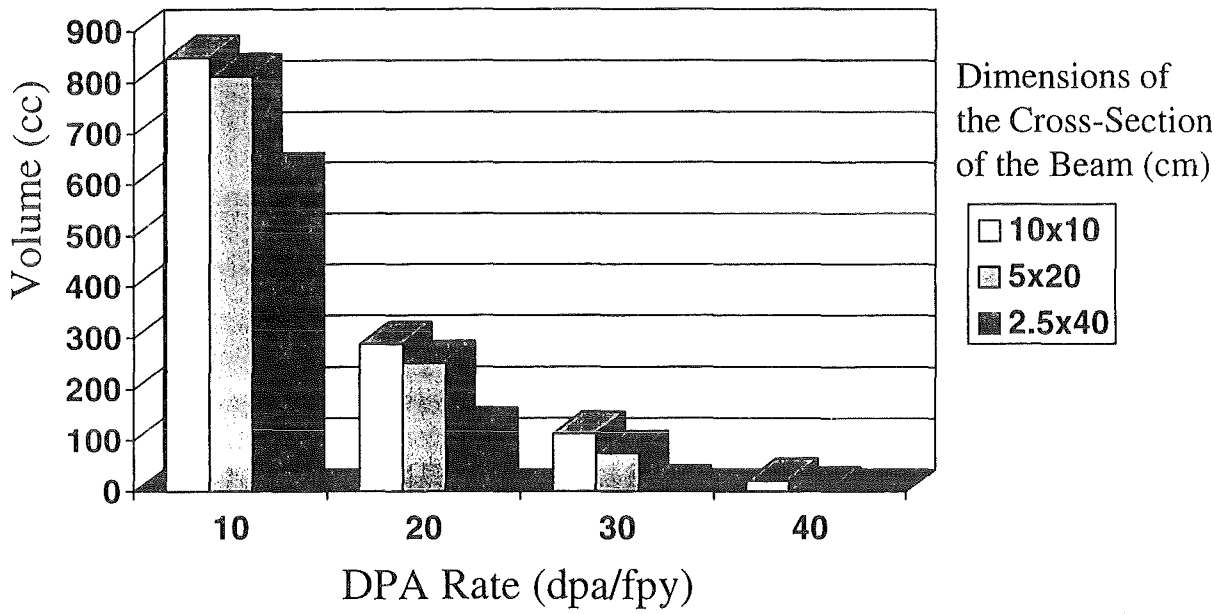

Variation of the Testing Volume with the Beam Cross-Sectional Shape - 40 MeV Deuterons - 250 mA Current

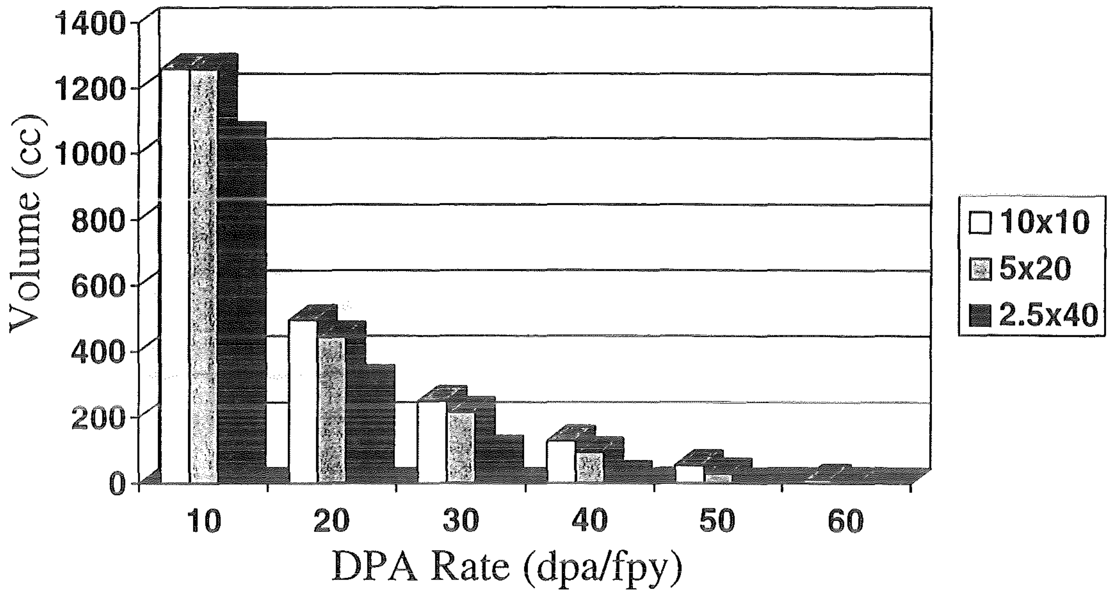

I.C.Gomes - Argonne National Laboratory

Recommendations

- It is strongly recommended to have 40 MeV incident deuteron energy as the reference case for the IFMIF design.
- To keep as much flexibility in the design, in terms of beam spot area and duplicated test cells, to allow a broader application of the facility - including some flexibility on the deuteron energy.

I.C.Gomes - Argonne National Laboratory

Variation of the Testing Volume for a Few Fe densities

Cases Analyzed:

Fe 100% dense   Fe 75% dense

Fe 50% dense   Fe 25% dense

vacuum

I.C.Gomes - Argonne National Laboratory

Changes in Volume Due to Changes of the Fe Density in the Test Assembly Region
30 MeV Deuterons - 250mA - 10x10 beam

- c#1 = vacuum
- c#2 = 25% Fe
- c#3 = 50% Fe
- c#4 = 75% Fe
- c#5 = 100% Fe

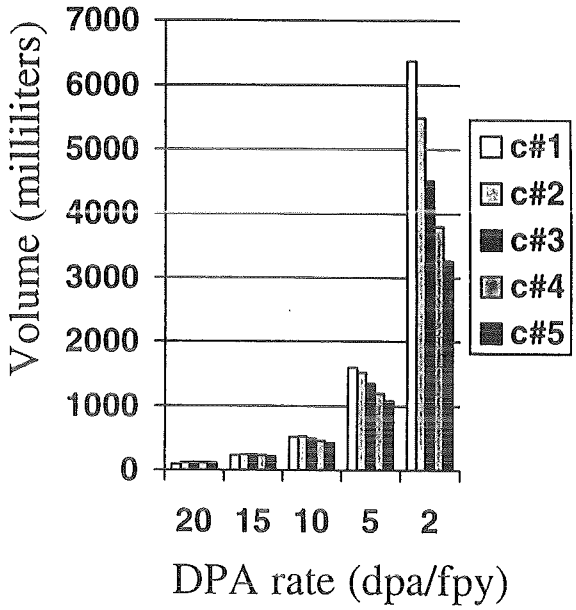

Changes in Volume of the High Flux Region Due to Changes in Fe Density
30 MeV Deuterons - 250mA - 10x10 beam

- c#1 = vacuum
- c#2 = 25% Fe
- c#3 = 50% Fe
- c#4 = 75% Fe
- c#5 = 100% Fe

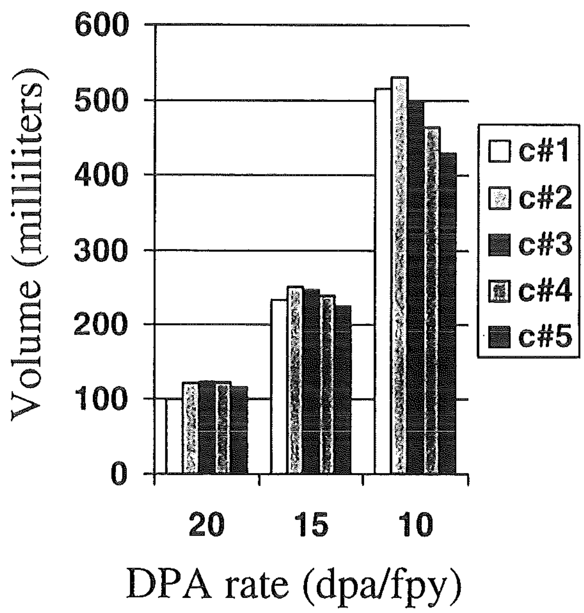

Changes in Volume Due to Changes in Fe Density in the Test Assembly Region 35 MeV deuterons - 250mA - 10x10 beam

- c#1 = vacuum
- c#2 = 25% Fe
- c#3 = 50% Fe
- c#4 = 75% Fe
- c#5 = 100% Fe

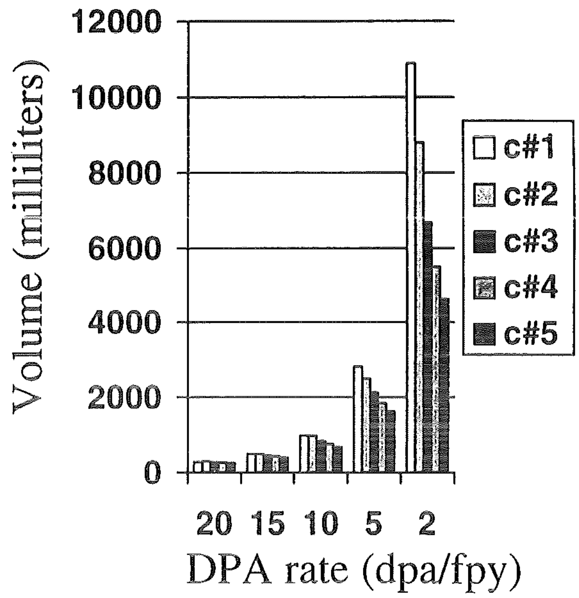

I.C.Gomes - Argonne National Laboratory

Changes in Volume of the High Flux Region Due to Changes in Fe Density 35 MeV Deuterons - 250mA - 10x10 beam

- c#1 = vacuum
- c#2 = 25% Fe
- c#3 = 50% Fe
- c#4 = 75% Fe
- c#5 = 100% Fe

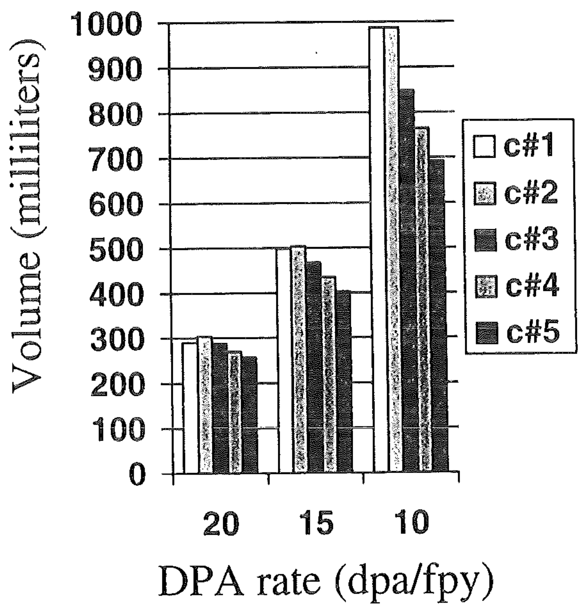

I.C.Gomes - Argonne National Laboratory

Change in Volume Due to Changes in Fe Density in the Test Assembly Region 40 MeV deuterons - 250mA - 10x10 beam

- c#1 = vacuum
- c#2 = 25% Fe
- c#3 = 50% Fe
- c#4 = 75% Fe
- c#5 = 100% Fe

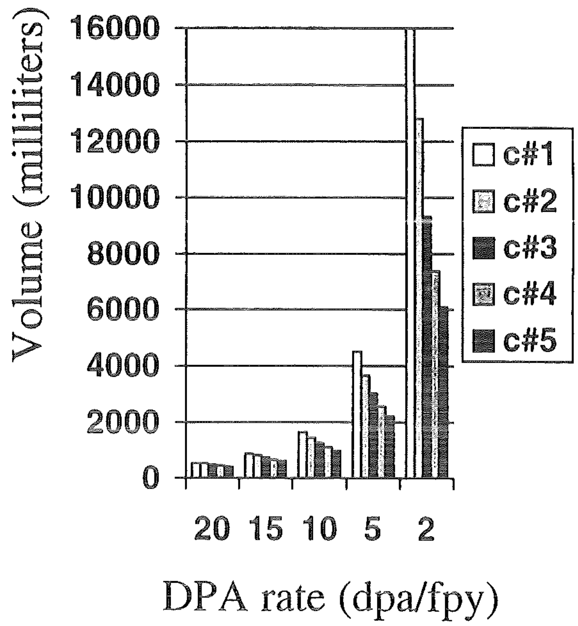

Changes in Volume of the High Flux Region Due to Changes in Fe Density - 40 MeV Deuterons - 250mA - 10x10 beam

- c#1 = vacuum
- c#2 = 25% Fe
- c#3 = 50% Fe
- c#4 = 75% Fe
- c#5 = 100% Fe

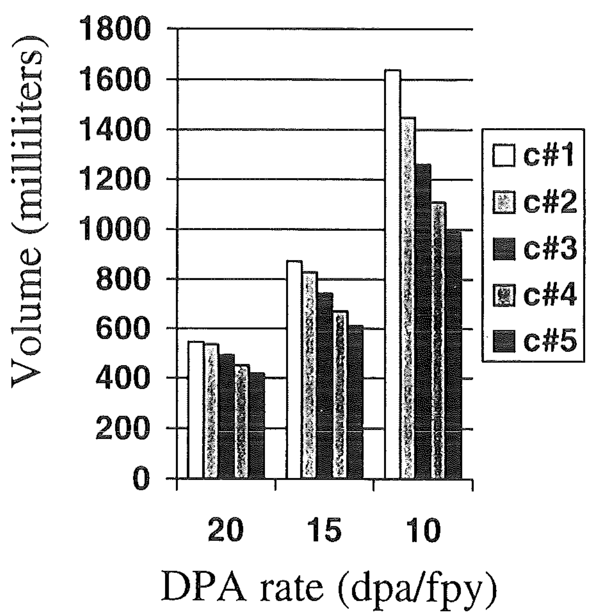

Volume (cc) with dpa rate above the indicated value for different deuteron energies
10cmx10cm beam - 250mA

Vacuum Deuteron Energy (MeV)	DPA / FPY 20	15	10	5	2
40	544	873	1640	4490	16000
35	290	499	987	2810	10900
30	99	233	516	1600	6380

25% Fe Deuteron Energy (MeV)	DPA / FPY 20	15	10	5	2
40	539	828	1450	3670	12800
35	304	504	987	2490	8790
30	121	251	531	1520	5490

Volume (cc) with dpa rate above the indicated value for different deuteron energies
10cmx10cm beam - 250mA

50% Fe Deuteron Energy (MeV)	DPA / FPY 20	15	10	5	2
40	493	743	1260	3020	9340
35	288	468	849	2120	6690
30	123	247	496	1350	4510

75% Fe Deuteron Energy (MeV)	DPA / FPY 20	15	10	5	2
40	453	671	1110	2570	7380
35	257	403	692	1610	4630
30	116	225	429	1080	3260

Volume (cc) with dpa rate above the indicated value for different deuteron energies 10cmx10cm beam - 250mA

100% Fe	DPA / FPY				
Deuteron Energy (MeV)	20	15	10	5	2
40	419	613	988	2220	6090
35	257	403	692	1610	4630
30	116	225	429	1080	3260

Conclusions

- The influence of the material loading scheme on the available volume for the high flux region (above 10-15 dpa/fpy) is small
- The volume of the low flux (below 2-5 dpa/fpy) region is heavily affected by the material composition and material density in the test assembly region.

Influence of the Angle of Incidence of the Beam on the Available Testing Volume

Cases analyzed:

1. Single footprint with beams overlapping
2. Single footprint without overlap

Angles to the normal to the jet analyzed:

5, 10, 15, 20, 30, and 40 degrees

I.C.Gomes - Argonne National Laboratory

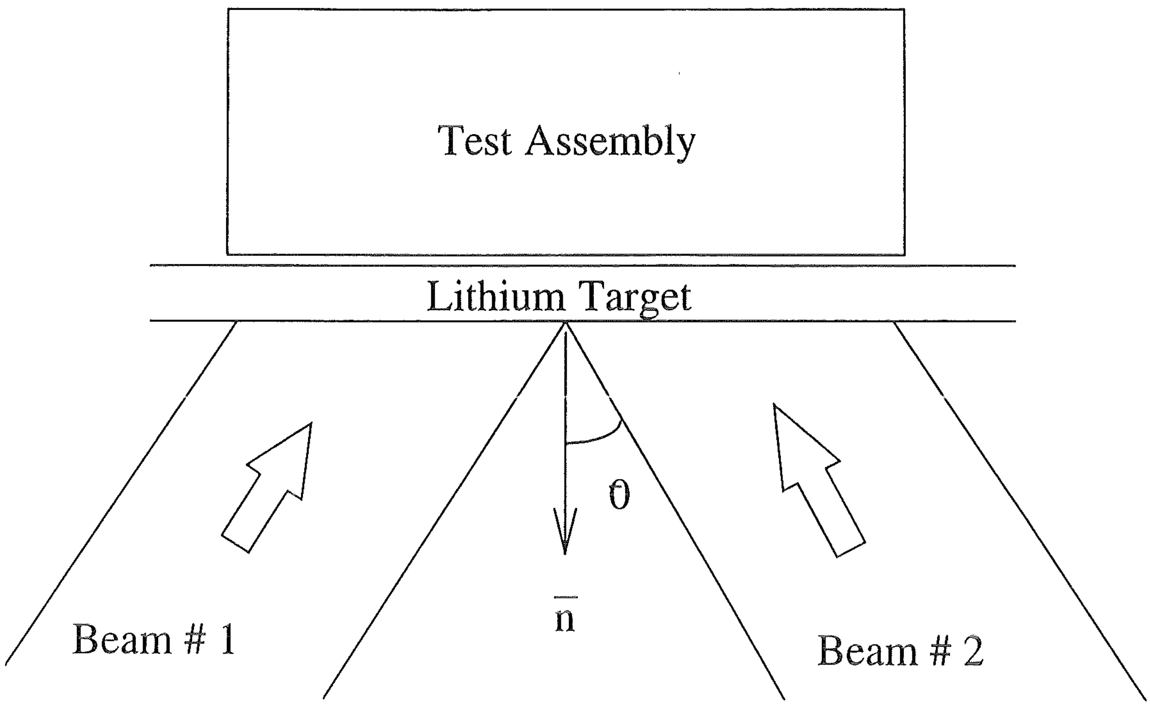

Two Beams Incident on the Same Target Without Overlapping the Footprint

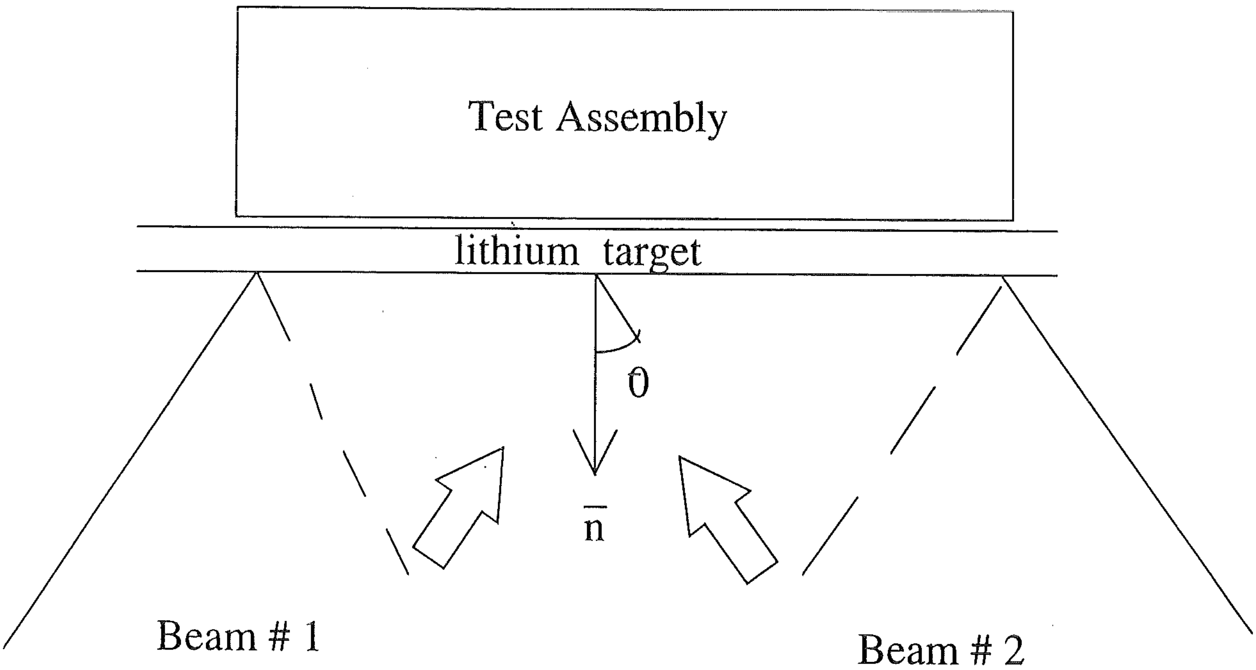

Two Beams on the Same Target Overlapping the Footprints

Influence of the Angle of Incidence of 2 Beams on the Testing Volume with dpa rate above 40 dpa/fpy

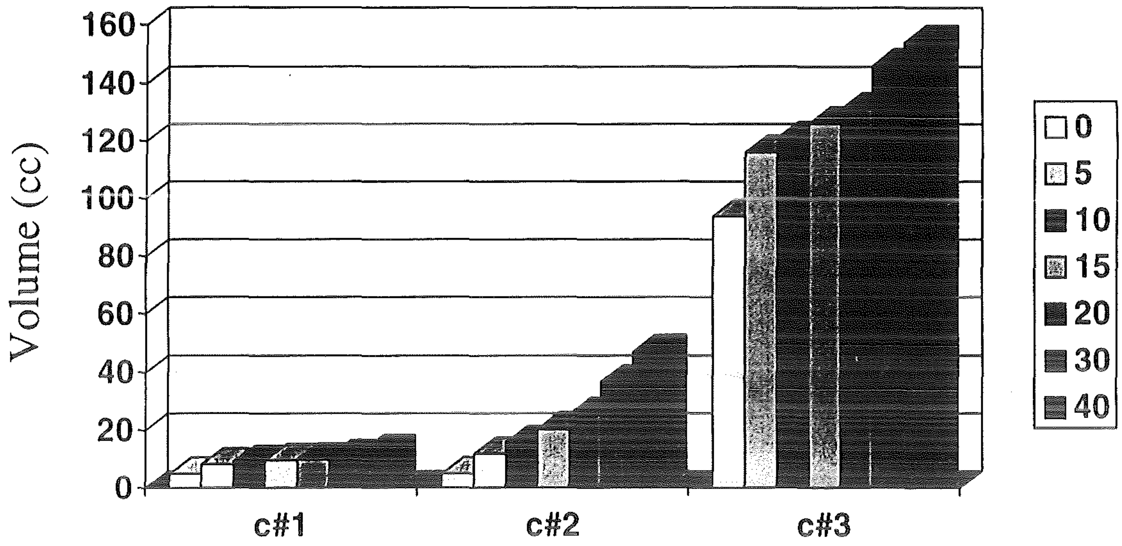

35 MeV -with overlapping | 35 MeV - w/o overlapping | 40 MeV - w/o overlapping

I.C.Gomes - Argonne National Laboratory

Influence of the Angle of Incidence, for 2 Beams, on the Testing Volume with dpa rate above 30dpa/fpy

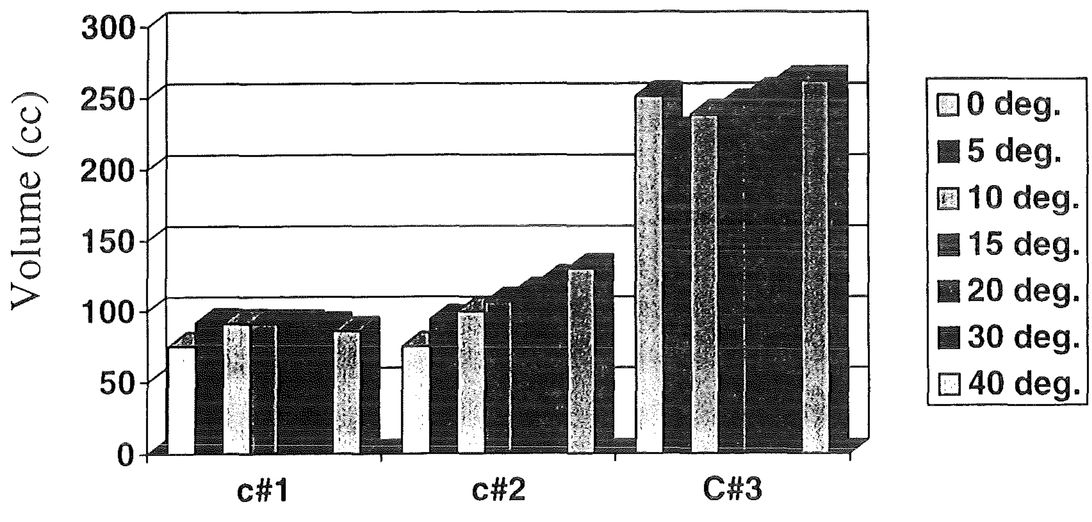

35 MeV - with overlapping | 35 MeV - w/o overlapping | 40 MeV - w/o overlapping

I.C.Gomes - Argonne National Laboratory

Influence of the Angle of Incidence, for 2 Beams, on the Testing Volume with DPA rate above 20 dpa/fpy

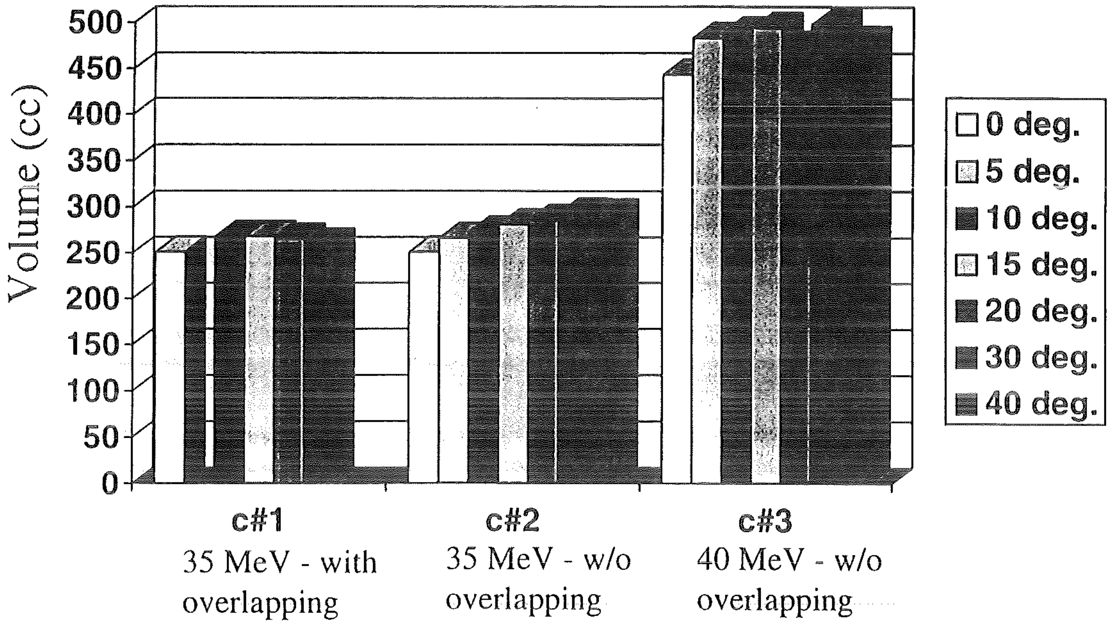

I.C.Gomes - Argonne National Laboratory

Influence of the Angle of Incidence, for 2 Beams, on the Testing Volume with DPA rate above 15 dpa/fpy

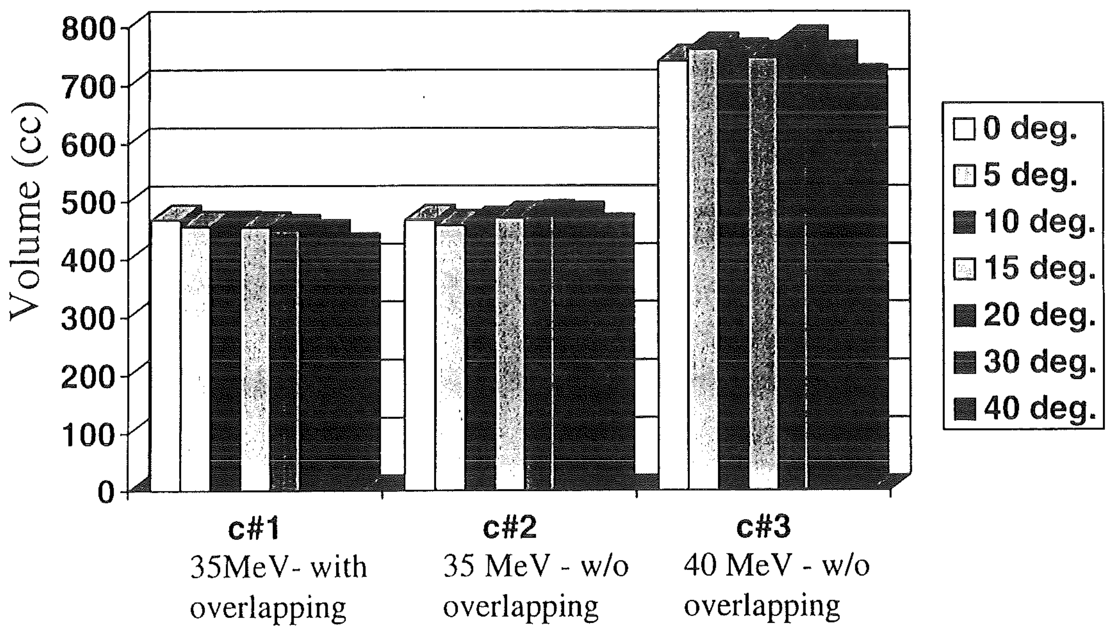

I.C.Gomes - Argonne National Laboratory

Conclusions

- The angle of incidence, for 2 beams incident on the same target case, does not not have a strong influence on the testing volume.
- For large dpa threshold values the increase in volume is significative when using large angles, but the volume is small.
- For small dpa threshold values the uni-directional beam or beams at small angles have a slightly advantage over large angles.

I.C.Gomes - Argonne National Laboratory

Helium to DPA ratio

- Throughout the high flux region He/DPA ratio varies from 10 to 14 (SS-316).
- From the materials analyzed (SS-316, V, Nb, Fe) he to DPA ratios similar to the fusion environment were calculated.
- For 250mA a beam spot area of 100 cm2 produces a very good agreement with the fusion environment (in the high flux region)

I.C.Gomes - Argonne National Laboratory

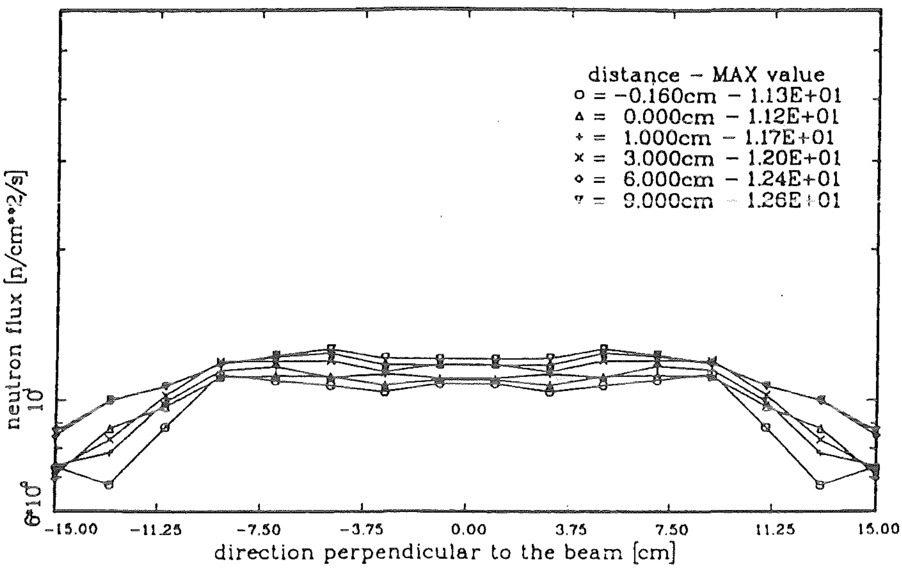

Figure 9 Helium production (appm/yr) to DPA rate (DPA/yr) ratio. Profile perpendicular to the beam and to the Jet for a 250 mA, 35 MeV, 10 x 10 cm^2 deuteron beam.

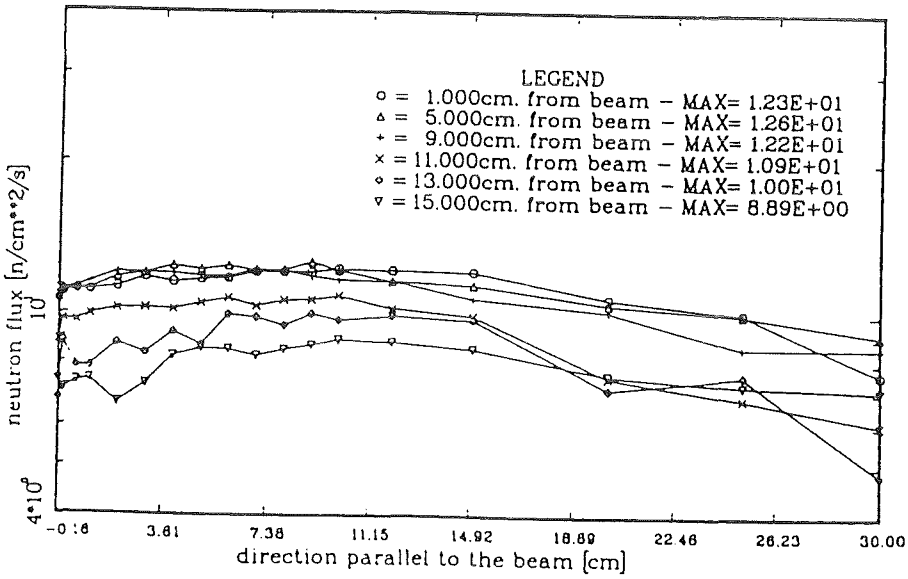

Figure 8 Helium production (appm/yr) to DPA rate (dpa/yr) ratio Profile along the beam direction for a 250 mA, 35 MeV, 10 x 10 cm^2 deuteron beam.

Transmutation Rate in Different Irradiation Facilities

I.C.Gomes - Argonne National Laboratory

Different neutron energy spectra
⇒ Different transmutation rates

- Vanadium transmutation cross-section

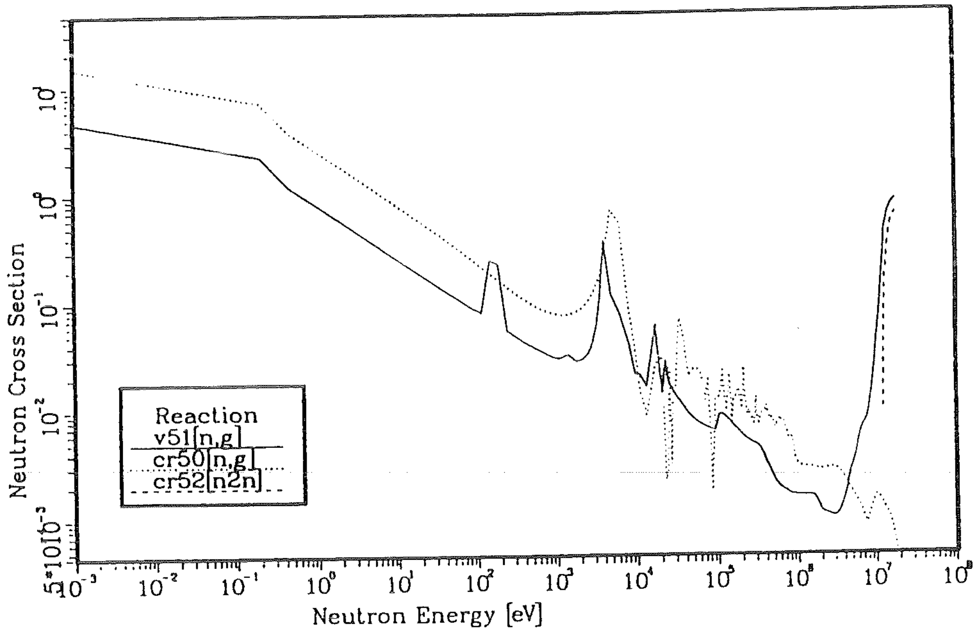

- Typical neutron energy spectra for fission and fusion devices

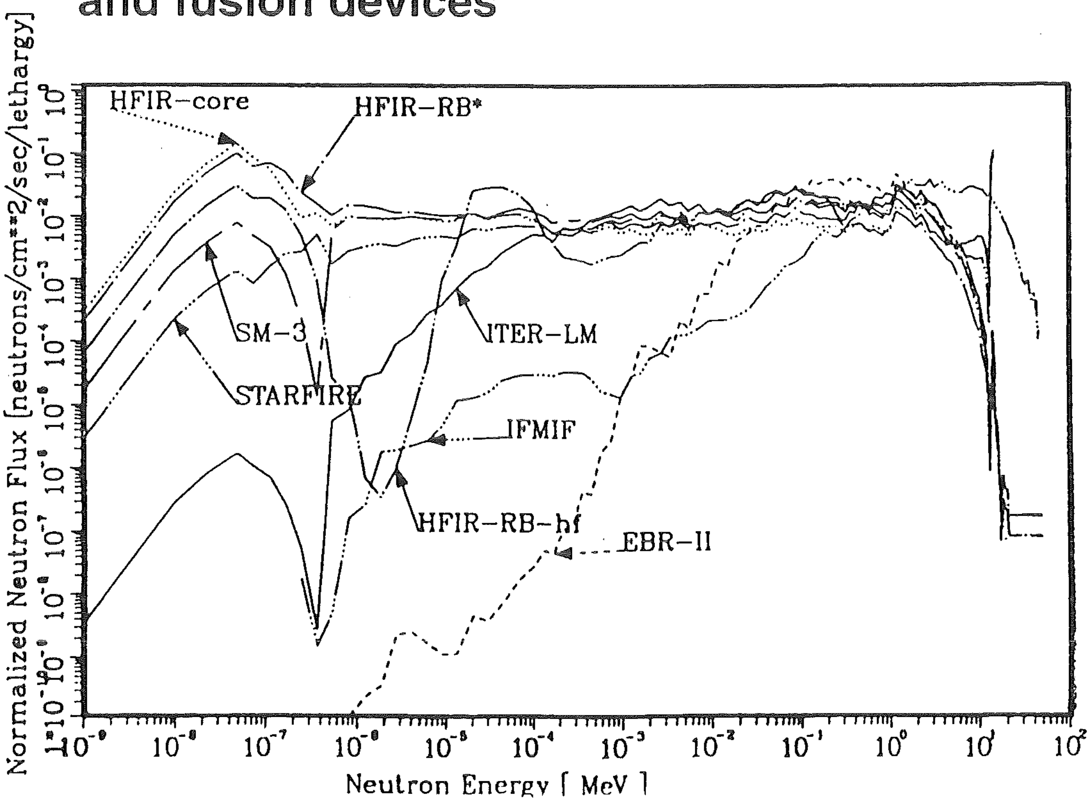

V4Cr4Ti at HFIR, ITER–LM, SM–3, FMIF, and EBR–II
RB bare/Hf cover, EBR row 1, SM–3 core, FMIF 10x10, ITER 1st

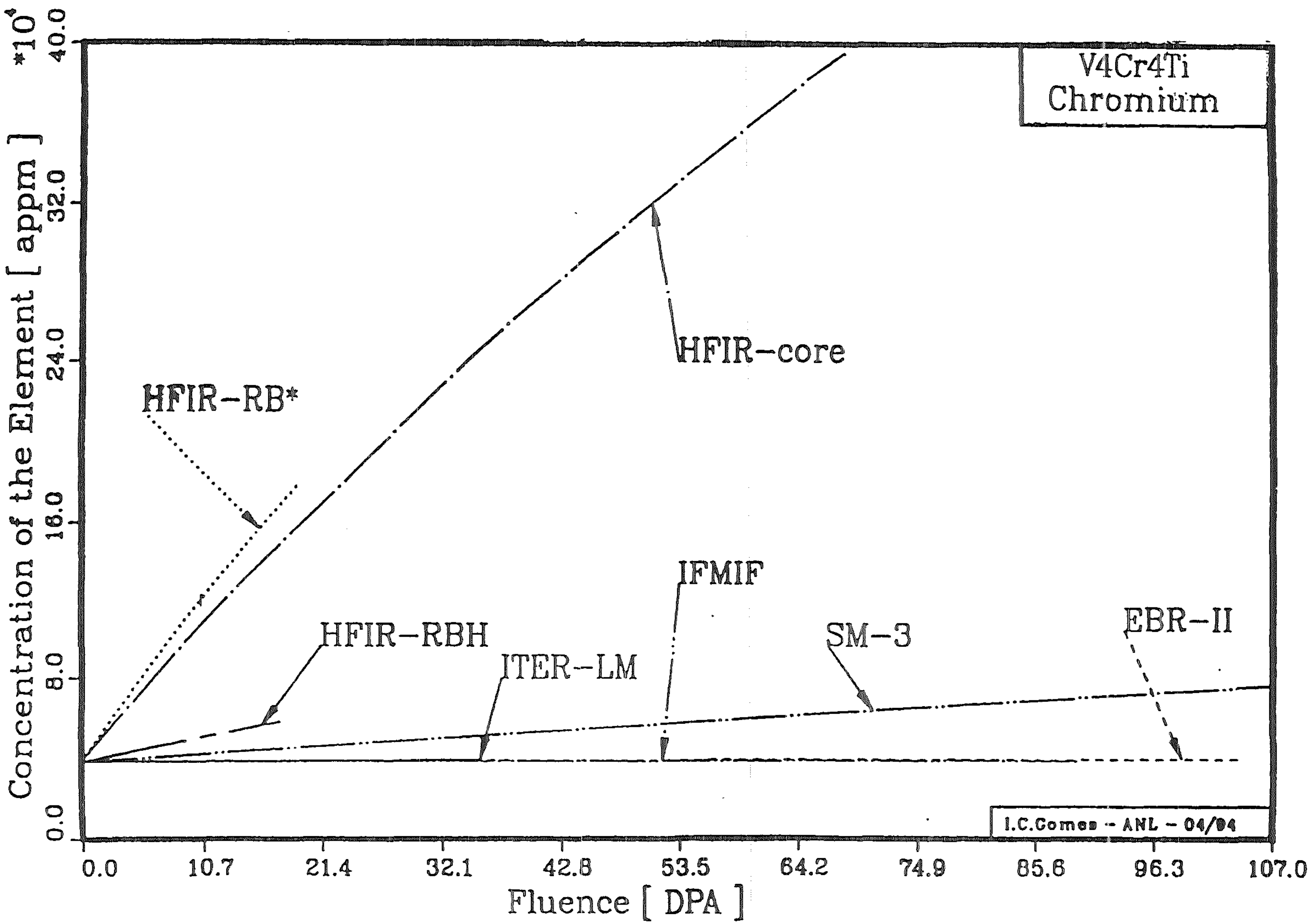

Figure 8
Gomes and Smith (ANL)
Characterization of Nuclear...

Cu0.5Cr0.3Zr at HFIR, ITER–LM, SM–3, FMIF, and EBR–II
RB bare/Hf cover, EBR row 1, SM–3 core, FMIF 10x10, ITER 1st

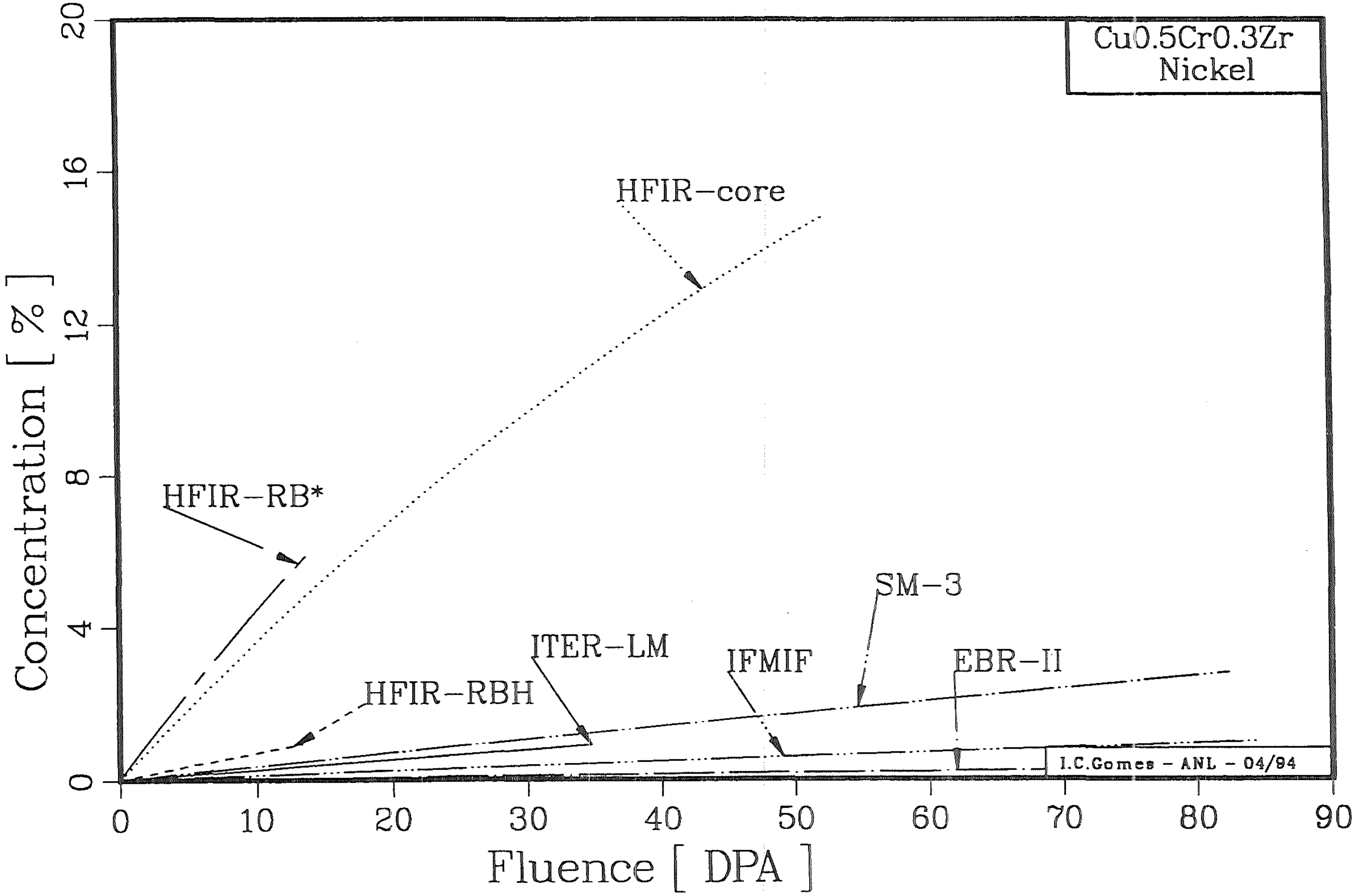

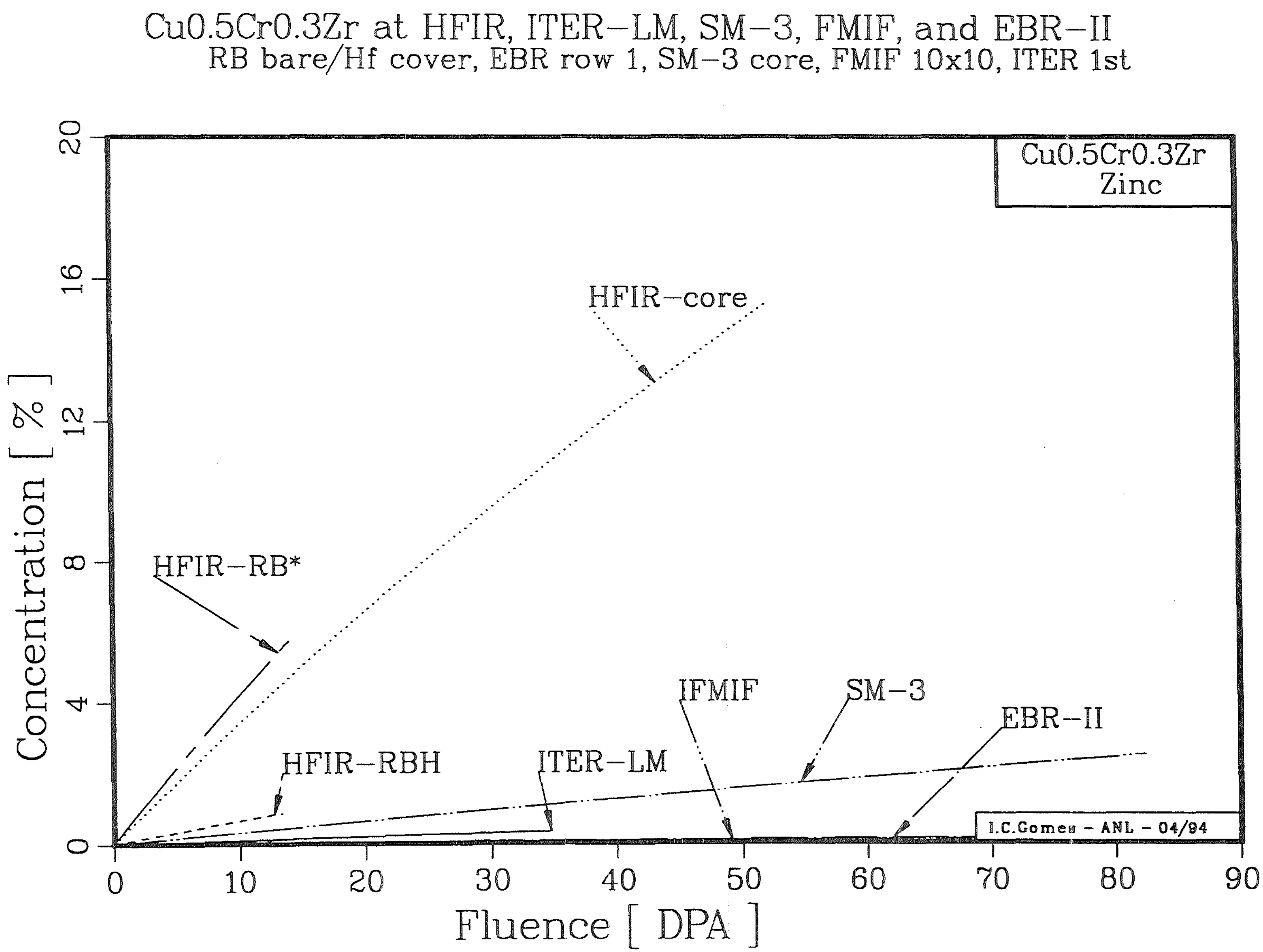
Cu0.5Cr0.3Zr at HFIR, ITER–LM, SM–3, FMIF, and EBR–II
RB bare/Hf cover, EBR row 1, SM–3 core, FMIF 10x10, ITER 1st
Cu0.5Cr0.3Zr
Zinc
HFIR–core
HFIR–RB*
HFIR–RBH
ITER–LM
IFMIF
SM–3
EBR–II
I.C.Gomes – ANL – 04/94
Concentration [%]
Fluence [DPA]
0
4
8
12
16
20
0
10
20
30
40
50
60
70
80
90

SiC at HFIR, ITER–LM, SM–3, FMIF, and EBR–II
RB bare/Hf cover, EBR row 1, SM–3 core, FMIF 10x10, ITER 1st

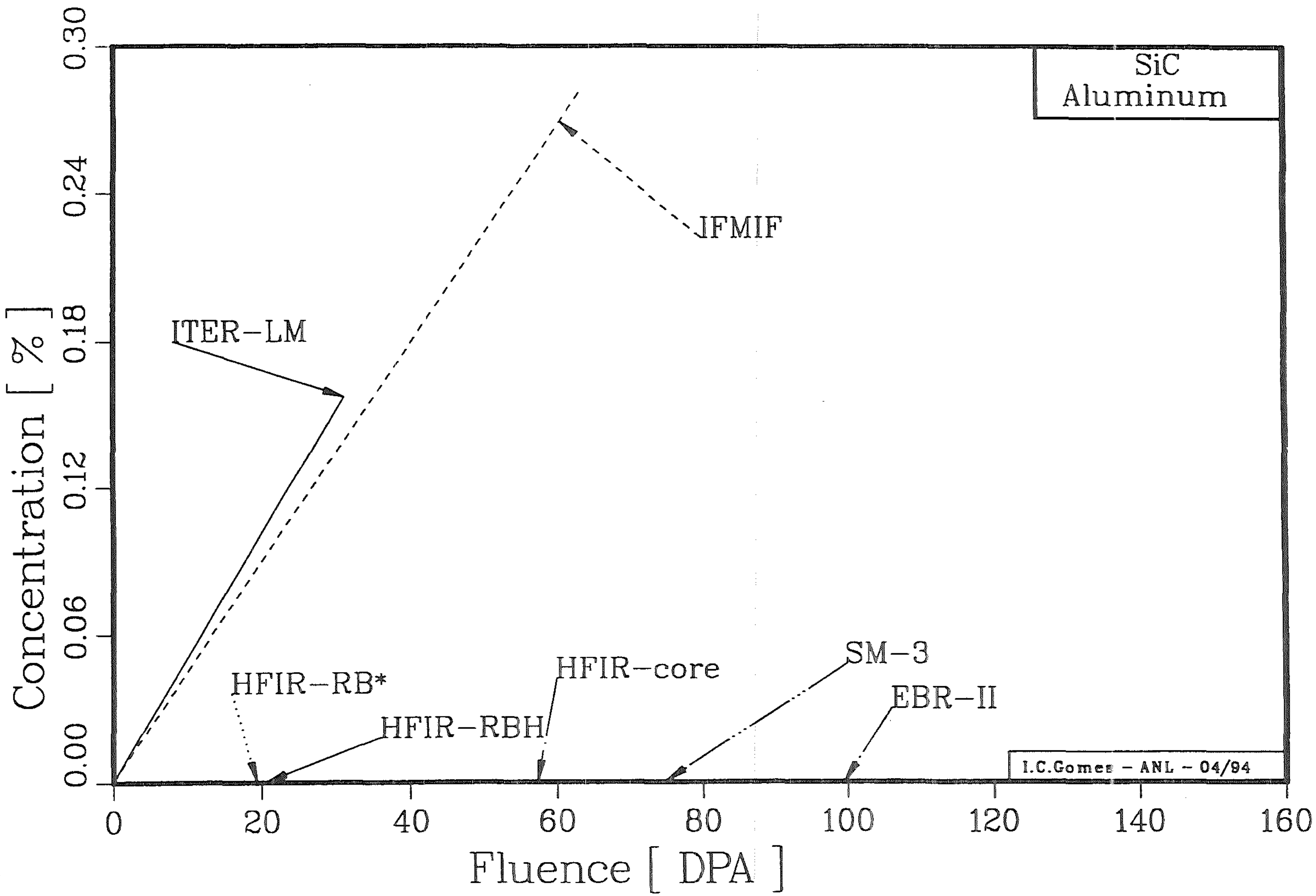

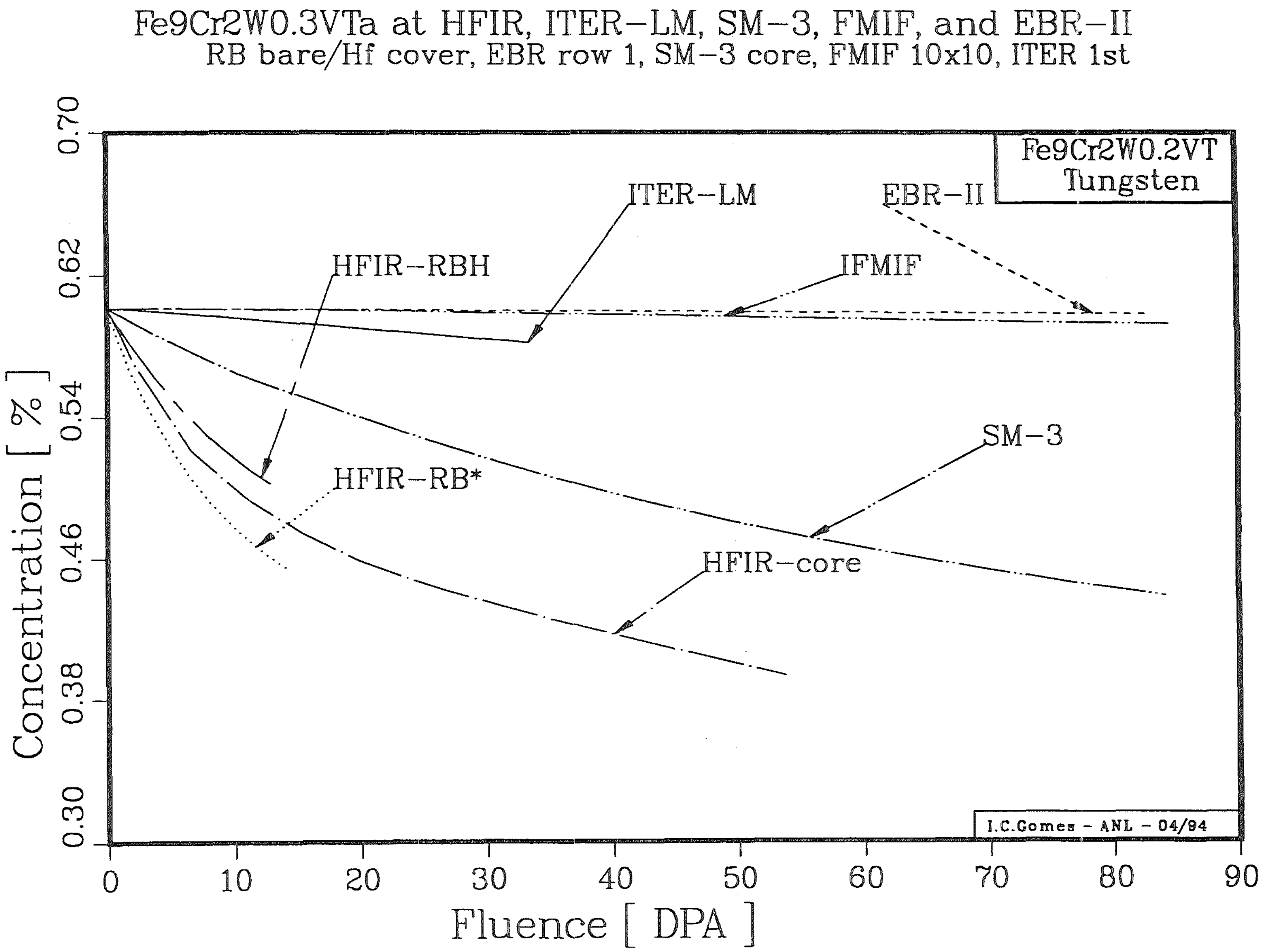

Fe9Cr2W0.3VTa at HFIR, ITER-LM, SM-3, FMIF, and EBR-II
RB bare/Hf cover, EBR row 1, SM-3 core, FMIF 10x10, ITER 1st
Fe9Cr2W0.2VT
Tungsten
ITER-LM
EBR-II
HFIR-RBH
IFMIF
SM-3
HFIR-RB*
HFIR-core
I.C.Gomes - ANL - 04/94
Concentration [%]
0.70
0.62
0.54
0.46
0.38
0.30
0
10
20
30
40
50
60
70
80
90
Fluence [DPA]

Gradient of the Damage Rate

10x10, 5x20, and 2.5x40 beams

30, 35, and 40 MeV

I.C.Gomes - Argonne National Laboratory

Maximum DPA Rate for Different Beam Spot Shapes

- The square beam shape gives the highest dpa rate at the back plate.
- The larger aspect ratio the smaller the maximum dpa value.

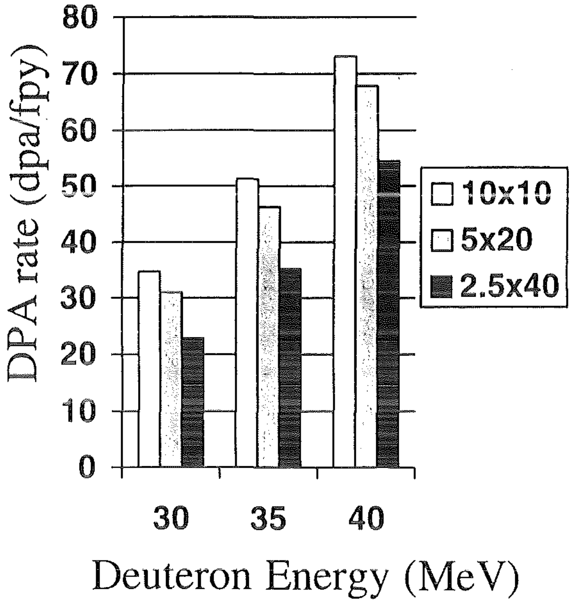

Coordinate System Used to Plot the DPA rate profiles.

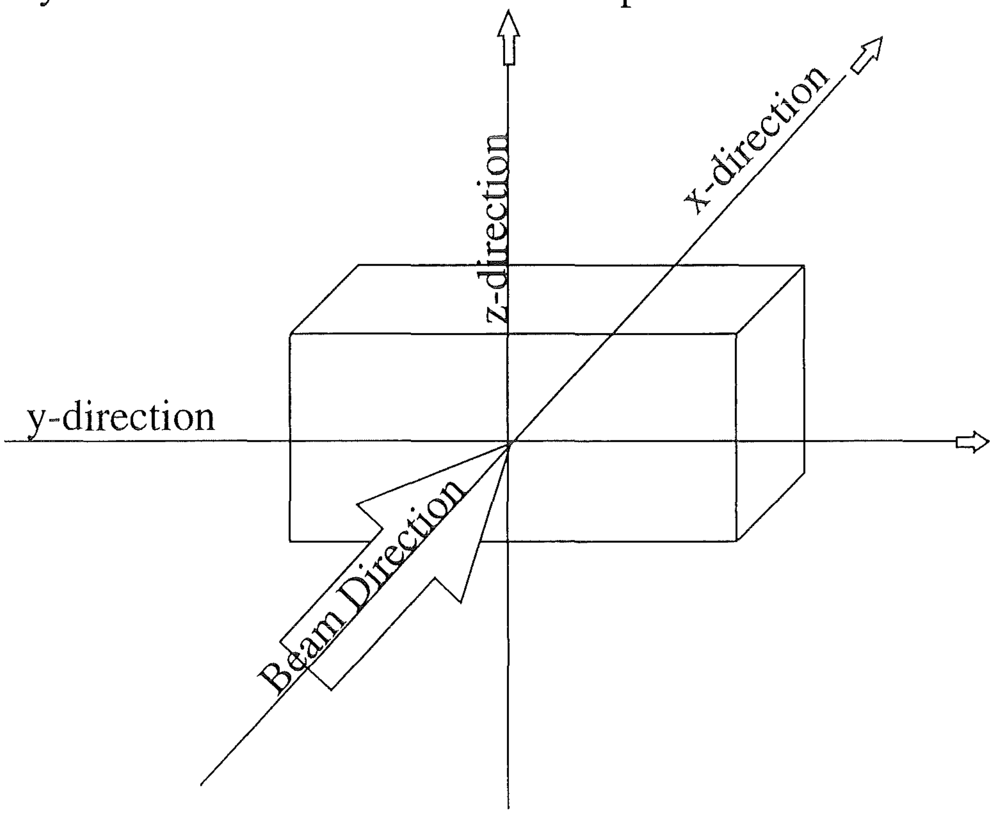

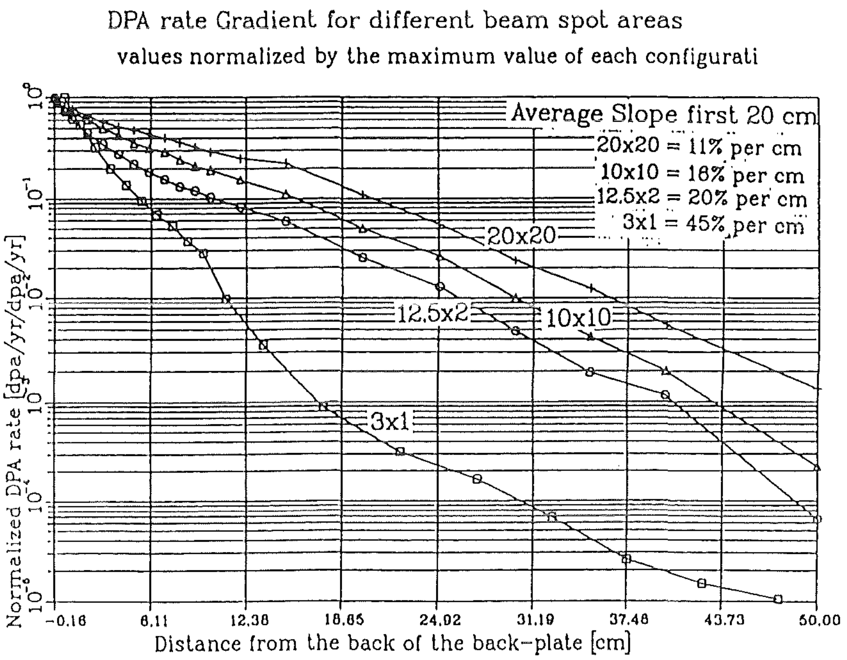

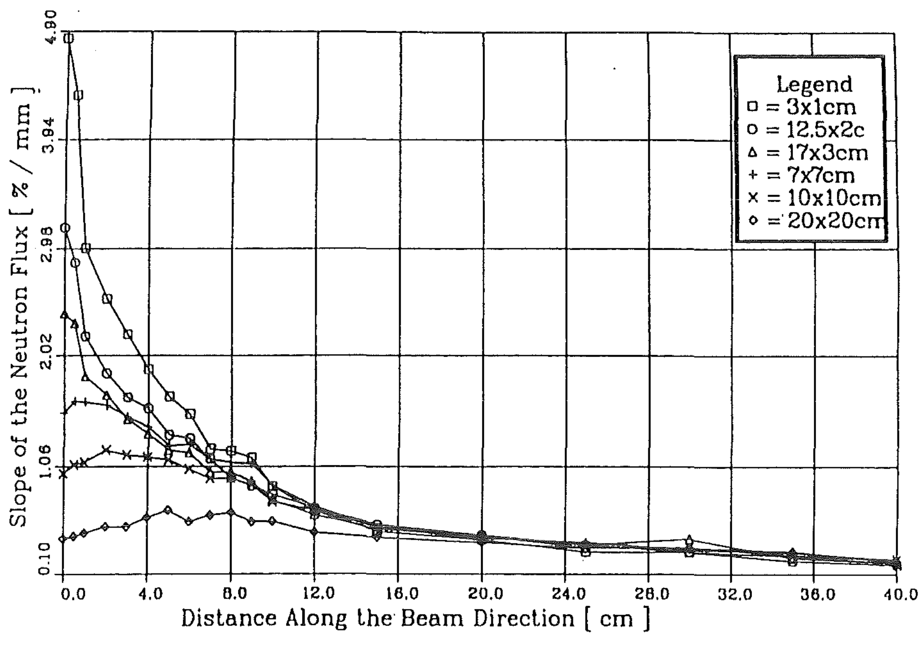

Figure 4. Uncollided neutron flux gradient in percentile per millimeter for six different beam cross sectional areas with the same 250 mA current, and same 35 MeV incident deuteron energy.

Fe DPA along the Beam direction – 35 MeV deuteron energy
250mA current – Fe 50% – 10cmx10cm beam size
Z Distance from the center of the beam = 0.65 cm.

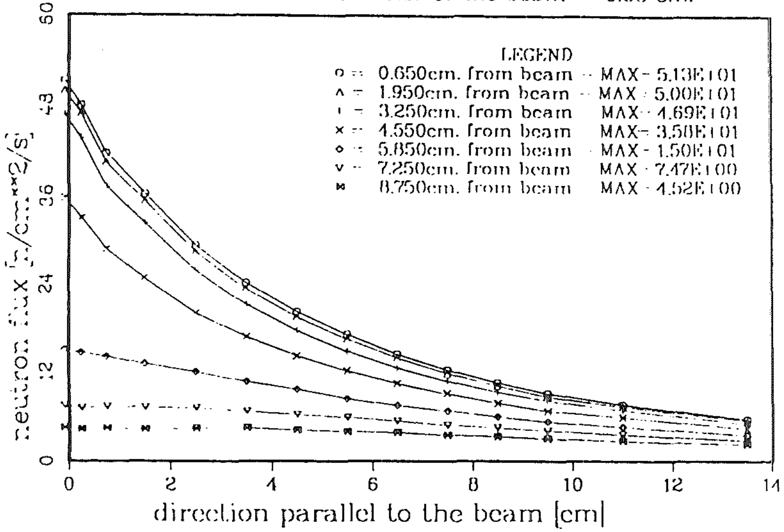

Fe DPA along the Beam direction – 35 MeV deuteron energy
250mA current – Fe 50% – 5cmx20cm beam size
Z -Distance from the center of the beam = 0.69 cm.

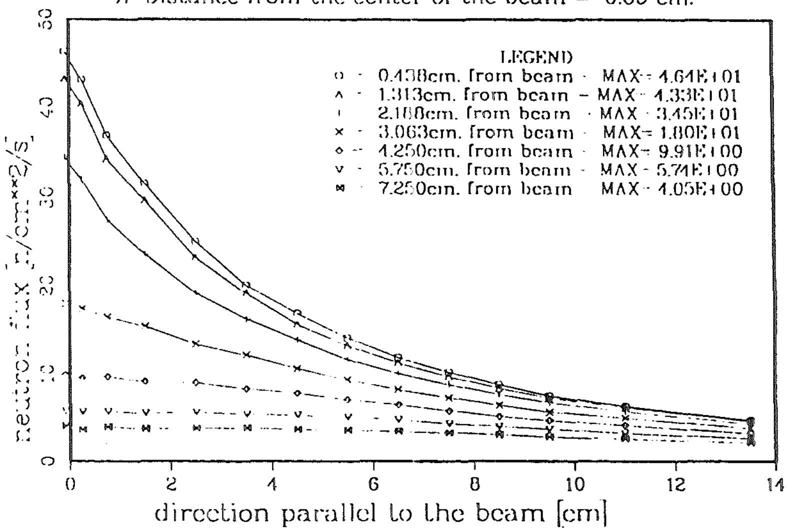

Fe DPA along the Beam direction – 35 MeV deuteron energy
250mA current – Fe 50% – 2.5cmx40cm beam size
Z–Distance from the center of the beam = 1.00 cm.

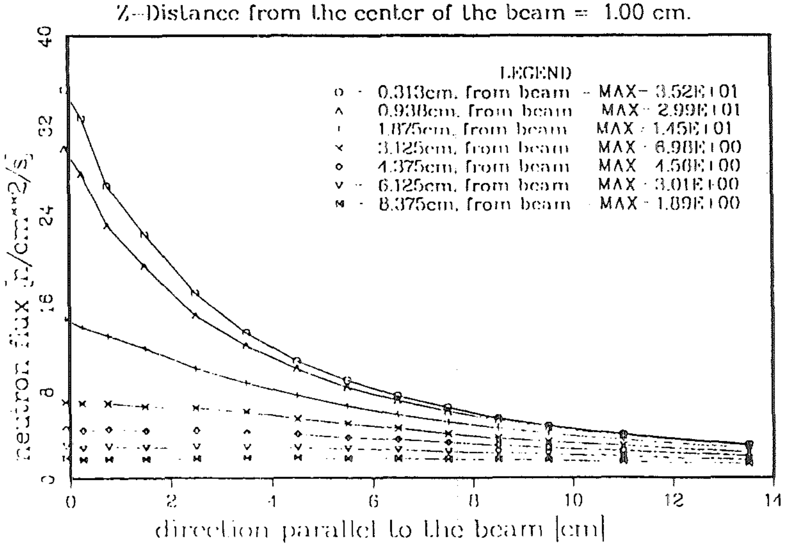

Fe DPA along the Beam direction - 40 MeV deuteron energy
250mA current -- Fe 50% - 10cmx10cm beam size
% Distance from the center of the beam = 0.65 cm.

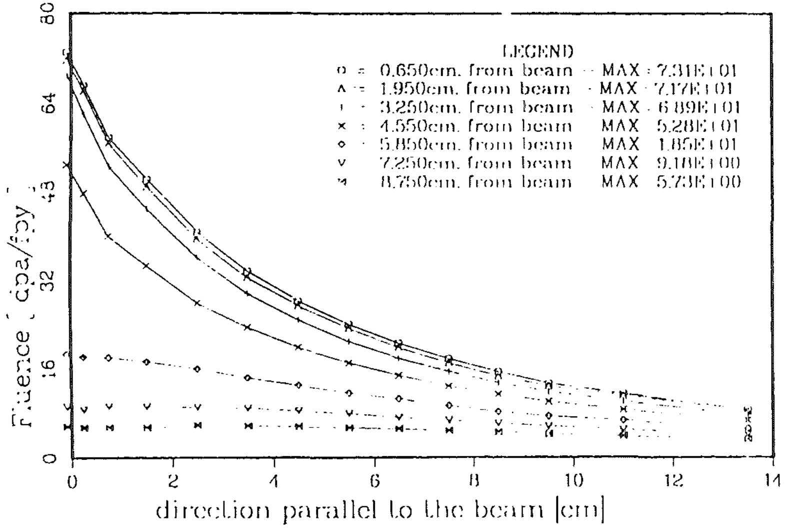

Fe DPA along the Beam direction - 40 MeV deuteron energy
250mA current - Fe 50% -- 5cmx20cm beam size
% Distance from the center of the beam = 0.69 cm.

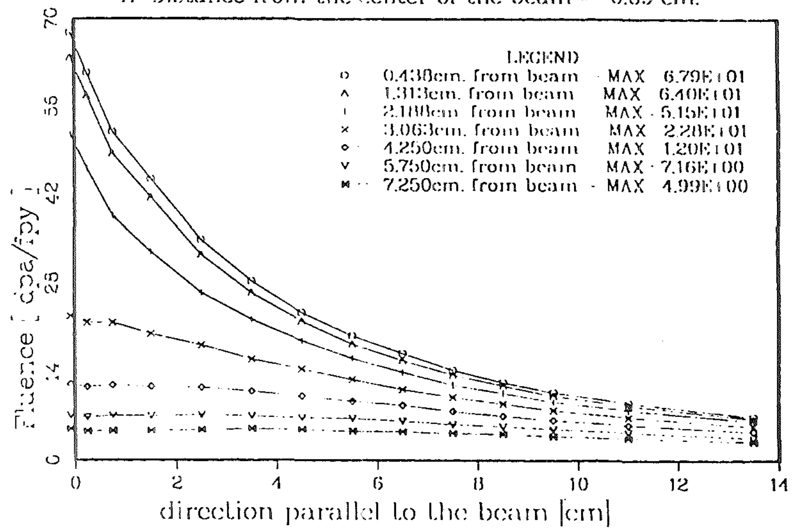

Fe DPA along the Beam direction 40 MeV deuteron energy
250mA current - Fe 50% - 2.5cmx40cm beam size
% Distance from the center of the beam = 1.00 cm.

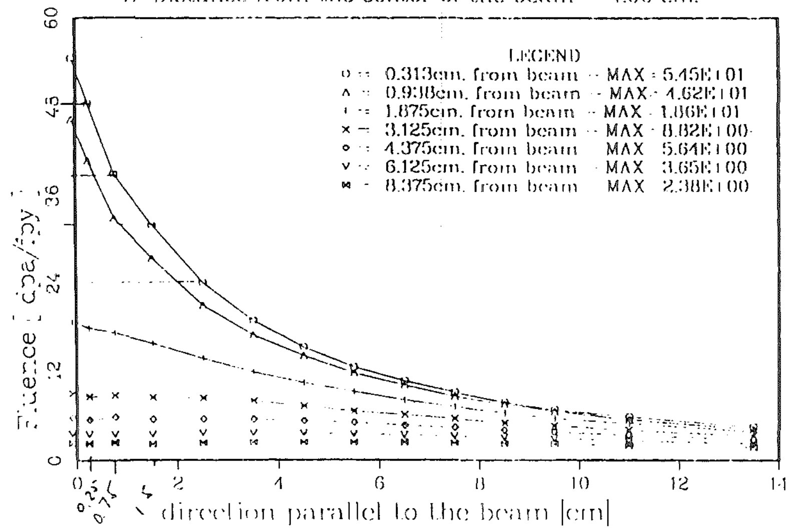

Fe DPA along the Beam direction -- 40 MeV deuteron energy
250mA current -- Fe 50% -- 5cmx20cm beam size
Z- Distance from the center of the beam = 0.69 cm.

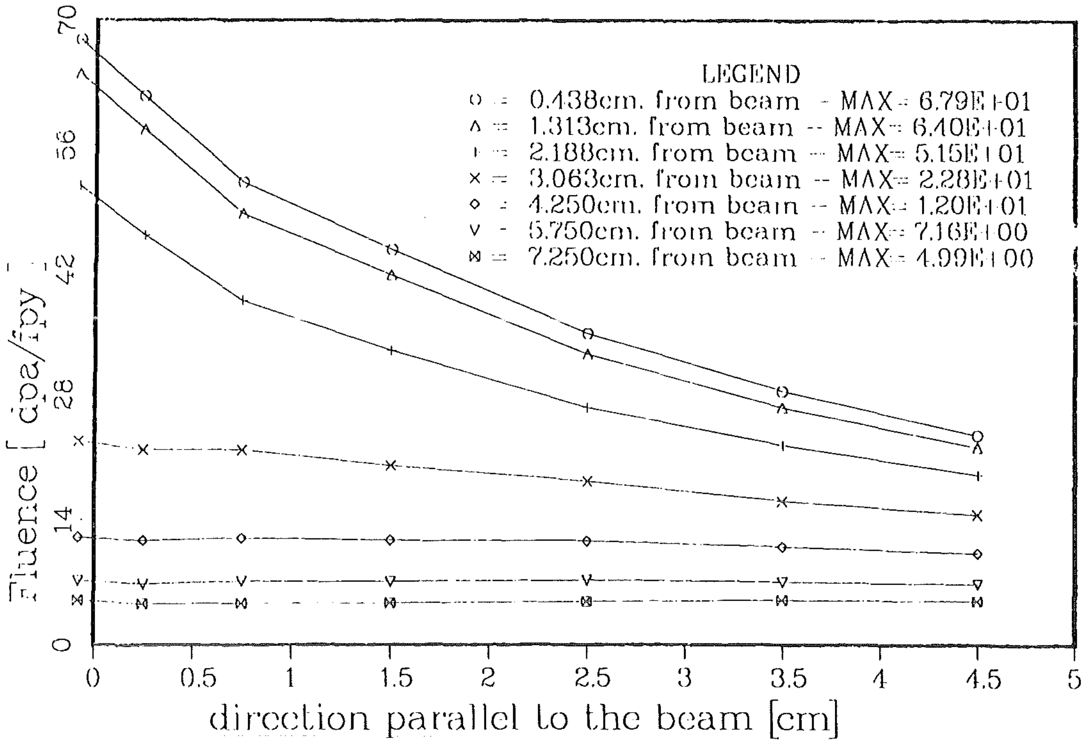

Fe DPA along the Beam direction -- 40 MeV deuteron energy
250mA current -- Fe 50% -- 5cmx20cm beam size
Z- Distance from the center of the beam = 0.69 cm.

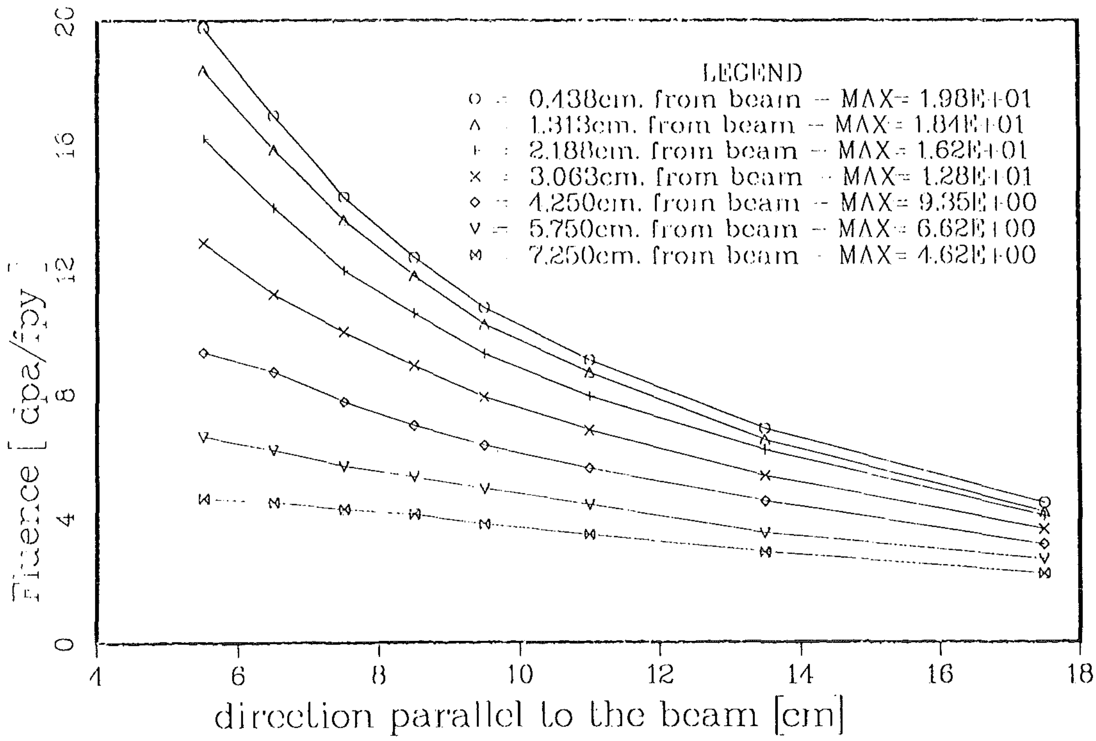

Fe DPA perpendicular to the beam — 35 MeV deuteron energy
250mA current - Fe 50% - 10cmx10cm beam size - z direction
Z Distance from the center of the beam - 0.65 cm.

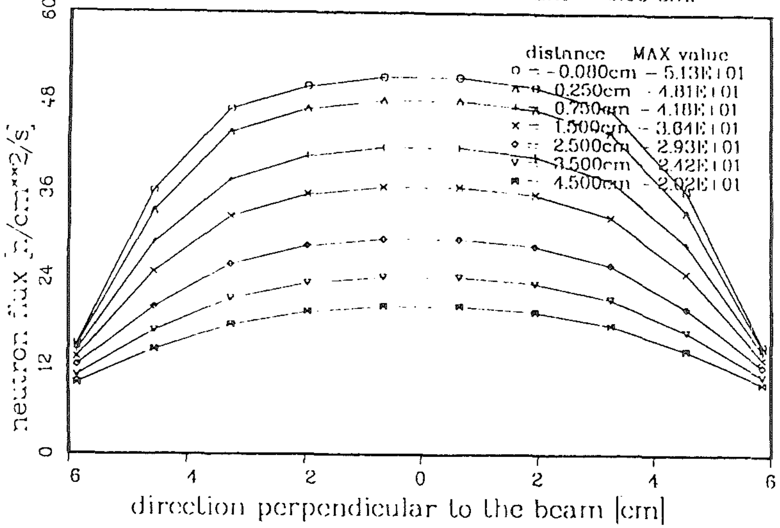

Fe DPA perpendicular to the beam — 35 MeV deuteron energy
250mA current - Fe 50% 5cmx20cm beam size z-direction
Z Distance from the center of the beam - 0.44 cm.

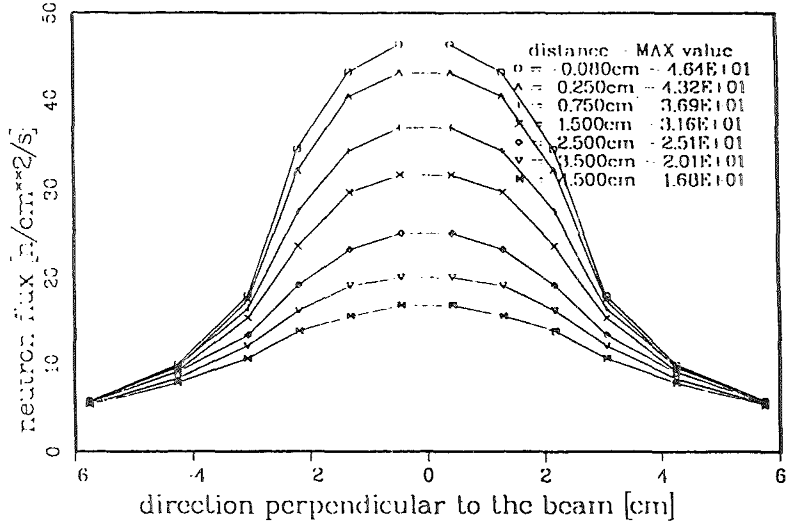

Fe DPA perpendicular to the beam — 35 MeV deuteron energy
250mA current - Fe 50% - 2.5cmx40cm beam size - z-direction
Z- Distance from the center of the beam = 0.31 cm.

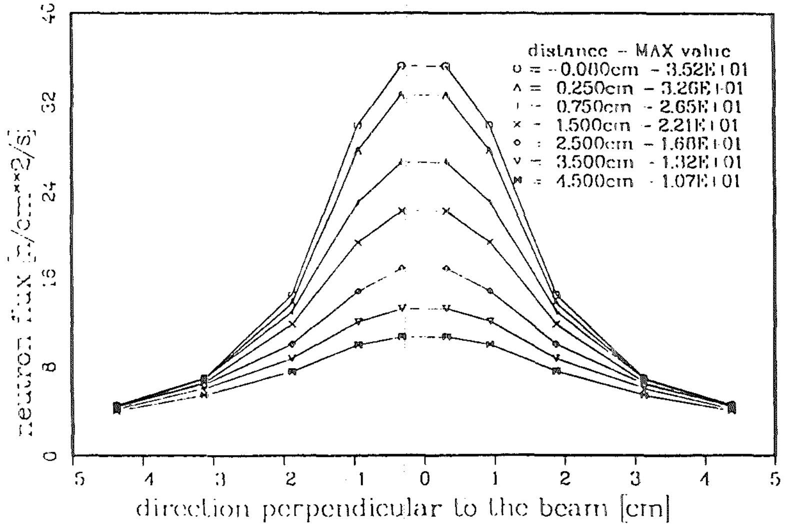

Fe DPA perpendicular to the beam - 40 MeV deuteron energy
250mA current Fe 50% - 10cmx10cm beam size - z direction
Z Distance from the center of the beam = 0.65 cm.

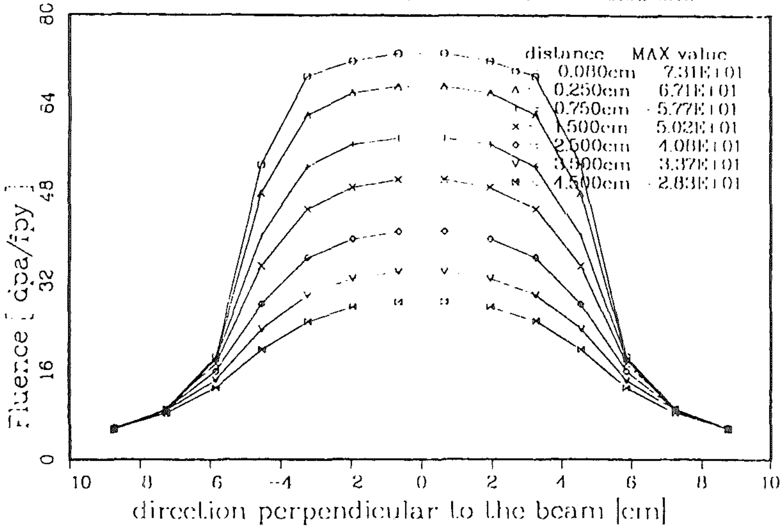

Fe DPA perpendicular to the beam - 40 MeV deuteron energy
250mA current - Fe 50% - 5cmx20cm beam size - z direction
Z Distance from the center of the beam = 0.44 cm.

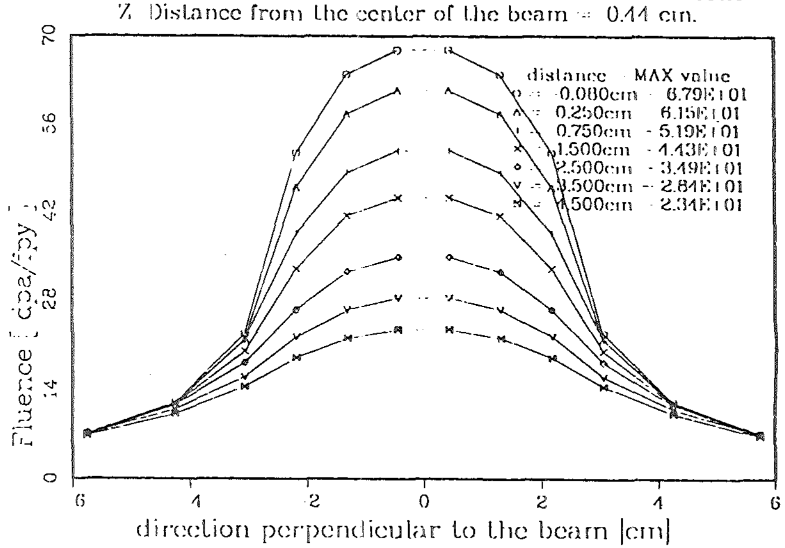

Fe DPA perpendicular to the beam - 40 MeV deuteron energy
250mA current - Fe 50% - 2.5cmx40cm beam size - z-direction
Z Distance from the center of the beam = 0.31 cm.

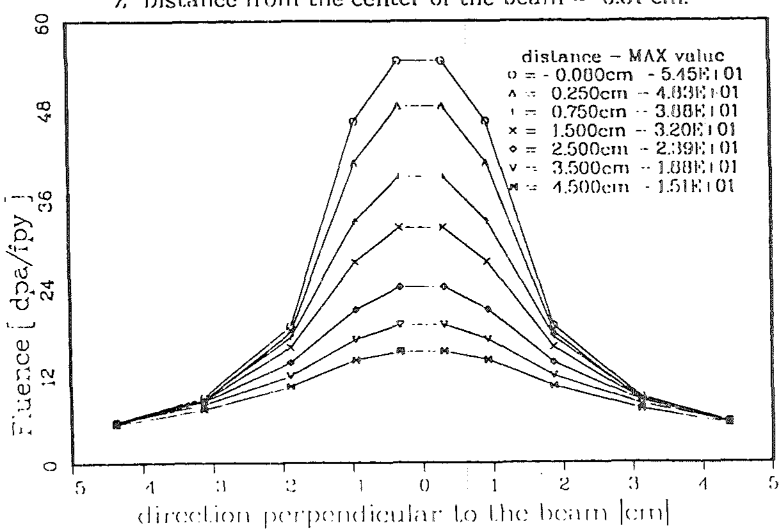

Fe DPA perpendicular to the beam – 40 MeV deuteron energy
250mA current – Fe 50% – 5cmx20cm beam size – z–direction
Z–Distance from the center of the beam = 0.44 cm.

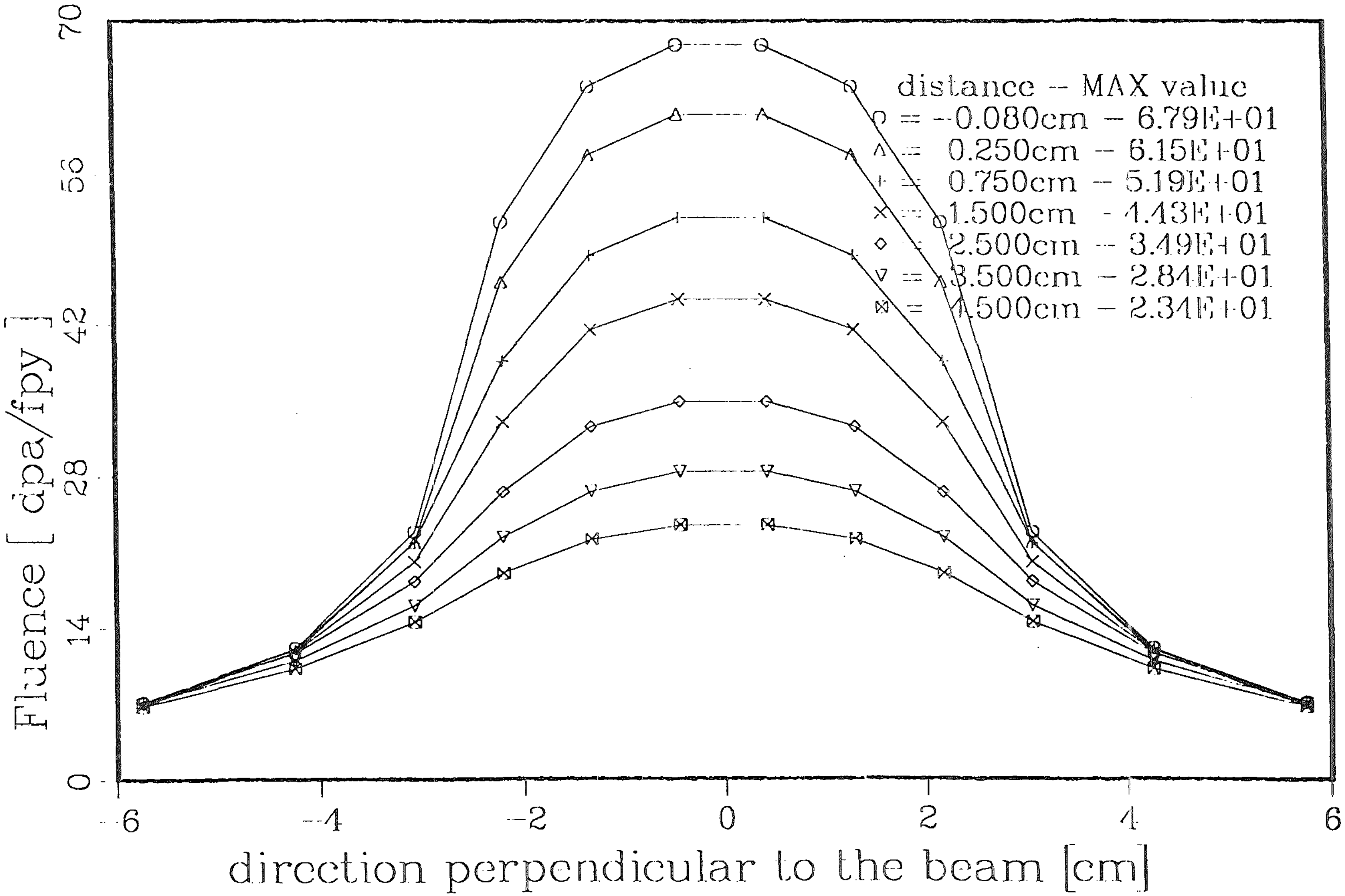

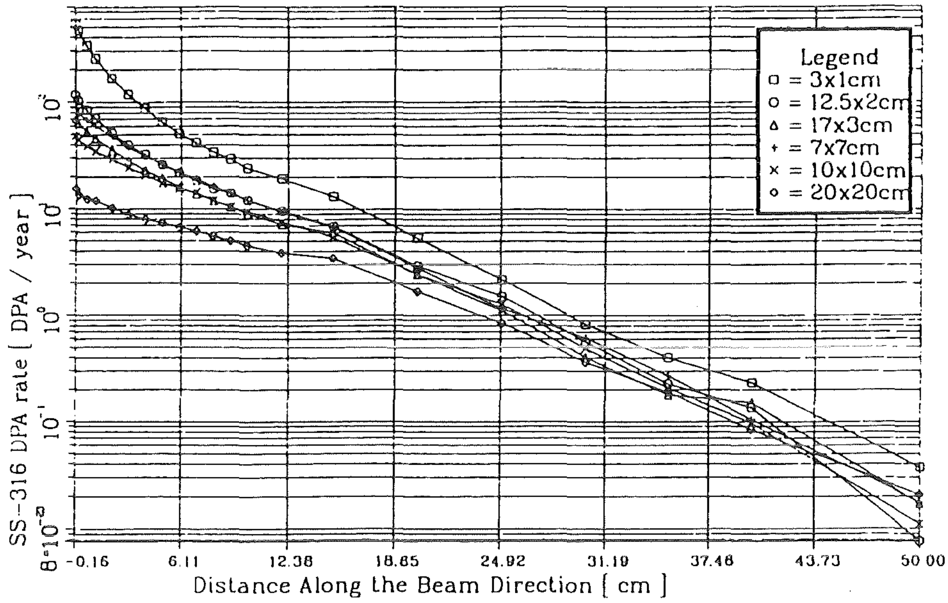

Figure 6 SS 316 DPA rate profile along the beam direction for four different beam cross sectional areas with 250 mA of current and 35 MeV deuteron energy.

16

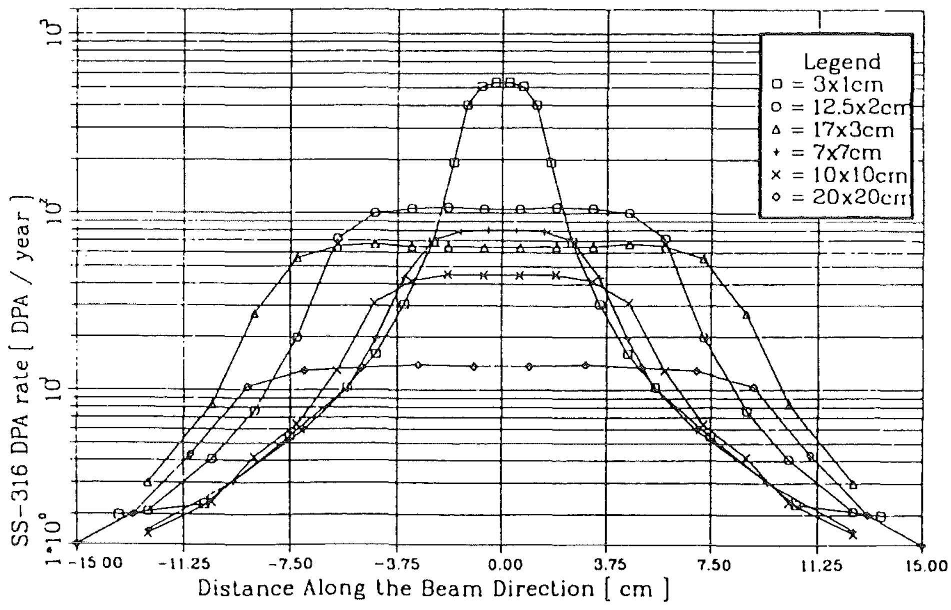

Figure 7 SS 316 DPA profile in the direction perpendicular to the beam and to the jet for four beam cross sectional areas with 250 mA of current and 35 MeV deuterons.

Conclusions

- The gradient value, in the direction of the beam, does not differ too much from the 10x10 to 5x20.
- The gradient value, in the direction of the smallest dimension perpendicular to the beam, is much larger in the cases of 2.5x40 and 5x20 than in the 10x10 case.

I.C.Gomes - Argonne National Laboratory

U. Fischer, FZK-INR

Detailed neutronics analysis for a test cell with standard loading configuration

Objective

Principal purpose is to establish a relationship between neutron source strength or neutron flux density and a reactor equivalent neutron wall loading of 2 MW/m^2, taking into account a suitable fusion reactor spectrum or spectra.

Methodological approach

I. Perform three-dimensional neutronic calculations for fusion reactor model (ITER and/or Demo power reactor)

- Normalise to 2.0 MW/m^2 neutron wall load at first wall

- Calculate neutron flux spectra, damage rates, gas production rates etc.

- Establish relationship damage parameters / neutron wall loading - different materials & different spectra

Methodological approach (cont'd)

II. Perform three-dimensional neutronic calculations for IFMIF test cell using standard loading configuration

- Normalise to the first wall neutron flux density of fusion reactor
- Calculate neutron flux spectra, damage rates, gas production rates etc.
- Establish relationship damage parameters IFMIF / fusion reactor

III. Re-adjust IFMIF design parameters to achieve required neutron fluxes/fluences, damage, gas production and transmutation rates

Computational approach

- **3d Monte Carlo calculations (MCNP-code)**
  - Torus sector model for fusion reactor calculations
  - Target - test cell model with/without wall scattering
- **Nuclear cross-section data for MCNP transport calculations**
  - EFF-1, -2 & FENDL data libraries for E<20 MeV
  - To be provided & processed for E>20 MeV (task D7)
- **Damage, gas production & transmutation rate calculations using 3d-MCNP spectra**
  - SPECTER, FISPACT
  - Nuclear data for damage & activation calculations
    - Available for E<20 MeV (EAF-3,-4, RFL-1, -2)
    - To be provided for E> 20 MeV (task D7)

Status of D2-task (EU-FZK)

- **3d Monte Carlo calculations performed for fusion reactors**
  - ITER: Water-steel shielding blanket
  - European Demo power reactor: Helium-cooled solid breeder blanket with beryllium neutron multiplier
  - Neutron wall loading, first wall neutron fluxes, damage & gas production rates
  - Damage parameters vs. neutron wall loading

- **3d Monte Carlo calculations for IFMIF test cell pending**
  - Lack of nuclear cross-section data E>20 MeV for MCNP-calculation of neutron transport
  - Further strategy:
    - Provide & process data for major isotopes of standard test cell: ^{56}Fe, ^{22}N, ^{39}K (task D7)
    - Obtain data from IFMIF-partners (EU-ENEA, JAERI)
    - Perform MCNP-calculations for IFMIF test cell

Neutron wall loading, first wall flux & current density

$$W_L\left[\frac{MW}{m^2}\right] = N_\Phi \cdot J_{14}\left[cm^{-2}s^{-1}\right]$$

$$N_\Phi = 14.06 MeV \cdot 1.6021 \cdot 10^{-19}\frac{Ws}{eV} \cdot 10^4 \frac{cm^2}{m^2}$$

J_{14} = 14 MeV neutron current density

$$J_{14} = \langle\mu\rangle \cdot \Phi_{14}$$

ϕ_{14} = 14 MeV neutron flux density

$<\mu>$ = cosine of neutron flight direction and surface normal

	W_L[MW/m^2]	J_{14}[cm^{-2} s^{-1}]	ϕ_{14}[cm^{-2} s^{-1}]	ϕ_{tot}[cm^{-2} s^{-1}]
ITER (inboard)	2.0	$8.88 \cdot 10^{13}$	$1.44 \cdot 10^{14}$	$8.00 \cdot 10^{14}$
Demo (outboard)	2.0	$8.88 \cdot 10^{13}$	$1.15 \cdot 10^{14}$	$7.14 \cdot 10^{14}$

Results of 3d Monte Carlo calculations normalised to a neutron wall loading of 2.0 MW/m^2

1 2/21/95 8:28:37
ITER 3D GLOBAL MODEL WITH
UPDATED SHIELDING BLANKET AND
DIVERTOR 2/95
PROBID - 1 2/21/95 8:26:36
BASIS:
(0.997857, 0.065440, 0.000000)
(0.000000, 0.000000, 1.000000)
ORIGIN:
(850.00, 50.00, 0.00)
EXTENT - (900.00, 900.00)

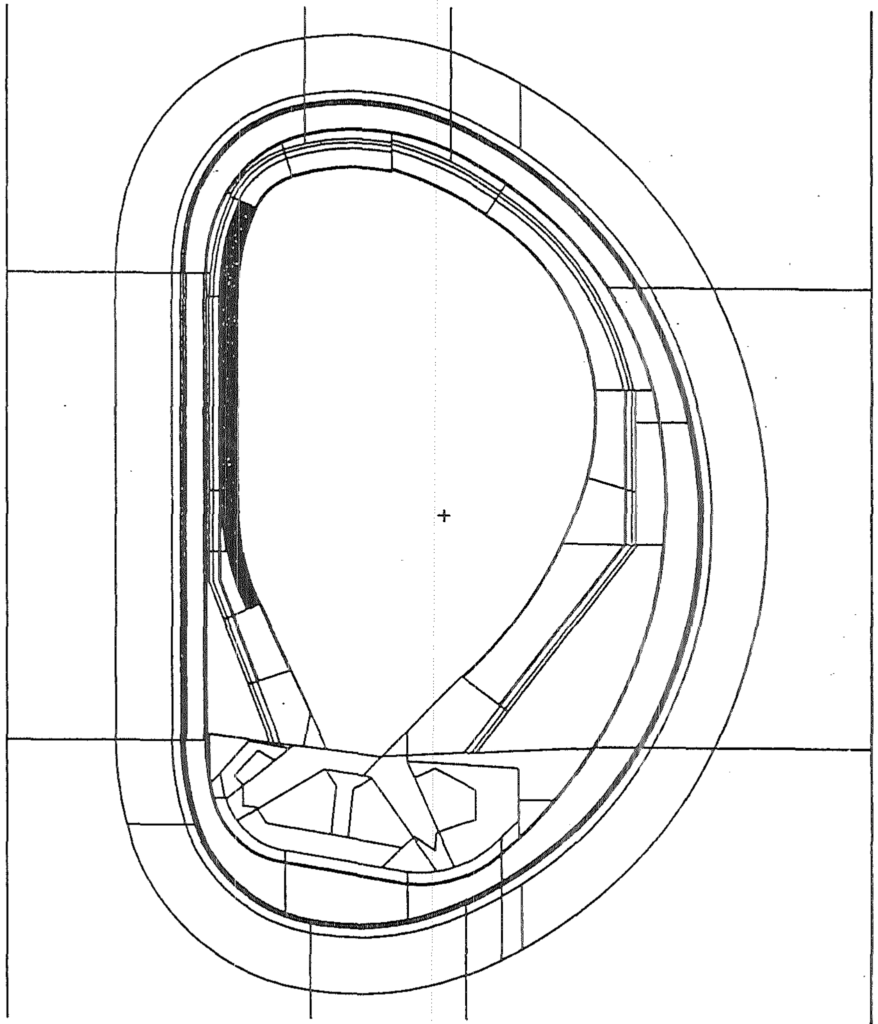

PLOT 1 08.28.37 TUES 21 FEB, 1995 JOB-IMR297 , KERNFORSCHUNGSZENTRUM - KA DISSPLA 11.0

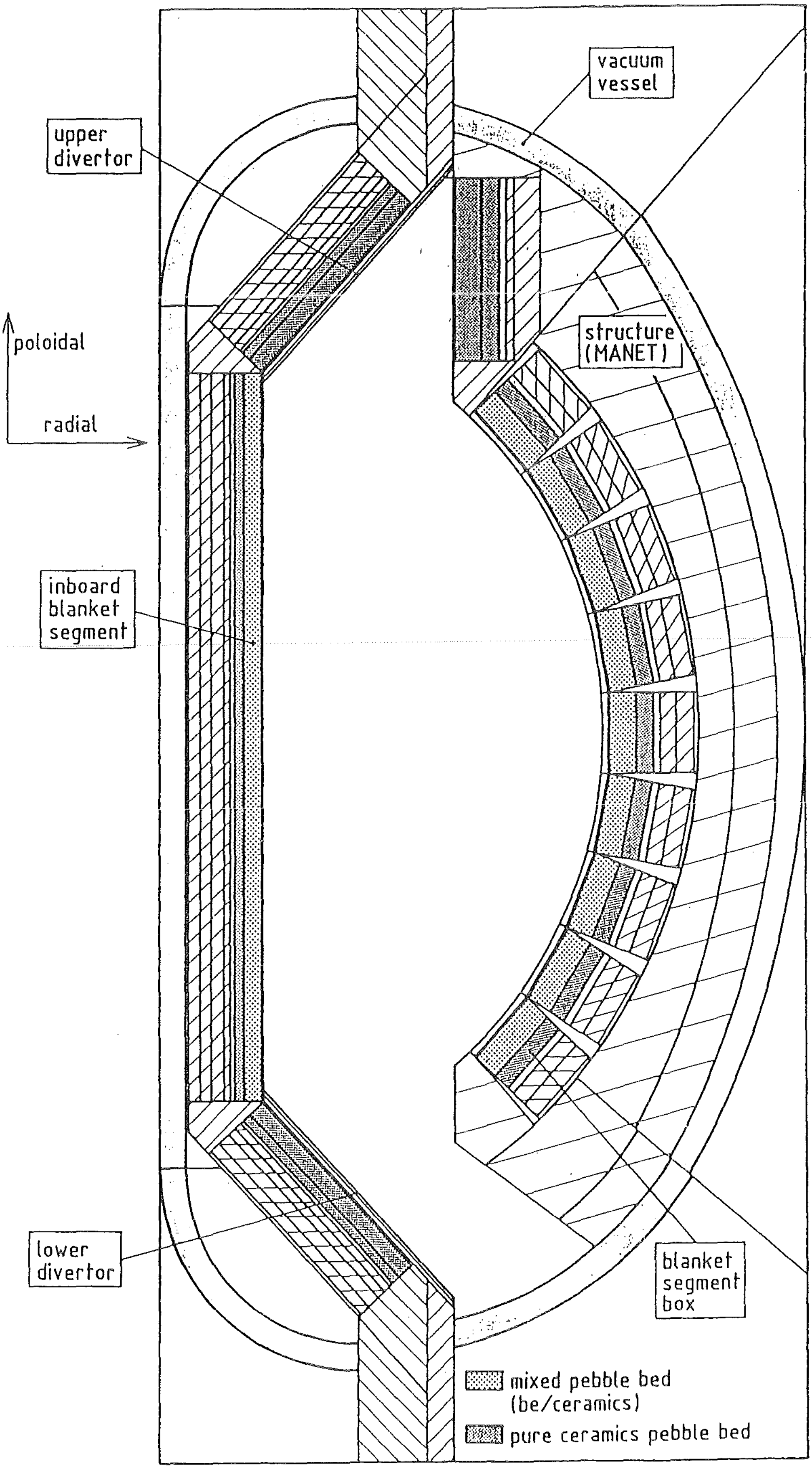
vacuum vessel
upper divertor
poloidal
radial
structure (MANET)
inboard blanket segment
lower divertor
blanket segment box
mixed pebble bed (be/ceramics)
pure ceramics pebble bed

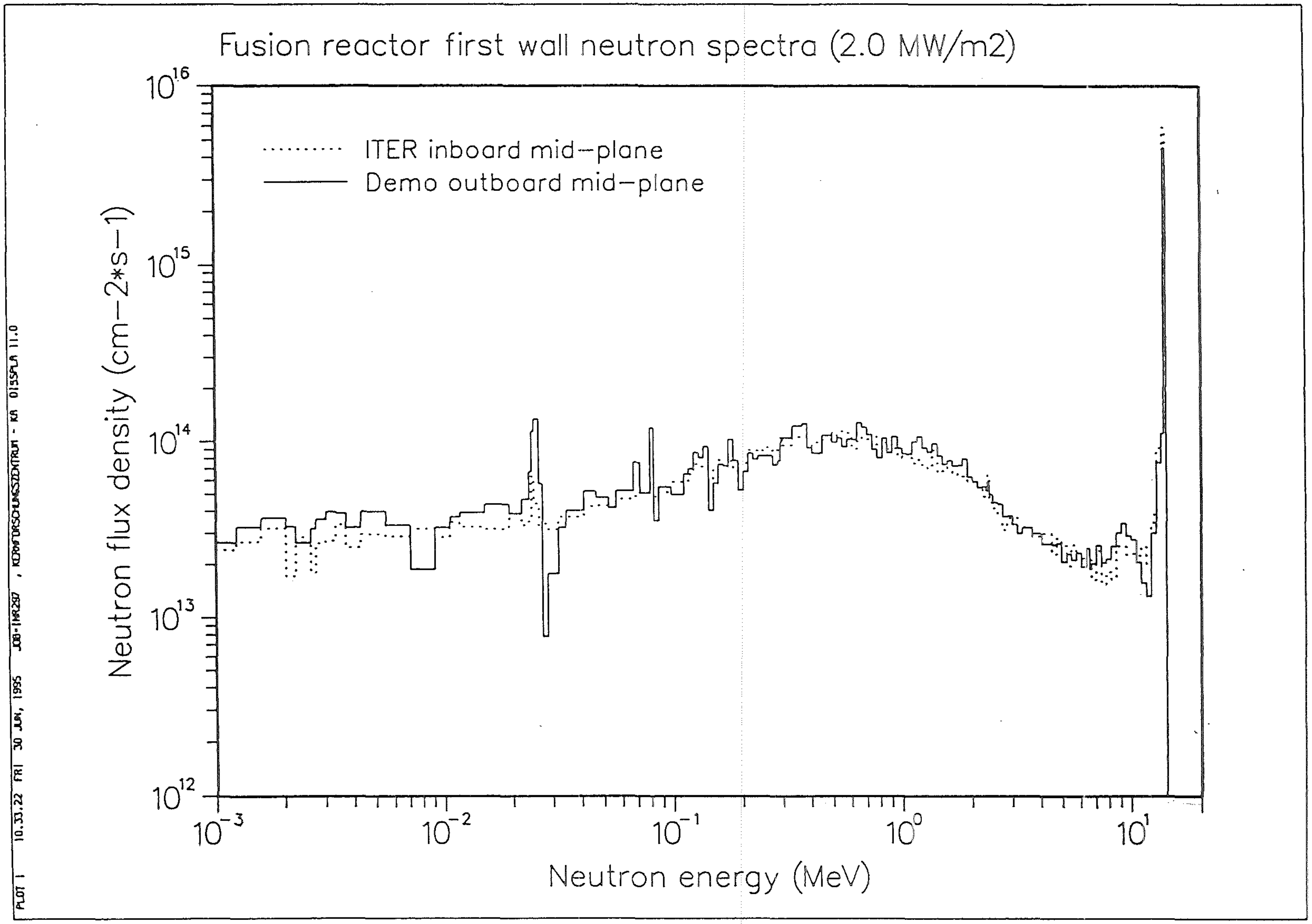

Fusion reactor first wall neutron spectra (2.0 MW/m2)
ITER inboard mid-plane
Demo outboard mid-plane
Neutron flux density (cm-2*s-1)
Neutron energy (MeV)
10^{12}
10^{13}
10^{14}
10^{15}
10^{16}
10^{-3}
10^{-2}
10^{-1}
10^{0}
10^{1}

First wall neutron fluxes and fluences

$2.0\ MW/m^2$ $\Delta t = 1a$	ITER inboard mid-plane	Demo outboard mid-plane
$\phi_{fast}\ [10^{14}\ cm^{-2}\ s^{-1}]$	4.65	4.40
$\phi_{tot}\ [10^{14}\ cm^{-2}\ s^{-1}]$	8.00	7.14
$\phi_{fast} \cdot \Delta t [10^{22}\ cm^{-2}]$	1.47	1.39
$\phi_{tot} \cdot \Delta t [10^{22}\ cm^{-2}]$	2.52	2.25

Results of 3d Monte Carlo calculations normalised to a neutron wall loading of 2.0 MW/m^2 and an integral irradiation time of one year.

Displacement damage [dpa] in first wall spectra

2.0 MW/m^2 $\Delta t = 1a$	ITER inboard mid-plane	Demo outboard mid-plane
SS-316 steel	20.3	17.5
MANET steel	20.2	17.3
V15Cr5Ti	20.9	18.4
Al_2O_3	18.8	17.6
Li_4SiO_4	9.4	5.7
BeO	11.1	10.8
Cu_3Au	2.52	2.25

Results of SPECTER calculations using first wall spectra provided by 3d Monte Carlo calculations.

Normalised to a neutron wall loading of 2.0 MW/m^2 and an integral irradiation time of one year.

Helium production [appm] in first wall spectra

$2.0\ MW/m^2$ $\Delta t = 1a$	ITER inboard mid-plane	Demo outboard mid-plane
Iron	227.5	180.0
Chromium	360.8	281.9
Nickel	789.9	634.0
Copper	250.5	198.1
Vanadium	113.9	88.8
Beryllium	6510.0	5424.2
Carbon	4301.7	3371.1
Silicon	859.8	692.5

Results of SPECTER calculations using first wall spectra provided by 3d Monte Carlo calculations.

Normalised to a neutron wall loading of $2.0\ MW/m^2$ and an integral irradiation time of one year.

Hydrogen production [appm] in first wall spectra

$2.0\ MW/m^2$ $\Delta t = 1a$	ITER inboard mid-plane	Demo outboard mid-plane
Iron	890.4	708.5
Chromium	905.1	722.0
Nickel	3994.3	3222.3
Copper	1262.6	1006.1
Vanadium	477.0	374.0
Beryllium	98.0	76.2
Carbon	1.15	0.884
Silicon	1912.2	1523.7

Results of SPECTER calculations using first wall spectra provided by 3d Monte Carlo calculations.

Normalised to a neutron wall loading of $2.0\ MW/m^2$ and an integral irradiation time of one year.

Displacement damage [dpa] in first wall spectra

2.0 MW/m^2 $\Delta t = 1a$	ITER inboard mid-plane	Demo outboard mid-plane
Iron	20.2	17.3
Chromium	20.2	17.5
Nickel	21.4	18.6
Copper	20.5	17.7
Vanadium	20.7	18.3
Beryllium	6.93	6.92
Carbon	9.35	9.16
Silicon	27.0	24.3

Results of SPECTER calculations using first wall spectra provided by 3d Monte Carlo calculations.

Normalised to a neutron wall loading of 2.0 MW/m^2 and an integral irradiation time of one year.

Conclusions & future work programme

- **Results of calculations performed for different fusion reactors and spectra**
  - Neutron fluxes and spectra different at same neutron wall loading
  - Unique trend for gas production rates
    - Corresponds to differences in ϕ_{14}
  - Non-unique trend for dpa-rates
    - Corresponds to differences in ϕ_{tot} for structural materials
    - No effect for light materials (Be, C)

- **Further work programme**
  - Extend analysis to IFMIF test cell
  - Establish relationship damage parameters IFMIF / fusion reactor

ITER 3-D Shielding Analysis - Main Results for Nuclear Responses to the Inboard TF-Coil

U. Fischer, KfK
February 27, 1995

Basis: Updated global model (7.5° torus sector) including new shielding blanket and divertor cassette design.

Computational procedure: 3-D MCNP-calculation using importance sampling techniques (geometry/particle splitting with Russian Roulette); 320000 source neutron histories, 10h CPU computing time on IBM 9021 mainframe .

Main results for nuclear response to the inboard TF-coil - maximum values at the highest loaded part (120 - 200 cm above torus mid-plane). Normalisation performed for fusion power of 1500 MW, integral operation time of 3 years is assumed.

Peak fast neutron (E>0.1 MeV) fluence to the SC:	$6.52\ 10^{17}\ cm^{-2}$
Peak insulator radiation dose (Epoxy resin):	$5.85\ 10^{8}$ rad
Peak heating rate of magnet:	$0.134\ mW\ cm^{-3}$
Peak displacement damage in the copper stabiliser:	$4.15\ 10^{-4}$ dpa
Peak total neutron flux density at the front of he SC:	$1.02\ 10^{10}\ cm^{-2}\ s^{-1}$

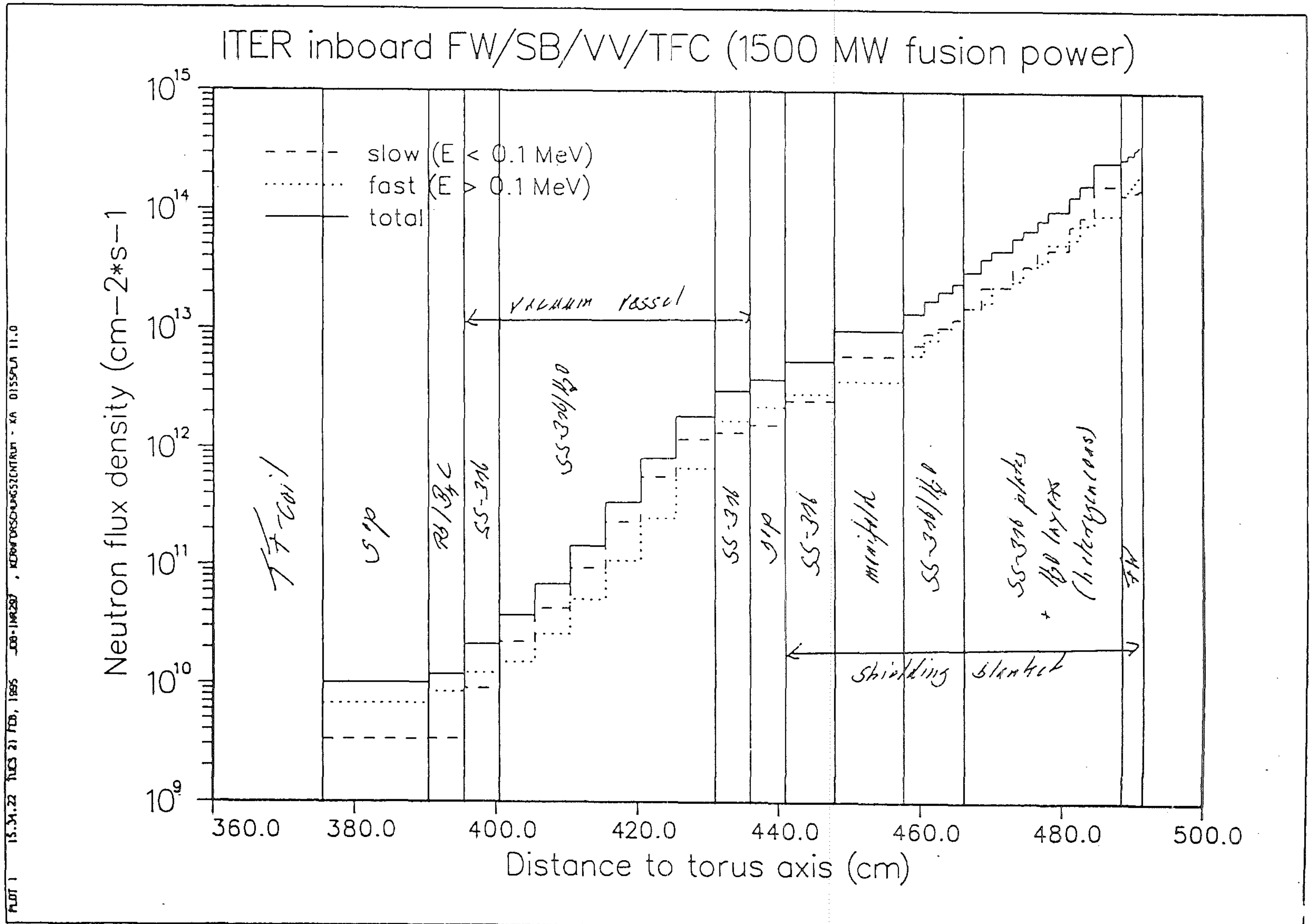

Radial flux distribution, averaged over a poloidal height from z = 120 to 200 cm above torus mid-plane (maximum neutron wall loading)

U. Fischer, KfK

IFMIF-CDA Test Cell/Users Task CDA-D-3

Specimen Geometry/Cell Configuration (Test Matrix for Materials Selection, Miniaturized Specimens and Specimen Arrangement Plan in Test Cell)

S. Jitsukawa
IFMIF-CDA Test Cell/Users Group of JAERI

1. Introduction

Extensive use of miniaturized specimens is very important for materials testing using IFMIF, since test volume of irradiation field of IFMIF is very limited especially for the high flux region, in which irradiation tests of structural materials are performed. In this task, configurations and sizes of standard miniaturized specimens of structural materials for irradiation testing are identified, and specimen loading plan at the high flux region is described for the miniaturized specimens of structural materials.

2. Test Matrix for Materials Selection

Irradiation effect on the (mostly) mechanical properties of following structural materials will be examined for selecting out candidate materials for prototype and demonstration fusion reactors. Possible service temperature ranges for the materials are indicated in the parenthesis.

(I) Low activation ferrite/martensite steels	(300~500C)
(II) Vanadium alloys	(400~600C)
(III) SiC/SiC-composites	(600~1000C)
(IV) Innovative materials; not specified	(300~1000C)

Two to three heats are expected for each material.

Properties to be examined are,

(1) Tensile properties (including temperature and strain rate dependencies)
(2) Creep under irradiation
(3) Fracture toughness
(4) Impact properties (Ductile to brittle transition temperature; DBTT, Displacement rate dependence of fracture toughness)
(5) Fatigue properties (Fatigue life, Fatigue crack growth rate)
(6) Microstructure (Transmission electron microscopy)

(7) Corrosion properties
(8) Physical properties (Thermal and electrical conductivitys)

Properties for (7) and (8) will be examined using specimens for the other tests, such as tensile (IASCC by SSRT), fatigue (corrosion fatigue) and other specimens. Specimens for only (1) to (6) will be treated in CDA-D-3.

For the designing of reactors, information of strain (displacement) rate effect on tensile properties and their temperature dependencies will be required. Characteristic events for fusion reactor, such as plasma disruption can cause the temperature and rate ranges to widen, and multiplicity of specimens for irradiation experiments to evaluate model material behavior for designing seems to increase. For instance, multiplicity of tensile specimens will be of 25 to 35. The multiplicity for fatigue specimens will be larger. Also, in-situ tests occupying large space will be required.

It seems to be unrealistic to plan irradiation experiments with such a large multiplicity. It may be reasonable to conduct irradiation experiments with smaller test matrix not for obtaining design data but for selecting candidate materials. Smaller test matrices are proposed in table D3J-1 to D3J-9.

After the selection stage, a larger matrix (see table D9J-1) may be applied to obtain design data base (or model behavior of material). An example of the very small test matrices is also shown in table D9J-2.

3. Miniaturized Specimens

3-1. Miniaturized specimens and configuration of specimen packets

Miniaturized specimens are listed in Fig. D3J-1. Most of the specimens are the same as those proposed by Grossbeck (ORNL) in 1993 for IFMIF, however specimens for creep, fatigue and crack growth were changed. Configuration of the miniaturized hour glass fatigue specimen is also shown in the figure. It should be noted that the developments of the fatigue and crack growth specimens have not completed yet.

Specimens will be packed to specimen packet, and the specimen packets will be arranged in the test module for irradiation. Each packet will contain one to six specimens. The geometry of the specimen packet is determined by extending the outside dimensions of the specimen bundle proportionally so as to make the specimen volume fraction of 50% in the packet. The volume fraction of 50% was proposed in the last workshop at FZK but the fraction may be reduced in view of specimen temperature control.

The total volume of the specimen packets for the test matrix is about twice as much as the volume of 500 cc proposed at FZK, and the specimen packets will be irradiated dividing into two or three groups. It may be required to make the test matrix smaller.

3-2. Arrangement of the specimen packets

Three reference beam foot prints were proposed at FZK. Plans of specimen packet arrangement for these three beam foot prints are shown in Figs. D3J-2 to D3J-7 and in tables D3J-10 to D3J-12.

A preliminary evaluation about the feasibility of specimen temperature control was carried out in CDA-D-4. The result indicates that side by side arrangement of specimen packets with different irradiation temperatures may cause some difficulty for the temperature control. Therefore, specimen packets were arranged in blocks for every irradiation temperature. In the preliminary evaluation on temperature control, helium gas was used as heat exchanging medium. For different media, such as liquid metals, the result may be changed because of the suitable thermo-physical properties for temperature control.

3-3. About the size effect of specimens for fracture properties tests

Values of fracture toughness and DBTT are rather readily affected by the specimen size. Therefore, the size effects of the specimens for these properties should be examined. The size effects for fatigue specimens may also be important.

Resistance for fracture of the structure is thought to depend on toughness of the material (fracture toughness, DBTT, etc.), flaw size, configuration and size of the structure. And, the size effect on the fracture mechanism of the component of the structure mainly depends on the minimum dimension. Wall thickness of FBW at the plasma facing side is smaller than 10 mm in most of the current designs. On the other hand, the minimum dimensions of fracture toughness and 1/3 Charpy specimens are 4.6 and 3.3 mm, respectively. This indicates that the specimen size is large enough to obtain fracture properties of the material to estimate the stability of FWB with the materials.

However, fracture criteria in elastic plastic region and fracture mechanisms of FWB, and effect of specimen size and configuration should be examined to optimize test method and specimen size/configuration. Following items may be examined for the optimization.

(1) Application (ability) to the part of blanket structure with larger wall thickness
(2) Comparison between DBTTs with 1/3 Charpy and (model) blanket structure

(3) Optimization of Charpy (bend) specimens; notch size, pre-cracking, side groove, configuration at minimum cross section
(4) Structural strength of FWB in elastic plastic region
(5) Application of 1/3 Charpy specimen to evaluate temperature and displacement rate dependence of fracture toughness

3-4. Other specimens

Because of the rather large estimated irradiation volume for the test matrix, further miniaturization of the specimens may be required. Also, developments of miniaturized fatigue and crack growth specimen is important. Deformation and fracture mechanisms for composite materials are different from most of metallic structural materials. For instance, plastic deformation of non-metallic composite material is often accompanied with micro-cracking rather than plastic flow, which is common for metallic materials. This may lead that structural design criteria for structures with composites is different from that with conventional metallic materials. In addition, microstructures of composites are also different. Therefore, miniaturized specimen test techniques optimized for composites as fusion reactor material should be developed. R&D issues for test specimens and technique are as follows.

(1) Miniaturization of tensile and creep specimens (to half as much as current small specimens in volume; this seems to be possible)
(2) Development and demonstration of fatigue and crack growth specimens
(3) Development of miniaturized specimen test technique for composite materials

Table D3J-1 J-Test Matrix / Materials

Marerials	Dose (dpa)*	Temperature (C)
F1, F2, F3, I1	50	300
	100	
	150	
F1, F2, F3, V1, V2, V3, I1, I2	50	400
	100	
	150	
F1, F2, F3, V1, V2, V3, I1, I2	50	500
	100	
	150	
V1, V2, V3, SIC1, SIC2, I2, I3	50	600
	100	
	150	
SIC1, SIC2, I3	50	800
	100	
	150	
SIC1, SIC2, I3	50	1000
	100	
	150	
		Number of heats
F1, F2, F3	Ferritic	3
V1, V2, V3	Vanadium alloys	3
SIC1, SIC2	SiC/SiC Composites	2
I1, I2, I3	Innovative alloys**	3
	Total	11

* Goal doses Structural materials of test modules can be danaged by irradiation,
and Reloading of specimens into new test modules may be carried out at 25, 50, 75, 100 and 125 dpa.

** Innovative alloys of I1, I2 and I3 are not specified, but are supposed to be compatible with Ferrite/Martensite steels, Vanadium alloys and SiC/SiC composites in view of cross contamination, respectively

Tabe 1&2/1

Table D3J-2 Volume of Specimens and Specimen Packets				
Properties	Configuration	Specimen Volume	Packet Configuration*	No. of Specimens / Packet
	(mm)	(cm3)	(mm) [Cross section(mm2)]	
Microstructure	TEM disk / 3 dia. x 0.25 t	0.0018	13.5 x 4 x 4 [54]	50
Tensile	SS-3 / 25 x 4.8x 0.76 (1.52 for SiC)	0.1	6.5 x 6.5 x 28 [182]	6
		0.2 for SiC-tensile		3 for SiC
Fatigue	25 x 4.8 x 1.52	0.2	6.5 x 6.5 x 28 [182]	3
Fracture toughness	0.18 DCT / 12.7 dia. x 4.6 t	0.57	15 x 15 x 15.5 [233]	3
Crack Growth	0.09 DCT / 12.7 dia. x 2.3 t	0.57	15 x 15 x 15.5 [233]	6
Bend/Charpy	1/3-Charpy / 3.3 x 3.3 x 25	0.28	9 x 9 x 28 [252]	4
Creep	0.7-Pressurized Tube / 25 x 2.5 dia.	0.12	3.5 x 3.5 x 27 [95]	1

* Dimentions were determined by extending them isotropically so as to make the volume twice as much as that of specimen
** Number of specimens in a packet x specimen volume x 2

Properties	Number of Packets	Total Packet Vol.	Total Packet Area	
	300C/400C/500C/600C/800C/1000C (Total)	(cm3)	(cm2)	
Microstructure	3/3/3/3/3/3 (18)	3.9	9.72	
Tensile	9/15/15/9/3/3 (54)	63.9	98.3	
Fatigue	12/18/18/12/6/6 (72)	89	137	
Fracture toughness	18/27/27/15/6/6 (99)	346	231	
Crack Growth	6/9/9/6/3/3 (36)	126	84	
Bend/Charpy	15/21/21/12/6/6 (81)	184	204	
Creep	18/27/27/15/6/6 (99)	32.67	94.05	

Tabe 1&2/1

Packet Volume**
(cm3)
0.216
1.183
1.183
3.49
3.49
2.27
0.33

Table 3-14/1

Table D3J-3 J-Test Matrix / TEM disks					
Marerials	Dose (dpa)	Temperature (C)	No. of specimens*	No. of packets**	
F1, F2, F3, I1	50	300	20	1	
	100		20	1	
	150		20	1	
F1, F2, F3, V1, V2, V3, I1, I2	50	400	40	2	1 for F+I1 and 1 for V+I2
	100		40	2	
	150		40	2	
F1, F2, F3, V1, V2, V3, I1, I2	50	500	40	2	1 for F+I1 and 1 for V+I2
	100		40	2	
	150		40	2	
V1, V2, V3, SIC1, SIC2, I2, I3	50	600	35	2	1 for V+I2 and 1 for SIC+I3
	100		35	2	
	150		35	2	
SIC1, SIC2, I3	50	800	15	1	
	100		15	1	
	150		15	1	
SIC1, SIC2, I3	50	1000	15	1	
	100		15	1	
	150		15	1	
			495	27	

* Multiplication > 5
** Each packet will contain upto 50 specimens. And, will contain spacers, which will be located to separate different materials.
To avoid cross contamination, Ferrite/Martensite steels + I1, Vanadium alloys + I2 and SiC/SiC composite + I3 are supposed to be loaded in separate packets.

Total Packet Vol. (cm3)	3.9
Total Packet Area(cm2)	9.72

Table 3-14/1

Table D3J-4 J-Test Matrix / Tensile specimen					
Marerials	Dose (dpa)	Temperature (C)	No. of specimens*	No. of packets**	
F1, F2, F3, I1	50	300	12	2	
	100		12	2	
	150		12	2	
F1, F2, F3, V1, V2, V3, I1, I2	50	400	24	4	2 for F+I1 and 2 for V+I2
	100		24	4	
	150		24	4	
F1, F2, F3, V1, V2, V3, I1, I2	50	500	24	4	2 for F+I1 and 2 for V+I2
	100		24	4	
	150		24	4	
V1, V2, V3, SIC1***, SIC2***,	50	600	21	5	2 for V+I2 and 3 for SIC+I3
	100		21	5	
	150		21	5	
SIC1***, SIC2***, I3	50	800	9	3	
	100		9	3	
	150		9	3	
SIC1***, SIC2***, I3	50	1000	9	3	
	100		9	3	
	150		9	3	
			297	63	

* Multiplication = 3

** Each packet will contain 3 to 6 specimens. And, similar materials will be loaded into a same packet

To avoid cross contamination, Ferrite/Martensite steels + I1, Vanadium alloys + I2 and SiC/SiC composite + I3 are supposed to be loaded in separate packets.

*** Thickness of the tensile specimens for SiC/SiC-composite is twice as much as that for the other materials

Total Packet Vol. (cm3)	74.529
Total Packet Area (cm2)	114.66

Table 3-14/1

Table D3J-5 J-Test Matrix / Creep specimens				
Marerials	Dose (dpa)	Temperature (C)	No. of specimens*	No. of packets**
F1, F2, F3, I1	50-150	300	12	12
F1, F2, F3, V1, V2, V3, I1, I2	50-150	400	24	24
F1, F2, F3, V1, V2, V3, I1, I2	50-150	500	24	24
V1, V2, V3, SIC1, SIC2, I2, I3	50-150	600	21	21
SIC1, SIC2, I3	50-150	800	9	9
SIC1, SIC2, I3	50-150	1000	9	9
			99	99

* Multiplication =3 (Test = 3)
** Each packet will contain 1 specimen.

Total Packet Vol.(cm3)	32.67
Total Packet Area(cm2)	94.05

Table 3-14/1

Table D3J-6 J-Test Matrix / Fracture toughness specimens					
Marerials	Dose (dpa)	Temperature (C)	No. of specimens*	No. of packets**	
F1, F2, F3, I1	50	300	12	4	
	100		12	4	
	150		12	4	
F1, F2, F3, V1, V2, V3, I1, I2	50	400	24	8	4 for F+I1 and 4 for V+I2
	100		24	8	
	150		24	8	
F1, F2, F3, V1, V2, V3, I1, I2	50	500	24	8	4 for F+I1 and 4 for V+I2
	100		24	8	
	150		24	8	
V1, V2, V3, SIC1, SIC2, I2, I3	50	600	21	7	4 for V+I2 and 3 for SIC+I3
	100		21	7	
	150		21	7	
SIC1, SIC2, I3	50	800	9	3	
	100		9	3	
	150		9	3	
SIC1, SIC2, I3	50	1000	9	3	
	100		9	3	
	150		9	3	
			297	99	

* Multiplication = 3 (Test =3)
** Each packet will contain upto 3 specimens.
To avoid cross contamination, Ferrite/Martensite steels + I1, Vanadium alloys + I2 and SiC/SiC composite + I3 are supposed to be loaded in separate packets.

Total Packet Vol.(cm3)	345.51
Total Packet Area(cm2)	230.67

Table 3-14/1

Table D3J-7 J-Test Matrix / Crack growth specimens***					
Marerials	Dose (dpa)	Temperature (C)	No. of specimens*	No. of packets**	
F1, F2, F3, I1	50	300	8	2	
	100		8	2	
	150		8	2	
F1, F2, F3, V1, V2, V3, I1, I2	50	400	16	4	2 for F+I1 and 2 for V+I2
	100		16	4	
	150		16	4	
F1, F2, F3, V1, V2, V3, I1, I2	50	500	16	4	2 for F+I1 and 2 for V+I2
	100		16	4	
	150		16	4	
V1, V2, V3, SIC1, SIC2, I2, I3	50	600	14	3	2 for V+I2 and 1 for SIC+I3
	100		14	3	
	150		14	3	
SIC1, SIC2, I3	50	800	6	1	
	100		6	1	
	150		6	1	
SIC1, SIC2, I3	50	1000	6	1	
	100		6	1	
	150		6	1	
			198	45	

* Test = 1 (Duplication = 2)
** Each packet will contain upto 6 specimens.
To avoid cross contamination, Ferrite/Martensite steels + I1, Vanadium alloys + I2 and SiC/SiC composite + I3 are supposed to be loaded in separate packets.
*** Half as thick as Fracture toughness specimen

Total Packet Vol.(cm3)	157.05
Total Packet Area(cm2)	104.85

Table 3-14/1

Table D3J-8 J-Test Matrix / Fatigue specimens

Marerials	Dose (dpa)	Temperature (C)	No. of specimens*	No. of packets**	
F1, F2, F3, I1	50	300	8	3	
	100		8	3	
	150		8	3	
F1, F2, F3, V1, V2, V3, I1, I2	50	400	16	6	3 for F+I1 and 3 for V+I2
	100		16	6	
	150		16	6	
F1, F2, F3, V1, V2, V3, I1, I2	50	500	16	6	3 for F+I1 and 3 for V+I2
	100		16	6	
	150		16	6	
V1, V2, V3, SIC1, SIC2, I2, I3	50	600	14	5	3 for V+I2 and 2 for SIC+I3
	100		14	5	
	150		14	5	
SIC1, SIC2, I3	50	800	6	2	
	100		6	2	
	150		6	2	
SIC1, SIC2, I3	50	1000	6	2	
	100		6	2	
	150		6	2	
			198	72	

* Test = 2 (Duplication = 1)

** Each packet will contain upto 3 specimens.

To avoid cross contamination, Ferrite/Martensite steels + I1, Vanadium alloys + I2 and SiC/SiC composite + I3 are supposed to be loaded in separate packets.

Total Packet Vol. (cm3)	85.176
Total Packet Area (cm2)	131.04

Table 3-14/1

Table D3J-9 J-Test Matrix / Crack growth specimens***					
Marerials	Dose (dpa)	Temperature (C)	No. of specimens*	No. of packets**	
F1, F2, F3, I1	50	300	8	2	
	100		8	2	
	150		8	2	
F1, F2, F3, V1, V2, V3, I1, I2	50	400	16	4	2 for F+I1 and 2 for V+I2
	100		16	4	
	150		16	4	
F1, F2, F3, V1, V2, V3, I1, I2	50	500	16	4	2 for F+I1 and 2 for V+I2
	100		16	4	
	150		16	4	
V1, V2, V3, SIC1, SIC2, I2, I3	50	600	14	3	2 for V+I2 and 1 for SIC+I3
	100		14	3	
	150		14	3	
SIC1, SIC2, I3	50	800	6	1	
	100		6	1	
	150		6	1	
SIC1, SIC2, I3	50	1000	6	1	
	100		6	1	
	150		6	1	
			198	45	

* Test = 1 (Duplication = 2)
** Each packet will contain upto 6 specimens.
To avoid cross contamination, Ferrite/Martensite steels + I1, Vanadium alloys + I2 and SiC/SiC composite + I3 are supposed to be loaded in separate packets.
*** Half as thick as Fracture toughness specimen

Total Packet Vol.(cm3)	157.05
Total Packet Area(cm2)	104.85

Table 3-14/1

Table D3J-10 100 x 100 mm Beam foot print

Temperature (C)	Specimen	Number of packets in the row X x Z	Y*	Number of packets	Number of Specimens	
300	TEM	1	6	3		60
	Tensile/Fatigue	5	3	15	36/24	
	Creep	3	4	12		12
	Fracture toughness/Crack growth	3	6	18	36/24	
	1/3 Charpy	3	4	9		36
400	TEM	1	6	6		120
	Tensile/Fatigue	10	3	30	72/48	
	Creep	6	4	24		24
	Fracture toughness/Crack growth	6	6	36	72/48	
	1/3 Charpy	5	4	18		72
500	TEM	1	6	6		120
	Tensile/Fatigue	10	3	30	72/48	
	Creep	6	4	24		24
	Fracture toughness/Crack growth	6	6	36	72/48	
	1/3 Charpy	5	4	18		72
600	TEM	1	6	6		105
	Tensile/Fatigue	10	3	30	63/42	
	Creep	6	4	21		21
	Fracture toughness/Crack growth	5	6	30	63/42	
	1/3 Charpy	5	4	18		63
800	TEM	1	6	3		45
	Tensile/Fatigue	5	3	15	27/18	
	Creep	3	4	9		9
	Fracture toughness/Crack growth	2	6	12	27/18	
	1/3 Charpy	3	4	9		27
1000	TEM	1	6	3		45
	Tensile/Fatigue	5	3	15	27/18	
	Creep	3	4	9		9
	Fracture toughness/Crack growth	2	6	12	27/18	
	1/3 Charpy	3	4	9		27

* Y and Z corresponds to the beam thickness and beam incident direction, respectively.

Table 3-14/1

Table D3J-11 200 x 50 mm Beam foot print

Temperature (C)	Specimen	Number of packets in the row X x Z	Y*	Number of packets	Number of Specimens	
300	TEM	1	3	3		60
	Tensile/Fatigue	8	2	15	36/24	
	Creep	6	2	12		12
	Fracture toughness/Crack growth	6	3	18	36/24	
	1/3 Charpy	5	2	9		36
400	TEM	2	3	6		120
	Tensile/Fatigue	15	2	30	72/48	
	Creep	12	2	24		24
	Fracture toughness/Crack growth	12	3	36	72/48	
	1/3 Charpy	9	2	18		72
500	TEM	2	3	6		120
	Tensile/Fatigue	15	2	30	72/48	
	Creep	12	2	24		24
	Fracture toughness/Crack growth	12	3	36	72/48	
	1/3 Charpy	9	2	18		72
600	TEM	2	3	6		105
	Tensile/Fatigue	15	2	30	63/42	
	Creep	11	2	21		21
	Fracture toughness/Crack growth	10	3	30	63/42	
	1/3 Charpy	9	2	18		63
800	TEM	1	3	3		45
	Tensile/Fatigue	8	2	15	27/18	
	Creep	5	2	9		9
	Fracture toughness/Crack growth	4	3	12	27/18	
	1/3 Charpy	5	2	9		27
1000	TEM	1	3	3		45
	Tensile/Fatigue	8	2	15	27/18	
	Creep	5	2	9		9
	Fracture toughness/Crack growth	4	3	12	27/18	
	1/3 Charpy	5	2	9		27

* Y and Z corresponds to the beam thickness and beam incident direction, respectively.

Table 3-14/1

Table D3J-12 400 x 25 mm Beam foot print

Temperature (C)	Specimen	Number of packets in the row X x Z	Y*	Number of packets	Number of Specimens	
300	TEM	3	1	3		60
	Tensile/Fatigue	15	1	15	36/24	
	Creep	12	1	12		12
	Fracture toughness/Crack growth	9	2	18	36/24	
	1/3 Charpy	9	1	9		36
400	TEM	6	1	6		120
	Tensile/Fatigue	30	1	30	72/48	
	Creep	24	1	24		24
	Fracture toughness/Crack growth	18	2	36	72/48	
	1/3 Charpy	18	1	18		72
500	TEM	6	1	6		120
	Tensile/Fatigue	30	1	30	72/48	
	Creep	24	1	24		24
	Fracture toughness/Crack growth	18	2	36	72/48	
	1/3 Charpy	18	1	18		72
600	TEM	6	1	6		105
	Tensile/Fatigue	30	1	30	63/42	
	Creep	21	1	21		21
	Fracture toughness/Crack growth	15	2	30	63/42	
	1/3 Charpy	18	1	18		63
800	TEM	3	1	3		45
	Tensile/Fatigue	15	1	15	27/18	
	Creep	9	1	9		9
	Fracture toughness/Crack growth	6	2	12	27/18	
	1/3 Charpy	9	1	9		27
1000	TEM	3	1	3		45
	Tensile/Fatigue	15	1	15	27/18	
	Creep	9	1	9		9
	Fracture toughness/Crack growth	6	2	12	27/18	
	1/3 Charpy	9	1	9		27

* Y and Z corresponds to the beam thickness and beam incident direction, respectively.

Miniaturized specimens

Microstructure: TEM disk 3mm diameter
Tensile: SS-3(25x5x0.75) or smaller specimen
Creep: Pressurized tube (2.5-3mm diameter)
Fracture toughness: DCT (4.5mm thick)
Impact (DBTT): 1/3-Charpy or Pre-cracked
Fatigue: Miniaturized hour glass
Crack growth: Half thickness DCT

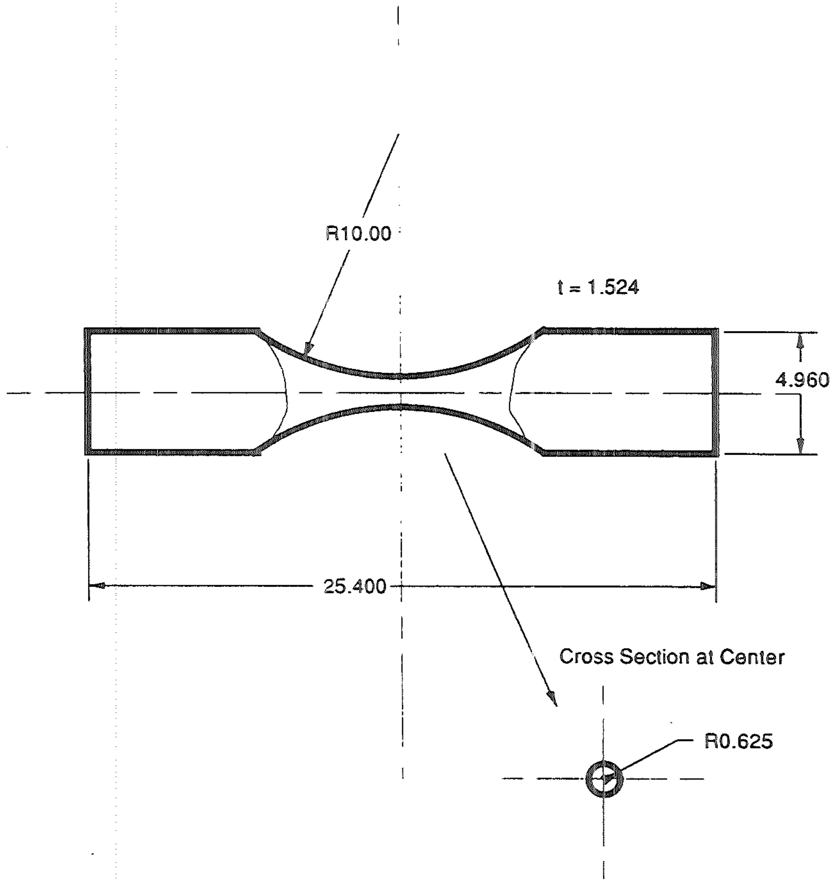

Fig. D3J-1 A miniaturized hour glass fatigue specimen

Fig. 2 Arrangement of specimen packets (mm)
100 x 100 beam foot print, 50% specimen volume fraction

Fig. D3J-2

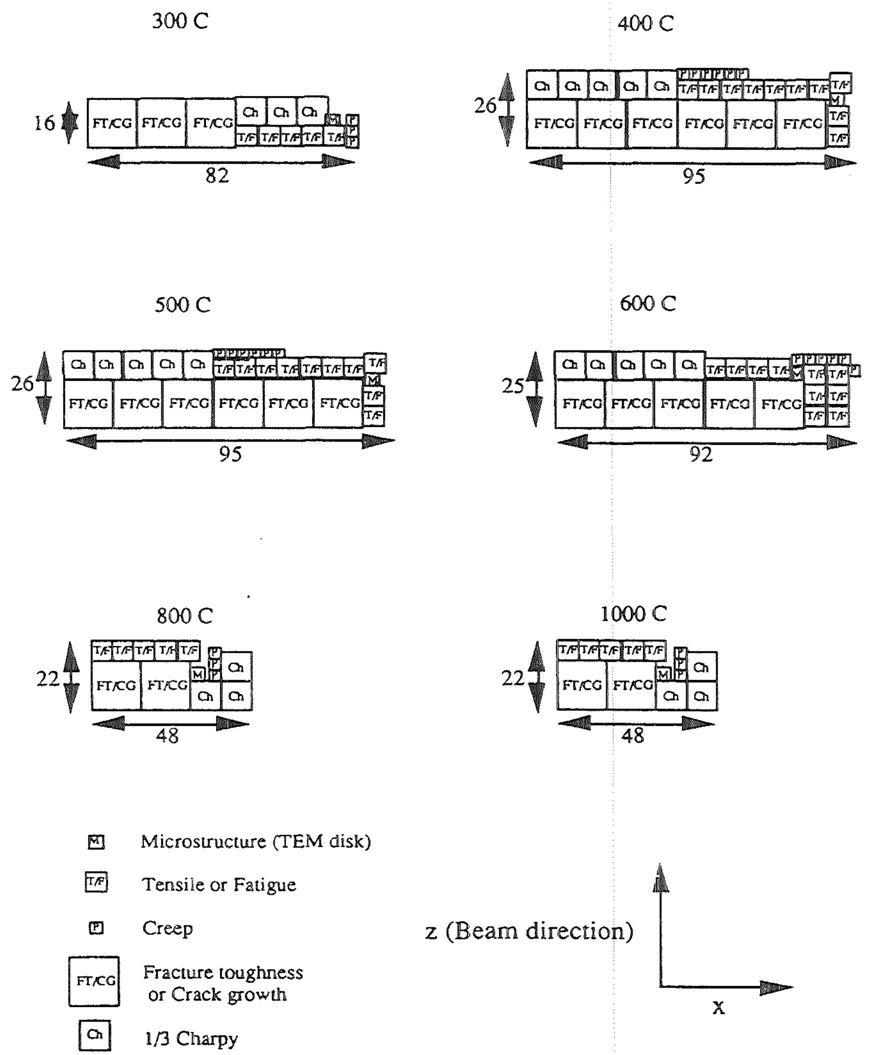

Maximum dimension in y direction is 120 mm.

Fig. D3J-3

Fig. 3 Arrangement of specimen packets(mm)
200 x 50 beam foot print, 50% specimen volume fraction

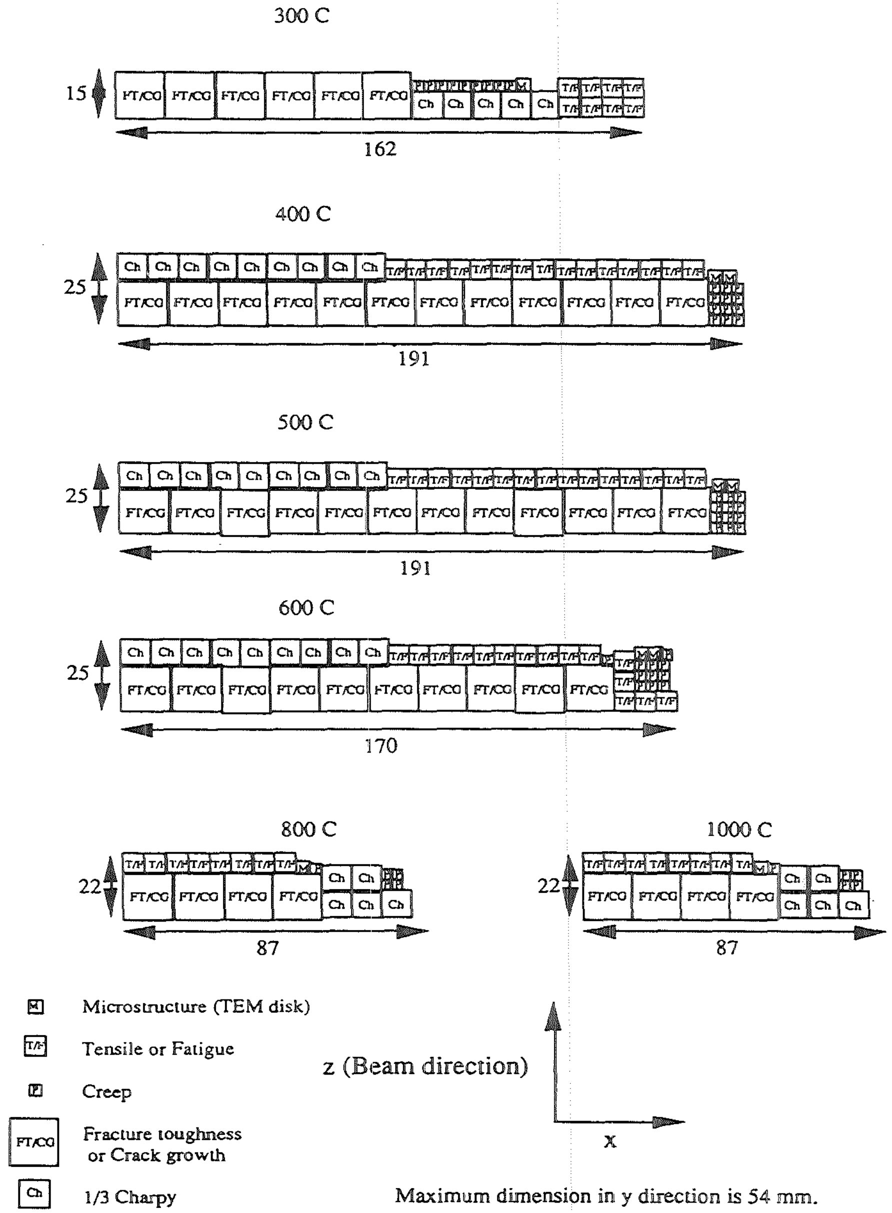

Fig. D3J-4

Fig. 4 Arrangement of specimen packets (mm)
400 x 25 beam foot print, 50% specimen volume fraction

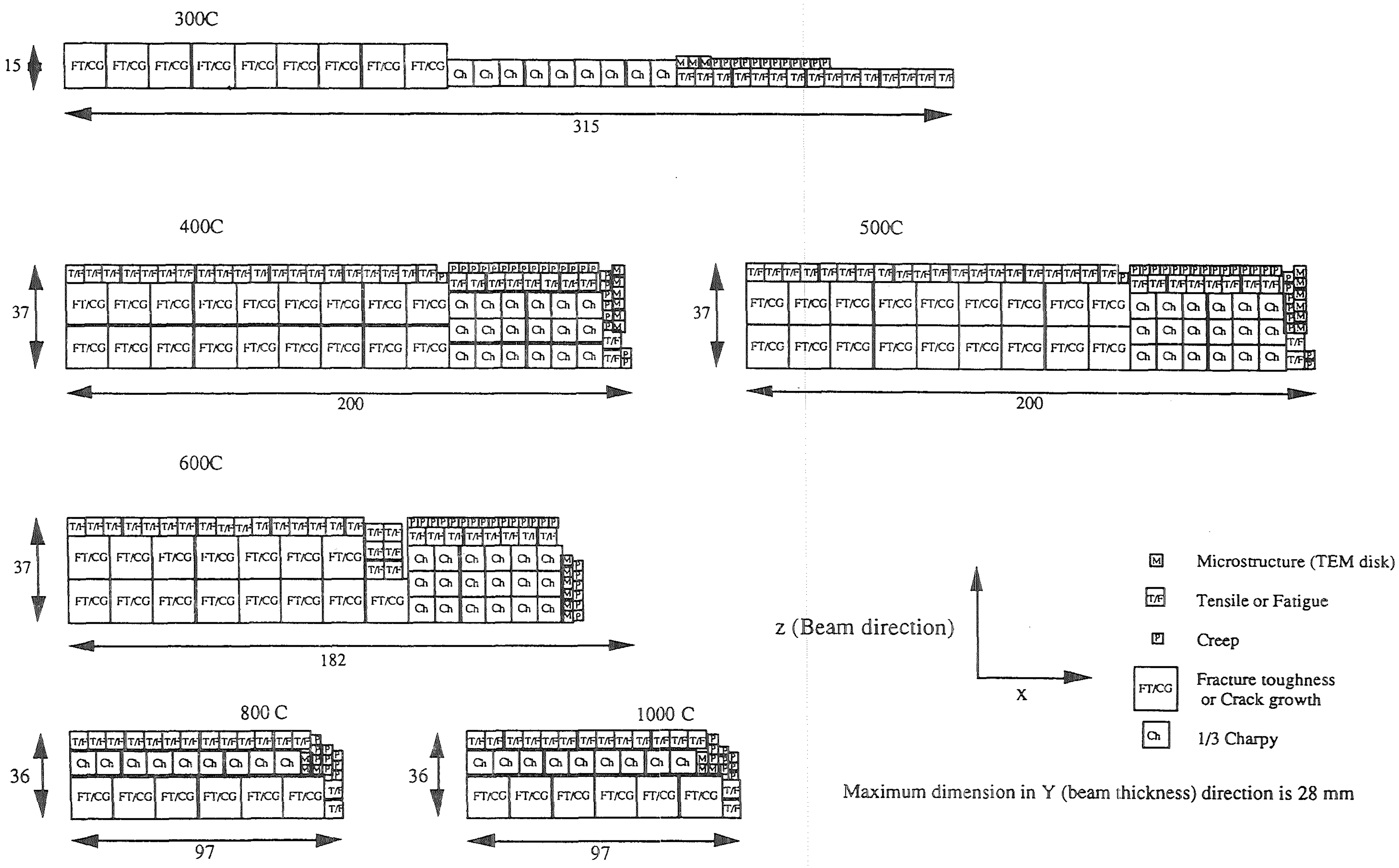

Fig. D3J-5

Fig. 5 Arrangement of specimen packets II
100 x 100 beam foot print (mm), 50% specimen volume fraction

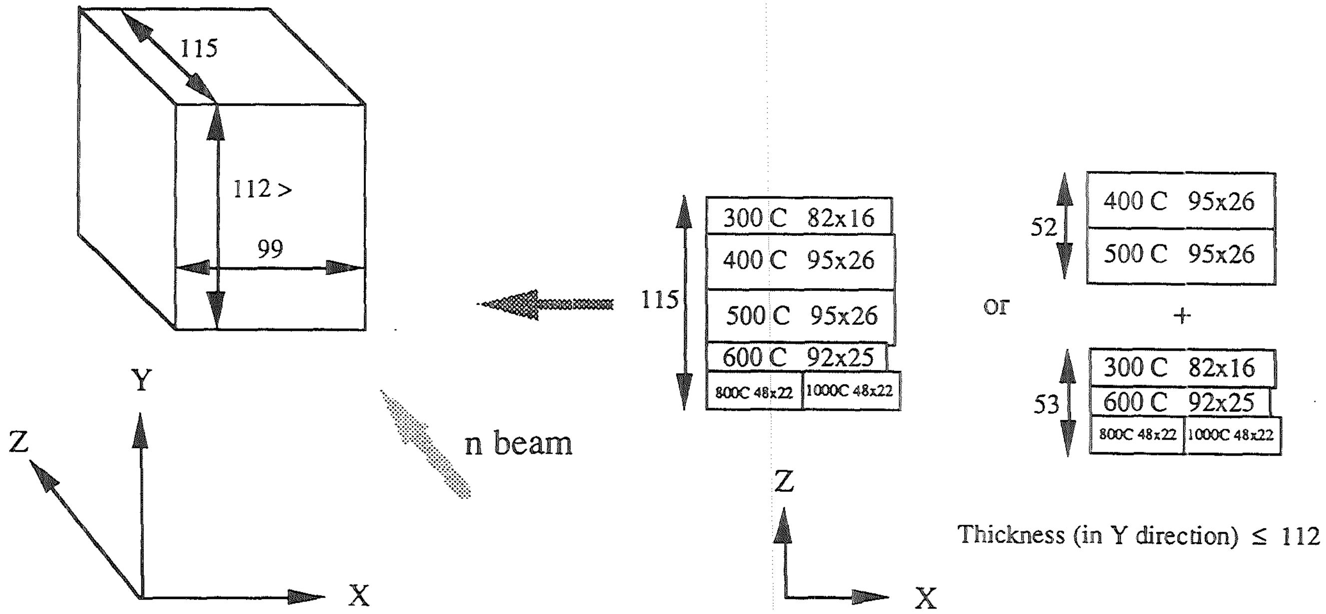

Fig. D3J-6

Fig. 6 Arrangement of specimen packets II
200 x 50 beam foot print (mm), 50% specimen volume fraction

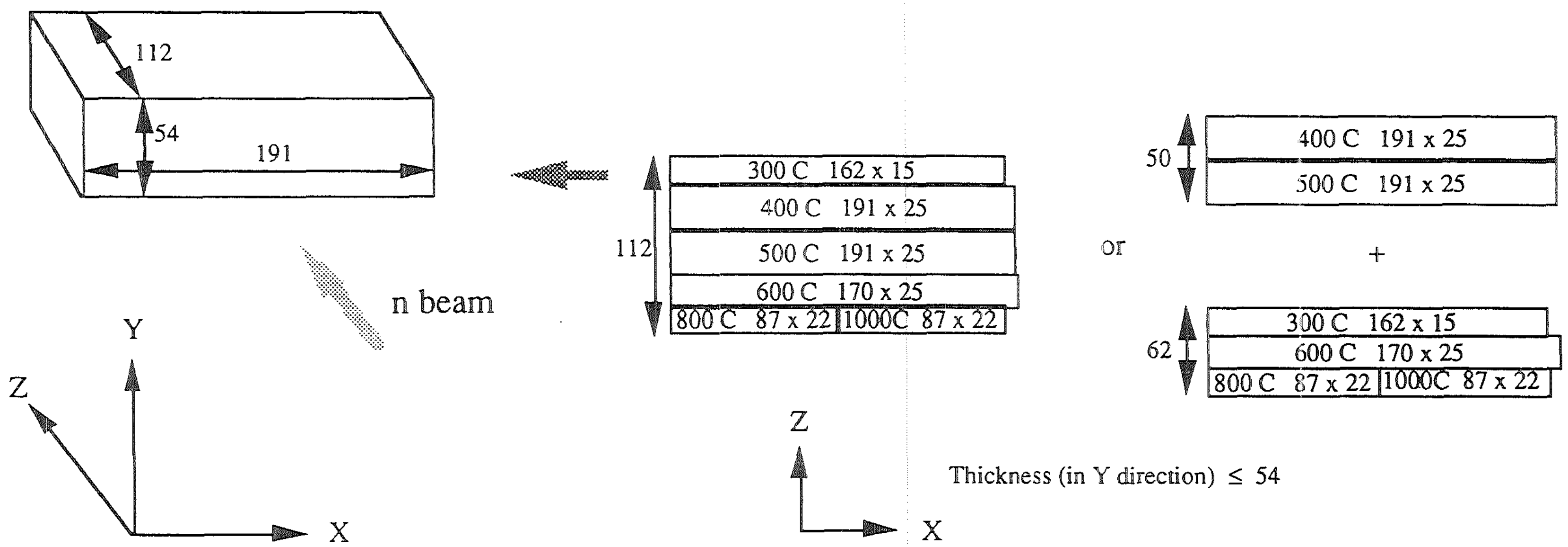

Fig. D3J-7

Fig. 7 Arrangement of specimen packets II
400 x 25 beam foot print (mm), 50% specimen volume fraction

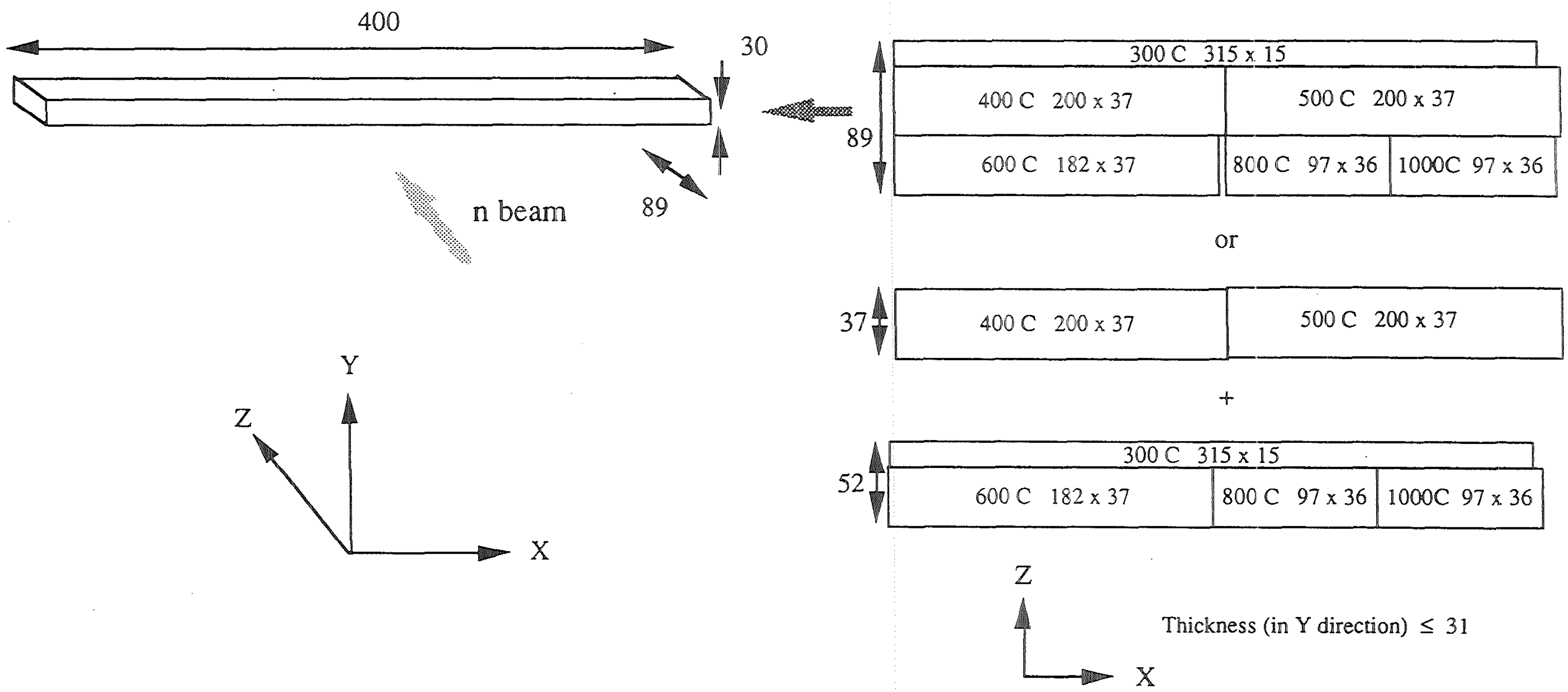

Summary (CDA-D-3)

1. Small specimens are listed.
   SS-3 tensile, SF-1 fatigue, 1/3 pre-cracked Charpy (Bending), etc.

2. Test matrices are listed.
   11 heats including Ferrite/Martensite steel, Vanadium alloys,
   SiC/SiC composites plus not specified Innovative materials
   Temperature range 300 to 1000C
   Goal dose 150 dpa

3. Total volume for the matrix is estimated.
   about 1000 cc

4. Future work is proposed.
   Volume fraction of the specimen:
   samller fraction for temperature control may be required
   Test matrix: large total volume
   Small specimen: needs for further development;
   Fracture specimen and Specimens for composites.

Difference from U.S. proposal for CDA-D-3

1. Bundle of specimens

U.S.	Smaller maximum thickness of specimen bundle is employed for a small temperature distribution.

2. Irradition plan

U.S.	2 batches
Japan	1 to 3 batches; not specified

3. Fatigue specimen

U.S.	SF-1 and HFIR hour glass (not for materials selection)
Japan	SF-1

PROPOSED REFERENCE SPECIMEN GEOMETRIES AND TEST MATRIX FOR THE HIGH-FLUX REGIONS OF IFMIF

S.J. Zinkle
Oak Ridge National Laboratory
Oak Ridge, TN 37831-6376

1st CDA Workshop on IFMIF Test Cell System
Forschungszentrum Karlsruhe
Karlsruhe, Germany
July 3-6, 1995

IFMIF Users/Test Cell Subgroup Task CDA-D3: Reference Specimen Loading Matrix

The purpose of this document is to outline a prototypic specimen loading matrix for the high flux (equivalent to >2 MW/m^2 first wall neutron loading) region of the International Fusion Materials Irradiation Facility (IFMIF) as part of the conceptual design activity for this facility (Users/Test Cell subgroup task CDA-D3). This document relies heavily on a previous evaluation performed in 1993 by the Neutron Source Working Group under Annex II of the Implementing Agreement for Research and Development on Fusion Reactor Materials for the International Energy Agency ("Test Volume Considerations for an IFMIF", D.G. Doran, chairman, May 1993). The specific objectives of the present document are twofold, namely 1) to identify reference miniaturized specimen geometries for IFMIF, and 2) to develop a preliminary reference test module loading for the high flux region of IFMIF based on accepted miniaturized specimens. For the purposes of this document, the conversion between first wall neutron loading and displacements per atom is taken to be 1 MWa/m^2=11 dpa (this is the appropriate relation for Fe and V in the STARFIRE first wall fusion neutron spectrum). The reference specimen loading matrix for the lower flux regions of IFMIF will be developed in the near future, and will be incorporated into this document at a later date.

Preliminary neutron flux calculations for the IFMIF test cell suggest that the high flux region will have a volume of $\leq$ 0.5 liter. This irradiation volume is comparable to (or slightly smaller than) the typical irradiation volumes available in existing fission neutron reactors, e.g., ~0.6 liter for the Removable Beryllium positions in the HFIR reactor. It is therefore clear that extensive use of miniaturized specimens will be required for the IFMIF tests, and that only a limited number of materials can be tested. Establishment of an irradiated properties data base for DEMO will certainly require extensive use of both IFMIF and fission reactor irradiation sources. It is assumed that fission reactor facilities will continue to be available to perform scoping irradiation tests on experimental or innovative alloys, and that IFMIF will only be used to test materials that have demonstrated good radiation resistance during high-dose (>50 dpa) fission neutron irradiation.

Table 1 lists a tentative test matrix of the materials, irradiation temperatures and doses (in dpa) for the high flux region of IFMIF. A total of 6 irradiation temperatures ranging from 300 to 1000°C are considered to be of interest for evaluating the radiation resistance of first wall (including divertor and limiter) and blanket structural materials. From an engineering viewpoint, it does not appear to be feasible to simultaneously control with good accuracy these 6 widely different temperatures within a limited test volume of ~0.5 liter. Therefore, it is assumed that this range of temperature would be accomplished in separate "low-temperature" and "high-temperature" irradiation campaigns. The "low-temperature" irradiations would utilize 3 side-by side test chambers that would operate at coolant temperatures of 300, 400 and 500°C, whereas the "high-temperature" irradiation series would be performed at 600, 800 and 1000°C. Suitable insulation would be utilized to inhibit heat transfer between the test assembly chambers. Figure 1 shows a schematic of the proposed reference set of 3 side-by-side irradiation chambers, assuming a deuteron beam "footprint" of 5 cm by 20 cm. A thermal insulation layer of 1 cm thickness is assumed between the irradiation chambers.

Considering the reference availability for IFMIF of 70%, the high flux region would produce a damage level of ~15 dpa in vanadium and ferritic/martensitic steel in one calendar year. Therefore, approximately 10 years would be required to achieve a DEMO-relevant lifetime dose of ~150 dpa. Given the uncertainties of the radiation resistance of the capsule containers and test assembly materials, it would appear to be prudent to plan for periodic (i.e., every one to two years) removal of the test assemblies for inspection and possible replacement. A subset of the irradiated specimen matrix could be removed for testing at these times, and the remaining specimens could be re-encapsulated (along with some additional unirradiated specimens) for further irradiation. Maximum utilization of the IFMIF could be achieved by sequential cycling between the "low-temperature" (300-500°C) and "high-temperature" (600-1000°C) irradiation assemblies. For example, the "high temperature" assemblies could be inserted into IFMIF immediately after the withdrawal of the "low-temperature" assemblies. Inspection (and replacement, if necessary) of the test assemblies, removal of specimens for testing, and specimen re-encapsulation could be performed on the "low temperature" assemblies during the subsequent one to two years that the "high temperature" assemblies are being irradiated. If any of the alloys exhibited poor radiation resistance during the postirradiation specimen testing, all specimens for that alloy could be replaced with unirradiated specimens of a more promising alloy (depending on programmatic requirements). The total irradiation program would require a facility lifetime of about 20 years to achieve doses of 150 dpa at all temperatures. By selective streamlining of the specimen matrix at periodic intervals (and replacement of tested specimens with new specimens), the complete dose-dependent behavior up to ~150 dpa of two or more of the most promising fusion structural materials could be obtained at dose increments of ~20 dpa during this time frame. An example of a possible facility schedule for alternating low-temperature and high-temperature irradiation campaigns is shown in Table 2.

Although the detailed specimen matrix for IFMIF will be dependent on alloy developments that occur over the next 10 years, the three leading candidates for the first wall and blanket structure of DEMO are considered to be ferritic/martensitic steels, vanadium alloys, and SiC/SiC composites. Two to three variants of each of these materials are included in the reference IFMIF specimen matrix. Some space is also reserved for a limited number of unspecified alternative materials ("innovative alloys"). It is unlikely that this specimen matrix can be significantly reduced, since IFMIF must meet the needs of more than one DEMO design.

The tentative reference specimen geometries are shown in Figs. 2-8. It is anticipated that seven different specimen geometries will be used for investigation of key properties such as density and microstructure, tensile properties, fatigue strength, fracture toughness, crack growth, impact behavior, and irradiation creep. It is anticipated that further development will be required on several of the specimen geometries to verify their suitability for providing engineering design data. In particular, the miniature SF-1 push-pull fatigue specimen shown in Fig. 4 is still under development at JAERI and has not yet been tested. However, it is anticipated that the miniature SF-1 fatigue specimens would at least provide qualitative information that could be used to compare the fatigue behavior of the various candidate materials and could be correlated with fission reactor irradiations. Larger push-pull hourglass fatigue specimens could be irradiated at later times (e.g., 10-15 years after the start of facility operation) on one or two materials that show the most promising overall radiation resistance behavior.

The tentative reference geometries for the specimen packets that house the various specimen types are shown in Figs. 9-15, and the results are summarized in Table 3. With the exception of the TEM disk packets (which would contain up to ~80 specimens), a total of one to six specimens would be encapsulated in each packet. It is anticipated that the exterior of these packets would be kept at a constant temperature by liquid metal coolant. The maximum thickness of the specimen packets may be limited by nuclear heating effects, depending on the method of specimen encapsulation in the packets (He vs. liquid metal encapsulation). Preliminary calculations indicate that the maximum nuclear heating in the high flux region of IFMIF will be ~3.2 W/g (25 W/cm^3 in ferritic/martensitic steel). Therefore, the maximum specimen thickness that will keep temperature gradients below 1°C is ~3 mm for a specimen cooled with liquid metal on both faces. Specimen encapsulation in He gas would produce larger differences between the specimen temperature and the temperature at the exterior of the packet, due to thermal contact resistances. For example, using a He gas-gap thickness of ~75 μm between the stacked TEM disks and the packet wall (Fig.9) in order to accomodate void swelling up to ~10%, the temperature difference between steel TEM disks and the packet wall would be ~10 °C. The packet dimensions shown in Figs. 9-15 have been sized so that the maximum temperature difference between the specimens and the packet wall is <10°C for He gas

Table 1. IFMIF Test Matrix / Materials		
Materials	Dose (dpa)	Temperature (°C)
FM1, FM2, FM3*, I1, I2*	20-150	300
FM1, FM2, FM3*, Van1, Van2, Van3*, I1, I2*, SiC1	20-150	400
FM1, FM2, FM3*, Van1, Van2, Van3*, I1, I2*	20-150	500
Van1, Van2, Van3*, SiC1, SiC2, I3	20-150	600
SiC1, SiC2, I3	20-150	800
SiC1, SiC2, I3	20-150	1000

		Number of heats
FM1, FM2, FM3*	Ferritic/martensitic steel	3
Van1, Van2, Van3*	Vanadium alloys	3
SIC1, SIC2	SiC/SiC composites	2
I1, I2*, I3	Innovative alloys	4
	Total	12

* TEM and tensile specimens only

Table 2. Calendar Years of operation (assuming 70% facility availability at 2 MW/m2)

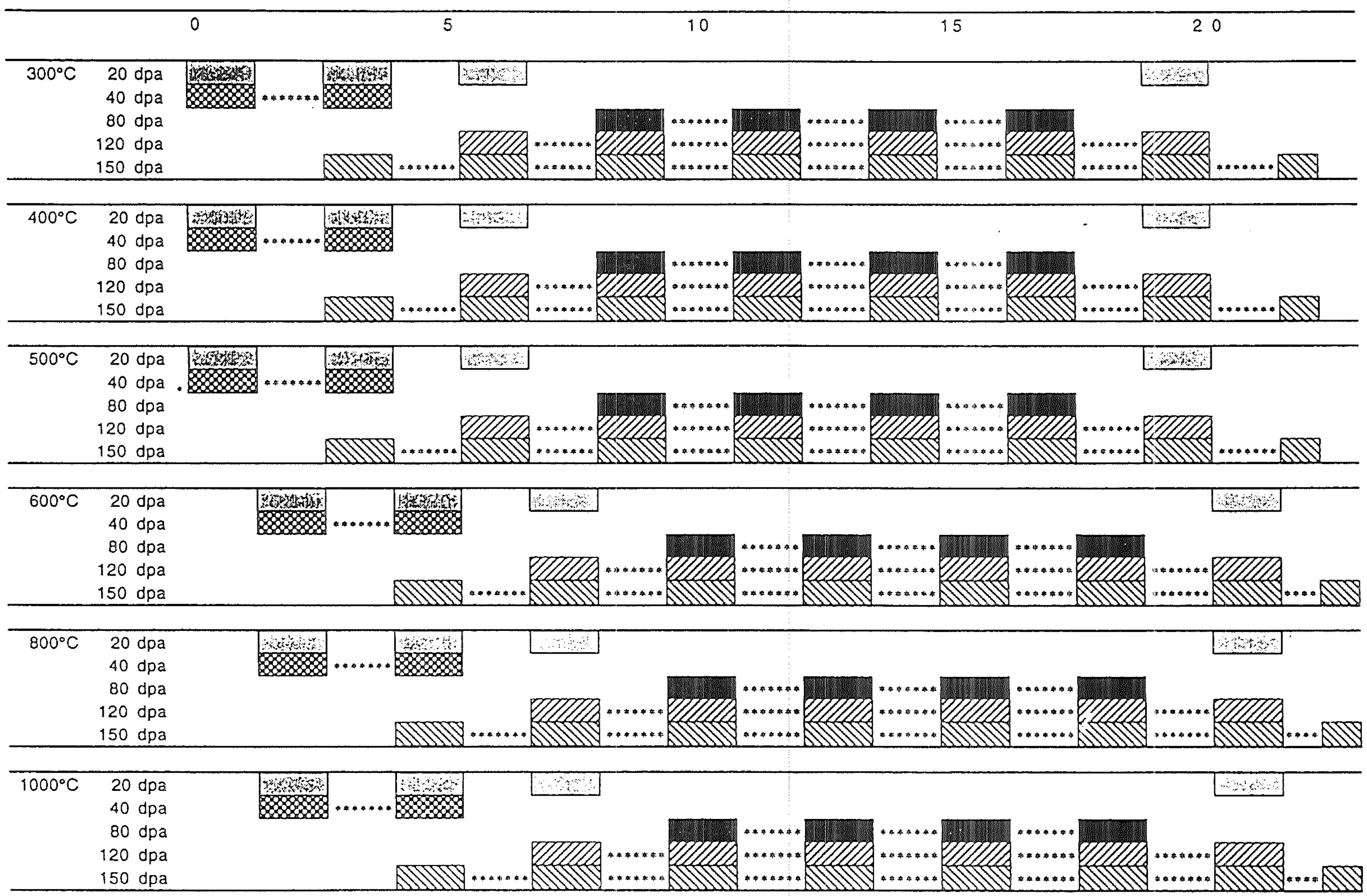

Table 3. Volume of Specimens and Specimen Packets

Properties	Geometry (dimensions in mm)	Specimen Volume (cm^3)	Packet Configuration* (cm) [cross-section area, cm^2]	No. of Specimens per Packet	Packet Volume** (cm^3)
Microstructure	TEM disk (3 diam. x 0.25 t)	0.0018	0.4 diam x 2.5 [1.00]	≤80	0.4
Tensile	SS-3 (25 x 4.8x 0.76)	0.091	0.55 x 0.7 x 3.0 [2.10]	4	1.16
Fatigue	SF-1 hourglass (25 x 4.8 x 1.52)	0.18	0.55 x 0.7 x 3.0 [2.10]	2	1.16
Fracture toughness	0.18 DCT (12.5 diam. x 4.6 t)	0.57	0.6 x 1.5 x 3.0 [1.80]	2	2.7
Crack Growth	0.09 DCT (12.5 diam. x 2.3 t)	0.28	0.7 x 1.5 x 3.0 [2.10]	4	3.15
Bend/Charpy/DFT	1/3-Charpy (3.3 x 3.3 x 25)	0.28	0.9 x1.2 x 2.85 [2.56]	6	3.08
Creep	0.7-Pressurized Tube (25 x 2.5 diam.)	0.13	0.4 diam x 2.85 [1.14]	1	0.36

* Dimensions were determined according to standard packing arrangements used for fission neutron irradiation capsules (see accompanying text)

** Includes space occupied by the specimen container

Properties	Number of Packets 300C/400C/500C/600C/800C/1000C (low temp. + high temp. loadings total)	Total Packet Vol. low T + high T (cm^3)	Total Number of Specimens (low temp. + high temp. loading)
Microstructure	2/4/4/4/2/2 (1st loadings: 10+8 packets)	4+3.2	up to 800+640
	3/5/5/5/3/3 (2nd loadings: 13+11 packets)	5.2+4.4	up to 1040+880
Tensile	9/15/15/10/5/5 (1st loadings: 39+20 packets)	45.2+23.2	156+80
	12/18/18/12/7/7 (2nd loadings: 48+26 packets)	55.7+30.2	192+104
Fatigue	10/20/18/18/10/10 (1st loadings: 48+38 packets)	55.7+44.1	96+76
	10/20/16/16/12/12 (2nd loadings: 46+40 packets)	53.4+46.4	92+80
Fracture toughness	7/13/13/9/5/5 (1st loadings: 33+19 packets)	89.1+51.3	66+38
	8/14/12/10/8/8 (2nd loadings: 34+26 packets)	91.8+70.2	68+52
Crack Growth	2/4/4/4/2/2 (1st loadings: 10+8 packets)	31.5+25.2	40+32
	3/5/5/5/3/3 (2nd loadings: 13+11 packets)	41.0+34.6	52+44
Bend/Charpy/DFT	4/8/8/8/4/4 (1st loadings: 20+16 packets)	61.6+49.3	120+96
	4/8/7/7/4/4 (2nd loadings: 19+15 packets)	58.5+46.2	114+90
Creep	20/44/40/48/20/20 (1st loadings: 104+88 packets)	37.4+31.7	104+88
	16/36/28/36/16/16 (2nd loadings: 80+68 packets)	28.8+24.5	80+68
	Totals: 1st loadings: 264+197 packets	325+228	up to 1382+1050
	2nd loadings: 253+197 packets	334+256	up to 1638+1318

Table 4. IFMIF Test Matrix / TEM disks

Materials	Dose (dpa)	Temperature (°C)	No. of specimens*	No. of packets**
FM1, FM2, FM3, SiC1, etc.	20	300	35+	1
I1, I2, I3	20 (2nd set)			1
FM1, FM2, FM3, SiC1, I1, I2, I3	40		35+	1
	80		35+	1
	120		35+	1
	150		35+	1
FM1, FM2, FM3, Van1, Van2, Van3, SiC1, etc.	20	400	50	2
I1, I2, I3	20 (2nd set)			1
	40		50	2
	80		50	2
	120		50	2
	150		50	2
FM1, FM2, FM3, Van1, Van2, Van3, SiC1, etc.	20	500	50	2
I1, I2, I3	20 (2nd set)			1
	40		50	2
	80		50	2
	120		50	2
	150		50	2
Van1, Van2, Van3, SiC1, SiC2, I3, etc.	20	600	30+	2
	20 (2nd set)			1
	40		30+	2
	80		30+	2
	120		30+	2
	150		30+	2
SiC1, SiC2, I3, etc.	20	800	15+	1
	20 (2nd set)			1
	40		15+	1
	80		15+	1
	120		15+	1
	150		15+	1
SiC1, SiC2, I3, etc.	20	1000	15+	1
	20 (2nd set)			1
	40		15+	1
	80		15+	1
	120		15+	1
	150		15+	1

* Multiplicity ≥ 5. Additional alloys may also be irradiated in these capsules, assuming they have chemical compatibility with the main candidate materials.
** Each packet will contain up to 50 specimens of the same alloy class (or otherwise compatible materials). Inert refractory TEM disks will be used to separate different materials. Vanadium alloys will be packaged separate from other materials.

Total number of packets —
Total Packet Vol. (cm^3) —

Table 5. IFMIF Test Matrix / SS-3 Sheet Tensile specimen				
Materials	Dose (dpa)	Temperature (°C)	No. of specimens*	No. of packets**
FM1, FM2, FM3	20	300	12	3
I1, I2, SiC1	20 (2nd set)		12	3
FM1, FM2, FM3, I1, I2, SiC1	40		24	6
FM1, FM2, I1, SiC1	80		16	4
FM1, FM2	120		12	3
FM1, FM2	150		12	3
FM1, FM2, FM3, Van1, Van2, Van3	20	400	24	6
I1, I2, SiC1	20 (2nd set)		12	3
FM1, FM2, FM3, Van1, Van2, Van3, I1, I2, SiC1	40		36	9
FM1, FM2, Van1, Van2, I1, SiC1	80		24	6
FM1, FM2, Van1, Van2	120		24	6
FM1, FM2, Van1, Van2	150		24	6
FM1, FM2, FM3, Van1, Van2, Van3	20	500	24	6
I1, I2, SiC1	20 (2nd set)		12	3
FM1, FM2, FM3, Van1, Van2, Van3, I1, I2, SiC1	40		36	9
FM1, FM2, Van1, Van2, I1, SiC1	80		24	6
FM1, FM2, Van1, Van2	120		24	6
FM1, FM2, Van1, Van2	150		24	6
Van1, Van2, Van3, SiC1, SiC2	20	600	20	5
I3	20 (2nd set)		4	1
Van1, Van2, Van3, SiC1, SiC2, I3	40		20	5
Van1, Van2, SiC1, SiC2, I3	80		20	5
Van1, Van2, SiC1, SiC2	120		24	6
Van1, Van2, SiC1, SiC2	150		24	6
SiC1, SiC2	20	800	8	2
I3	20 (2nd set)		4	1
SiC1, SiC2, I3	40		12	3
SiC1, SiC2, I3	80		12	3
SiC1, SiC2	120		12	3
SiC1, SiC2	150		12	3
SiC1, SiC2	20	1000	8	2
I3	20 (2nd set)		4	1
SiC1, SiC2, I3	40		12	3
SiC1, SiC2, I3	80		12	3
SiC1, SiC2	120		12	3
SiC1, SiC2	150		12	3

* Multiplicity = 4 at low ($\leq$80 dpa) doses and 6 at high doses (duplicate specimens tested at different temperatures or strain rates); multiplicity =2 to 3 for SiC specimens (these specimens have twice the normal SS-3 thickness)
** Each packet will contain 4 specimens of the same alloy class

Total number of packets —
Total Packet Vol. (cm^3) —

Table 6. IFMIF Test Matrix / SF-1 push-pull fatigue specimens				
Materials	Dose (dpa)	Temperature (°C)	No. of specimens*	No. of packets**
FM1, FM2	20	300	8	4
I1	20 (2nd set)		4	2
FM1, FM2, I1	40		12	6
FM1, FM2, I1	80		12	6
FM1	120		4	2
FM1	150		4	2
FM1, FM2, Van1, Van2	20	400	16	8
I1, SiC1	20 (2nd set)		8	4
FM1, FM2, Van1, Van2, I1, SiC1	40		24	12
FM1, FM2, Van1, Van2, I1, SiC1	80		24	12
FM1, Van1	120		8	4
FM1, Van1	150		8	4
FM1, FM2, Van1, Van2	20	500	16	8
I1	20 (2nd set)		4	2
FM1, FM2, Van1, Van2, I1	40		20	10
FM1, FM2, Van1, Van2, I1	80		20	10
FM1, Van1	120		8	4
FM1, Van1	150		8	4
Van1, Van2, SiC1, SiC2	20	600	16	8
I3	20 (2nd set)		4	2
Van1, Van2, SiC1, SiC2, I3	40		20	10
Van1, Van2, SiC1, SiC2, I3	80		20	10
Van1, SiC1, SiC2	120		12	6
Van1, SiC1	150		8	4
SiC1, SiC2	20	800	8	4
I3	20 (2nd set)		4	2
SiC1, SiC2, I3	40		12	6
SiC1, SiC2, I3	80		12	6
SiC1, SiC2	120		8	4
SiC1, SiC2	150		8	4
SiC1, SiC2	20	1000	8	4
I3	20 (2nd set)		4	2
SiC1, SiC2, I3	40		12	6
SiC1, SiC2, I3	80		12	6
SiC1, SiC2	120		8	4
SiC1, SiC2	150		8	4

* Multiplicity = 4 (4 specimens tested at different strain ranges for each irradiation condition to roughly determine the fatigue curve)
** Each packet will contain 2 specimens of the same alloy class.

Total number of packets —
Total Packet Vol. (cm^3) —

Table 7. IFMIF Test Matrix / Disc Compact Tension Fracture Toughness specimens

Materials	Dose (dpa)	Temperature (°C)	No. of specimens*	No. of packets**
FM1, FM2	20	300	6	3
I1	20 (2nd set)		2	1
FM1, FM2, I1	40		8	4
FM1, FM2, I1	80		8	4
FM1	120		6	3
FM1	150		6	3
FM1, FM2, Van1, Van2	20	400	12	6
I1, SiC1	20 (2nd set)		6	3
FM1, FM2, Van1, Van2, I1	40		14	7
FM1, FM2, Van1, Van2, I1	80		14	7
FM1, Van1	120		8	4
FM1, Van1	150		8	4
FM1, FM2, Van1, Van2	20	500	12	6
I1	20 (2nd set)		2	1
FM1, FM2, Van1, Van2, I1	40		14	7
FM1, FM2, Van1, Van2	80		12	6
FM1, Van1	120		8	4
FM1, Van1	150		8	4
Van1, Van2, SiC1	20	600	8	4
SiC2, I3	20 (2nd set)		6	3
Van1, Van2, SiC1, SiC2	40		10	5
Van1, Van2	80		6	3
Van1, SiC1	120		4	2
Van1	150		4	2
SiC1	20	800	2	1
SiC2, I3	20 (2nd set)		6	3
SiC1, SiC2, I3	40		8	4
SiC1, I3	80		4	2
SiC1	120		2	1
SiC1	150		2	1
SiC1	20	1000	2	1
SiC2, I3	20 (2nd set)		6	3
SiC1, SiC2, I3	40		8	4
SiC1, I3	80		4	2
SiC1	120		2	1
SiC1	150		2	1

* Multiplicity = 3 (allows for testing at different temperatures and/or strain rates); multiplicity = 2 for I1, SiC alloys

** Each packet will contain 2 specimens of the same alloy class or otherwise compatible materials.

Total number of Packets —

Total Packet Vol. (cm^3) —

Table 8. IFMIF Test Matrix / Disc Compact Tension Crack Growth specimens (2.3 mm thick)				
Materials	Dose (dpa)	Temperature (°C)	No. of specimens*	No. of packets**
FM1, FM2	20	300	4	1
I1	20 (2nd set)		4	1
FM1, FM2	40		4	1
FM1, FM2	80		4	1
FM1	120		4	1
FM1	150		4	1
FM1, FM2, Van1, Van2	20	400	8	2
I1, SiC1	20 (2nd set)		4	1
FM1, FM2, Van1, Van2	40		8	2
FM1, FM2, Van1, Van2	80		8	2
FM1, Van1	120		8	2
FM1, Van1	150		8	2
FM1, FM2, Van1, Van2	20	500	8	2
I1	20 (2nd set)		4	1
FM1, FM2, Van1, Van2	40		8	2
FM1, FM2, Van1, Van2	80		8	2
FM1, Van1	120		8	2
FM1, Van1	150		8	2
Van1, Van2, SiC1, SiC2	20	600	8	2
I3	20 (2nd set)		4	1
Van1, Van2, SiC1, SiC2	40		8	2
Van1, Van2, SiC1, SiC2	80		8	2
Van1, SiC1	120		8	2
Van1, SiC1	150		8	2
SiC1, SiC2	20	800	4	1
I3	20 (2nd set)		4	1
SiC1, SiC2	40		4	1
SiC1, SiC2	80		4	1
SiC1, SiC2	120		4	1
SiC1, SiC2	150		4	1
SiC1, SiC2	20	1000	4	1
I3	20 (2nd set)		4	1
SiC1, SiC2	40		4	1
SiC1, SiC2	80		4	1
SiC1, SiC2	120		4	1
SiC1, SiC2	150		4	1

* Multiplicity = 2 (Duplicate specimens tested at each irradiation condition)
** Each packet will contain up to 4 specimens of the same alloy class.

Total number of packets	—
Total Packet Vol. (cm^3)	—

Table 9. IFMIF Test Matrix / Bend or Charpy (dynamic fracture toughness) specimens				
Materials	Dose (dpa)	Temperature (°C)	No. of specimens*	No. of packets**
FM1, FM2	20	300	12	2
I1	20 (2nd set)		6	1
FM1, FM2	40		12	2
FM1, FM2	80		12	2
FM1	120		6	1
FM1	150		6	1
FM1, FM2, Van1, Van2	20	400	24	4
I1, SiC1	20 (2nd set)		12	2
FM1, FM2, Van1, Van2, SiC1	40		24	4
FM1, FM2, Van1, Van2, SiC1	80		24	4
FM1, Van1	120		12	2
FM1, Van1	150		12	2
FM1, FM2, Van1, Van2	20	500	24	4
I1	20 (2nd set)		6	1
FM1, FM2, Van1, Van2	40		24	4
FM1, FM2, Van1, Van2	80		24	4
FM1, Van1	120		12	2
FM1, Van1	150		12	2
Van1, Van2, SiC1, SiC2	20	600	24	4
I3	20 (2nd set)		6	1
Van1, Van2, SiC1, SiC2	40		24	4
Van1, Van2, SiC1, SiC2	80		24	4
Van1, SiC1	120		12	2
Van1, SiC1	150		12	2
SiC1, SiC2	20	800	12	2
I3	20 (2nd set)		6	1
SiC1, SiC2, I3	40		12	2
SiC1, SiC2	80		12	2
SiC1, SiC2	120		12	2
SiC1	150		6	1
SiC1, SiC2	20	1000	12	2
I3	20 (2nd set)		6	1
SiC1, SiC2, I3	40		12	2
SiC1, SiC2	80		12	2
SiC1, SiC2	120		12	2
SiC1	150		4	1

* Multiplicity ≥ 4 (2 test temperatures, 2 loading rates)
** Each packet will contain up to 6 specimens of the same alloy class.

Total number of packets —
Total Packet Vol. (cm^3) —

Table 10. IFMIF Test Matrix / Pressurized Tube Irradiation Creep specimens

Materials	Dose (dpa)	Temperature (°C)	No. of specimens*	No. of packets**
FM1, FM2	20	300	12	12
I1	20 (2nd set)		4	4
FM1, FM2	40		8	8
FM1, FM2	80		8	8
FM1	120		4	4
FM1	150		4	4
FM1, FM2, Van1, Van2	20	400	24	24
I1, SiC1	20 (2nd set)		8	8
FM1, FM2, Van1, Van2, SiC1	40		20	20
FM1, FM2, Van1, Van2	80		16	16
FM1, Van1	120		8	8
FM1, Van1	150		8	8
FM1, FM2, Van1, Van2	20	500	24	24
I1	20 (2nd set)		4	4
FM1, FM2, Van1, Van2	40		16	16
FM1, FM2, Van1, Van2	80		16	16
FM1, Van1	120		8	8
FM1, Van1	150		8	8
Van1, Van2, SiC1, SiC2	20	600	24	24
I3	20 (2nd set)		4	4
Van1, Van2, SiC1, SiC2	40		24	24
Van1, Van2, SiC1, SiC2	80		16	16
Van1, SiC1	120		8	8
Van1, SiC1	150		8	8
SiC1, SiC2	20	800	12	12
I3	20 (2nd set)		4	4
SiC1, SiC2	40		8	8
SiC1, SiC2	80		8	8
SiC1	120		4	4
SiC1	150		4	4
SiC1, SiC2	20	1000	12	12
I3	20 (2nd set)		4	4
SiC1, SiC2	40		8	8
SiC1, SiC2	80		8	8
SiC1	120		4	4
SiC1	150		4	4

* Multiplicity ≥ 4 (specimens loaded with 4 or more different gas pressures)

** Each packet will contain 1 specimen. The SiC/SiC specimens will contain a metal bladder insert (further analysis is required to determine if meaningful creep data can be obtain from thin-wall SiC/SiC specimens, due to the limited number of plies).

Total number of packets —

Total Packet Vol. (cm^3) —

INTRODUCTION

- The reference IFMIF design assumes that the high-flux region (>2 MW/m^2 neutron wall loading)* will have a volume of ~0.5 liter

    - IFMIF high-flux irradiation volume is comparable to typical volumes in fission reactor capsules (e.g., ~0.6 liters in HFIR removable Be positions), but many capsules can be accommodated in fission reactors

- Miniaturized specimens must be extensively used in IFMIF

    -validity of miniaturized specimen data must be established

- Development of an irradiated properties data base for DEMO will require both IFMIF and fission reactor irradiation sources

    - IFMIF will be used to test materials that have demonstrated good radiation resistance during high-dose ((>50 dpa) fission neutron irradiation

---

*1 MWa/m^2 ~ 11 dpa in Fe, V (Starfire 1st wall neutron spectrum)
The mimimum damage rate in the high flux region would be ~15 dpa/CY, assuming the reference availability of 70% for IFMIF

The three leading US candidates for the 1st wall/blanket structure of DEMO are ferritic/martensitic steels, vanadium alloys, and SiC/SiC composites

- Each of these materials have a different range of operating temperatures

    - 300 to 500°C for ferritic/martensitic steel
    - 400 to 650°C for vanadium alloys
    - 600 to 1000°C for SiC/SiC composites (He coolant)

- An adequate assessment of these three materials requires a minimum of 6 irradiation temperatures (300, 400, 500, 600, 800, 1000°C)

- The proposed operation scheme for the high-flux region of IFMIF utilizes alternating "low-temperature" (300-500°C) and "high-temperature" (600-1000°C) campaigns

    - Irradiation campaigns are conducted in 10 to 20 dpa segments

    - test assemblies are inspected/replaced during the out cycles, and some of the irradiated specimens are tested (remainder are re-encapsulated)

    - Achievement of DEMO-relevant lifetime doses of ~150 dpa will require a facility lifetime of more than 20 years (40 year plant lifetime desirable)

KEY MATERIAL PROPERTIES CAN BE EXAMINED USING MINIATURIZED SPECIMENS

- Tensile properties (sheet tensile specimen)
- Push-pull fatigue properties (miniature hourglass specimen)
- Fracture toughness (disk compact tension specimen)
- Fatigue crack growth parameters (disk compact tension specimen)
- Dynamic fracture toughness/ flexural strength (notched bar)
- Irradiation creep (pressurized tube)
- Microstructural stability (TEM disk)

- Typically ~800 TEM disks and 400-600 specimens of the remaining geometries would be irradiated in each campaign in the high-flux region

  (note: FMIT high-flux matrix contained 4,450 specimens, with 3290 TEM disks and 1040 mini-tensiles)

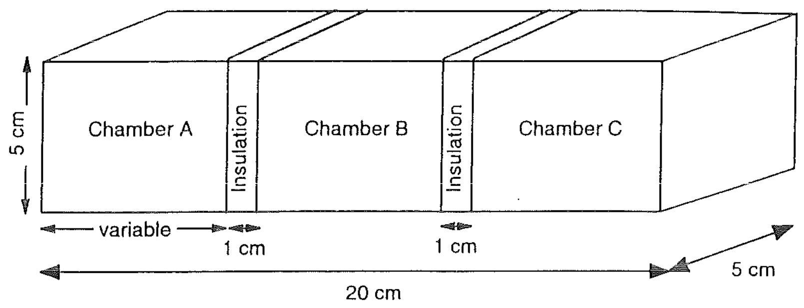

Fig. 1. Proposed reference 3-chamber geometry for high flux region of the IFMIF test cell

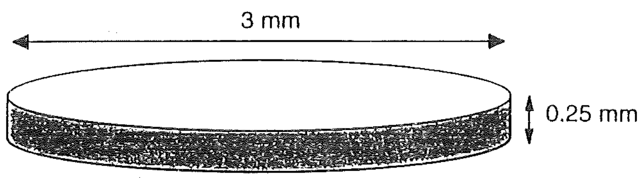

Fig. 2. Transmission electron microscopy disk

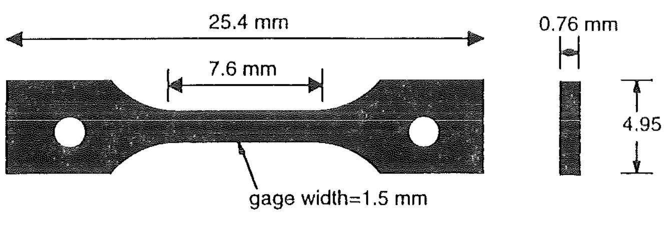

Fig. 3. SS-3 miniature sheet tensile specimen

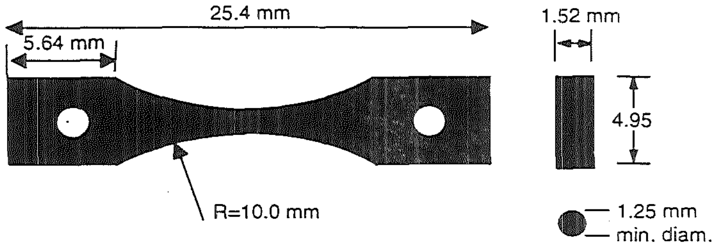

Fig. 4. SF-1 miniature push-pull fatigue specimen (hourglass gage region and sheet end tab regions)

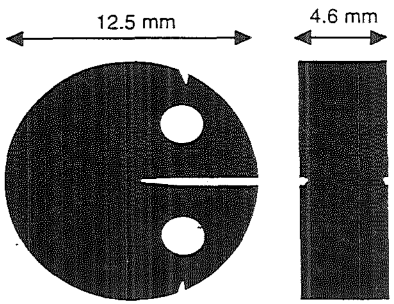

Fig. 5. Mini (0.18T) Disk Compact Tension Fracture Toughness Specimen

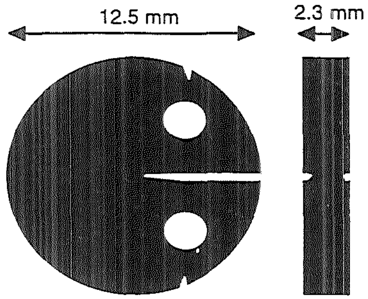

Fig. 6. Mini (0.09T) Disk Compact Tension Crack Growth Specimen

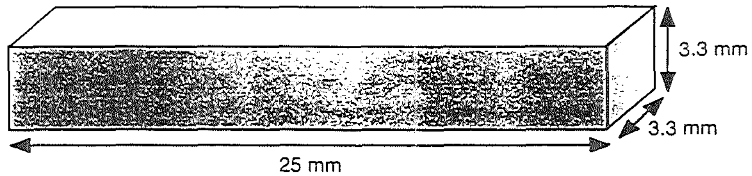

Figure 7. Charpy/bend bar/dynamic fracture toughness specimens (V-notch not shown for Charpy bars).

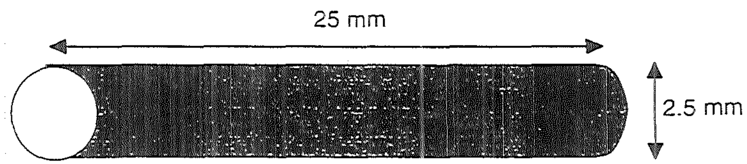

Fig. 8. Pressurized irradiation creep tube (0.25 mm wall thickness).

SUMMARY OF PROPOSED REFERENCE HIGH-FLUX SPECIMEN MATRIX

Property	Multiplicity at each irrad. condition	Volume occupied* (cm^3)	% of total volume
Microstructure/ swelling	≥ 5	0.025	0.2%
Tensile	4-6	1.2	10%
Fatigue	4	2.3	18%
Fracture toughness	3	4.0	32%
Crack growth	2	1.6	13%
Bend bar/ dynamic fracture toughness	≥ 4	2.0	16%
Creep	≥ 4	1.4	11%
		Total: 12.5 cm^3	

*includes space occupied by specimen container

SPECIMEN ENCAPSULATION

- individual specimens will be encapsulated in packets to avoid possible contamination from the test cell coolant (NaK/He)

- encapsulation medium is different for the 3 materials; therefore, each packet will typically contain only specimens from the same material

  - Na (or NaK or He) for ferritic/martensitic steel
  - Li for vanadium alloys (better scavenging of impurities, e.g. oxygen)
  - He for SiC/SiC (Li attacks grain boundaries in SiC)

- the maximum packet size is restricted due to nuclear heating effects for He-filled packets

  - all packets are sized so that the maximum temperature difference between the specimens and the packet wall is <10°C for He encapsulation

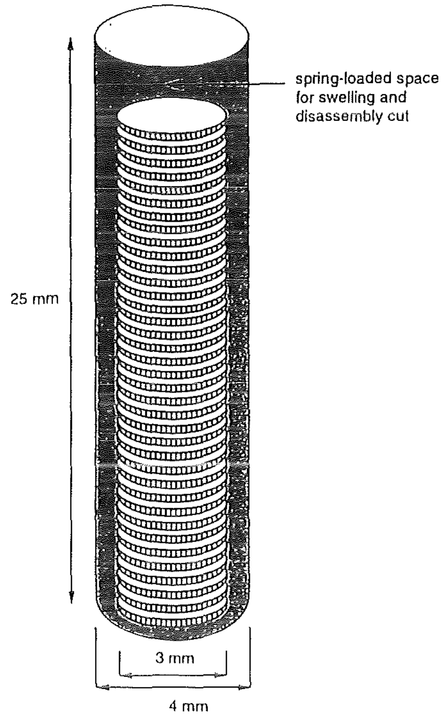

Fig. 9. TEM tube packet (up to 80 specimens per packet).

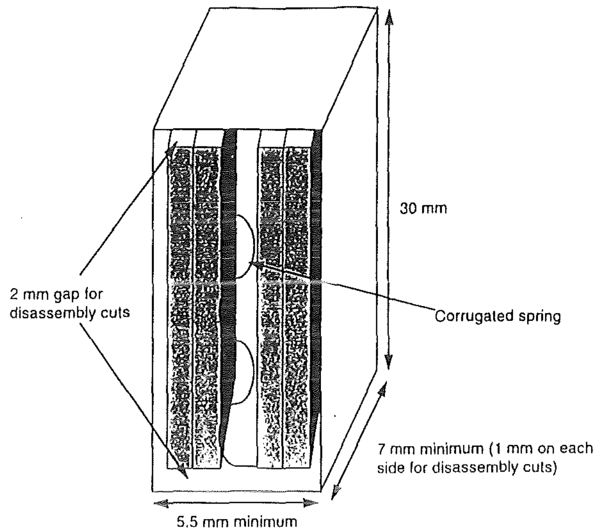

Fig. 10. SS-3 miniature sheet tensile specimen packet (4 specimens per packet). Packet wall thickness = 0.5 mm.

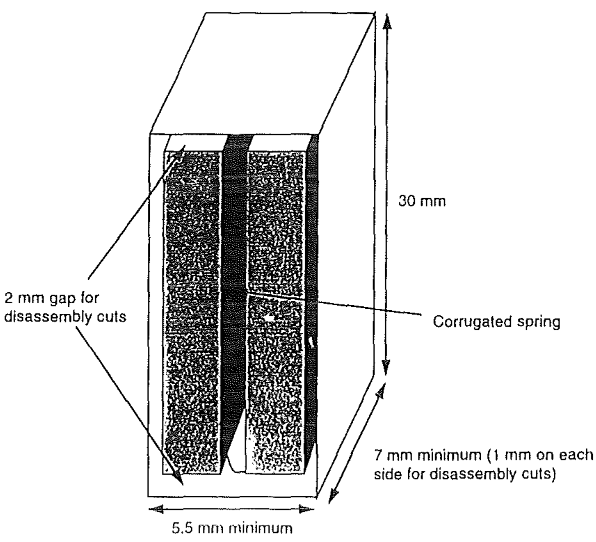

Fig. 11. Miniature SF-1 push-pull fatigue specimen packet (2 specimens per packet). Packet wall thickness = 0.5 mm.

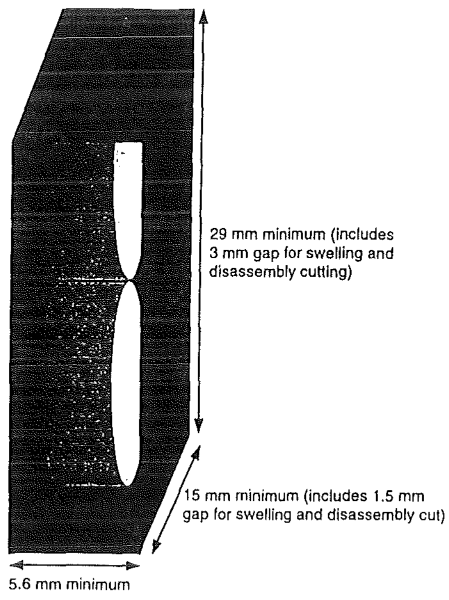

Fig. 12. Miniature (0.18T) disk compact tension specimen packet (2 specimens per packet). Packet wall thickness = 0.5 mm.

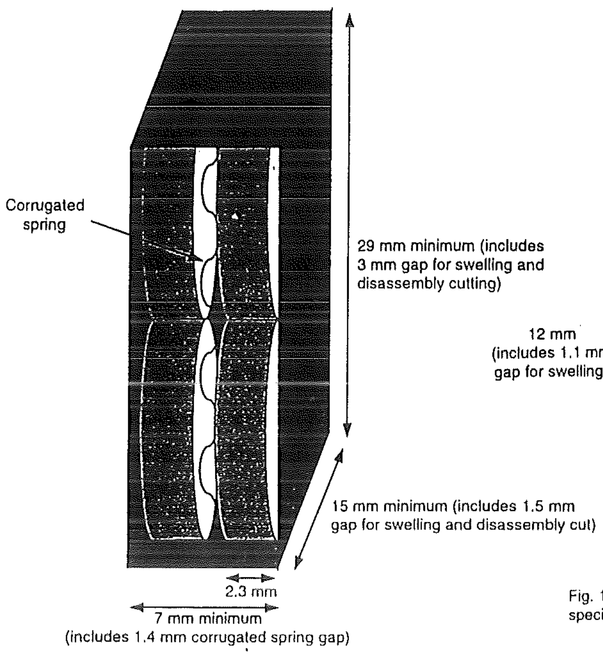

Fig. 13. Miniature (0.09T) disk compact tension specimen packet for crack growth measurements (4 specimens per packet). Packet wall thickness = 0.5 mm.

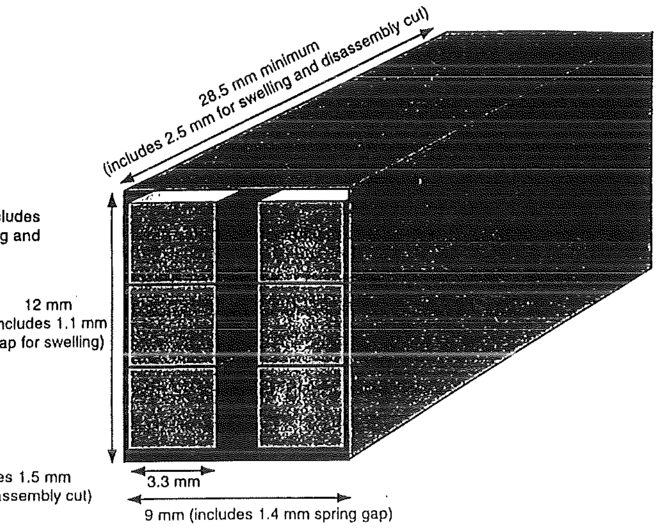

Fig. 14. Bend bar/ Charpy/ dynamic fracture toughness specimen packet (6 specimens per packet). Packet wall thickness = 0.5 mm.

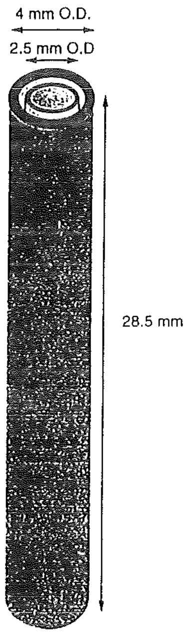

Fig. 15a. Specimen packet for pressurized creep tube (He gas option, 1 specimen per packet). The packet wall thickness is 0.5 mm and the He gas gap between the specimen and packet wall is 0.25 mm

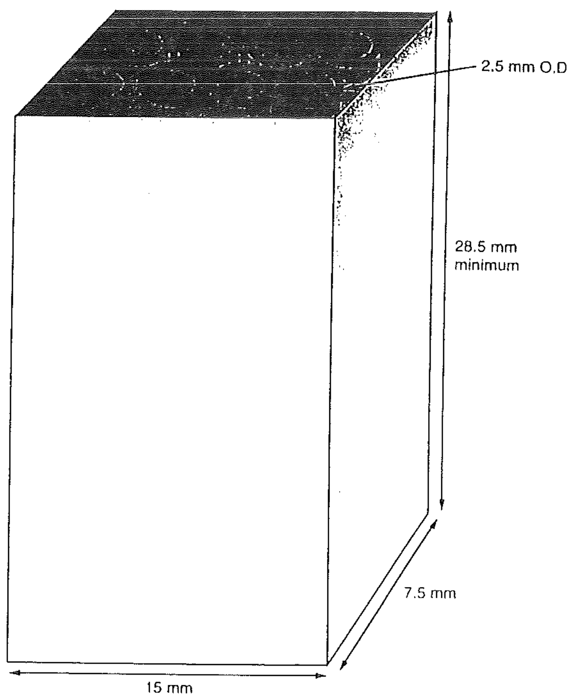

Fig. 15b. Specimen packet for pressurized creep tubes (liquid metal option, 8 tubes per packet). The packet wall thickness is 0.5 mm and the spacing between pressurized tubes is 0.5 mm

THE SPECIMEN PACKETS HAVE BEEN POSITIONED WITHIN EACH CHAMBER IN A COMPACT ARRANGEMENT 300° C, 400° C, 500° C MODULE I ST LOADING

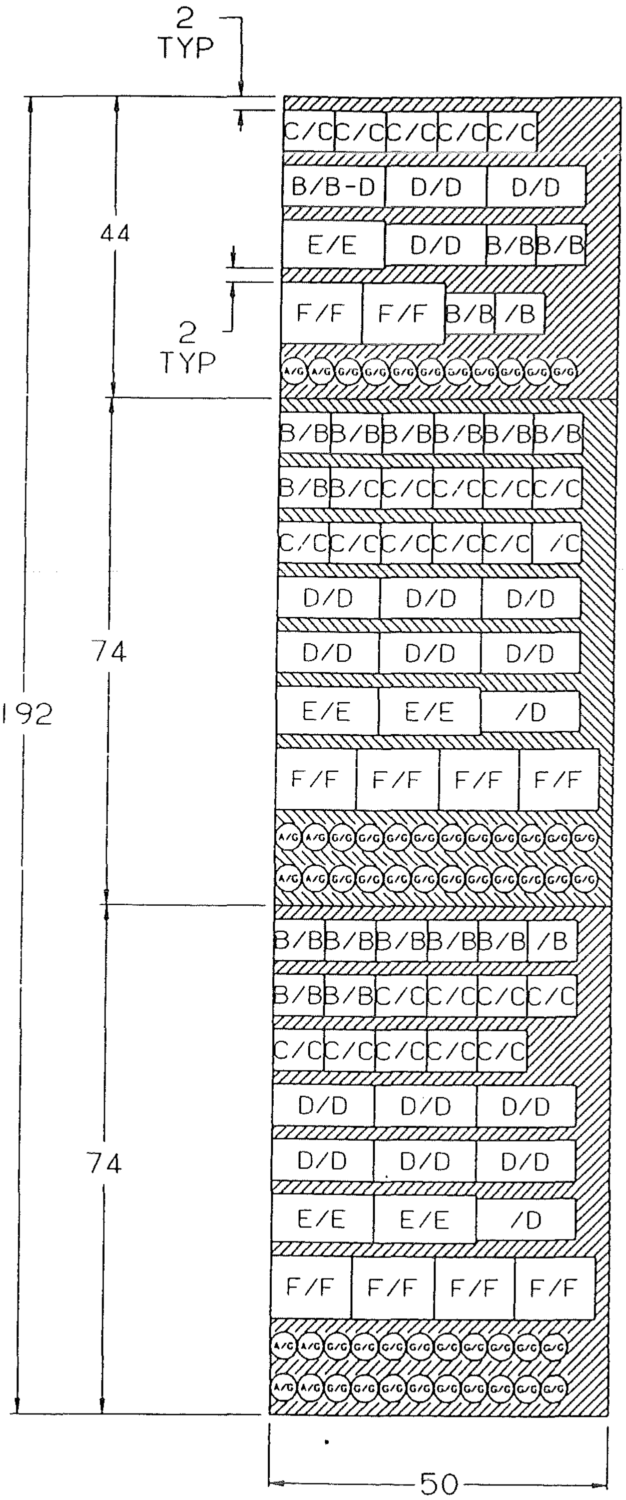

300° C

02- MICROSRTUCTURE (A)
09- TENSILE (B)
10- FATIGUE (BENDING) (C)
07- FRACTURE TOUGHNESS (D)
02- CRACK GROTH (E)
04- BEND/CHARPY/DFT (F)
20- CREEP (G)

400° C

04- MICROSRTUCTURE (A)
15- TENSILE (B)
20- FATIGUE (BENDING) (C)
13- FRACTURE TOUGHNESS (D)
04- CRACK GROTH (E)
08- BEND/CHARPY/DFT (F)
44- CREEP (G)

500° C

04- MICROSRTUCTURE (A)
15- TENSILE (B)
18- FATIGUE (BENDING) (C)
13- FRACTURE TOUGHNESS (D)
04- CRACK GROTH (E)
08- BEND/CHARPY/DFT (F)
40- CREEP (G)

THE SPECIMEN PACKETS HAVE BEEN POSITIONED WITHIN EACH CHAMBER IN A COMPACT ARRANGEMENT
300° C, 400° C, 500° C MODULE 2 ST LOADING

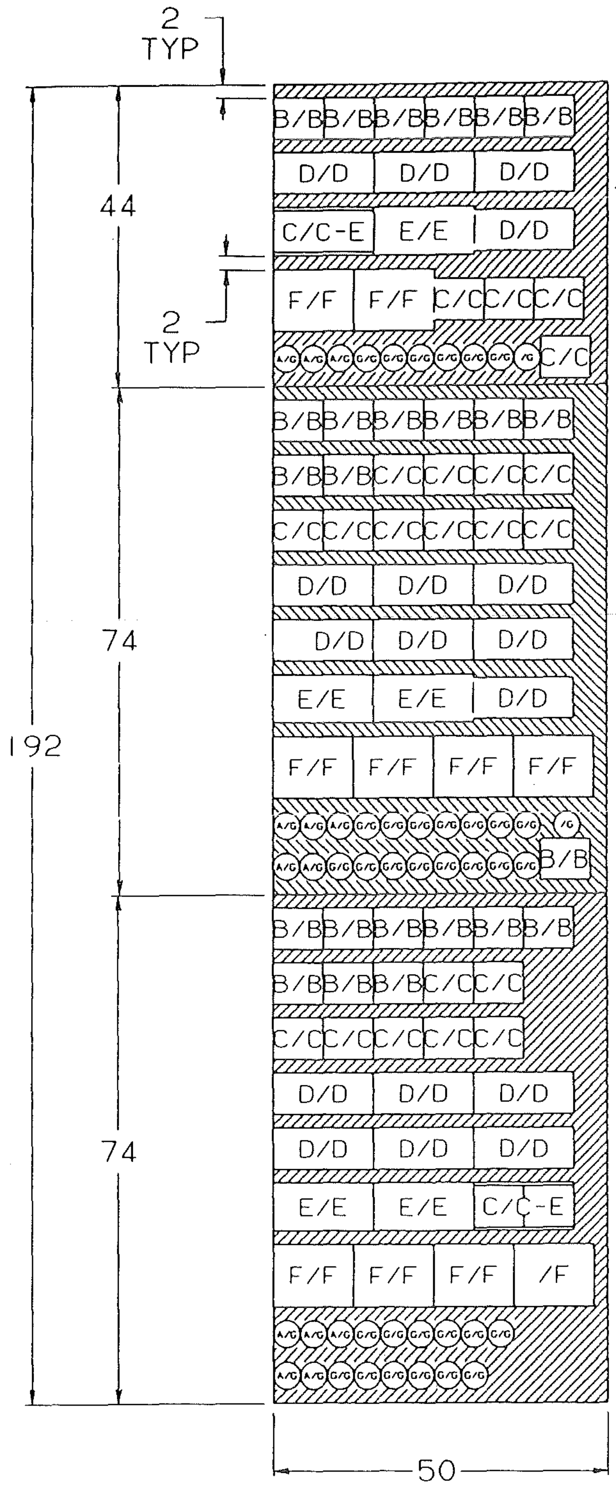

300° C

03- MICROSRTUCTURE (A)
12- TENSILE (B)
10- FATIGUE (BENDING) (C)
08- FRACTURE TOUGHNESS (D)
03- CRACK GROTH (E)
04- BEND/CHARPY/DFT (F)
16- CREEP (G)

400° C

05- MICROSRTUCTURE (A)
18- TENSILE (B)
20- FATIGUE (BENDING) (C)
14- FRACTURE TOUGHNESS (D)
05- CRACK GROTH (E)
08- BEND/CHARPY/DFT (F)
36- CREEP (G)

500° C

05- MICROSRTUCTURE (A)
18- TENSILE (B)
16- FATIGUE (BENDING) (C)
12 FRACTURE TOUGHNESS (D)
05- CRACK GROTH (E)
07- BEND/CHARPY/DFT (F)
28- CREEP (G)

THE SPECIMEN PACKETS HAVE BEEN POSITIONED WITHIN EACH CHAMBER IN A COMPACT ARRANGEMENT
600° C, 800° C, 1000° C MODULE 1 ST LOADING

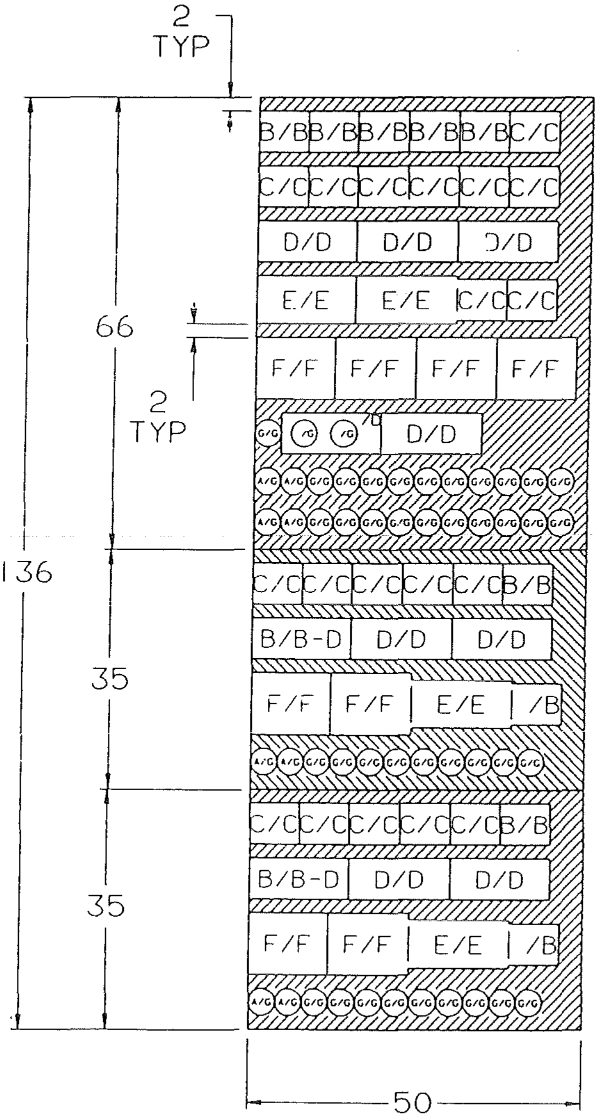

600° C

04- MICROSRTUCTURE (A)
10- TENSILE (B)
18- FATIGUE (BENDING) (C)
09- FRACTURE TOUGHNESS (D)
04- CRACK GROTH (E)
08- BEND/CHARPY/DFT (F)
48- CREEP (G)

800° C

02- MICROSRTUCTURE (A)
05- TENSILE (B)
10- FATIGUE (BENDING) (C)
05- FRACTURE TOUGHNESS (D)
02- CRACK GROTH (E)
04- BEND/CHARPY/DFT (F)
20- CREEP (G)

1000° C

02- MICROSRTUCTURE (A)
05- TENSILE (B)
10- FATIGUE (BENDING) (C)
05- FRACTURE TOUGHNESS (D)
02- CRACK GROTH (E)
04- BEND/CHARPY/DFT (F)
20- CREEP (G)

THE SPECIMEN PACKETS HAVE BEEN POSITIONED WITHIN EACH CHAMBER IN A COMPACT ARRANGEMENT 600° C, 800° C, 1000° C MODULE 2 ST LOADING

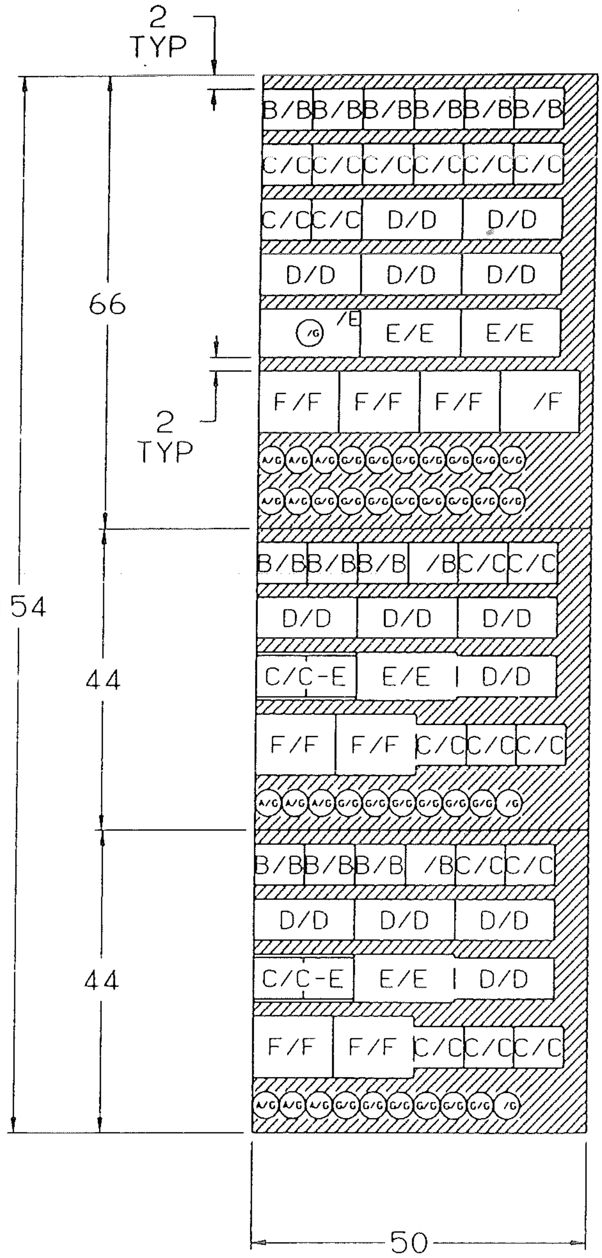

600° C

05- MICROSRTUCTURE (A)
12- TENSILE (B)
16- FATIGUE (BENDING) (C)
10- FRACTURE TOUGHNESS (D)
05- CRACK GROTH (E)
07- BEND/CHARPY/DFT (F)
36- CREEP (G)

800° C

03- MICROSRTUCTURE (A)
07- TENSILE (B)
12- FATIGUE (BENDING) (C)
08- FRACTURE TOUGHNESS (D)
03- CRACK GROTH (E)
04- BEND/CHARPY/DFT (F)
16- CREEP (G)

1000° C

03- MICROSRTUCTURE (A)
07- TENSILE (B)
12- FATIGUE (BENDING) (C)
08- FRACTURE TOUGHNESS (D)
03- CRACK GROTH (E)
04- BEND/CHARPY/DFT (F)
16- CREEP (G)

CONCLUSIONS

- A high-flux irradiation volume of ~0.5 liter is considered to be the minimum acceptable size for performing qualifying lifetime irradiation tests on materials for DEMO

  - capability for future upgrades of IFMIF should be a priority

- Flux gradients within the high-flux region should generally be less than 1%/mm (larger gradients are allowable near the periphery of the beam footprint)

- Although the primary mission for IFMIF is evaluation of irradiated materials for fusion energy applications, the US believes that consideration should be given during the design for other potential users (basic science programs, accelerator-based spallation neutron sources, etc.)

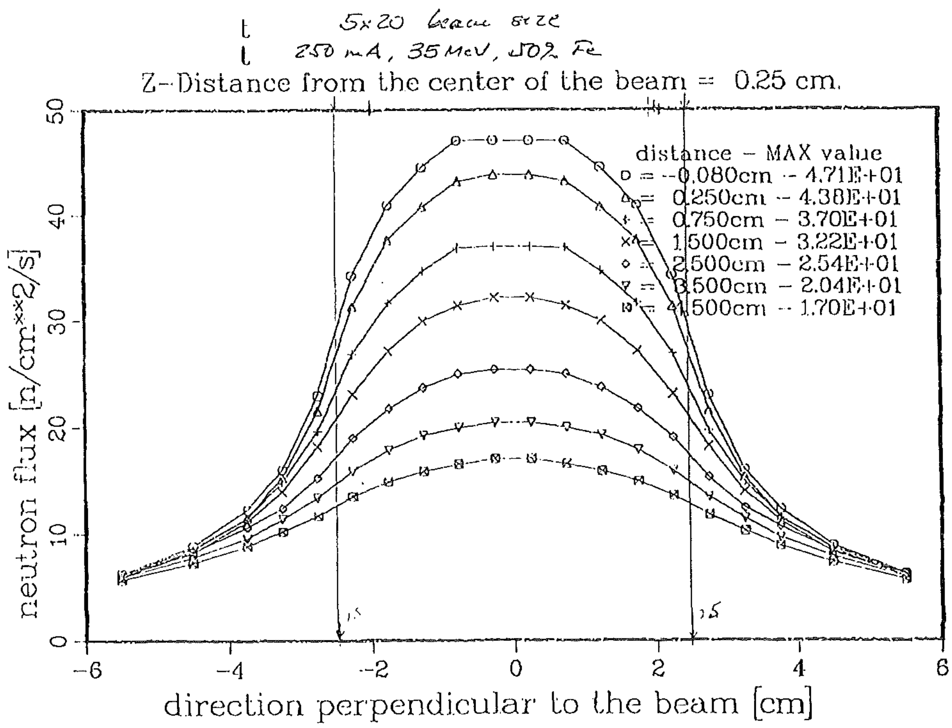

HIGH FLUX TEST SPECIMEN PACKETS

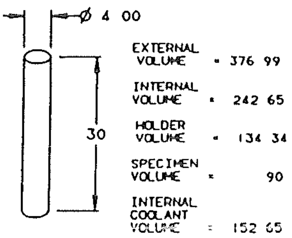

MICROSTRUCTURE
"A"

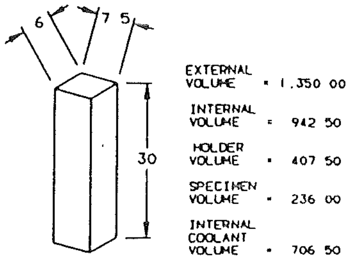

TENSILE
"B"

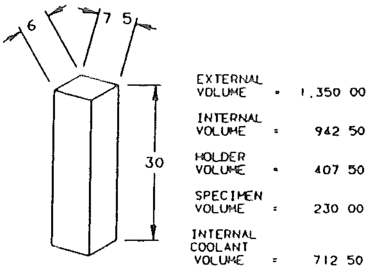

FATIGUE
(BENDING)
"C"

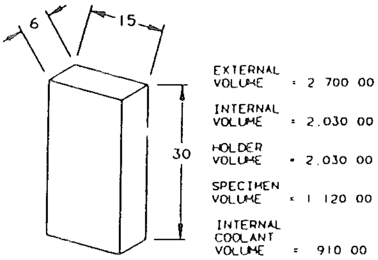

FRACTURE
TOUGHNESS
"D"

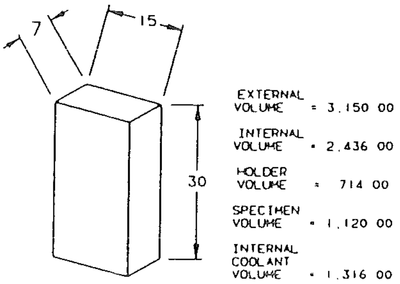

CRACK GROWTH
"E"

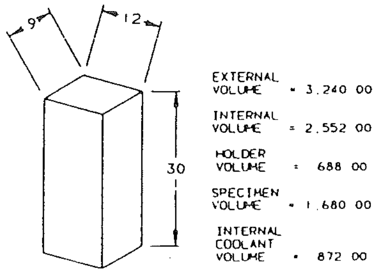

BEND/CHARPY/DFT
"F"

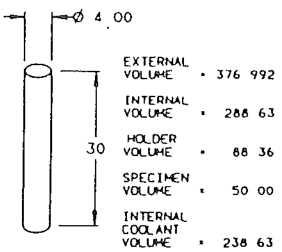

CREEP
"G"

Porter + Hudman
Trans. ANS (1980) 230

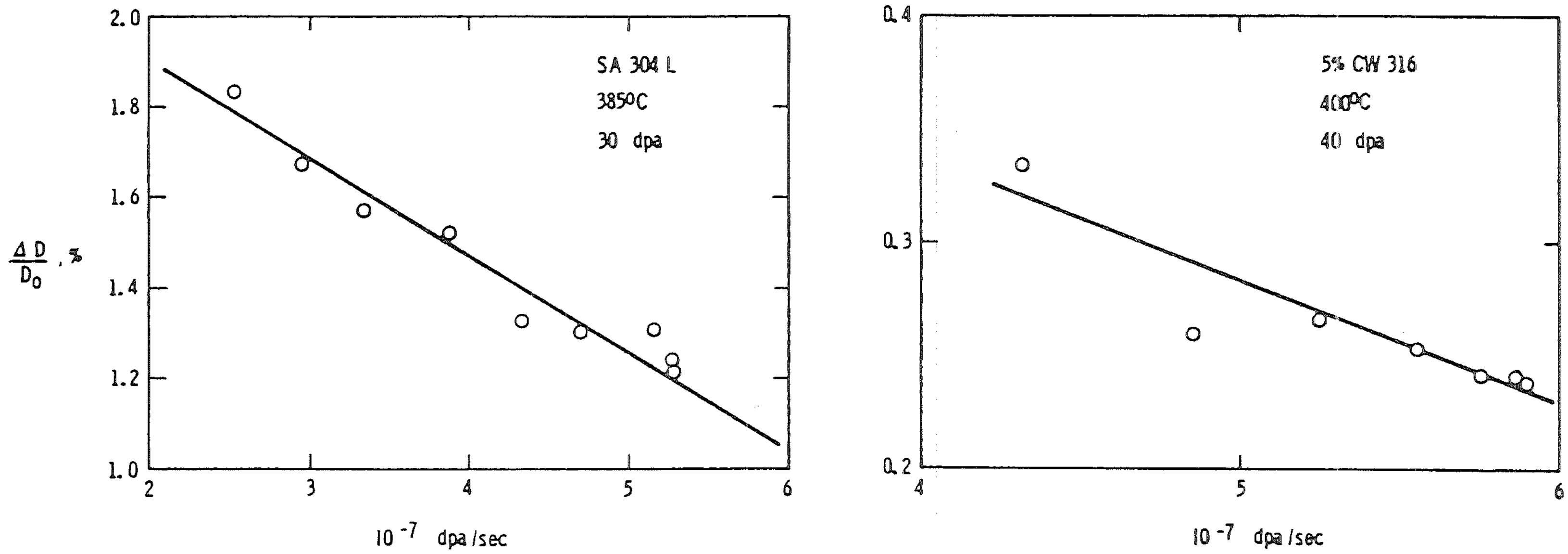

FIGURE 9. Influence of Displacement Rate on Swelling of Annealed AISI 304L and 5% Cold-Worked AISI 316 in EBR-II.[6]

Seran + Dupouy (1982)

EFFECTS OF RADIATION OF MATERIALS (11TH CONF.)

ASTM STP 782, p. 5

R1 STEEL

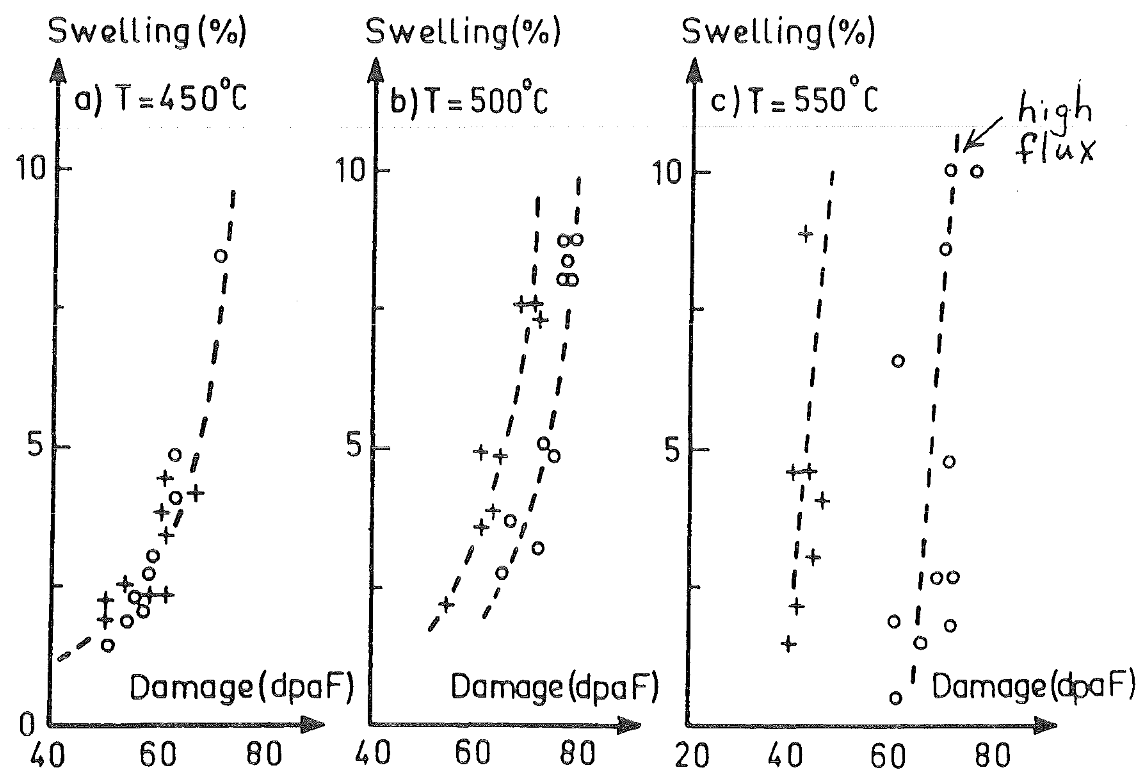

Figure 2 : Isothermal swelling of the R1 steel irradiated as central (O) or pheriphereal (+) positions in RAPSODIE core

Stoller et al.
J. Nucl. Mater 155-157 (1988)

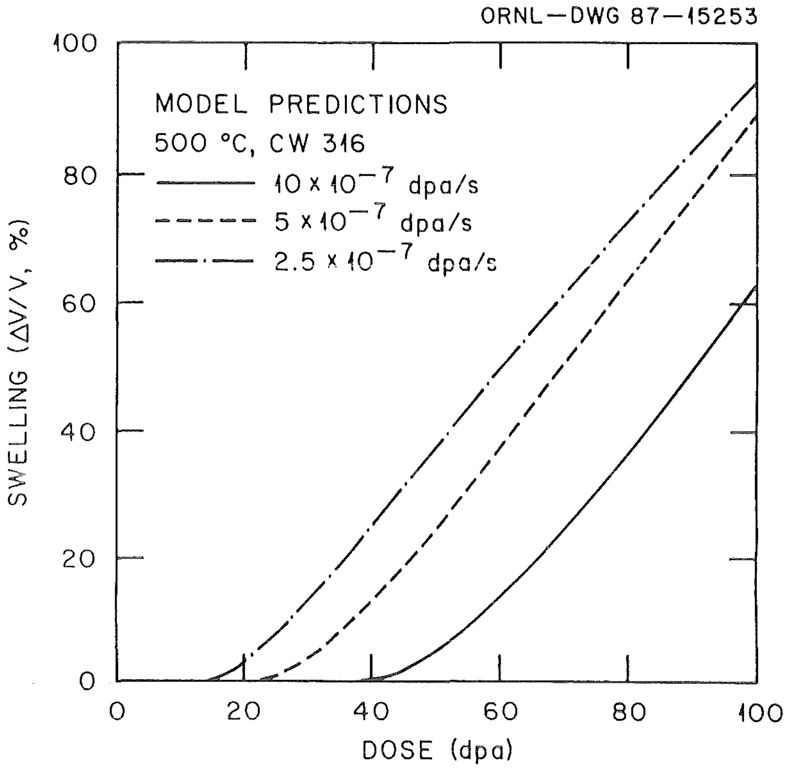

Stoller et al.
J. Nucl. Mater. 155-157 (1988)

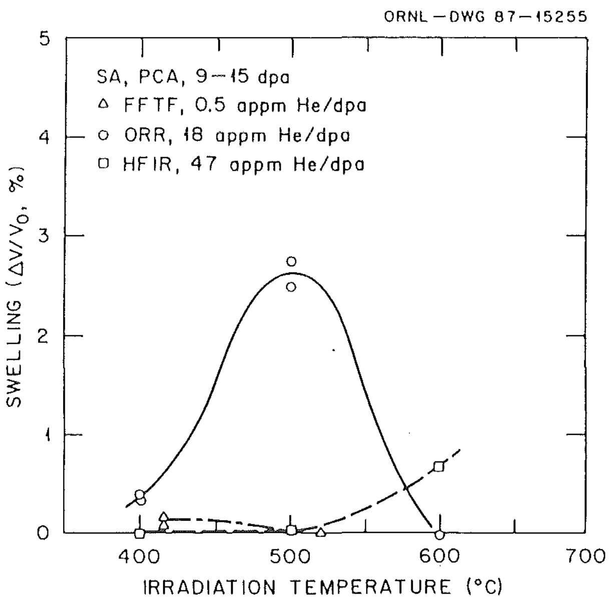

Temperature dependence of swelling observed in HFIR, FFTF and spectral tailoring experiment also indicates need for appropriate He/dpa ratio. and damage rate.

R. E. Stoller
J. Nucl. Mater. 174 (199c

Possible confounding factor, damage rate in MFE-4 was ~1/8 that in FFTF or HFIR; but,

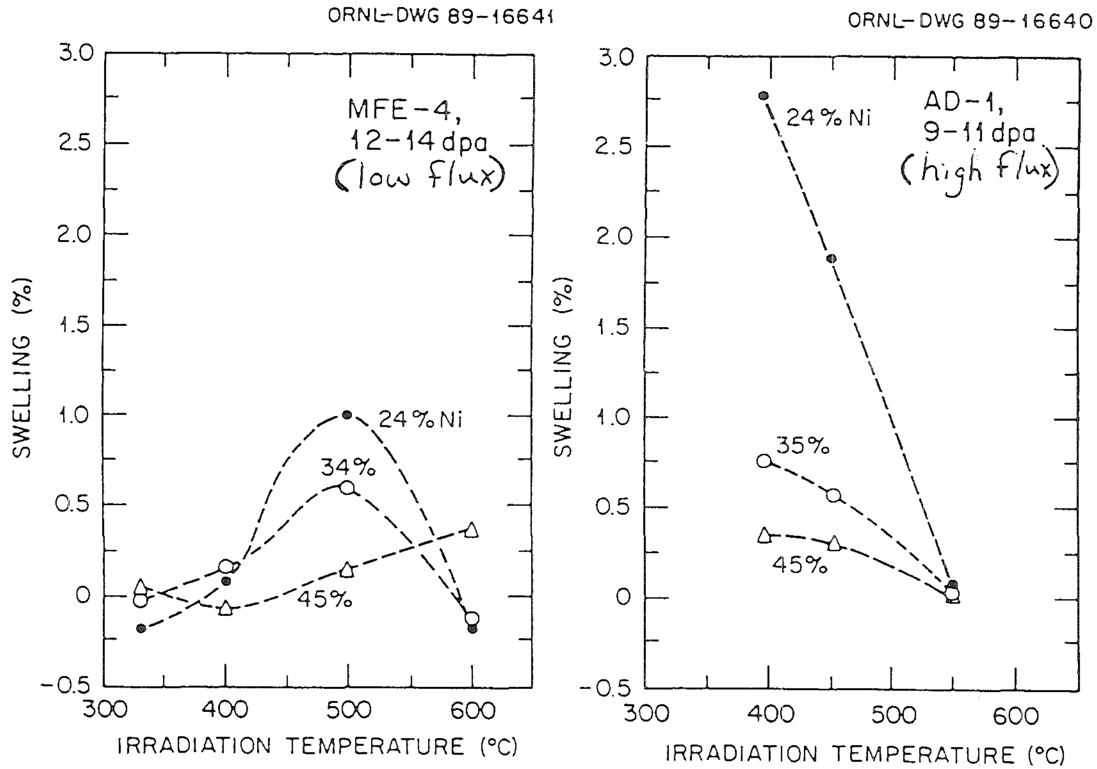

- temperature dependence of swelling change and higher loop densities observed in MFE-4 not consistent with damage rate explanation.
- similar comparison of Fe-Ni-Cr ternary alloys irradiated in MFE-4 and AD-1 (EBR-II) indicates that lower damage rate did not increase swelling (Hamilton, et al, 1989)
- higher Helium led to somewhat lower swelling and altered temperature dependence

IFMIF-CDA Test Cell/Users Task CDA-D-4

Engineering Concept for Standard Loading (Feasibility of Specimen Temperature Control)

S. Jitsukawa
IFMIF-CDA Test Cell/Users Group of JAERI

1. Introduction

Specimen temperatures can be controlled for prescribed irradiation temperatures during stable neutron beam generation. For specimen packets in CDA-D-3, cooling by flowing helium gas is available for specimen temperature control during irradiation.

Pulse operation and plasma disruption may introduce temperature change of FWB. To evaluate irradiation effect on materials including the effect by such temperature changes, it is desirable to have an ability of specimen temperature control independent from beam heating. This may be excess for irradiation experiment for materials selection, but it seems to be necessary for the irradiation tests to obtain design data base.

Temperature change during irradiation accompanied by beam intensity change or beam interruption may introduce unexpected effects on the irradiation-induced microstructural and property changes. Beam interruption for about 1 s is thought to be occurred several times per week for IFMIF. For such short beam interruption, annealing of radiation damage would not occur substantially, and the specimen temperatures should be maintained for the prescribed irradiation temperature for restarting of irradiation. Beam interruption with much longer period should to be taken into account in terms of annealing out of damage structure. For the beam interruption, ability of specimen temperature control independent from beam intensity may be required.

Allowable range of temperature change during irradiation and beam interruption has been discussed but not yet concluded. This is true for the duration allowable in terms of annealing out of radiation induced microstructure by keeping specimen temperature to an elevated temperature during longer beam interruption time. Following items may be discussed with respect to temperature control of the specimens.

(1) Allowable range of temperature fluctuation
(2) Allowable duration to prevent from annealing out of radiation effect after beam stop
(3) Ability of temperature control for simulating pulse operation and plasma disruption

Feasibility of specimen temperature control at various beam intensity levels including beam interruption condition will be examined. Major material of the test module is supposed to be austenitic stainless steel. To minimize irradiation induced degradation, the temperature may be kept below 400 C for the module structural material of austenitic stainless steel. Helium gas is selected as a heat exchanging medium. Although helium gas cooling can cause problems for vanadium alloys, it allows rather easy maintenance comparing with liquid metal as a coolant.

2. Method of temperature control and the feasibility

Ability of temperature control by flowing helium gas was estimated by numerical calculations. Specimen bundle was modeled to be semi-infinite cylinder in shape with cross sectional area corresponding to that of bundle of six tensile specimens. Specimens are located in pipes to separate two gas flow systems. Figure D4J-1 illustrates the model for the numerical calculation.

It was estimated to be feasible to control the specimen temperatures when beam heating was of about 50 W/cc. However, it was difficult to control the temperatures without beam heating (some of helium gas flows were supposed to heat the specimens to keep the specimen temperature). Figures D4J-2-1 to D4J-2-4 show the results. The temperature gradients along the helium gas flow and the temperatures of the pipes were calculated in the case of the inlet temperatures of 750 C, 350 C and 20 C for flowing gas in gas gap 2. The calculated temperature gradient for the inlet temperature of 750 C is too large. Conclusions obtained from the calculation are as follows.

(1) Because it seems rather difficult to keep temperature of the structural materials of test modules low enough to minimize radiation induced degradation, the test modules should be designed for easy exchange.
(2) Specimen packets should be arranged in the test module to make the temperature difference between adjacent specimen packets small. It may be good to arrange specimen packets into blocks for every irradiation temperature.
(3) It may be better to use beam foot print (beam spot) of smaller height.

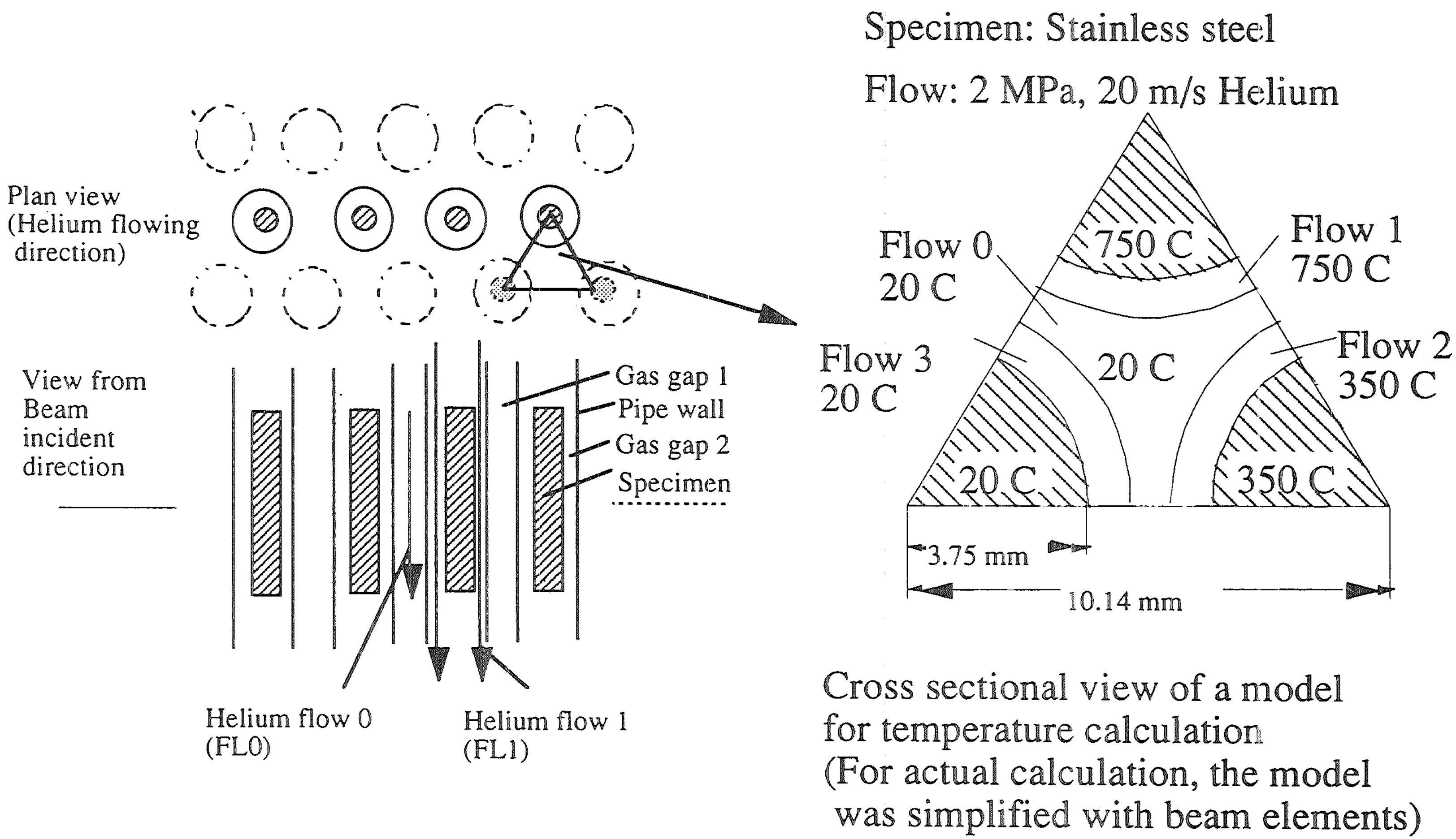

Fig. D4J-1 The model for specimen temperature calculation

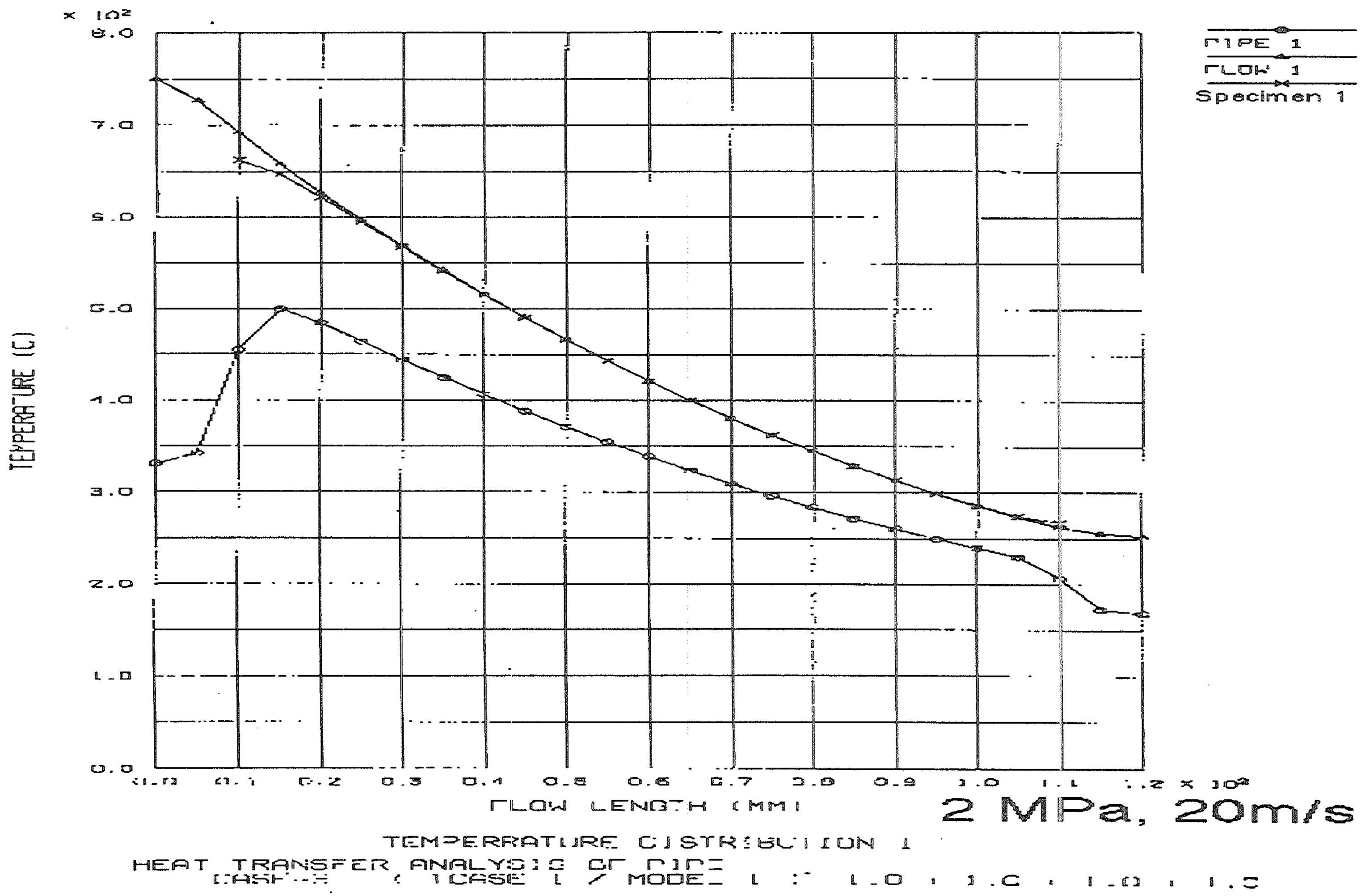

Fig.D4J-2-1Temperature distribution in the model specimen (A result of the numerical calculation)
Beam OFF, Specimen 1, Flow 1: 2MPa 20m/s Helium

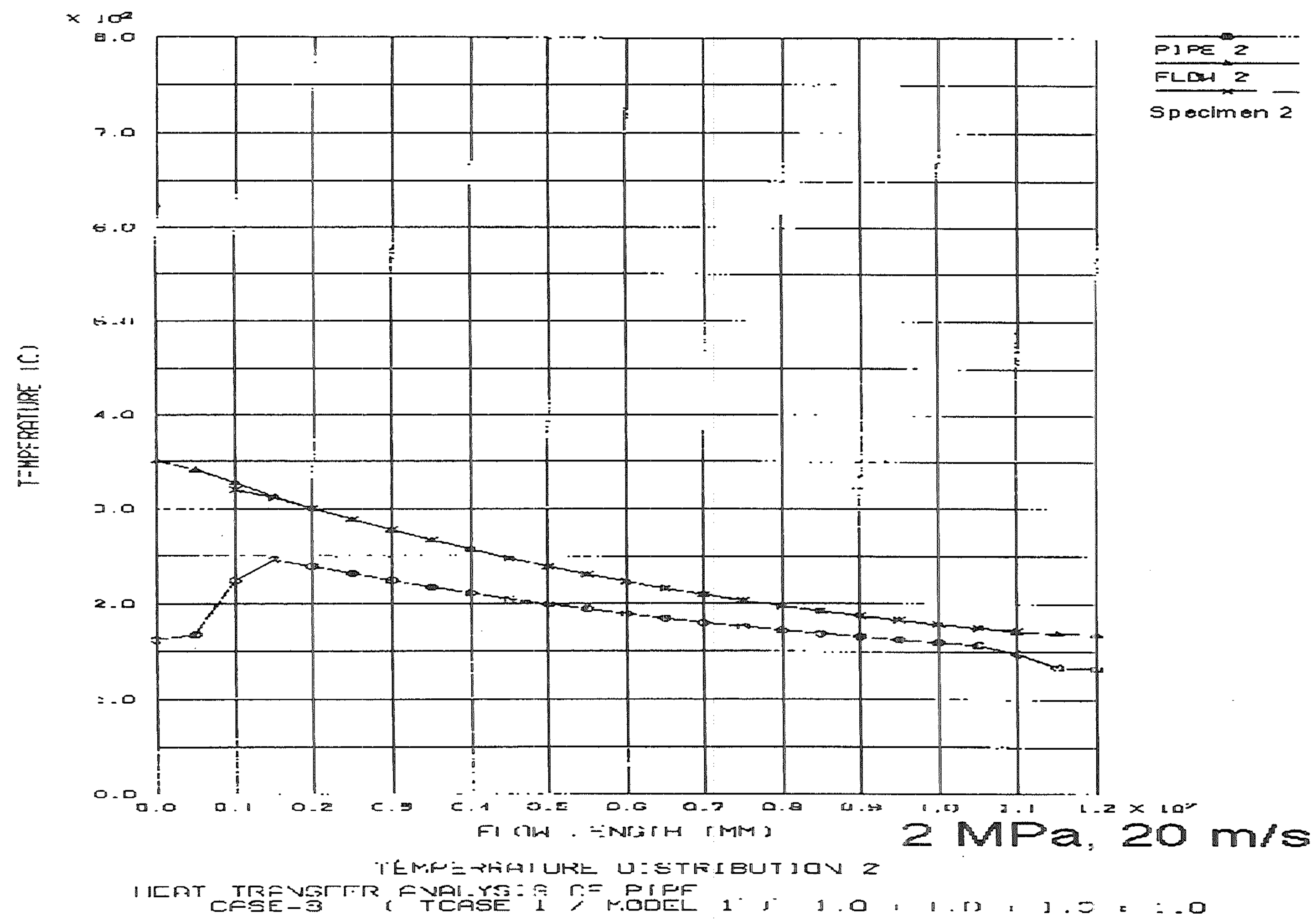

Fig.D4J-2-2Temperature distribution in the model specimen (A result of the numerical calculation)

Beam Off, Specimen 2, Flow 2: 2MPa 20m/s Helium

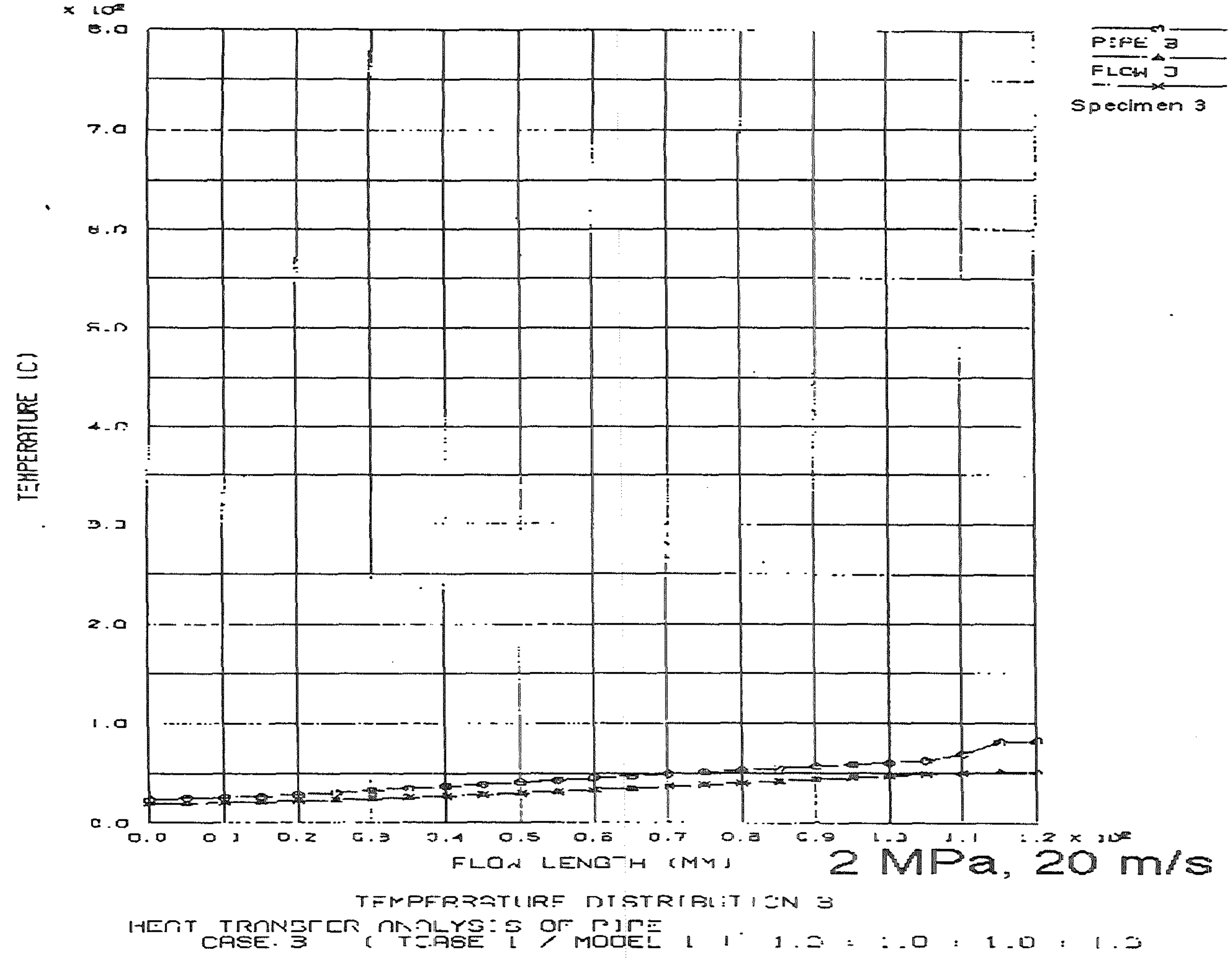

Fig.D4J-2-3Temperature distribution in the model specimen (A result of the numerical calculation)
Beam OFF, Specimen 3, Flow 3: 2MPa 20m/s Helium

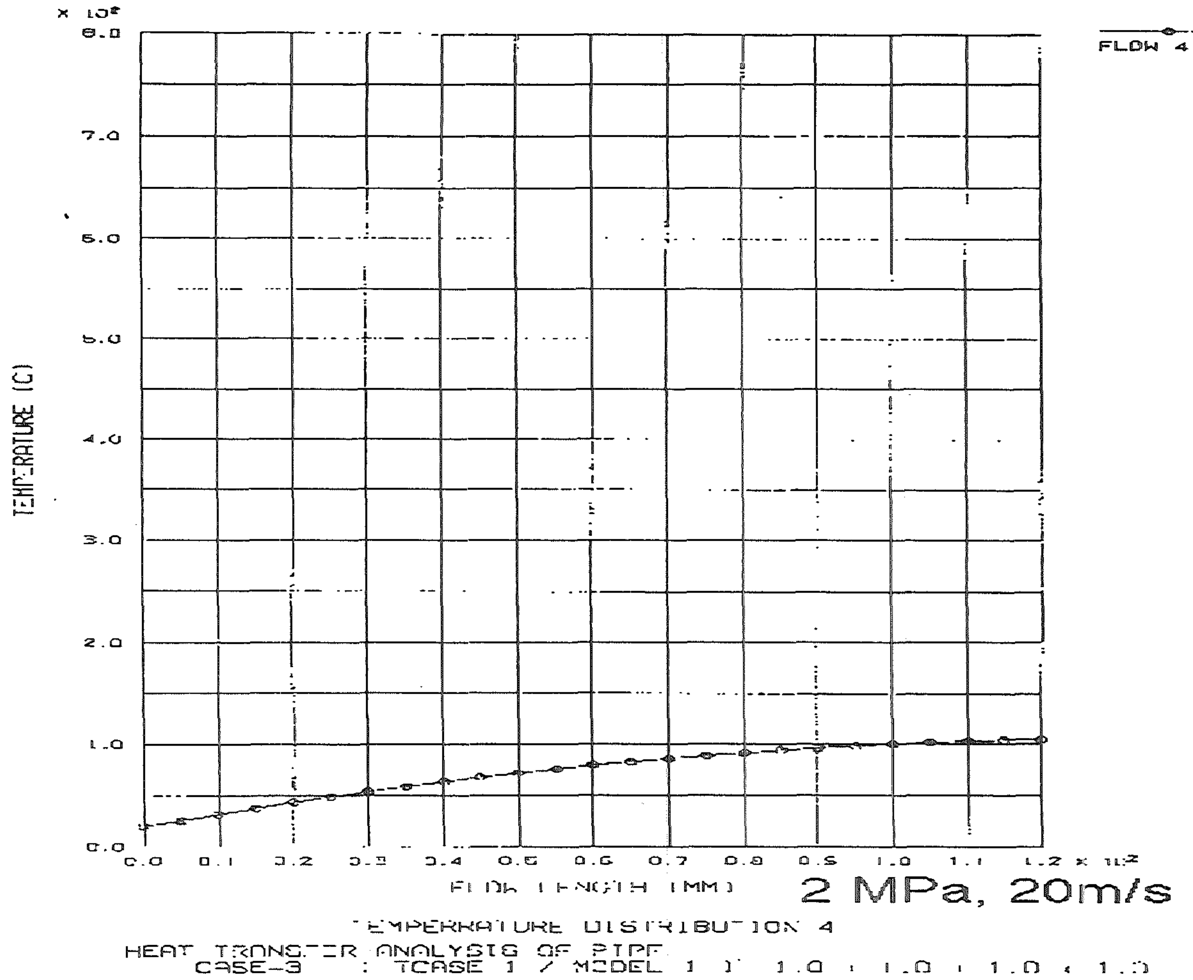

Fig.D4J-2-4Temperature distribution in the model specimen (A result of the numerical calculation)

Beam OFF, Flow 0: 2MPa 20m/s Helium

Summary (CDA-D-4)

Numerical calculation was conducted on a close packed model

Side by side specimen arrangement (with different temperature)

Helium gas as a heat exchnaging medium

Temperature control without beam intensity fluctuation

Temperature gradient along He (at high temperature) flow with zero beam heating is estimated to be considerably large.

Direct heating by electric current or electric heater may be necessary.

Task CDA-D-4: Design Concept for the High Flux Test Chambers

Presented by
J. R. Haines (ORNL)
at the
IFMIF-CDA Technical Workshop
on the Test Cell System
July 5, 1995

High Flux Test Chamber Design Topics

- Assumptions and design features
- Test specimens and holders
- Chambers
- Thermal/hydraulic performance

Assumptions / Design Parameters for High Flux Test Module Design

- Three chambers/module each operating at a different temperature
  - Low temperature module - 300°C, 400°C, 500°C
  - High temperature module - 600°C, 800°C, 1000°C
- Coolant - NaK (78% Na, 22% K)
- Low temperature chambers (≤ 600°C) constructed from HT-9 ferritic steel
- High temperature chambers constructed from Nb-1Zr
  - Requires high vacuum ($<10^{-7}$ torr) or extremely pure inert environment to prevent oxygen embrittlement

Guidelines Used for Arranging Specimen Holders in High Flux Test Module

- Depth = 50 mm, based on damage rate ~ 20 dpa/yr
- Height = 50 mm, based on beam size
- Width treated as an independent variable
  - Determined based on providing the required number/types of specimens, wall thicknesses, space for coolant and insulation between chambers

Key Issues for Test Cell Design

- Is there enough high-flux test volume?
- Dilemma: Structural material for test modules should withstand the neutron fluence for testing lifetime - but - this material will not exist (at least in the sense of being qualified) until IFMIF is operated
  - Test specimens may have to be removed periodically and installed in new modules
- Requirement for high temperature (> 650°C) tests creates major difficulties
  - Refractory material required for structure
    - Nb-1Zr alloy rapidly embrittles at these temperatures
    - Must have extremely pure inert gas environment or high vacuum
    - Vacuum barrier wall reduces neutron flux to test chambers and must be cooled
    - High activation
  - High temperature coolant line couplings must be developed
  - High pressures required to avoid boiling NaK

HIGH FLUX TEST SPECIMEN PACKETS

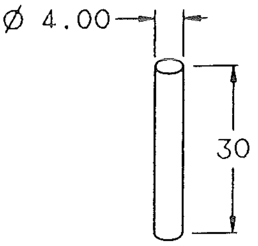

MICROSTRUCTURE
"A"

EXTERNAL VOLUME = 376.99
INTERNAL VOLUME = 242.65
HOLDER VOLUME = 134.34
SPECIMEN VOLUME = 90
INTERNAL COOLANT VOLUME = 152.65

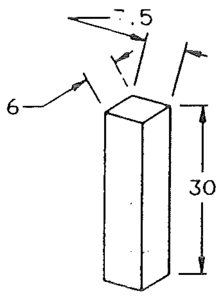

TENSILE
"B"

EXTERNAL VOLUME = 1,350.00
INTERNAL VOLUME = 942.50
HOLDER VOLUME = 407.50
SPECIMEN VOLUME = 236.00
INTERNAL COOLANT VOLUME = 706.50

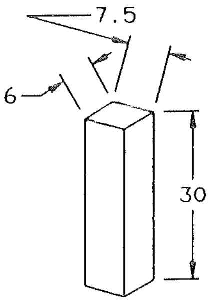

FATIGUE
(BENDING)
"C"

EXTERNAL VOLUME = 1,350.00
INTERNAL VOLUME = 942.50
HOLDER VOLUME = 407.50
SPECIMEN VOLUME = 230.00
INTERNAL COOLANT VOLUME = 712.50

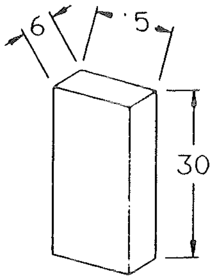

FRACTURE
TOUGHNESS
"D"

EXTERNAL VOLUME = 2,700.00
INTERNAL VOLUME = 2,030.00
HOLDER VOLUME = 2,030.00
SPECIMEN VOLUME = 1,120.00
INTERNAL COOLANT VOLUME = 910.00

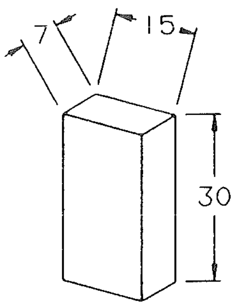

CRACK GROWTH
"E"

EXTERNAL VOLUME = 3,150.00
INTERNAL VOLUME = 2,436.00
HOLDER VOLUME = 714.00
SPECIMEN VOLUME = 1,120.00
INTERNAL COOLANT VOLUME = 1,316.00

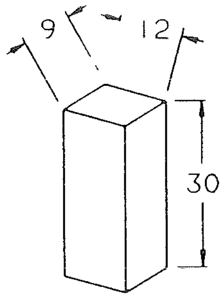

BEND CHARPY/DFT
"F"

EXTERNAL VOLUME = 3,240.00
INTERNAL VOLUME = 2,552.00
HOLDER VOLUME = 688.00
SPECIMEN VOLUME = 1,680.00
INTERNAL COOLANT VOLUME = 872.00

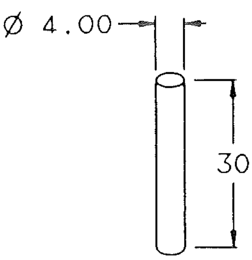

CREEP
"G"

EXTERNAL VOLUME = 376.992
INTERNAL VOLUME = 288.63
HOLDER VOLUME = 88.36
SPECIMEN VOLUME = 50.00
INTERNAL COOLANT VOLUME = 238.63

THE SPECIMEN PACKETS HAVE BEEN POSITIONED WITHIN EACH CHAMBER IN A COMPACT ARRANGEMENT 300° C,400° C,500° C MODULE I ST LOADING

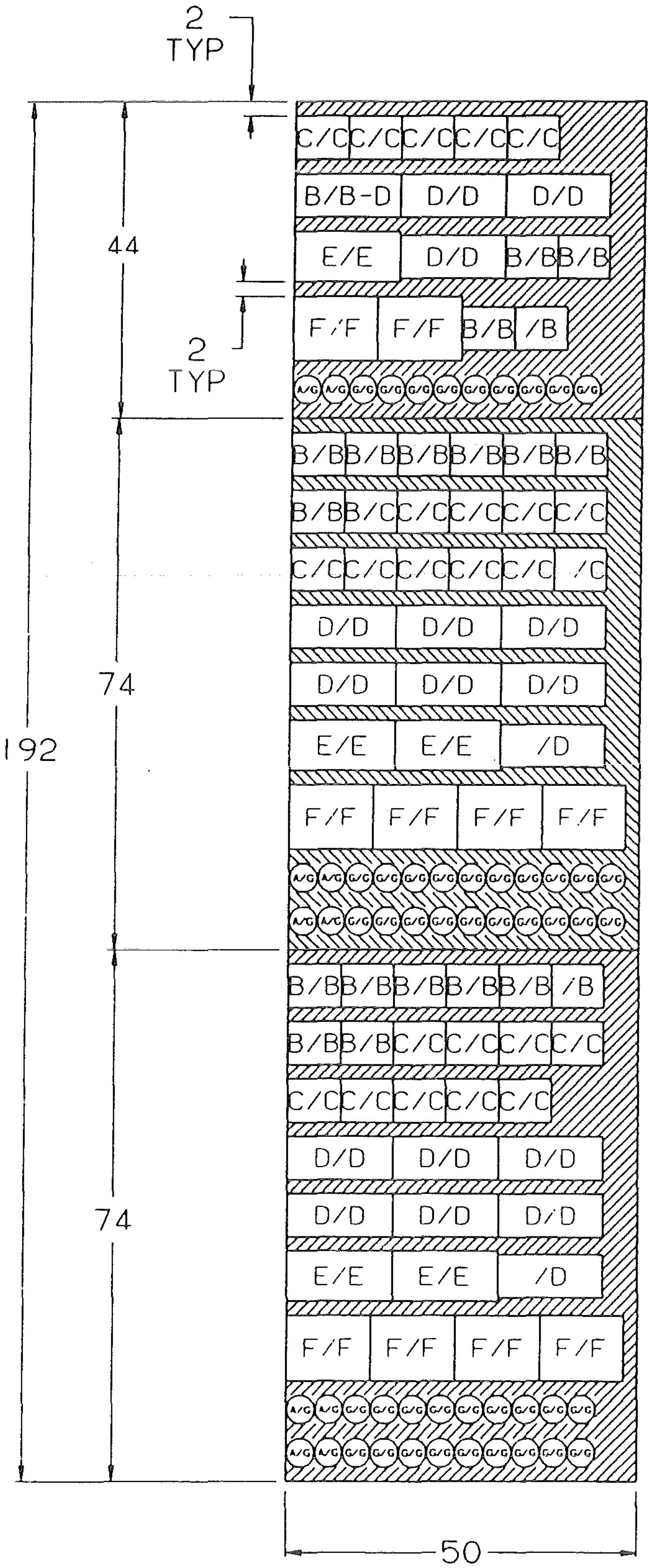

300° C

02- MICROSTRUCTURE (A)
09- TENSILE (B)
10- FATIGUE (BENDING) (C)
07- FRACTURE TOUGHNESS (D)
02- CRACK GROWTH (E)
04- BEND/CHARPY/DFT (F)
20- CREEP (G)

400° C

04- MICROSTRUCTURE (A)
15- TENSILE (B)
20- FATIGUE (BENDING) (C)
13- FRACTURE TOUGHNESS (D)
04- CRACK GROWTH (E)
08- BEND/CHARPY/DFT (F)
14- CREEP (G)

500° C

04- MICROSTRUCTURE (A)
15- TENSILE (B)
18- FATIGUE (BENDING) (C)
13- FRACTURE TOUGHNESS (D)
04- CRACK GROWTH (E)
08- BEND/CHARPY/DFT (F)
40- CREEP (G)

THE SPECIMEN PACKETS HAVE BEEN POSITIONED WITHIN EACH CHAMBER IN A COMPACT ARRANGEMENT 600° C, 800° C, 1000° C MODULE 1 ST LOADING

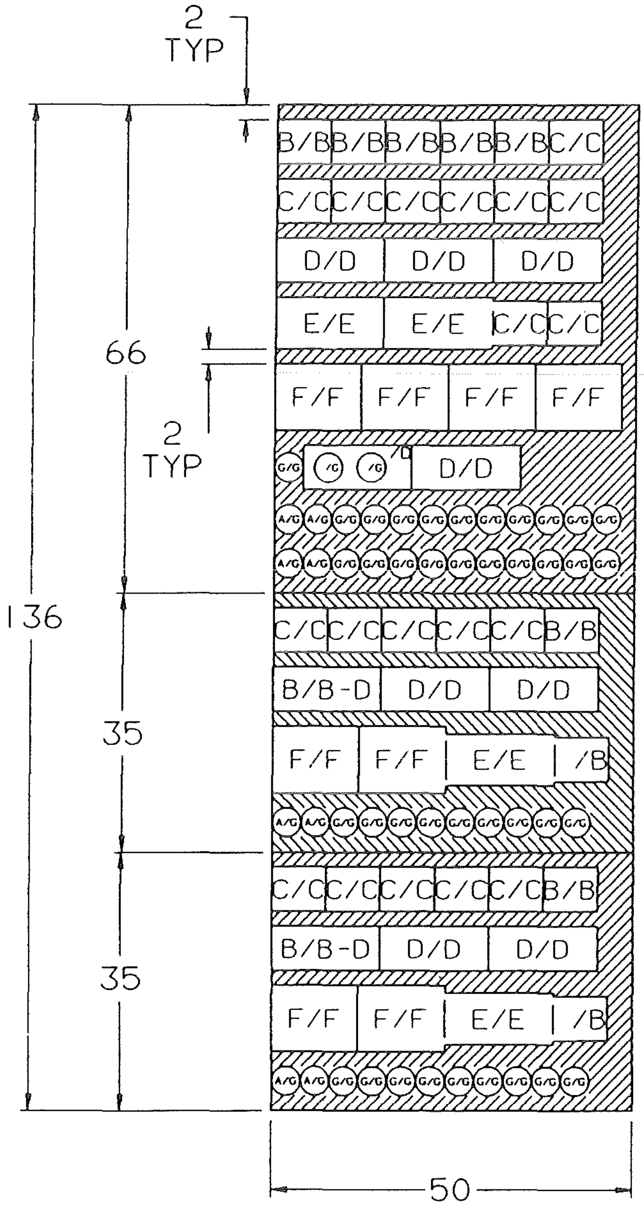

600° C

04- MICROSTRUCTURE (A)
10- TENSILE (B)
18- FATIGUE (BENDING) (C)
09- FRACTURE TOUGHNESS (D)
04- CRACK GROWTH (E)
08- BEND/CHARPY/DFT (F)
48- CREEP (G)

800° C

02- MICROSTRUCTURE (A)
05- TENSILE (B)
10- FATIGUE (BENDING) (C)
05- FRACTURE TOUGHNESS (D)
02- CRACK GROWTH (E)
04- BEND/CHARPY/DFT (F)
20- CREEP (G)

1000° C

02- MICROSTRUCTURE (A)
05- TENSILE (B)
10- FATIGUE (BENDING) (C)
05- FRACTURE TOUGHNESS (D)
02- CRACK GROWTH (E)
04- BEND/CHARPY/DFT (F)
20- CREEP (G)

THE SPECIMEN PACKETS HAVE BEEN ARRANGED IN ROWS TO ACCOMMODATE COOLING

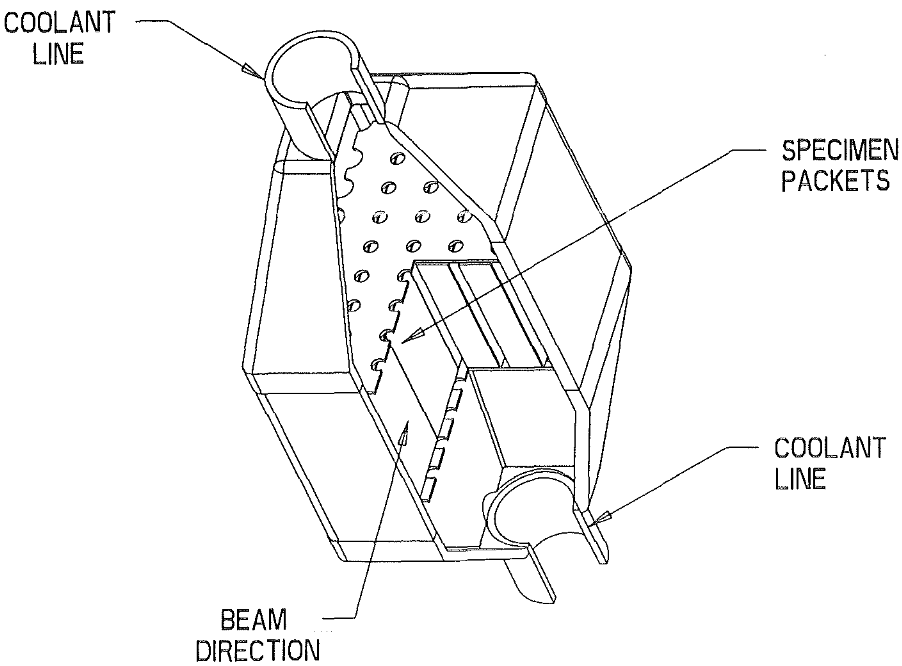

THE HIGH FLUX TEST MODULE IS DIVIDED INTO THREE CHAMBERS

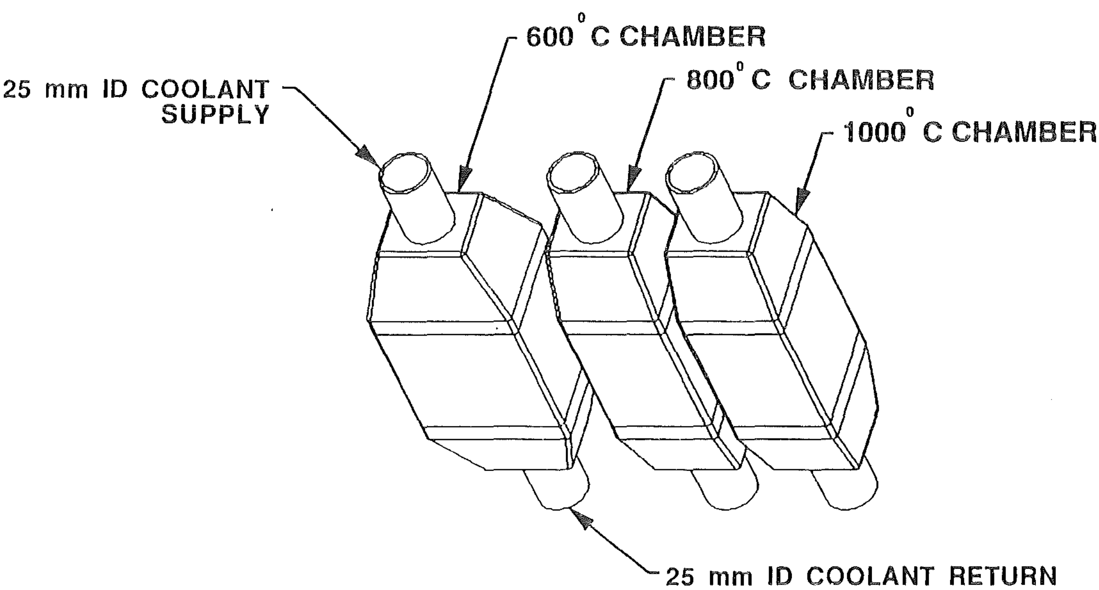

600°C – 800°C – 1000°C MODULE

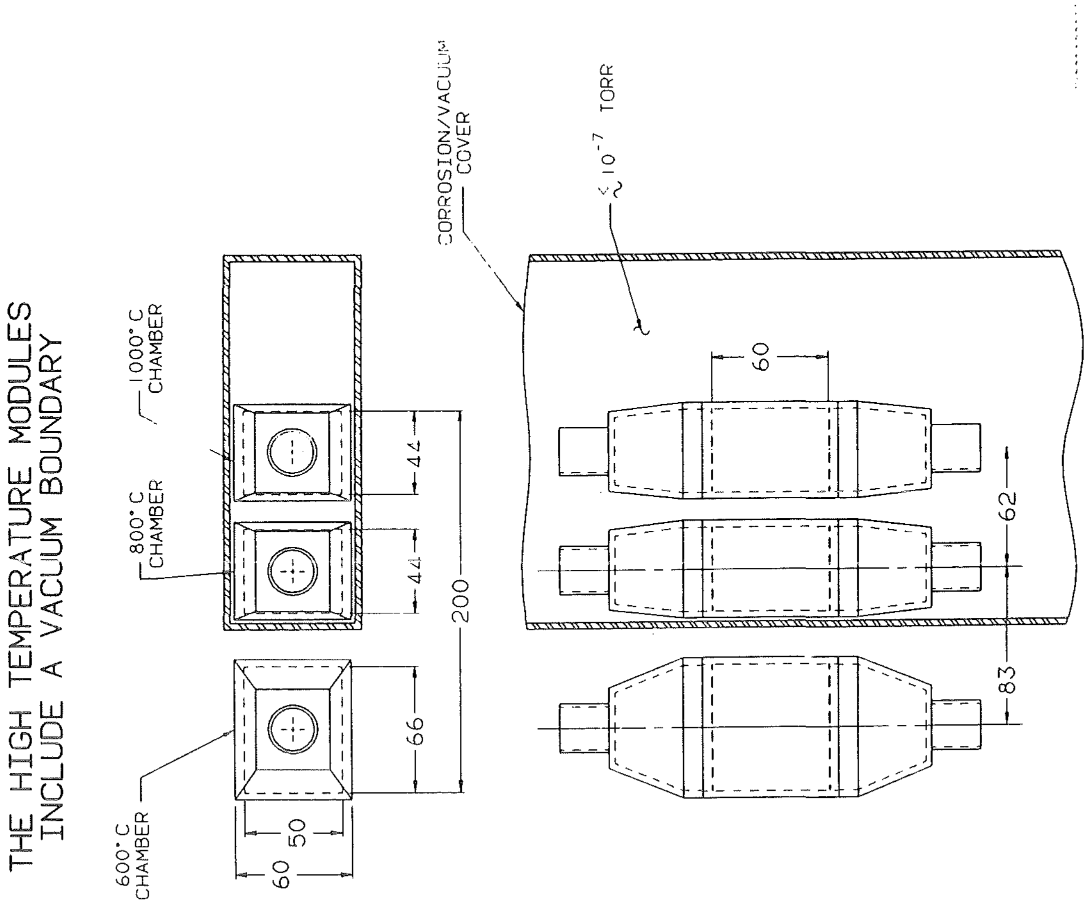

Module Sizes and Concentrations for First Four Loadings

Loading No.	Ext. Dimensions (mm)			Concentrations		
	Width	Depth	Height	Structure + Specimens	NaK Coolant	Void
1st Low Temp	214	54	64	44%	31%	25%
2nd Low Temp	214	54	64	45%	30%	25%
1st High Temp	158	54	64	44%	30%	26%
2nd High Temp	176	54	64	44%	31%	25%

These results agree well with the guess made at Oct 94 Karlsruhe Meeting:

50% Fe, 30% NaK, 20% Void

Thermal Hydraulic Analyses Assumptions

Coolant	NaK
Velocity in High-Flux Chamber	3 m/s
Velocity in Feedlines	2 m/s
Peak Nuclear Heating Rate	50 MW/m^3
Decay Length for Nuclear Heating	88 mm
Chamber Wall Thickness	2 mm
Min Temperature Margin Below Saturation	10 °C

Saturation Pressure for NaK and Na

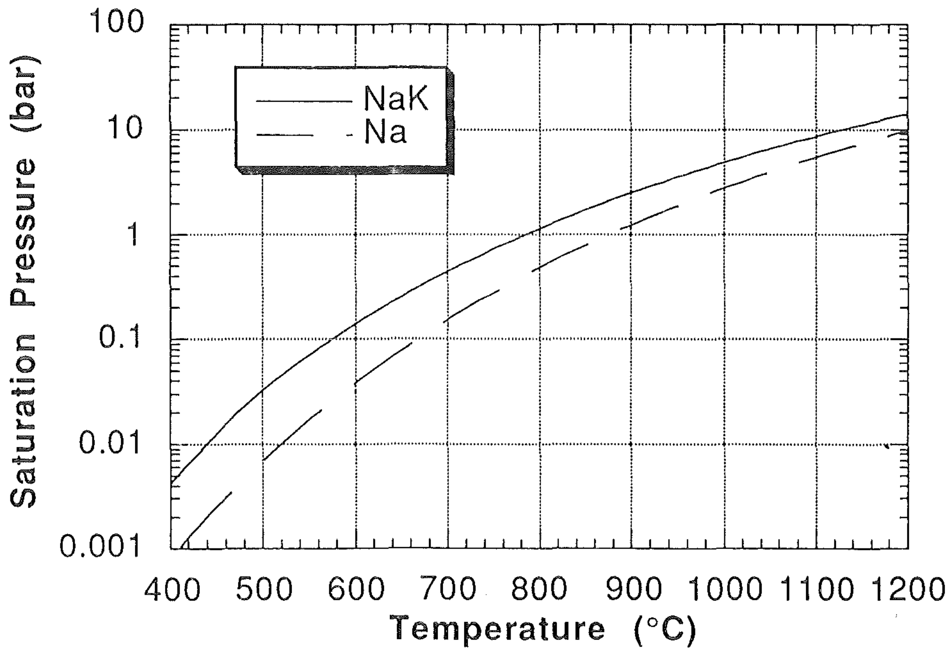

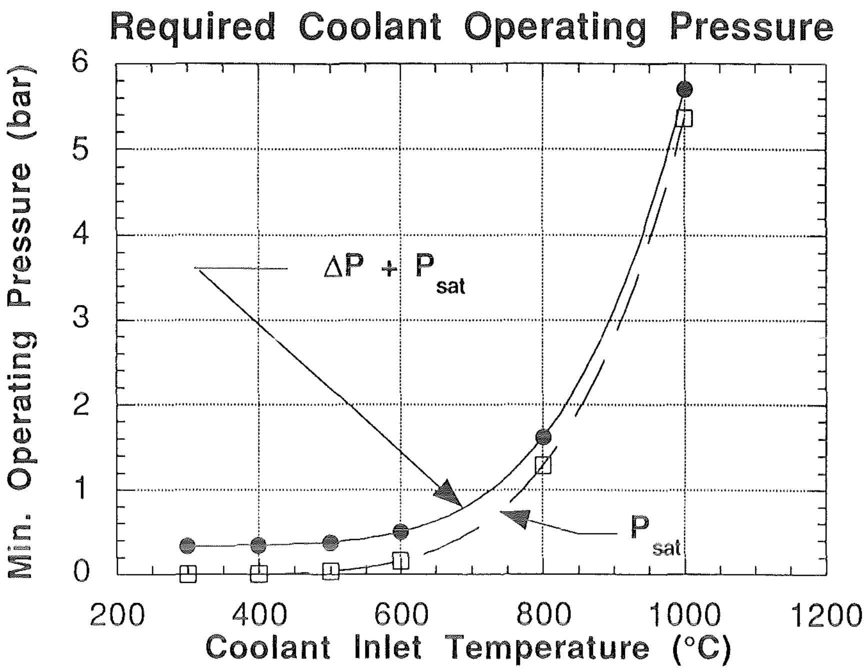

NaK Coolant Performance Is Acceptable for Temperatures ≤ 800 °C

- Pressure drop ~ 0.03 MPa (5 psi)
- Flow rate to high-flux module ~ 6.8 kg/s (9 L/s)
- All specimen temperatures are held within 20°C of coolant inlet temperature
    - Coolant temperature rise through high-flux chamber < 5 °C
    - Temperature difference through specimen holders < 10 °C
    - Convection film drop along 2 mm thick walls < 2 °C
- Inlet pressure of 0.2 MPa adequate for all testing temperatures except 1000°C case
    - Inlet pressure of 0.6 MPa required for 1000°C tests

HELIUM COOLED AND MODULAR DESIGN TEST CELL FOR IFMIF HIGH FLUX REGION

R. Conrad, R. Viola

CEC-JRC IAM Petten

1st IFMIF-CDA Technical Workshop on Test Cell System

Forschungszentrum Karlsruhe

July 3-6 1995

REQUIREMENTS FOR AN IFMIF IRRADIATION TEST CELL

-OPERATIONAL FLEXIBILITY

- PROPER SPECIMEN IRRADIATION ENVIRONMENT

-INTEGRATION WITH THE OVERALL CYCLE (ASSEMBLY, IRRADIATION CONTROL, PIE)

-REMOTE HANDLING

-REDUCED RISK FOR OVERALL FAILURE. MECHANICAL SIMPLICITY

-ABILITY FOR UPGRADING

-EASY MODELLING

PROPOSAL:

A HELIUM-COOLED MODULAR DESIGN TEST CELL FOR IFMIF HIGH FLUX REGION

-HELIUM ENSURES GOOD COMPATIBILITY WITH STRUCTURAL MATERIALS.

-NO NEUTRON SPECTRUM DISTORTION

-NO SAFETY IMPLICATIONS. LICENSING

-MUCH EXPERIENCE ON HELIUM COOLING

-MODULAR DESIGN

-RELOAD IRRADIATION RIGS

-INDEPENDENT TEMPERATURE CONTROL

-REDUCED ENGINEERING RISK

HIGH FLUX REGION - TEST CELL LAYOUT

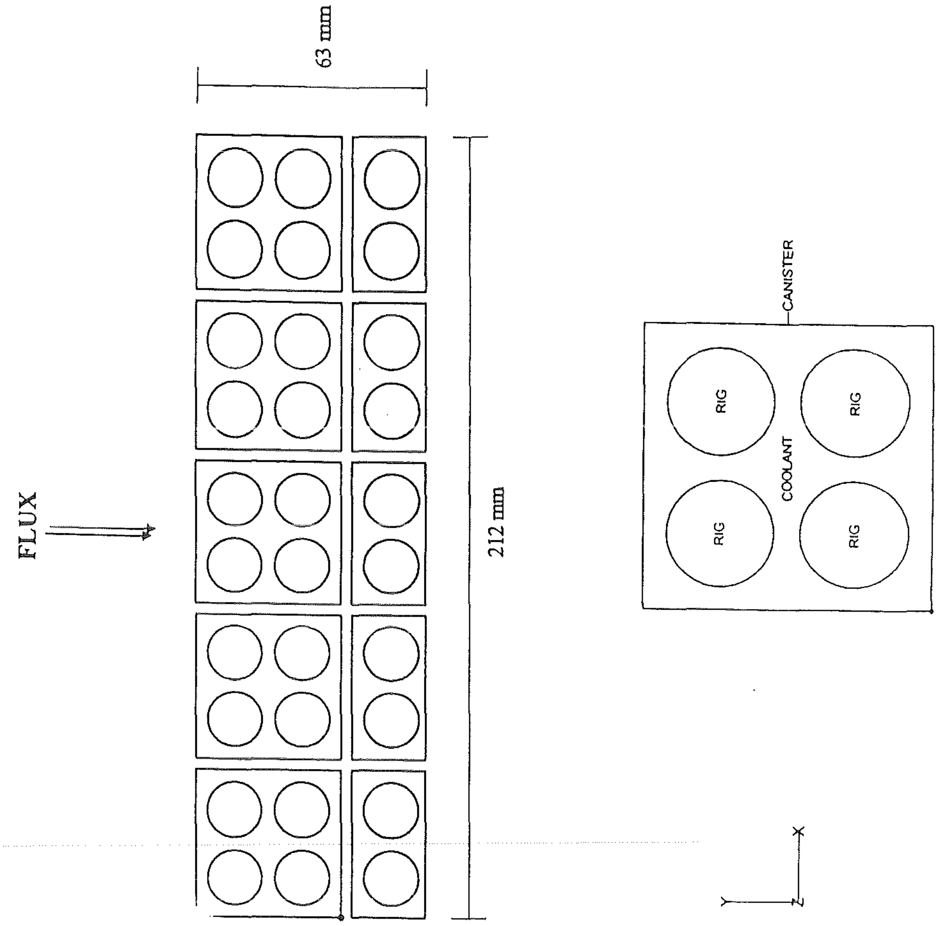

V1

IFMIF TEST CELL - GENERAL VIEW

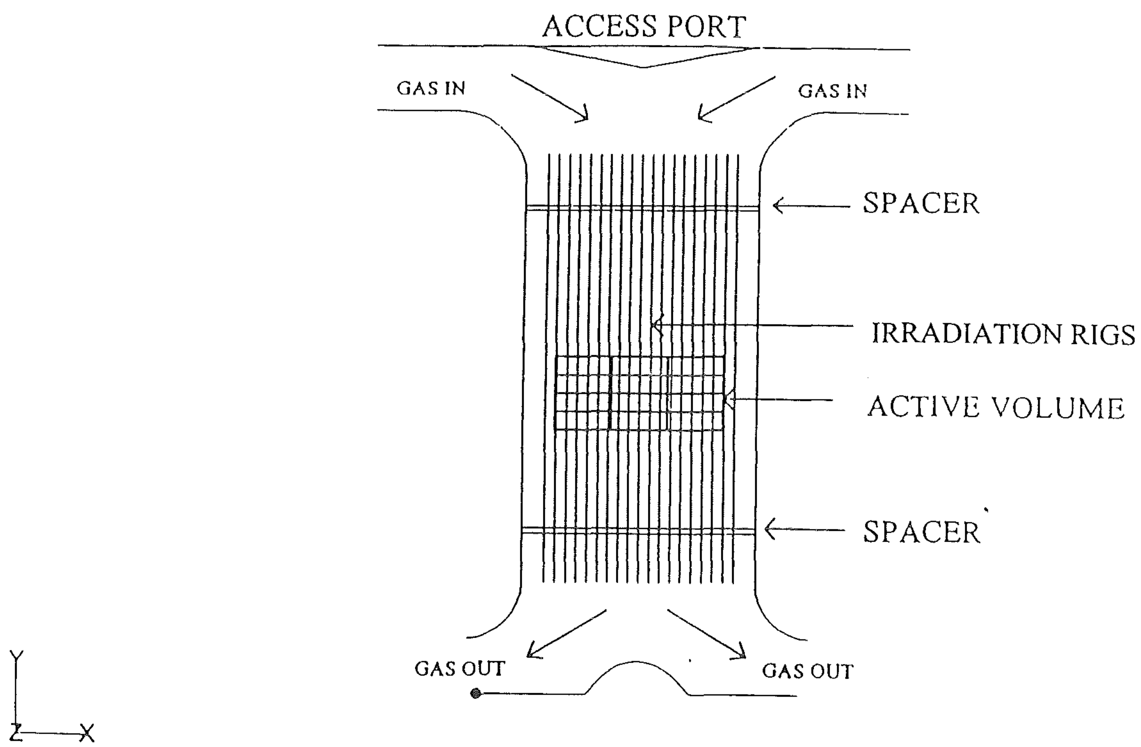

CANISTER WITH RECTANGULAR RIGS

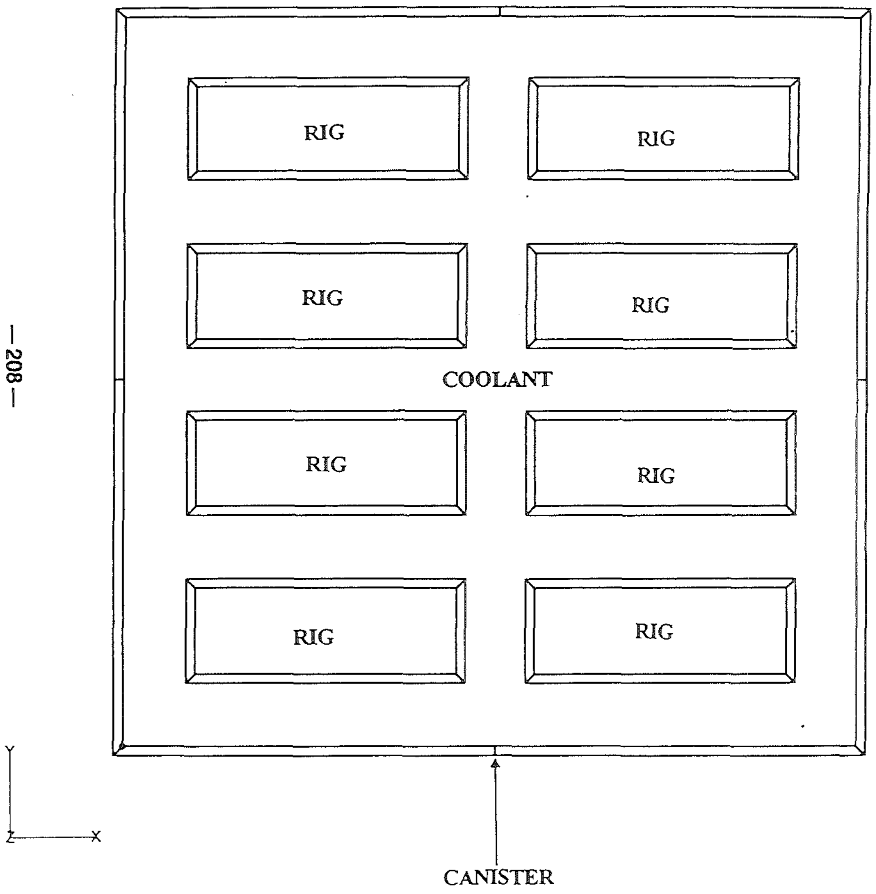

HIGH FLUX REGION - CANISTER WITH 10 mm RIGS

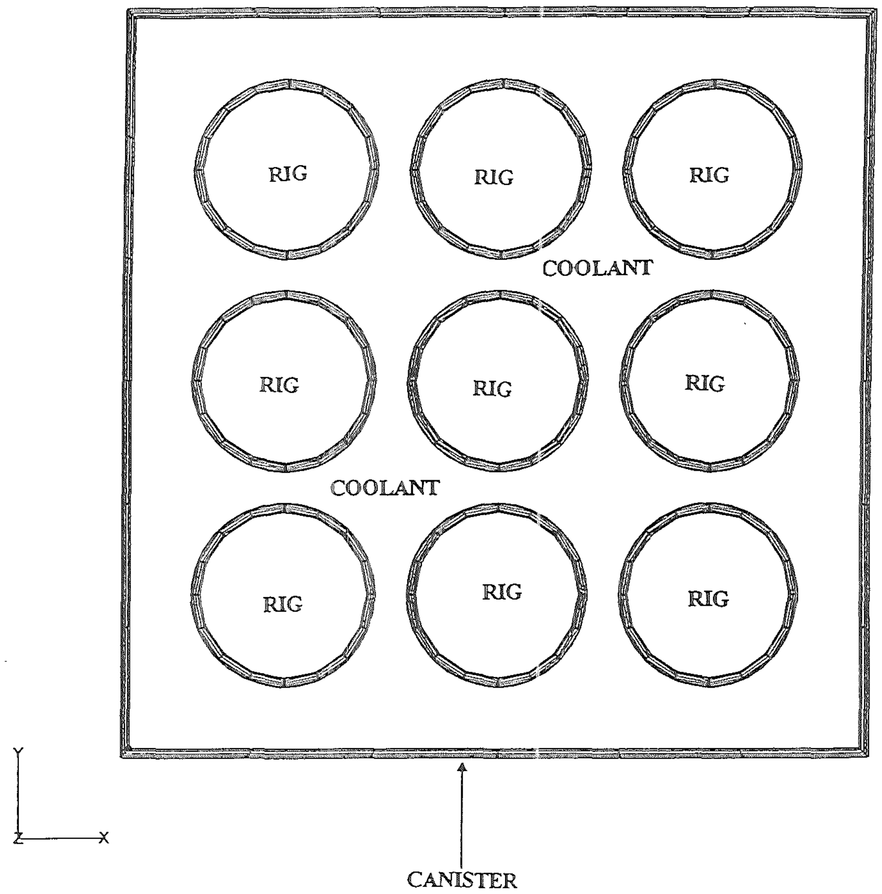

REQUIREMENTS

*ASSUMPTIONS:

-NUCLEAR HEATING: 5 W/g

-15 mm DIAMETER RIGS

-SPECIMEN DENSITY: 10 g/cm^3

-IRRADIATION TEMPERATURE ⩾250 °C.

-COOLANT INLET TEMPERATURE: 50 °C

*COOLING REQUIREMENTS:

-MINIMUM CONVECTION COEFFICIENT:

h ~800 W/m^{2}K

-OPERATING CONDITIONS FOR h = 2000 W/m^2 K

-PUMPED COOLANT VELOCITY: Vp ~ 22 m/s

-COOLANT PRESSURE: P ~ 10 bar

-COOLANT FLOW RATE: 0.3 kg/s

-COOLANT OUTLET TEMPERATURE: ~51 °C

-PRESSURE DROP (SPACERS, ELBOWS, RIGS):

$\Delta P < 0.2$ bar

TEMPERATURE CONTROL

-TEMPERATURE GRADIENT DEPENDS ON THE NUMBER: hV/kA

-ABSOLUTE TEMPERATURE CAN BE CONTROLLED WITH GAS OR LIQUID METAL GAPS

-FINE TUNING CAN BE ACHIEVED VARYING GAS COMPOSITION (He, %He/(1-%)Ne, Ne, etc..) IN GAPS

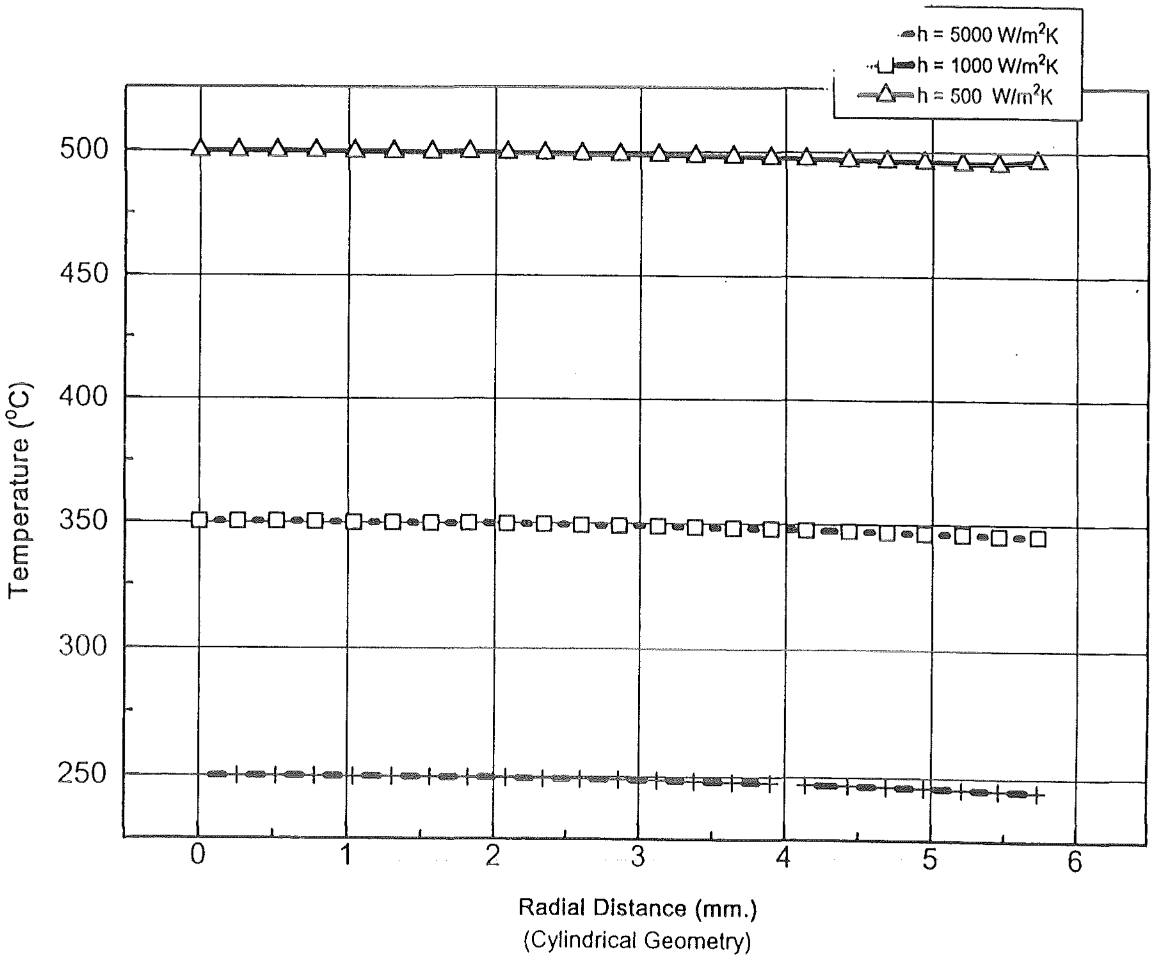
h = 5000 W/m²K
h = 1000 W/m²K
h = 500 W/m²K
Temperature (°C)
500
450
400
350
300
250
0
1
2
3
4
5
6
Radial Distance (mm.)
(Cylindrical Geometry)

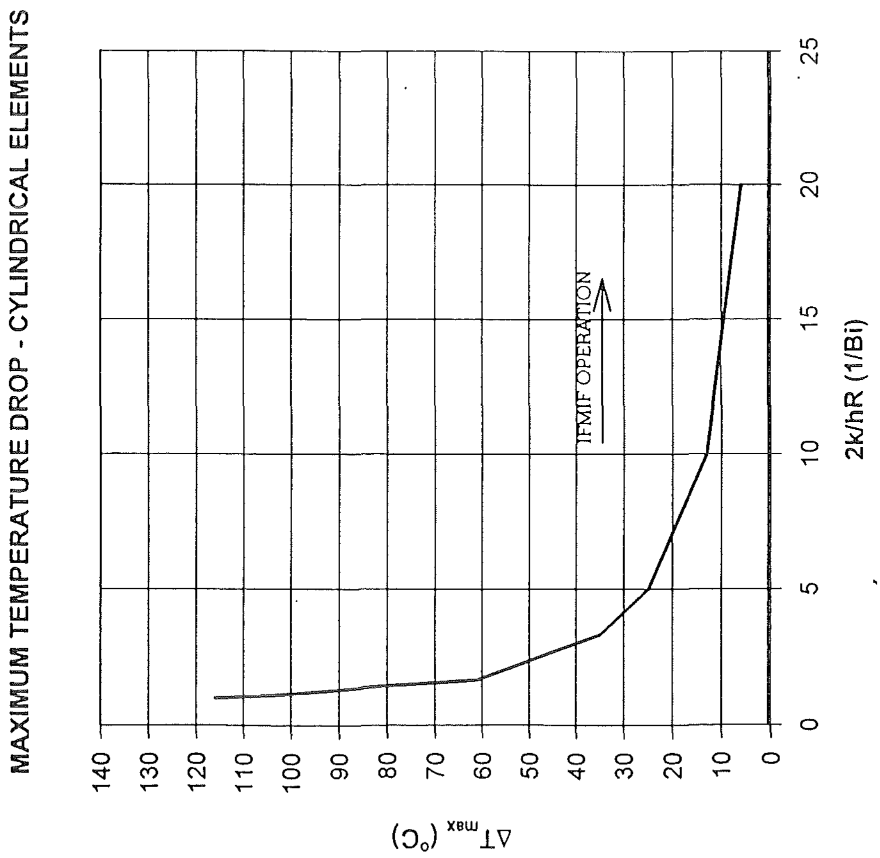
MAXIMUM TEMPERATURE DROP - CYLINDRICAL ELEMENTS
IFMIF OPERATION
2k/hR (1/Bi)
0
5
10
15
20
25
ΔTmax (°C)
140
130
120
110
100
90
80
70
60
50
40
30
20
10
0

LOW CONDUCTIVITY MATERIAL (SS 316) AXIAL TEMPERATURES

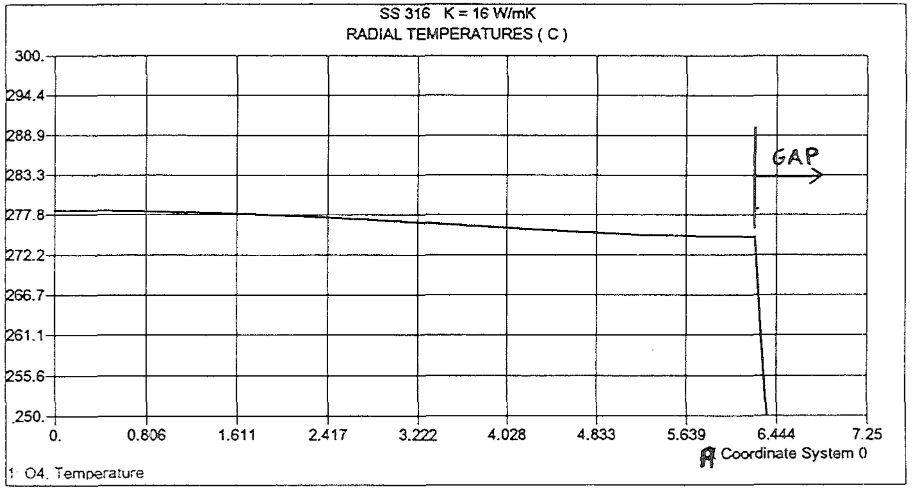

LOW CONDUCTIVITY MATERIAL (SS 316) AXIAL TEMPERATURES

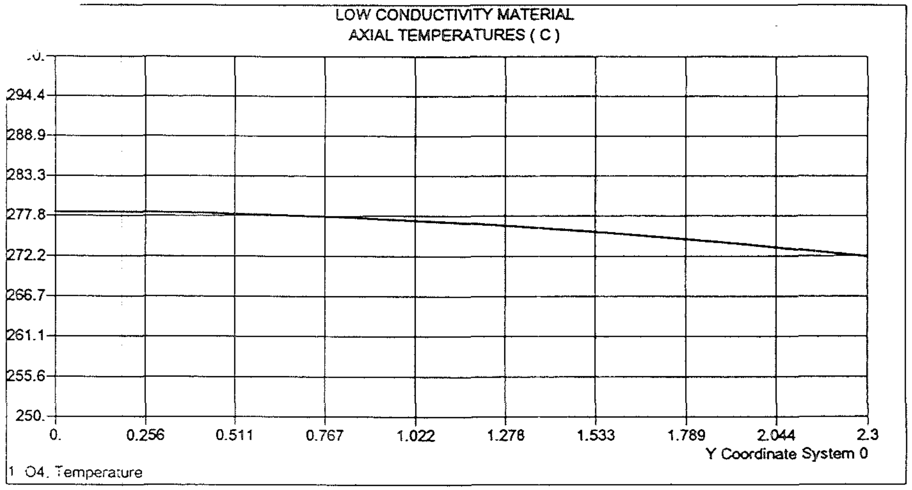

TEMPERATURE DISTRIBUTION FOR A 3x3xL (mm) BAR IN A ROW
h = 1000 W/sq m K - 0.3 mm Gap
(only 1/4th shown)
MAXIMUM TEMPERARURE DROP = 4.0 Deg. C

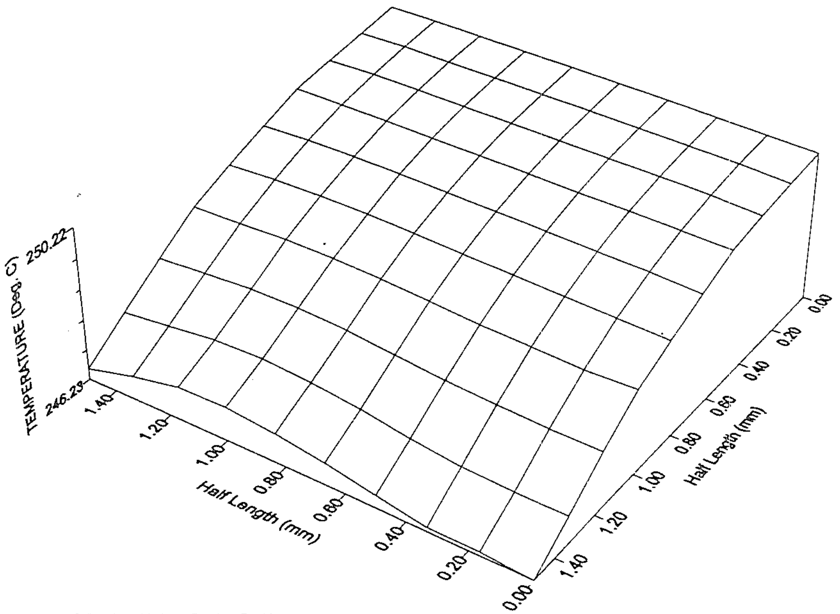

IRRADIATION ELEMENT
(TOP VIEW)

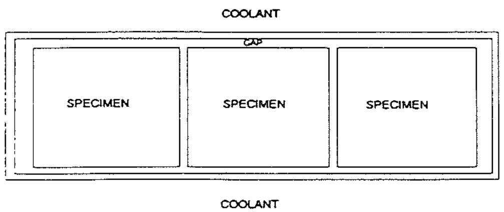

TEMPERATURE DISTRIBUTION FOR ONE SS 3x3xL (mm) BAR
h = 1000 W/sqm K - 0.6 mm Gap
(only 1/4th shown)
MAXIMUM TEMPERATURE DROP = 3.5 Deg. C

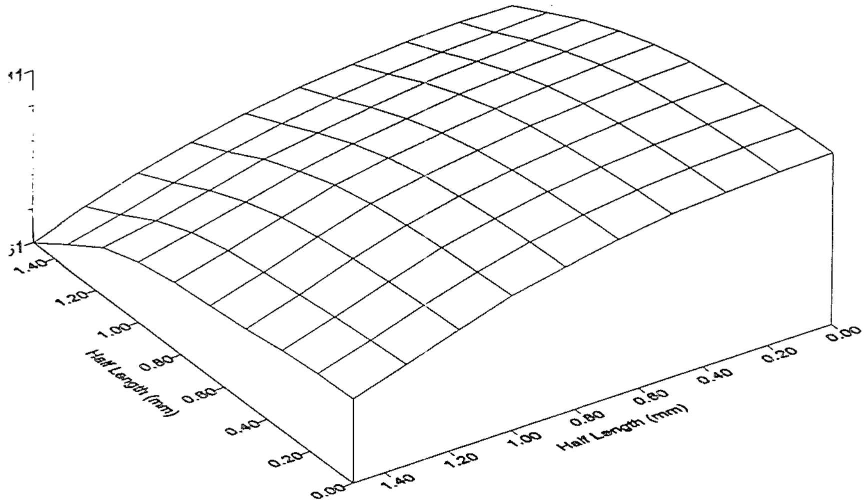

IRRADIATION ELEMENT
(TOP VIEW)

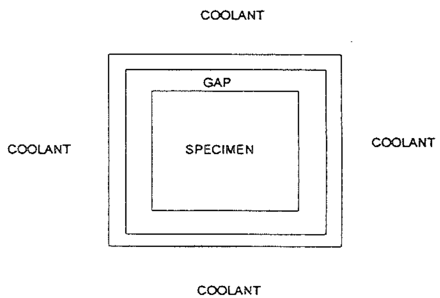

CONCLUSIONS

-HELIUM COOLED TEST CELL IS A VIABLE OPTION FOR IFMIF

-MECHANICALLY SIMPLE (RELIABILITY, EASY MAINTENANCE, COST)

-OPERATIONAL FLEXIBILITY

-INDEPENDENT TEMPERATURE CONTROL

-REDUCED RISK DUE TO OVERALL FAILURE

-SCALEABLE CONCEPT

PRELIMINARY WORK ON REFERENCE IN-SITU EXPERIMENTS AND TEST FACILITIES FOR IFMIF

S.J. Zinkle
Oak Ridge National Laboratory
Oak Ridge, TN 37831-6376

1st CDA Workshop on IFMIF Test Cell System
Forschungszentrum Karlsruhe
Karlsruhe, Germany
July 3-6, 1995

INTRODUCTION

- Numerous in-situ tests are required to establish the design data base of materials

- It is assumed that only a few in-situ tests will be necessary for structural materials; present analysis concentrates on "special purpose materials"

  - ceramic insulators

  - Rf windows and feedthroughs

  - diagnostic materials (fiberoptic cables, windows, magnetic coils, etc.)

  - ceramic breeding materials

- Development of an irradiated properties data base for DEMO will require both IFMIF and fission reactor irradiation sources

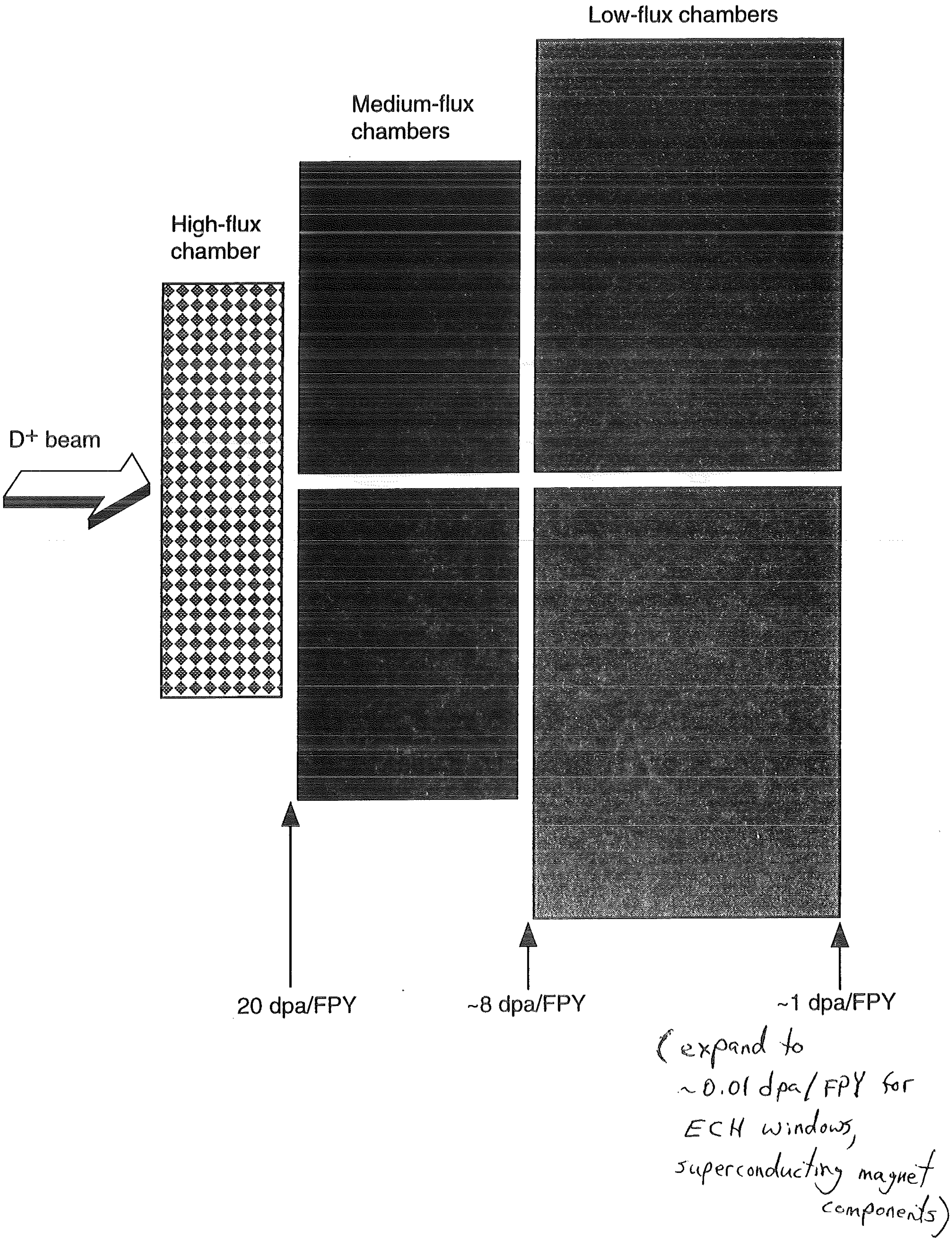
Low-flux chambers
Medium-flux chambers
High-flux chamber
D+ beam
20 dpa/FPY
~8 dpa/FPY
~1 dpa/FPY
(expand to ~0.01 dpa/FPY for ECH windows, superconducting magnet components)

PARTIAL LIST OF IN-SITU TESTS

- Ceramic insulators
  T_{irr}~20 to 500°C; doses ~0.1 to 10 dpa

  - radiation induced conductivity/radiation induced electrical degradation

  - mechanical properties/ IASCC (known to be severe in ceramics for aqueous environments

- Dielectric windows/ feedthroughs for Rf heating systems (mainly ceramics)
  ICRH, LHRH: T_{irr}~20 to 400°C; doses ~0.1 to 10 dpa
  ECH: T_{irr}~77 K; doses <0.1 dpa

  - loss tangent, thermal conductivity (measure in-situ or after low-temperature transfer to avoid point defect annealing effects)

  - mechanical properties/ IASCC

  - tritium diffusion (ionization enhanced diffusion effects)

TRIST in-situ Electrical Conductivity Capsule

OTE:

FOR CORRECT LOCATION WHERE TRIAX CABLE PART NO.63 & 64. TE'S PART NO.65 AND GAS TUBES PART NO.11.12.13.14 & 15. ENTER INTO SUBCAPSULES AREA. SEE DWG X3E020977A089 AND DETAILS "A"."B"."C" AND "D" ON THIS DWG.

LOWER SECTION OF THE LOW TEMPERATURE FACILITY SEE DWG X3E020977A044

EXISTING H.I.F.I. LARGE R.B. LINER TUBE ASSY. HFIR PART NO.41-11. DWG NO.M-11506-ØH-211-E-1

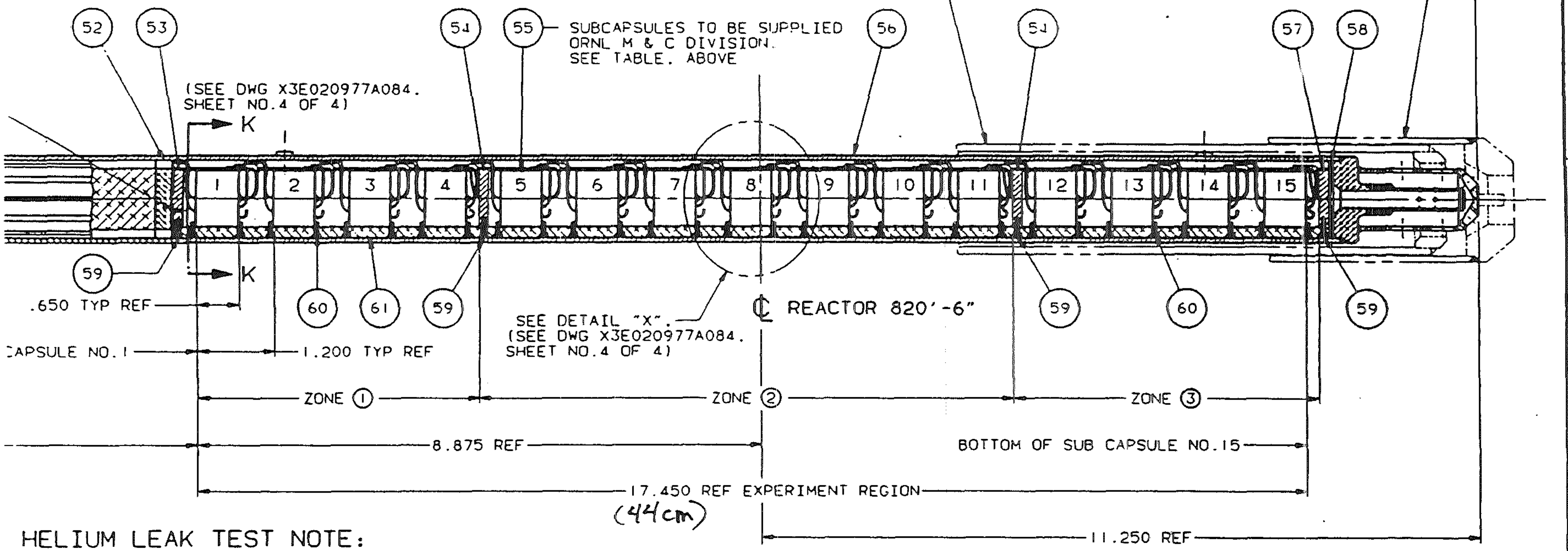

HELIUM LEAK TEST NOTE:

AFTER MAKING WELD NO.1. THE LOWER SECTION OF THE CAPSULE. FROM THE LOWER BULKHEAD (PART NO.50) DOWN. ALONG WITH BRAZED JOINTS AT BULKHEAD AND GAS TUBES (PART NO.11. 12.13.14 AND 15) SHALL BE HELIUM LEAK TESTED WITH A MASS SPECTROMETER. NO LEAKAGE GREATER THAN 10^{-8} STD CC/SEC PERMITTED A PRESSURE DIFFERENTIAL OF ONE ATOMPSPHERE. SEE ASSEMBLY/MANUFACTURING PLAN AP-ETD-20977-003-0.

FOR QA REQUIREMENTS SEE DWG X3E020977A084. SHEET NO.1 OF 4 AND/OR DWG THAT PART IS DETAILED ON.

CERTIFIED FOR CONSTRUCTION

ISSUE DATE: / /

ASSY/MANUF PLAN	AP-ETD-20977-003-0
DESIGN CALCULATIONS	X-OE-712
HOLDER SLEEVE SHEET NO.3	X3E020977A090
HOLDER SLEEVE SHEET NO.2	X3E020977A089
ASSEMBLY SHEET NO.4 OF 4	X3E020977A084
ASSEMBLY SHEET NO.3 OF 4	X3E020977A084
ASSEMBLY SHEET NO.1 OF 4	X3E020977A084

B

DES J COBUN A LONGEST K FARLEY 12/94
DRW K L FARLEY 12/94

KLF

REVISION APPROVALS — SOUND CHECK — DRAWING APPROVALS

MARTIN MARIETTA ENERGY SYSTEMS, INC.

HFIR-MFE RB* IN-SITU LOW TEMP IRRADIATION CAPSULE- PART NO.1 OVERALL ASSEMBLY

A

HFIR-MFE RB* IN-SITU IRRAD FACS

SCALE	ID	PLANT	BLDG	FL	SHEET	OF	DWG	REV
AS NOTED	20977	ORNL	7900	A	2	4	X3E020977A084	0

4 3 2

NUMBER OF MODELS IN THIS DRAWING= 7

Assembly Drawing for TRIST in-situ electrical conductivity expt. subcapsules and electrical connections. (draft 1/6/95)

NOTE:

THE CONNECTIONS TO THE SUBCAPSULE ASSEMBLIES AS SHOWN ON THE DRAWING ARE PESPRESENTATIVE. ACTUAL CONNECTIONS ARE TO BE MADE UNDER THE DIRECTION OF MMES METALS AND CERAMICS DIV AT ORNL.

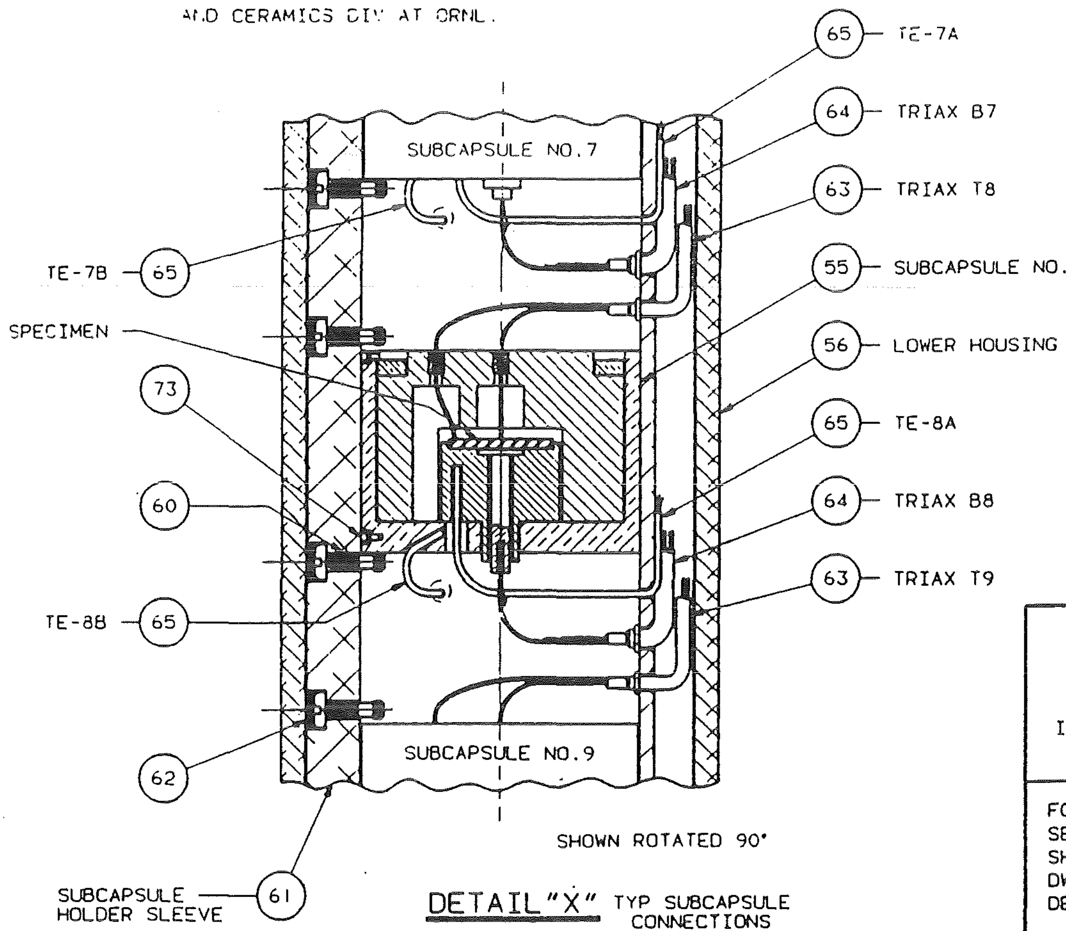

DETAIL "X" TYP SUBCAPSULE CONNECTIONS (SEE NOTE)

SCALE: 4"=1"

(SEE DWG X3E020977A084, SHEET NO.2 OF 4)

CERTIFIED FOR CONSTRUCTION

ISSUE DATE: / /

FOR QA REQUIREMENTS SEE DWG X3E020977A084, SHEET NO.1 OF 4 AND/OR DWG THAT PART IS DETAILED ON.

ASSY/MANUF PLAN	AP-ETD-20977-003-0
ASSEMBLY SHEET NO.3 OF 4	X3E020977A084
ASSEMBLY SHEET NO.2 OF 4	X3E020977A084
ASSEMBLY SHEET NO.1 OF 4	X3E020977A084

DES J CORUM & LORETT K FARLEY 12/94
DRW K L FARLEY 12/94
CHK J E CORUM
SECT J W MOORE
DEPT & PLANT

MARTIN MARIETTA ENERGY SYSTEMS, INC

HFIR-MFE RB• IN-SITU LOW TEMP IRRADIATION CAPSULE- OVERALL ASSY SECTIONS & DETAILS

HFIR-MFE RB• IN-SITU IRRAD FACS

TYPE A | PLANT ORNL | BLDG 7900 | FL A | SHEET 4 OF 4 | CLASS U

SCALE AS NOTED | TD 20977 | X3E020977A084 | REV 0

NUMBER OF MODELS IN THIS DRAWING= 2

PARTIAL LIST OF IN-SITU TESTS (continued)

- Optical materials (fiberoptic cables, silica windows, etc.)
  T_{irr}~20 to 400°C; doses ~0.001 to 1 dpa

  - optical absorption

  - luminescence

- various plasma diagnostics (magnetic coils, etc.)
  T_{irr}~20 to 400°C; doses ~0.01 to 10 dpa

- Blanket materials (ceramic breeders)
  T_{irr}~300 to 700°C?; doses ~1 to 50 dpa

  - tritium release rate in the presence of different sweep gases

- Superconducting magnet components (ex-situ testing after cryotransfer?)
  T_{irr}~4 to 100 K; doses <0.1 dpa

UNRESOLVED QUESTIONS

- What is the minimum "useful" irradiation flux for potential tests in IFMIF

  - anticipated maximum dose for organic insulation, superconductors, and ECRH windows is ~10^{-3} dpa; this implies that irradiation fluxes as low as ~0.01 dpa/FPY (10^{-3} dpa month) might be useful

  - need calculations of neutron flux in the low-dose regions of the test cell

- What provisions should be made for modifying the neutron and gamma ray spectrum in the different test regions

  - maintain a highly moderated neutron spectrum in one of the low-flux chambers, and a "hard" neutron spectrum on the other chamber?

IFMIF-CDA Technical Workshop
on
Test Cell System

Karlsruhe, July 3-6 1995

A. Möslang

In-situ tests (CDA-D-5)

— Preliminary Report —

- Introduction
- Categories of in-situ experiments
- Specimen development
- Feasibility studies
- Test matrix considerations

Introduction

In-situ experiments are the closest approach to real fusion conditions. Although fully instrumented material property tests under irradiation often imply a sophisticated technology, there is a strong need to investigate selected in-situ properties. Relevant in-situ experiments should address urgent material problems which cannot be investigated by other techniques.

➡ Interaction with blanket designers

With respect to Tokamak specific loading conditions, postirradiation tests often are a significant simplification, since the irradiation and (creep-)fatigue load are separated, i.e., the irradiation modified microstructure is completely developed before the mechanical test is started.
Several in-situ mechanical tests from light ion irradiation facilities indicate, that the material response on simultaneous long-term irradiation and mechanical loading cannot be simulated by conventional postirradiation tests and that in-situ experiments therefore are really needed for a valuable material development.

Selected in-situ push-pull (creep-)fatigue and stress corrosion tests on structural materials can also confirm whether the bulk of the postirradiation data are conservative with respect to real fusion conditions, and to what extend safety margins can be reduced, if fusion devices can hardly be constructed because of too conservative materials data.

With respect to ceramics, again available results from charged particle and neutron sources confirm the fundamental difference between e.g. in-beam and postirradiation electrical properties.

Categories of necessary in-situ experiments

In-situ irradiation tests include any simultaneous combination with at least one of the following loadings:

Properties	Proposed geometry
Thermally and/or mechanically induced (dynamic) stresses and stains	hollow push pull fatigue specimen
Corrosion in gaseous or liquid environments: Irradiation induced stress corrosion (IISC)	Crack growth specimen *
Coolant-coating compatibility	hollow push pull fatigue specimen with coating
Test of modules & mock-up's	requires blanket relevant dimensions*; too large for IFMIF test cell

*disregarded in the following

A universal testing machine in combination with a hollow push-pull fatigue specimen meet the bulk of the above requirements and offers a large field of possible loading conditions.

Practically independent of the irradiation the universal testing machine allows the following creep-fatigue modes:

- push-pull; e.g. R = -1
- stress/strain controlled
- with/without dwell periods
- thermal fatigue
- beam cycling experiments

Specimen development

A suitable specimen design has been already developed

(Ref: "Development of miniaturized specimens for in-situ creep fatigue tests in an intense neutron source;" E. Daum, E. Diegele and A. Möslang; IEA Internat. Symp.on Miniaturized Specimens for Testing of Irradiated Materials; H. Ullmaier, P. Jung (eds); 22-23. Sept. Jülich, Germany.), p.168.

<u>Hollow push-pull fatigue specimens</u> ensure high flexibility with respect to

- **choice of coolant (gaseous or liquid)**
- **dynamic temperature variations;**
  T is measured with small thermocouples welded at different parts of the gauge length and controlled by the flow rate of the coolant inside the tubular specimen
- **T-stability;**
  an additional ohmic heating system (a.c.-power) ensures T-stability nearly independend of γ– heat flux
- **coolant-coating interactions**
  by using specimens coated at the inner surface

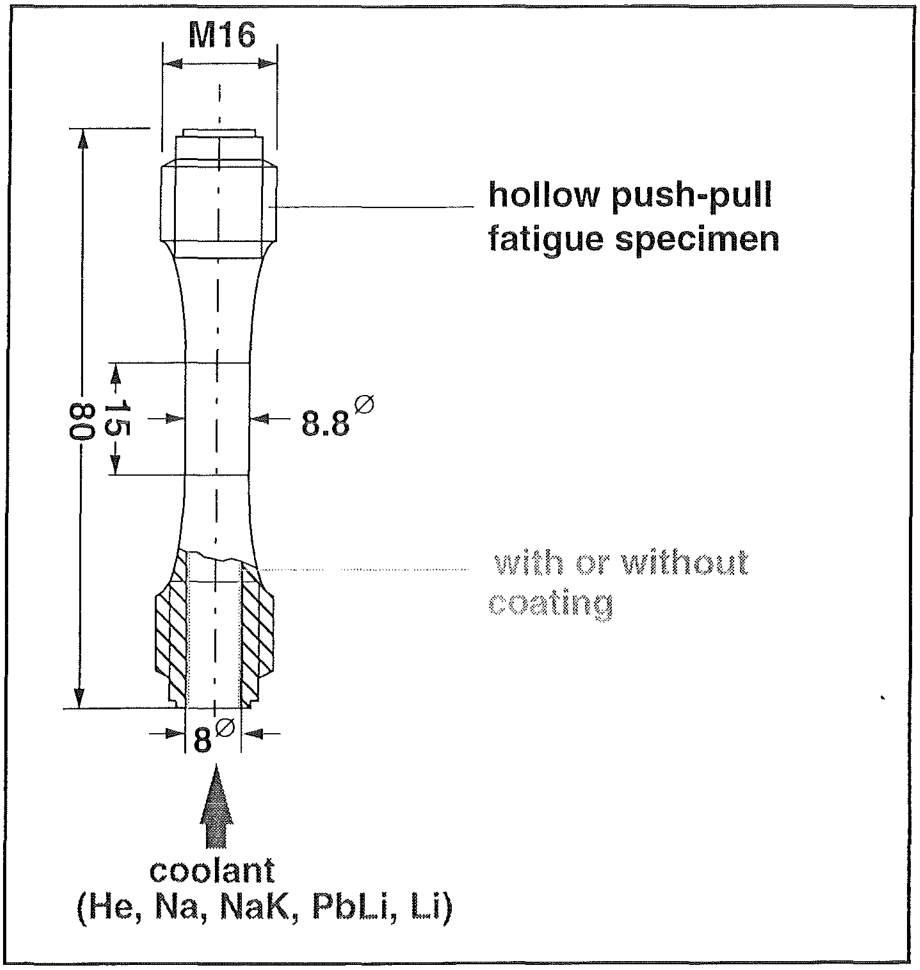

Specimen development (cont'd)

Elastic and elasto-plastic calculations were performed with the FE code ABAQUS to develop and optimize the specimen geometry. Only the active deformation volume of the push-pull fatigue specimen is assumed to be irradiated. For the calculations austenitic steel has been used with a Young's modulus of 175,000 MPa in the elastic regime, a plastic tangent modulus of 17,500 MPa beyond that limit, a heat load of $\dot{Q} = 100W/cm^3$ and a specimen temperature of 300 °C. This assumptions are certainly conservative for ferritic/martensitic steels or V alloys and the heat deposition can easily be removed using e.g. room temperature He-gas with 2 atm pressure as coolant inside the tubular specimen. An advantage of the proposed set-up is the possible replacement of gaseous coolants by liquid ones to study radiation assisted crack corrosion or to investigate the compatibility with ceramic coatings under fusion relevant conditions.

For specimens with a cylindrical length of 10 mm, a diameter of 8 mm and 0.4 mm wall thickness the FE calculations performed show that excellent homogeneous thermo-mechanical test conditions can be achieved The temperature variation in the irradiated volume is 10 K maximum. Thermal stresses induced by the temperature field are less than 2 MPa (axial as well as hoop), cf. figs. a,b. In contrast, a wall thickness of 2.4 mm (instead of 0.4 mm) results in a temperature field with objectionable high gradients of up to 78 K as fig. c shows. Finally, the homogeneity of stress fields under push-pull test is demonstrated under elastic and elasto-plastic material behaviour. Under elastic conditions (see fig. d) the deviation of axial stress from nominal stress is less than 2% within the irradiated volume, whereas under cyclic fatigue conditions of $\Delta\varepsilon_t$ = 1% (i.e. under elastic-plastic conditions), there is a moderate variation in axial and hoop stress especially at the end of the gauge volume of up to 8% (e)

To improve this stress-strain transition at the end of the gauge volume, the radius of curvature is increased to 100 mm for the fabricated fatigue specimens made of the tempered ferritic/martensitic steel MANET I. Standard strain controlled push-pull fatigue tests with R=-1 at elevated temperatures have already shown (see fig.), that within a broad load range all fatigue properties of such hollow specimens are similar to conventional solid specimens, that is, the generated data can be regarded as material specific. The average surface roughness was 3-5 mm for both specimen types. Although the application of hollow specimens is limited in the low cycle fatigue regime, where total strain amplitudes above about $\Delta\varepsilon_t$ = 0.9-1% leads to specimen buckling at elevated temperatures, this is no real limitation for near term fusion devices, which require in the present design concepts a fatigue life of at least 10,000 cycles and consequently much lower stain loadings.

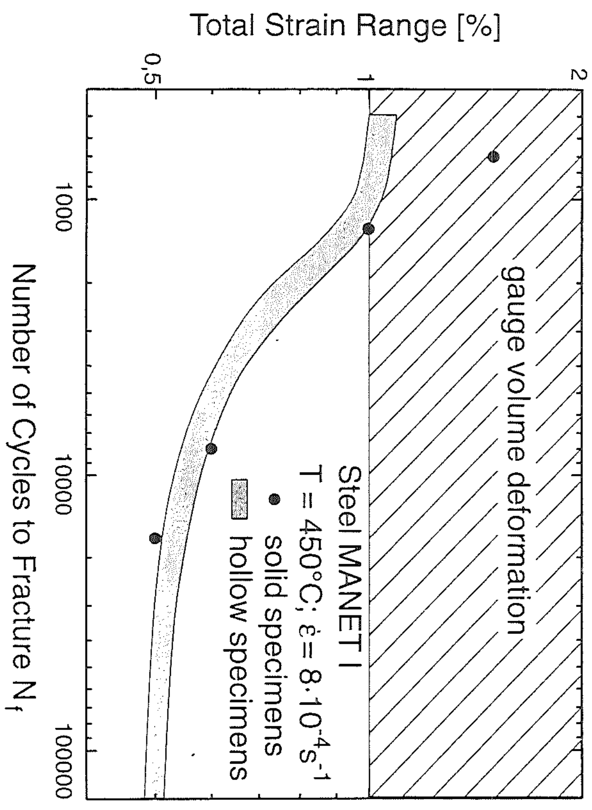

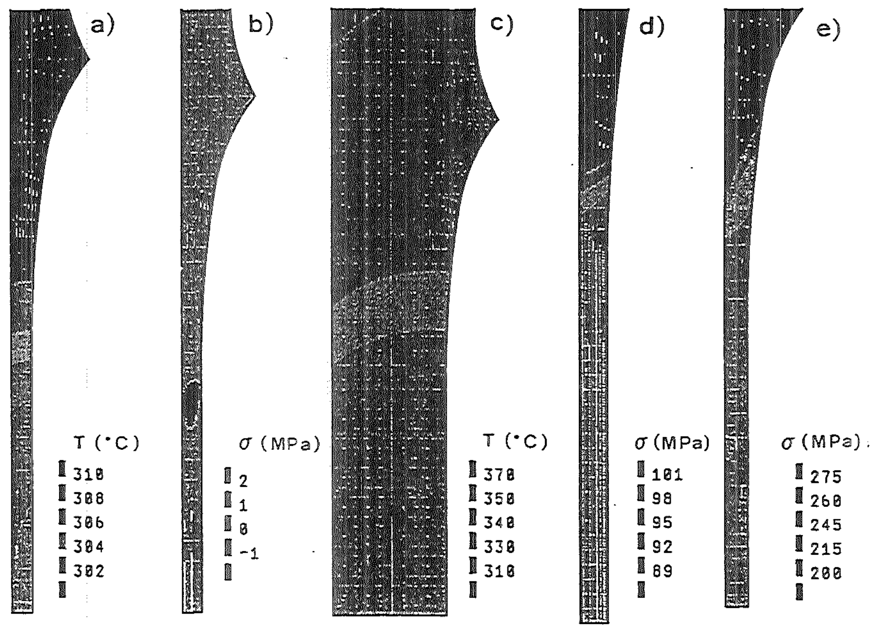

Fig: Calculated temperature and stress fields of a hollow fatigue specimen (austenitic steel) during irradiation at 300 °C in an intense neutron field (100 W/cm^3). Distribution of temperature (a) and thermal stresses (b) in a 0.4 mm thin specimen, temperature distribution in a 2.4 mm thick specimen (c), stress distribution assuming a tensile stress of 100 MPa (d), and stress distribution assuming a total strain of $\Delta\varepsilon_t$ = 1% (e).

Feasibility considerations

Background

- In-situ push-pull fatigue experiments with sophisticated technologies are already running in some high energy light ion facilities.
- All these facilities are fully instrumented and remote controlled.
- Small temperature gradients up to high heat loads $\dot{Q}$ (e.g. $\dot{Q} \leq 90$ W/cm^3 at 450°C) are achieved routinely already with Helium-gas ($T_{He} \cong$ R.T., $p_{He} \cong 2.5$ bar) as coolant.

Critical aspects

- Miniaturization is controlled by the size of the push pull rods rather than by the specimen dimensions.
  - ⇒ Within a foot print of 5x20 cm^2 only about three simultaneously running in-situ (creep-)fatigue tests seem to be realistic.
- Long-term experience (>4000 h) under irradiation for critical aspects already available, e.g;
  - seals of specimen under fatigue conditions
  - thermocouples (0.1 mm ∅)
  - load cell (stress- measurement
  - Extensometer (strain measurement)
  - Specimen failure scenario
  - Helium gas coolant concept
- γ-heat production outside the foot print area can be removed by additional coolant channels e.g. in the push-pull rods or the load frame.
- Final construction of overall in-situ test facility (load frame, coolant concept, equipment, vacuum chamber) needs feedback from P.I.E. assembling.

Load Cell

Sufficiently small load cells are already tested in strong radiation environment, e.g. :

Load cell U9A (HBM® GmbH, Darmstadt)

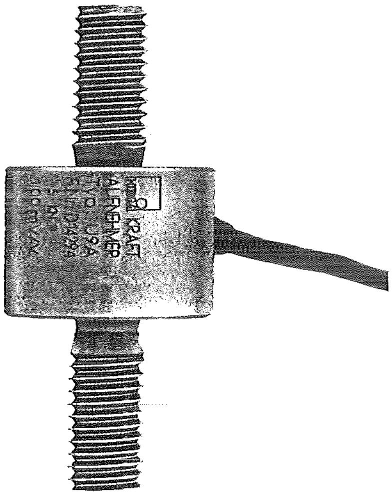

Nennkräfte:
2 kN...20 kN

Dimensions

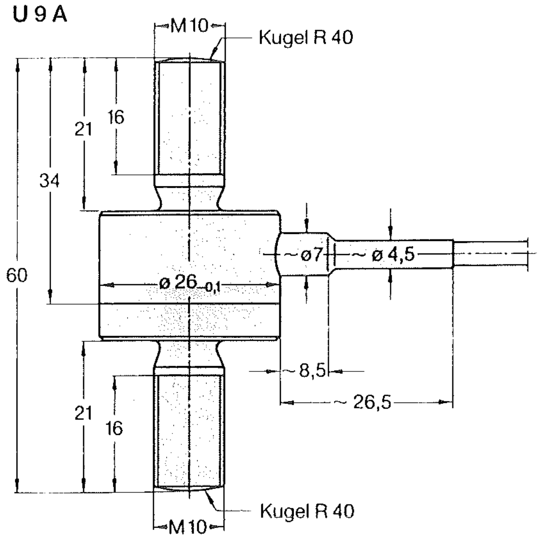

Helium gas coolant loop

Long-term experience for He-loops operating in neutron and light ion irradiation facilities is available.

According to the proposed in-situ fatigue design, the following lay-out of a He-gas loop was found to be sufficient ($T_{specimen} \geq 250$ °C) for the med-flux region (≤8 dpa/year) of IFMIF downstream the P.I.E. module:

❍ He inlet (pressure pipe)	≤2.5 bar_{abs}	25 °C
❍ He outlet (suction pipe)	≥1.5 bar_{abs}	≤35 °C*
❍ He pressure drop (specimen & rods)	≤0.9 bar	
❍ He-gas throughput	12 x 10^{-3} kg/s	
❍ Compressor size	240 m^3/h	25 kW
❍ He-gas purity (C, N, O)	≤ 0.1 appm	

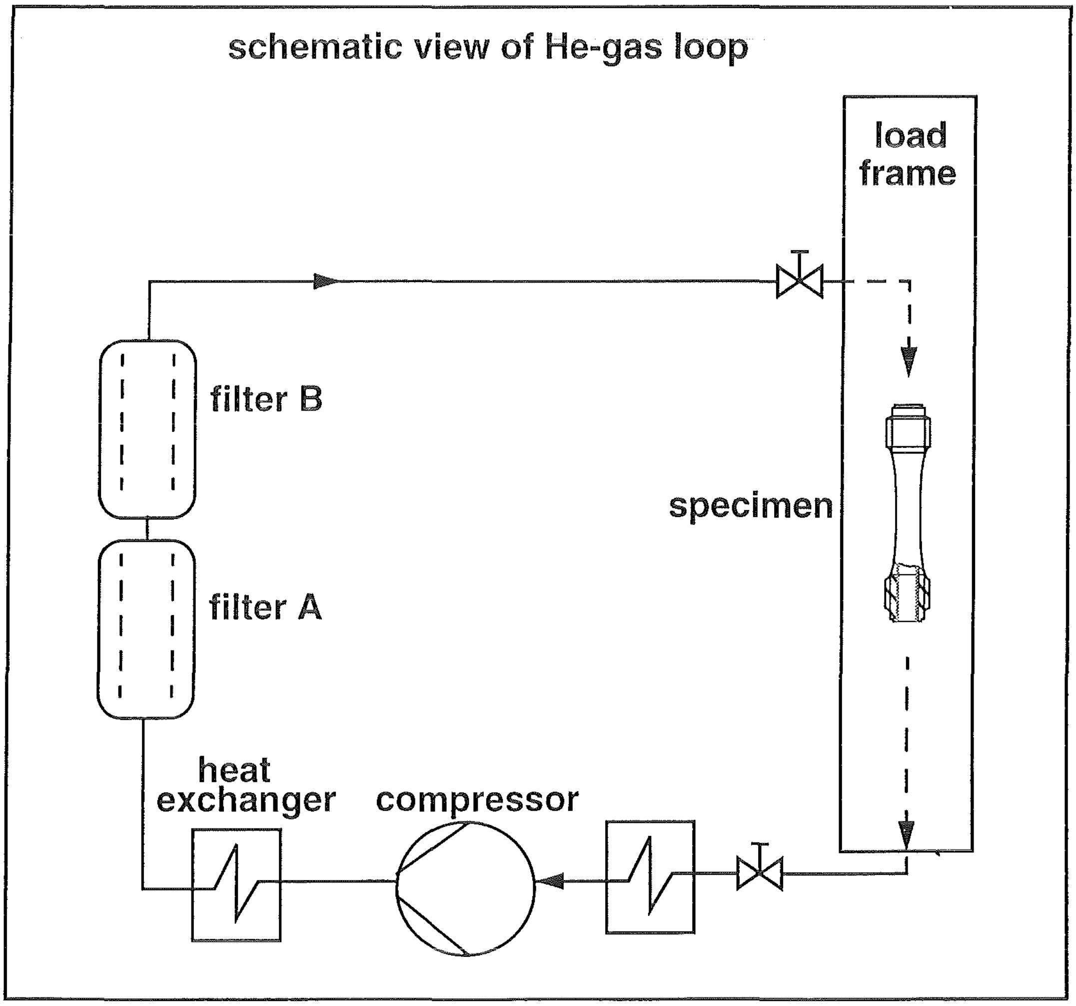

* at specimen outlet

Forschungszentrum Karlsruhe
Technik und Umwelt

IFMIF - In-Situ - Experiments
Preliminary design of rod drive

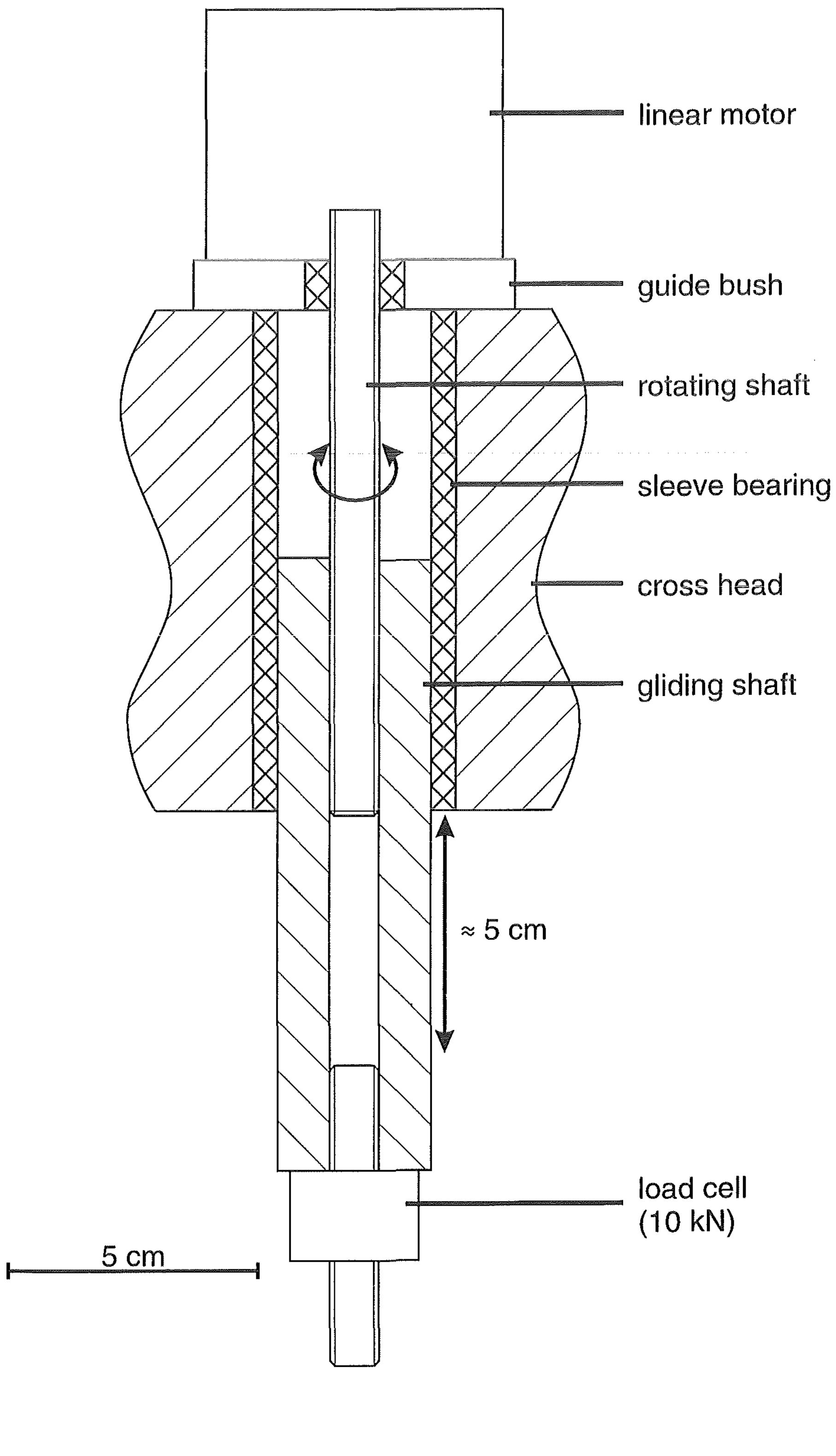

Forschungszentrum Karlsruhe
Technik und Umwelt

IFMIF - In-Situ - Experiments
Proposed design of push pull rod

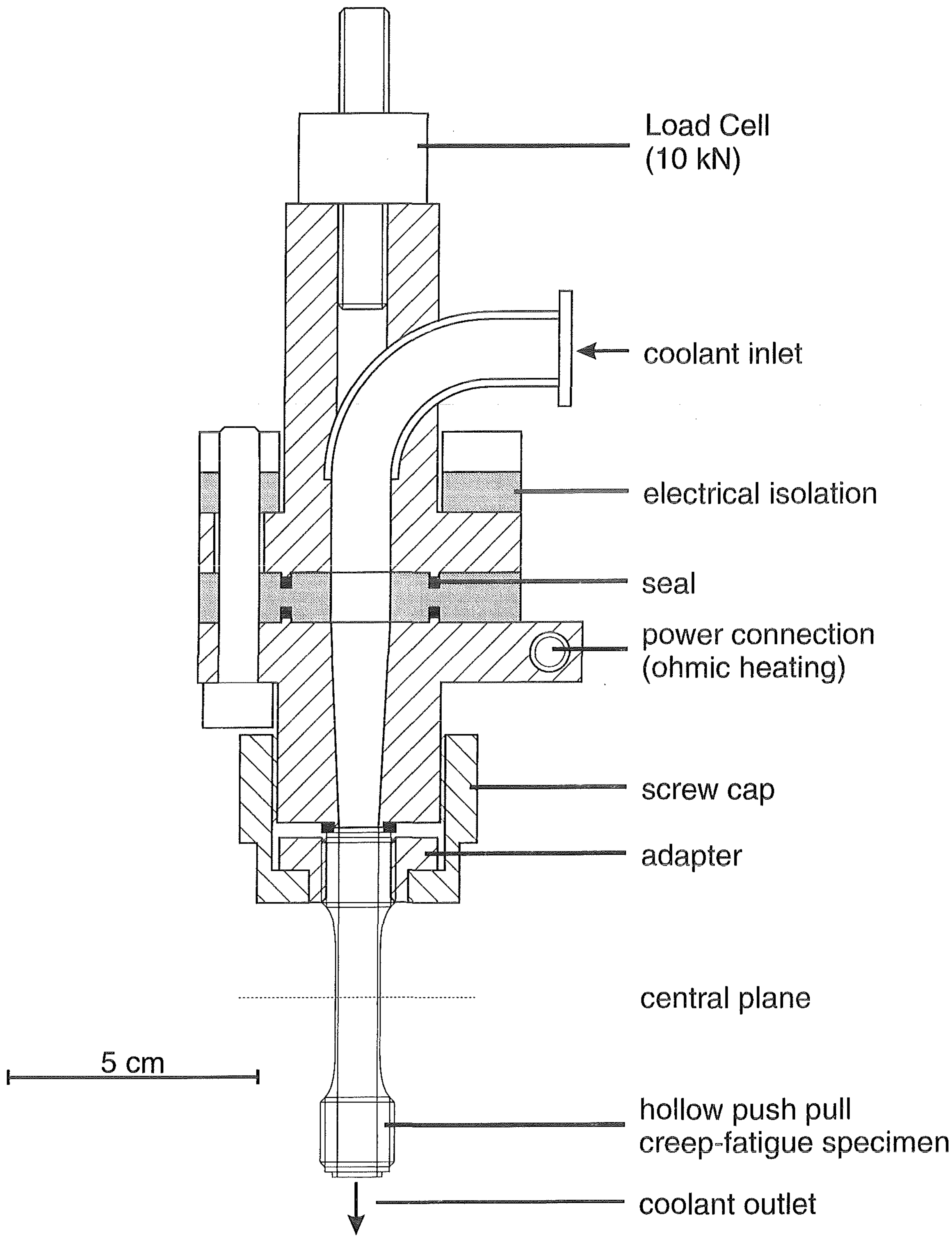

Forschungszentrum Karlsruhe
Technik und Umwelt

IFMIF - In-Situ - Experiments
Preliminary design of universal testing machine

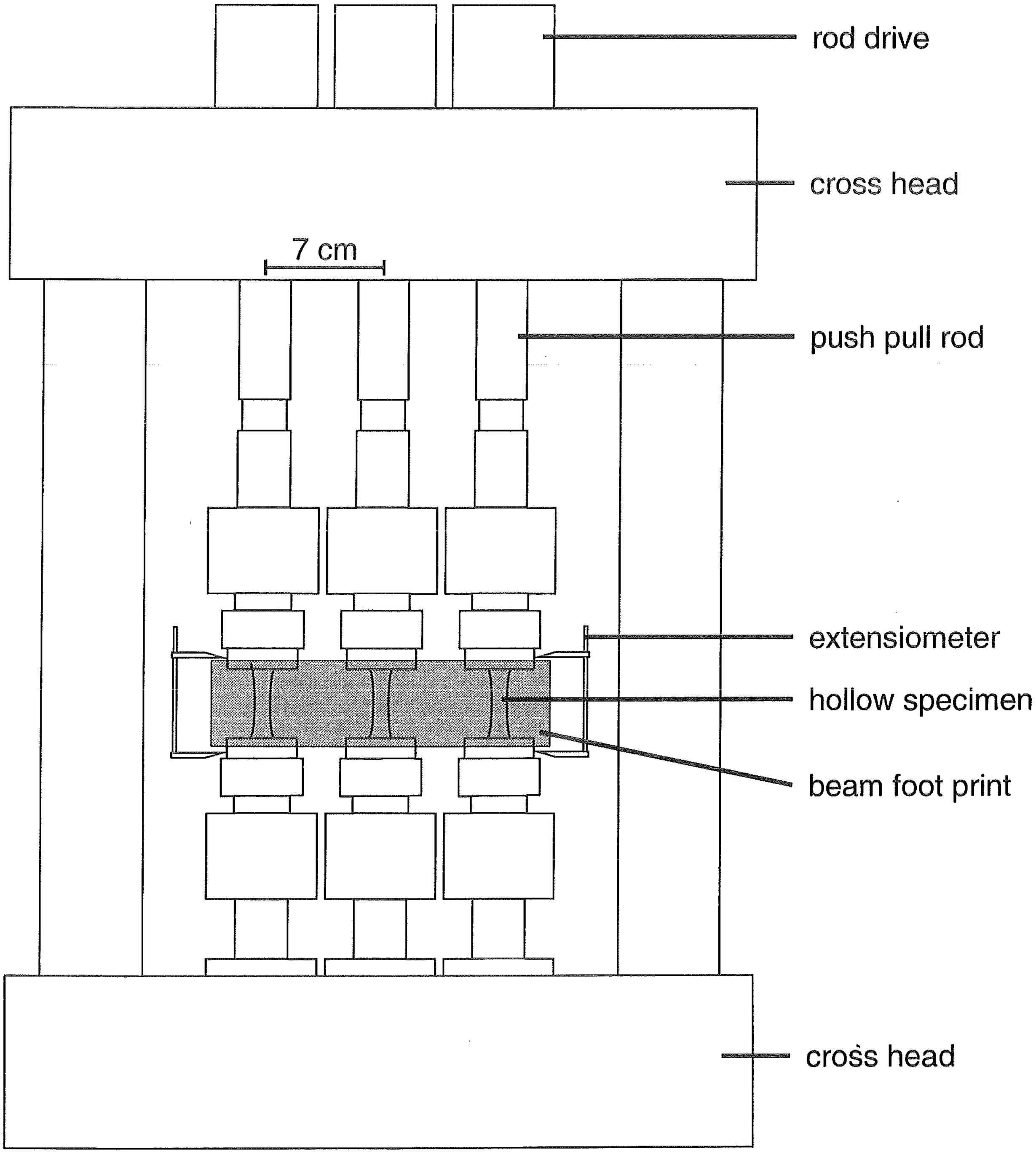

IFMIF In-Situ Experiments   Top view schematic

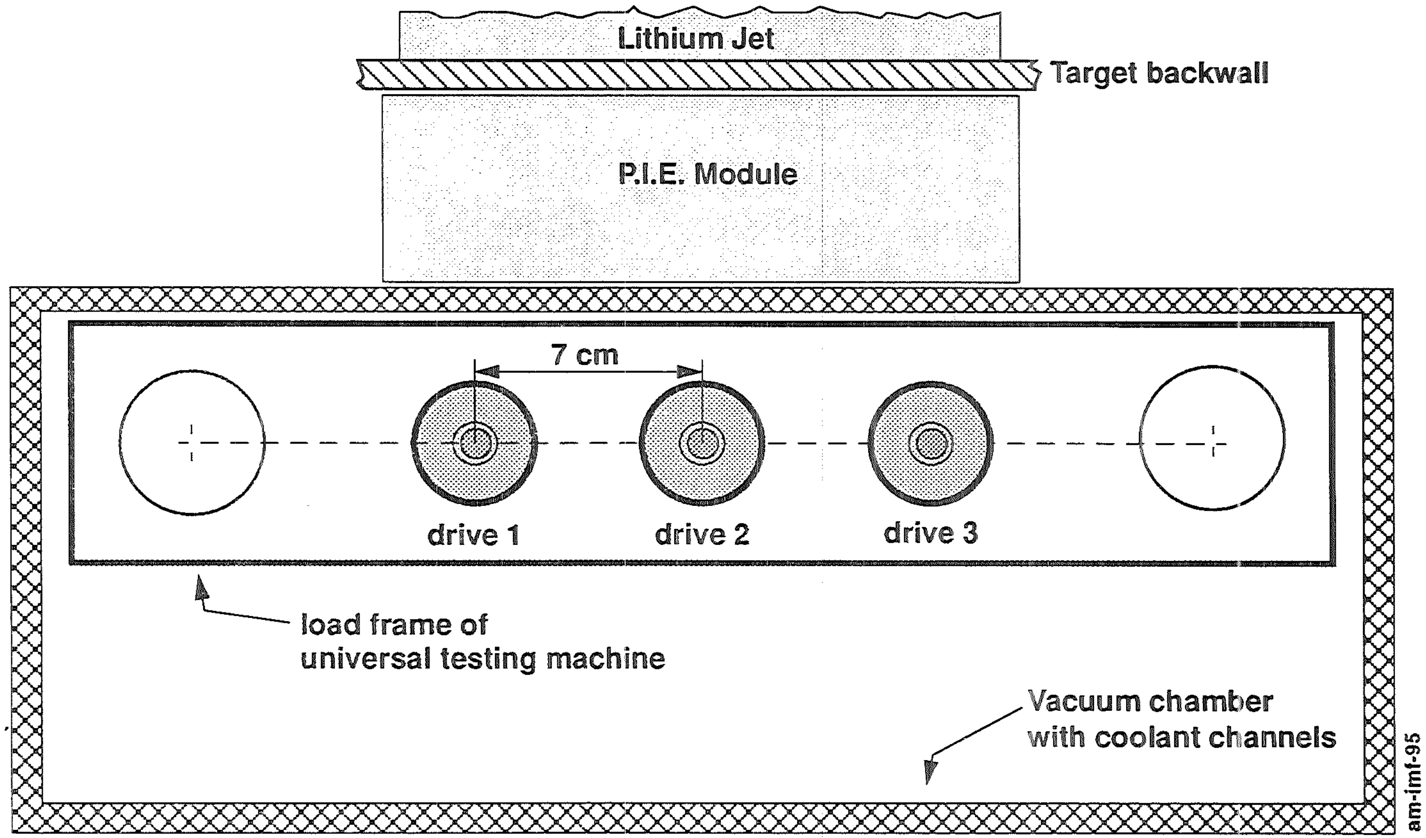

Test matrix considerations for instrumented tests

- In contrast to the postirradiation module only very few specimens can be irradiated in an in-situ test assembly.

- "Accommodation for instrumented tests in the lower flux region" (see user requirements, D.G. Doran 1994).
  As a consequence displacement damage accumulation will be only moderate (Actual values needs to be determined by MCNP code on the basis of more detailed designs).

Implications of these strong boundary conditions are:

➡ End-of-life dpa levels seem to be unrealistic.

➡ Broad database production on "in-situ properties" not the goal of instrumented tests in IFMIF.

➡ However, on the basis of a formal interaction and a close cooperation with the design community, selected in-situ experiments should give relevant answers on urgent and critical problems which cannot be solved by conventional tests.

Therefore, in contrast to P.I.E. needs, a detailed and complete definition of a final test matrix for a 10-15 years irradiation programme already during the CDA phase seems not to be necessary.
We should rather arrive on feasible concepts for highly flexible in-situ test facilities

Nevertheless, requirements for a preliminary test matrix on critical material problems will be given.

Preliminary matrix* for in situ test facility

Experiment 1: Material development; Creep-fatigue; Holdtime at T_{max}

Test No.	Comments	Target Coating Coolant	Parameter Definition	Expected Duration
1.1	Low T irradiation embrittlement: does it occur under these conditions? fatigue life	f/m steel 1 - He	Thermal (evtl. thermo-mechanical), uniaxial T_{min} = 250 °C, T_{max} = 550 °C t_{dwell} = 2 h (at T_{max}) Clamping at $T_m = (T_{min} + T_{max})/2$ T = command variable; $\sigma(t)$, $\varepsilon(t)$ measurement	10^4 cycles, 2 years
1.2	Irradiation embrittlement, interstitial pick-up	V alloy 1 to be defined He	Thermal (evtl. thermo-mechanical), uniaxial T_{min} = 350 °C, T_{max} = 700 °C t_{dwell} = 2 h (at T_{max}), Clamping at $T_m = (T_{min} + T_{max})/2$ T = command variable; $\sigma(t)$, $\varepsilon(t)$ measurement	10^4 cycles, 2 years
1.3	Irradiation embrittlement	Innov. alloy 1 to be defined He	Thermal (evtl. thermo-mechanical), uniaxial T_{min} =coolant inlet, T_{max} coolant outlet t_{dwell} = 2 h (at T_{max}) Clamping at $T_m = (T_{min} + T_{max})/2$ T = command variable; $\sigma(t)$, $\varepsilon(t)$ measurement	10^4 cycles, 2 years

* Depending strongly on actual blanket designs

- If irradiation hardening is expected to control fatigue life, it might be sufficient to reach the quasi saturation of the irradiation induced hardening (<10 dpa in many alloys) for an accepted assessment of long-term creep-fatigue properties. That is, to "adjust" the thermal or thermo-mechanical load to about 10^4 cycles.
- During maintenance periods the (polished) specimen surface can be examined in detail with a long range optical microscope (e.g. QUESTAR©, 1-2 μm resolution) in order to evaluate crack initiation and propagation.

Experiment 2: Material development; Creep-fatigue; Holdtime at T_{min}

Test No.	Comments	Target Coating Coolant	Parameter Definition	Expected Duration
2.1	Low T irradiation embrittlement: does it occur under these conditions?	f/m steel 1 - He	Thermal (evtl. thermo-mechanical), uniaxial T_{min} = 250 °C, T_{max} = 550 °C t_{dwell} = 2 h (at T_{min}) Clamping at $T_m = (T_{min} + T_{max})/2$ T = command variable; $\sigma(t)$, $\varepsilon(t)$ measurement	10^4 cycles, 2 years
2.2	Irradiation embrittlement, interstitial pick-up	V alloy 1 to be defined He	Thermal (evtl. thermo-mechanical), uniaxial T_{min} = 350 °C, T_{max} = 700 °C t_{dwell} = 2 h (at T_{min}), Clamping at $T_m = (T_{min} + T_{max})/2$ T = command variable; $\sigma(t)$, $\varepsilon(t)$ measurement	10^4 cycles, 2 years
2.3	Irradiation embrittlement	Innov. alloy 1 to be defined He	Thermal (evtl. thermo-mechanical), uniaxial T_{min} = coolant inlet, T_{max} = coolant outlet t_{dwell} = 2 h (at T_{min}) Clamping at $T_m = (T_{min} + T_{max})/2$ T = command variable; $\sigma(t)$, $\varepsilon(t)$ measurement	10^4 cycles, 2 years

Experiment 3: Material development; Welds & Joints; Creep-fatigue

Test No.	Comments	Target Coating Coolant	Parameter Definition	Expected Duration
3.1	Welded/ joined deformation volume; stress/strain concentrations or embrittlement in/near heat affected zones?	f/m steel 1 - He	Thermal (evtl. thermo-mechanical), uniaxial T_{min} = 250 °C, T_{max} = 550 °C t_{dwell} = 2 h, T_{dwell} to be defined Clamping at $T_m = (T_{min} + T_{max})/2$ T = command variable; $\sigma(t)$, $\varepsilon(t)$ measurement	10^4 cycles, 2 years
3.2	Welded/ joined deformation volume; stress/strain concentrations or embrittlement in/near heat affected zones?	V alloy 1 to be defined He	Thermal (evtl. thermo-mechanical), uniaxial T_{min} = 350 °C, T_{max} = 700 °C t_{dwell} = 2 h, T_{dwell} to be defined Clamping at $T_m = (T_{min} + T_{max})/2$ T = command variable; $\sigma(t)$, $\varepsilon(t)$ measurement	10^4 cycles, 2 years
3.3	Welded/ joined deformation volume; stress/strain concentrations or embrittlement in/near heat affected zones?	Innov. alloy 1 to be defined He	Thermal (evtl. thermo-mechanical), uniaxial T_{min} = coolant inlet, T_{max} = coolant outlet t_{dwell} = 2 h T_{dwell} to be defined Clamping at $T_m = (T_{min} + T_{max})/2$ T = command variable; $\sigma(t)$, $\varepsilon(t)$ measurement	10^4 cycles, 2 years

Experiment 4: Material development; Coolant coating compatibility

Test No.	Comments	Target Coating* Coolant*	Parameter Definition	Expected Duration
4.1	Suitable instrumentation to measure electrical conductivity of coating	f/m steel 1 to be defined liquid metal	Thermal (evtl. thermo-mechanical), uniaxial T_{min} = 250 °C, T_{max} = 550 °C t_{dwell} = 2 h, T_{dwell} to be defined Clamping at $T_m = (T_{min} + T_{max})/2$ T = command variable; $\sigma(t)$, $\varepsilon(t)$ measurement	10^4 cycles, 2 years
4.2	Suitable instrumentation to measure electrical conductivity of coating	V alloy 1 to be defined liquid metal	Thermal (evtl. thermo-mechanical), uniaxial T_{min} = 350 °C, T_{max} = 700 °C t_{dwell} = 2 h, T_{dwell} to be defined Clamping at $T_m = (T_{min} + T_{max})/2$ T = command variable; $\sigma(t)$, $\varepsilon(t)$ measurement	10^4 cycles, 2 years
4.3	Suitable instrumentation to measure electrical conductivity of coating	Innov. alloy 1 to be defined liquid metal	Thermal (evtl. thermo-mechanical), uniaxial T_{min} = coolant inlet, T_{max} = coolant outlet t_{dwell} = 2 h T_{dwell} to be defined Clamping at $T_m = (T_{min} + T_{max})/2$ T = command variable; $\sigma(t)$, $\varepsilon(t)$ measurement	10^4 cycles, 2 years

* Depending on actual blanket designs and progress in coating development

Experiment 5: Critical design issues

To be defined; e.g. adjust loading conditions of of-normal operation events

Preliminary Conclusions

- In-situ experiments are the closest approach to real fusion conditions. In-situ fatigue properties e.g. can differ fundamentally from those of postirradiation tests.

- A suitable hollow push-pull (creep-)fatigue specimen meets together with a novel concept for a miniaturized universal testing machine inside a vacuum chamber the requirements for:
  - simultaneous and independent in-situ tests on 3 fully instrumented specimens
  - efficient heat remove and temperature control
  - design relevant standard material characterization tests under in-situ conditions
  - flexibility with respect to
    specimen - coating - coolant combinations, and
    irradiation - heat - mechanical load combinations.

- The hollow fatigue specimen is already tested and feasibility considerations on the universal testing machine and a helium gas coolant loop has been done.

- Not the level of specimen miniaturization limits the number of in-situ tests but the size of the push-pull rods and the specimen instrumentation.

- Categories of necessary in-situ experiments and boundary conditions for a test matrix has been discussed.
  An initial test matrix for a 8-10 years program on 12-15 specimens was proposed; *requires further discussions.*
  Final test matrix needs close and ongoing cooperation with the design and SSTT communities.

IFMIF-CDA Test Cell/Users Task CDA-D-5

Necessary In-situ Experiments for All Classes of Materials Investigated and Concepts for In-situ Test Facilities

S. Hamada, K. Noda, Y. Katano
IFMIF-CDA Test Cell/Users Group of JAERI

1. Introduction

In-situ experiments using IFMIF are important to evaluated materials irradiation behavior during operation of fusion reactors, since some materials properties are substantially affected by radiation effects under irradiation. In this task, necessary in-situ experiments for structural materials, ceramic breeders and ceramic insulators/diagnostic materials are identified, and some preliminary concepts of in-situ experiment facilities are described.

2. Structural Materials

(1) In-situ experiments for structural materials

The objects of in-situ experiments are phenomena which may occur by the interaction between irradiation damages and other environmental conditions during irradiation. In-situ experiment items are as follows:

(1) Creep
(2) Stress-Cracking Corrosion
(3) Fatigue
(4) Corrosion Fatigue
(5) Creep-Fatigue
(6) Creep-Fatigue in Corrosion Environment

Creep tests under irradiation could be replaced by creep tests using pressurized tube specimens for which creep is evaluated by PIE.

(2) Requirements for in-situ experimental facilities.

- Usage of miniaturized specimens is desirable.
- Temperature control and monitor during irradiation.
- Systems to detect strain and load.
- Consideration of life time of these systems under irradiation.
- Size and volume of facilities are as small as possible.
- Good remote-handling.
- Structure for easy sample exchange and maintenance.
- Control of water quality in IASCC tests.

(3) Experimental conditions

1) Materials

Low activation ferritic steels, Vanadium alloys, SiC/SiC composites, Innovative materials

2) Specimen size/shapes

Usage of specimens with a rod shape such as hourglass type specimens is desirable for tests related to fatigue.

3) Test conditions

- Temperature :

Ferritic steels	(300 - 500 C, corrosion;100-300 C)
Vanadium alloys	(400 - 600 C)
SiC/SiC composites	(600 - 1000 C)
Innovative materials	(300 - 1000 C)

- Atmosphere :
  Helium gas for experiments of fatigue and creep- fatigue.
  High temperature and high pressure water for tests in corrosion atmosphere.

- Strain rate
  Fatigue; 0.1%/s
  Stress-cracking corrosion: $1X10^{-7}$

- Flux and Fluence; 5-20 dpa/y and 50- 150 dpa

In-situ experiments up to high fluence are somewhat difficult (unrealistic) from standpoints of measurements for long period and occupation of large test volume. Some ideas to shorten in-situ test period are required. In case of IASCC, combination of irradiation up to medium fluence levels in the stress/corrosion environment applied state without in-situ measurement (simple jig may be needed but the occupied space is not so large.) and in-situ experiment at high fluence levels may be useful.

4) In-situ measurements
- Strain
- Temperature
- Load
- Cycle number for fatigue tests

(4) Proposed concept of the in-situ test facility for structural materials

1) Measurement systems
- Strain measurement system
- Temperature monitoring system

2) Control systems
- Temperature control system
  including coolant gas and heating system
- Loading system
- Maintenance system of water quality for tests in corrosion environment

3. Ceramic Breeders

(1) Necessary In-situ Experiments for Ceramic Breeders
-Materials development phase-

*Most designs of fusion blanket are made with concept of continuous tritium recovery during operation.

*In-situ tritium recovery experiments up to end of life are important for materials development and fusion blanket design.

*Moisture (HTO/H_2O) in environment has large influence on materials properties of ceramic breeders.

*All irradiation tests for both in-situ measurements and PIE to evaluate tritium release performance and durability should be carried out in in-situ experiment systems in which moisture level can be controlled by sweep gas.

(2) Requirements for In-situ Experiments

1) Materials

Present candidate materials ; Li_2O, Li_2ZrO_3, Li_2TiO_3, $LiAlO_2$, Li_4SiO_4
Innovative materials

2) Specimen sizes/shapes

Various shapes of ceramic breeders (blocks, pebbles, tubes) are used for fusion blanket designs. Specimen sizes/shapes affect temperature gradient during irradiation. Microstructures development in irradiated specimens was found to depend on temperatures and temperature gradients. So, specimens with some kinds of sizes/shapes should be examined.

*Disks (10 mm in diam. X 2 mm in thick.)

*Pellets (10 mm in diam. X10 mm in height)

* Pebbles (1 mm in diam.)

*Compatibility test specimens;
Breeder (disks, 5 mm in diam. X 1.5 mm in thick.)
Structural (disks, 5 mm in diam. X 0.5 mm in thick.)

3) Test conditions:

*Neutron flux; 5-10 dpa/y (Medium to low flux region)
*Neutron fluence; Max. 40 dpa
*Temperature; 300-900 C
*Sweep gas; He, He+H_2 (0.1-1 %)

4) In-situ measurements:

*Tritium release rate
*Temperature of specimens

5) PIE:

Mechanical integrity, Dimensional change, Density change, Microstructural change, Fracture strength, Tritium/Helium retention, Thermal conductivity, Radiation damage, Compatibility, Li burn-up, etc.

6) Others

*Size/volume of in-situ experiment capsules is as small as possible.
*Neutron fluence/spectrum is monitored at proper specimen position by measurements after irradiation.
*Neutron flux monitor during irradiation.

(3) Proposed Concept of the In-situ Test Facility for Ceramic Breeder
-Materials development phase-

1) Irradiation capsule of In-situ experiments

a) Irradiation capsule for disk specimens

*Sweep gas capsule with gas gap for specimen temperature control.
*3 capsules at 3 different temperatures for each materials.
*1 capsule contains 5 specimens.

b) Irradiation capsule for pellet specimens

*Sweep gas capsule with gas gap for outer specimen surface temperature.
*1 capsule at 1 temperature gradient for each materials.
*1 capsule contains 2 specimens.

c) Irradiation capsule for pebble specimens

*Sweep gas capsule with gas gap for temp. at outer surface of pebble bed.
*1 capsule at 1 temperature gradient for each materials.
*1 capsule contains a pebble bed (1 cm in diam. x1 cm in height).

d) Irradiation capsule for compatibility test specimens

*Sweep gas capsule with gas gap for control of specimen sets temperature.
*3 capsules at 3 different temperatures.
*1 capsule contains 12 specimen sets for 6 kinds of breeders and 3 kinds of structural materials.

2) Measurement/control system

*Sweep gas supply system
*Released tritium measurement/monitor system
*Temperature control system (including coolant gas and gap gas control system)

(4) Necessary In-situ Experiments for Ceramic Breeders and Requirement for Them
-Design database acquisition phase-

*In-situ tritium recovery tests up to end of life should be preformed for selected materials with selected shapes at selected temperature and atmosphere conditions for the reference blanket design.

*Irradiation tests are desired to be carried out in spectrum-tailored neutronic conditions using specimen sets (breeder, coolant, neutron multiplier, structural materials) and specially-designed irradiation capsules, from the standpoint dpa and Li burnup.

(5) Proposed Concept of the In-situ Test Facility for Ceramic Breeder
-Design database acquisition phase-

1) Irradiation capsule of in-situ tritium recovery tests.

2) Sweep gas capsule with gas gap for specimen set temperature control.

3) Specimen sets consisting of breeders, coolant, neutron multiplier, structural materials

4) Measurement /control system including sweep gas supply system, tritium release measurement system, temperature control system.

4. Insulator Ceramics/Diagnostic Materials

(1) Necessary In-situ Experiments for Insulator Ceramics/Diagnostic Material

*Radiation Induced Conductivity (RIC) and Radiation Induced Electrical Degradation (RIED) degrade electrical insulation properties of ceramics during irradiation. RIC can be measured only during irradiation. Although RIED can be measured after irradiation, it is expected to occur at low fluence. IFMIF cannot be frequently stopped to check RIED. Thus, in-situ experiments for electrical resistivity of insulator ceramics are necessary to investigate RIC and RIED.

*Since dielectric loss changes due to RIC and RIED, in-situ experiments for dielectric loss of insulator ceramics are required.

*Luminescence due to irradiation can be measured only during irradiation. Optical absorption due to radiation-induced defects can be detected after irradiation, but optical degradation of optical diagnostics materials occurs at low fluence. In the same reason as the case of electrical resistivity, in-situ experiments for optical properties of optical diagnostics materials are needed.

(2) Requirements for In-situ Experiments

1) Materials:

Al_2O_3, MgO, AlN, $MgAl_2O_4$, SiO_2, Si_3N_4, Optical fiber (Currently available material, materials development)

2) Specimen sizes/shapes:

Disks (8.5 mm in diam. x 0.2 mm in thick); Electrical resistivity
Rectangular (25^l x 10^w x 3 and 5^t mm^3); Dielectric loss
Fiber wire (0.25 mm in diam. 30 pieces x ~8000 mm); Optical properties

3) Test conditions:

Neutron flux: 10^{-5} to 20dpa/y (Medium to low flux region)
Neutron fluence: 10^{-3} to 50dpa
Temperature: RT-800C (Design depend)
Liq.He to -180C (Cryogenic window)

Additional condition:
Applied electric field (for RIED) 1-1.5kV/cm

4)In-situ measurements:

Electrical resistivity (RIC/RIED)
Dielectric loss
Optical absorption/Luminescence

(3) Proposed Concept of In-situ Test Facility for Insulator Ceramics/Diagnostic Materials

1) Irradiation capsules

a) Irradiation capsule for electrical resistivity (disk specimens)

* RIC/RIED measurement specimen holders with gas gap/heater for specimens temperature control.
* One specimen holder contains 16 specimens. (2/material x 8 materials)
* 4 specimen holders at 4 different temperatures.
* One capsule contains 4 specimen holders.

b) Irradiation capsules for dielectric loss (rectangular specimens)

*Dielectric loss capsule with gas gap/heater for specimens temperature control.

c) Irradiation capsule for optical properties (optical fiber)

* Optical absorption/luminescence capsule with gas gap for specimens temperature control.
* One capsules contains 3 specimens.
* 4 capsules at 4 different temperatures.

2) Measurement/control system

* Temperature control system
* RIC/RIED measurement system
* Optical absorption/luminescence measurement system
* Dielectric loss measurement system

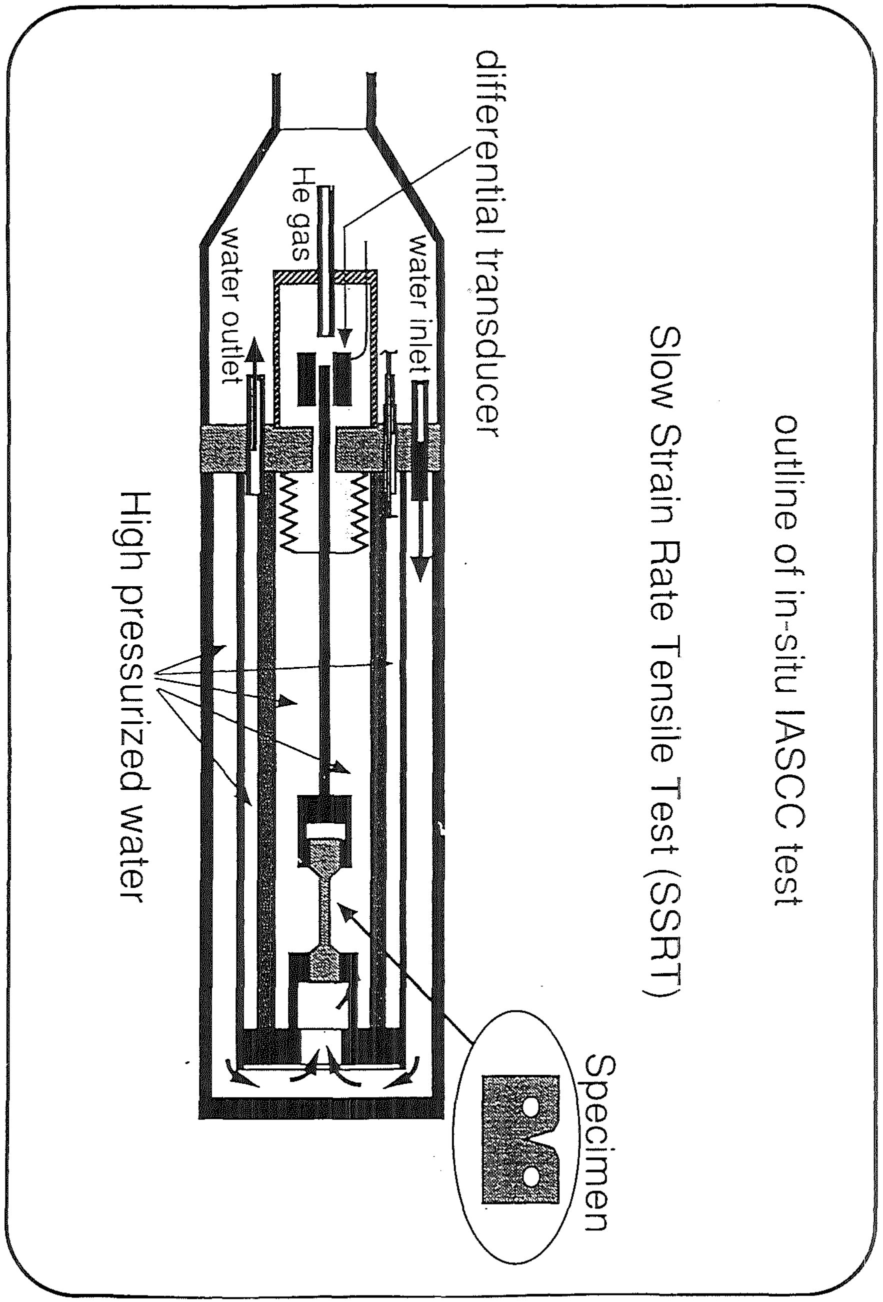

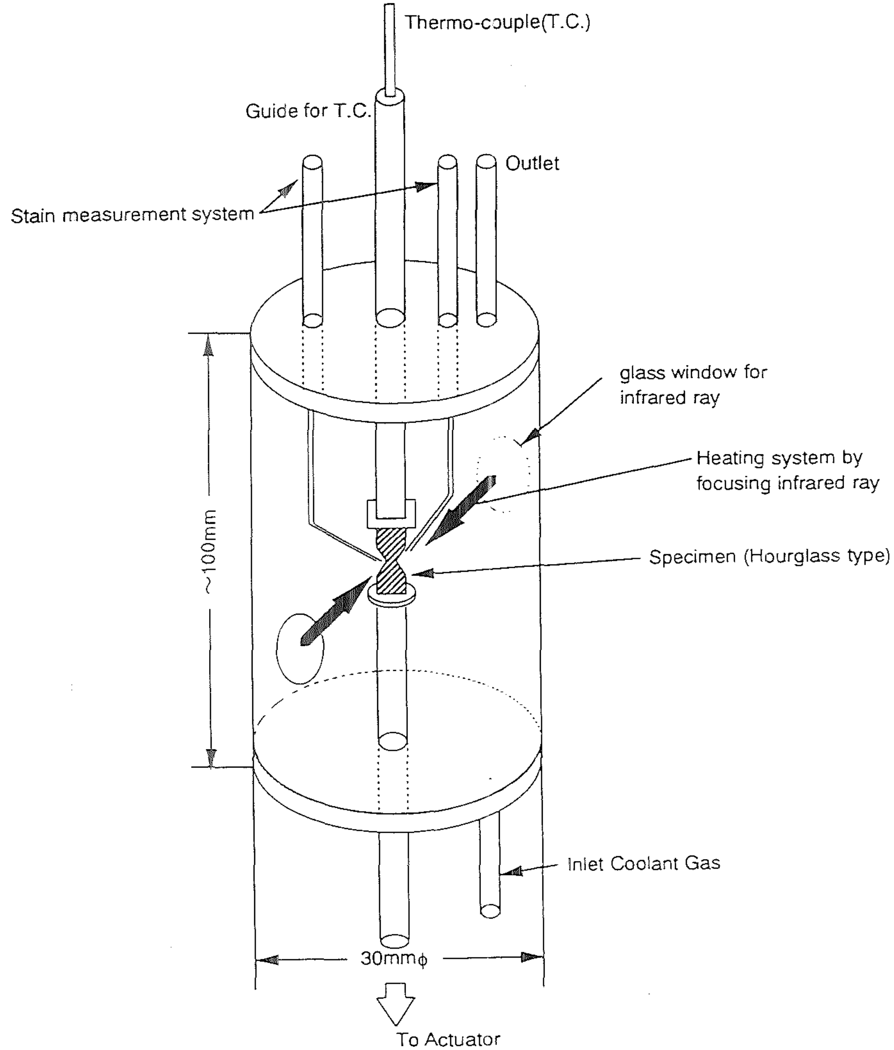

Concept of in-situ fatigue experiment

Irradiation Capsule for Disk Specimens

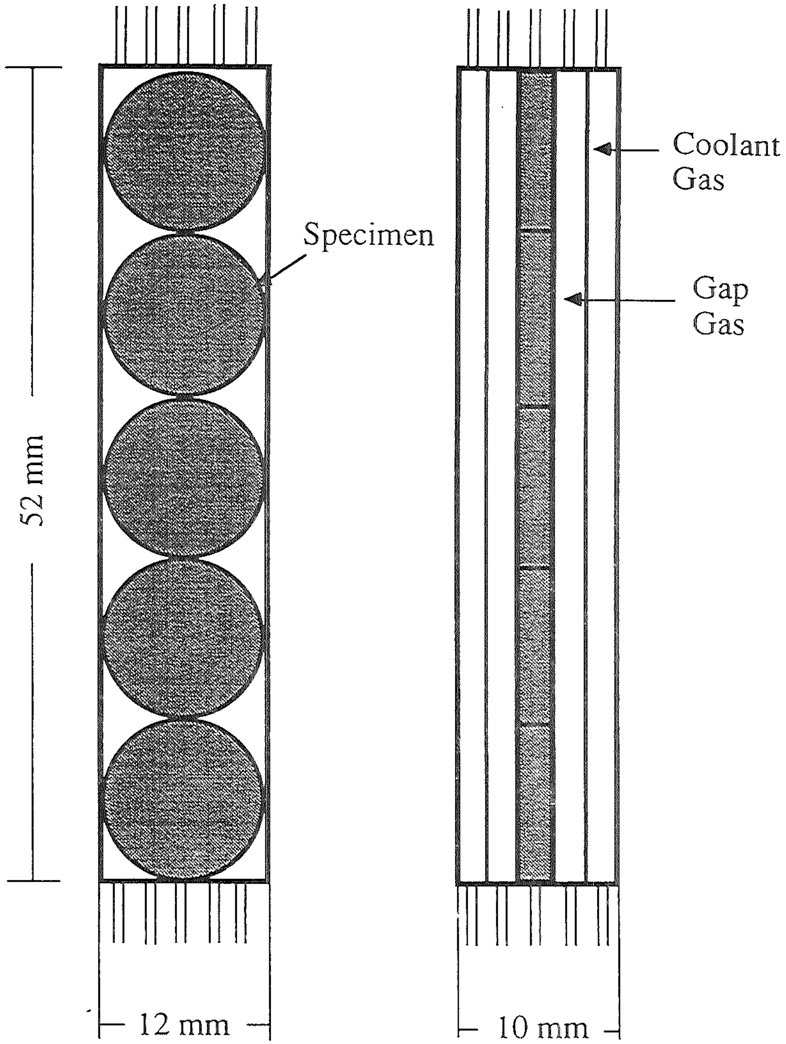

Disk Specimens:10 mm in diam. x2 mm in thick.

Irradiation Capsule for Pellet Specimens

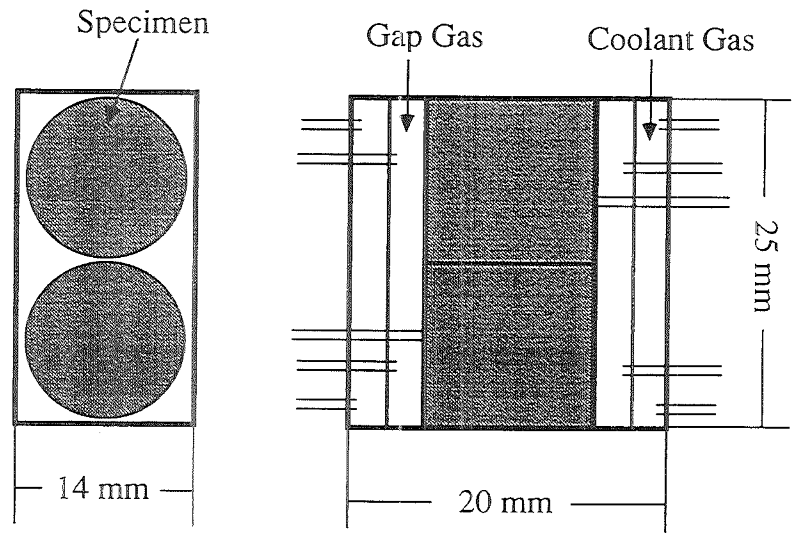

Pellet Specimens:10 mm in diam. x 10 mm in thick.

Irradiation Capsule for Pebble Bed

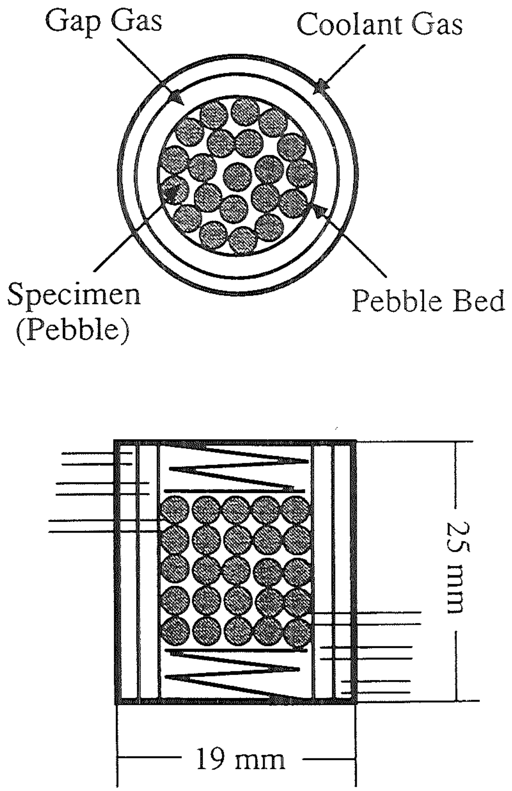

Pebble: 1 mm in diam.
Pebble Bed: 10 mm in diam. x 10 mm in height

Irradiation capsule for compatibility test specimens

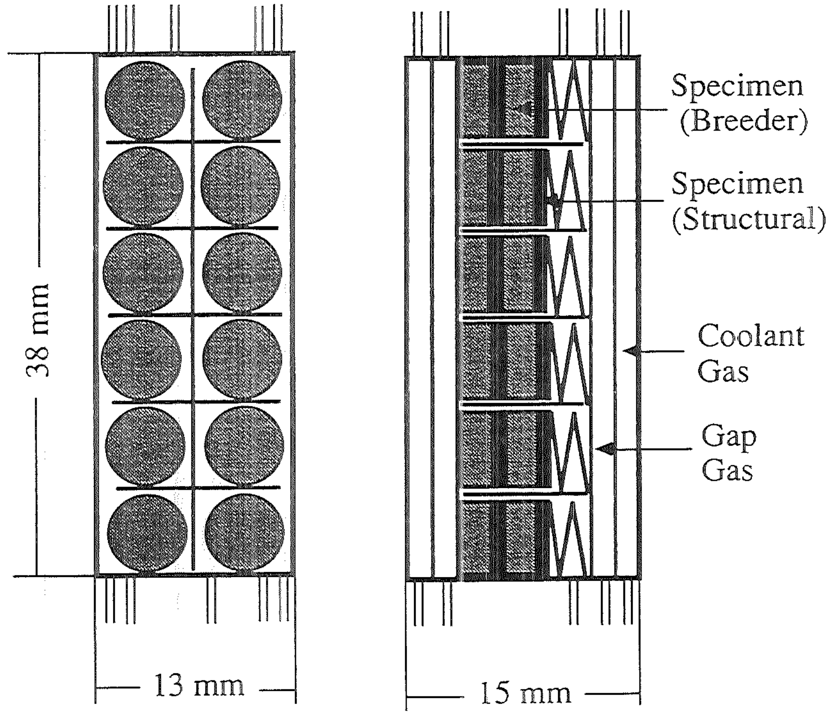

Compatibility Specimens:
Breeder (disks, 5 mm in diam. X 1.5 mm in thick.)
Structural (disks, 5 mm in diam. X 0.5 mm in thick.)

Irradiation Test Volume for In-situ experiments of Ceramic Breeder

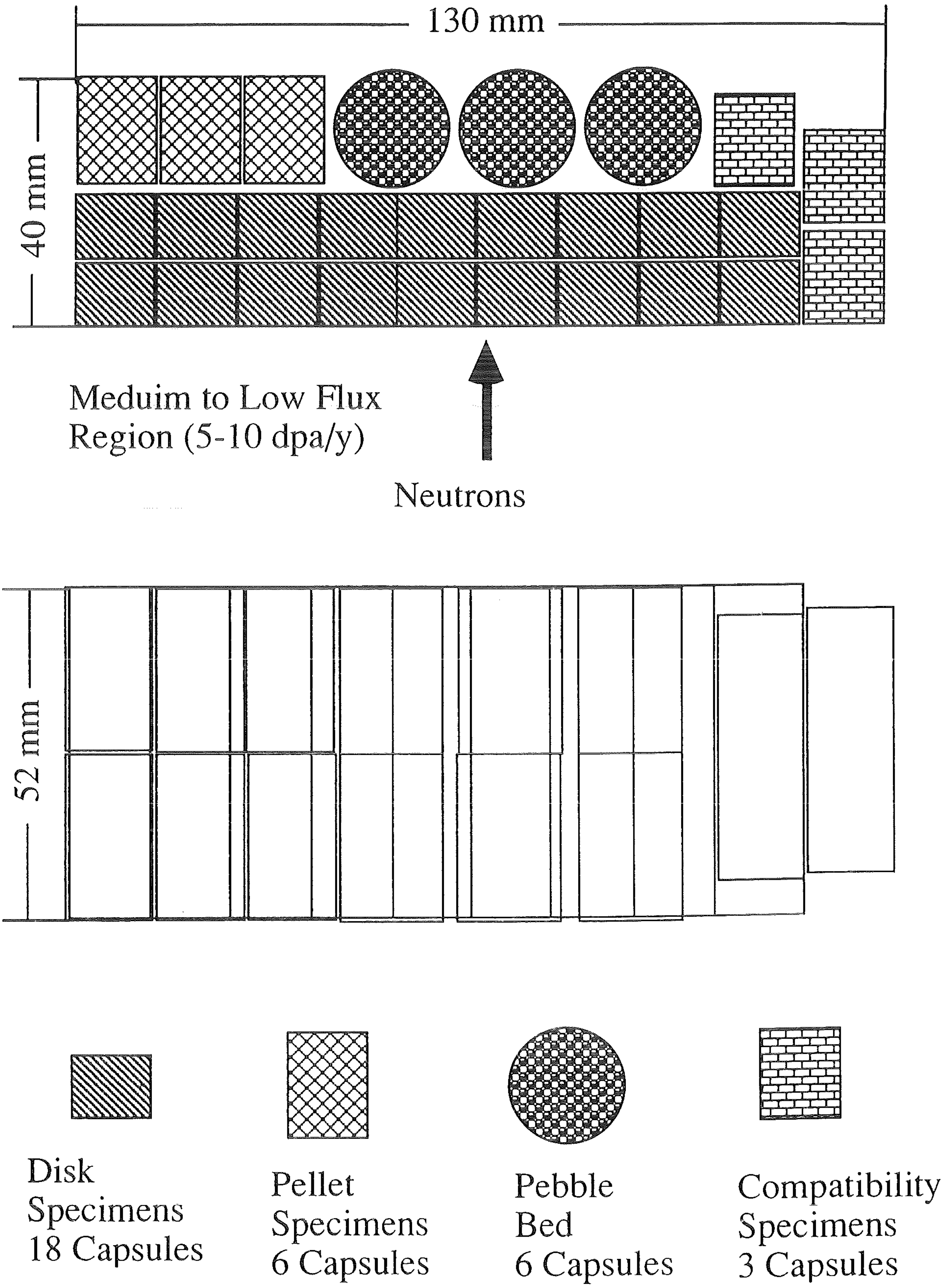

Irradiation capsule of In-situ electrical conductivity

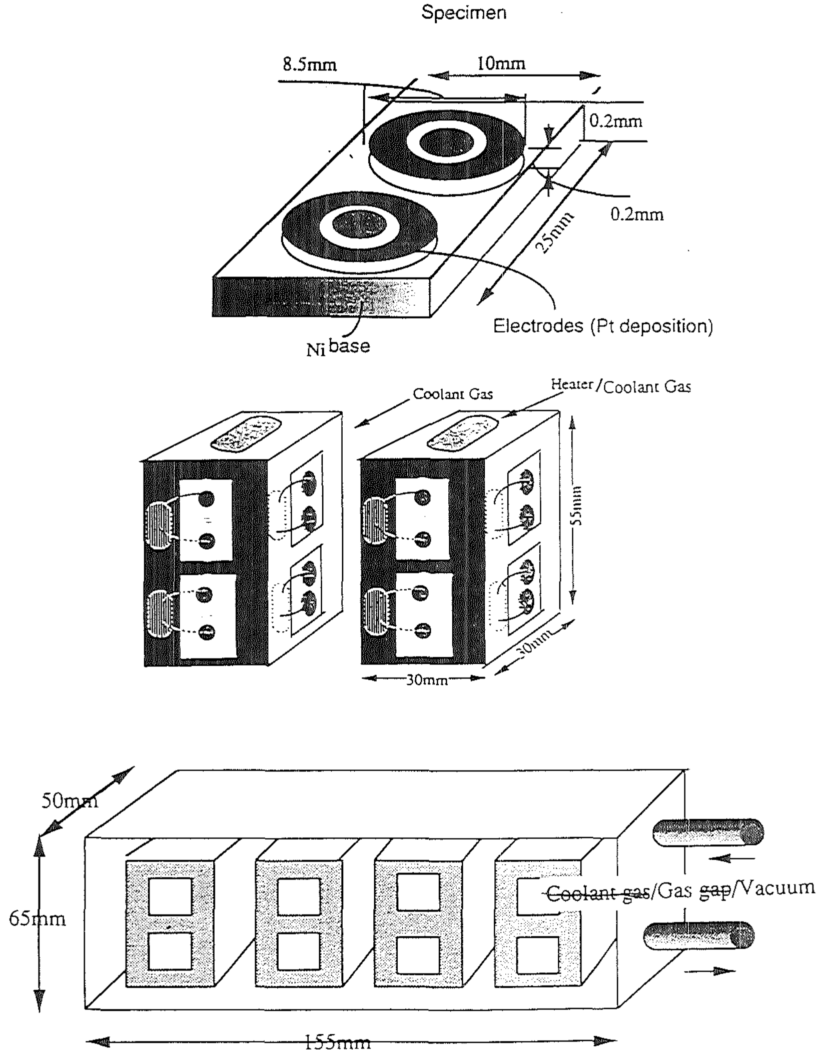

Irradiation capsule of In-situ and PIE optical fiber

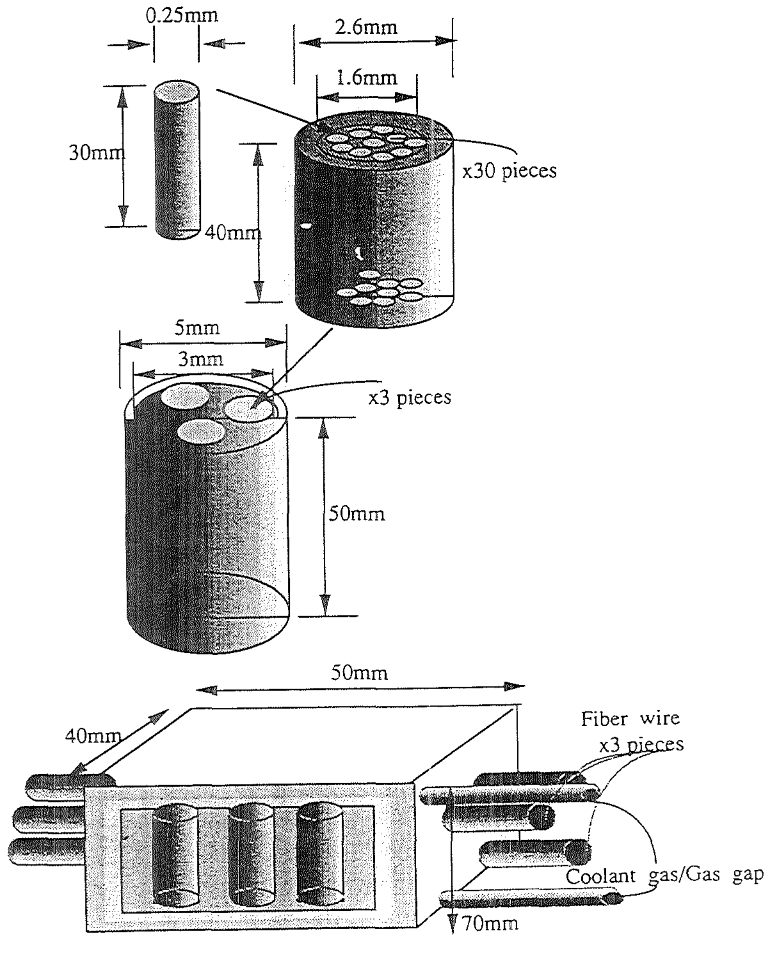

Specimen packet

IFMIF-CDA Test Cell/Users Task CDA-D-6

Design Concepts for Typical Test Modules and Their Interface with Test Cell
(Proposed Concepts for Test Modules and Their Interface with Test Cell)

T. Hoshiya, K. Noda
IFMIF-CDA Test Cell/Users Group of JAERI

1. Required Functions for Test Modules

Test modules have to include necessary functions to carry out all the irradiation experiments for several kinds of specimens in packets; structural materials, ceramic breeders, insulator ceramics, diagnostic materials and advanced materials. For structural materials, it is important to carry out heavy irradiation experiments (fluence dependent experiment) and the Post Irradiation Examination (PIE) for the design of the structure of fusion reactors. For ceramic breeders, insulator and diagnostic materials, the in-situ experiments (CDA-D-5) is also indispensable for analyzing time dependent phenomena such as continuous tritium recovery during operation.

It is also key issues for improvement of performance of test module to provide good interfaces with Test Assembly and Test Cell and also to shorten the time required for the replacement and maintenance of test module from the standpoint of function desired for test modules.

2. Test Modules and Their Interface with Test Cell

(1) Required items of test modules

Test modules have to possess the sufficient removal capacity for heat generation of packets to realize proper specimen temperature control.

It is also necessary to provide the good performance of quick and easy insertion / removal of test modules, because replacement and maintenance time governs all the function of the test module, test assembly and test cell in terms of the efficiency and the reliability.

Required items of test modules are as follows:

- Realization of goal temperature and neutron fluence (dpa) of specimens
- Removal of heat generation by nuclear heating and gamma-ray heating
- Quick and easy replacement (insertion and removal) of test modules
- Monitoring / diagnostic system
- Coherent interfaces with test assembly and test cell
- Cleanup system to prevent radioactive contamination in remote replacement and maintenance procedures

(2) Proposed Concepts of the Test Module

1) Monitoring / diagnostic system

- Temperature and fluence monitoring during irradiation

-Taking into account of proposed packet volume (CDA-D-3), flux region have to be separated into two parts; high flux region and medium and low flux region as shown in the contour map of neutron flux (Fig. D6J-1) with respect with standard beam size (20 x 5 cm^2).

- Temperature regions in test modules are needed to be separated into three parts; high temperature region, medium temperature region and extremely low temperature region.

- Usage of multiple thermocouple which can be used for the synchronous measurement of multi-point of specimen

- Usage of fluence monitor and the Self Powered Neutron Detector (SPND)

- Usage of the Close Circuit TV (CCTV) system including SiO_2 optical fiber with irradiation resistance

2) Quick and easy replacement (insertion and removal) of test modules

By using shape memory alloy (SMA) driving element, the quick replacement technique can extensively apply to the design of test modules, test assembly and test cell. The SMA joints can be used for connecting and disconnecting the coupling in a few minutes by simply controlling the SMA temperature. Two different kinds of SMA can be used for driving element of joints or connectors in medium temperature region (RT - 373K) and in high temperature region (373K - 873K). One is Ti-Ni based SMA for use in the medium temperature region and the other is Ti-Pd based high temperature SMA (HTSMA) for use in the high temperature region.

- Quick Replacement Technique (including remote handling and maintenance) using SMA driving element

- Remote handling robotics

3) Re-instrumentation and Re-irradiation technique

- Re-instrumentation system with re-installed thermocouple, SPND and fluence monitor

- Re-irradiation system after irradiation of specimens with medium and low fluence to obtain heavy damage of specimens

4) Homogenization technique of damage levels of specimens in IFMIF irradiation field with flux gradient (See CDA-D-9)

- Rotating system of test module during irradiation

- Exchange system of specimen irradiation position in test modules

5) Differentiation in function between test modules

- In-situ test module --------- special test module

- Heavy irradiation test module --------- same above

- Re-irradiation test module --------- same above

- Re-instrumentation test module -------- same above

- Sweeping gas test module --------- same above

- Cryogenic temperature test module --------- same above

- Pulse irradiation test module --------- same above

- Normal irradiation test module

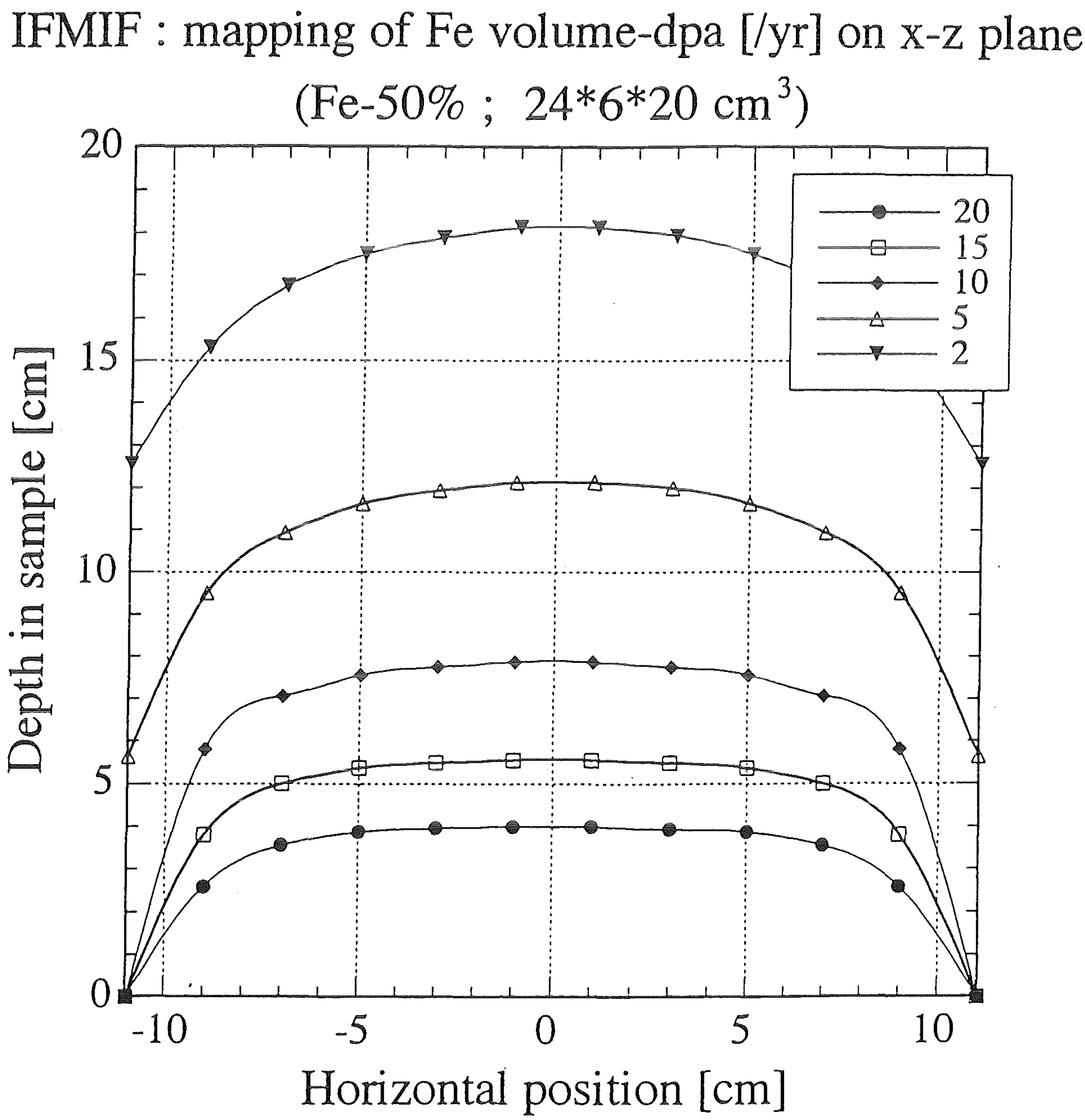

IFMIF : mapping of Fe volume-dpa [/yr] on x-z plane
(Fe-50% ; 24*6*20 cm³)
20
15
10
5
0
-10
-5
0
5
10
Depth in sample [cm]
Horizontal position [cm]
20
15
10
5
2

Fig. D6J-1

Task CDA-D-6: Design Concept for Typical Test Modules

Presented by
J. R. Haines (ORNL)
at the
IFMIF-CDA Technical Workshop
on the Test Cell System
July 5, 1995

Topics for Typical Test Module Design Concepts

- Assumptions/design features

- Arrangement of modules

- Cooling system equipment

Assumptions and Design Features for Test Modules

- Five modules including the high-flux module

Region	Number of Modules	Number of Chambers per Module	Total Volume (L)
High-flux	1	3	0.5
Intermed.-flux	2	2	6
Low-flux	2	1	8

THE TEST CELL CONSISTS OF FIVE TEST MODULES

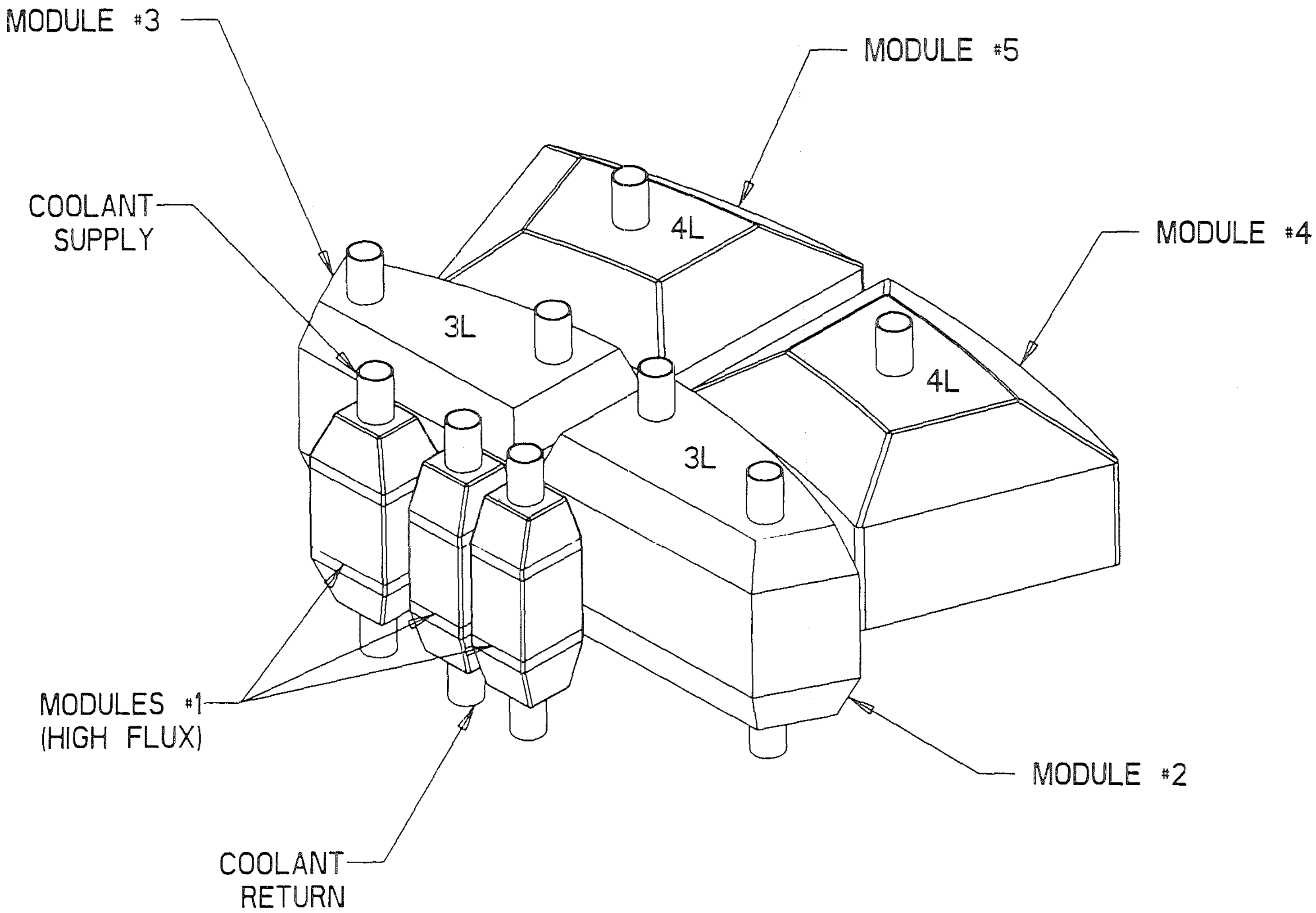

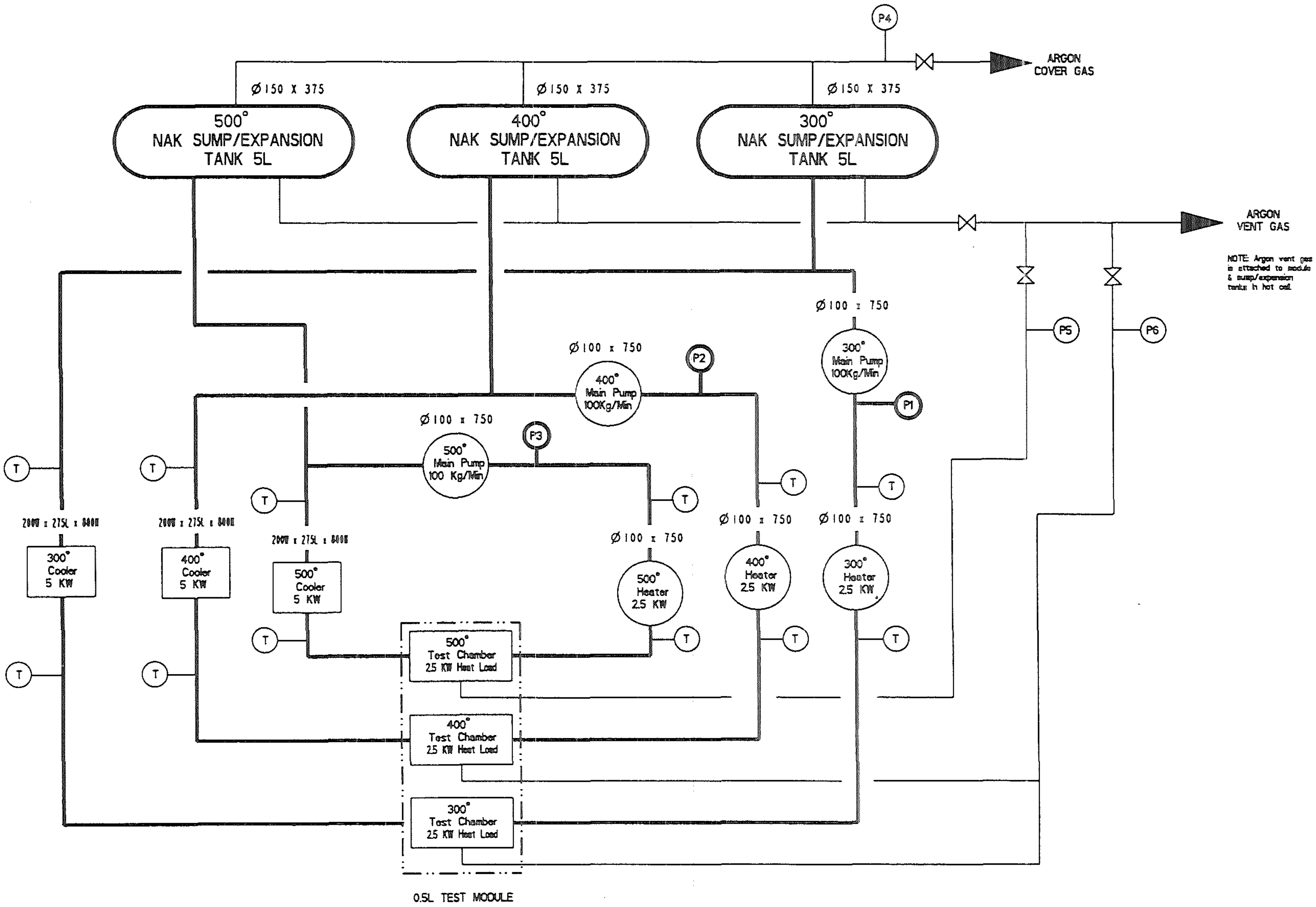

P4
ARGON COVER GAS
Ø150 X 375
Ø150 X 375
Ø150 X 375
500° NAK SUMP/EXPANSION TANK 5L
400° NAK SUMP/EXPANSION TANK 5L
300° NAK SUMP/EXPANSION TANK 5L
ARGON VENT GAS
NOTE: Argon vent gas is attached to module & sump/expansion tanks in hot cell.
Ø100 x 750
300° Main Pump 100Kg/Min
P1
P5
P6
Ø100 x 750
400° Main Pump 100Kg/Min
P2
Ø100 x 750
500° Main Pump 100 Kg/Min
P3
T
200W x 275L x 840H
300° Cooler 5 KW
200W x 275L x 840H
400° Cooler 5 KW
200W x 275L x 840H
500° Cooler 5 KW
Ø100 x 750
500° Heater 2.5 KW
Ø100 x 750
400° Heater 2.5 KW
Ø100 x 750
300° Heater 2.5 KW
500° Test Chamber 2.5 KW Heat Load
400° Test Chamber 2.5 KW Heat Load
300° Test Chamber 2.5 KW Heat Load
0.5L TEST MODULE

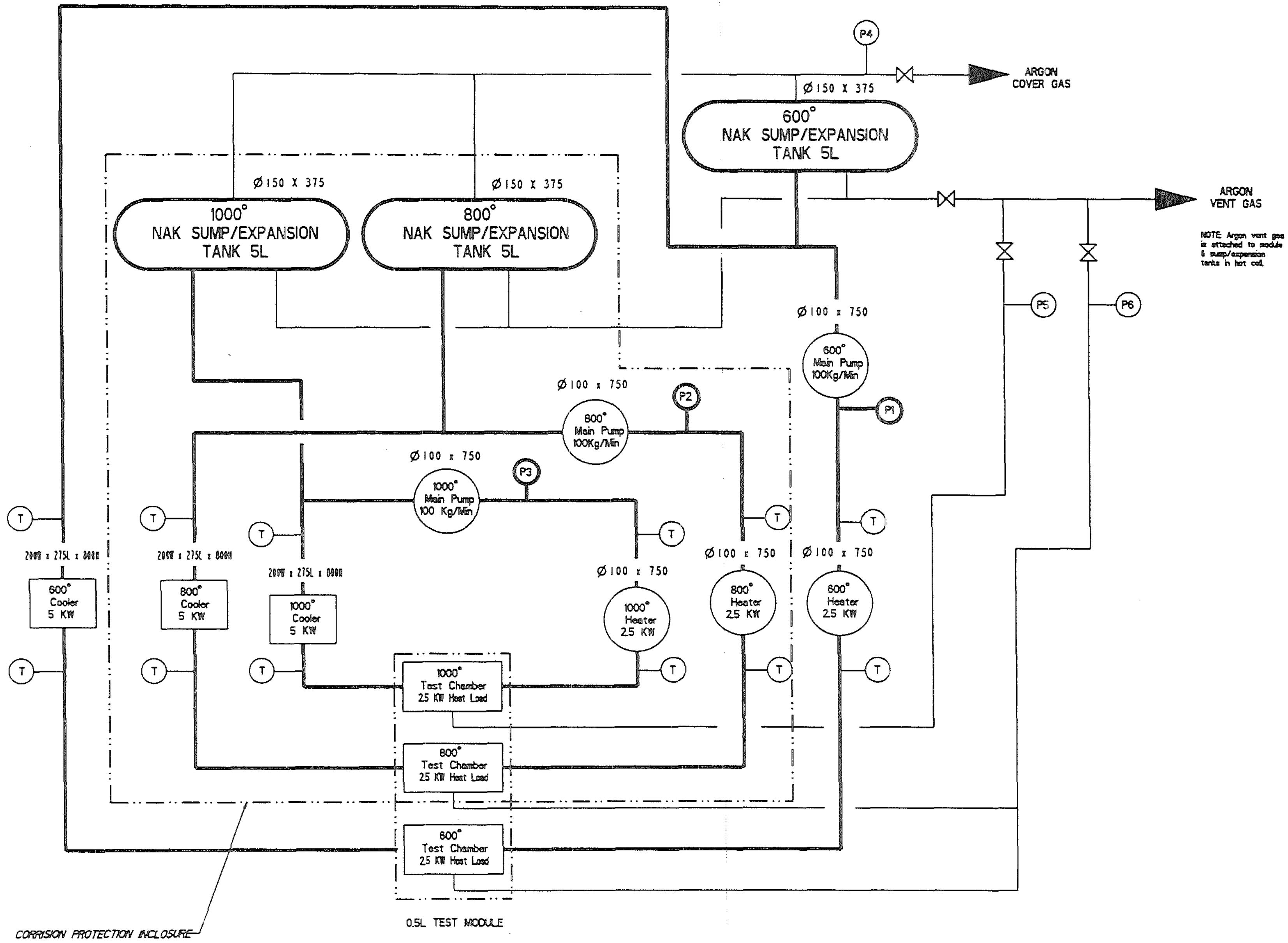
ARGON
COVER GAS
P4
Ø150 X 375
600°
NAK SUMP/EXPANSION
TANK 5L
ARGON
VENT GAS
NOTE: Argon vent gas is attached to module & sump/expansion tanks in hot cell.
Ø150 X 375
1000°
NAK SUMP/EXPANSION
TANK 5L
Ø150 X 375
800°
NAK SUMP/EXPANSION
TANK 5L
Ø100 x 750
600°
Main Pump
100Kg/Min
P1
P5
P6
Ø100 x 750
800°
Main Pump
100Kg/Min
P2
Ø100 x 750
1000°
Main Pump
100 Kg/Min
P3
T
200W x 275L x 800H
600°
Cooler
5 KW
200W x 275L x 800H
800°
Cooler
5 KW
200W x 275L x 800H
1000°
Cooler
5 KW
Ø100 x 750
1000°
Heater
2.5 KW
Ø100 x 750
800°
Heater
2.5 KW
Ø100 x 750
600°
Heater
2.5 KW
1000°
Test Chamber
2.5 KW Heat Load
800°
Test Chamber
2.5 KW Heat Load
600°
Test Chamber
2.5 KW Heat Load
0.5L TEST MODULE
CORRISION PROTECTION INCLOSURE

THE COOLING SYSTEM OF EACH TEST MODULE IS SELF CONTAINED AND MOUNTED TO THE TOP OF THE VTA

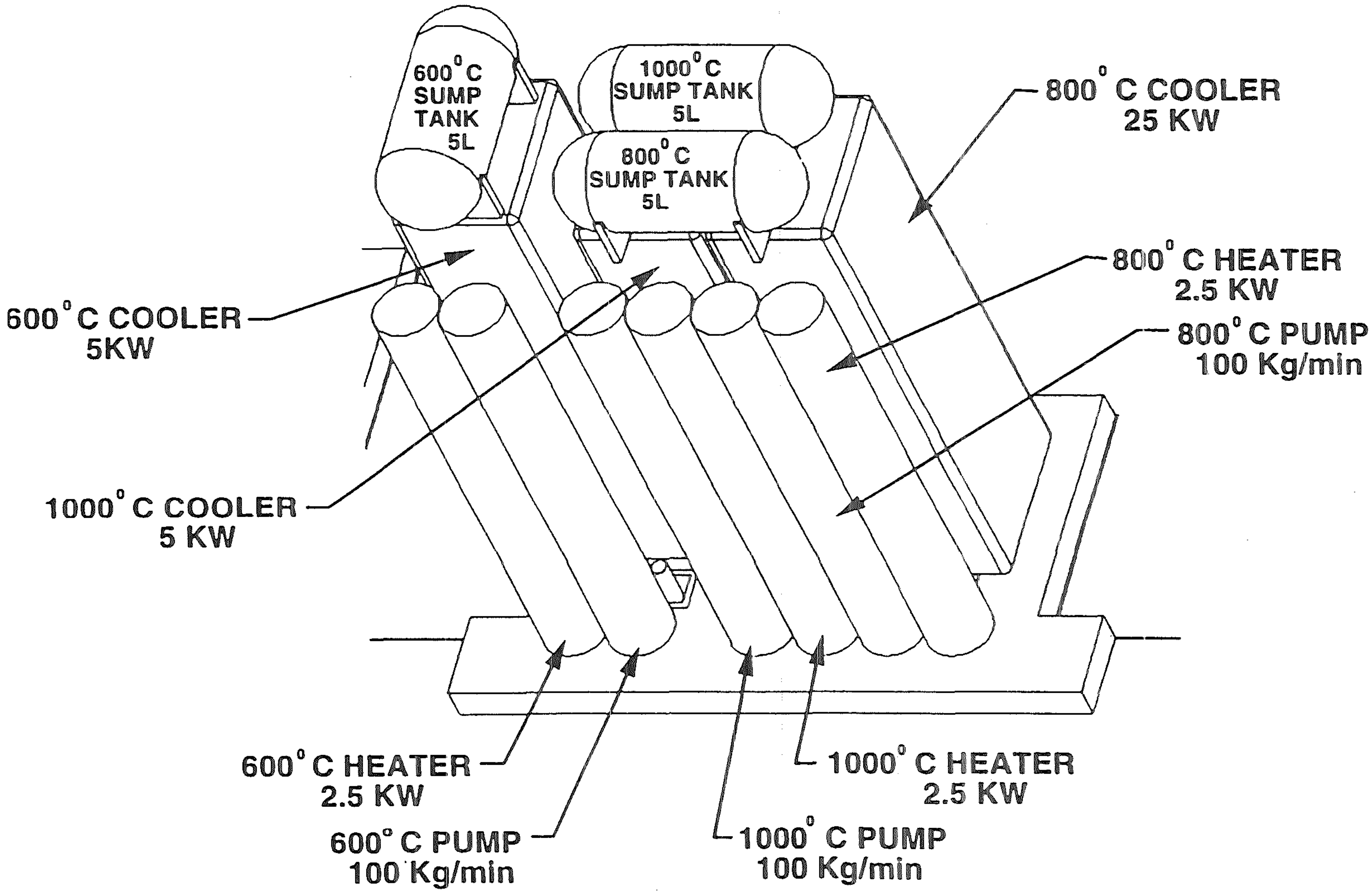

THE TEST CELL CEILING PENETRATION CONSIST OF FIVE VERTICAL TEST ASSEMBLIES AND A FLOOR PLUG

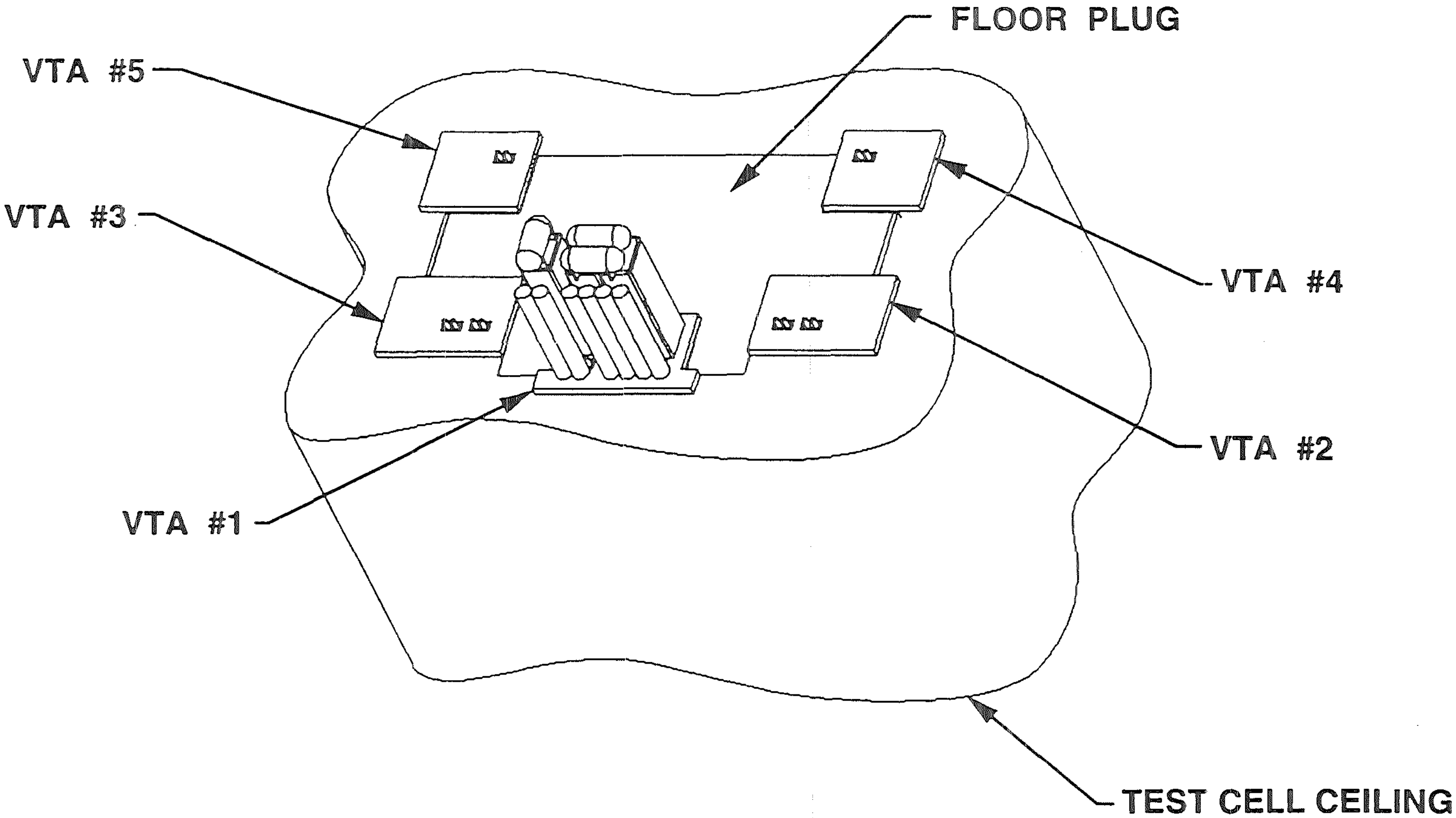

THE HIGH FLUX TEST MODULE IS SUPPORTED BY VERTICAL TEST ASSEMBLY #1 (VTA)

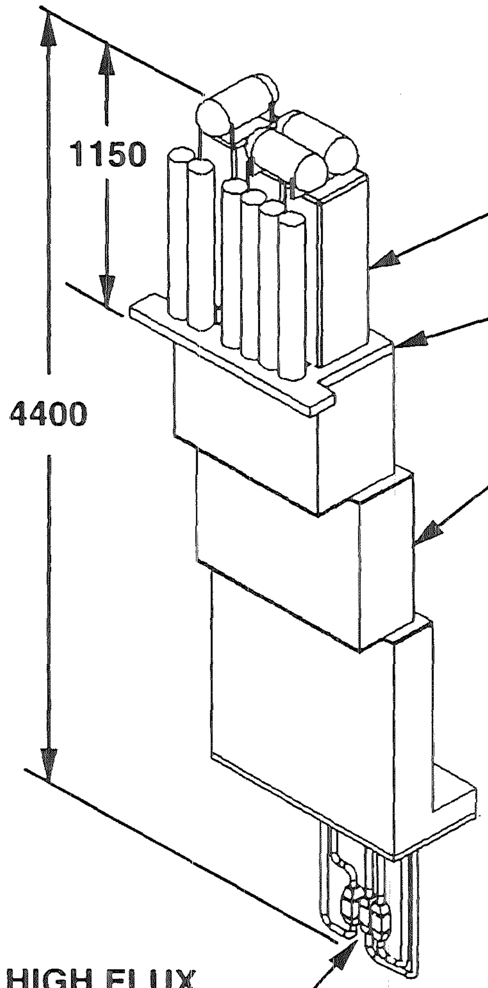

TOTAL WEIGHT APPROXIMATELY 3000 Kg

IFMIF Test Cell/Users Task CDA-D-7 (Interim):

Provide Processed Nuclear Data between 20-50 MeV for Relevant Elements

Task Responsible: Y. Oyama
IFMIF Test Cell/Users Group of JAERI

1. Introduction

Energy of neutrons generated by IFMIF includes higher energy than 20 MeV, i.e. to about 50 MeV. Thus nuclear data of neutron cross sections up to 50 MeV is required to esimate irradiation conditions and to design the facility itself for shielding and safety. However, the present available nuclear data library with high energy is the ENDF/B-VI high energy file but it includes only four nuclides. Since 1990, evaluations of high energy neutron nuclear data have been attempted under Japanese Nuclear Data Commitee, according to request by ESNIT group for the purpose of damage characteristics evaluation study. The process of evaluation usually needs long period due to iteration by reviewing. This activity was taken over by IFMIF CDA task. The evaluations were repeated together with modification or correction of the evaluation code EGNASH. The code was finally established to the SINCROS-II system with the EGNASH-IV code.

2. Nuclides to be included

Priority of nuclides to be evaluated was selected by two ways:

1) Cross Section for Neutron Transport

This includes nuclides for damage analysis of a test matrix, e.g., stainless steel (Fe, Cr, Ni, Mo, V, Ti) and alumina (Al, O), for shielding design, e.g., stainless steel, concrete (H, O, Al, Si, Ca, C, Na, K, Mg), and for acceleartor components (Cu, Fe, Li). From these materials, the following priority was assigned:

1st priority	H, O, Al, Si, Fe
2nd priority	Ca, Cr, Cu, Ni
3rd priority	Li, C, N, Na, Mg, K, Ti, Mn, V, Mo

2) PKA Spectrum and Transmutation Cross Section

This includes nuclides for damage analysis of stainless steel, alumina, etc. and for activation estimation of the accelerator facility. The following priority was assigned:

1st priority	Li, N, O, Si, Al, Fe, Cr, Ni, Cu
2nd priority	Ca, C, Na
3rd priority	Mg, K, Ti, Mn, V, Mo

Finally the following nuclides were selected for evaluation.

H, Li, Be, C, N, O

and

Al, Si, Ca, Na, Mg, K, Ti, Cr, Mn, Fe, Ni, Cu, V, Y, Mo, W

For light nuclides, Monte Carlo code SCINFUL
For intermediate nuclides, SINCROS-II system (including EGNASH-IV)

The file format follows the format for intermadiate energy nuclear data proposed in the NEANSC working party. (Appendix 1)

4. Processed Library

The processed library for neutron transport calculation will be prepared for the library of the MCNP code. The PKA spectrum file is also prepared from the evaluated nuclear data file by using the ESPERANT code.

5. Progress

The first set of evaluated files will be released by the end of March, 1996, and the version-up will be performed with addition of new evaluations. The first set will includes Fe, Cr and Ni, at least.

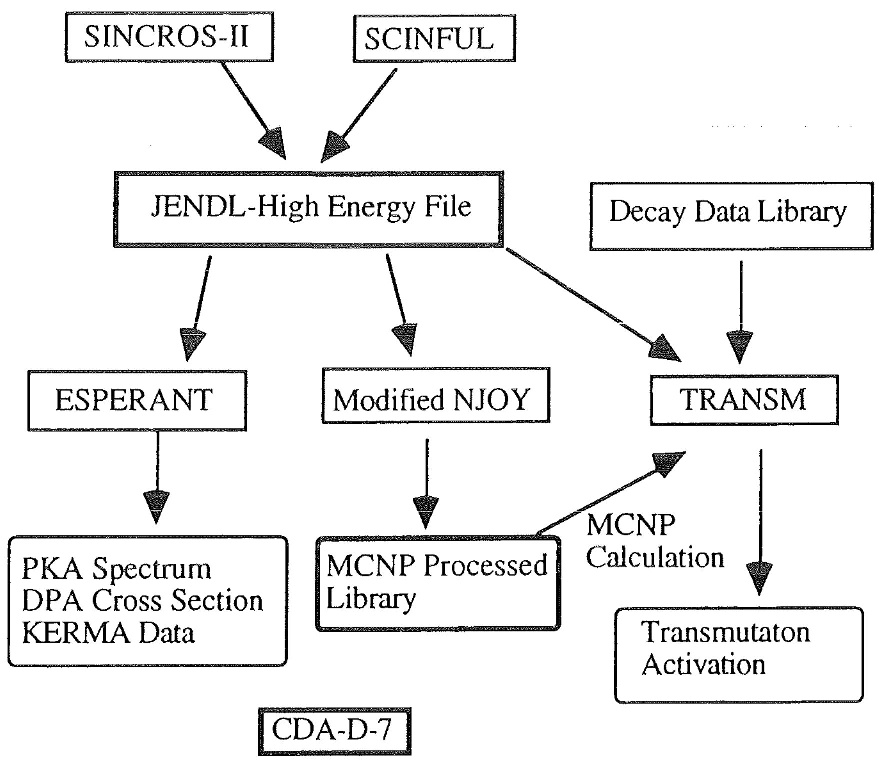

Needs of cross section task for IFMIF

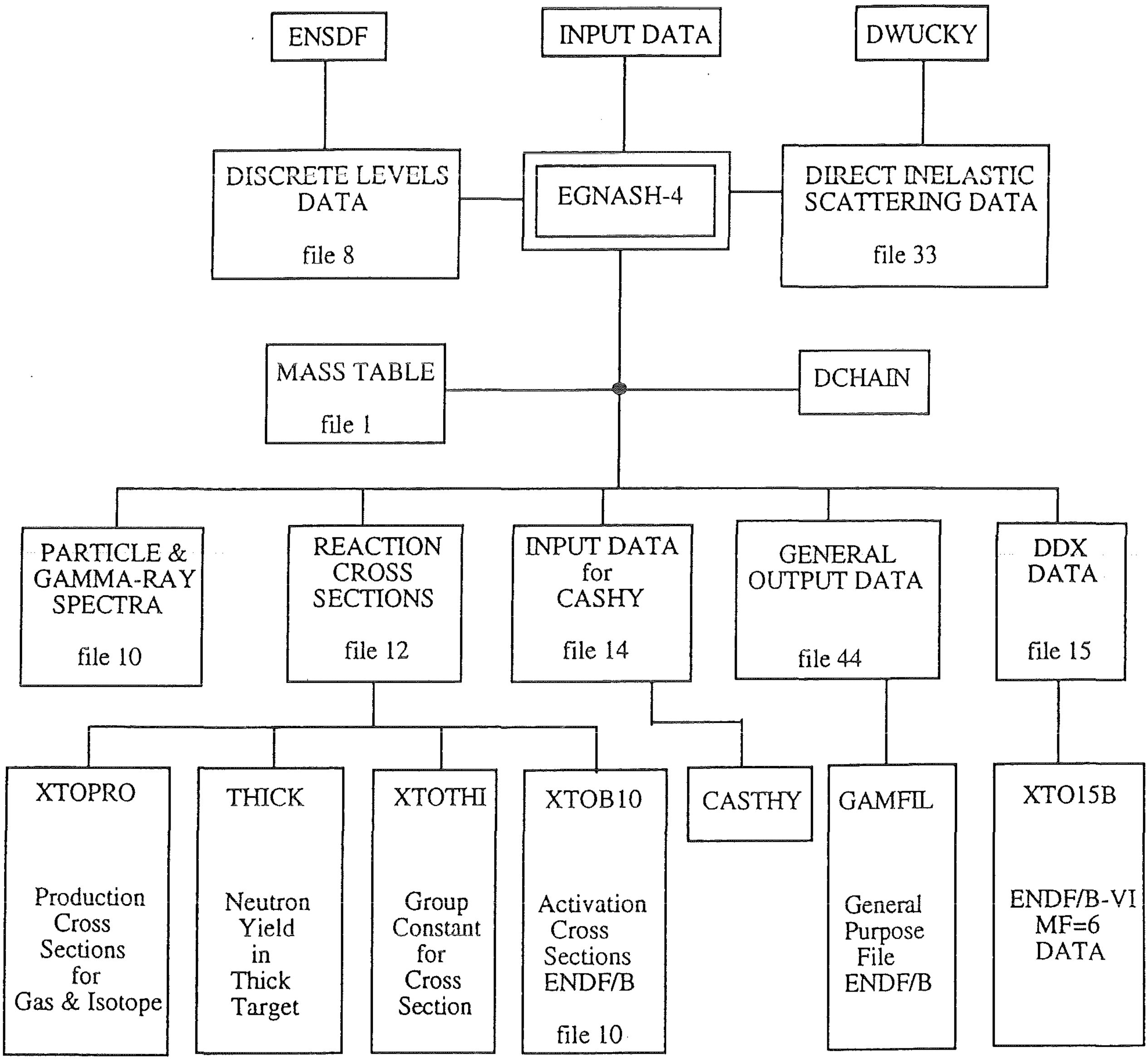

Flow of Data processing in SINCROS-II system

to be submitted to the NEANSC/WPIEC/SG13 meeting at Data Bank on Dec. 9, 1994

Proposal of Format for Intermediate Energy Nuclear Data

T. Fukahori
Nuclear Data Center, Department of Reactor Engineering,
Japan Atomic Energy Research Institute,
Tokai-mura, Naka-gun, Ibaraki-ken, 319-11 Japan

and

A.J. Koning
Netherlands Energy Research Foundation ECN
P.O. Box 1, 1755 ZG Petten, The Netherlands

1. Introduction

NEANSC Working Party on International Evaluation Cooperation (WPIEC) has started a research cooperation on the intermediate energy nuclear data (IEND) as subgroup 13 (SG13). SG13 is organized to research and solve common problems about the IEND evaluation. One of the common problems of SG13 is to make recommendation of IEND format. A survey has been made on the requirements for an evaluated nuclear data file for accelerator-based transmutation by Koning[1], and the report included the format of existing evaluated IEND and recommendations. A few status and reviewal reports[2,3] for evaluated IEND file were presented in the Gatlinburg Conference.

From the summary of inquiry collected by Kikuchi[4], the major applications of IEND are medical use, accelerator-related applications; i.e. spallation neutron source, waste management, and space and astrophysics. These applications need isotope production cross section and double differential light particle, gamma-ray, meson and primary knock-on atom (PKA) spectra for neutron-, proton- and photo-induced reactions, fundamentally. Though it is necessary to include individual product nuclides for isotope production cross sections, it seems that composite particle spectra, which are not identified the emitted reaction and summing up the same particle from all the reaction channels, might be enough to use for each application. It is no meaning to separate the energy region in consideration of format. From these points of view, physical quantities which should be included in evaluated IEND files are defined and their format is proposed in this report.

2. Included Physical Quantities and Format for IEND

2.1 Physical Quantities

The physical quantities which are necessary for evaluated IEND files are roughly classified into cross section (MF=3), angular distribution (MF=4), energy spectrum (MF=5) and double differential particle, gamma-ray, meson and PKA emission spectra (MF=6). Since MF=4 and MF=5 can be combined into MF=6 in ENDF-6 format, only MF=6 should be considered in this report.

For the cross section, total (neutron-induced reaction only), elastic scattering, total reaction (non-elastic), discrete inelastic scattering (not always) and fission channels should be included, and isotope and particle production cross sections are also important. In the case of combination with existing lower energy evaluated file, neutron capture and (n,z) reaction, where z is light charged particle from proton to alpha, cross sections are might be included as an neutron disappearance cross section.

The angular distributions for elastic and discrete inelastic scattering, and fission neutron spectrum should be considered. The double differential cross sections must be included for neutron, gamma-ray, proton, deuteron, triton, He-3, alpha, pi+, pi0, pi-, (K+, K0, K-). Fission related quantities are also included.

2.2 Format and Some Rules

ENDF-6 format must be selected fundamentally. For evaluated IEND file, some quantities must be newly defined. The MF number is defined in section 2.1, and MT number is as following.

MT	MF	quantities
1	3	total (only for neutron-induced reaction)
2	3,6	elastic scattering
3	3	total reaction
5	3,6	isotope production by spallation and evaporation processes
18	3,6	fission (FP yield is stored in MF=6, MT=18)
51-90	3,6	discrete inelastic scattering (not always)
102	3,6	capture (only for neutron-induced reaction)
103-107	3,6	(n,z) reactions (only for neutron-induced reaction)
151	2	resonance information (only for neutron-induced reaction)
201	3,6	neutron production
202	3,6	gamma production
203	3,6	proton production
204	3,6	deuteron production
205	3,6	triton production
206	3,6	He-3 production
207	3,6	alpha production
208	3,6	pi+ production (if necessary)
209	3,6	pi0 production (if necessary)
210	3,6	pi- production (if necessary)
211	3,6	K+ production (if necessary)
212	3,6	K0 production (if necessary)
213	3,6	K- production (if necessary)
451	1	general information
452-458	1	fission-related quantities

For conservation of consistency, some rules should be promised inside the format, for instance, sum rule. The evaluation information and comments are included in MF=1. If fission reaction channel is included, the fission-related quantities, for example, fission neutron spectra (MF=5, MT=18), average prompt neutron number (MF=1, MT=452,455,456), fission product distribution (MF=6, MT=18), etc., should be compiled. For sum rule, 1) (MF=3, MT=1) = (MF=3, MT=2) + (MF=3, MT=3), 2) (MF=3, MT=3) = (MF=3, MT=5) + (MF=3, MT=18), 3) For MF=3, MT=201, 203, 204, 205, 206 and 207, the contributions of elastic scattering and fission channels are not included. For the angular distributions of elastic and discrete inelastic scattering channels, it can be compiled both in MF=4 and in MF=6, LAW=2. For fission neutron spectrum, both MF=5 and MF=6 can be used. Other detail of rules for MF=6 are listed below:

MF=6, LAW=0:	in the case of only the isotope production ratio (MT=5) to MF=3, MT=5 is included (unknown distribution).
MF=6, LAW=1:	for MT=201–213, using Legendre coefficients or Kalbach systematics.
MF=6, LAW=2:	for MT=2, 51–90 (discrete two-body scattering), using Legendre coefficients or tabular expression.
MF=6, LAW=5:	for MT=2 of charged particle (charged particle elastic scattering).
MF=6, LAW=7:	for MT=201–213, using table type format, and MT=5 in the case including the isotope production ratio to MF=3, MT=5, and the PKA spectra.

3. Summary

From the assumption which many applications for IEND require the physical quantities of cross section and double differential cross section, the format for evaluated IEND file is proposed. ENDF-6 format is fundamentally selected, and some rules on compiling evaluated data are discussed. Though it is one of compiling options, the discussions for physical quantities and their format are very helpful to evaluate IEND and generate evaluated IEND files.

References

[1] A.J. Koning: "Requirements for an Evaluated Nuclear Data File for Accelerator-Based Transmutation", NEA/NSC/DOC(93)6, ECN-C-93-041 (1993).

[2] T. Fukahori, S. Chiba, M. Kawai, Y. Kikuchi and Japanese Nuclear Data Committee: "Status of Nuclear Data Evaluations for JENDL High Energy File", Proc. of Int. Conf. on Nuclear Data for Science and Engineering, May 9-13, 1994, Gatlinburg, U.S.A., (to be published)

[3] A.J. Koning: "Present Status of Intermediate Energy Data Evaluation for Accelerator-Based Transmutation of Radioactive Waste", Proc. of Int. Conf. on Nuclear Data for Science and Engineering, May 9-13, 1994, Gatlinburg, U.S.A., (to be published)

[4] Y. Kikuchi and T. Fukahori: "Result of Inquiry on Intermediate Nuclear Data Needs for Various Applications as Start-up Task of SG13", SG13 documents #?? (1994).

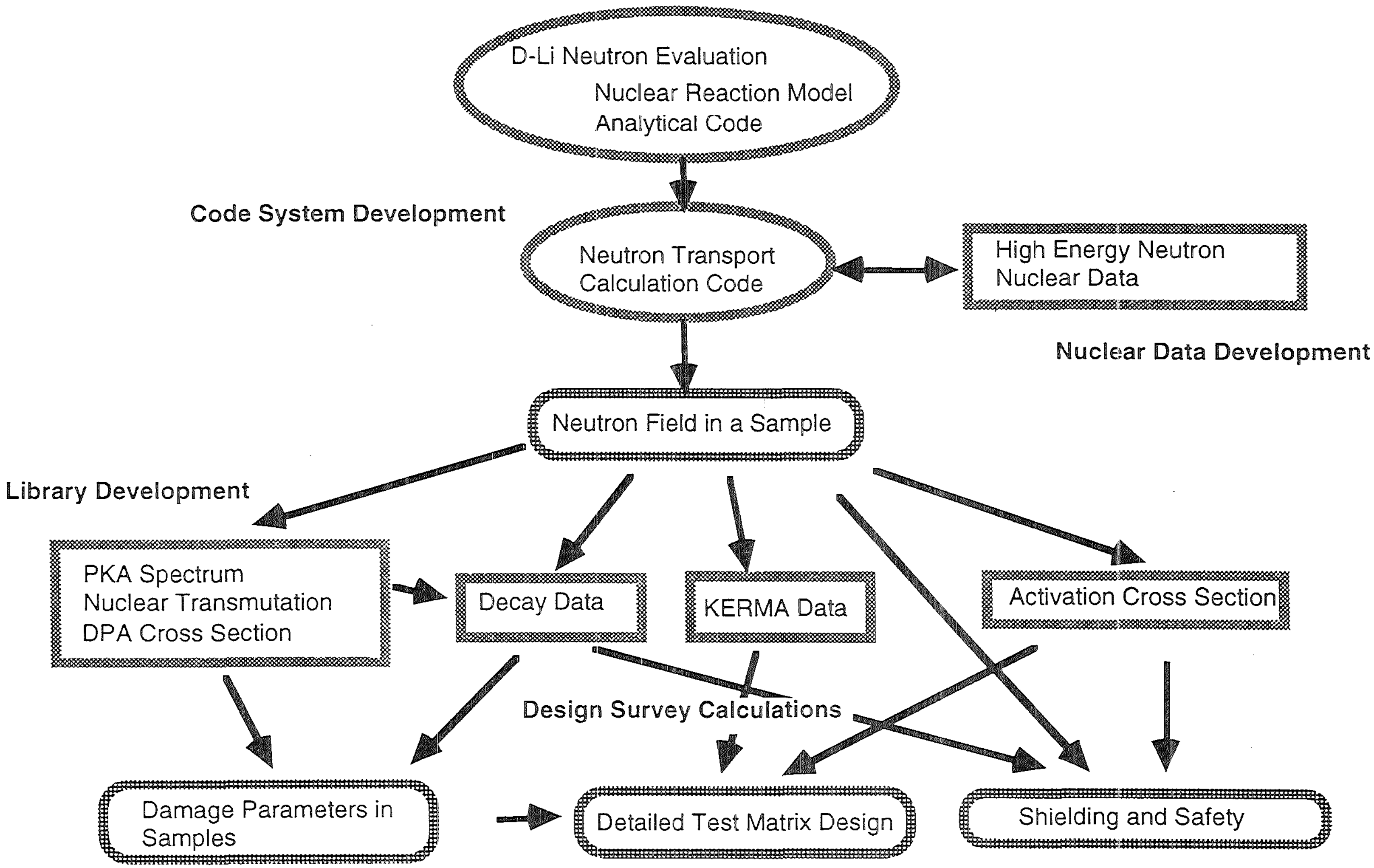

Development Flow of Neutron Related Issues

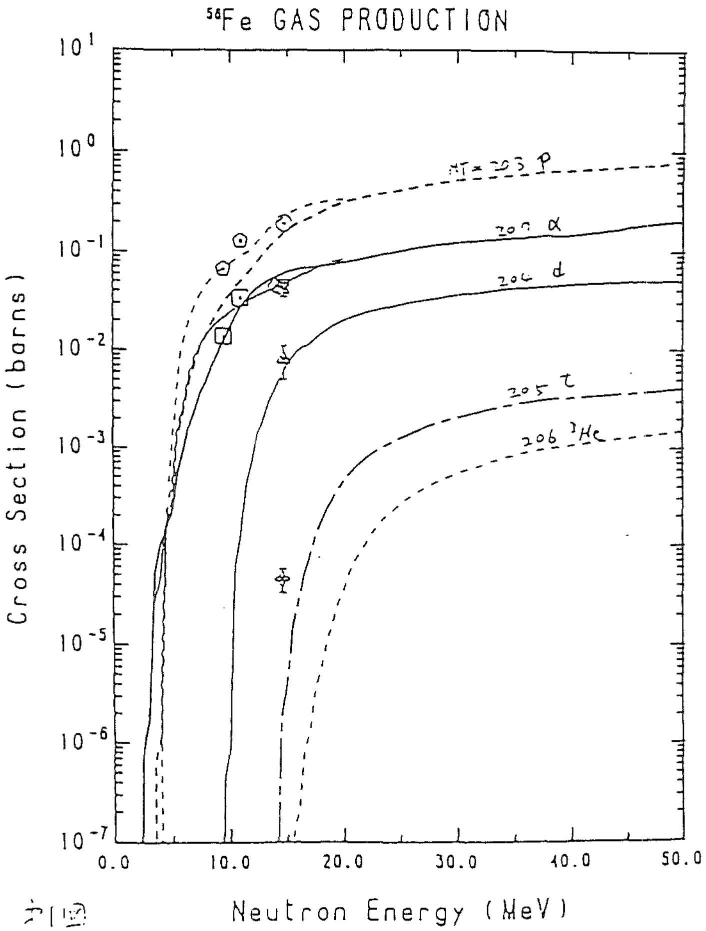
⁵⁶Fe GAS PRODUCTION
Cross Section (barns)
Neutron Energy (MeV)
MT=203 p
207 α
204 d
205 t
206 ³He

第1図

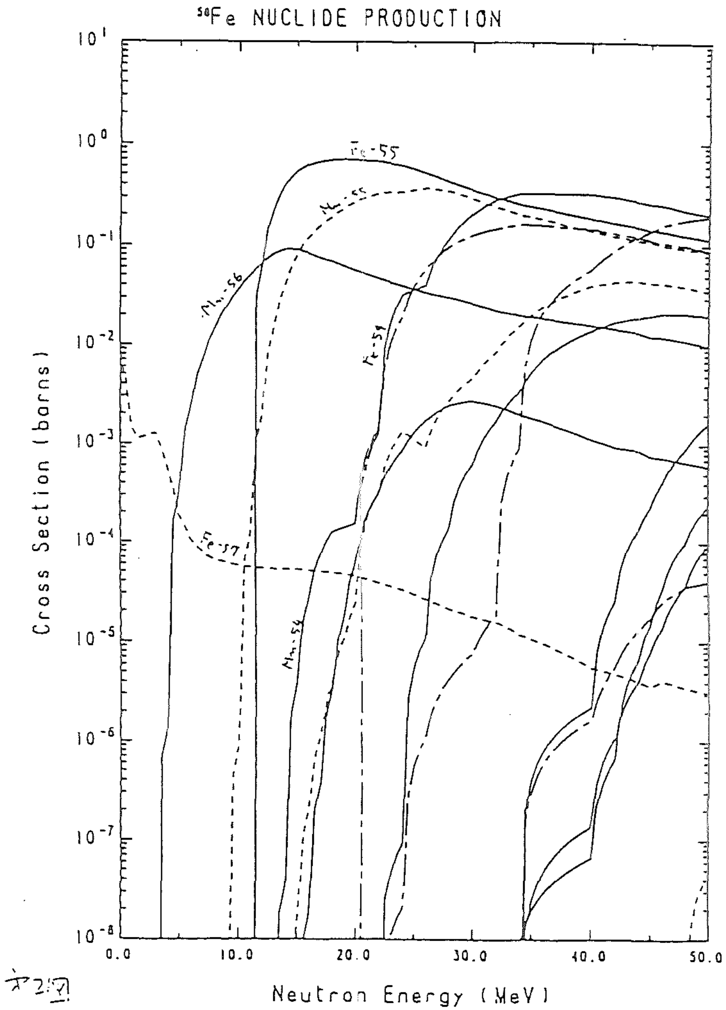
⁵⁶Fe NUCLIDE PRODUCTION
Cross Section (barns)
Neutron Energy (MeV)
Fe-55
Mn-55
Mn-56
Fe-57
Mn-54

第2図

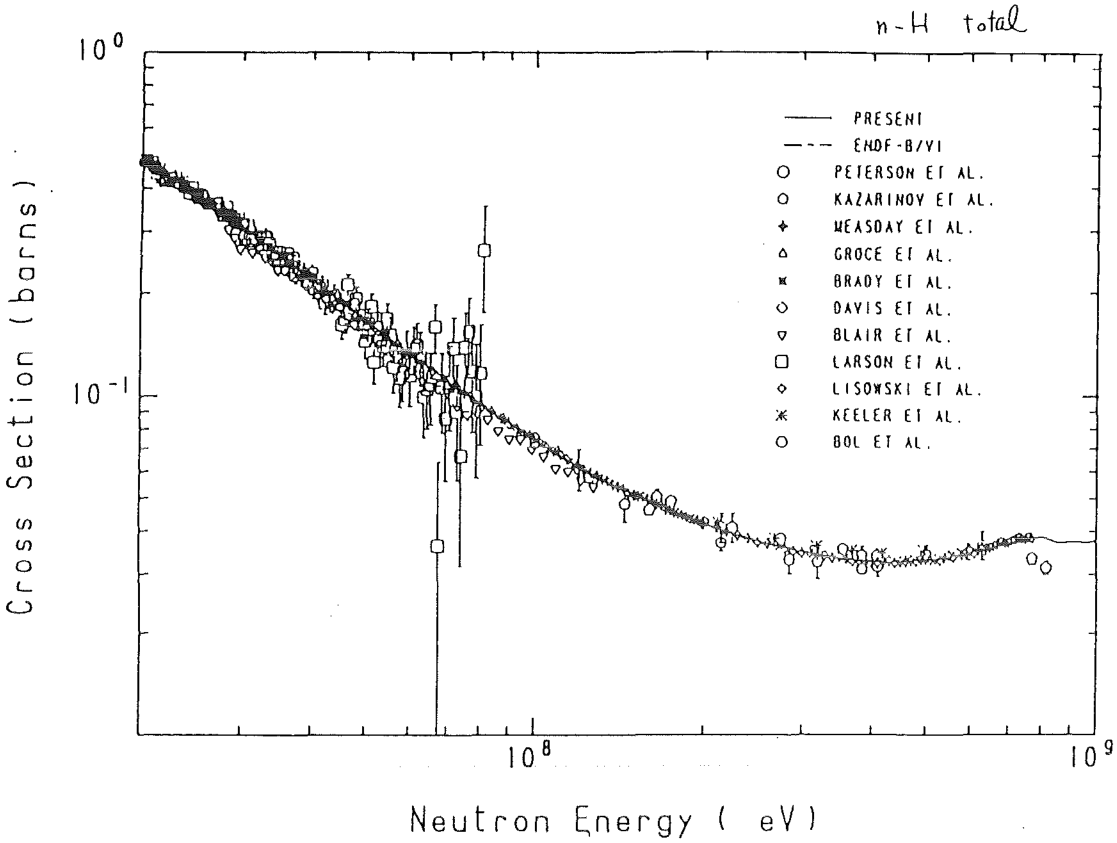
n-H total
PRESENT
ENDF-B/VI
PETERSON ET AL.
KAZARINOV ET AL.
MEASDAY ET AL.
GROCE ET AL.
BRADY ET AL.
DAVIS ET AL.
BLAIR ET AL.
LARSON ET AL.
LISOWSKI ET AL.
KEELER ET AL.
BOL ET AL.
Cross Section (barns)
Neutron Energy (eV)
10^0
10^{-1}
10^8
10^9

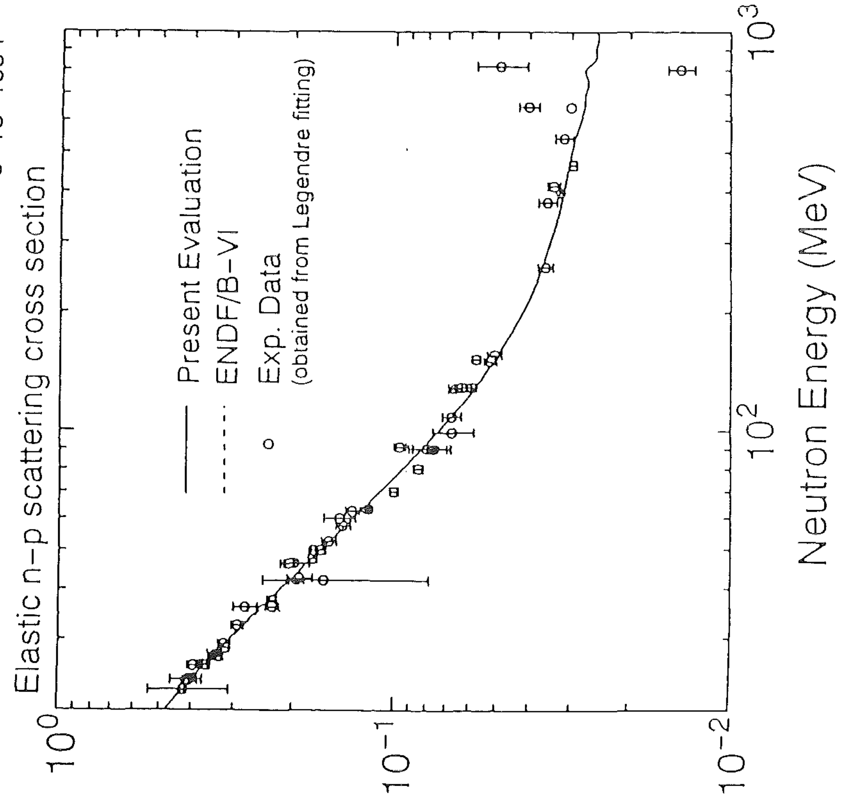
Elastic n–p scattering cross section
5-16-1994
Present Evaluation
ENDF/B–VI
Exp. Data
(obtained from Legendre fitting)
Cross Section (barns)
Neutron Energy (MeV)
10^0
10^{-1}
10^{-2}
10^2
10^3

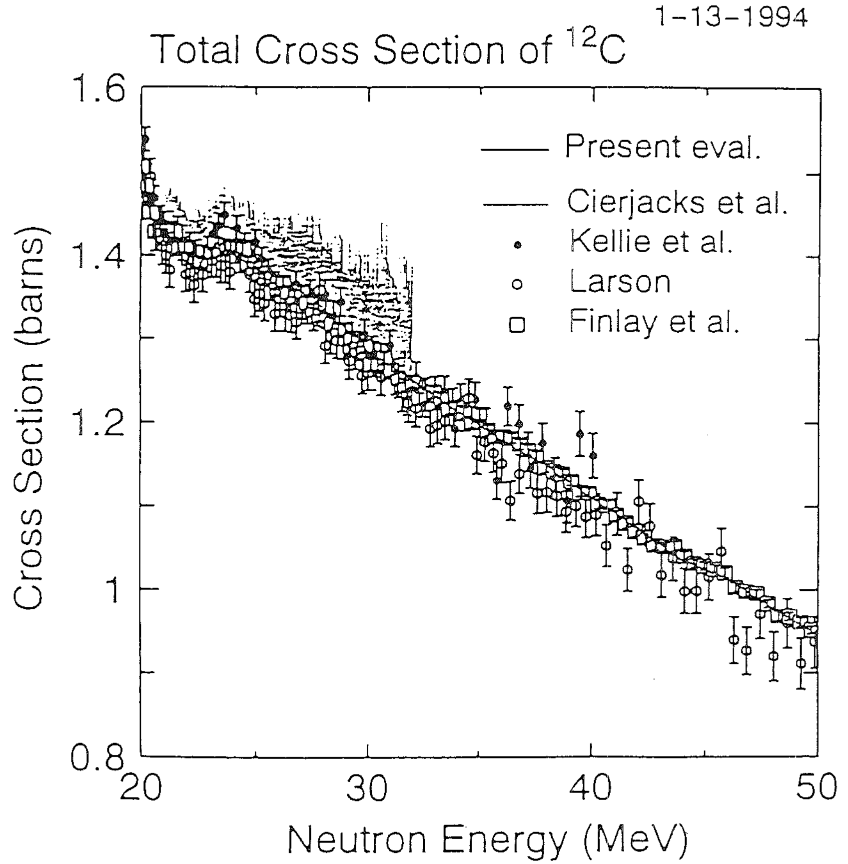
1-13-1994
Total Cross Section of ^{12}C
Present eval.
Cierjacks et al.
Kellie et al.
Larson
Finlay et al.
Cross Section (barns)
Neutron Energy (MeV)
1.6
1.4
1.2
1
0.8
20
30
40
50

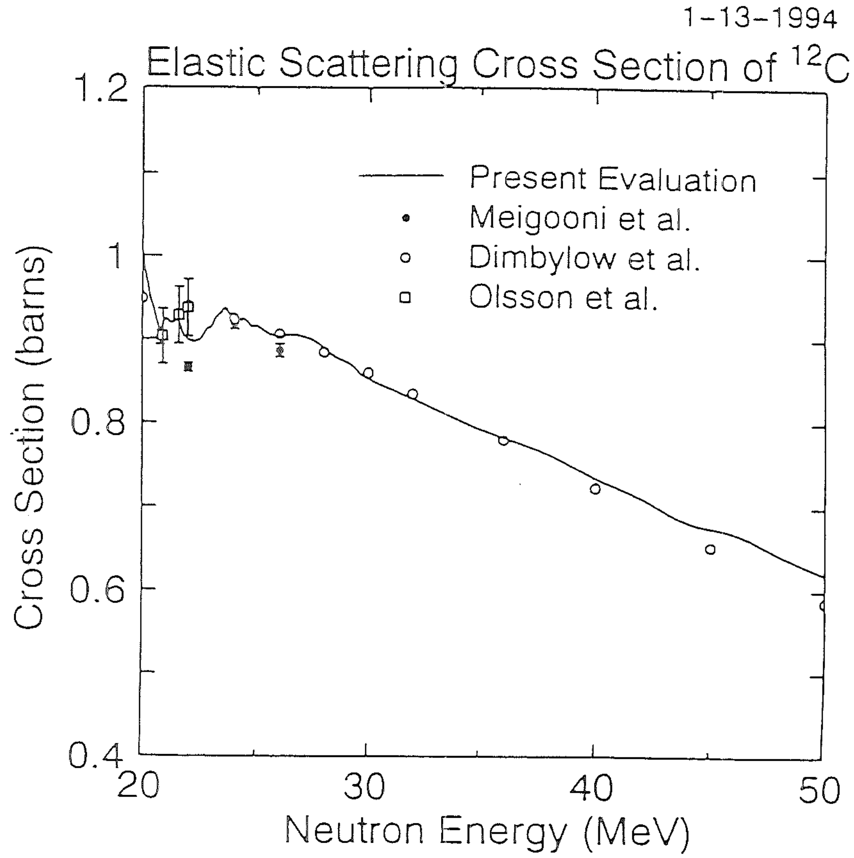
1-13-1994
Elastic Scattering Cross Section of ^{12}C
Present Evaluation
Meigooni et al.
Dimbylow et al.
Olsson et al.
Cross Section (barns)
Neutron Energy (MeV)
1.2
1
0.8
0.6
0.4
20
30
40
50

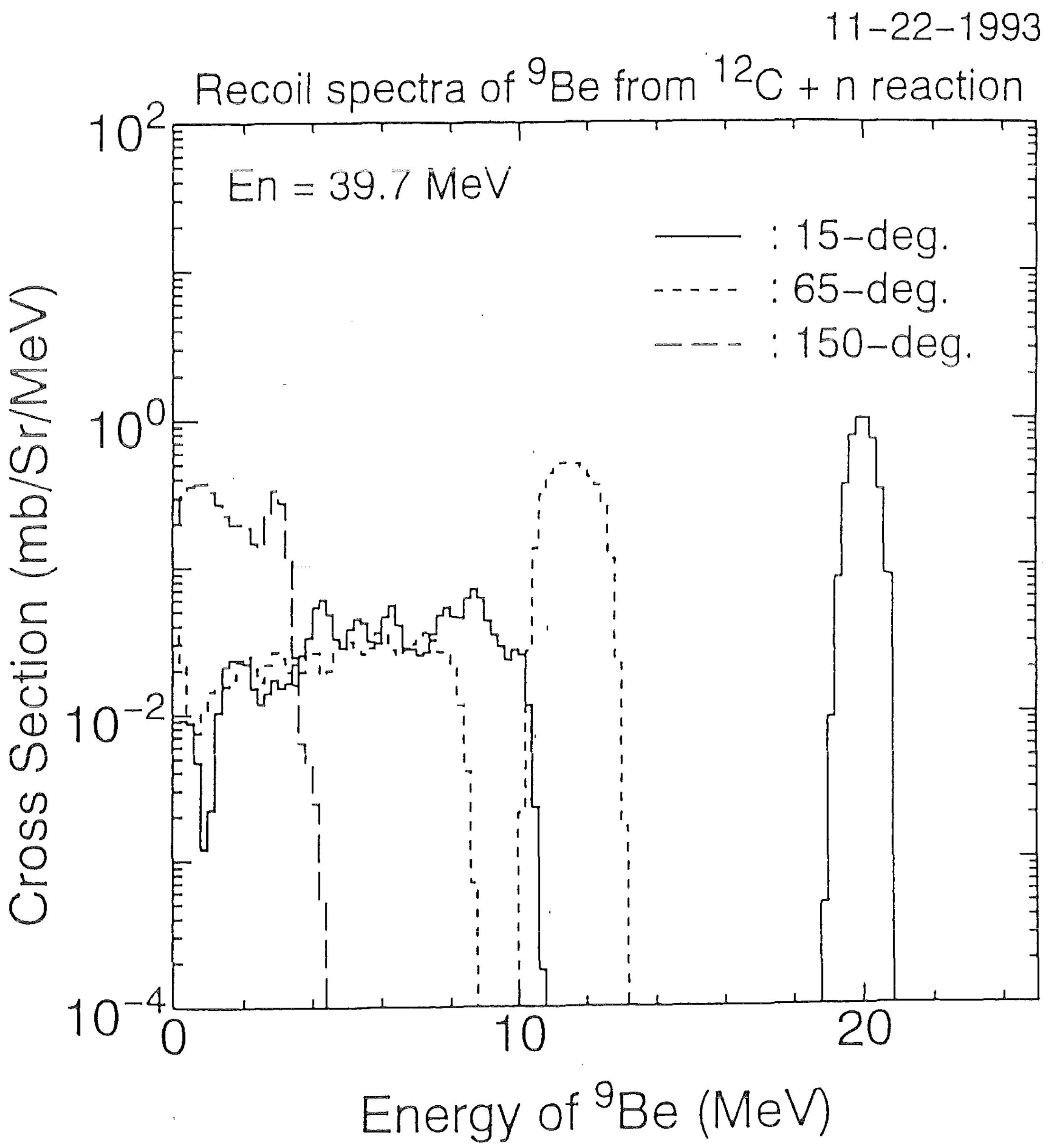

11-22-1993
Recoil spectra of ^{9}Be from ^{12}C + n reaction
En = 39.7 MeV
: 15-deg.
: 65-deg.
: 150-deg.
Cross Section (mb/Sr/MeV)
10^{2}
10^{0}
10^{-2}
10^{-4}
0
10
20
Energy of ^{9}Be (MeV)

CDA-D7 - Neutron Cross Sections up to 50 MeV

IFMIF International Workshop on the Test Cell Design

Karlsruhe - Germany

Itacil C. Gomes

Argonne National Laboratory

July 3-6

Required Neutron Cross Section Information

- Transport Cross Section for Neutrons up to
- 50-70 MeV - this would include:
  1. Total
  2. Scattering
  3. Neutron Emission - (n,xn)
- Activation Cross Section - would include all possible reactions and products cross sections.

Available Information in US - Neutron Transport Cross Section: HILO Library

- R.G.Asmiller, J.M.Barnes,and J.D.Drischler
- Up to 400 MeV
- Elements: H, B-10, B-11, C, N, O, Na, Mg, Al, S, K, Ca, Cr, Fe, Ni, W, and Pb.
- 66 neutron groups and 22 photon groups.
- Except for S and Pb, the cross sections below 20 MeV are based on the ENDF-BV with P5 Legendre expansion (sulfur and lead are based on ENDF-BIV with P3)

I.C.Gomes - Argonne National Laboratory

Available Information in US - Neutron Transport Cross Section: HILO Library

- The data show that the total cross sections tend to decrease above 20 MeV.
- The HILO multigroup cross sections present a general good agreement with experimental data - Figure.
- The tabulated values of the elastic and nonelastic cross section show a significant decrease as the neutron energy goes higher.

Available Information in US - Activation Cross Section: REAC Library

- F.M.Mann/B.Wilson(LANL)
- Cross Sections up to 50 MeV are available in two different group structures: 99 and 63 neutron groups.

Problems with the Available Cross Section Libraries

- They are mostly based on nuclear models without enough nuclear data to validate the models.
- It is an agreement that more experimental data is required, but the availability of funds is very limited in this area.
- HILO contains only a few elements and more elements are required for truly represent the D-Li NS environment.

Current US Activities in Nuclear Data Field

- Most of the work being developed in the nuclear data field is basically theoretical.
- Many experimental facilities were shut down and there is no perspective of a change in this scenario.
- There still are a number of experts highly qualified, in both, data acquisition and data analysis.

I.C.Gomes - Argonne National Laboratory

Current US Activities in the Nuclear Data Field

- ANL - most of the nuclear data activity was eliminated, only Donald Smith still in the laboratory.
- LLNL - R.White, M.Chadwick, D.Resler, M.Blann and others. Neutron scattering, (n,xn),..... mostly for medical applications.
- LANL - T2 Division. P.Young, G.Hale, R.MacFarlane. High energy, some exp's

Current US Activities in the Nuclear Data Field

- There is a current mentality that nuclear data acquisition is not needed anymore, and that the available data can fulfill the requirements for present and future designs.
- The fusion community, despite being aware of the problems, does not see as an immediate need and very low or none investment is made to improve the available data.

I.C.Gomes - Argonne National Laboratory

Current US Activities in the Nuclear Data Field

- Lately, most of the activities in US, in the fusion area, are product of international collaboration.
- Collaboration in terms of acquiring, analyzing, and processing "high energy" neutron nuclear data is desirable for US.
- JAERI-Tokai has a major program to develop data > 20 MeV - Satoshi Chiba.
- A closer interaction and information exchange in this activity can produce beneficial results for all parties.

I.C.Gomes - Argonne National Laboratory

U. von Möllendorff
Forschungszentrum Karlsruhe
Institut für Neutronenphysik und Reaktortechnik

3 July 1995

IFMIF-CDA Task D-7

Provide processed nuclear data for neutron energies 20 - 50 MeV

Status at FZK:

The data are to be used in neutron transport calculations, Task D-2. For the combined tasks, D-7 + D-2, **three possible pathways** were identified:

(1)

Obtain calculated nuclear data for E_n = 20 ... 50 MeV for Fe-56, Na-23 and K-39 from ***Inst. of Nuclear Power Engineering (INPE)***, Obninsk, Russia;

combine these with available data in < 20 MeV range;

process combined data by suitable NJOY version for MCNP-4A code;

perform Task D-2 using this processed library + MCNP-4A code.

(2)

Calculate data for E_n = 20 ... 50 MeV using ALICE code;

other steps as in way (1)

(3)

Perform D-2 using PROSDOR, an available combination of the MCNP and HETC codes. HETC is a Monte-Carlo code that calculates itself the cross sections as they are required. In PROSDOR, a neutron treated by HETC is handed over to MCNP as its energy goes < 20 MeV.

Expected quality differences between ways (1), (2), (3):

- Way (3) is questionable for $E_n \lesssim 50$ MeV because reactions in HETC are modeled for $E_n \gg E_{bind}$.

- Way (1) is likely superior to way (2) because of refined modeling. INPE uses an ALICE version modified in several aspects, as e.g.

  to include cluster emission algorithms (d, t, He-3, He-4),

  to use the Generalized Superfluid Model for level densities,

  and others.

→ **Way (1) = Stage 1 in FZK D-7 Task Description**

Stage 2 = fully evaluated nuclear data and
more nuclides;
input from ENEA and/or JAERI

Present status, way (1):

- Fe-56 data in ENDF/B-VI format obtained from INPE.

- Na-23 and K-39 data expected by 31 July 1995

The next three pages show the integral cross sections of some of the $^{56}Fe + n$ reactions as functions of E_n.

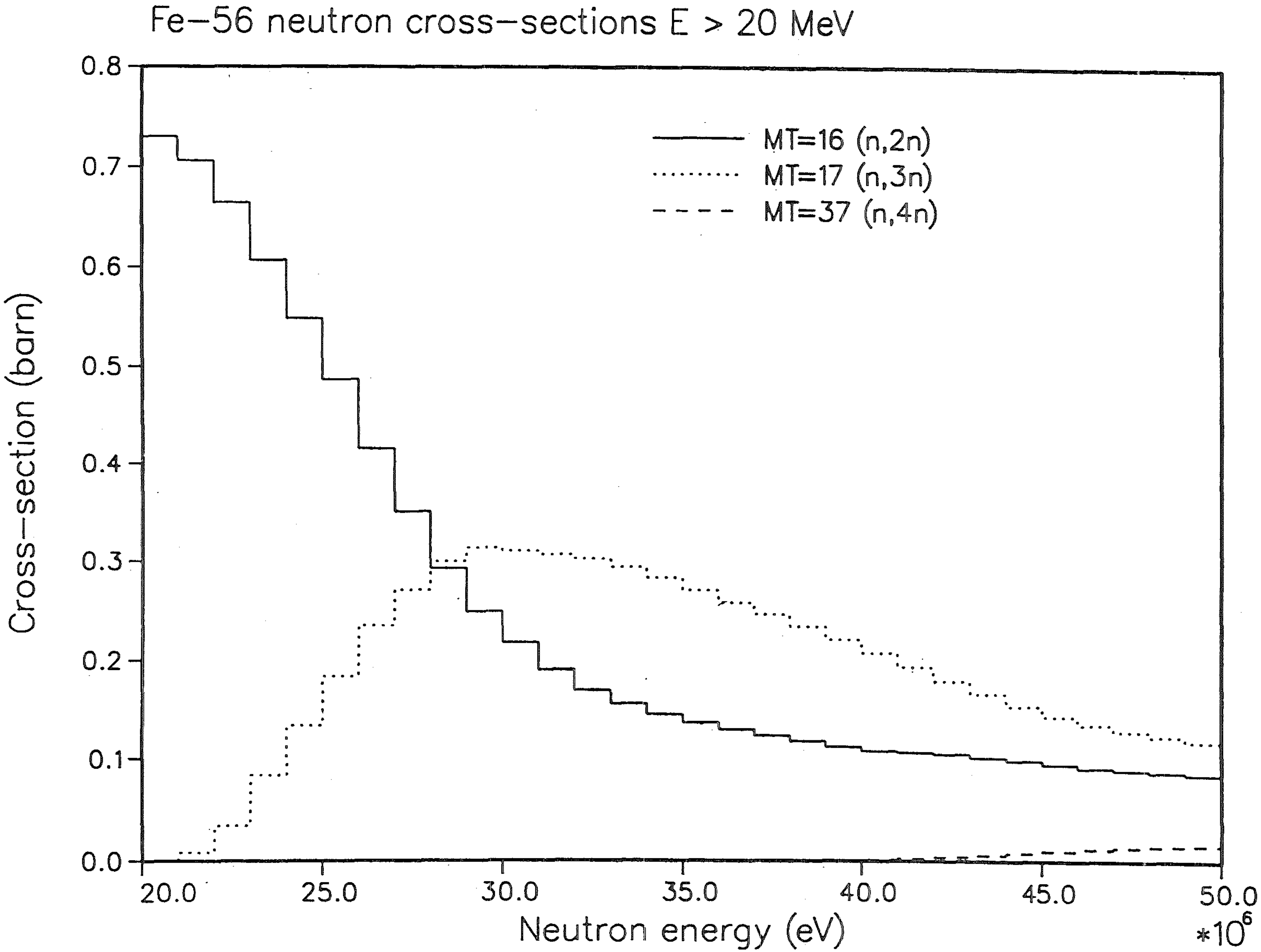
Fe-56 neutron cross-sections E > 20 MeV
MT=16 (n,2n)
MT=17 (n,3n)
MT=37 (n,4n)
Cross-section (barn)
0.8
0.7
0.6
0.5
0.4
0.3
0.2
0.1
0.0
20.0
25.0
30.0
35.0
40.0
45.0
50.0
Neutron energy (eV)
*10^6

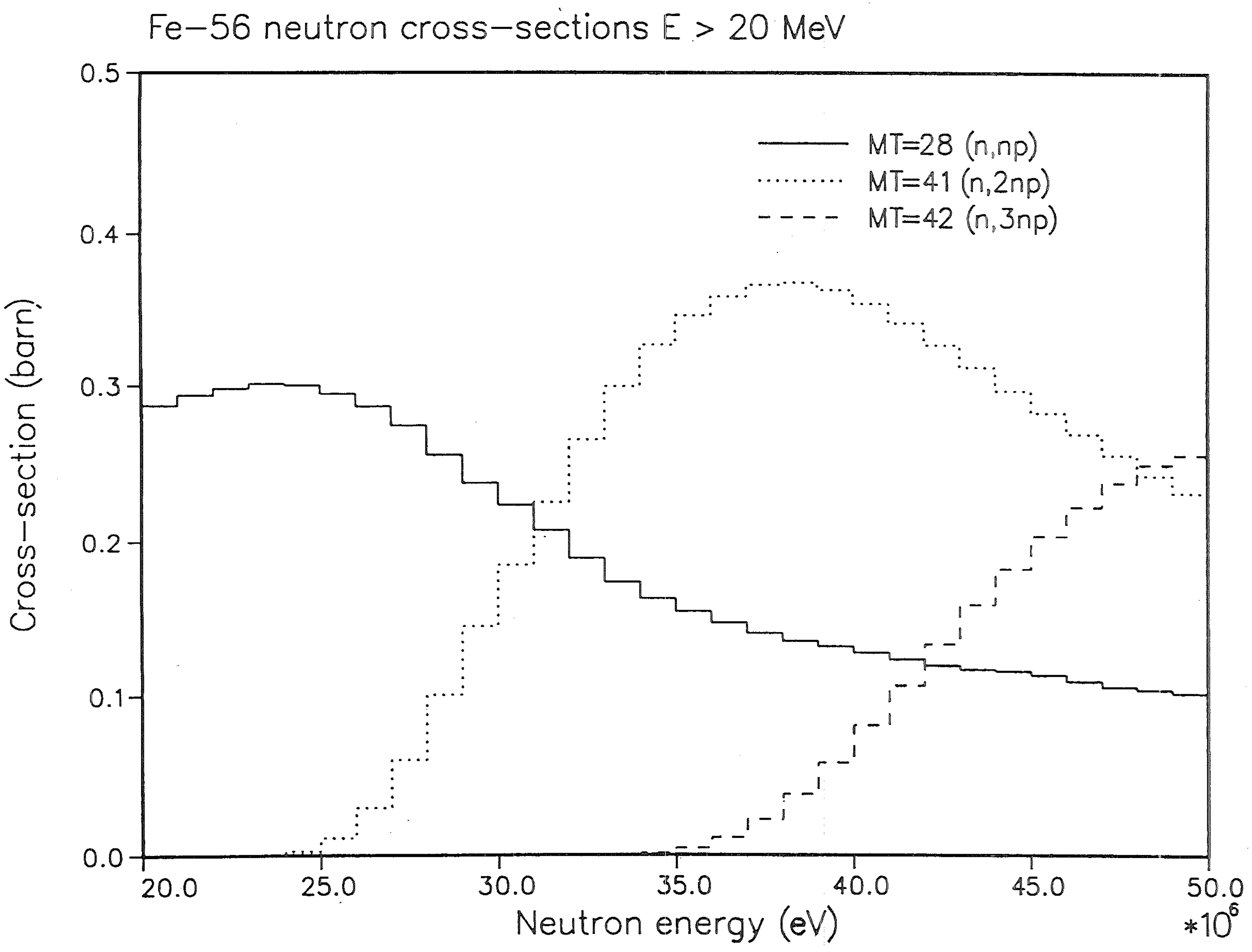

Fe–56 neutron cross–sections E > 20 MeV
MT=28 (n,np)
MT=41 (n,2np)
MT=42 (n,3np)
Cross–section (barn)
0.5
0.4
0.3
0.2
0.1
0.0
20.0
25.0
30.0
35.0
40.0
45.0
50.0
Neutron energy (eV)
*10^6

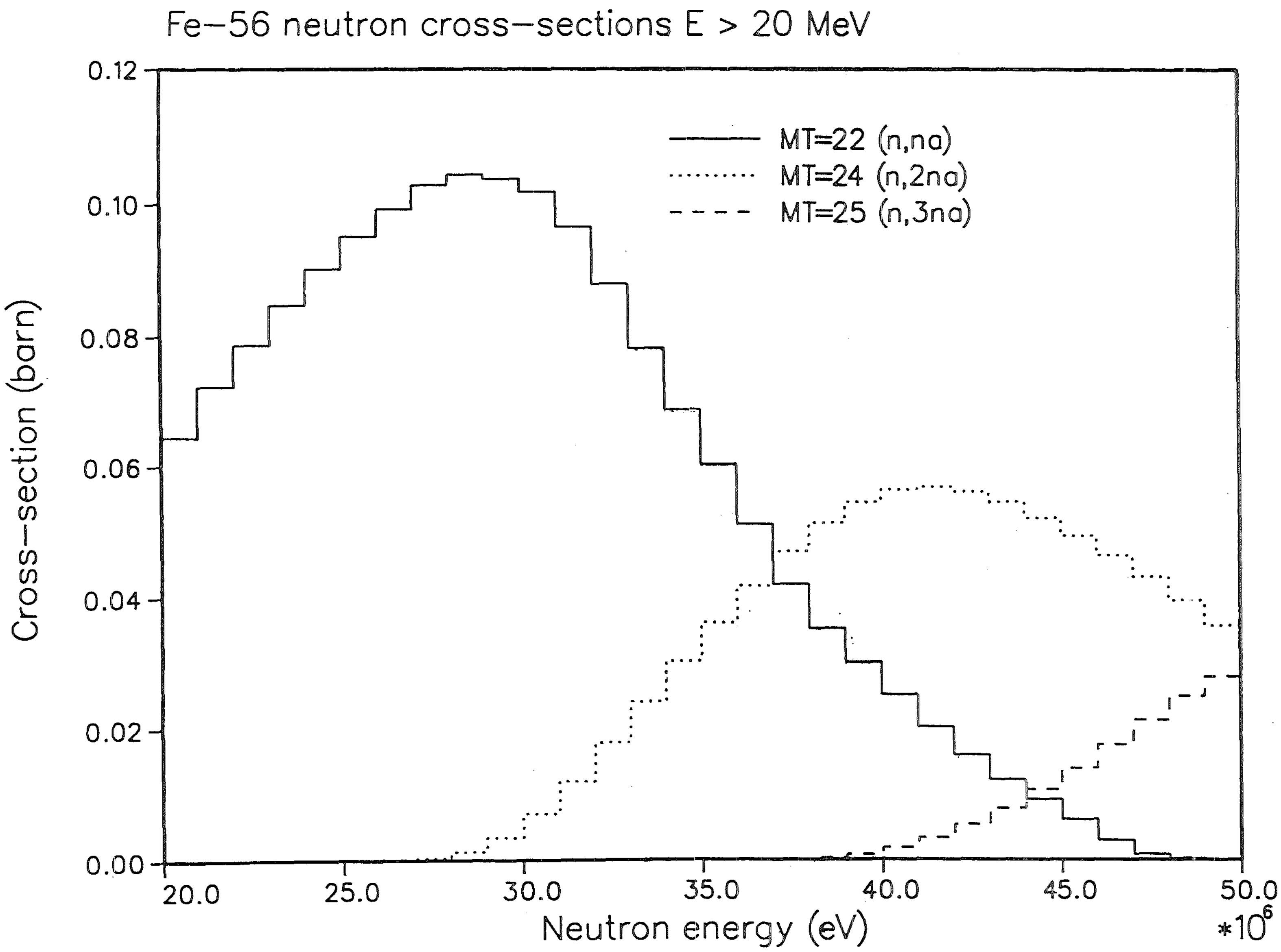
Fe–56 neutron cross–sections E > 20 MeV
MT=22 (n,nα)
MT=24 (n,2nα)
MT=25 (n,3nα)
Cross–section (barn)
0.12
0.10
0.08
0.06
0.04
0.02
0.00
20.0
25.0
30.0
35.0
40.0
45.0
50.0
Neutron energy (eV)
*10^6

1. Background and Objectives

Evaluated and processed nuclear data in the 20 to 50 MeV energy range have to be provided as these are not existing in standard fusion nuclear data files.

2. Technical outline of task

Calculation/evaluation of nuclear data relevant for neutron transport in 20-50 MeV incident neutron energy range; processing of such nuclear data into a library for use in the MCNP Monte-Carlo code.

3. Task description

For executing neutron transport calculations, the MCNP (or any other) code requires a library of the pertinent nuclear data, i.e., for every nuclide present, a multitude of integral, single-differential and double-differential cross sections of nuclear scattering and reaction processes as functions of incident neutron energy.

This library has to be produced using a Processing Code from a file or files of Evaluated Nuclear Data.

Evaluated nuclear data are cross section data that have been prepared for a given nuclide on a combined basis of theoretical and general systematical knowledge on one hand and experimental data from cross section measurements on the other. In the absence of experiments, nuclear data based only on theory and systematics can be used with a certain degree of confidence.

TASK CDA-D7
NUCLEAR DATA BASE

INTERMEDIATE REPORT ON REVIEW OF EXISTING DATA

G. REFFO

NUCLEAR DATA NEED

- particle spectra
- gamma-emmission spectra
- angular distributions

are needed for

- machine functioning
- material damage (gas production, transmutation)
- shielding
- activation

REVIEW OF EVALUATED FILES

TRANSPORT FILES

ENDFB-VI
EFF
JEF
JENDL-3
BROND
CENDL
FENDL

ACTIVATION FILES

ENDFB
EAF
JENDL
ADL
REAC

NEW FEN.DL!

OTHER PURPOSE FILES

ENDFHE6

- partial x-sections not given, only total n- and gamma-production,
- comparison with expt. data not possible
- ddx given only at 20 and 40 MeV
- spectra calculated with code ALICE
- ALICE covers a broad spectrum of energies at the expense of using simplified formulations. Preeq. mechanism in terms of hybrid model , with no MSC-MSD process treatment in terms of quantum mechanical approaches; C.N. no spin and parity conservation allowed, no nuclear structure details included.

HILO

- partial x-sections not given, only total n- and gamma-production, (400 and 20 MeV respectively
- intranuclear cascade evaporation model adopted, not suitable for low energies, same deficiencies like ALICE.

((24-CR-50(N,T)23-V-48,,SIG,,SPA) + (24-CR-50(N,N+D)23-V-48 ,,SIG,,SPA) + (24-CR-50(N,2N+P) 23-V-48,,SIG,,SPA))	2.2500E+01	(J,NP/A,295,150,7801)
(24-CR-53(N,HE3)22-TI-51,,SIG,,SPA)	2.2500E+01	(W,QAIM,8007)
(24-CR-0(N,X)1-H-3,,SIG,,SPA)	2.2500E+01	(W,QAIM,8007)

REVIEW OF EXPTL DATA

Table 2. Experimental and evaluated data status

REACTION	EXP. DATA (MAX. ENERGY) (MeV)	EVAL. DATA
IRON		
(26-FE-0(N,TOT),,SIG)	194	YES
(26-FE-0(N,EL),,SIG)	26	YES
(26-FE-0(N,NON),,SIG)	25.5	YES
(26-FE-54(N,INL)26-FE-54,PAR,DA)	26	NO
(26-FE-0(N,INL)26-FE-0,,SIG)	20.6	NO
(26-FE-56(N,2N)26-FE-55,,SIG)	21.8	NO
(26-FE-56(N,3N)26-FE-54,SIG)	NO	NO
(26-FE-0(N,3N)26-FE-0,SIG)	NO	NO
(26-FE-56(N,P)25-MN-56,,SIG)	20.3	NO
(26-FE-0(N,D)25-MN-0,,SIG)	NO	NO
(26-FE-0(N,X)1-H-3,,SIG,,SPA)	20	YES
(26-FE-0(N,X)0-G-0,PAR,SIG)	65	YES
VANADIUM		
(23-V-0(N,TOT),,SIG)	32	NO
(23-V-0(N,EL),,SIG)	NO	NO
(23-V-0(N,NON),,SIG)	NO	NO
(23-V-51(N,INL)23-V-51,PAR,DA)	NO	NO
(23-V-0(N,INL)23-V-0,,SIG)	NO	NO
(23-V-0(N,X)0-NN-1,EM,DA/DE)	25.7	NO
(23-V-0(N,X)0-NN-1,EM,DE)	25.7	NO
(23-V-51(N,2N)23-V-50,,SIG)	21	NO

(23-V-51(N,3N)23-V-49,,SIG)	NO	NO
(23-V-51(N,P)22-Ti-51,,SIG)	NO	NO
(23-V-51(N,D)22-Ti-50,,SIG)	NO	NO
(23-V-0(N,1-H-3),SIG,,SPA)	22.5	NO
(23-V-0(N,X)0-G-0,PAR,SIG)	NO	NO
CHROMIUM		
(24-Cr-0(N,TOT),,SIG)	81.4	NO
(24-Cr-0(N,EL),,SIG)	21.6	NO
(24-Cr-0(N,NON),,SIG)	NO	NO
(24-Cr-52(N,INL)24-Cr-52,PAR,SIG)	21.6	NO
(24-Cr-0(N,INL)24-Cr-0,PAR,DA)	21.6	NO
(24-Cr-0(N,2N)24-Cr-0,,SIG)	21.0	NO
(24-Cr-0(N,3N)24-Cr-0,,SIG)	22.5	NO
(24-Cr-56(N,P)23-V-56,,SIG)	NO	NO
(24-Cr-50(N,1-H-3),SIG,,SPA)	22.5	NO
(24-Cr-53(N,1-HE3)22-Ti-51,,SIG,SPA)	22.5	NO
(24-Cr-0(N,X)0-G-0,PAR,SIG)	NO	NO

Legend to Table 1 and 2

SIG - cross section

DA - angular distribution

PAR - partial cross section

SPA - spectrum

EM - emission (inclusive)

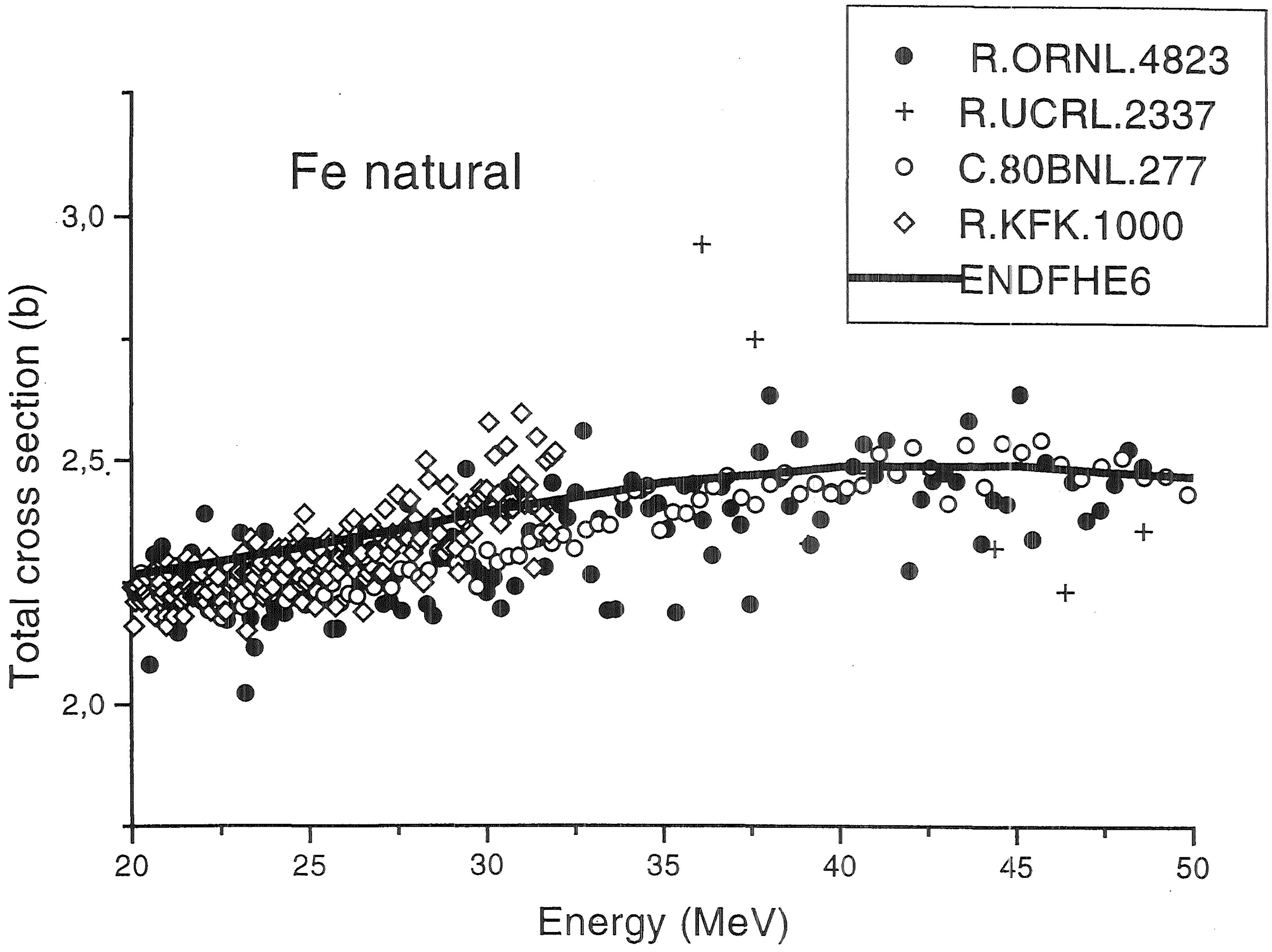
Fe natural
R.ORNL.4823
R.UCRL.2337
C.80BNL.277
R.KFK.1000
ENDFHE6
Total cross section (b)
3,0
2,5
2,0
20
25
30
35
40
45
50
Energy (MeV)

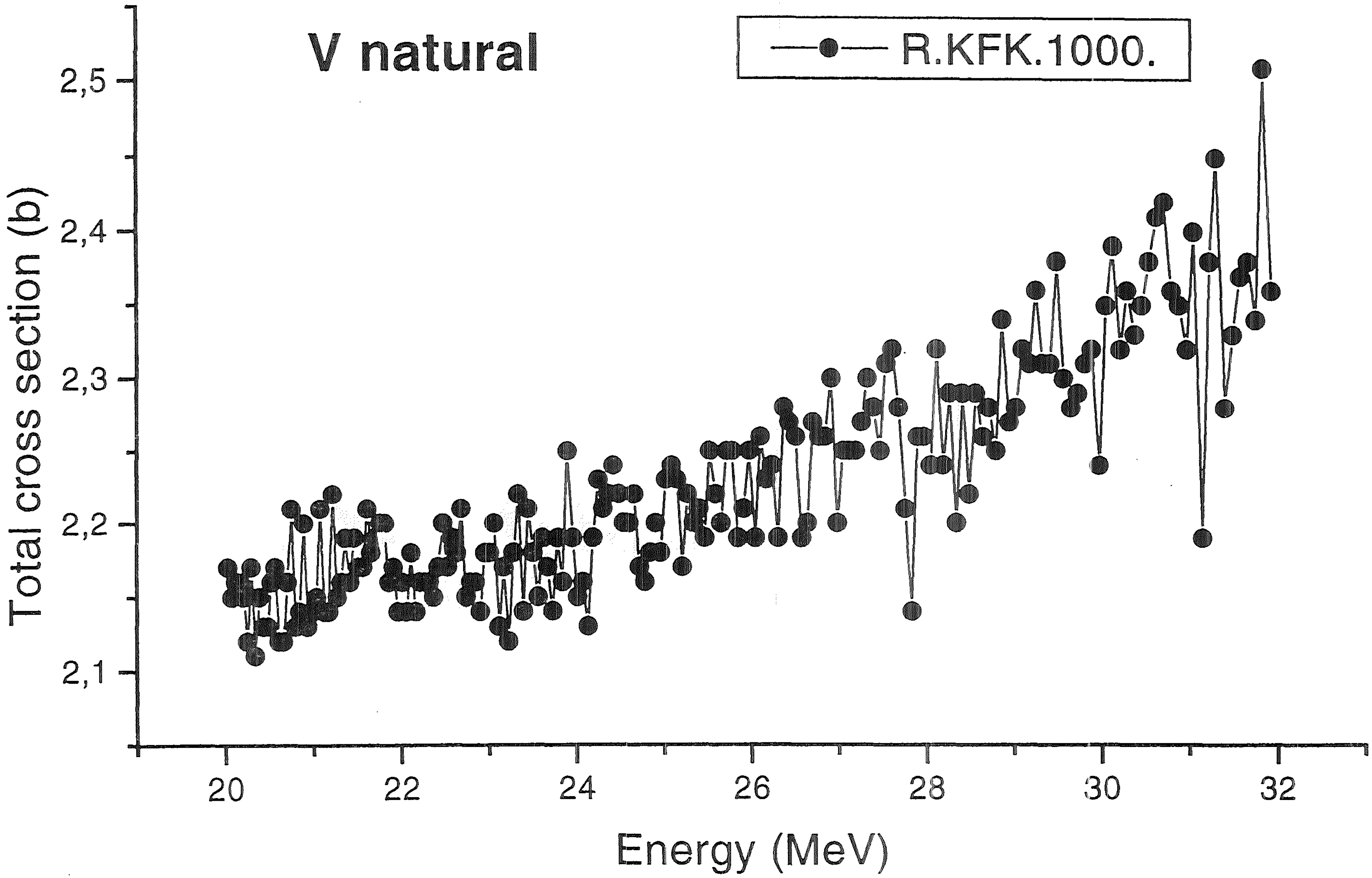
V natural
R.KFK.1000.
Total cross section (b)
2,1
2,2
2,3
2,4
2,5
Energy (MeV)
20
22
24
26
28
30
32

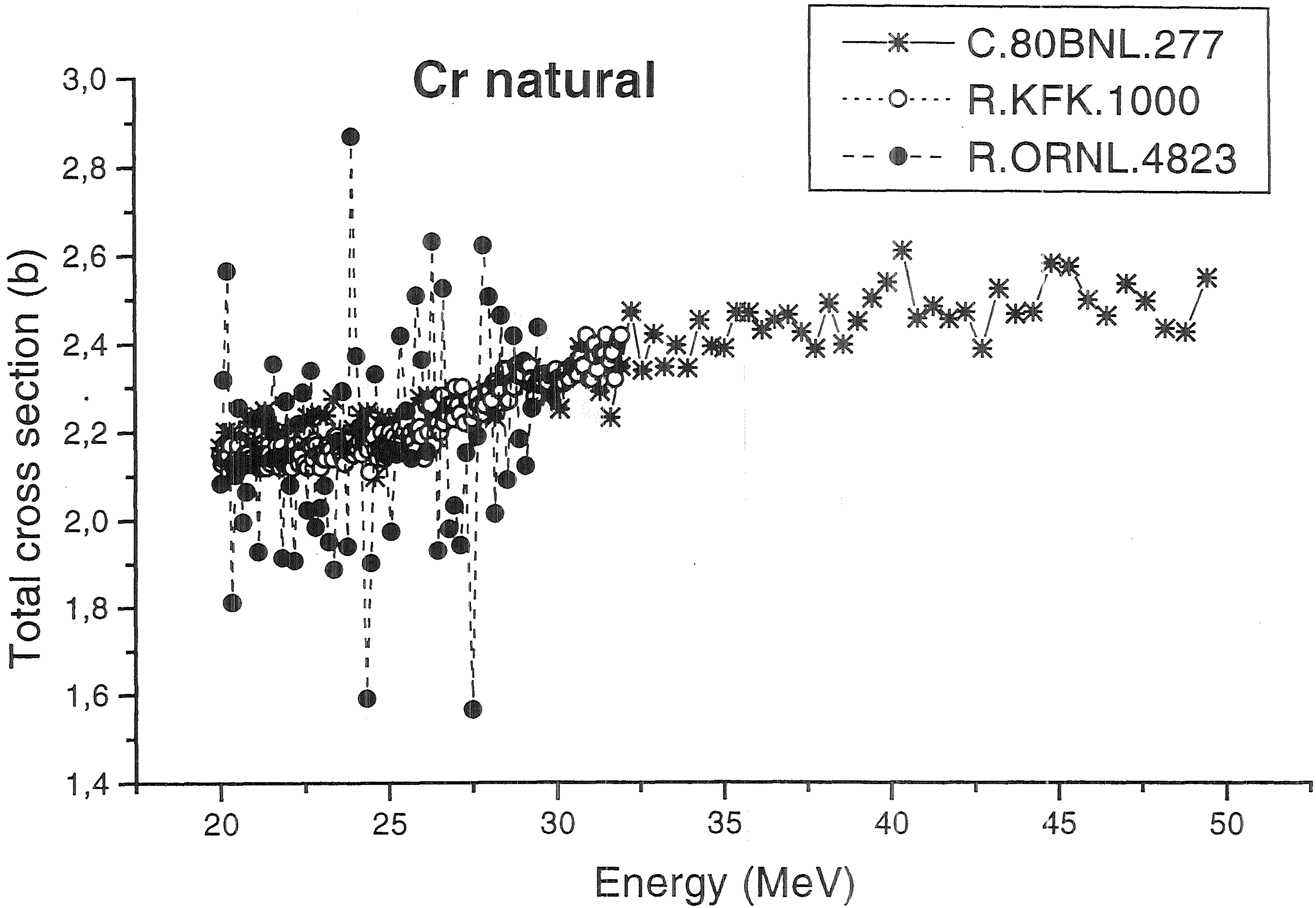

Cr natural
C.80BNL.277
R.KFK.1000
R.ORNL.4823
Total cross section (b)
3,0
2,8
2,6
2,4
2,2
2,0
1,8
1,6
1,4
20
25
30
35
40
45
50
Energy (MeV)

NEED FOR COORDINATION

What we are doing is an ad hoc file for IFMIF project i.e. an **IFMIF-FILE**

One should remind that

- the needs for IFMIF-file overlap with ongoing activities (national and) international (e.g. FENDL), except that IFMIF needs span a wider energy range
- which thing justifies additional work to be done for IFMIF.

One can imagine to proceed in two ways:

- performing independent evaluations and then choosing the best (duplications of work will occur)
- sharing the work
- a priority list is needed.

CONCLUSIONS

- The situation is acceptable below 20MeV.
- A lot has to be done above 20MeV if reasonable accuracy is needed.
- HILO can be adopted as a starter file useful also for sensitivity studies, provided large uncertainties are allowed.
- The activation file produced in ENEA can be taken as a starter file, allowing for large uncertainties

IFMIF Users/Test Cell Task CDA-D-8
Requirements for a common facility for materials testing at the IFMIF-site

K. Watanabe, K. Noda and T. Konishi
IFMIF Users/Test Cell Task Group of JAERI

1. Introduction

In the preparatory activity of IFMIF-CDA, a common facility for materials testing at IFMIF-site was considered to be required for effective use of IFMIF. The objectives of CDA-D-8 task is to define needs of common facility for materials testing at International Fusion Materials Irradiation Facility (IFMIF) site and to develop the requirements for the facility and test equipments to be installed .

2. Needs of A Common Facility for Materials Testing at IFMIF-site

IFMIF will be only one intense neutron irradiation facility to meet international demand for fusion reactor materials development and testing in the stage of development for fusion demonstration or prototype reactors. The test volume of IFMIF, especially for high flux region in which irradiation testing of structural materials will be carried out, will be very limited. In order to obtain various kinds of materials data in the limited test volume, a large number of miniaturized specimens will be irradiated especially in the high flux region of IFMIF, as described in CDA-D-3 task. In addition, various kinds of in-situ experiments will be carried out in neutron irradiation field of IFMIF to obtain data of materials properties during irradiation (i.e., during operation of fusion reactors).

An advanced Post Irradiation Examination (PIE) facility for the miniaturized specimens is required to perform the PIE of a large number of miniaturized specimens with high efficiency. In the PIE facility, testing equipments installed in specially-designed hot cells for PIE of the miniaturized specimens should be fully automatized to realize the testing with high efficiency. Such a special PIE facility, which is not currently available, is required as one of common facilities for materials testing at IFMIF site. Furthermore, it is desirable that the facility has functions to test materials properties before irradiation, from the standpoints of obtaining the data before irradiation with reliability and accuracy levels same as those for PIE.

In IFMIF, irradiation testing at various temperatures will be performed at various neutron fluences up to high damage levels such as 150 dpa. Therefore, the test modules and packets used for irradiation of the specimens have to be sometimes changed in the case of testing at high neutron fluences, in order to keep integrity of the test module and the packets. In respect of the specimens for low to intermediate damage levels, such specimens will be removed from the test module after the prescribed irradiation period such as around one year. So, a facility to reload the irradiated specimens to new or different test modules for further irradiation is required at IFMIF site as well as a facility to disassemble the test module and remove the specimens from the packets for PIE. Such facilities are very useful for reloading the irradiated specimens to test module after non-destructive PIE, which may realize acquisition of materials irradiation data with high reliability and high efficiency. In-situ experiments using the irradiated specimens will also be valuable to evaluate materials properties under irradiation at high neutron fluence. In order to perform such in-situ irradiation experiments, the above-mentioned facility for reloading the irradiated specimens needs to be constructed at IFMIF site.

3. Requirements for A Common Facility for Materials Testing at IFMIF-site

The main activity in this facility is focused on the examination of specimens irradiated with IFMIF. In IFMIF, the post irradiation examination (PIE) are supposed to be conducted for a larger number of miniaturized specimens, because of the limitation of irradiation volume which is common to the d-Li stripping reaction type intense neutron irradiation facilities. The PIE facility at IFMIF site should have the excellent function and capability for PIE of miniaturized specimens from viewpoint of operation and maintenance.

Very preliminary requirements for the PIE facility were developed by considering (1) handling and materials tests for miniaturized specimens, (2) process for PIE, i.e., loading , disassembling, classification, dosimetry, measurements, maintenance, machining of specimens, assembling of re-irradiation test module etc. , (3) three levels (low, medium and high) of radio-activity for irradiated materials, (4) tritium handling in PIE procedures (Materials without tritium contamination; structural materials [ferritic, SiC/SiC, gas-cooled vanadium alloy] , ceramic insulators and diagnostic materials, Materials containing tritium/with tritium contamination; ceramic breeders, Li-cooled vanadium alloy, etc.).

Tritium handling system for PIE will follow the regulation and design requirements specific for large amount of tritium that will be applied for the entire IFMIF facility. General feature of such system are, 1)Multiple (usually 3) confinement system 2)Inventory accountability and control and 3) Multiple detritiation systems. Besides the technical features for PIE facility, these three functions will be added to the equipments for handling of tritiated/tritium containing samples.

The preliminary requirements for hot cells and glove boxes in the PIE facility are as follows:

(1) Hot cells for miniaturized specimen tests

Handling of miniaturized specimens requires precise and sensitive handling, which may performed by fully-automatized test equipments or advanced manipulator systems. High efficiency of PIE for a large number of miniaturized specimens are also requested to obtain materials irradiation data by the time expected from the time schedule of prototype or demonstration fusion reactor development. Thus, miniaturized specimen tests are considered to need to be performed by fully-automatized test equipments. Such automatized test equipments required frequent maintenance for proper operation in hot cells. Therefore, the hot cell structure has to have capability for quick maintenance of test equipments in the cell. In Energy Selective Neutron Irradiation Test facility (ESNIT) program, modular type hot cells for materials PIE was proposed as advanced PIE facility with high efficiency and flexibility.

The modular type hot cell system consists of modular type cells, removable box, decontamination cell, maintenance room and removable box exchange system. The removal boxes which contain equipments are installed in modular type cells. The removable box exchange system enables rapid exchange of the removable box to carry out maintenance of the equipment. The box containing the equipment to be repaired is transferred to decontamination cell for decontamination of the equipment before repairing. On the other hand, another box containing the equipment in perfect condition is installed just after the removal of the former box. Such a rapid exchange of the removal boxes can realize to shorten maintenance /repair time of equipments. Thus, the modular type cells are required for effective use of fully-automatized test equipments for miniaturized specimens.

(2) Tritium handling hot cells

Irradiated ceramic breeders specimens contains tritium and some of them have high level radio- activity (Li_2ZrO_3, $LiAlO_2$ etc.). Irradiation tests of the ceramic breeders will be carried out using sweep gas capsules, and therefore most parts of tritium generated is expected to be released from the specimens. Thus, retained tritium levels may be not so large in normal irradiation condition. However, the ceramic breeders should not be handled in the cell same as that for the other specimens containing no tritium to avoid tritium contamination of the other specimens. This tritium handing cell will be conventional stationary type hot cell with high level airtight for tritium contamination of the leak rate no greater than 0.1 vol% / hour level. The cell will be filled with inert, nitrogen or air depending on the samples to be handled, and the gas will be continuously circulated maintaining negative pressure. Tritium in this stream, either in the form of hydrogen (HT) or chemically bound in moisture or hydrocarbon will be removed by catalyst or getter. Moisture of atmosphere in the cells should also be controlled, by the reason that moisture affects materials properties of ceramic breeders. Gas removed from the cell to maintain the negative pressure will be processed by a detritiation system and will be stacked.

In the primary enclosure, tritium generated in the sample will be contained in a highly gas tight containers. Since most of the samples are anticipated to be tested with sweep gas during irradiation, maximum amount of handling tritium are expected to be less than several grams. Amount of tritium entering and leaving from the cell will be assessed for accounting purpose. The handling of tritium enclosed in a container or bound form and the amount less than 100Ci per cell may not require closed cycle atmosphere processing.

Vanadium alloy specimens irradiated in packets with liq. Li bond will be also contaminated with tritium, and it will be better to handle such specimen in tritium handling hot cells. However, number of tritium handling hot cells should be minimized, because tritium handling facility requires tritium removal systems which is somewhat expensive. From this standpoint, use of gas cooling system for temperature control of vanadium alloy is desirable to avoid generation of unnecessary tritium.

(3) Glove box systems for low gamma-ray level specimens

Most of ceramics are low activation materials, and some ceramic materials will be irradiated in low flux region. So, some fraction of ceramics specimens will have only low gamma level. Some of ceramic breeders, i.e., Li_2O, have only very low level gamma-ray activity. Such specimens should be handled in glove box systems which enables easy handling. Atmosphere control for these gloveboxes will be same as for the above mentioned tritium hot cells. Some of the equipments for the atmosphere control and processing can be shared with both hot cells and gloveboxes.

(4) Loading /storage cell

This cell will be used for the loading and storage of the irradiated specimens and test modules. In addition, non-destructive examination of irradiated specimens, e.g., X-ray radiography, mensuration, etc., are also performed for further irradiation tests. For the loading /storage cell, separation of tritium-contaminated specimens from the other specimens is needed.

(5) Disassembly cell

This cell will be used for dismantling of test modules, machining of irradiated specimens and assembling of re-irradiation test module. In respect of disassembly cells, a cell for tritium handling (for ceramic breeders) should be built in addition to another cell for materials containing no tritium or without tritium contamination.

(6) Specific requirements for tritium handling

The rooms that will be equipped with tritium handling hot cells and gloveboxes are regarded as tertial containment of the tritium that works as a final boundary against tritium release to the environment in the case of emergency. Such rooms are air tight, and the negative pressure in it will be maintained. Necessity of tritium removal/recovery function in the room is currently uncertain. The inner surface of the tritium handling rooms should be painted or coated to prevent acute and chronological soaking of tritium.

It should be noted that the entire IFMIF facility will very likely be regarded as a major tritium handling facility and be subject to the regulation and design requirements specific for large amount of tritium. Tritium is anticipated to exist in almost all part of the IFMIF system. Major sources will be, Li target, irradiated blanket materials, and irradiated samples containing lithium. It is important that the tritium handling facility for PIE and test cells are to be consistent with the rest of the IFMIF facility .

4. Test Equipments required

Experimental matrices (specimen loading plan) for structural materials, ceramic breeders and ceramic insulators/diagnostic materials are described in CDA-D-3 and CDA-D-9. On the basis of the information described in CDA-D-3 and CDA-D-9, the following test equipments required for PIE were preliminarily identified. Development of test matrices for all kinds of fusion materials has just started. Information on required equipments will be further provided from CDA-D-9 task.

(1) For loading and storage for irradiated material and test modules, and non-destructive testing;

X-ray and neutron radiography, dosimetory, viewing tool (TV, periscope), mensuration tool, helium leak detector, etc.

(2) For dismantling of test modules, machining of irradiated specimens and assembling of re-irradiation test module;

Numerically controlled milling machine, electron beam welding apparatus, electric discharge processing apparatus, micro-cutter, etc.

(3) For sample preparation for metallography/ceramography;

Polishing apparatus (glinding, electrical etching, ion milling), diamond cutter, etc.

(4) For metallography/ceramography

Optical microscope, transmission electron microscope, scanning electron microscope, etc.

(5) For mechanical property measurements;

Miniaturized specimen test equipments (tensile test, Charpy impact test, fatigue test, corrosion fatigue test, etc.) , mensuration equipment, etc.

(6) For physical property measurements;

Thermal conductivity measurement apparatus, optical absorption measurement apparatus, electrical resistivity and dielectric loss measurement apparatus, X-ray diffractometer, etc.

(7) For chemical analysis;

Mass spectrometer, X-ray fluorescence analyzer, various spectroscopy apparatus, etc.

5. Summary

A common facility for materials testing at the IFMIF-site are needed for extensive PIE of miniaturized specimens with high efficiency, reloading of irradiated specimens for high fluence level irradiation, etc. Requirements for the PIE facility were preliminarily developed. Modular type hot cells are required for high efficient PIE of a large number of miniaturized specimens using fully automatized test equipments from the standpoint of quick maintenance of the equipment. Tritium handling hot cell and glove boxes are needed for handling of ceramic breeders, etc. In addition, test equipments required for the PIE facility were preliminarily identified.

Proposal of CDA-D-8 Task Schedule

(1) Development of preliminary needs and requirement for a common facility at IFMIF site

[July, 1995]

(2) Preliminary identification of required equipments for a common facility at IFMIF site

[July, 1995]

(3) Report on the requirements and required equipments for a common facility at IFMIF site based on CDA-D-9 task

[October, 1995]

(4) Design concept for PIE facility will be made from CDA-D-8 task

[Beginning of 1996]

(5) Conceptual design of a common facility at IFMIF site

[Summer, 1996]

Modular Type Cell without Shielded Window

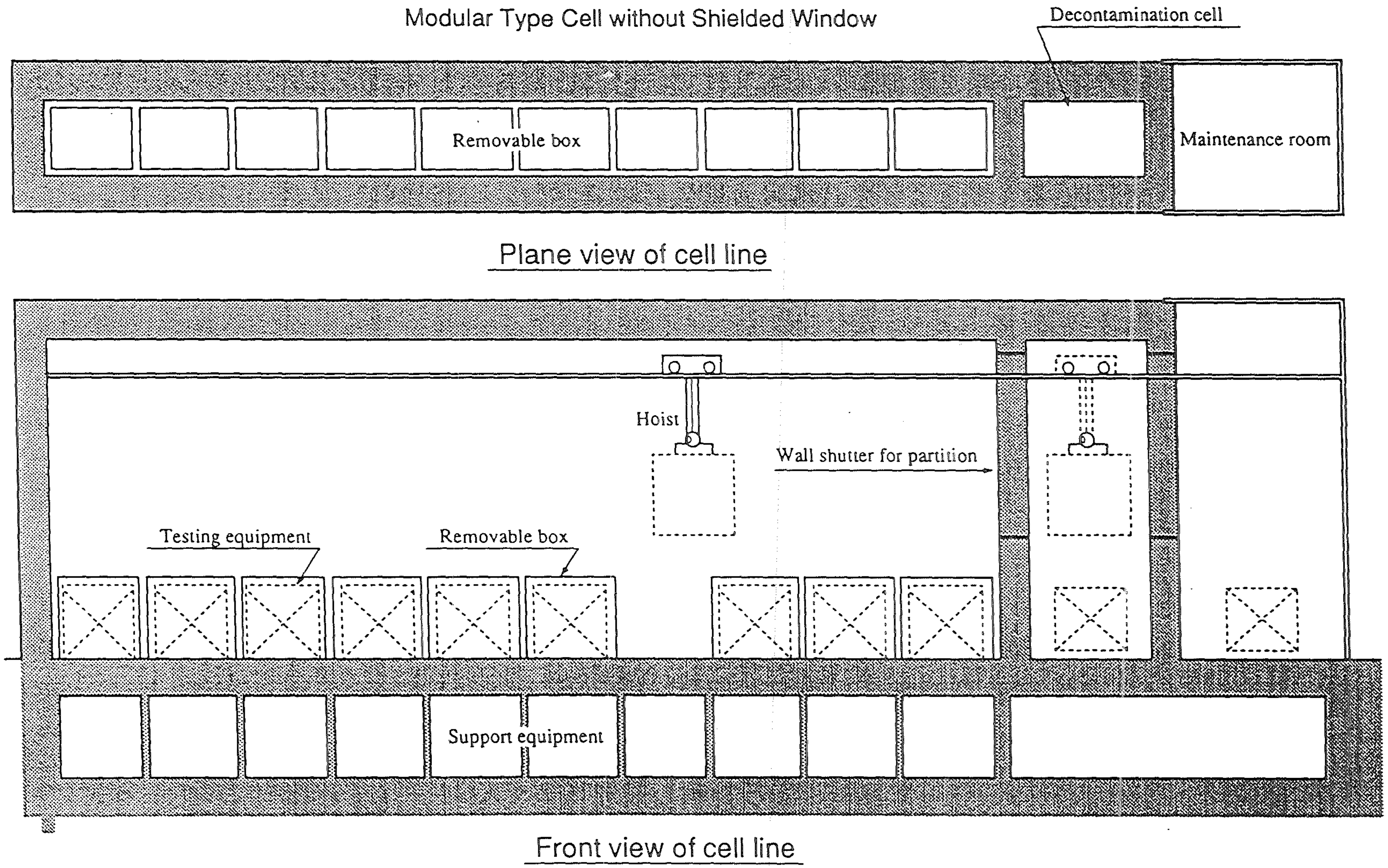

Fig. 1 Plane and front view of hot cell line in the modular-type cell.

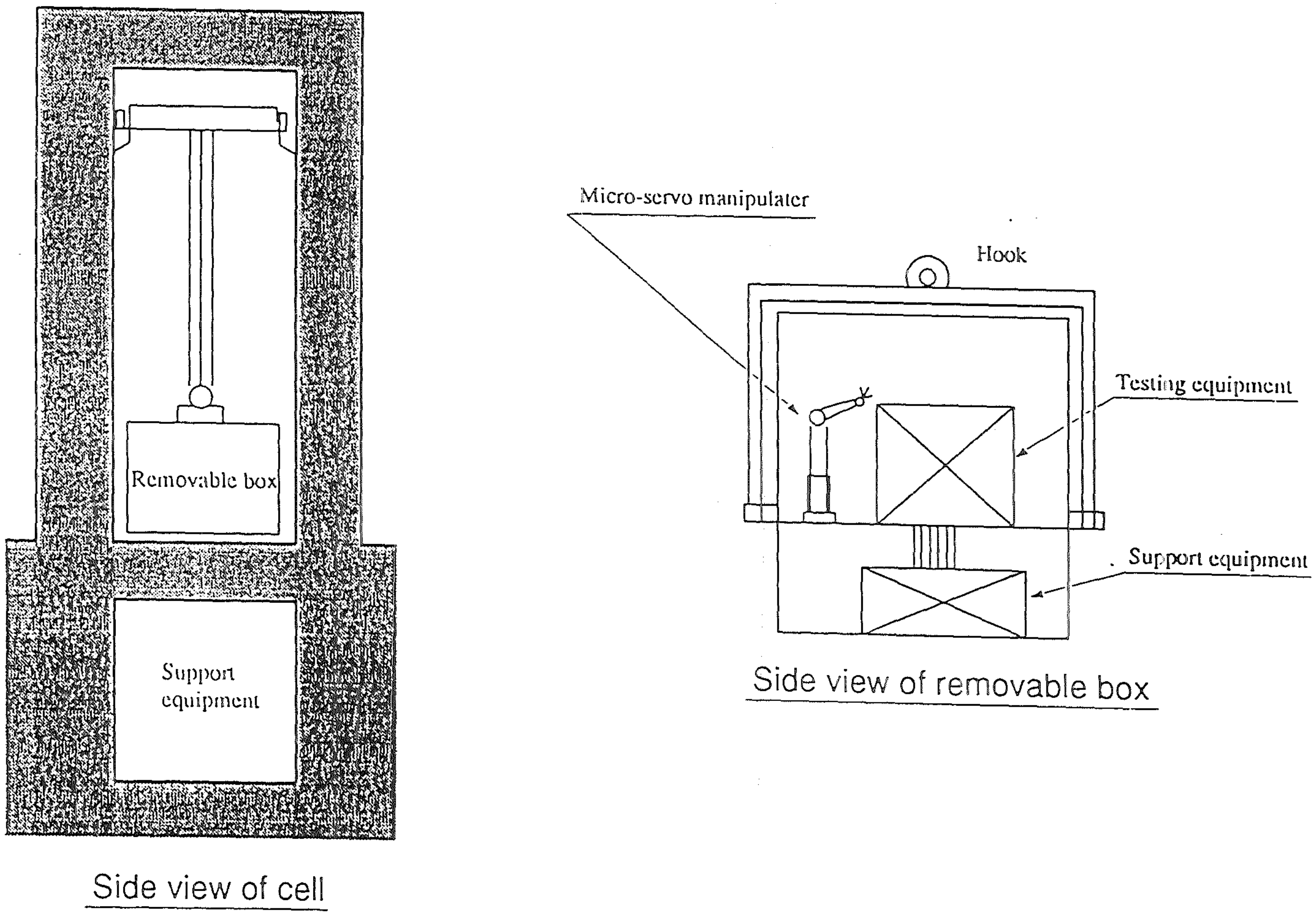

Fig. 2 Side view of hot cell and removable inner box.

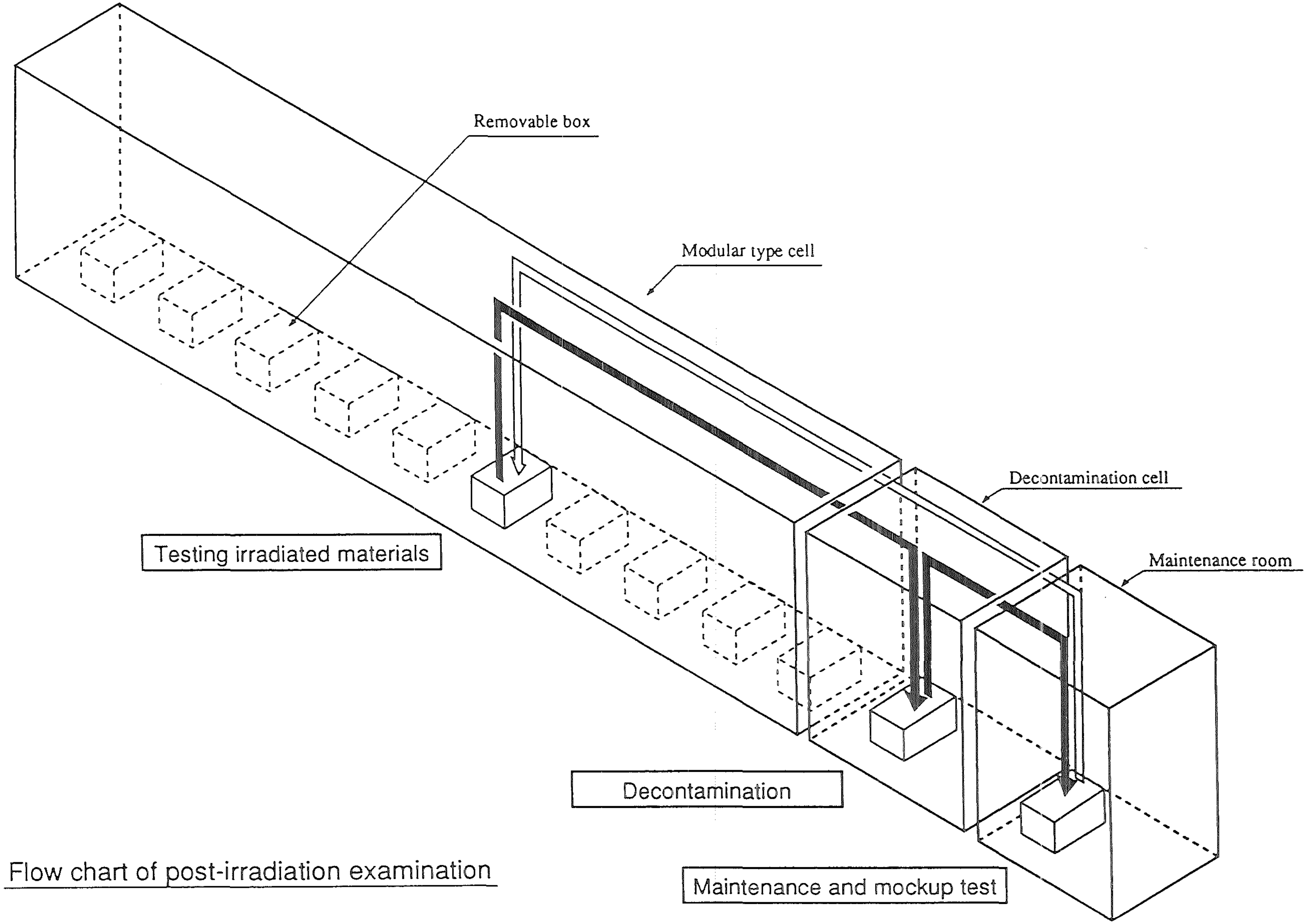

Fig. 3 Flow chart of post-irradiation examination in the modular-type cell line.

Tritium Confinement for PIE Facility

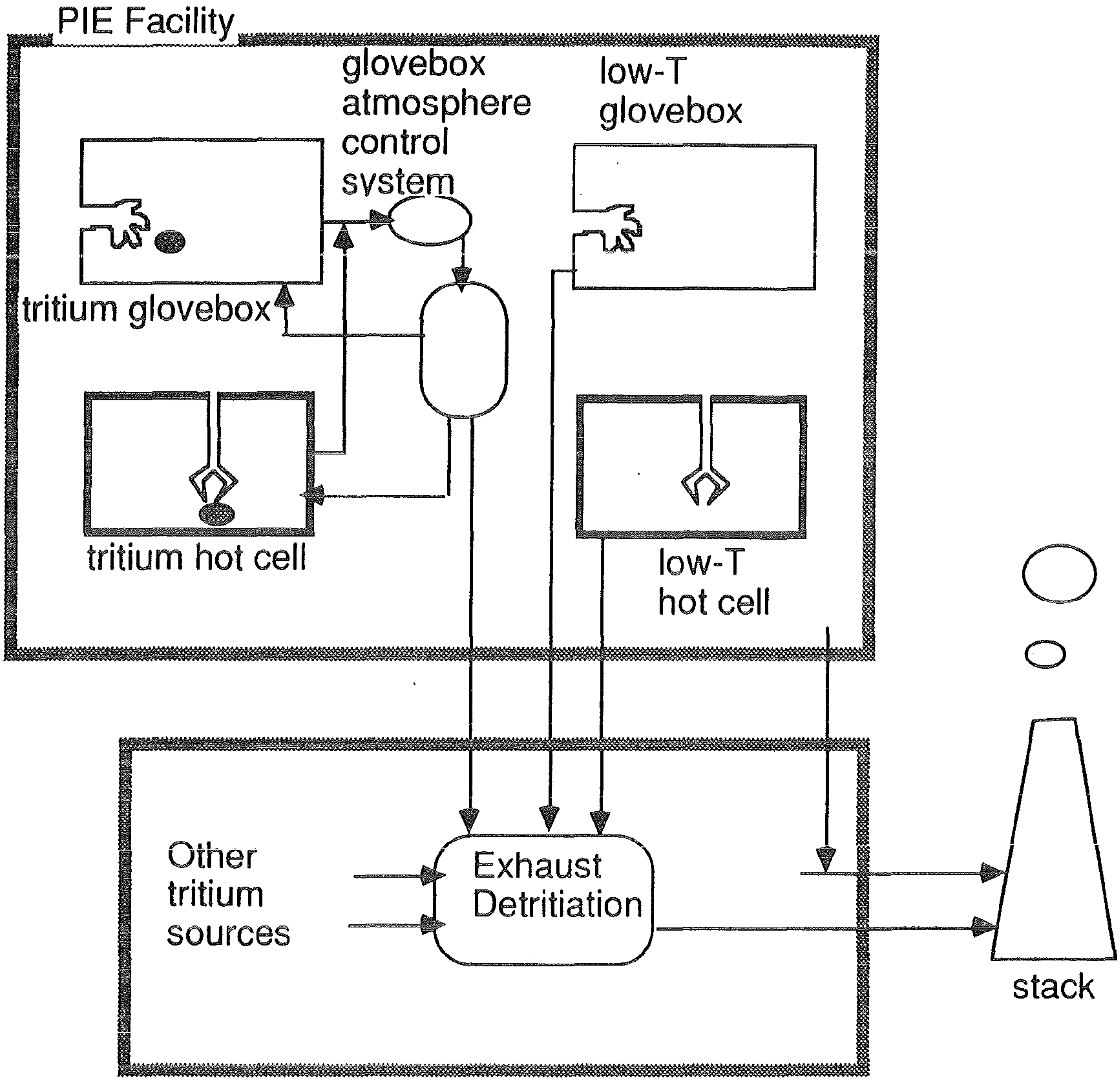

IFMIF-CDA Technical Workshop
on
Test Cell System

Karlsruhe, July 3-6 1995

Required Test Equipment for Materials Testing at IFMIF-Site

CDA-D-8

Preliminary Considerations

A. Möslang

Test equipment necessary for:

- Post irradiation examination (PIE) for all kinds of irradiated specimens
- Investigations on unirradiated control specimens in order to have references for postirradiated and in-beam irradiated specimens
- Quality control: - all kinds of specimens
  - instrumentation
  - irradiation devices

(● Capsulation and encapsulation of specimen packets)

Note: The overall test capacity should guarantee, that out-of-beam examinations are less time consuming than the irradiation experiments itself.

Tentative reference specimens to be tested

- Postirradiation tests (according to e.g. CDA-D-3):
  - ○ TEM disk — 0.25 mm x 3 mm ∅
  - ○ Sheet tensile specimen — 0.76 mm x 4.95 mm x 25.4 mm
  - ○ Disc compact tension crack growth — 2.3 mm x 12.5 mm ∅
  - ○ Disc compact tension fracture toughness — 4.6 mm x 12.5 mm ∅
  - ○ Charpy-V bars — 3.0 mm x 4.0 mm x 25 mm
  - ○ Pressurized tubes — 25 mm x 2.5 mm ∅
  - ○ Push-pull fatigue specimen — 3.0 mm x 4.95 mm x 25.4 mm
- In-situ tests (according to e.g. CDA-D-5), e.g.:
  - ○ push-pull creep-fatigue:
  - ○ coolant-coating compatibility:

    Tubular specimens:
    inner ∅: 8.00 mm
    outer ∅: 8.80 mm
  - ○ Irrad. Ind. Stress Corrosion:

    Crack growth specimens

Expected specimen yield

- Postirradiated specimens (according to CDA-D-3):

Properties	Average yield/year*
Microstructure (TEM disk)	370
Tensile	55
Crack growth	15
Fracture toughness	25
Charpy-V	45
Creep (pressurized tubes)	40
Fatigue	40

*assuming 150 dpa in 10 years

- In-Situ irradiated specimens (according to CDA-D-5):
  Analyses of fracture and microstructure;
  expected specimens: < 5/year

- Aged specimens:
  To minimize data scatter, about 2-3 times more mechanical tests on unirradiated reference specimens are usually necessary.

- Li-Target back plate *(to be discussed)*
  Investigations after intensive neutron exposure.

Hot Cell Test Equipment Considerations for IFMIF

Hot Lab (remote handled & controlled)	Investigations & Equipment	Required Space
Material Test Facilities	- Tensile tests: 2 universal testing machines (10 kN and 800 °C in vacuum) - Charpy-V tests: 2 instrumented devices (<50 Joule, -195 °C - 600 °C - Tension crack growth tests: 2 test devices - Fracture toughness tests: 2 test devices - Pressurized tubes: 1 size determination instrument; 1 leakage test device - Creep-fatigue tests thermal: 3 thermal fatigue devices Isothermal & thermomech.: 2 univers. testing machines (10 kN, 800 °C in vacuum)	Hot Labs: 50 m^2 Operation: 35 m^2 Charging: 35 m^2
Metallography	- specimen preparation TEM, REM - cutting: 1 lead box - punching, prethinning: 1 lead box - final thinning: 1 glove box - transfer locks for charging of devices and specimens - waste depository: 1 lead box - Metallographic investigations - surface morphology: 1 lead box - auto radiography: 1 lead box - 2 optical microscopes: 1 lead box	Hot Labs: 40 m^2 Operation: 30 m^2 Charging: 30 m^2
Microscopy	- Transmission Electron Microscopy - Scanning Electron Microscopy	50 m^2 (total) 35 m^2 (total)

Hot Cell Test Equipment Considerations for IFMIF (cont'd)

Hot Lab (remote handled & controlled)	Investigations & Equipment		Required Space
Non-destructive investigations	- Activation Analysis γ-Spectroscopy:	1 Ge-detector 1 SiLi- detector	25 m^2
	-Visual inspection, photo documentation	1 lead box	4
	- Weight determination	1 lead box	2
	- roughness determination	1 lead box	3
	- electrical and thermal conductivity analysis	1 lead box	5
	- Micro-hardness test device		2
Furnace equipment	- aging and annealing of specimens; capability for long-term thermal treatments at different temperatures in high vacuum:	8 furnaces	Hot Lab: 25 m^2 Operation: 15 m^2
Creep-Rupture Test Facility *(necessity to be discussed)*	- Creep-rupture test devices (<10KN) for long-term creep tests in vacuum	8 devices	Hot Lab: 32 m^2 Operation: 20 m^2
Specimen Treatment Facility	- specimen transfer lock - dismantling - storage capacity - welding equipment - specimen fabrication machining e.g. from Li-Target back plate (sawing, forming, spark erosion, polishing, etc.) - fabrication of coatings		Hot Labs: 50 m^2 Operation: 30 m^2 Charging: 30 m^2

Required Hot Cell Area - Preliminary Conclusions:

To investigate postirradiated and in-situ irradiated metal specimens at the IFMIF site, the following hot cell area is required. Existing hot cells are the basis of the area and test equipment considerations.

Hot Lab		Required space
Material test facilities		120 m^2
Metallography		100 m^2
Microscopy		85 m^2
Non-destructive investigations		40 m^2
Furnace equipment		40 m^2
Specimen treatment facility		110 m^2
Total area	Σ	495 m^2

Some additional area might be necessary for:

- postirradiation investigation of ceramics and composites,
- long-term creep rupture tests or any special tests necessary to establish an engineering data base,
- maintenance of activated accelerator & Li-target devices,
- quality control of specimens and equipment, and
- photographic laboratory.

The total estimated area is significantly above that one in the "Reference IFMIF Configuration" from 5 Dec 94, but still well below the hot cell areas in some Research Centers.

The discussed hot cell area and test equipment should be able to establish for the irradiated classes of materials all relevant data for an engineering data base at the IFMIF site within a sufficiently short time. ■

IFMIF-CDA Test Cell/Users Task CDA-D-9

Development of Overall Test Matrix

S. Jitsukawa, K. Noda, Y. Katano
IFMIF-CDA Test Cell/Users Group of JAERI

1. Introduction

Test matrices to obtain data base of FWB structural materials, ceramic breeders and insulator ceramics/diagnostic materials are treated in CDA-D-9.

Test matrices for selection of FWB structural materials are also described in this task. For design data base (model materials behavior), test matrices of in-situ tests may be included. However, test matrices of in-situ tests for structural materials are not treated in the following description. On the other hand, in-situ tests will be the major tests for ceramic breeders and insulator ceramics/diagnostic materials. These will be carried out at the areas with rather small dose rate, and the volume limitations for these tests may not be severe. Items and examples for these tests are shown in CDA-D-5.

2. FWB structural materials

(1) Irradiation period for test matrices in CDA-D-3 (standard matrix)

Figure D9J-1 (left) shows dose rate in collided condition as a function of distance from the target. Total volume for the standard test matrix in CDA-D-3 (STD matrix) is estimated to be about 1000 cc. The volume corresponds to occupy to the distance of about 100 mm from the Li target. Dose rate at about 100 mm will be 6 dpa/y. This will be 15 % of the rate at the target surface. To make even accumulated dose for the specimens loaded at different distances, specimens loaded at the position close to the target may be exchanged periodically for the specimens loaded at the position with lower dose rate. Averaged dose rate by the exchanging for the specimens (or the test matrix) loaded at positions up to 100 mm will be 15 dpa/y. That for the specimens at positions up to 50 mm will be 25 dpa/y. Average dose rate for the specimen group is also shown in Fig. D9J-1 (right) as a function of the distance or the thickness of specimen group. The availability of IFMIF is supposed to be 70 % in the figure.

Dose rate for each specimen will change by the position exchange. The ratio of dose rate in the change will be 6 and 2.6 for the thickness of 100 and 50 mm, respectively. The thickness for the ratio of two will be 35 mm. Dose rate change may introduce some effects on radiation damage, and the thickness should be limited by allowable level of the ratio.

For STD matrix, total irradiation period to 150 dpa will be 22.5y when specimens will be loaded to a thickness of 35 mm (specimens will be divided into three batches). The time will be 17 and 14.2 y with thicknesses of 50 (two batches) and 100 (one batch) mm, respectively. Irradiation period for STD matrix is estimated to be considerably long. In addition, the irradiation will be followed by the irradiation to obtain design data base including the space-occupying in-situ tests. An example of the test matrix for design data base (or model materials behavior) is shown in table D9J-1. This is an elemental test matrix in the test matrices to obtain materials data base for designing. For 2 heats, 3 temperature levels and 3 dose levels to 150 dpa (50, 100 and 150 dpa), total number of the elemental test matrix will be 18, corresponding to a total volume of about 1600 cc. Supposing that irradiation for 100 dpa will be carried out after those for 50 dpa (and the irradiation for 150 dpa will be finished at the same time), the number of elemental test matrix at one time and the total volume will be 12 and 1100 cc. And, the total irradiation time will be similar to that for STD matrix. To shorten irradiation time, irradiation with smaller test matrix may be considered.

(2) Test matrix with smaller irradiation volume

To shorten irradiation period, (i) further miniaturization of specimens and (ii) reduction of the number of properties may be considered.

(2-1) Specimen miniaturization

The test volumes of fracture toughness, 1/3 Charpy and crack growth specimens are relatively large, and further miniaturization of these specimens is apparently effective for the reduction of the irradiation volume. These tests are rather strongly depending on the specimen size, therefore progress of specimen miniaturization technology may be required for the further specimen miniaturization.

Temperature dependence of fracture toughness relating to properties of materials at relatively high deformation rate is obtained from the tests with 1/3 Charpy specimens. However, fracture toughness is not usually evaluated from Charpy tests due to the limitation of miniaturization of specimen arising from size effects and measurements. Development of techniques to evaluate temperature and displacement dependence of fracture toughness of the materials from 1/3 Charpy tests or sort of specimens will allow to remove DCT specimens from the test matrix and to result in reduction of irradiation volume.

Such technical feasibility may be examined by the communities of both small specimen technology and reactor design. The removal of DCT specimens reduces the volume of the elemental test matrix from 90 to 60 cc. In such a case, the total volume is 720 cc, corresponding to 11 y of irradiation period.

(2-2) Reduction of the numbers of properties to be tested and heats

STD test matrix contains most of the properties common for post irradiation tests. The materials properties rather sensitive to irradiation damage are thought to be flow stress and embrittlement at both low and elevated temperatures. These have close relation to reactor safety, and are indispensable to obtain prototypic design criteria. Comparing with these properties, fatigue, corrosion and creep properties are not very sensitive to irradiation.

A very small (elemental) test matrix only for materials selection is shown in table D9J-2. For 8 heats, 3 temperature levels and 3 dose levels, total irradiation volume is estimated to be about 500 cc, corresponding to irradiation period of 8.2 y to 150 dpa.

Reduction of the number of heats is of course effective for the reduction of the test volume. Total volume of the very small test matrices for 5 heats, 2 temperature levels and 3 dose levels is about 100 cc corresponding to 6 y of irradiation period to 150 dpa. Specimen block thickness for 100 cc is 10 mm. Dose rate at the back side of the specimen block may be a high value of 32 dpa/y. In-situ tests at a high dose rate and preliminary irradiation of the test matrix for design data base with limited number of heats may be carried out in the back side area of the specimens for the very small test matrix. Test volume for 1 heat, 3 temperature levels and 3 dose levels to 150 dpa is about 300 cc corresponding to irradiation period of about 8 y.

(3) Issues for reduction of test matrix volume

(i) Further specimen miniaturization may be necessary, including development of techniques to evaluate fracture toughness and its temperature and displacement rate dependencies using 1/3 Charpy specimen.

(ii) Limition of properties to be evaluated

(iii) Allowable range of dose rate change accompanied by the exchange of position of the specimens may be examined.

3. Ceramic breeders

(1) A Strategy of Ceramic Breeder Materials Development for DEMO Fusion Reactors

[Ceramic Breeders and Their Operation Conditions in Various types of Blanket Design]

1)Various types of ceramic breeders are considered for various blanket designs.

a) Shapes: pebble bed, block, tube (annular pellet)

b) Materials; Li_2O, Li_2ZrO_3, Li_4SiO_4, $LiAlO_2$, Li_2TiO_3

2)Various conditions for ceramic breeders in various blanket designs

a) Temperature: 300 to 900 C

b) Neutron Fluence: 5 to 30 (40) dpa

c) Li Burnup: several to 30 %

d) Sweep gas:He+H_2 (0-0.1%)

[Current R&D Status of Ceramic Breeder Irradiation Performance]

1) Good tritium release performance and irradiation durability of Li_2O and Li_2ZrO_3 were demonstrated up to 4% Li BU (burnup) (equivalent Li BU level in ITER blanket designs) in fast neutron reactor environment by IEA collaborative irradiation tests (BEATRIX-II).

2) Temperature and temperature gradient affect microstructure in irradiated specimens substantially. Temperature gradient depends on shape and size of specimens.

3) No data for Li_2O and Li_2ZrO_3 at fluences higher than 4 % BU.

4) No data for Li_4SiO_4, $LiAlO_2$, Li_2TiO_3 at high burnup (high fluence).

5) No data for radiation effects due to high energy neutrons (higher than 2 MeV)

[Required R&D for Ceramic Breeders for DEMO Fusion Reactors]

1) Fraction of high energy neutrons in neutron spectra for ceramic breeders is somewhat smaller than that for structural materials. High fluence irradiation tests using fast reactors are needed to evaluate tritium release performance and durability up to DEMO relevant high burnup.

2) High fluence irradiation tests using IFMIF up to DEMO relevant high dpa using IFMIF were required to evaluate high energy neutron irradiation effects on tritium release performance and durability.

3) Development of innovative ceramic breeders (high radiation-resistance, low activation) .

4) Above-mentioned irradiation tests using fast reactors and IFMIF are needed to be carried out for present candidate materials (Li_2O, Li_2ZrO_3, Li_4SiO_4, $LiAlO_2$, Li_2TiO_3) and innovative materials with various shapes (disks, cylindrical pellets, pebbles) in materials development/selection phase.

5) Irradiation tests of selected materials in selected shapes for a reference blanket design using IFMIF are required to be performed up to the end of life (DEMO relevant Li burnup and dpa) in spectrum-tailored neutronic conditions using specimen sets (breeders, neutron multiplier, coolant,

structural materials) and specially-designed irradiation capsules and in temperature/atmosphere conditions in the reference blanket design to obtain materials database for the DEMO blanket design.

(2) Irradiation Tests of Ceramic Breeders using IFMIF
(Materials Development/Selection Phase)

1) Irradiation

All irradiation tests should be carried out by in-situ experiments to examine irradiation performance (in- situ tritium release, durability, etc.) under controlled moisture conditions. (see CDA-D-5)

2) Materials

*Present candidate materials; Li_2O, Li_2ZrO_3, Li_2TiO_3, $LiAlO_2$, Li_4SiO_4,

*Innovative materials

3) Specimen sizes/shapes:

*Disks (10 mm in diam. X 2 mm in thick.)

*Pellets (10 mm in diam. X10 mm in height)

*Pebbles (1 mm in diam.)

*Compatibility test specimens;
Breeder (disks, 5 mm in diam. X 1.5 mm in thick.)
Structural (disks, 5 mm in diam. X 0.5 mm in thick.)

4)Test conditions:

*Neutron flux; 5-10 dpa/y (Medium to low flux region)
*Neutron fluence; Max 40 dpa#
*Temperature; 300-900 C (e.g., 400 C, 600 C, 800 C)
*Sweep gas; He, He+H_2 (0.1-1 %) (Reference; He+0.1%H_2)

#Specimen integrity is checked at end of every irradiation cycles (e.g., once a year) non-destructively (neutron radiography). Irradiation is stopped when severe degradation is found.

5)In-situ measurements:

*Tritium release rate
*Temperature of specimens

6)PIE:

Mechanical integrity, Dimensional change, Density change, Microstructural change, Fracture strength, Tritium/Helium retention, Thermal conductivity, Radiation damage, Compatibility, Li burn-up, etc.

(3) Test Matrices for Ceramic Breeders
(Materials Development/Selection Phase)

(see Table D9J-3 and Table D9J-4)

4. Insulator Ceramics/Diagnostic Materials

(1) A Strategy for Insulator Ceramics/Diagnostic Materials Development

1) Many kinds of insulator ceramics and diagnostic materials will be used for for various components at various conditions in fusion reactors. Extensive and flexible materials development should be performed.

2) Functional properties (electrical; and optical) are substantially affected under irradiation. (flux effects effects) Functional properties of insulator ceramic and diagnostic materials degraded at low fluence in comparison with metallic materials. (fluence effects) Functional effects must be tested with in-situ tests, and then durability of materials with acceptable radiation resistance of functional properties should be examined by PIE.

3) Evaluation of irradiation properties of various ceramics available is carried out in terms of functional properties and durability. On the basis of materials data of ceramics available, innovative materials with high level of radiation resistance should be developed.

(2) Irradiation Test of Insulator Ceramics/Diagnostic Materials Using IFMIF

All irradiation tests for functional properties (electrical resistivity (RIC/RIED), dielectric loss, optical absorption/luminescence) should be carried out by in-situ experiments under controlled test conditions (see CDA-D-5)

PIE are needed to be performed for evaluation of durability and radiation damage.

1) Materials:

Al_2O_3, MgO, AlN, $MgAl_2O_4$, SiO_2, Si_3N_4,
Optical fibers (Currently available materials), Innovative materials

2) Test Items:

a) In-situ experiments

-Electrical resistivity (IER)
-Dielectric loss (IDl)
-Optical properties (IOP)

b)PIE

-Thermal conductivity (PTC)
-Mechanical integrity (PMI)
-Dimensional change (PDC)
-Fracture strength (PFS)
-Radiation damage studies (PRD)
(Damage structure, point defects)

(3) Specimen size/shapes:

Disks (8.5mm in diam. x 0.2mm in thick.): IEP, PRD
(8.5mm in diam. x 0.5mm and 3mm in thick.): PTC, PMI, PFS

Rectangular (25' x 10" x 3mm and 5'mm^3): IDl, PMI, PDC, PFS, PRD

Fiber wires (0.25mm in diam. x 30 pieces x 8,000mm): IOP
(0.25mm in diam. x 30 pieces x 30mm): PMI, PDC, PRD

(4) Test conditions:

Neutron flux: 10^{-5} to 20 dpa/y (Medium to low flux region)
Neutron fluence: 10^{-3} to 50dpa
Temperature: RT - 800C (Design depend)
Liq.He to -180C (Cryogenic window)
Additional condition:
Applied electric filed (for RIED) 1,000 to 1,500V/cm

-Specimen temperature control of In-situ experiments may be examined with gas gap controled.

(3) Test Matrices for Insulator Ceramics/Diagmostic Materials

(TBD.)

Table 3-14/1

Table D9J-1 An example of the large test matrix for design data accumulation (Post irradiation test)

Specimen		Mulitiplicity	Number of specimen packet	Packet volume for each heat, temperature and dose
TEM	Microstructure, Buldge test for a	25	1	0.216
Tensile	Temperature/strain rate depende	35	6	7.098
Fracture toughness	Temperature/displacement rate d	30	10	34.9
1/3 Charpy	Temperature/displacement rate d	30	8	18.16
Creep	Creep strain (four stress levels),	20	20	6.6
Fatigue	Fatigue life, Cyclic stress-strain	40	14	16.562
Crack growth	Crack growth rate, Corrosion fai	12	2	6.98
				90.516

(in cm^3)

For three temperatures and three dose levels, total volume will be 810 (cm^3)

Table D9J-2 An example of the very small test matrix for materials selection

Specimen		Multiplicity	Number of specimen packet	Packet volume for each heat, temperature and dose
TEM	Microstructure, Buldge test	10	0.2	0.0432
Tensile	Stress-strain relation	3	0.5	0.5915
Creep	Creep strain	3	3	0.99
1/3 Charpy	Temperature dependence of dyn	6	1.5	3.405
				5.0297

The total number of irradiation condition is 99, and the total volume for this vs matrix will be 500 (cm^3) for 50% of specimen volume fraction

Table D9J-3 Test Matrices (Ceramic Breeder)

Materials	Specimen type	Test Items	Dose (dpa)	Sweep Gas	Temmperature(C)
Li_2O (L1) Li_2ZrO_3 (L2) Li_4SiO_4 (L3) $LiAlO_2$ (L4) Li_2TiO_3 (L5) Innovative (I)	Disk (10mm diam.) (2mm thick.)	- In-situ tritium release - Neutron radiography - Mechanical integrity - Dimensional Change - Density Change - Microstructural Change - Fracture Strength - Tritium/Helium retention - Thermal Conductivity - Radiation damage - Li burn up	Max 40 dpa*	He+0.1% H_2 (reference)	400 600 800
	Pellet (10mm diam.) (10mm height)				Temp. gradient (400 - 900C) for Li_2O (300 - 900C) for Others
	Pebble (1mm diam.)				Temp. gradient (400 - 900C) for Li_2O (300 - 900C) for Others
	Compatibility Breeder (5mm diam.) (1.5mm thick.) Structural (5mm diam.) (0.5mm thick.)	-Compatibility			400 600 800

* Specimen integrity is checked at end of every irradiation cycle. Irradiation is stopped when severe degradation of specimen integrity is found.

Table D9J-4 Specimen and Capsule Volume (Ceramic Breeder)

Specimen Type	Specimen Volume	Capsule Configuration and Volume	No of Specimens in Capsule	No. of Capsules	Materials	Temperature	Total Volume
Disl (10mm diam.) (2mm Thick.)	$157 mm^3$ $0.16 cm^3$	10 x 12 x 52mm = $6240 mm^3$ =$6.3 cm^3$	6	1 capsule for each materials and temp. =1 x 6 x 3 =18	L1,L2, L3, L4,. L5, I	400 C 600 C 800 C	$114 cm^3$
Pellet (10mm diam.) (10mm height)	$785 mm^3$ $0.79 cm^3$	14 x 20 x 25mm =$7000 mm^3$ =$7 cm^3$	2	1 capsule for each materials =1 x 6 = 6	L1, L2, L3, L4, L5, I	Temp. gradient	$42 cm^3$
Pebble (1mm diam.)	$0.26 mm^3$ $0.00026 mm^3$	9.5x9.5x3.14x25mm =$7085 mm^3$ =$7.1 cm^3$	Pebble bed	1 capsule for each material =1 x 6 = 6	L1, L2, L3, L4, L5, I	Temp. gradient	$43 cm^3$
Compatibility Breeder (5mm diam.) (1.5mm thick.) Structural (5mm diam.) (0.5mm thick.)	2 Breeder $29 mm^3$ x2 = $58 mm^3$ 2 Structural $10 mm^3$x2 =$20 mm^3$	13 x 15 x 38mm =$7410 mm^3$ =$7.4 cm^3$	12 specimen sets	1 capsule for each temp.	L1, L2, L3, L4, L5, I	400 C 600 C 800 C	$22 cm^3$

L1:Li_2O, L2:Li_2ZrO_3, L3: Li_4SiO_4
L4 : $LiAlO_2$, L5: Li_2TiO_3, I: Innovative

Total $221 cm^3$

Dose rate

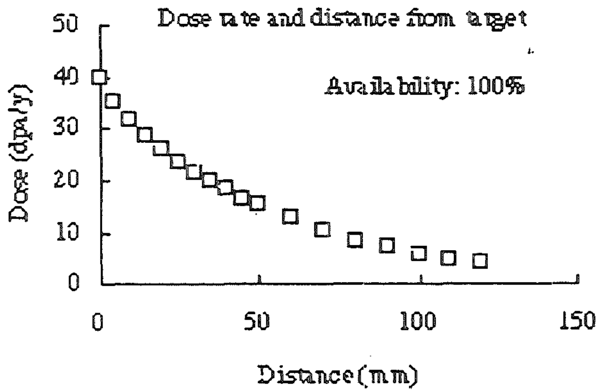

Dose rate with specimen position exchange for uniform dose level distribution

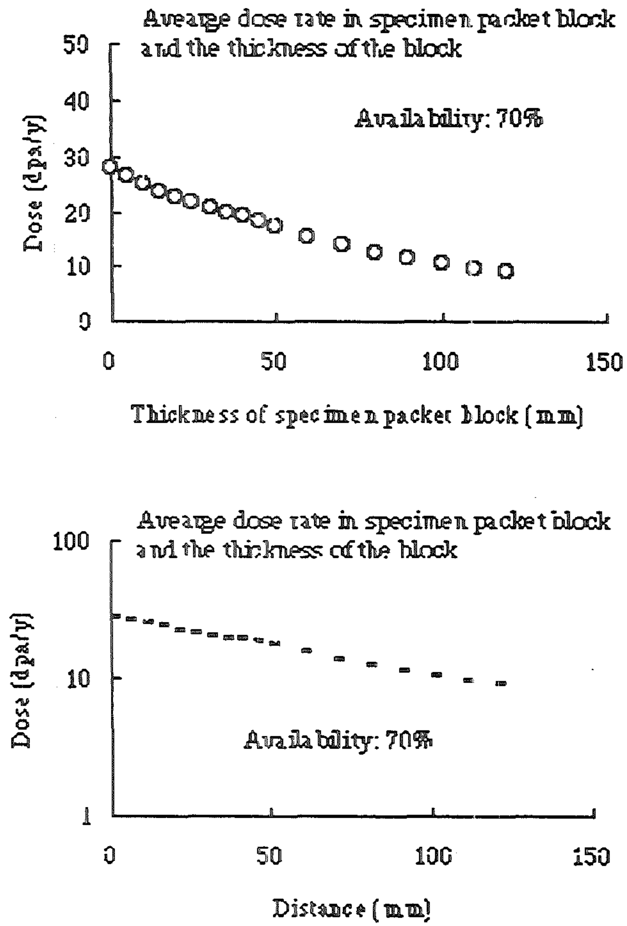

Fig. D9J-1 Dose rate as functions of the distance from the target

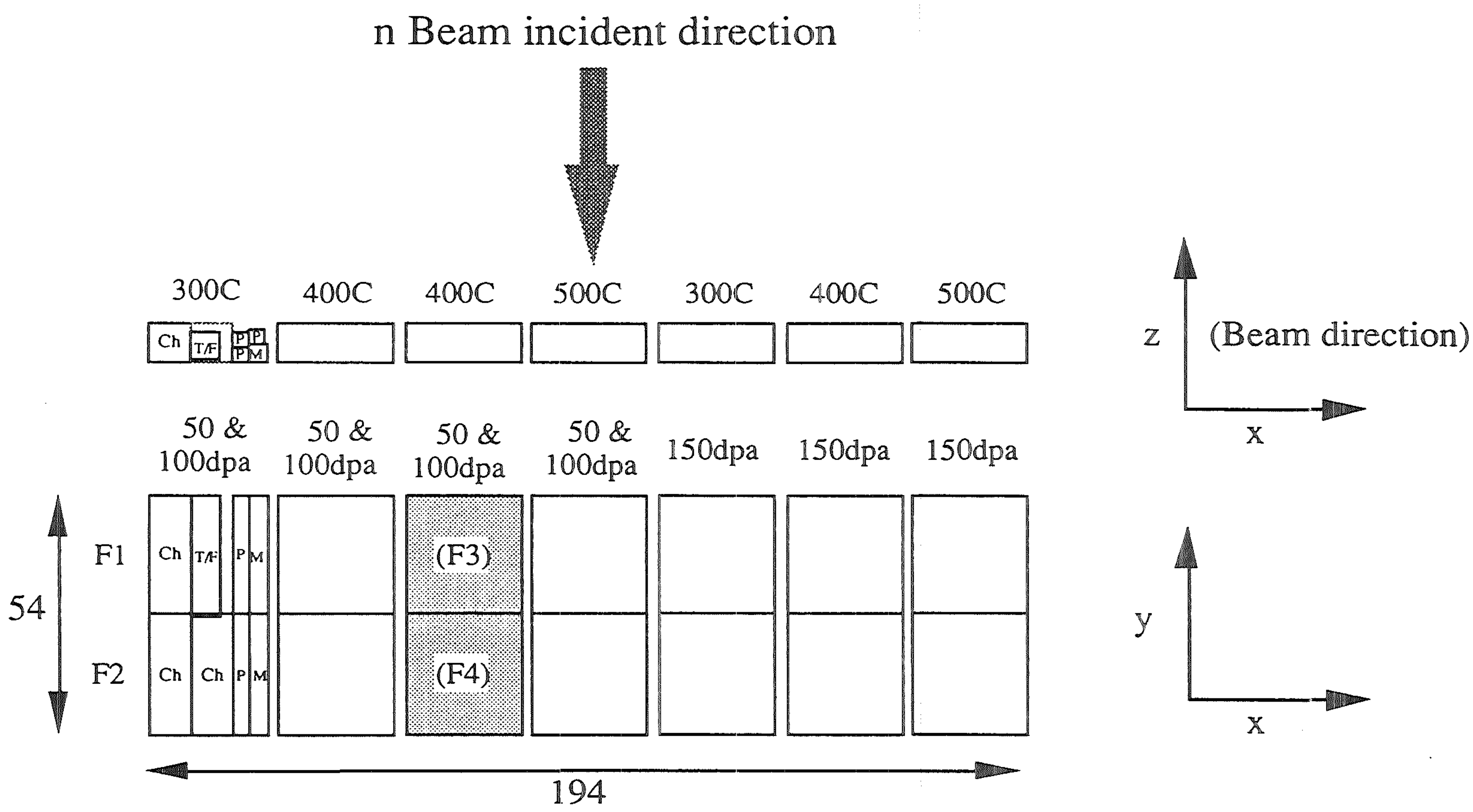

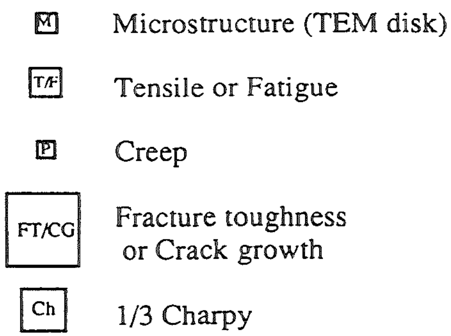

Fig. D9J-2-1 Arrangement of specimen packets

Very small test matrix

Case 1: One material, two (four) heats

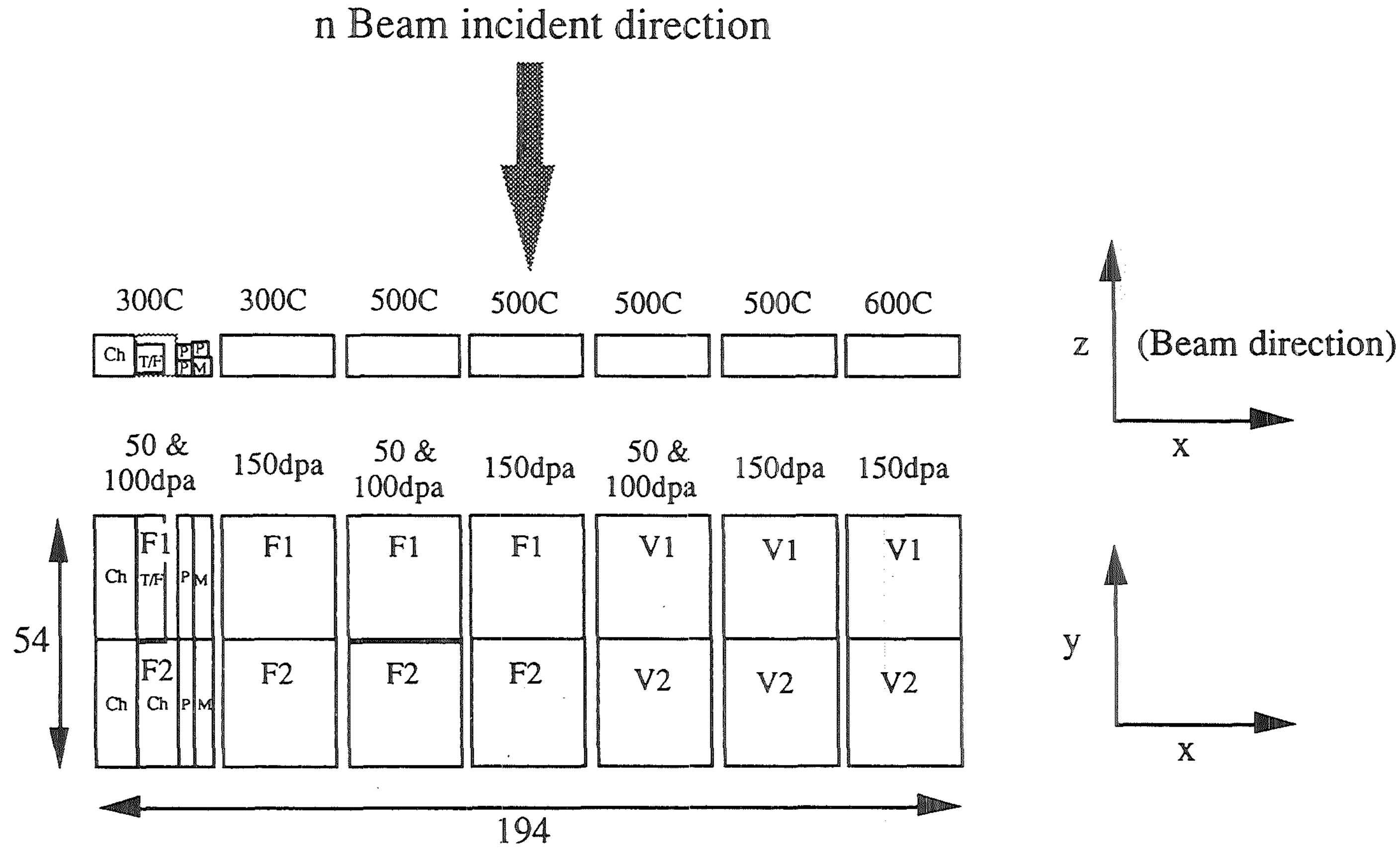

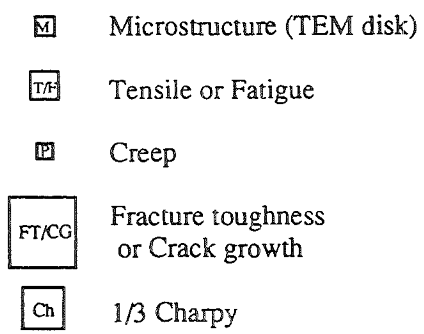

Fig. D9J-2-2 Arrangement of specimen packets

Very small test matrix

Case 2: Two material, two heats

Irradiation Test Volume for In-situ experiments of Ceramic Breeder

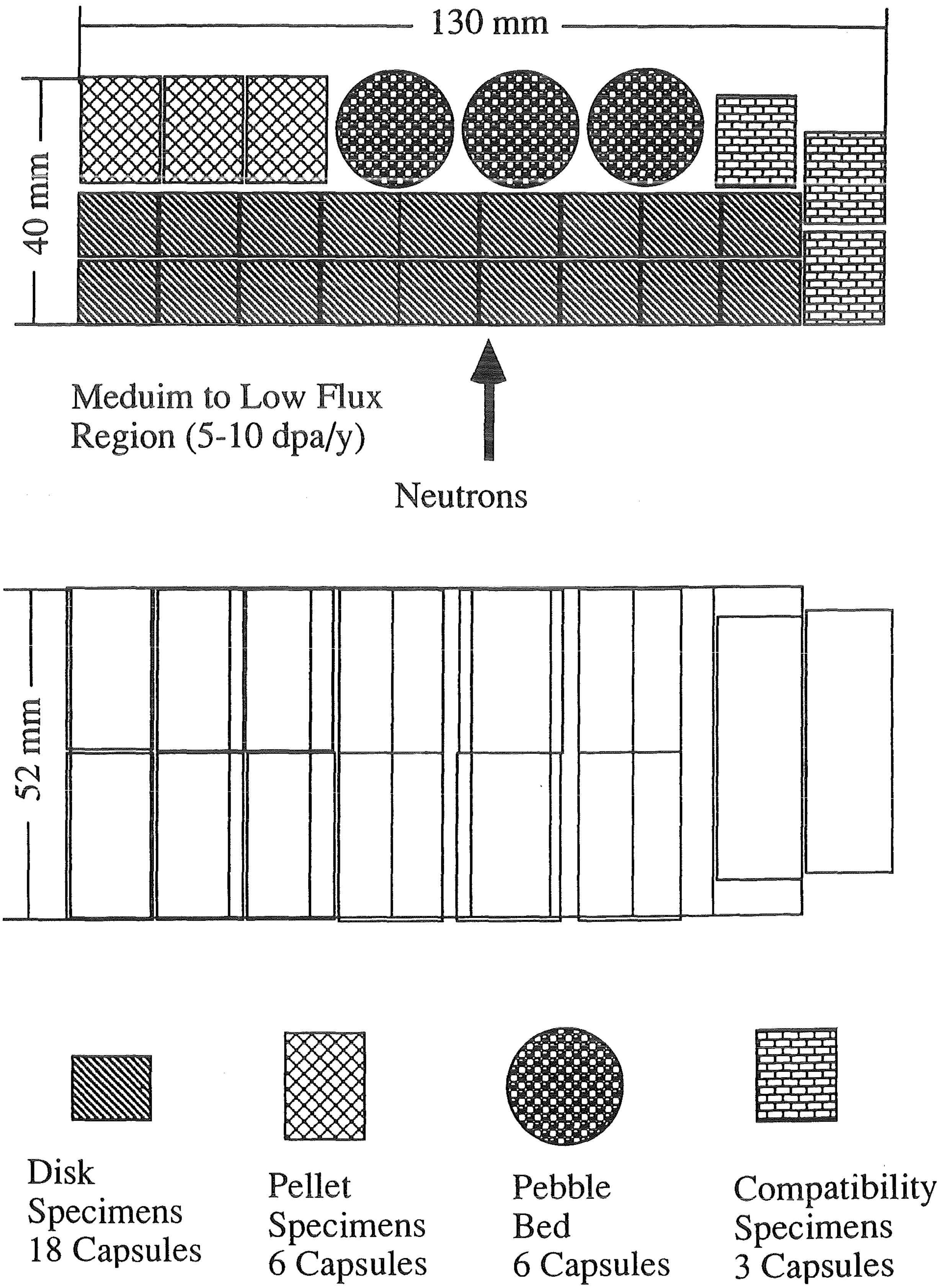

Irradiation capsule of PIE specimens

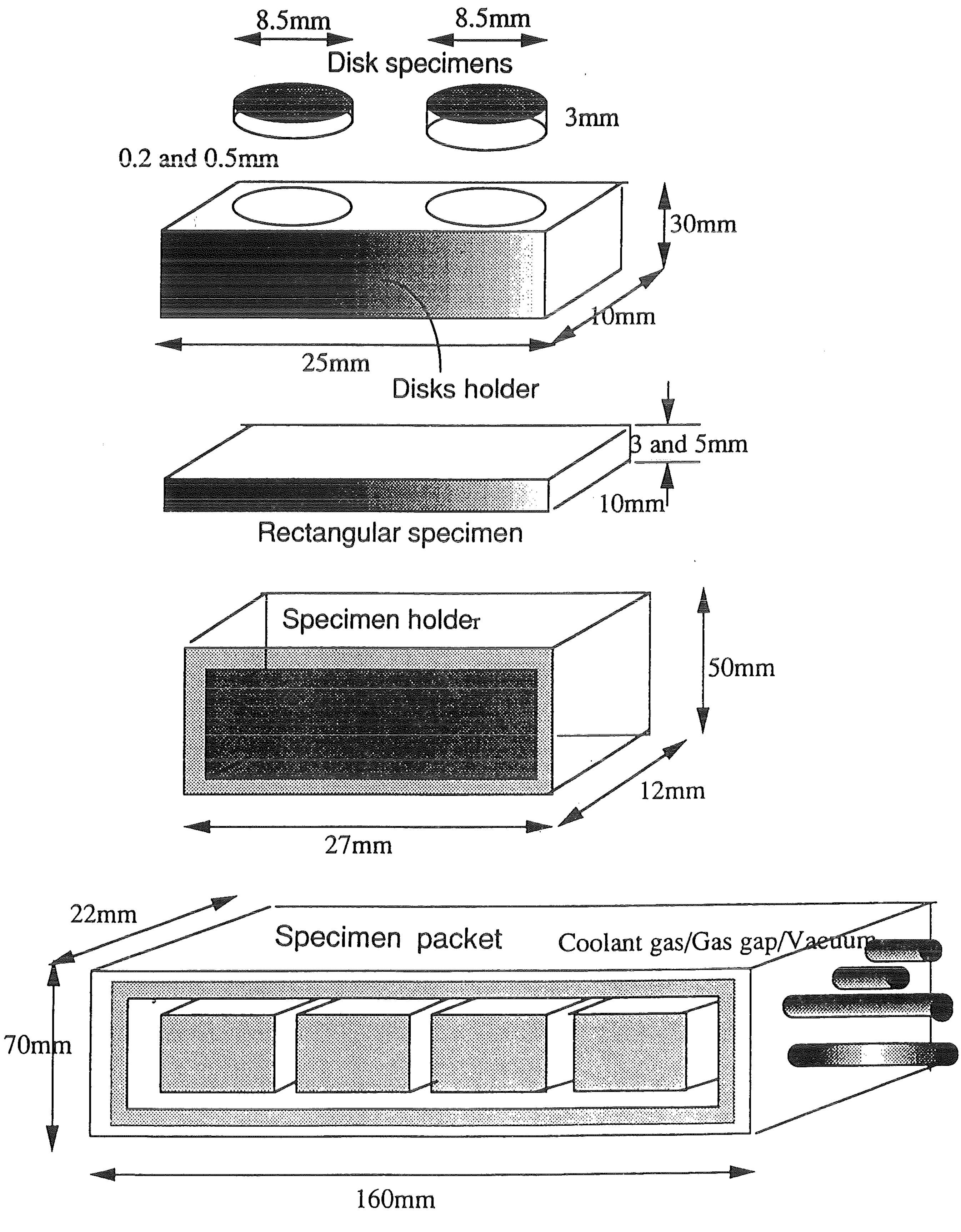

ENEA
ENTE PER LE NUOVE TECNOLOGIE
L'ENERGIA E L'AMBIENTE
Associazione EURATOM-ENEA sulla Fusione

ENEA Contributions to the Conceptual Design Activity (CDA)
of the International Fusion Material Irradiation Facility
(IFMIF)

INTERMEDIATE REPORT

of

Test Cell Task D-10 , Define Design Concept for Dosimetry

(B. Esposito)

CONTRACT
ERB5000
CT 950012 NET

(NET/94-365)

May 1995

Executive Summary

The final goal of the task is to provide a detection system suitable for the measurement of the neutron flux and energy spectrum experienced by irradiated specimens in the IFMIF test cell.

The neutron foil activation method is proposed as a simple and reliable measuring system. In this frame, two issues have been addressed so far: a) the assessment of constraints and b) the identification of suitable activation reactions.

A list of key parameters and requirements (available from official documents) concerning neutron measurements in the test cell has been produced; this list should, however, still be modified according to updated specifications and/or inputs from participants in the joint task and other related tasks.

On the basis of such parameters, a literature search of suitable neutron activation reaction has been undertaken.

This report focuses on reactions with thresholds above 10 MeV, as for lower energies several reactions are already well known and have been routinely used in various experiments.

A table with 46 candidate reactions, mainly (n,xn), above 10 MeV has been produced; for each reaction, the table gives the half-life of the product nuclide, the energy threshold, the energy of the emitted γ-rays, the peak cross section and the literature references.

Almost all the reactions included in the list have experimentally measured cross sections (experimental data are believed more reliable than theoretical calculations or evaluations).

However, there is a lack of experimental cross section data in the region between 20 MeV and 50 MeV. Cross section plots (derived from published papers up to 1994) have also been attached to the report.

1. Introduction

The proposed dosimetric system for the IFMIF test cell is the neutron activation technique. The method consists in the neutron irradiation of a set of foils of different materials and energy thresholds and in the subsequent measurement of the induced γ-ray activity. The neutron flux (and its energy distribution) in different locations within the test cell is then easily derived by means of a deconvolution algorithm.

The choice of such method is primarily due to its semplicity: it provides an energy spectrum determination which can be accurate within ~10% (of course the measured activities must have similar uncertainties); the foils require no electrical connection to the outer world: they can be very thin and located close to the actual samples which are under neutron irradiation testing; also, the method does not require any manipulation or check during the irradiation run and the foils can be transferred to the counting station after any irradiation by means of a remote handling system, together with the samples under test; the foils are not affected by the high radiation field. However, some materials might be not suitable to the high temperature within the test cell.

Two different types of measurements can be performed:

- pre-irradiation or short term measurement: this measurement is needed to check and confirm the calculations of the neutron flux in the test cell prior to any irradiation test, during the initial phase of testing of the IFMIF source: foils producing short-lived nuclides (i.e. whose half-lives are of the order of hours) should be used in this case.

- in-irradiation or long term measurement: this is the standard measurement mode; a stack of foils is assembled in various positions in the test cell and removed only after the irradiation run is completed. Foils producing long-lived nuclides (i.e. whose half lives are comparable to the irradiation duration) should be used if information on the integrated neutron flux is required; the use of short-lived nuclides is also possible:

a) as a complementary measurement of the energy spectrum (assuming its global stability during the irradiation run), or

b) if multiple measurements are required at different times during the irradiation runs.

2. Constraints

A minimum set of test cell parameters, which should be known in advance for a proper final design of the activation system, is listed below (in brackets are the data presently available in official documents [1]):

1) neutron flux spatial distribution (wall loading of ~2 MW/m^2);

2) neutron energy spectrum;

3) temperature distribution;

4) available volume (min. 0.4 l --> high flux, 1 l total);

5) access and internal structure;

6) typical duration of irradiation runs.

The knowledge of items 1), 2), 3) and 6) is necessary to optimise the choice of the activation foil material and size (calculations of 1) and 2) should be provided by tasks D-1 and D-2). Items 4) and 5) are related to the actual design of the system and the choice of foil locations.

In addition, some questions should be answered concerning the required output of information from neutron measurements. For example:

- do we simply require the knowledge of the time-integrated neutron flux (and energy spectrum) or also its time evolution?

3. Spectrum Analysis

Neutron activation threshold reactions have been successfully used in a fast fission reactor environment to determine the energy spectrum and the absolute magnitude of the neutron flux; the maximum neutron energy in the fission reactors is approximately 10 MeV and several activation reactions are available with threshold up to this energy and are routinely used [2].

A code such as SAND-II [3] (Spectrum Analysis by Neutron Detectors - II) can be employed for the deconvolution of the measurements of neutron induced γ-ray activity in the foils and to obtain the neutron energy spectrum. The SAND-II code is normally run in combination with a 640 energy-group cross sections from different libraries; it uses an iteration method with an initial trial spectrum, subsequently modified until a solution spectrum is found which provides calculated γ-ray activities in agreement with the measured activities. The code is a useful tool also in the selection of the best set of foils, as it can give the limits of sensitivity of the foils in a given neutron field.

In the case of the Li(d,n) neutron source used in the IFMIF project, the neutron energy upper limit is about 50 MeV [4]. Therefore, although the same technique can be applied as in fission reactors, additional activation reactions, with thresholds extending up to ~50 MeV, are needed. A literature search has been performed in order to obtain such reactions. The main requirements in the search have been the following:

- availability in published papers of experimental determinations of cross sections;
- energy threshold in the range: 10 MeV÷ 50 MeV.

Two problems have been encountered:

- lack of reactions with published cross section data above ~30 MeV;
- poor quality of cross section data for reactions with threshold above ~20 MeV.

An effort in providing new experimental data must be certainly undertaken.

At the same time, libraries with cross sections (also evaluated or calculated) extending up to 50 MeV should be produced (task D-7). The few existing libraries available above 20 MeV, such as DLC-119/HILO86 [5], are based on calculations only.

4. Activation reaction list

A list of 46 neutron activation reactions with experimentally measured cross sections and threshold above 10 MeV is given in Table I. The eight columns give respectively: type of neutron activation reaction, half-life of product nuclide, energy threshold of reaction, peak value of cross section (roughly), accuracy of cross section data (see note in Table I), energy of main γ-ray lines, latest references with experimental cross section data, latest reference describing dosimetry applications of the reaction. The list is not meant to be complete and addition of further reactions is necessary, especially with thresholds above 30 MeV. The cross sections of the reactions listed in Table I are plotted in Figs. 1-45.

The half-lives show a large spread, from ~9 min to ~3 years; however, only few of them have "long" (i.e. > ~100 days) half lives: ^{55}Mn(n,2n), ^{89}Y(n,2n), ^{23}Na(n,2n), ^{175}Lu(n,3n), ^{151}Eu(n,3n), ^{197}Au(n,3n), ^{209}Bi(n,3n), ^{59}Co(n,3n), ^{27}Al(n,spall).

The accuracy of the cross section data is decreasing with increasing reaction threshold. Most of the reactions have cross sections values (in the region of interest) in the range ~0.1-1 barns.

Further work is in progress to select a proper subset of reactions from Table I, taking into account all constraints previously discussed and the need mainly for reactions producing long-lived nuclides, i.e. with lives comparable to typical irradiation times. In this phase, the SAND-II code will be employed (with a restricted energy-group cross section data): the predicted IFMIF spectrum will be used as input. The aim is to verify the feasibility and the quality of the determination of the IFMIF neutron spectrum energy spectrum by using the foil activation method.

References

[1] IFMIF Neutron Source Planning Meeting, Tokai, Japan, 13-15 June 1994

[2] J.G. Kelly, P.J. Griffin and W.C. Fan, IEEE Trans. Nuc. Sci., **40**(6), 1993

[3] W.N. McElroy, S. Berg, T. Crockett, R.G Hawkins, "A computer-Automated Iterative Method for Neutron Flux Spectra Determination by Foil Activation", AFWL-TR-67-41, Sandia National Laboratories, 1967

[4] G.L. Varsamis et al., Nuc. Sci. Eng., **106**, 160, 1990

[5] R.G. Alsmiller, Jr., J.M. Barnes and J.D. Drischler, "Neutron-Photon Multigroup Cross Sections for Neutron Energies ≤400 MeV", ORNL/TM-9801, Oak Ridge National Laboratory, 1986

Table I: Activation reactions (>10 MeV threshold) with experimentally[a)] measured cross sections

Reaction	Half-life	Threshold (MeV)	Cross Section (barn)	Cross Section Quality[b)]	Gamma Ray Energy (MeV)	Cross Section Reference[c)]	Activation Reference
$^{14}N(n,2n)^{13}N$	9.96 min	~10	0.01 @ 15 MeV	5	β^+ 1.19	* Ry78	Ku77
$^{127}I(n,2n)^{126}I$	13 d	~10	2 @ 14 MeV	11	0.39, 0.67	* Lu79	
$^{64}Zn(n,t)^{62}Cu$	9.73 min	10.2	0.3-0.5 @ 34 MeV	1	0.51	Uw92	
$^{55}Mn(n,2n)^{54}Mn$	312 d	10.4	~0.8 @ 20 MeV	6	0.84	* Uw92, Gr85, Lu80	
$^{65}Cu(n,2n)^{64}Cu$	12.7 h	10.3	1 @ 14-20 MeV	11	0.51, 1.35	* Cs82, Ry78b ENDF/B-V	
$^{59}Co(n,2n)^{58}Co$	70.8 d	10.3	0.9 @ 16-20 MeV	13	0.51, 0.81	* Gr85, Hu81, Ve77 ENDF/B-V	
$^{63}Cu(n,2n)^{62}Cu$	9.76 min	11.3	0.7-1.0 @ 18 MeV	15	0.51, 1.17	* Uw92, Ja78, Ry78b	Ku77, Ho95
$^{70}Ge(n,2n)^{69}Ge$	1.6 d	11.5	1.4 @ 15 MeV	2	1.11	* Bo76, Pr61	Ku77, Ho95
$^{45}Sc(n,2n)^{44}Sc^m$	2.44 d	11.6	0.5 @ 17 MeV	5	0.27	* Ma80, Ve77, ENDF/B-V	
$^{89}Y(n,2n)^{88}Y$	106.6 d	11.6	1.2 @ 18-22 MeV	9	1.84	* Hu80, Ve77	
$^{64}Zn(n,2n)^{63}Zn$	38 min	12.0	0.2-0.5 @ 20 MeV	10	0.67	* Uw92, Bo69	
$^{90}Zr(n,2n)^{89}Zr^{g+m}$	78.4 h	12.1	1.2 @ 19-22 MeV	9	0.91	*Ik85, Zh84, Pa82 ENDF/B-V	Ke93
$^{52}Cr(n,2n)^{51}Cr$	27.7 d	12.4	~0.5 @ 16 MeV	1	0.32	* Bo68 ENDF/B-V	
$^{58}Ni(n,2n)^{57}Ni$	36 h	12.6	0.08 @ 18 MeV	17	0.51, 1.37	* Gr85, Pa85 ENDF/B-V	Ku77
$^{23}Na(n,2n)^{22}Na$	2.6 a	13.0	~0.1 @ 20 MeV	5	1.28	* Uw92, Ad80 ENDF/B-V	
$^{46}Ti(n,2n)^{45}Ti$	3.08 h	~13	0.2 @ 20 MeV	5	1.41	* Cs82, Pa75, Pa66	
$^{19}F(n,2n)^{18}F$	109.7 min	13.1	0.95 @ 20 MeV	4	0.51	* Ha91, Ry78, Me67	Ku77
$^{50}Cr(n,2n)^{49}Cr$	41.9 min	13.5	0.1 @ 25 MeV	2	0.15	* Uw92, Bo65	
$^{54}Fe(n,2n)^{53}Fe$	8.53 min	13.9	0.1-0.2 @ 18 MeV	4	0.38	* Gr85b, Ry78, Bo76	
$^{191}Ir(n,3n)^{189}Ir$	13.1 d	14.4	1.8 @ 24 MeV	1	0.24	* Ba75	
$^{175}Lu(n,3n)^{173}Lu$	499 d	14.5	1.8 @ 24 MeV	2	0.27	* Ve77, Ba75	
$^{151}Eu(n,3n)^{149}Eu$	97.3 d	14.5	1.6 @ 23 MeV	1	0.27	* Ba75	
$^{203}Tl(n,3n)^{201}Tl$	3.05 d	14.7	2.0 @ 24.5 MeV	1	0.17	* Ba75	
$^{197}Au(n,3n)^{195}Au$	183 d	14.8	1.9 @ 24 MeV	2	0.10	* Lu82, Ve77, Ba75	
$^{169}Tm(n,3n)^{167}Tm$	9.25 d	15	1.6 @ 24 MeV	3	0.21	* Lu85, Ve77, Ba75	

^{209}Bi(n,3n)^{207}Bi	38 a	~16	1.6 @ 24 MeV	1	0.57	* Ve77	
^{107}Ag(n,3n)^{105}Ag	41.3 d	17.6	~1 @ 28 MeV	1	0.34, 0.44	* Ba75, Li68	
^{103}Rh(n,3n)^{101}Rh	3.3 a	~18	0.8 @ 24 MeV	1	0.13, 0.20	* Ve77	
^{16}O(n,2n)^{15}O	122.1 s	~20	0.02 @ 35 MeV	1	β^+ 1.7	* Br61	
^{59}Co(n,3n)^{57}Co	271.6 d	20	0.1 @ 24 MeV	1	0.12	* Ve77	
^{12}C(n,2n)^{11}C	20.3 min	20	0.02 @ 30 MeV	3	0.51	* An81, Br61	Th88, Ba57
^{93}Nb(n,3n)^{91}Nb^{m}	62 d	~20	0.7 @ 24 MeV	1	1.2	* Fr80, Ve77	
^{63}Cu(n,3n)^{61}Cu	3.41 h	20.1	0.01 @ 32 MeV	1	0.28	Uw92	
^{89}Y(n,3n)^{87}Y	80 h	21.1	0.6 @ 28 MeV	0	0.48	* Ba75	
^{64}Zn(n,3n)^{62}Zn	9.13 h	21.3	0.03 @ 33 MeV	1	0.6	Uw92	
^{90}Zr(n,3n)^{88}Zr	83.4 d	21.5	0.3 @ 28 MeV	1	0.39	* Ve77	
^{191}Ir(n,4n)^{188}Ir	41.5 h	22.7	0.6 @ 28 MeV	0	0.15	* Ve77	
^{151}Eu(n,4n)^{148}Eu	54 d	22.8	0.4 @ 28 MeV	0	0.55, 0.63	* Ba75	
^{203}Tl(n,4n)^{200}Tl	26.1 h	23	0.03 @ 24 MeV	0	0.58	* Ba75	
^{169}Tm(n,4n)^{166}Tm	7.85 h	23.7	0.2 @ 28 MeV	0	2.05	* Ve77	
^{197}Au(n,4n)^{194}Au	39.5 h	24	1 @ 34 MeV	0	0.33	Uw92	
^{50}Cr(n,3n)^{48}Cr	21.6 h	24.1	0.005 @ 34 MeV	1	0.31	Uw92	
^{27}Al(n,spall)^{22}Na	2.62 a	25	0.01 @ ~ 50 MeV	calc only	0.51,1.28	Ho85	Th88
^{12}C(n,spall)^{7}Be	53.6 d	30	0.01 @ ~ 50 MeV	calc only	0.48	Ho85	Th88
^{55}Mn(n,4n)^{52}Mn	5.59 d	31.8	0.01 @ 38 MeV	1	0.74, 0.94, 1.43	Uw92	
^{209}Bi(n,f)	> 2 10^{8} a	~50	2 x 10^{-6} @ 24 MeV	2		* Vo84, Ke48	Th88

a) In published papers.

b) The listed numbers are an (arbitrary) qualitative measure of the accuracy of cross section data: they represent the number of published measurements with more than five experimental energy points.

c) Only references giving more than five energy points are listed; '*' indicates listing in: Neutron Cross Sections, vol. 2: Neutron Cross Section Curves, V. McLane, C.L. Dunford and P.F. Rose eds., Academic Press, Inc, London (1988).

References of Table I :

[Ad80] Adamski, Annals of Nuclear Energy, 7(7), 397, (1981)
[An81] Anders et al., Zeitsch. f. Physik/A, **301**(4), 353, (1981)
[Bo65] Bormann, Hamburg, (1965)
[Ba57] P.S. Baranov et al., Rev. Sci. Instrum. **28**(12), 1029, (1957)
[Bo68] Bormann, Nuclear Physics/A, **115**, 309, (1968)
[Bo69] Bormann, Nuclear Physics/A, **130**, 195, (1969)
[Bo76] Bormann et al., Zeitsch. f. Physik/A, **277**, 203, (1976)
[Br61] Brill et al., Sov. Phys.- Doklady, **6**(1), 24, (1961)
[Cs82] Csikai, Nuclear Data for Science and Technology, Antwerp, 414, (1982)
[Fr80] Frehaut et al., Neutron Cross Sections at 10-50 MeV, Brookhaven, 399, (1980)
[Gr85] Greenwood, DOE-ER-0046-21, (1985)
[Gr85b] Greenwood, Conf. on Nuclear Data for Basic & Applied Sci., Santa Fe, **1**, 163, (1985)
[Ho85] Holt P.D., Radiat. Prot. Dosim., **10**, 251, (1985)
[Ho95] Hoek M., Rev. Sci. Instrum., **66**(1), 885, (1995)
[Hu81] Huang Jian, Chinese Journal of Nuclear Physics, **3**(1), 59, (1981)
[Ik85] Ikeda, Conference on Nuclear Data for Basic & Applied Sci., Santa Fe, **1**, 175, (1985)
[Ja78] Jarjis et al., Journal of Phys./G-Nucl. Phys. **4**(3), 445, (1978)
[Ke48] E.L. Kelly and C. Wiegand, Phys. Rev., 73(10), 1135 (1948)
[Ke93] J.G. Kelly et al., IEEE Trans. on Nucl. Sci., **40**(6), 1418 (1993)
[Ku77] L. Kuijpers et al., NIM, **144**, 215, (1977)
[Li68] Liskien, Nucl. Phys. A, **118**, 379, (1968)
[Lu79] Lu Hanlin et al., Physica Energ. Fortis et Nuclearis, 3(1), 88, (1985)
[Lu85] Lu Hanlin et al., Nuc. Sci. Eng., **90**, 304, (1985)
[Lu82] Lu Hanlin et al., IAEA-NDS, 30637, (1982)
[Me67] H.O. Menlove et al., Phys. Rev., 163, **4**, 1308, (1967)
[Ma80] Ma Hong, Chinese Journal of Nuclear Physics, 2(1), 47, (1980)
[Pa66] Pai, Canadian Journal of Physics **44**, 2337, (1966)
[Pa82] Pavlik, Journal of Phys./G-Nucl. Phys. **8**, 1283, (1982)
[Pa85] Pavlik, Nuc. Sci. Eng., **90**, 186, (1985)
[Pa75] Paulsen, Atomkenenergie, **26**, 34, (1975)
[Pr61] R.J. Prestwood and B.P. Bayhurst, Phys. Rev., **121**, 1438, (1961)
[Ry78] T.B. Ryves et al., Journal of Phys./G-Nucl. Phys. 4(11), 1783, (1978)
[Ry78b] T.B. Ryves et al., Metrologia, **14**(3), 27, (1978)
[Th88] R.H. Thomas and G.R. Stevenson, Technical Report Series, n.283, IAEA, Vienna, (1988)
[Vo84] Vorotnikov et al., YF **40**(4), 867, (1984)
[Uw92] Y. Uwamino et al., Nuc. Sci. Eng., **111**, 391, (1992)
[Zh84] Zhao Wen, Chinese Journal of Nuclear Physics, 6(1), 80, (1984)

Figures: Cross Sections Plots

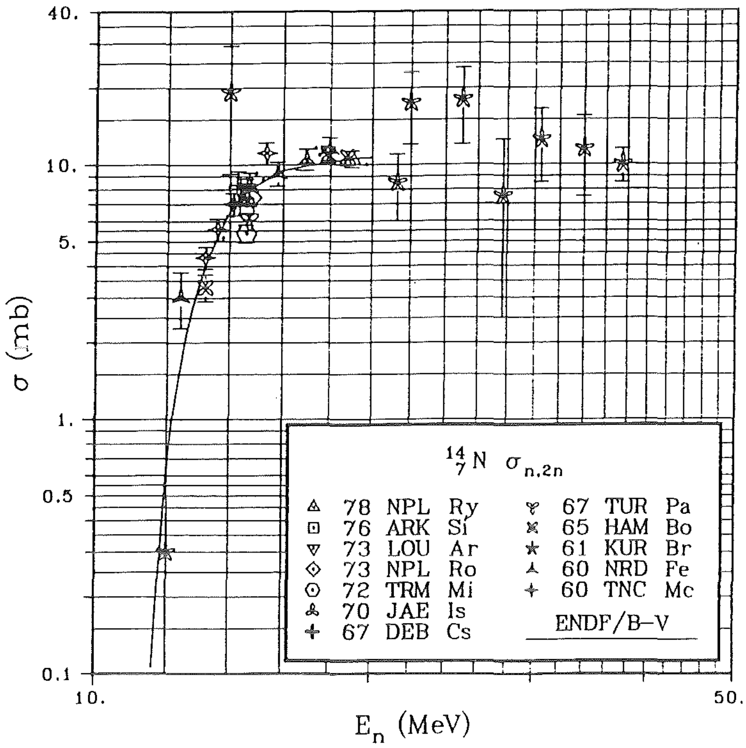
40.
10.
5.
1.
0.5
0.1
σ (mb)
10.
50.
E_n (MeV)
$^{14}_{7}$N $\sigma_{n,2n}$
78 NPL Ry
76 ARK Si
73 LOU Ar
73 NPL Ro
72 TRM Mi
70 JAE Is
67 DEB Cs
67 TUR Pa
65 HAM Bo
61 KUR Br
60 NRD Fe
60 TNC Mc
ENDF/B-V

Fig. 1

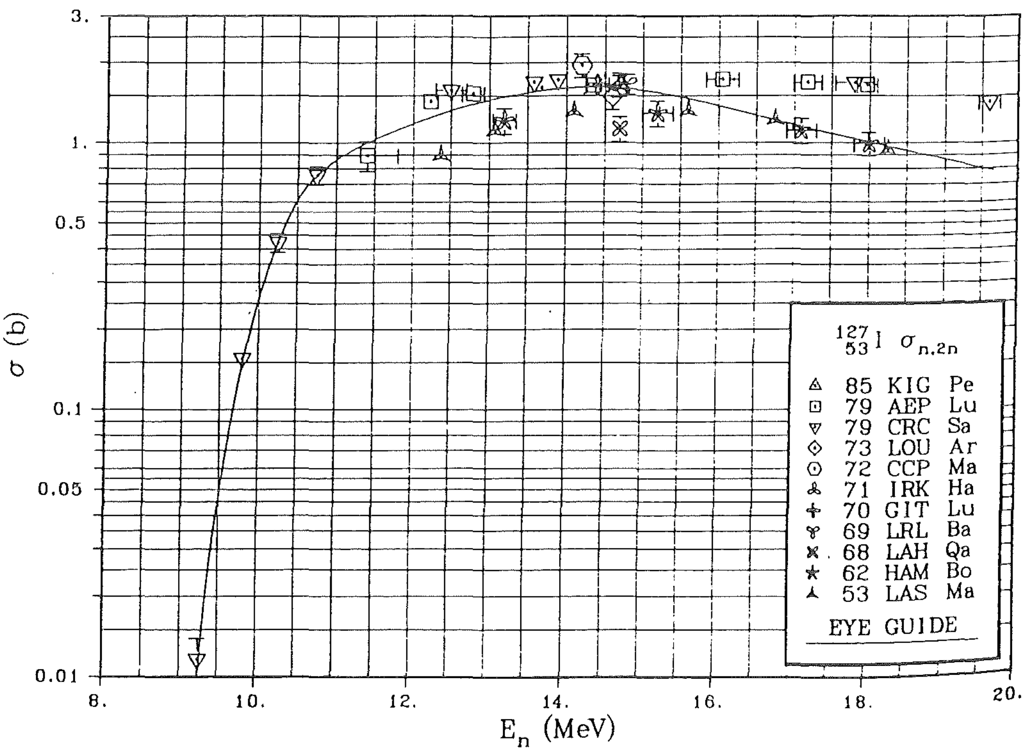
3.
1.
0.5
0.1
0.05
0.01
σ (b)
8.
10.
12.
14.
16.
18.
20.
E_n (MeV)
$^{127}_{53}$I $\sigma_{n,2n}$
85 KIG Pe
79 AEP Lu
79 CRC Sa
73 LOU Ar
72 CCP Ma
71 IRK Ha
70 GIT Lu
69 LRL Ba
68 LAH Qa
62 HAM Bo
53 LAS Ma
EYE GUIDE

Fig. 2

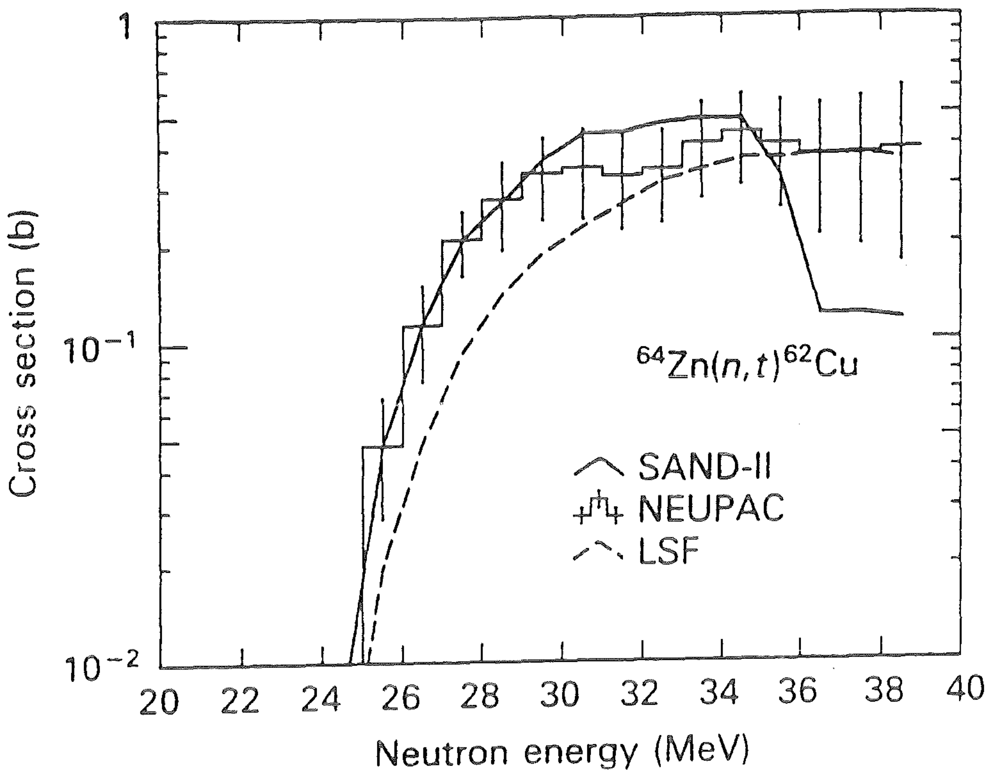

Cross section (b)
Neutron energy (MeV)
$^{64}Zn(n,t)^{62}Cu$
SAND-II
NEUPAC
LSF

Fig. 3

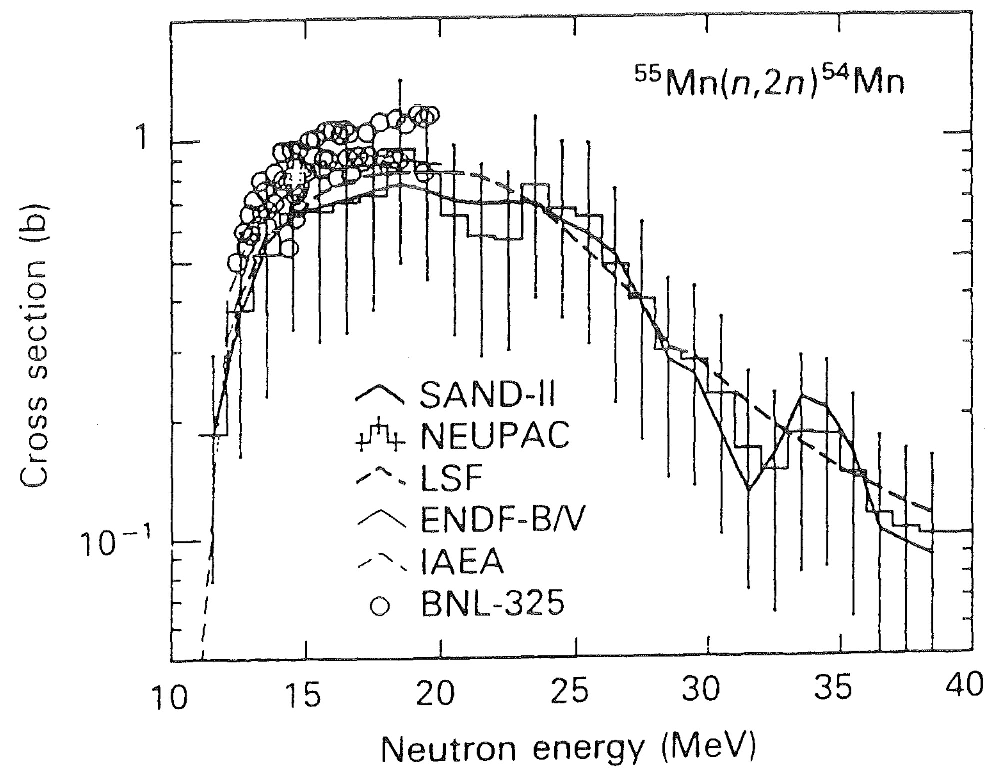

Cross section (b)
Neutron energy (MeV)
$^{55}Mn(n,2n)^{54}Mn$
SAND-II
NEUPAC
LSF
ENDF-B/V
IAEA
BNL-325

Fig. 4

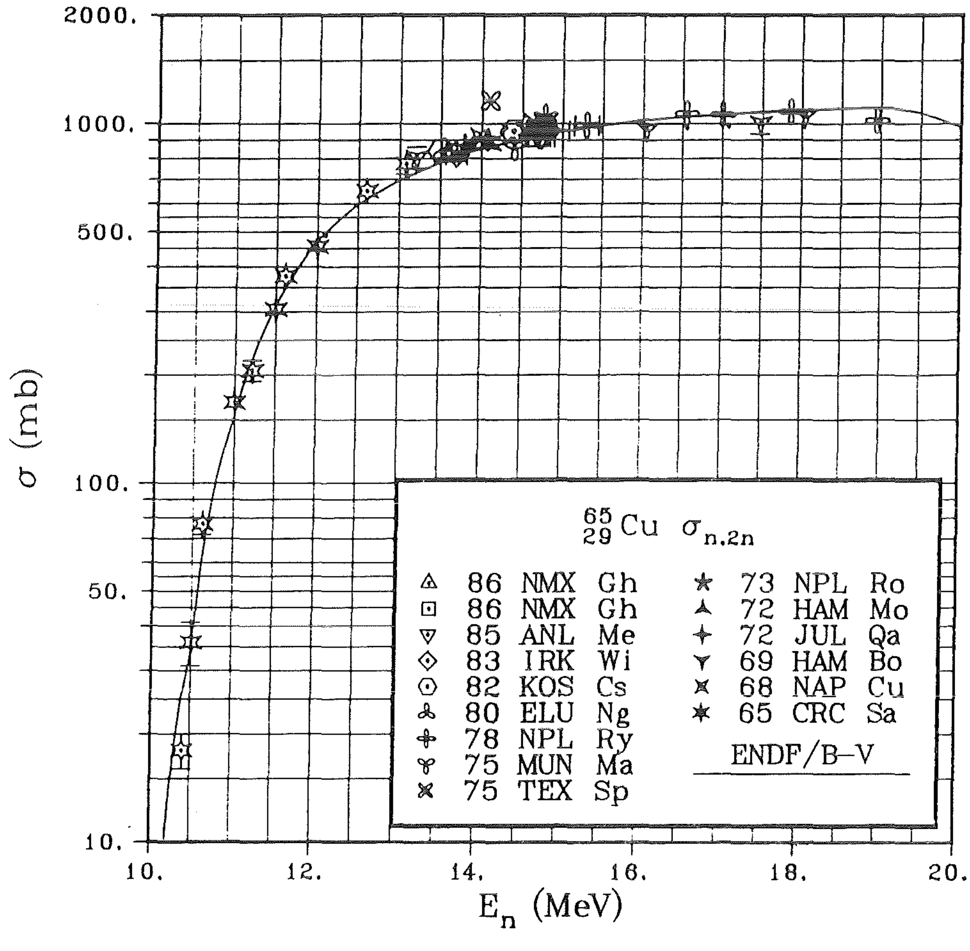

2000.
1000.
500.
100.
50.
10.
10.
12.
14.
16.
18.
20.
σ (mb)
E_n (MeV)
$^{65}_{29}$Cu $\sigma_{n,2n}$
86 NMX Gh
86 NMX Gh
85 ANL Me
83 IRK Wi
82 KOS Cs
80 ELU Ng
78 NPL Ry
75 MUN Ma
75 TEX Sp
73 NPL Ro
72 HAM Mo
72 JUL Qa
69 HAM Bo
68 NAP Cu
65 CRC Sa
ENDF/B-V

Fig. 5

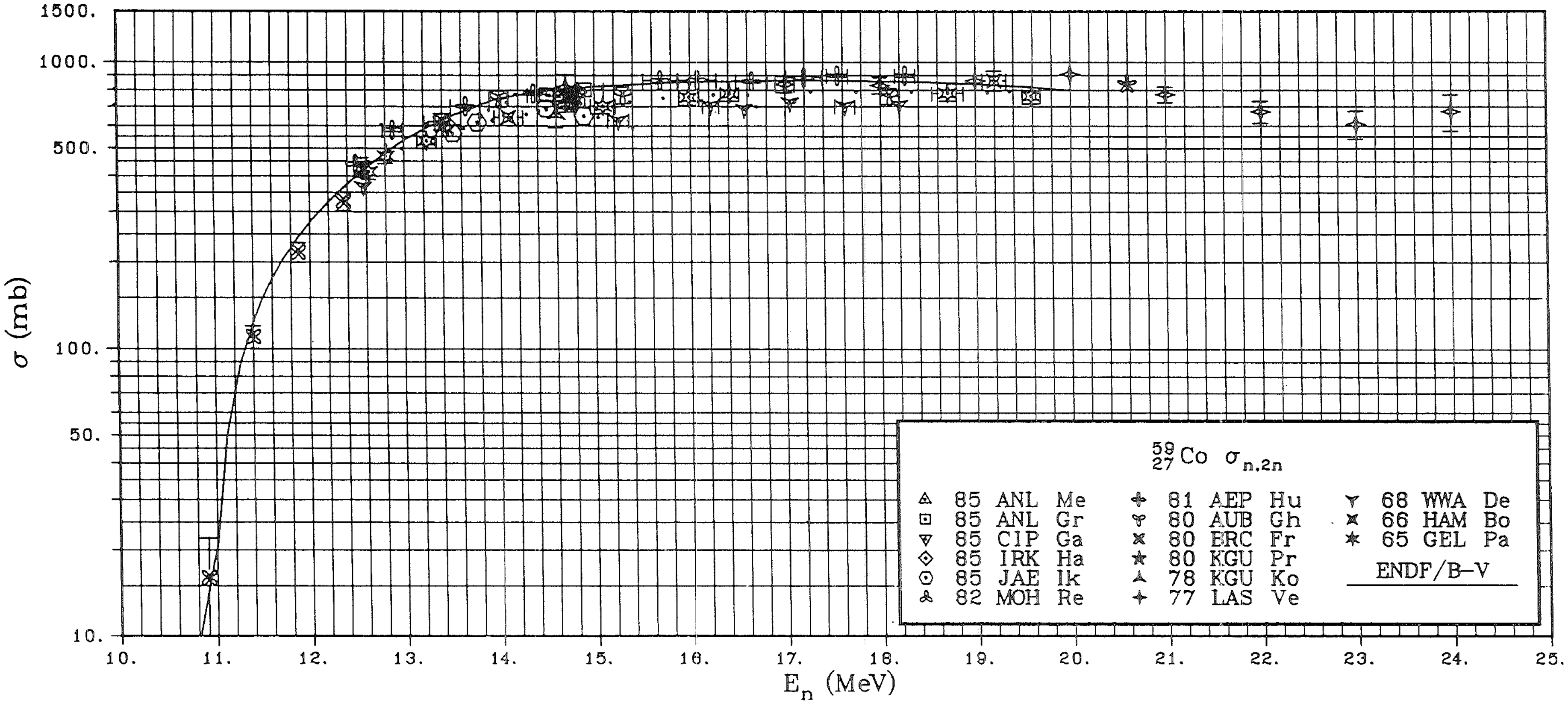
1500.
1000.
500.
100.
50.
10.
σ (mb)
10. 11. 12. 13. 14. 15. 16. 17. 18. 19. 20. 21. 22. 23. 24. 25.
E_n (MeV)
$^{59}_{27}$Co $\sigma_{n,2n}$
85 ANL Me
85 ANL Gr
85 CIP Ga
85 IRK Ha
85 JAE Ik
82 MOH Re
81 AEP Hu
80 AUB Gh
80 BRC Fr
80 KGU Pr
78 KGU Ko
77 LAS Ve
68 WWA De
66 HAM Bo
65 GEL Pa
ENDF/B-V

Fig. 6

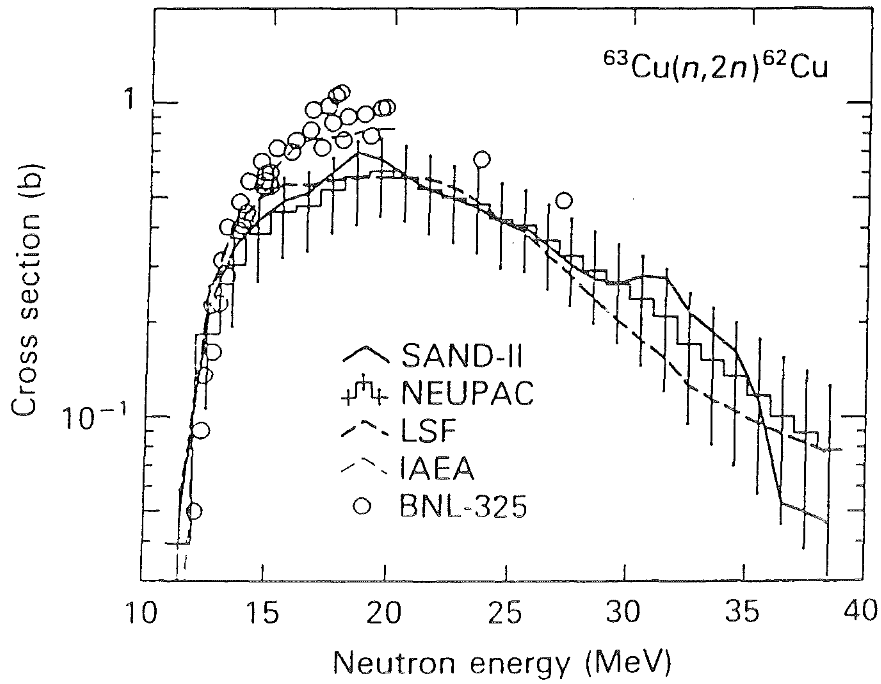
$^{63}Cu(n,2n)^{62}Cu$
1
10^{-1}
Cross section (b)
SAND-II
NEUPAC
LSF
IAEA
BNL-325
10
15
20
25
30
35
40
Neutron energy (MeV)

Fig. 7

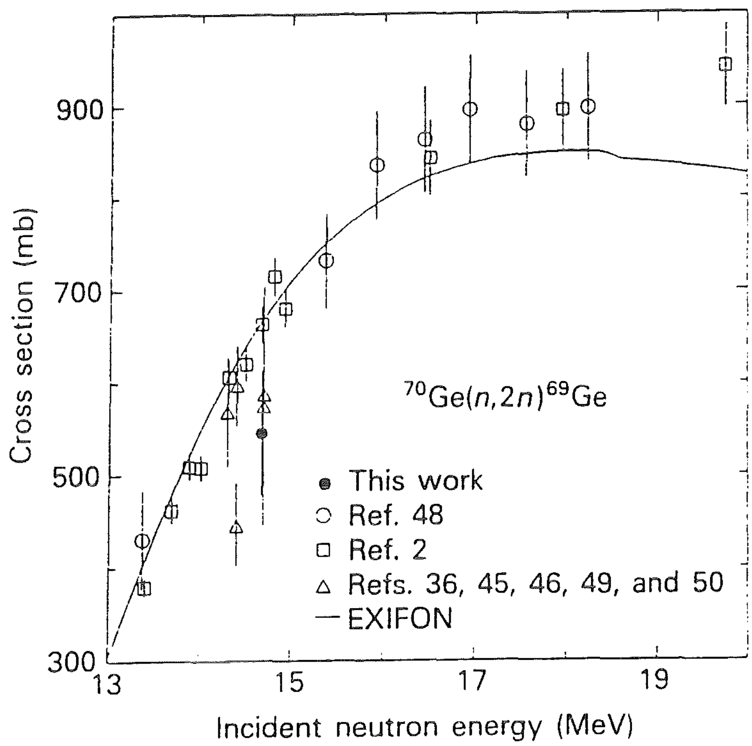
900
700
500
300
Cross section (mb)
$^{70}Ge(n,2n)^{69}Ge$
This work
Ref. 48
Ref. 2
Refs. 36, 45, 46, 49, and 50
EXIFON
13
15
17
19
Incident neutron energy (MeV)

Fig. 8

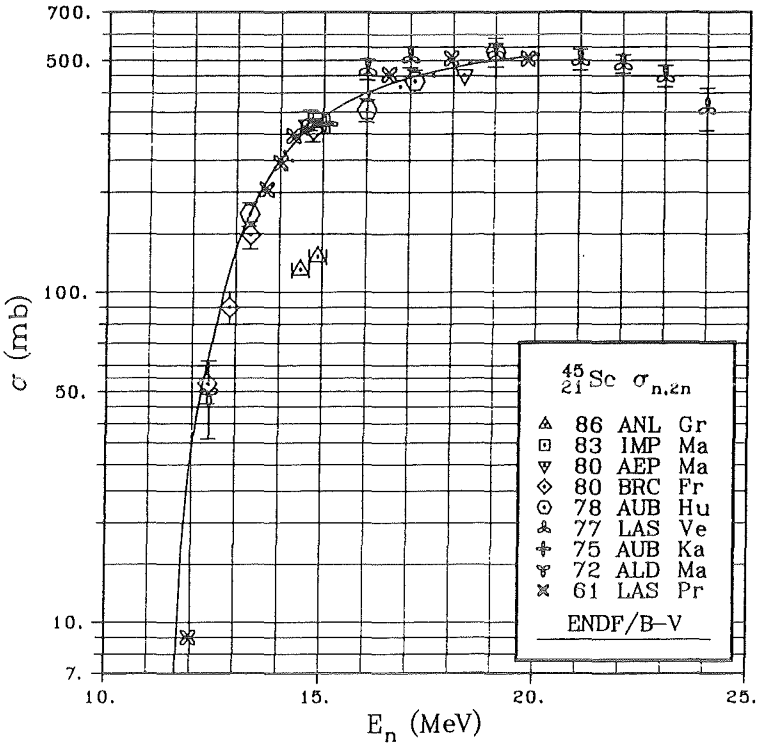

700.
500.
100.
50.
10.
7.
10.
15.
20.
25.
σ (mb)
E_n (MeV)
$^{45}_{21}$Sc $\sigma_{n,2n}$
86 ANL Gr
83 IMP Ma
80 AEP Ma
80 BRC Fr
78 AUB Hu
77 LAS Ve
75 AUB Ka
72 ALD Ma
61 LAS Pr
ENDF/B-V

Fig. 9

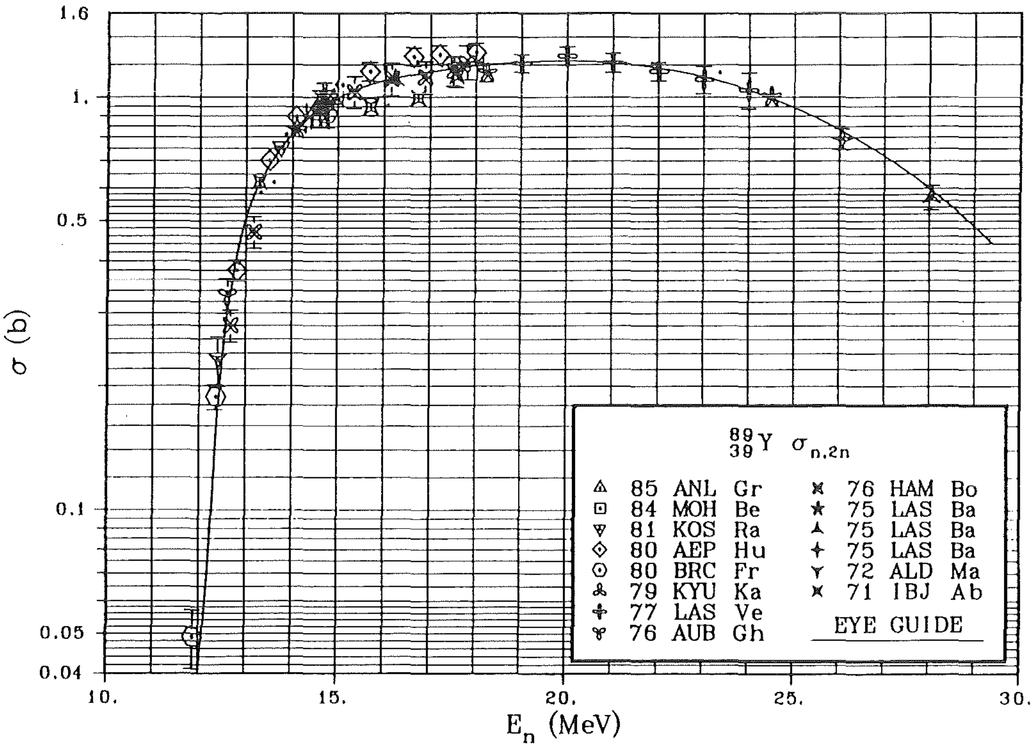

1.6
1.
0.5
0.1
0.05
0.04
10.
15.
20.
25.
30.
σ (b)
E_n (MeV)
$^{89}_{39}$Y $\sigma_{n,2n}$
85 ANL Gr
84 MOH Be
81 KOS Ra
80 AEP Hu
80 BRC Fr
79 KYU Ka
77 LAS Ve
76 AUB Gh
76 HAM Bo
75 LAS Ba
75 LAS Ba
75 LAS Ba
72 ALD Ma
71 IBJ Ab
EYE GUIDE

Fig. 10

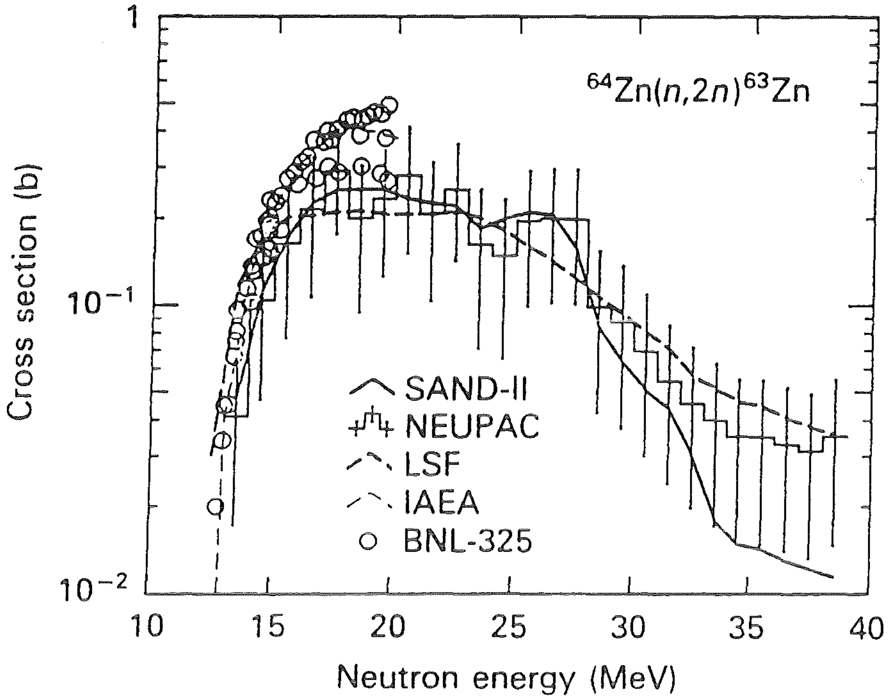

$^{64}Zn(n,2n)^{63}Zn$
SAND-II
NEUPAC
LSF
IAEA
BNL-325
Cross section (b)
Neutron energy (MeV)
1
10^{-1}
10^{-2}
10
15
20
25
30
35
40

Fig. 11

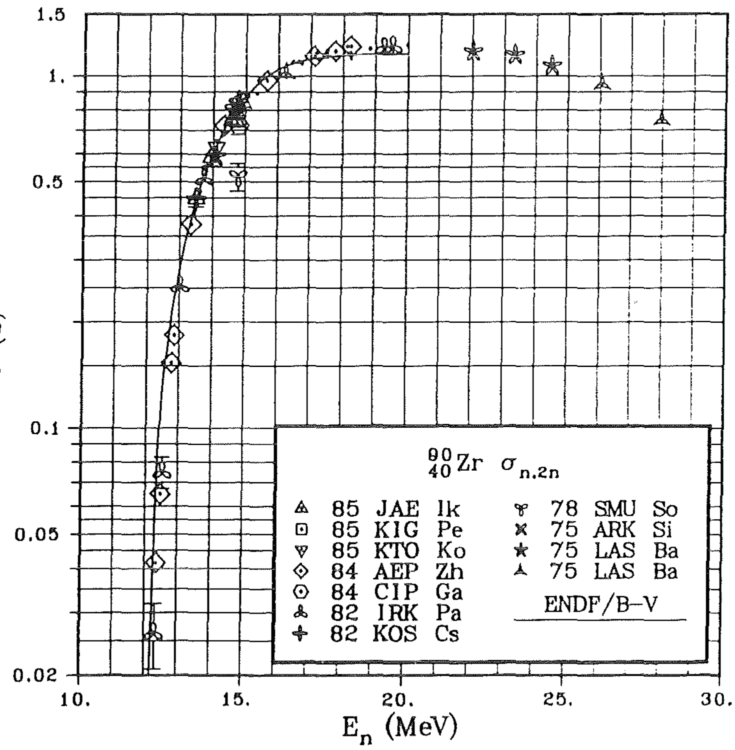

$^{90}_{40}Zr$ $\sigma_{n,2n}$
85 JAE Ik
85 KIG Pe
85 KTO Ko
84 AEP Zh
84 CIP Ga
82 IRK Pa
82 KOS Cs
78 SMU So
75 ARK Si
75 LAS Ba
75 LAS Ba
ENDF/B-V
σ (b)
E_n (MeV)
1.5
1.
0.5
0.1
0.05
0.02
10.
15.
20.
25.
30.

Fig. 12

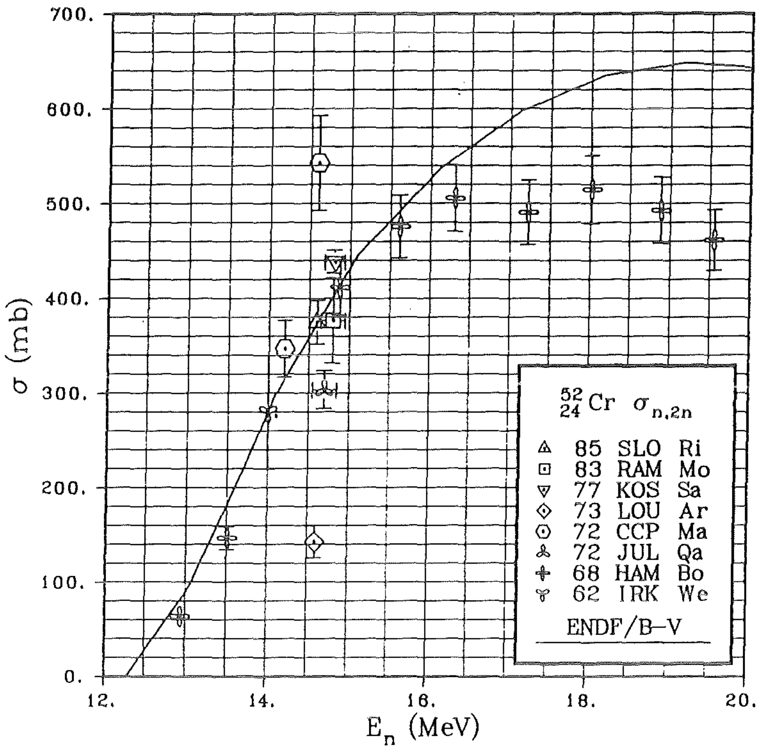
700.
600.
500.
400.
300.
200.
100.
0.
12.
14.
16.
18.
20.
σ (mb)
E_n (MeV)
$^{52}_{24}$Cr $\sigma_{n,2n}$
85 SLO Ri
83 RAM Mo
77 KOS Sa
73 LOU Ar
72 CCP Ma
72 JUL Qa
68 HAM Bo
62 IRK We
ENDF/B-V

Fig. 13

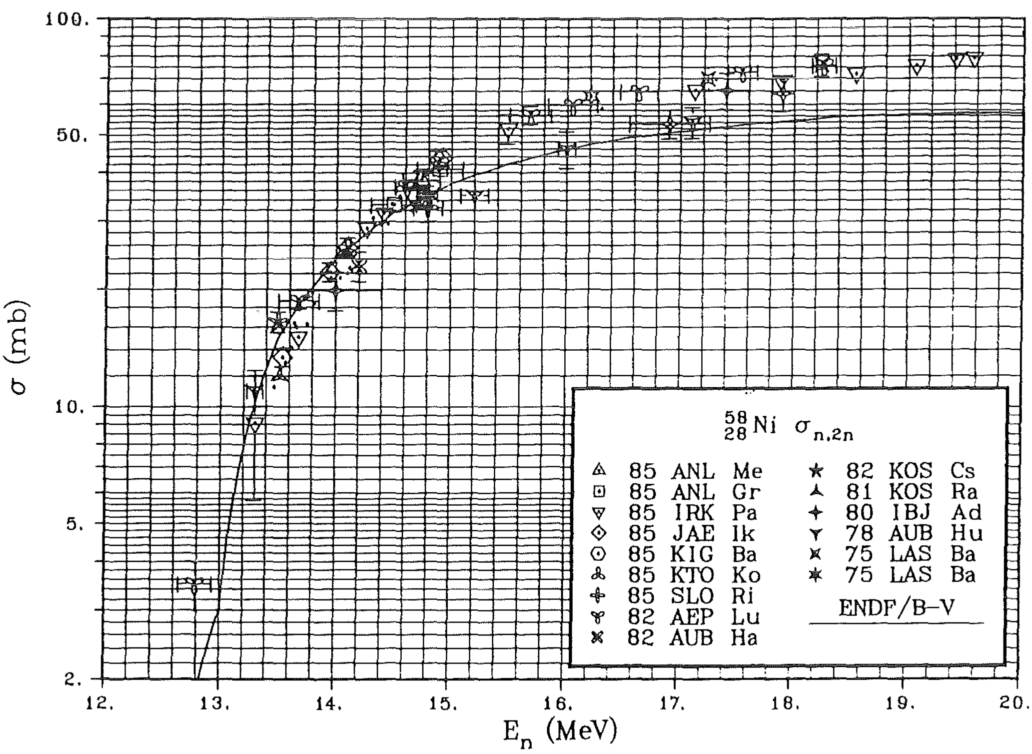
100.
50.
10.
5.
2.
12.
13.
14.
15.
16.
17.
18.
19.
20.
σ (mb)
E_n (MeV)
$^{58}_{28}$Ni $\sigma_{n,2n}$
85 ANL Me
85 ANL Gr
85 IRK Pa
85 JAE Ik
85 KIG Ba
85 KTO Ko
85 SLO Ri
82 AEP Lu
82 AUB Ha
82 KOS Cs
81 KOS Ra
80 IBJ Ad
78 AUB Hu
75 LAS Ba
75 LAS Ba
ENDF/B-V

Fig. 14

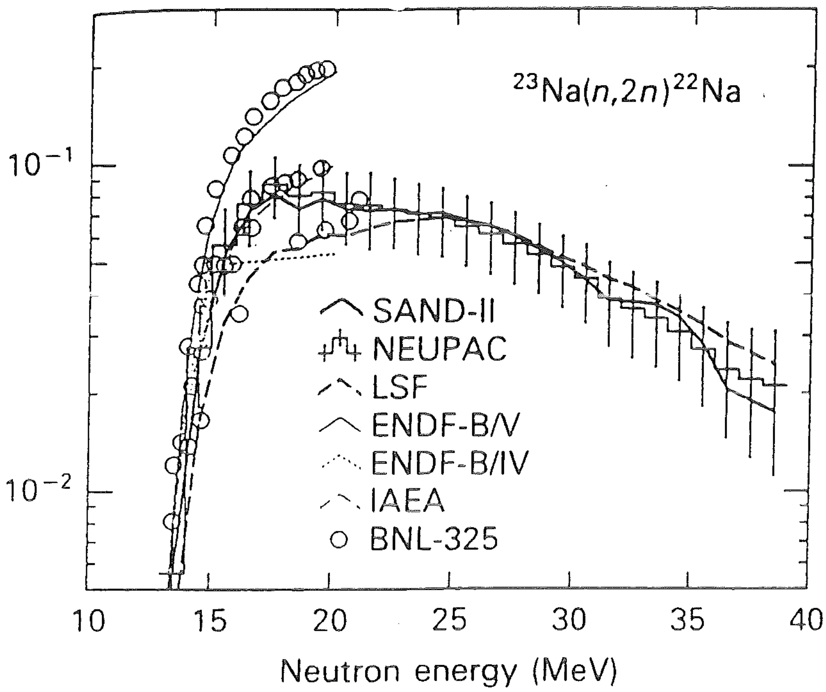
$^{23}Na(n,2n)^{22}Na$
10^{-1}
10^{-2}
SAND-II
NEUPAC
LSF
ENDF-B/V
ENDF-B/IV
IAEA
BNL-325
10
15
20
25
30
35
40
Neutron energy (MeV)

Fig. 15

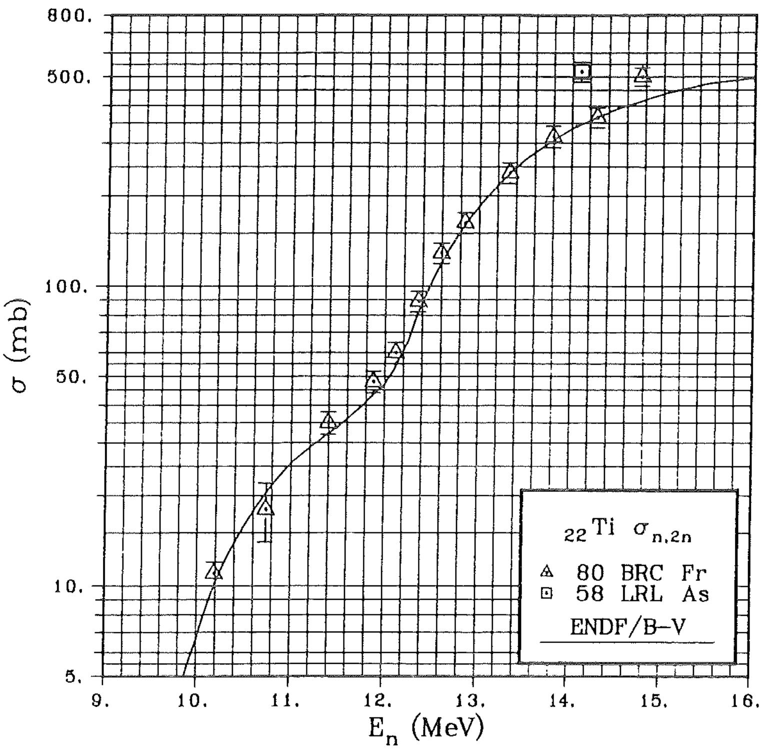
800.
500.
100.
50.
10.
5.
σ (mb)
$_{22}Ti$ $\sigma_{n,2n}$
80 BRC Fr
58 LRL As
ENDF/B-V
9.
10.
11.
12.
13.
14.
15.
16.
E_n (MeV)

Fig. 16

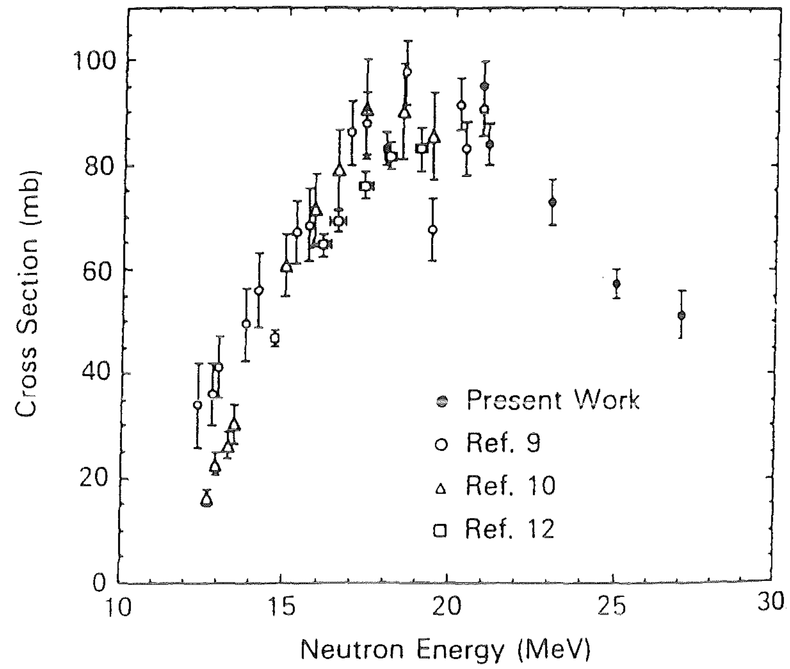

The $^{19}F(n,2n)^{18}F$ cross-section values plotted against neutron energy. Besides the present work, values reported in Refs. 9, 10, and 12 are indicated.

Fig. 17

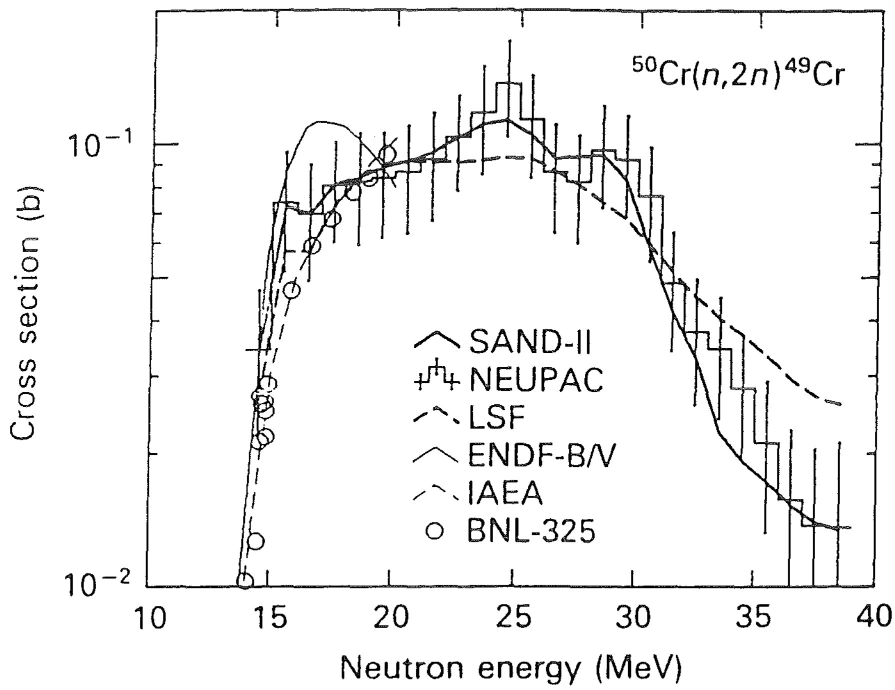

Fig. 18

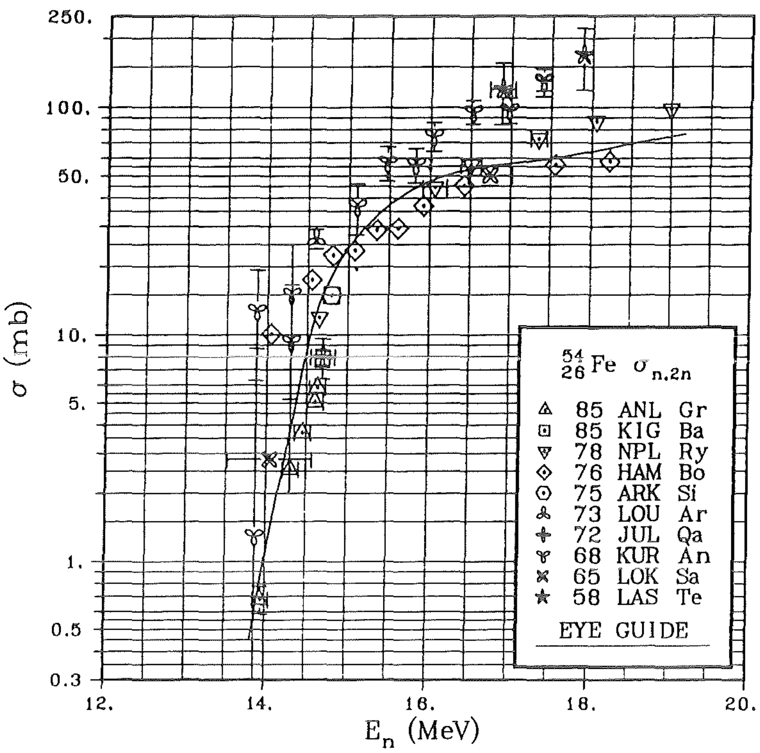
250.
100.
50.
10.
5.
1.
0.5
0.3
12.
14.
16.
18.
20.
σ (mb)
E$_n$ (MeV)
$^{54}_{26}$Fe $\sigma_{n,2n}$
85 ANL Gr
85 KIG Ba
78 NPL Ry
76 HAM Bo
75 ARK Si
73 LOU Ar
72 JUL Qa
68 KUR An
65 LOK Sa
58 LAS Te
EYE GUIDE

Fig. 19

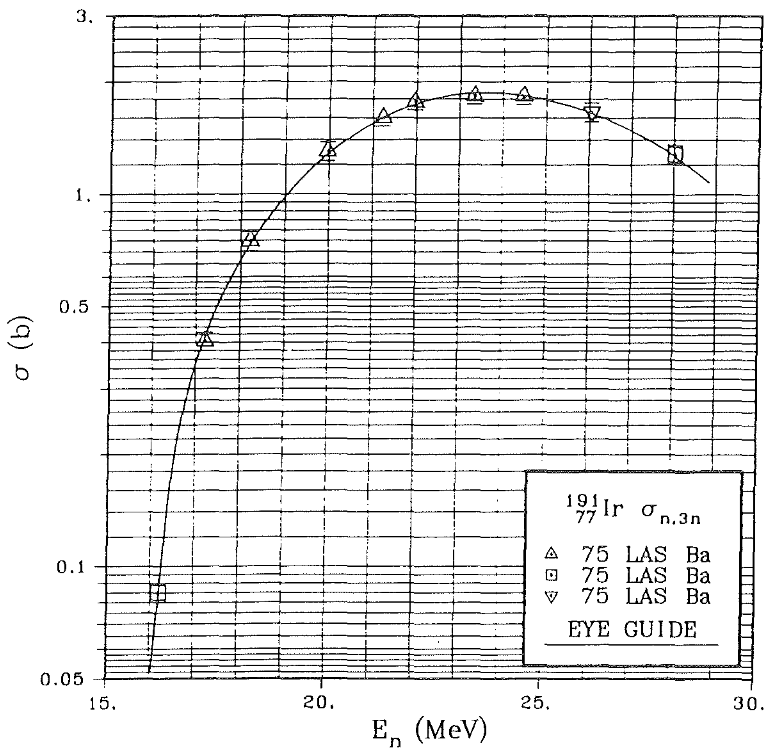
3.
1.
0.5
0.1
0.05
15.
20.
25.
30.
σ (b)
E$_n$ (MeV)
$^{191}_{77}$Ir $\sigma_{n,3n}$
75 LAS Ba
75 LAS Ba
75 LAS Ba
EYE GUIDE

Fig. 20

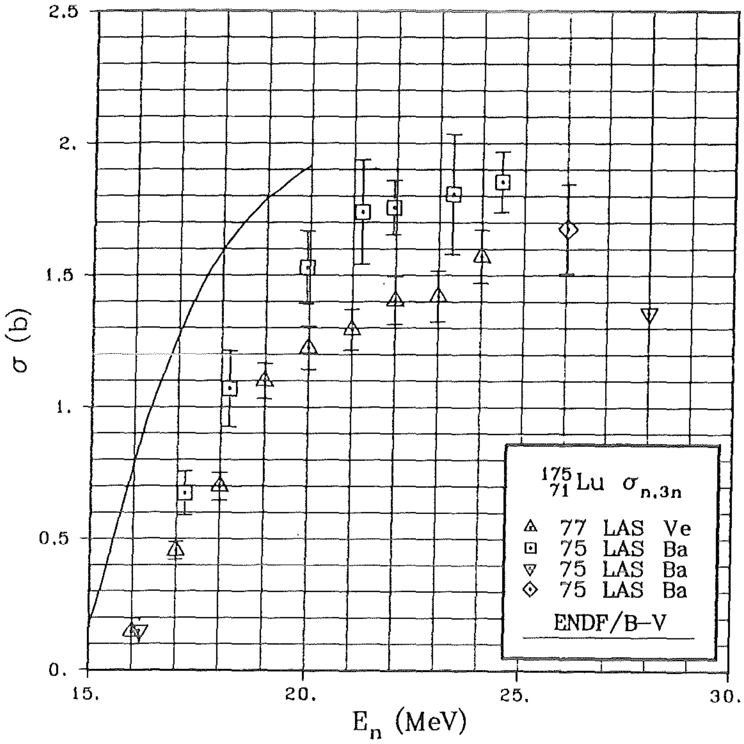

2.5
2.
1.5
1.
0.5
0.
σ (b)
15.
20.
25.
30.
E_n (MeV)
175 71 Lu σ n,3n
77 LAS Ve
75 LAS Ba
75 LAS Ba
75 LAS Ba
ENDF/B-V

Fig. 21

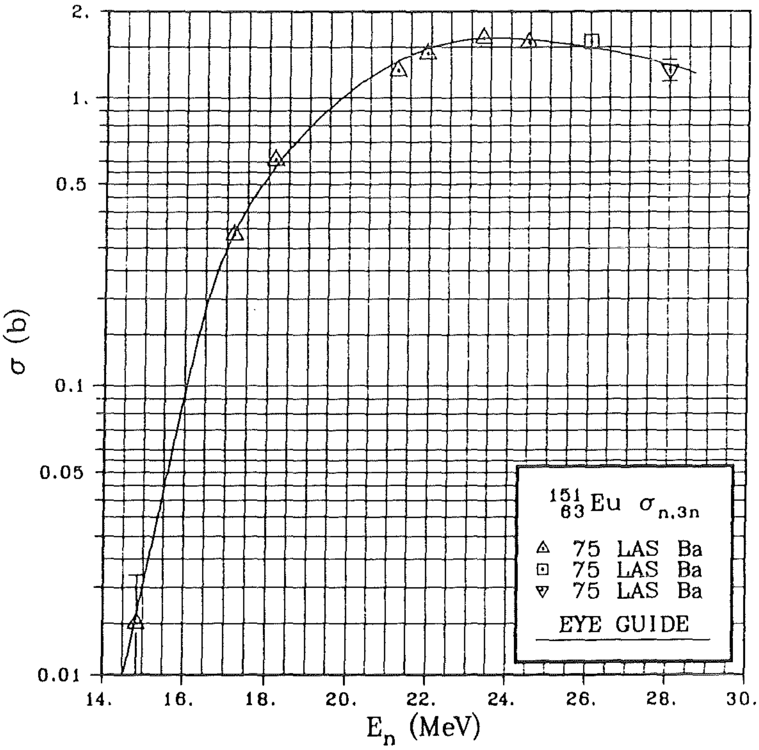

2.
1.
0.5
0.1
0.05
0.01
σ (b)
14.
16.
18.
20.
22.
24.
26.
28.
30.
E_n (MeV)
151 63 Eu σ n,3n
75 LAS Ba
75 LAS Ba
75 LAS Ba
EYE GUIDE

Fig. 22

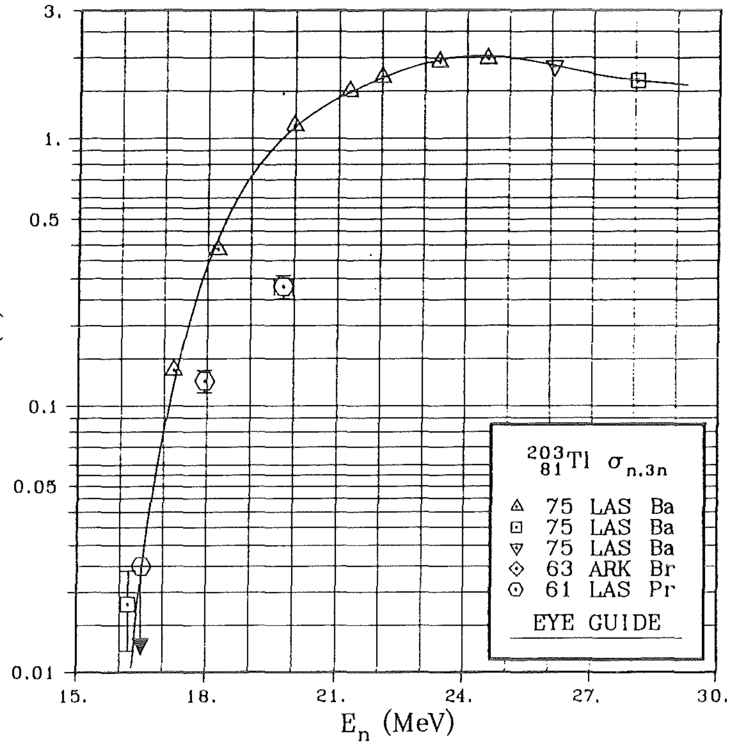

3.
1.
0.5
0.1
0.05
0.01
15.
18.
21.
24.
27.
30.
σ (b)
E_n (MeV)
$^{203}_{81}$Tl $\sigma_{n,3n}$
75 LAS Ba
75 LAS Ba
75 LAS Ba
63 ARK Br
61 LAS Pr
EYE GUIDE

Fig. 23

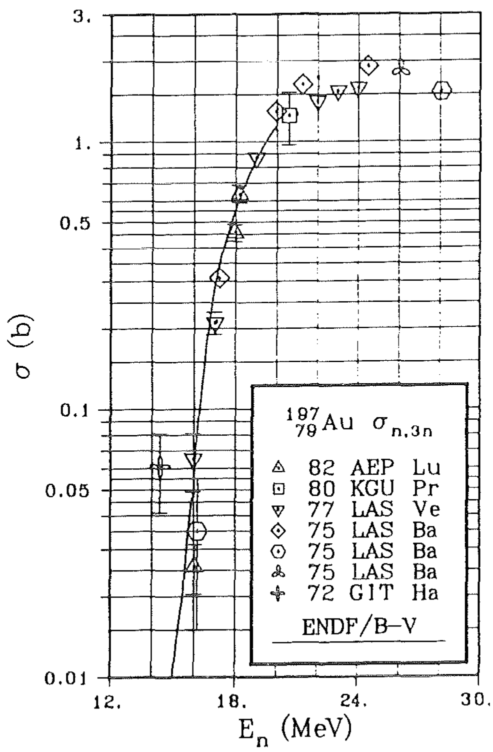

3.
1.
0.5
0.1
0.05
0.01
12.
18.
24.
30.
σ (b)
E_n (MeV)
$^{197}_{79}$Au $\sigma_{n,3n}$
82 AEP Lu
80 KGU Pr
77 LAS Ve
75 LAS Ba
75 LAS Ba
75 LAS Ba
72 GIT Ha
ENDF/B-V

Fig. 24

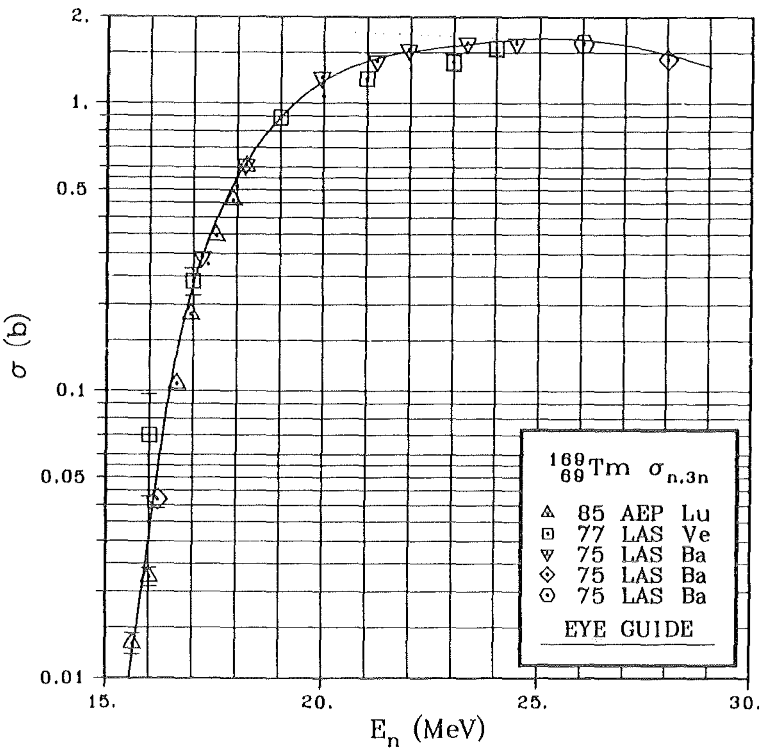

2.
1.
0.5
0.1
0.05
0.01
15.
20.
25.
30.
σ (b)
E_n (MeV)
$^{169}_{69}$Tm $\sigma_{n,3n}$
85 AEP Lu
77 LAS Ve
75 LAS Ba
75 LAS Ba
75 LAS Ba
EYE GUIDE

Fig. 25

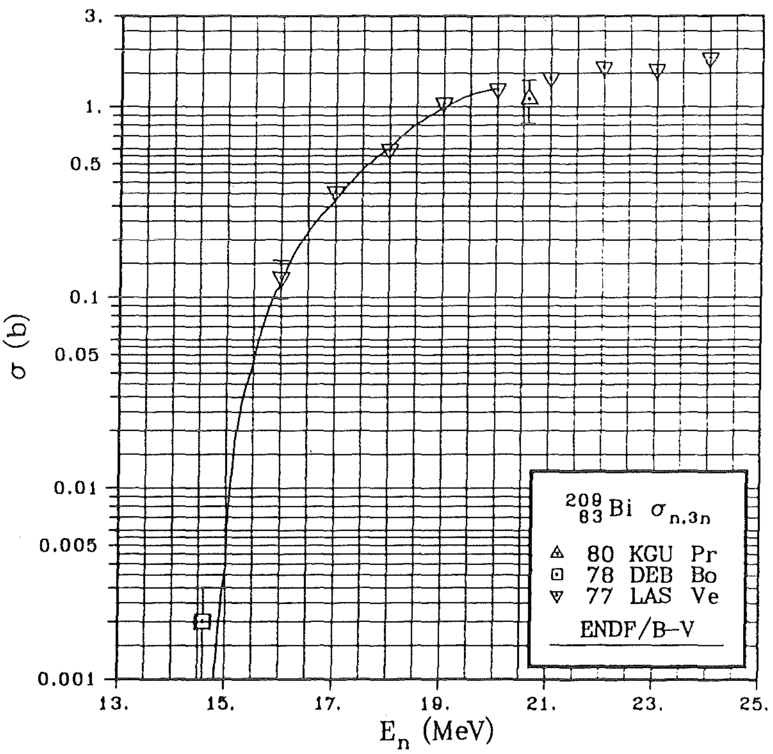

3.
1.
0.5
0.1
0.05
0.01
0.005
0.001
13.
15.
17.
19.
21.
23.
25.
σ (b)
E_n (MeV)
$^{209}_{83}$Bi $\sigma_{n,3n}$
80 KGU Pr
78 DEB Bo
77 LAS Ve
ENDF/B-V

Fig. 26

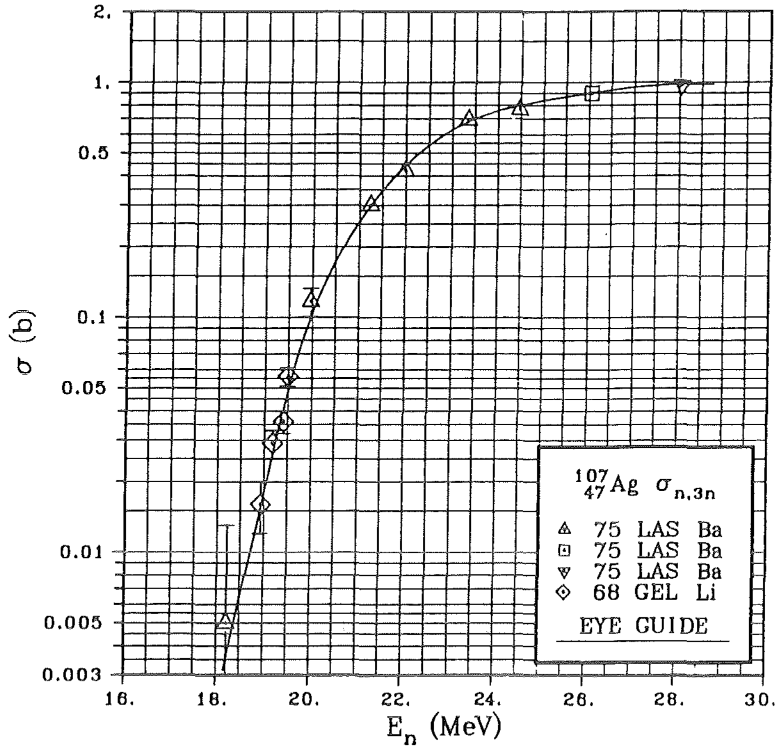

2.
1.
0.5
0.1
0.05
0.01
0.005
0.003
σ (b)
16.
18.
20.
22.
24.
26.
28.
30.
E_n (MeV)
$^{107}_{47}Ag$ $\sigma_{n,3n}$
75 LAS Ba
75 LAS Ba
75 LAS Ba
68 GEL Li
EYE GUIDE

Fig. 27

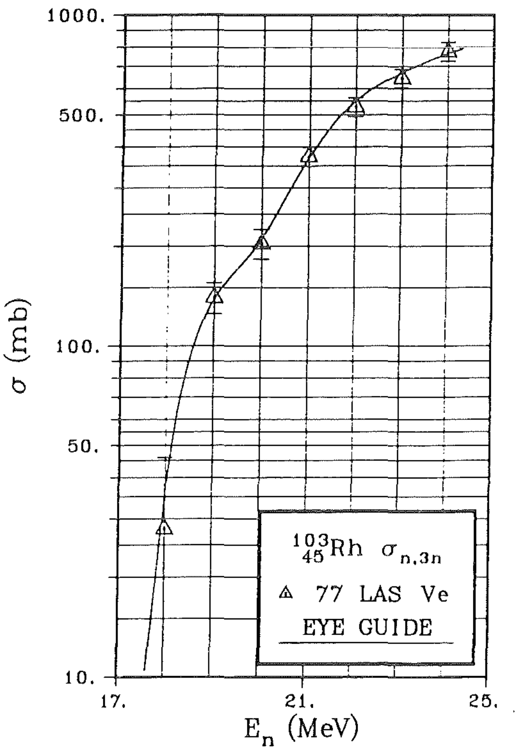

1000.
500.
100.
50.
10.
σ (mb)
17.
21.
25.
E_n (MeV)
$^{103}_{45}Rh$ $\sigma_{n,3n}$
77 LAS Ve
EYE GUIDE

Fig. 28

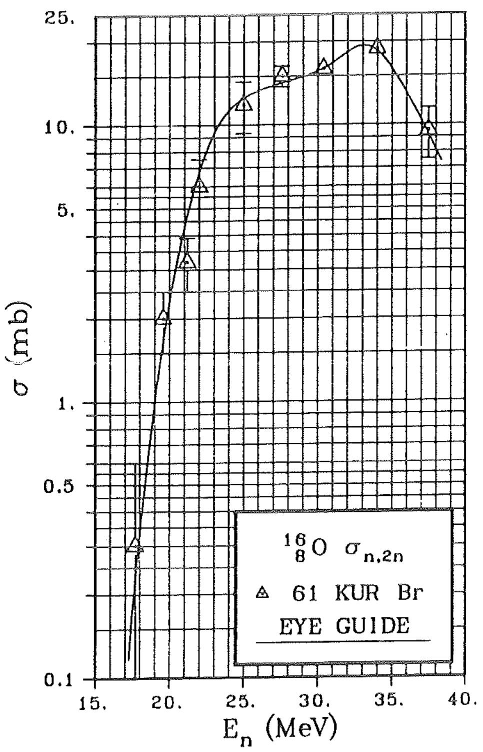

25.
10.
5.
1.
0.5
0.1
15.
20.
25.
30.
35.
40.
σ (mb)
En (MeV)
16 8 O σ n,2n
61 KUR Br
EYE GUIDE

Fig. 29

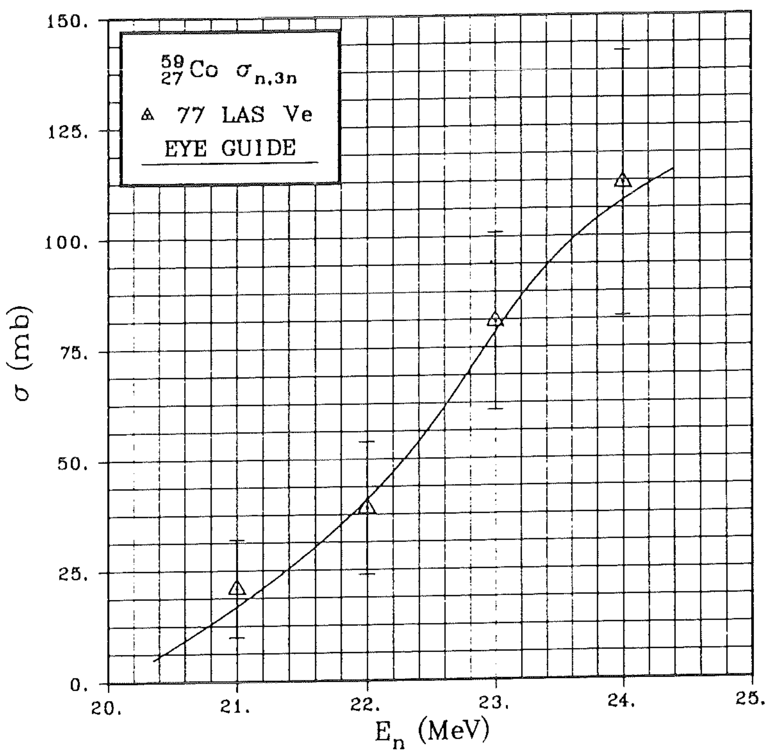

150.
125.
100.
75.
50.
25.
0.
20.
21.
22.
23.
24.
25.
σ (mb)
En (MeV)
59 27 Co σ n,3n
77 LAS Ve
EYE GUIDE

Fig. 30

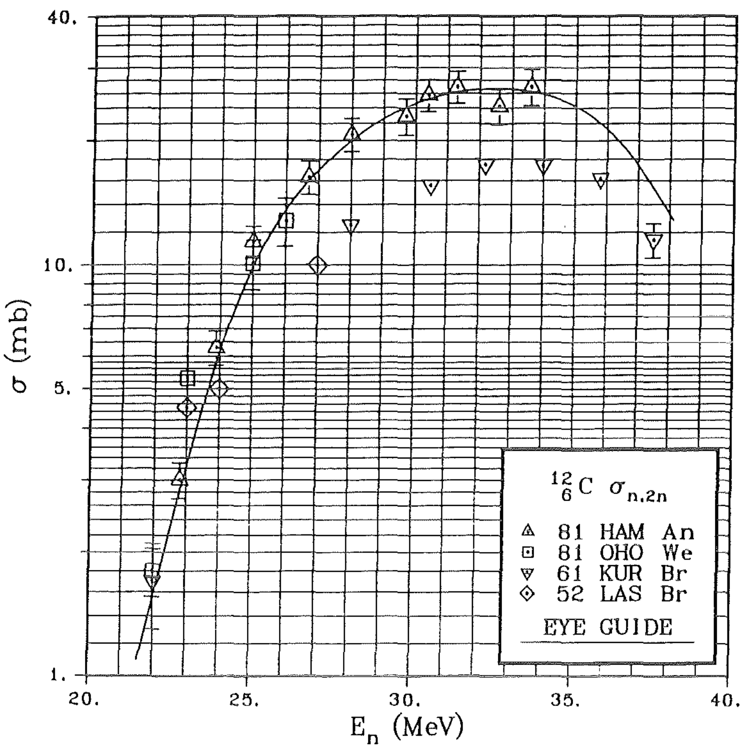
40.
10.
5.
1.
σ (mb)
20.
25.
30.
35.
40.
En (MeV)
12 6 C σn,2n
81 HAM An
81 OHO We
61 KUR Br
52 LAS Br
EYE GUIDE

Fig. 31

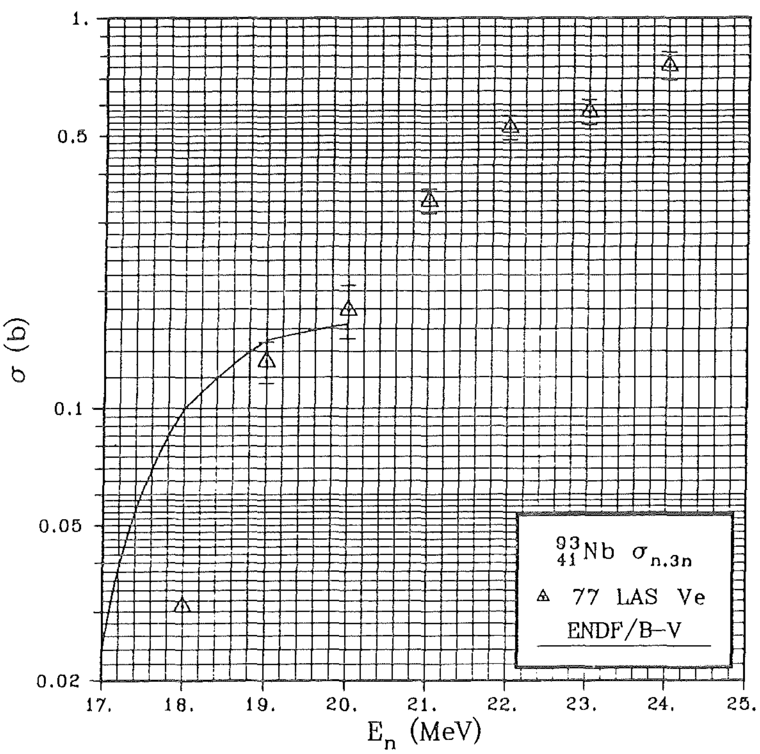
1.
0.5
0.1
0.05
0.02
σ (b)
17.
18.
19.
20.
21.
22.
23.
24.
25.
En (MeV)
93 41 Nb σn,3n
77 LAS Ve
ENDF/B-V

Fig. 32

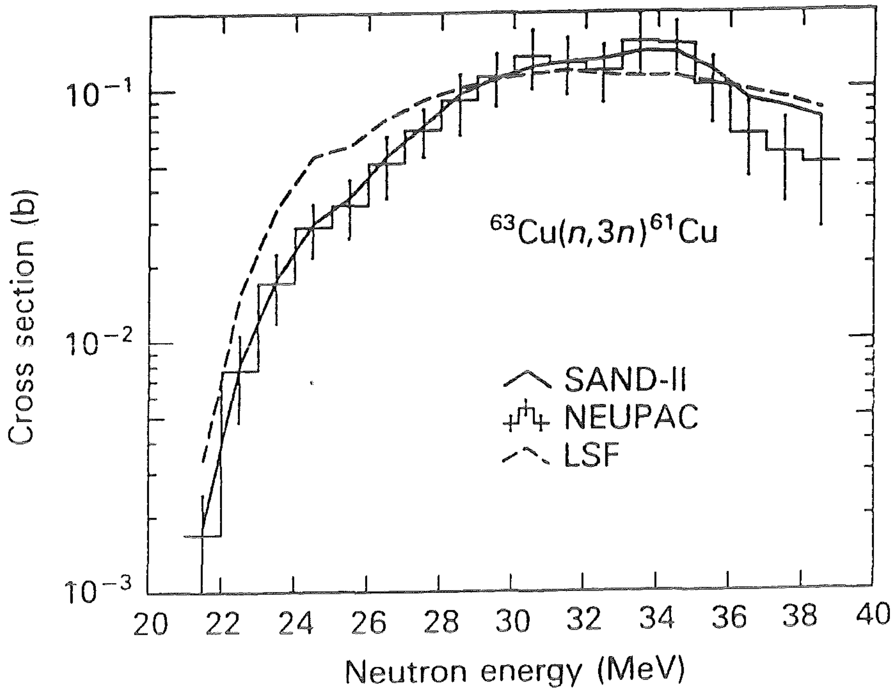

10^{-1}
10^{-2}
10^{-3}
Cross section (b)
$^{63}Cu(n,3n)^{61}Cu$
SAND-II
NEUPAC
LSF
20 22 24 26 28 30 32 34 36 38 40
Neutron energy (MeV)

Fig. 33

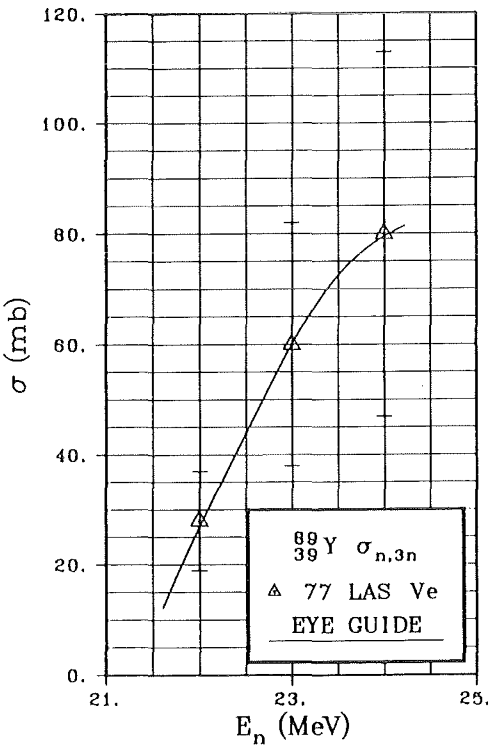

120.
100.
80.
60.
40.
20.
0.
σ (mb)
$^{89}_{39}Y$ $\sigma_{n,3n}$
77 LAS Ve
EYE GUIDE
21.
23.
25.
E_n (MeV)

Fig. 34

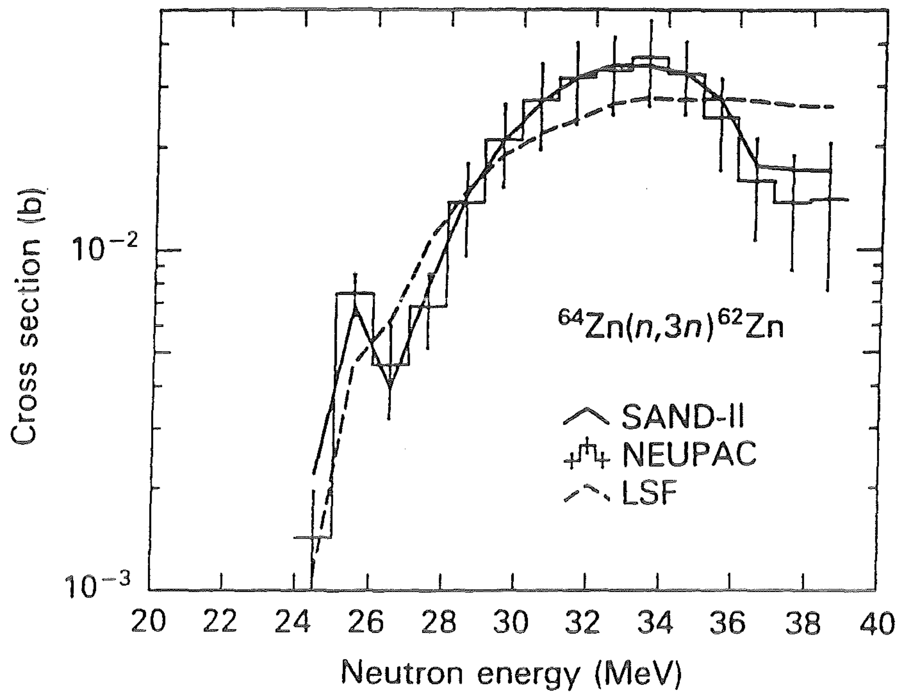
Cross section (b)
10^{-2}
10^{-3}
20 22 24 26 28 30 32 34 36 38 40
Neutron energy (MeV)
$^{64}Zn(n,3n)^{62}Zn$
SAND-II
NEUPAC
LSF

Fig. 35

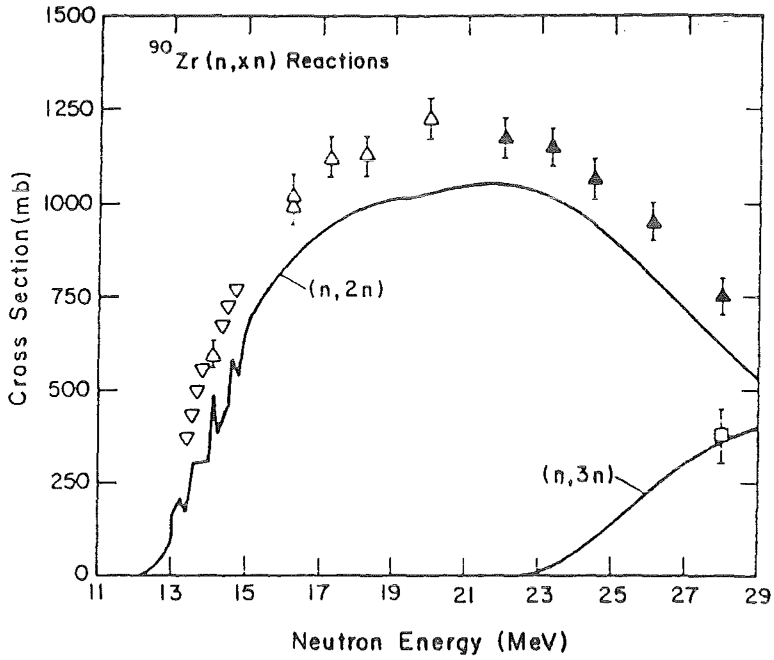
1500
1250
1000
750
500
250
0
^{90}Zr (n,xn) Reactions
Cross Section (mb)
(n,2n)
(n,3n)
11 13 15 17 19 21 23 25 27 29
Neutron Energy (MeV)

Fig. 36

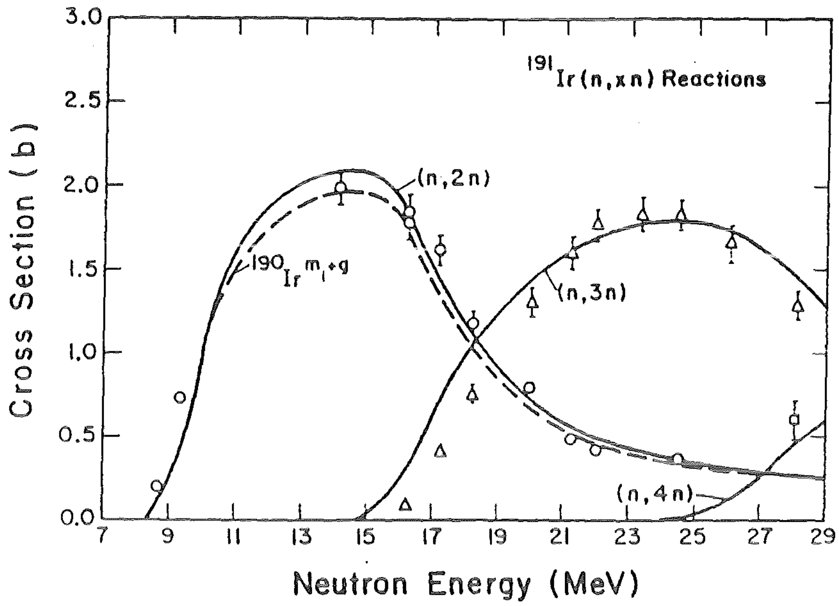
3.0
2.5
2.0
1.5
1.0
0.5
0.0
Cross Section (b)
191Ir (n, xn) Reactions
(n, 2n)
190Ir m1+g
(n, 3n)
(n, 4n)
7
9
11
13
15
17
19
21
23
25
27
29
Neutron Energy (MeV)

Fig. 37

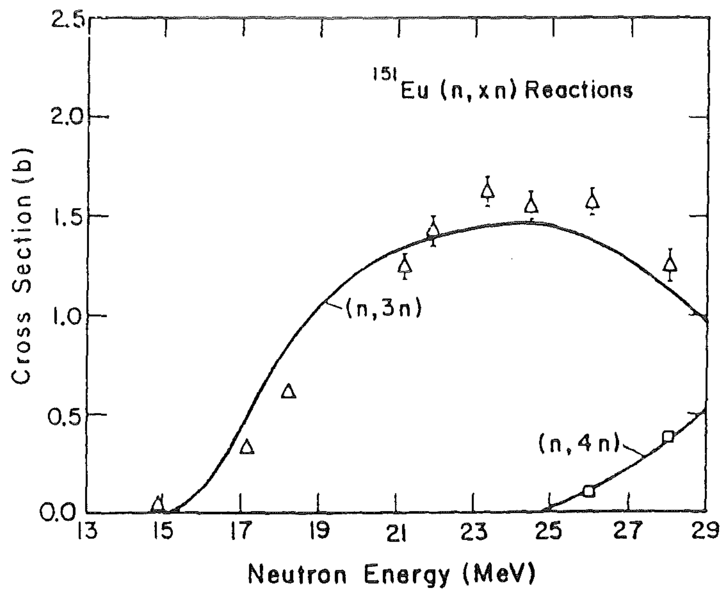
2.5
2.0
1.5
1.0
0.5
0.0
Cross Section (b)
151Eu (n, xn) Reactions
(n, 3n)
(n, 4n)
13
15
17
19
21
23
25
27
29
Neutron Energy (MeV)

Fig. 38

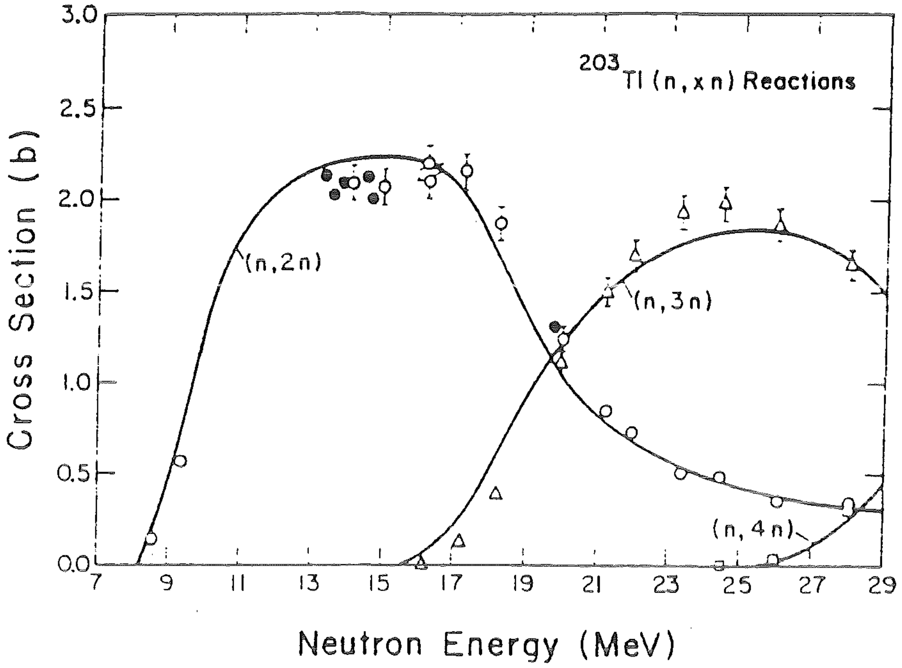

^{203}Tl (n, x n) Reactions
Cross Section (b)
Neutron Energy (MeV)
(n,2n)
(n,3n)
(n,4n)
3.0
2.5
2.0
1.5
1.0
0.5
0.0
7
9
11
13
15
17
19
21
23
25
27
29

Fig. 39

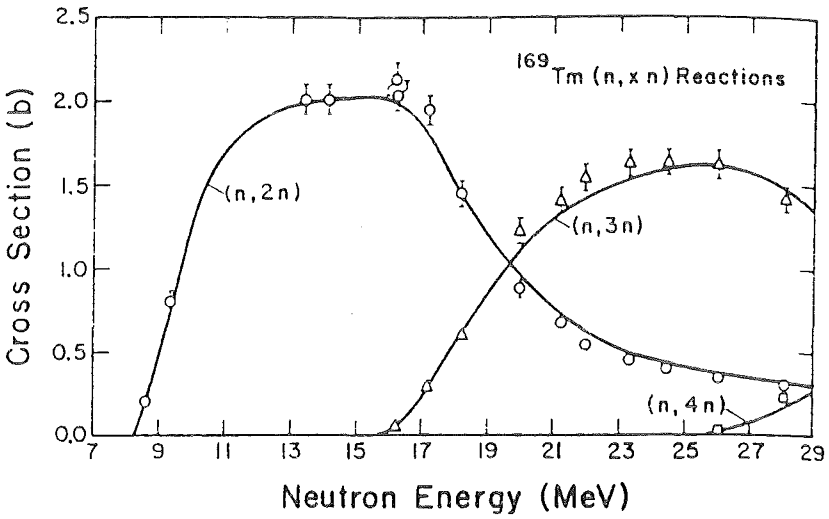

^{169}Tm (n, x n) Reactions
Cross Section (b)
Neutron Energy (MeV)
(n,2n)
(n,3n)
(n,4n)
2.5
2.0
1.5
1.0
0.5
0.0
7
9
11
13
15
17
19
21
23
25
27
29

Fig. 40

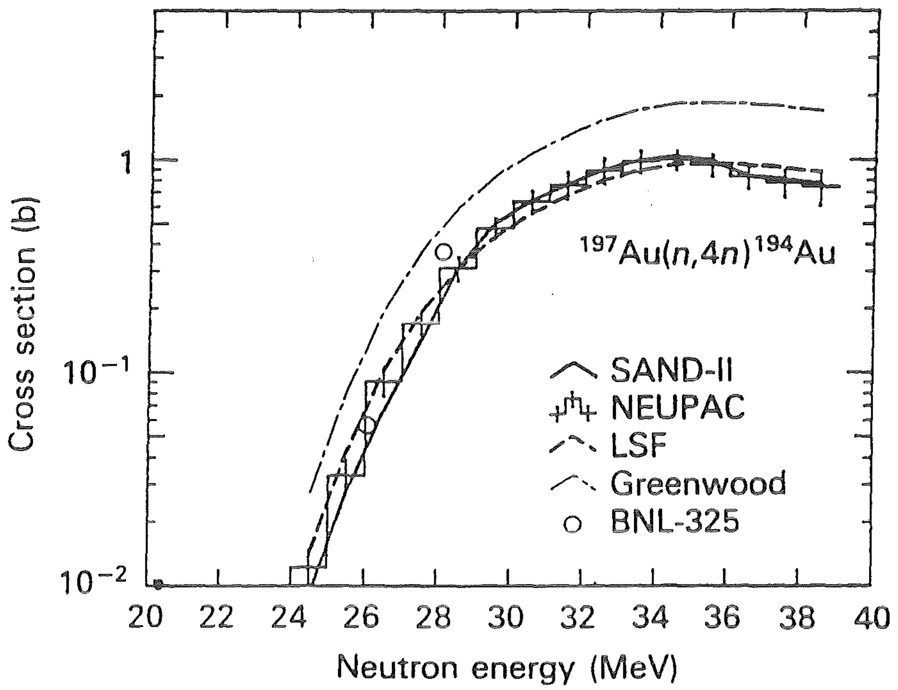

1
10^{-1}
10^{-2}
Cross section (b)
$^{197}Au(n,4n)^{194}Au$
SAND-II
NEUPAC
LSF
Greenwood
BNL-325
20
22
24
26
28
30
32
34
36
38
40
Neutron energy (MeV)

Fig. 41

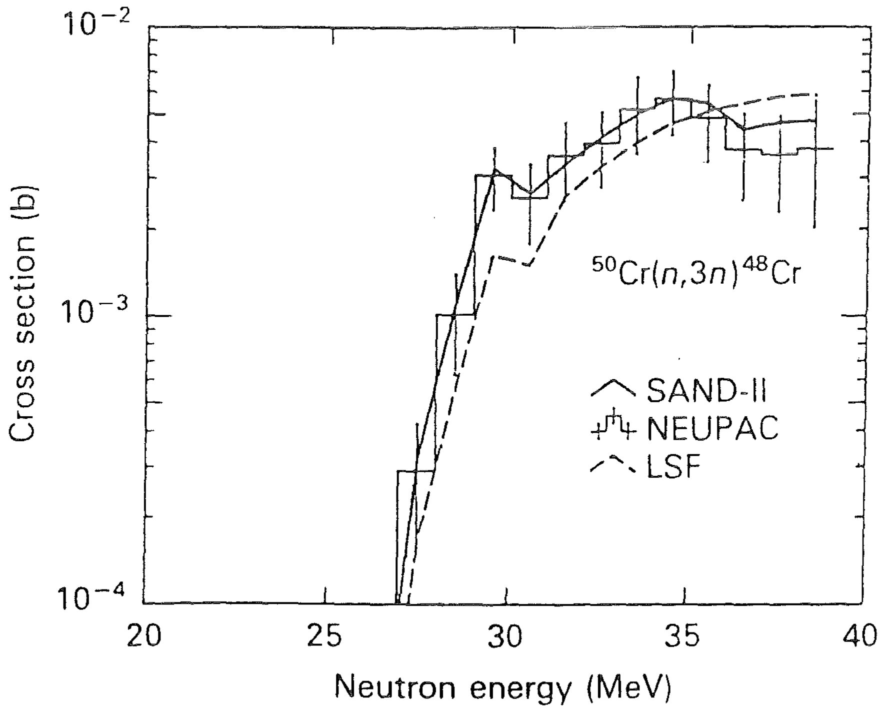

10^{-2}
10^{-3}
10^{-4}
Cross section (b)
$^{50}Cr(n,3n)^{48}Cr$
SAND-II
NEUPAC
LSF
20
25
30
35
40
Neutron energy (MeV)

Fig. 42

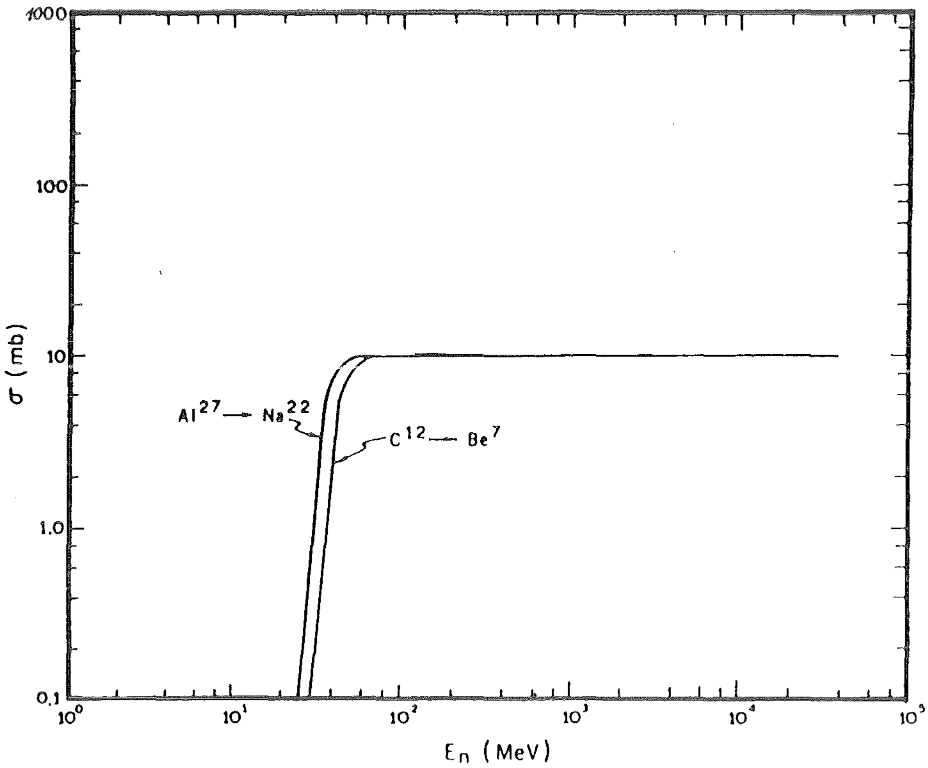
1000
100
10
1.0
0.1
σ (mb)
Al^{27} — Na^{22}
C^{12} — Be^{7}
10^0
10^1
10^2
10^3
10^4
10^5
En (MeV)

Fig. 43

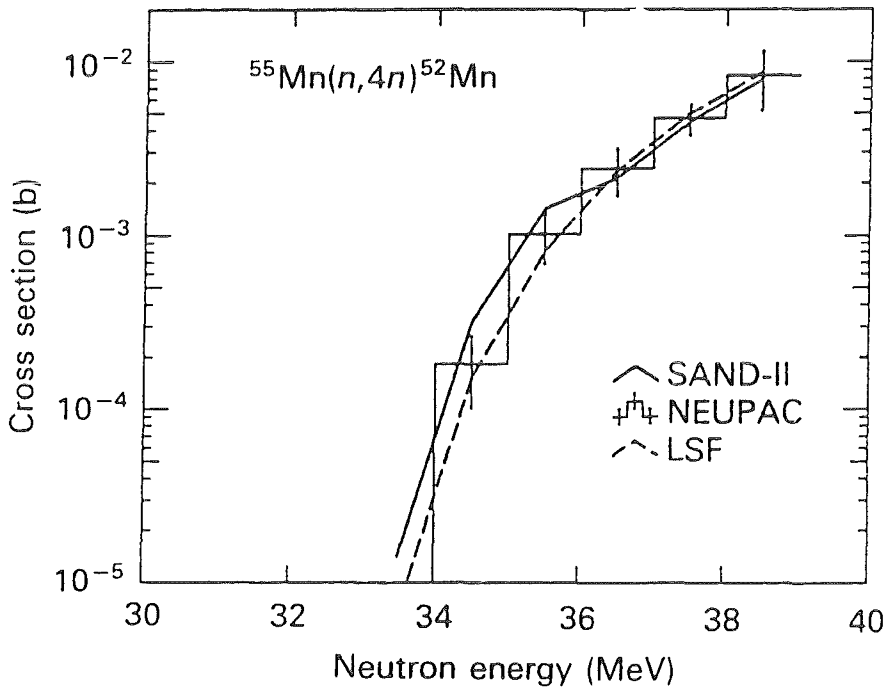
$^{55}Mn(n,4n)^{52}Mn$
10^{-2}
10^{-3}
10^{-4}
10^{-5}
Cross section (b)
SAND-II
NEUPAC
LSF
30
32
34
36
38
40
Neutron energy (MeV)

Fig. 44

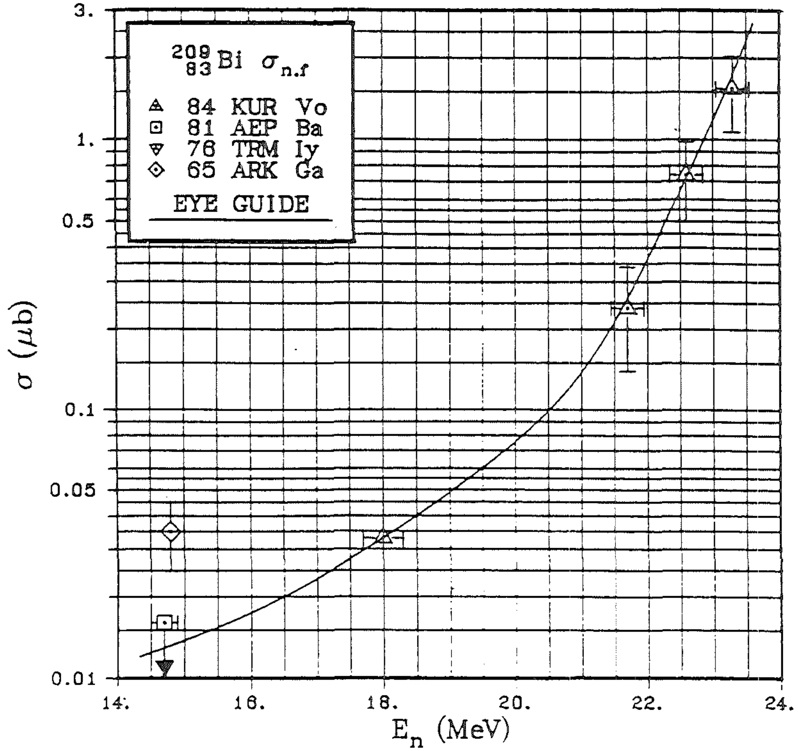

$^{209}_{83}$Bi $\sigma_{n,f}$
84 KUR Vo
81 AEP Ba
76 TRM Iy
65 ARK Ga
EYE GUIDE
σ (μb)
E$_n$ (MeV)

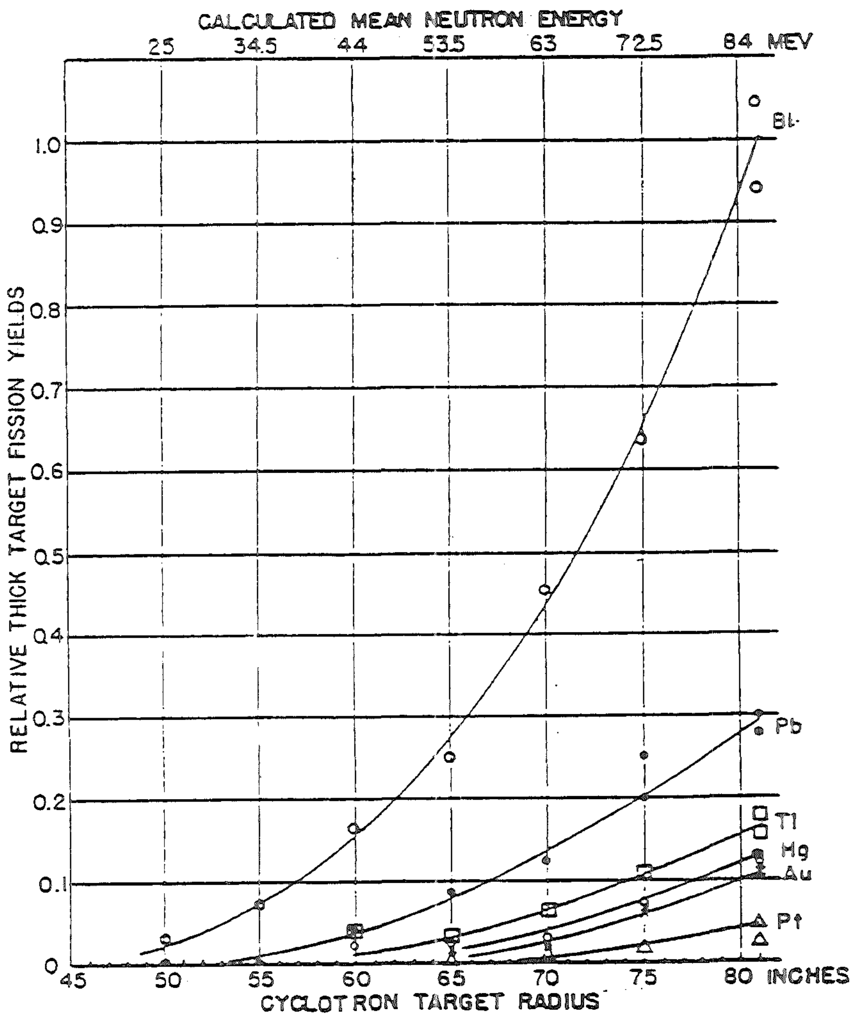

CALCULATED MEAN NEUTRON ENERGY
25 34.5 44 53.5 63 72.5 84 MEV
RELATIVE THICK TARGET FISSION YIELDS
Bi
Pb
Tl
Hg
Au
Pt
CYCLOTRON TARGET RADIUS
80 INCHES

Fig. 45

IFMIF Test Cell/Users Task CDA-D-10 :

Define Design Concept for Dosimetry

Y. Oyama
IFMIF Test Cell/Users Group of JAERI

1st IFMIF-CDA Technical Workshop
on Test Cell System

July 3-6, 1995
FZK, Germany

1. Objectives

1. Define dosimetry method requirements to estimate irradiation conditions, e.g.,

   Flux, Fluence, Neutron Spectrum,
   Gamma-ray Spectrum
   Absorption Dose and Dose Rate (Neutron and Gamma-rays)

2. Specify R&D needs for EDA because there are techniques and data base needed to be developed due to high energy and specific configurations relevant to IFMIF

2. Necessary Conditions for IFMIF Dosimetry

1. Time integrated response for post irradiation experiment

   fluence, total dose up to how much ?

   5×10^{14} n/cm^2/s x 3 month = 4×10^{21} n/cm^2 ?

2. Real time response/resolution for in-situ experiment

   flux, dose rate,
   sec ?, msec ? μsec ?
   flux level ? (10^{14} or 10^{12} n/cm^2/s)

3. Problems for IFMIF Dosimetry

1. Spectrum information/resolution

   neutron and gamma-ray spectrum

   energy range ? thermal to 50 MeV ?
   need high energy dosimetry cross section data

   resolution 5 MeV or 1MeV ?
   appropriate set of dosimetry reactions for MFA

2. Spatial information/resolution

   necessary detector size
   1 mm ==> activation foil or wire for time integration
   but real time monitor ? fiber ? resistivity detector ?
   new detector required

5. Accuracy
   may be, 10% or more ==> enough ?

4. Work plan for IFMIF Dosimetry

1. Review status of existing techniques
2. Review status of high energy dosimetry reaction
3. Review candidate of applicable detectors
4. Make combination strategy of detecors as a dosimetry system

Fluence

1) High threshold activation foils
   MFA spectrum unfolding $\Delta E \sim$ 4-5 MeV?
2) Single activation foil detector
   ex., $^{197}Au(n,\gamma)$, (n,p), (n,2n), (n,3n), (n,4n)
   $^{59}Co(n, \alpha)$, (n,p), (n,2n), (n,3n), (n,4n)

Flux

Fission chamber : U-238 , Th-232

He Gas Production

He mass spectrometer

Beam Profile

Plate track detector
Activation plate + radiography

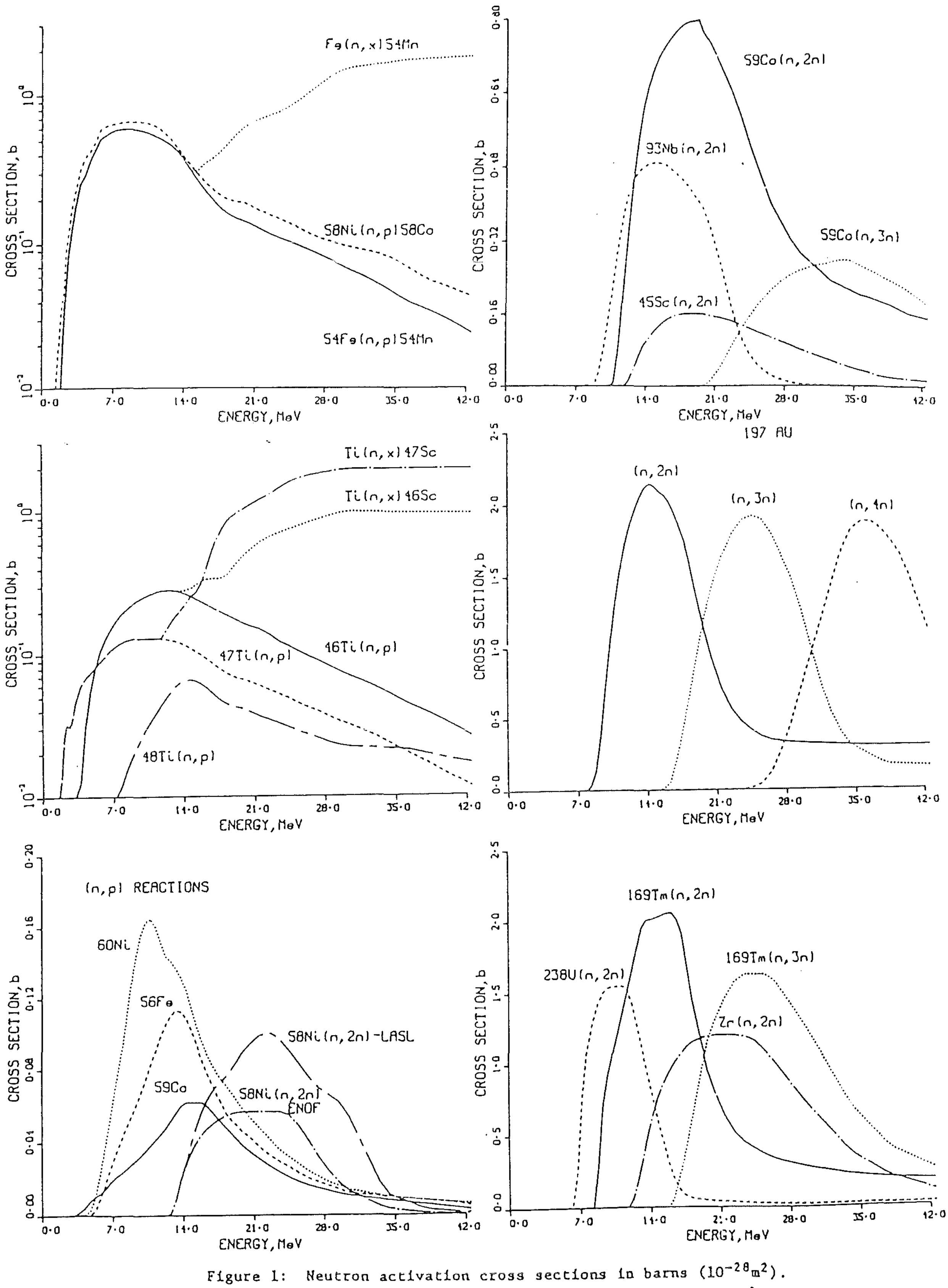

Figure 1: Neutron activation cross sections in barns ($10^{-28} m^2$).

TABLE III

Measured and Competing Reactions, Threshold Energies, Natural Abundances, and Recommendations of the Unfolding Method

Measured and Competing Reactions	Threshold Energy (MeV)	Natural Abundance (%)	Recommendation of the Best Result
^{23}Na$(n,2n)^{22}$Na	13.0	^{23}Na 100	NEUPAC
^{27}Al$(n,\alpha)^{24}$Na	3.2	^{27}Al 100	SAND-II
$(n,n^3\mathrm{He})$	24.6		
$(n,2d)$	28.0		
(n,npd)	30.3		
$(n,2n2p)$	32.6		
^{51}V$(n,\alpha)^{48}$Sc	2.1	^{51}V 99.750	SAND-II
$(n,n^3\mathrm{He})$	23.1	^{50}V 0.250	
$(n,2d)$	26.4		
(n,npd)	28.7		
$(n,2n2p)$	30.9		
^{50}V$(n,^3\mathrm{He})$	11.8		
(n,pd)	17.4		
$(n,2pn)$	19.7		
^{51}V$(n,p)^{51}$Ti	1.7		NEUPAC
^{50}Cr$(n,3n)^{48}$Cr	24.1	^{50}Cr 4.345	SAND-II
^{52}Cr$(n,5n)$	45.7	^{52}Cr 83.789	
		^{53}Cr 9.501	
^{50}Cr$(n,2n)^{49}$Cr	13.3	^{54}Cr 2.365	SAND-II
^{52}Cr$(n,4n)$	35.0		
^{53}Cr$(n,5n)$	43.0		
^{55}Mn$(n,p\alpha)^{51}$Ti	9.2	^{55}Mn 100	SAND-II
$(n,d^3\mathrm{He})$	28.5		
$(n,p2d)$	34.1		
$(n,n2pd)$	36.3		
$(n,2n3p)$	38.6		
^{55}Mn$(n,4n)^{52}$Mn	31.8		NEUPAC
^{55}Mn$(n,2n)^{54}$Mn	10.4		LSF
^{63}Cu$(n,3n)^{61}$Cu	20.1	^{63}Cu 69.17	SAND-II
^{65}Cu$(n,5n)$	38.1	^{65}Cu 30.83	
^{63}Cu$(n,2n)^{62}$Cu	11.0		SAND-II
^{65}Cu$(n,4n)$	29.1		
^{65}Cu$(n,p)^{65}$Ni	1.4		NEUPAC
^{64}Zn$(n,t)^{62}$Cu	10.2	^{64}Zn 48.6	NEUPAC
(n,nd)	16.6	^{66}Zn 27.9	
$(n,2np)$	18.9	^{67}Zn 4.1	
^{66}Zn$(n,2nt)$	29.6	^{68}Zn 18.8	
$(n,3nd)$	35.9	^{70}Zn 0.6	
$(n,4np)$	38.2		
^{67}Zn$(n,3nt)$	36.7		
$(n,4nd)$	43.1		
^{68}Zn$(n,4nt)$	47.1		
^{64}Zn$(n,3n)^{62}$Zn	21.3		SAND-II
^{66}Zn$(n,5n)$	40.6		
^{64}Zn$(n,2n)^{63}$Zn	12.0		NEUPAC
^{66}Zn$(n,4n)$	31.4		
^{67}Zn$(n,5n)$	38.5		
^{68}Zn$(n,6n)$	48.9		
^{197}Au$(n,4n)^{194}$Au	23.2	^{197}Au 100	NEUPAC
^{197}Au$(n,2n)^{196}$Au	8.1		NEUPAC

Table 2 Observed productions, competing reactions, threshold energies, natural abundances, sources of initial guesses for unfolding process and recommendations for best result

Production	Reaction	Threshold energy (MeV)	Natural abundance (%)	Source of unfolding initial guess	Recommendation for best result
Mg→^{24}Na	^{24}Mg(n,p)* ^{25}Mg(n,d) ^{26}Mg(n,t)	4.93 12.54 15.24	^{24}Mg 78.99 ^{25}Mg 10.00 ^{26}Mg 11.01	<15 MeV IAEA of ^{24}Mg(n,p) >15 MeV LSF	<10 MeV NEUPAC >10 MeV LSF
Si→^{27}Mg	^{28}Si($n,2p$)† ^{29}Si($n,{}^3$He)† ^{30}Si(n,α)*	13.89 14.66 4.34	^{28}Si 92.23 ^{29}Si 4.67 ^{30}Si 3.10	LSF	NEUPAC
Si→^{28}Al	^{28}Si(n,p)* ^{29}Si(n,d) ^{30}Si(n,t)	4.00 10.46 14.94		<16 MeV IAEA of ^{28}Si(n,p) >16 MeV LSF	NEUPAC
Si→^{29}Al	^{29}Si(n,p)* ^{30}Si(n,d)†	3.00 11.66		LSF	SAND-II
Ca→^{42}K	^{42}Ca(n,p)* ^{43}Ca(n,d)† ^{44}Ca(n,t)† ^{46}Ca($n,2nt$) ^{48}Ca($n,4nt$)	2.80 8.64 13.62 31.81 49.36	^{40}Ca 96.94 ^{42}Ca 0.647 ^{43}Ca 0.135 ^{44}Ca 2.09 ^{46}Ca 0.004 ^{48}Ca 0.187	<12 MeV IAEA of ^{42}Ca(n,p) >12 MeV LSF	NEUPAC
Ca→^{43}K	^{43}Ca(n,p)* ^{44}Ca(n,d)† ^{46}Ca(n,nt) ^{48}Ca($n,3nt$)	1.06 10.17 21.97 39.53		LSF	see text
V→^{46}Sc	^{50}V($n,n\alpha$)† ^{51}V($n,2n\alpha$)*	10.09 21.35	^{50}V 0.25 ^{51}V 99.75	LSF	LSF
V→^{47}Sc	^{50}V(n,α)† ^{51}V($n,n\alpha$)*	0 (Q=0.76) 10.50		LSF	LSF
Cr→^{52}V	^{52}Cr(n,p)* ^{53}Cr(n,d) ^{54}Cr(n,t)	3.26 9.08 12.60	^{50}Cr 4.35 ^{52}Cr 83.79 ^{53}Cr 9.50 ^{54}Cr 2.36	<15 MeV IAEA of ^{52}Cr(n,p) >15 MeV LSF	<15 MeV SAND-II >15 MeV LSF
Cr→^{53}V	^{53}Cr(n,p)* ^{54}Cr(n,d)†	2.69 10.32		<15 MeV BNL eye-guide of ^{53}Cr(n,p) >15 MeV LSF	NEUPAC
Cu→^{62m}Co $T_{1/2}$=14 min	^{63}Cu($n,2p$) ^{65}Cu(n,α)*	10.85 0.21	^{63}Cu 69.2 ^{65}Cu 30.8	<20 MeV IAEA of ^{65}Cu(n,α) >20 MeV LSF	NEUPAC
Zn→^{65}Ni	^{66}Zn($n,2p$)† ^{67}Zn($n,{}^3$He) ^{68}Zn(n,α)* ^{70}Zn($n,2n\alpha$)	10.44 9.76 0 (Q=0.77) 15.15	^{64}Zn 48.6 ^{66}Zn 27.9 ^{67}Zn 4.10 ^{68}Zn 18.8 ^{70}Zn 0.62	LSF	<20 MeV SAND-II >20 MeV NEUPAC
Zn→^{64}Cu	^{64}Zn(n,p)* ^{66}Zn(n,t)† ^{67}Zn(n,nt) ^{68}Zn($n,2nt$) ^{70}Zn($n,4nt$)	0 (Q=0.20) 10.51 17.67 28.01 43.92		<17 MeV IAEA of ^{64}Zn(n,p) >17 MeV LSF	NEUPAC
Zn→^{66}Cu	^{66}Zn(n,p)* ^{67}Zn(n,d) ^{68}Zn(n,t)† ^{70}Zn($n,2nt$)	1.89 6.79 10.78 26.70		LSF	NEUPAC
Zn→^{68m}Cu $T_{1/2}$=3.8 min	^{68}Zn(n,p)* ^{70}Zn(n,t)	4.63 11.95		LSF	NEUPAC

* Dominant reaction; † Supplemental observed reaction.

IFMIF-CDA Test Cell/Users Task CDA-D-11

Design Concept of Entire Test Cell

K. Noda
IFMIF-CDA Test Cell/Users Group of JAERI

1. Status of CDA-D-11 Task in Japan

IFMIF-CDA Test Cell Group at JAERI is making effort to get some budget for CDA-D-11 task. JAERI intends to provide some technical contribution for CDA-D-11, when the budget is secured.

Design concepts of entire test cell (test assembly, test cell structure and shielding, test cell coolant loop, etc.) do not have a large influence on accelerator and Li target design concepts. Testing requirements for irradiation tests for PIE and in-situ experiments, and outcomes of CDA-D-4, CDA-D-5, CDA-D-6 should be reflected to CDA-D-11. Design concepts of entire test cell should maintain flexibility by final stage of CDA.

2. Japanese View for CDA-D-11

Preliminary Requirements for Test Cell

(1) Capability for irradiation test of specimens for PIE

-Proper shielding for test assembly for irradiation test of specimens for PIE

-Quick change of test modules and the test assembly
(Period for changing:1 days)

-Specimen temperature measurement and control system with liq. metal coolant and gas coolant are attached to the test assembly.
(Temp. range;RT to 1000 C, Accuracy: ±5 C)

-Precise positioning of test module by the test assembly.
(Accuracy: ±1 mm)

- Reliable operation of test assembly.

-Neutron fluence/spectra can be monitored at various specimen positions.

-Hot cell systems for PIE, etc.

(2) Capability for in-situ experiments

-Loading system/ test assembly for in-situ experiment apparatus with precise positioning function.
(Period for changing: Several days)
(Positioning accuracy: ±1 mm)

-Ample space of test cells for various types of in-situ experiments.
(Larger than FMIT test cell volume of 2.8X1.8X1.5 m)

-Specimen temperature control system with liq. metal coolant and gas coolant can be used.
(Temp. range;RT to 1000 C, Accuracy:±5 C)

-Various kinds of measurement and service leads (electrical, optical, sweep gas, vacuum, hydraulic, pneumatic, coolant, etc.) for various in-situ measurements (creep, fatigue, electrical, optical, gas release, IASCC, etc.)

(3) Capability for maintenance of Li target

-Exchange system of Li target

-Hot cell systems for maintenance of Li target

Li Target Group will provide requirements for capability for maintenabce of Li target.

(4) Others

-Test cell atmosphere; Inert gas (He, N_2)

Japanese Preliminary View for Design Concept of Entire Test Cell

Although design concept of test cells in FMIT is good reference for test cells in IFMIF, the concept in FMIT has to be improved to meet new needs for fusion materials R&D which were identified for IFMIF, i.e., needs for development of advanced low activation structural materials such as SiC/SiC composites and ceramics materials and for various in-situ experiments.

-Test cells for IFMIF should be somewhat larger than those of FMIT for various kinds of in-situ experiments.

-Concept of Vertical Test Assembly (VTA) of FMIT may be still suitable technology for the test assembly of IFMIF for irradiation tests of specimens for PIE.

-Specimen temperature control system has to cover very wide temperature range, e.g., liq. nitrogen temperature to 1000 C from consideration for SiC/SiC composites and use of RF window materials at cryogenic temperatures.

-Remote handling is one of key technology for test cell of IFMIF. Current robotics technology should be applied for remote handling system as well as conventional master-slave manipulator systems.

Task CDA-D-11: Design Configuration for the Test Cell Assembly

Presented by
J. R. Haines (ORNL)
at the
IFMIF-CDA Technical Workshop
on the Test Cell System
July 5, 1995

Topics for Test Cell Assembly Design

- Assumptions/design features
- Typical vertical test assembly (VTA) configuration
- Arrangement/integration of five VTA's
- Removal and installation scheme
- Target system interface issues
- VTA Handling issues
- Test Cell Shielding - See Gomes' presentation

Assumptions and Design Features for Test Cell Assembly Configuration

- Modules/Assemblies removed with a simple vertical motion
- Each vertical test assembly (VTA) can be removed separately
- Coolant lines stepped (3 steps) to prevent neutron streaming
- Concrete ceiling shield thickness ~ 2.2 m

THE HIGH FLUX TEST MODULE IS SUPPORTED BY VERTICAL TEST ASSEMBLY #1 (VTA)

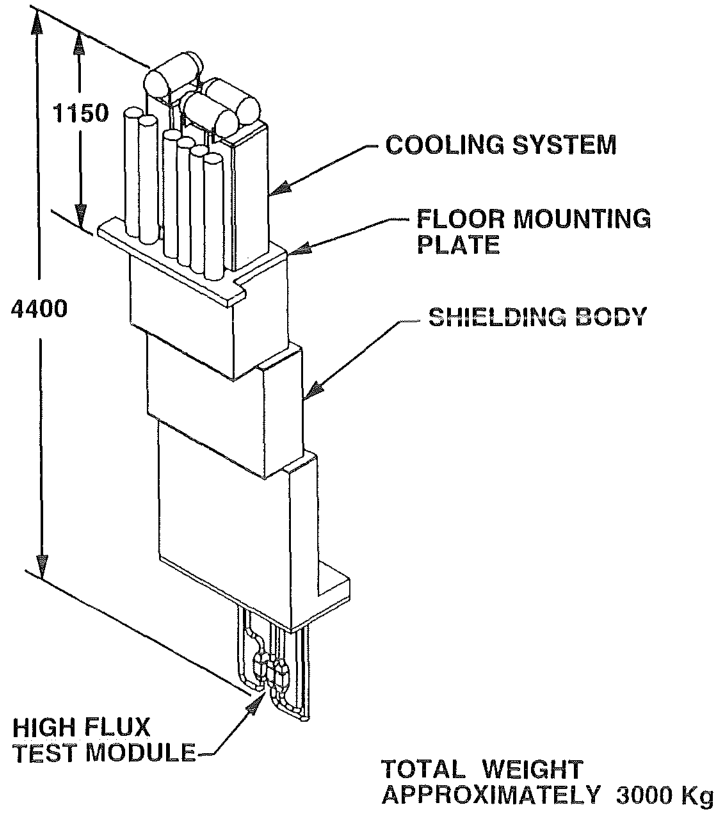

THE TEST CELL CEILING PENETRATION CONSIST OF FIVE VERTICAL TEST ASSEMBLIES AND A FLOOR PLUG

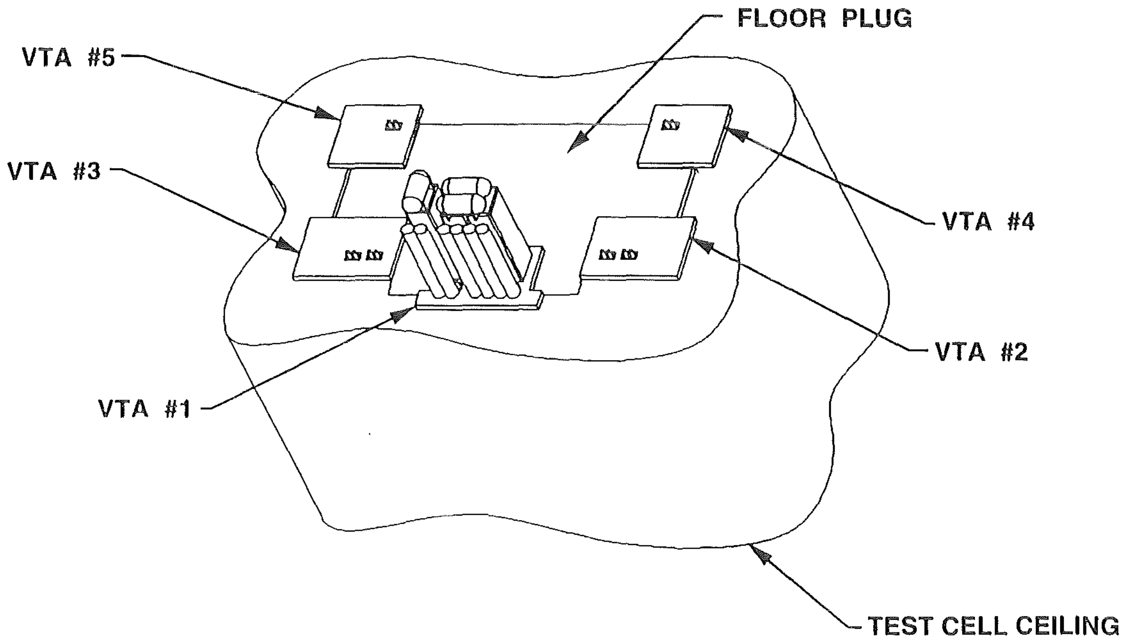

THE FLOOR SHIELD PLUG INTERLOCKS WITH ALL FIVE VTA'S AND THE FLOOR TO PREVENT RADIATION STREAMING

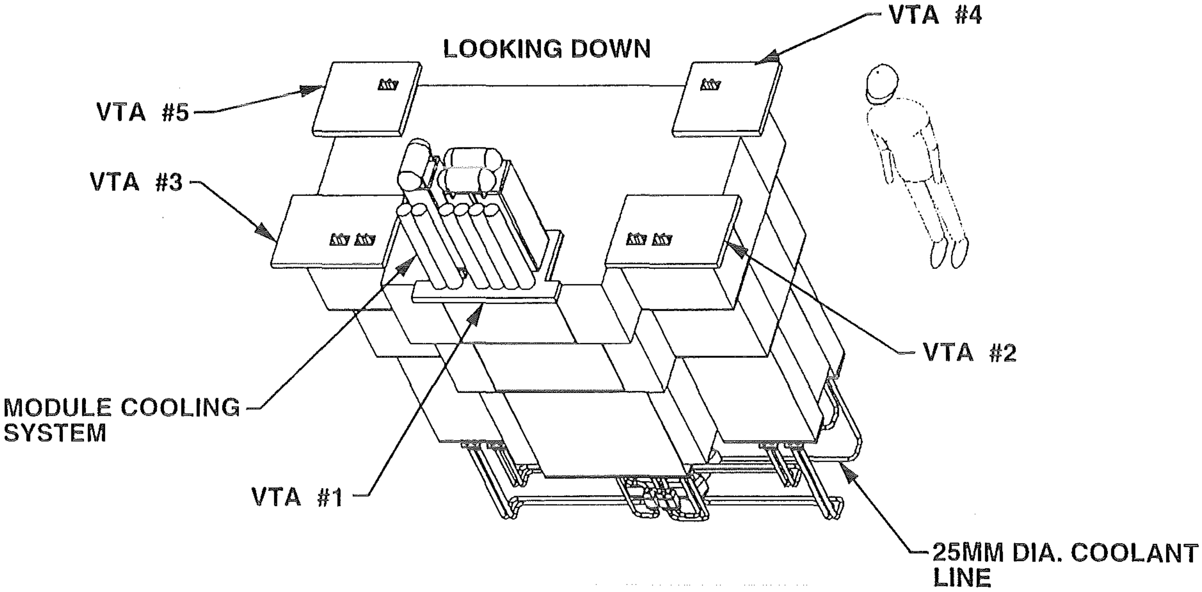

EACH TEST MODULE IS ATTACHED TO THE VTA'S WITH EASILY DECOUPLED FITTINGS

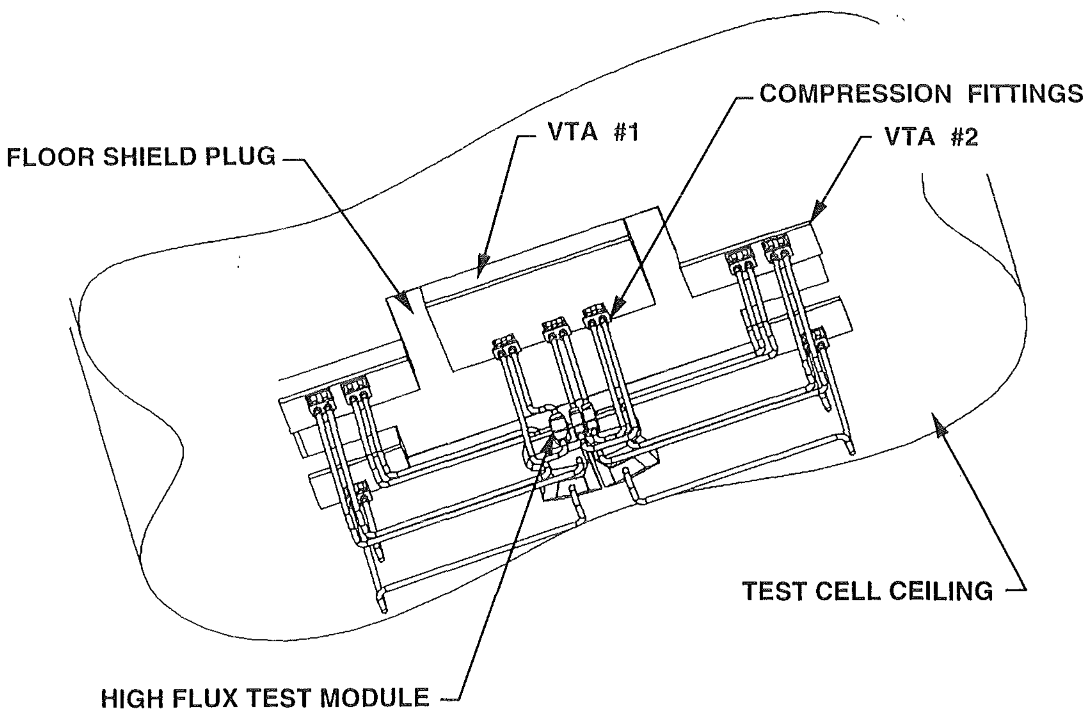

UNDERSIDE VIEW

THE FLOOR SHIELD PLUG IS STEPPED TO PREVENT RADIATION STREAMING AND ACCOMMODATE VERTICAL TEST ASSEMBLY REMOVAL

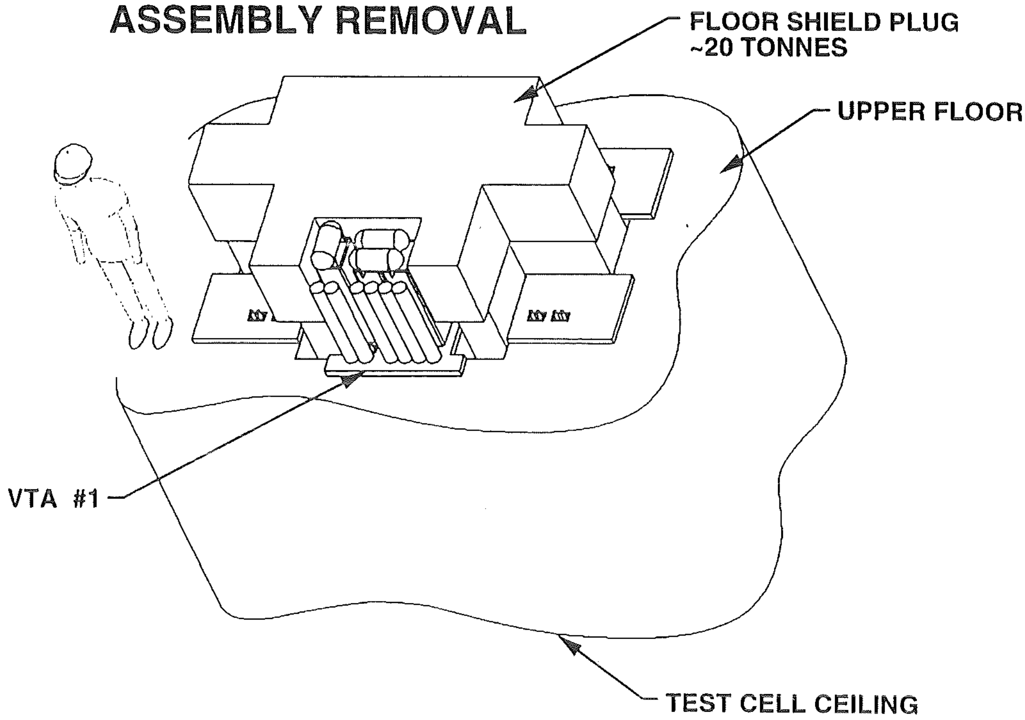

THE FLOOR SHIELD PLUG IS STEPPED TO PREVENT RADIATION STREAMING AND ACCOMMODATE VERTICAL TEST ASSEMBLY REMOVAL

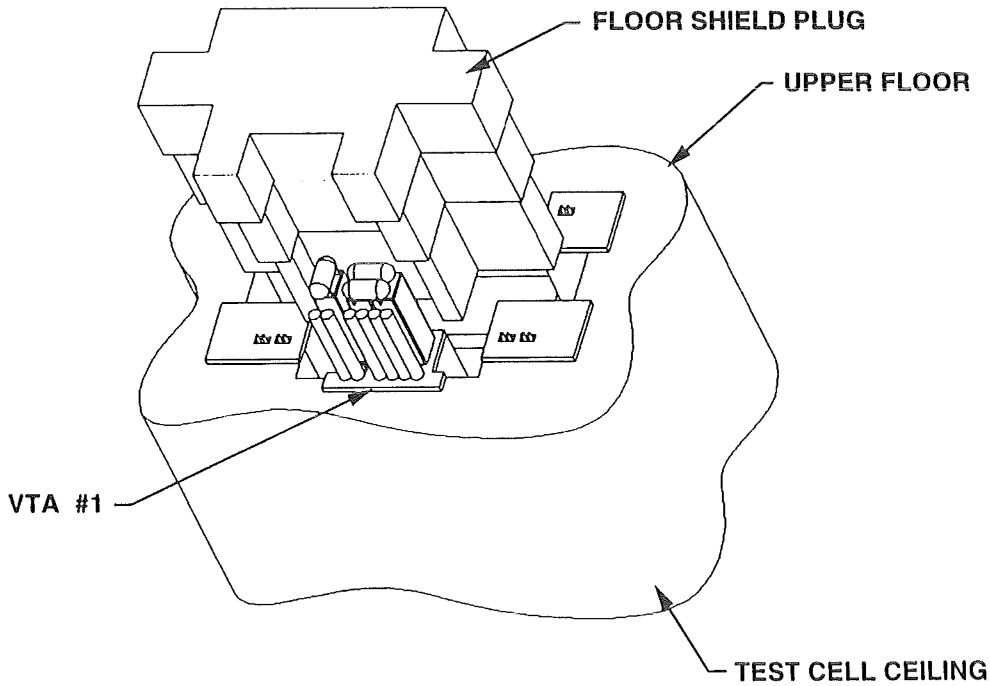

EACH VTA IS STEPPED TO PREVENT RADIATION STREAMING

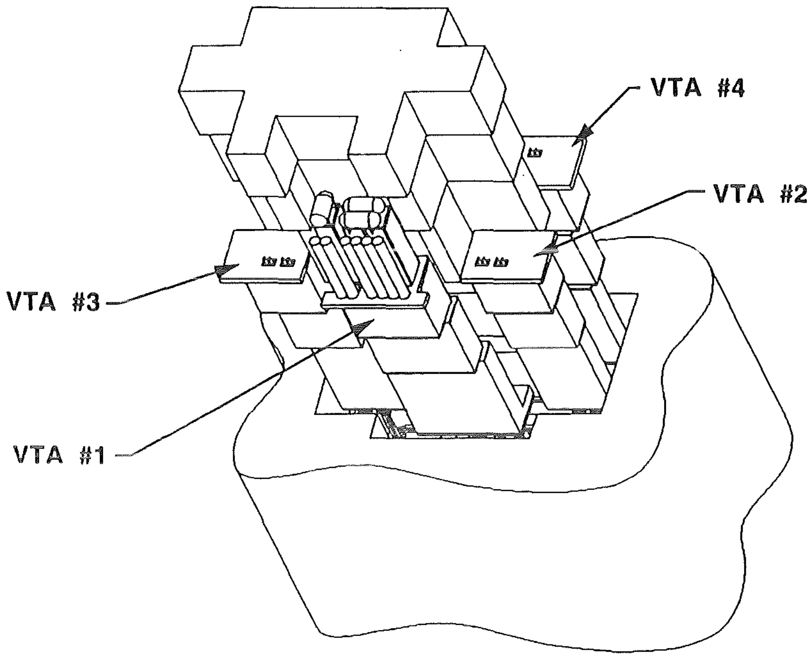

EACH VTA CAN BE RAISED VERTICALLY WITHOUT INTERFERING WITH THE REMAINING VTA'S

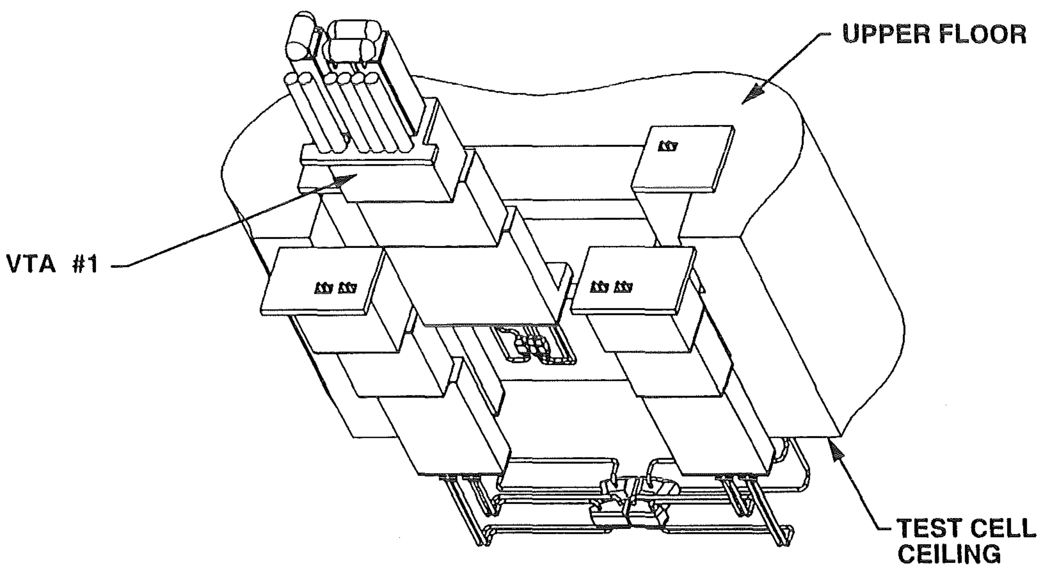

THE HIGH FLUX TEST MODULE #1 IS POSITIONED AS CLOSE TO THE TARGET BACK WALL AS POSSIBLE.

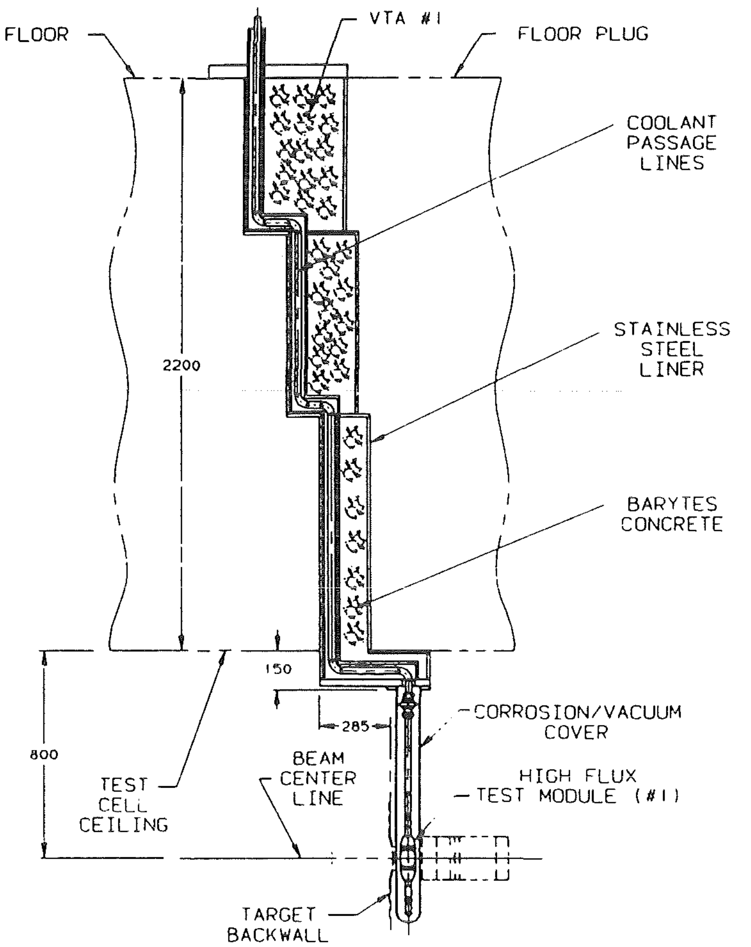

High-Flux Module Configuration Prevents Vertical Removal of Target Assembly Without Removing VTA #1

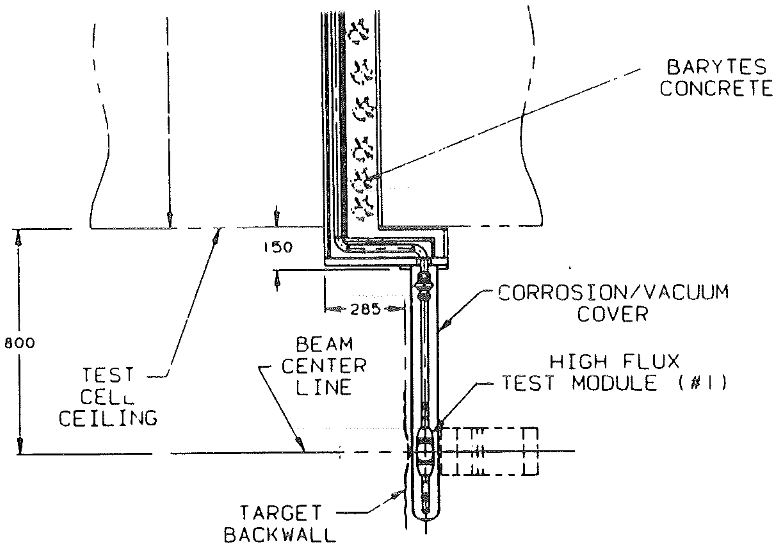

EACH VTA IS INVERTED DURING THE TEST MODULE REMOVAL OPERATION

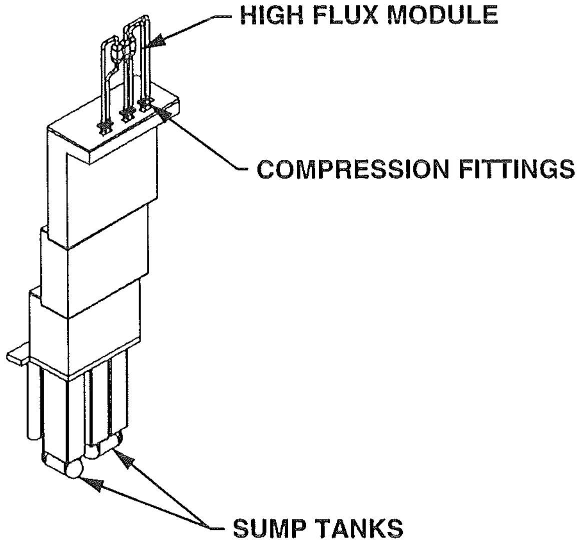

VTA Handling Issues

- There should be at least three different hot cells or hot cell regions for the test cell
    - Module removal (replacement) from VTA
    - Maintenance of VTA's and handling system
    - Removal/assembly of specimens into modules
- Handler design approach
    - Single handler approach - single piece of equipment lifts VTA, transports it to the hot cell, and installs/removes it from hot cell
- Multiple handling equipment approach, e.g.. crane for lifting, rails for transporting, inserter/remover performs handling in the hot cell

CDA-D11: Shielding Analysis of the Test Cell

IFMIF Test Cell Design Meeting

Karlsruhe - Germany

Itacil C. Gomes

Argonne National Laboratory

July 3-6, 1995

Shielding Analysis - Bulk Shield

- Simple estimations of the thickness of the test cell walls can be done based on FMIT results - around 3 meters depending on the dose levels outside the walls.
- A more realistic analysis can be done only after the design parameters concerning the test cell are set.
- Special attention has to be taken when designing access routes to the test cell.

Shielding Analysis - Penetrations

- Several penetrations will be present for:
  1. Instrumentation
  2. Lithium loop
  3. Remote maintenance
  4. Vehicle for test assembly
  5. Accelerator, among others
- Reducing radiation streaming to minimal levels must be the goal.

I.C.Gomes - Argonne National Laboratory

Shielding Analysis - Activation

- Inside the test cell the activation levels are going to be very high
- It is important to use materials which will reduce the decommission and disposal problems to the lowest levels.
- Activation of structure/equipment in areas close to the test cell has to be avoid.
- The goal is to keep the radioactive inventory to a minimum.

I.C.Gomes - Argonne National Laboratory

Shielding Analysis - Activation

- Test cell activation products, such as gases, must be prevented to enter other areas.
- Liquid lithium loop is going to carry a fair amount of activation products, as such a special attention must be taken to avoid further contamination.
- Replaceable parts are to be made of low activation materials.

I.C.Gomes - Argonne National Laboratory

Shielding Analysis - Maintenance

- Many service areas can be affected by the radiation from the test cell.
- As far it is possible, hands-on maintenance is highly desirable.
- A throughout analysis of the facility has to be conducted to ensure adequate shielding in all areas and avoid remote maintenance as much as possible.

I.C.Gomes - Argonne National Laboratory

IFMIF TASK CDA-D-11: PRELIMINARY ACTIVITIES ON SHIELDING CALCULATIONS

S. MONTI

In order to guarantee the accessibility of IFMIF during operation and the respect of the dose limits inside and outside the facility, the neutron and gamma shields around the facility have to be defined. An estimate of the shields aimed at the peculiar structure of IFMIF is of primary importance for meeting the two opposite requirements of ensuring doses below the recommended limits in the requested environments and reducing the construction costs. To this end, a set of Monte Carlo simulations has to be performed by considering the real geometry of the designed facility (see fig. 1) and the neutron source distribution inside the test cell environment. In this way the shielding of neutrons scattering on the room walls will also be taken into account.

According to ICRP recommendations, the maximum alowable equivalent dose rate to personnel employed at the installation will be below 50 mSv per year corresponding to 25 μSv/h for personnel working full time for 2000 h/year. This equivalent dose rate will be assumed for dimensioning the shielding thicknesses. However, it should be noted that the recent ICRP60 recommends an equivalent dose below 20 mSv/year.

Accessibility with occupancy factor equal to 1 has been assumed in Auxiliary Equipment & Facilities Room and outside the Test Cell Areas and the Beam Turning Room. Conservatively, also the use factor of the facility has been assumed equal to 1.

The neutron distribution due to two deuteron beams of 35 MeV impinging on the same lithium target at 10 degrees was provided by JAERI to FZK and transmitted to ENEA at the beginning of June. The neutron spectrum is devided into 19 energy bins and varies either in azimuthal and polar angle (30 azimuthal bins and 26 polar bins). In shielding calculations the same point neutron source with the above spectrum will be considered, alternatevely, in the target n° 1 or n° 2 or in the beam dump location.

All the simulations refer to the neutron and gamma radiations produced in the lithium target / Test Cell areas: neutron sources due to deuteron losses in the accelerators or other adjacent structures will not be here taken into account and will be treated in the framework of accelerator design.

At the present moment, shieldings around the neutron source are all assumed of concrete TSF-5.5 which elemental composition in units of 10^{21} atoms cm^{-3} is as follows:

H	8.5
C	20.20
O	35.5
Mg	1.86
Al	0.60
Si	1.70
Ca	11.30
Fe	0.19

Percent water, by weight	5.5
Density (g cm^{-3})	2.31

Other shielding materials, such as iron or polyethilene, will be eventually considered in a second step of the design, if required.

As no specific nuclear data library in the range of 0-50 MeV is still available, at present it is not possible to use only the well known MCNP code coupled with the usual libraries. Thus, it has been decided to also use a Monte Carlo high energy transport code such as FLUKA or LCS (Lahet Code System). The first was developped at CERN (Geneve, Switzerland) and INFN (Italy), the second at LosAlamos Laboratories (USA). In these codes, neutrons with energy below 20 MeV are transported in the same way as in MCNP code, making use of evaluated nuclear data libraries. Particularly, LCS makes use of MCNP itself and its libraries, while FLUKA adopts a Monte Carlo scheme with a dedicated nuclear data file based on ENDFB and JEF libraries, set up at ENEA-Bologna. Above 20 MeV both codes, still in a Monte Carlo scheme, calculate reaction cross sections using various nuclear reaction models (depending on the energy range) such as: Intranuclear Cascade, Precompound decay, Evaporation, Fission, etc.. Of course, a dedicated library for IFMIF calculations in a readble form for MCNP4A would be derirable. If and when task CDA-D-7 will provide such a library, a final check of shielding calculations will be performed.

The actual geometry of the facility has been reproduced in Monte Carlo simulations. The geometry has been first defined in MCNP4A environment (surfaces and cells: see plant and cuts in figs. 2, 3 & 4) but, making use of a geometry translator program developped at ENEA-

Bologna, the same geometry was got ready for FLUKA code too. This allow to perform calculations with MCNP and FLUKA in parallel.

All the calculations will be carry out taking into account the strong forward anisotropy of the neutron source. Particularly, in order to limit the needed thicknesses of concrete shield in the various directions, four different set of tallies will be assumed for frontal and lateral walls, ceiling and floor. Also the neutron streaming in backward direction will be checked.

Fig. 1

ce IFMIF Configuration

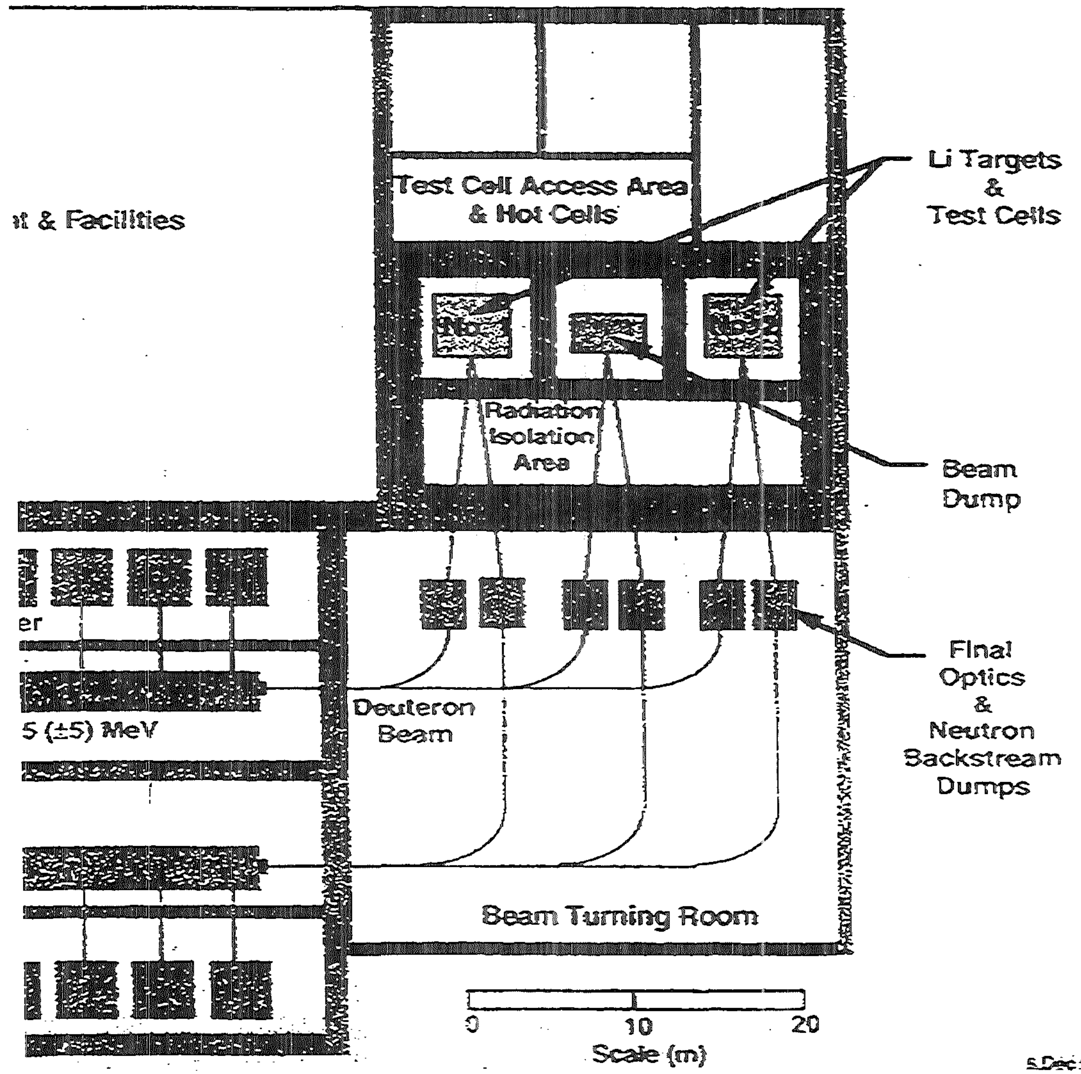

IFMIF-CDA
Design Integration Meeting
FZK Karlsrule
July 4, 1995

1. Meeting Objective

The objective of this meeting was to meet with specialists in the EU who are involved in the design integration activity and to discuss the status of tasks and planning in preparation for the design integration workshop to be held at ORNL October 16-27, 1995. T. E. Shannon reviewed the scope of the Design Integration Activity (Attachment 1) and the strategy for developing the Baseline Design in 1995 as prepared for the Executive Committee in February, 1995 (Attachment 2).

2. Attendees

C. Antonucci	ENEA Bologna	39-10-6098591
F. Cozzani	EC Brussels	32-2-295 06 76
F. Filotto	ENEA Brasimone	39-534-801337
M. Martone	ENEA Frascati	39-6-94005355
T. Shannon	University of Tenn.	615-974-7572
U. von Möllendorff	FZK Karlsrule	49-7247-82-2739

3. CDA Cost Estimate

An important task for the Design integration group in 1996 will be the coordination of the cost estimate for the IFMIF project. The suggestion was made that outside experts should be contacted to develop an accounting system to be used for organization of the estimate. It was furthur recommended that consideration be given to using the ITER home teams as a resource for the cost estimate so that some standardation could be obtained with the ITER project estimate.

4. CY 1995 Documentation

It was recommended that the project adopt an outline to describe the initial Baseline Design that will form the framework for the CDA report. M. Martone will provide the first draft of the document outline (Table of Contents) by the end of July.

5. Electronic Files and Data Base

F. Filotto from ENEA presented a proposal to provide a dedicated work station at Frascati for the use of the IFMIF project to use, store and maintain all documents, drawings and data developed by the project. The proposal is summarized in the Attachment 3. An FTP server will provide access in several formats including PC and Macintosh. There was a tentative agreement to accept the proposal pending approval by the IFMIF Subcommittee Shannon will contact the Committee members by the end of July. Hopefully, the System will be operational by August. It was suggested that some trial transfer of drawing and word processing files be carried out over the next several weeks.

6. Initial Facility Layout

M. Martoni presented preliminary general layout drawings prepared on the software Autocad 12 at Frascati (Attachment 4). He offered to extend this work to include the results of the three workshops through September. These layouts will be brought to Oak Ridge in October to be the starting point for the Design Integration working meeting.

SCOPE OF THE DESIGN INTEGRATION GROUP ACTIVITY

1. Develop and maintain Design Requirements and Standards, Interface and Configuration Control, and the Work Breakdown Structure (WBS).

2. Develop and maintain Assembly Drawings for the major systems.

3. Provide integrated layouts of the primary equipment and overall plant facility including:
   - Accelerator
   - Target
   - Test Cell
   - Power Systems
   - Instrumentation and Controls
   - Shielding
   - Remote Handling
   - Test Facilities
   - Utilities
   - Buildings and Structures

4. Coordinate project cost estimate and schedule.

5. Define Safety, Environmental and Health Requirements.

6. Coordinate documentation of the CDA.

7. Communications Protocal and Software.

Attachment 1

SCOPE OF THE DESIGN INTEGRATION GROUP ACTIVITY

1. Develop and maintain Design Requirements and Standards, Interface and Configuration Control, and the Work Breakdown Structure (WBS).

2. Develop and maintain Assembly Drawings for the major systems.

3. Provide integrated layouts of the primary equipment and overall plant facility including:
   - Accelerator
   - Target
   - Test Cell
   - Power Systems
   - Instrumentation and Controls
   - Shielding
   - Remote Handling
   - Test Facilities
   - Utilities
   - Buildings and Structures

4. Coordinate project cost estimate and schedule.

5. Define Safety, Environmental and Health Requirements.

6. Coordinate documentation of the CDA.

7. Communications Protocal and Software.

Draft
02/06/95

International Fusion Materials Irradiation Facility
Proposed Strategy for
the Development of a Baseline Design in 1995

1. Objective

The objective of this proposed strategy and plan is to complete the mechanical design layout and a written design description of a Baseline Design for the International Fusion Materials Irradiation Facility by December 31, 1995.

2. Scope of the Baseline Design Activity

The IFMIF Baseline Design will be the basis for developing the Conceptual Design in 1996. The Baseline Design will consist of an assembly drawing depicting the mechanical arrangement of the major equipment items and the supporting facilities. The drawing will also define the overall building structures and utilities. A written document will be produced to describe the design requirements and features of the systems as given in the Work Breakdown Structure. The resulting parameters and system interfaces will be established and controlled through a design integration activity.

3. Proposed Strategy

3.1 Resolve issues and perform the work defined at KfK workshop.

3.2 Develop and define reference design concepts for the three major systems
- Accelerator System
- Target System
- Test Cell System

3.3 Document design concepts for preliminary evaluation and study by the Design Integration Group.

3.4 Conduct an intense two-week design integration activity to produce the Baseline Design.

3.5 Document the description of the Baseline Design.

3.6 Define the issues and tasks for completion of the Conceptual Design Activity.

4. Outline of the Design Integration Working Meeting

4.1 The participants will be a limited group of experts (<20) representing the three major systems and facility design specialists.

4.2 Each of the three major systems will be represented by several experts with the background and knowledge necessary to design and integrate the systems.

4.3 Several facility specialists will provide design layouts for supporting equipment, building and utilities.

4.4 Layout Designers will produce CAD drawings.

4.5 ORNL will provide office and meeting space, CAD work stations, and two to three mechanical/facility designers.

5. Proposed Schedule

5.1	Technical Groups Perform work defined at KfK and develop reference design concepts	Jan-Oct/1995
5.2	Three major Systems Groups hold workshops and document reference designs	July-Sept/1995
5.3	Design Integration working meeting at ORNL	Oct 16-27/1995
5.4	Baseline Design Description Document	Dec/1995

ENEA
ENTE PER LE NUOVE TECNOLOGIE
L'ENERGIA E L'AMBIENTE
Associazione EURATOM-ENEA sulla Fusione

Design Integration:

Communication Protocols and Software, Project Documentation

F. Filotto (EU/ENEA)

IFMIF - CDA Technical Workshop on Test Cell System
Karlsruhe, July 3-6,1995

Design Integration:
Communication Protocols and Software, Project Documentation.

F. Filotto (EU/ENEA)

Progress Report

Offer of using for an FTP Server for storing the IFMIF Project Documentation.

1. Availability of an FTP Server.

In the ENEA Research Centre of Frascati is already available an FTP Server for storing the IFMIF Project Documentation (communications, reports, drawings, technical annexes, etc.);
The Server name is **ftp.frascati.enea.it**,
its IP Address is **192.107.51.13**.

2. FTP Server access typology.

Put and get files: access by entering a specific User ID and Password combination directly provided for the Project Leader;

Get files: access by entering the **anonymous** User ID.

Annexes 1 and 2 show suggested software for documents creation, respectively for Mac and for PC; show file exchange between them and the FTP Server and in general file exchange via Internet; Annexes 3 and 4 show access typology to the FTP Server, respectively from Mac and from PC.

3. Storing Directories for the IFMIF Project Documentation.

The complete pathname of the IFMIF directory in the FTP Server is **/pub /pub /IFMIF** if the access is by entering a specific User ID and Password combination for putting and getting files.

If the access is by entering the **anonymous** User ID (to get files only), the complete pathname of the IFMIF directory is **/pub /IFMIF**.

4. Content and composition of the IFMIF Project Documentation stored in the Frascati FTP Server.

README file with general informations: stored as **TEXT** file;

Documents created in Word, Word Perfect, etc.: stored as **WORD for Mac** files;

Documents created in Excel, Lotus 1-2-3, etc.: stored as **EXCEL for Mac** files;

CAD Drawings: stored as **AUTOCAD 12** files;

Tranfer files from and to the FTP Server have to be done in the **Binary** mode.

5. Next implementations.

Every Deputy Leader will be provided of a specific User ID and Password combination in order to put their own Team Documentation directly in the FTP Server, both in definitive or in in-progress types and in separated subdirectories.

Annex 1

Computer Apple Machintosh: Suggested software for document creation and file exchange via Internet.

Operating System:	7.1 or more;
Word Processor:	Word 6.0;
Electronic Sheet:	Excel 5.0;
Data Base:	File Maker 2.1;
CAD:	Autocad 12;
Internet Protocol:	Mac TCP;
FTP:	Fetch;
E-Mail:	PopMail, Eudora;
Connection to www servers:	Mosaic, Netscape.

Personal Computer IBM: Suggested software for document creation and file exchange via Internet.

Operating System:	Windows 3.1 (with MS DOS 6.2);
Word Processor:	Word 6.0;
Electronic Sheet:	Excel 5.0;
Data Base:	Access 2.0;
CAD:	Autocad 12;
Internet Protocol:	TCP/IP;
FTP:	FTP Client;
E-Mail:	PopMail, Eudora;
Connection to www servers:	Mosaic, Netscape.

How to connect to the IFMIF Frascati FTP Server from Macintosh.

1. **Access to the Frascati FTP Server.**
   Start Fetch application;
   As Host enter **ftp.frascati.enea.it** or **192.107.51.13.**

2. **Connection to get IFMIF files from the Frascati FTP Server.**
   As User ID enter **anonymous** and as Password enter your E-Mail Address;
   As Directory enter **/pub /IFMIF**;
   At the end of these steps press the **RETURN** key or click **OK**.

3. **Get a file from the FTP Server.**
   Left the transfer-mode switch at **Automatic**.
   Find the document you want to retrieve, either double click on its name in the list or click once to select it and click on **Get File**.
   This will open another window requesting the new location and name for the document on your local Mac.
   Select an appropriate disk and folder where to keep the document and click on the **Save** button.

4. **Content and composition of the IFMIF Project Documentation stored in the Frascati FTP Server.**

   README file with general informations: stored as **TEXT** file;
   Documents created in Word, Word Perfect, etc.: stored as **WORD for Mac** files;
   Documents created in Excel, Lotus 1-2-3, etc.: stored as **EXCEL for Mac** files;
   CAD Drawings: stored as **AUTOCAD 12** files;

5. **Connection to get files from and put files in the Frascati FTP Server.**

   Enter the specific User ID and Password combination provided for the Project Leader;
   As Directory enter **/pub /pub /IFMIF**;
   At the end of these steps press the **RETURN** key or click **OK**.

6. **Put a file.**

   Left the transfer-mode switch at **Automatic**.
   Select on your local Mac the document you want to put in the FTP Server and click on **Put File**.
   This will open another window requesting the new location and name for the document on the FTP Server.

7. **Get a file from the FTP Server.**

   Left the transfer-mode switch at **Automatic**.

Find the document you want to retrieve, either double click on its name in the list or click once to select it and click on **Get File**.
This will open another window requesting the new location and name for the document on your local Mac.
Select an appropriate disk and folder where to keep the document and click on the **Save** button.

How to connect to the IFMIF Frascati FTP Server from PC.

1. **Access to the Frascati FTP Server from Windows 3.1.**
   Open **Internet** window;
   Start **Trumpet Windsock** and reduce to icon;
   Start **FTP** application;
   As Host enter **ftp.frascati.enea.it** or **192.107.51.13.**

2. **Connection to get IFMIF files from the Frascati FTP Server.**
   As User ID enter **anonymous** and as Password enter your E-Mail Address;
   As Directory enter **/pub /IFMIF**;
   At the end of these steps press the **RETURN** key or click **OK**.

3. **Get a file from the FTP Server.**
   Select **Binary** transfer mode;
   Select the document and click on the **Receive** button or ← button that will be transfer on your local PC.
   Set your FTP application with transfer file dialog box switched on in the OPTION Selection; so you can give an appropriate name to the document

you are getting on your local PC from the FTP Server.

4. **Content and composition of the IFMIF Project Documentation stored in the Frascati FTP Server.**
   README file with general informations: stored as **TEXT** file;
   Documents created in Word, Word Perfect, etc.: stored as **WORD for Mac** files;
   Documents created in Excel, Lotus 1-2-3, etc.: stored as **EXCEL for Mac** files;
   CAD Drawings: stored as **AUTOCAD 12** files;

5. **Connection to get files from and put files in the Frascati FTP Server.**
   Enter the specific User ID and Password combination provided for the Project Leader;
   As Directory enter /pub /pub /IFMIF;
   At the end of these steps press the RETURN key or click OK.

6. **Put a file.**
   Select **Binary** transfer mode;
   Select a document on your local PC and click on the Send button or → button that will be transfer on the FTP Server.
   Set your FTP application with transfer file dialog box switched on in the OPTION Selection; so you can give an appropriate name to the

document you are putting in the FTP Server from your local PC.

7. **Get a file from the FTP Server.**
   Select **Binary** transfer mode;
   Select the document and click on the Receive button or ← button that will be transfer on your local PC.
   Set your FTP application with transfer file dialog box switched on in the OPTION Selection; so you can give an appropriate name to the document you are getting on your local PC from the FTP Server.

ENEA
ENTE PER LE NUOVE TECNOLOGIE
L'ENERGIA E L'AMBIENTE
Associazione EURATOM-ENEA sulla Fusione

Design Integration
General Layout

M. Martone (EU/ENEA)

IFMIF-CDA Technical Workshop on Test Cell System
Karlsruhe, July 3-6,1995

Design Integration: General Layout

M. Martone (EU/ENEA)

Progress Report

On the basis of:

-the Reference IFMIF Configuration,

-the documents released:
at the Planning Meeting in Tokai (June,1994),
at the Karlsruhe Technical Meeting (September, 1994),

an attempt has been made at drawing up a Very Preliminar General Layout of IFMIF using Autocad 12.

The following inputs have been considered:

- Deuteron beams impinge on the targets at an angle of 15°;
- Available room into the Test Cell, 2x2x2 m^3;
- Test Cell shielding designed for an easy access to the Li-target, for maintenance (sliding cover and the walls can be dismantled).

The following information allow us to make a further step:

- How much room into the Test Cell, is needed for the in situ experiment?

- How close to the Li-target the quench tank must be located?

- How far from the Li-target the final element of HEBT/EDC sistems must be located?

- Which areas must be accessible within a few hours since the source is switched off? (Beam Turning Room?, Radiation Isolation Area?, Accelerator Area?)

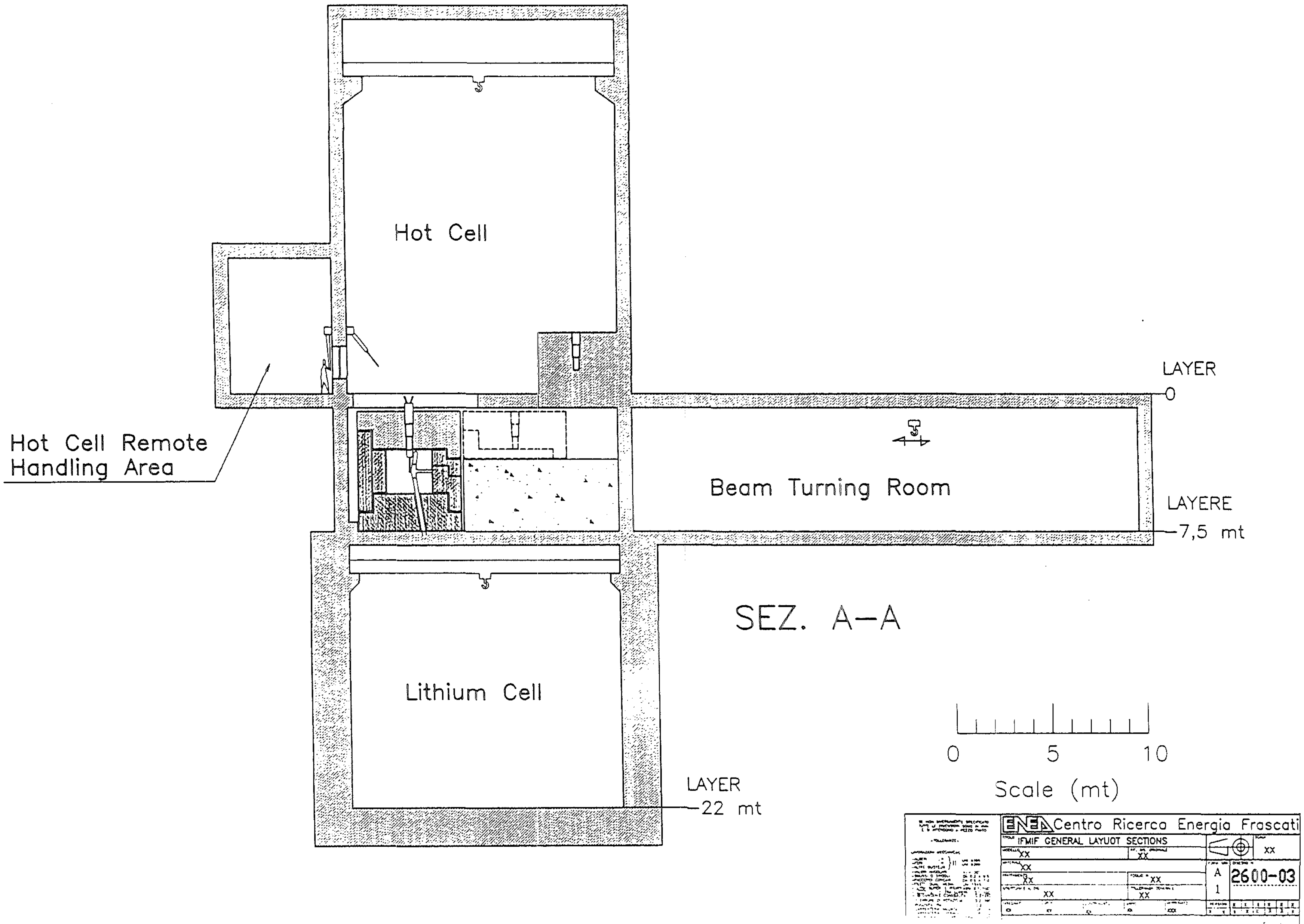
Hot Cell
Hot Cell Remote
Handling Area
LAYER
0
Beam Turning Room
LAYERE
-7,5 mt
SEZ. A-A
Lithium Cell
0
5
10
Scale (mt)
LAYER
-22 mt
Centro Ricerca Energia Frascati
IFMIF GENERAL LAYUOT SECTIONS
2600-03

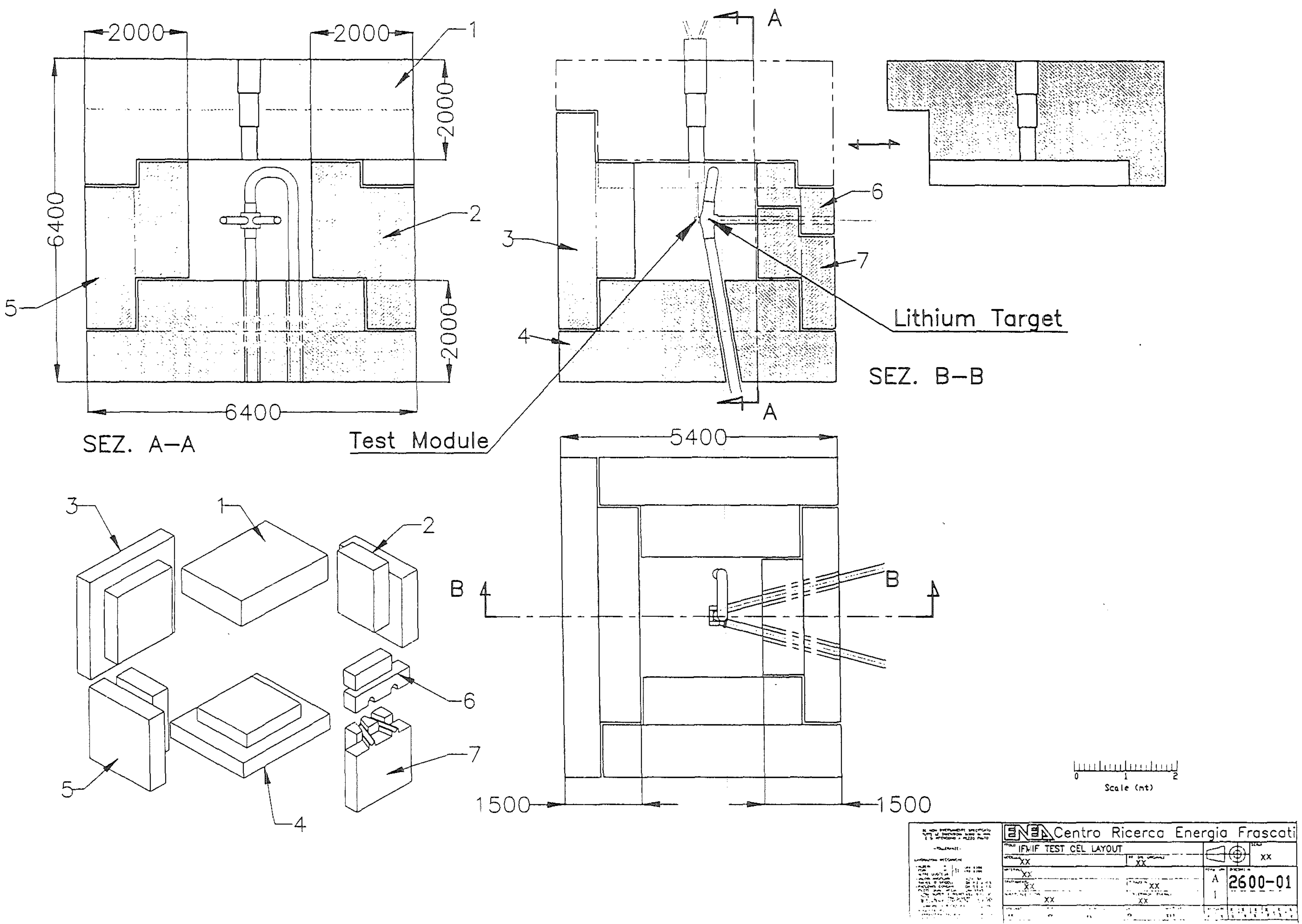

2000
2000
6400
6400
SEZ. A–A
1
2
3
4
5
6
7
A
A
Lithium Target
Test Module
SEZ. B–B
5400
B
B
1500
1500
Scale (mt)
Centro Ricerca Energia Frascati
IFMIF TEST CEL LAYOUT
2600-01

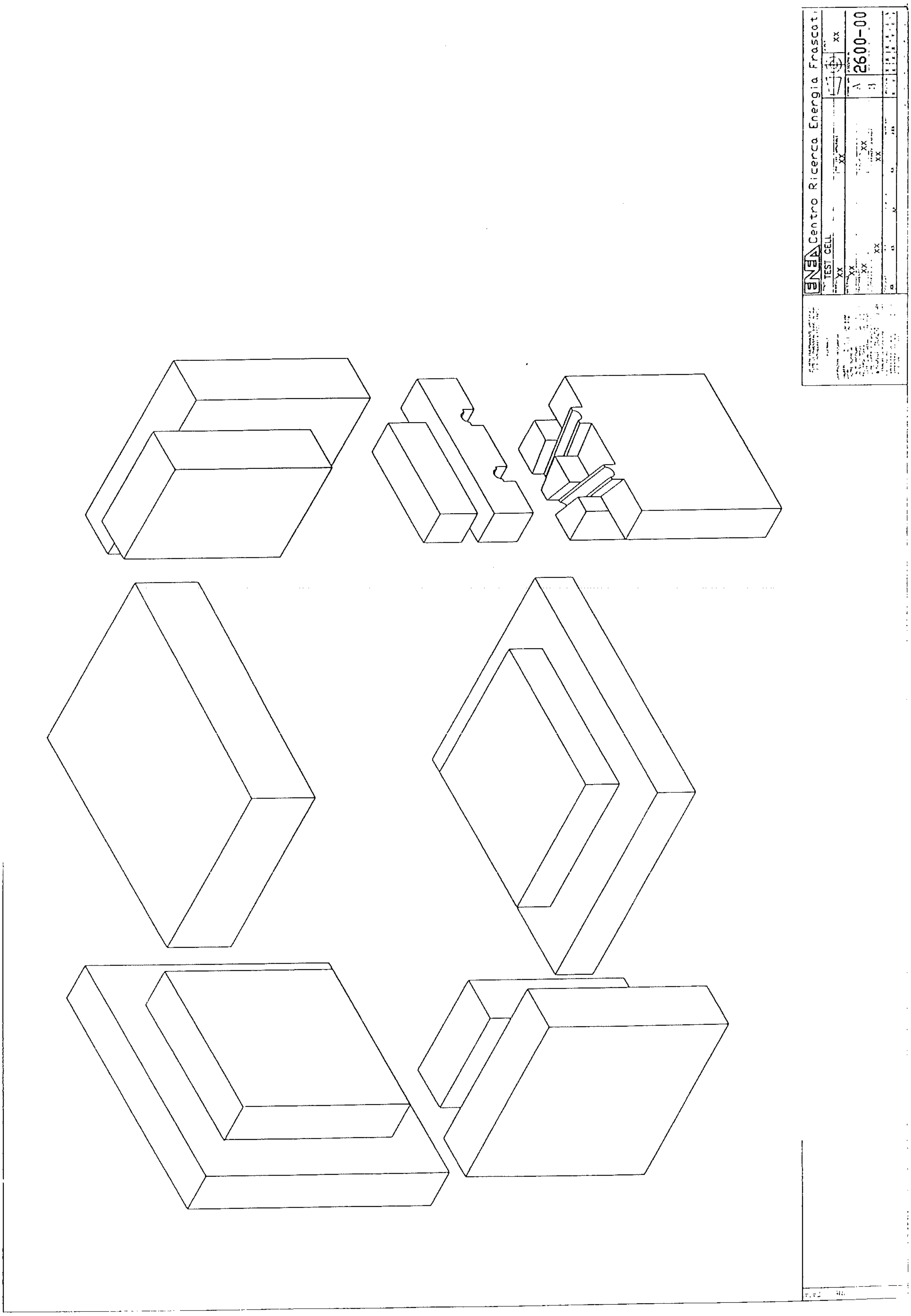
ENEA Centro Ricerca Energia Frascati
TEST CELL
2600-00

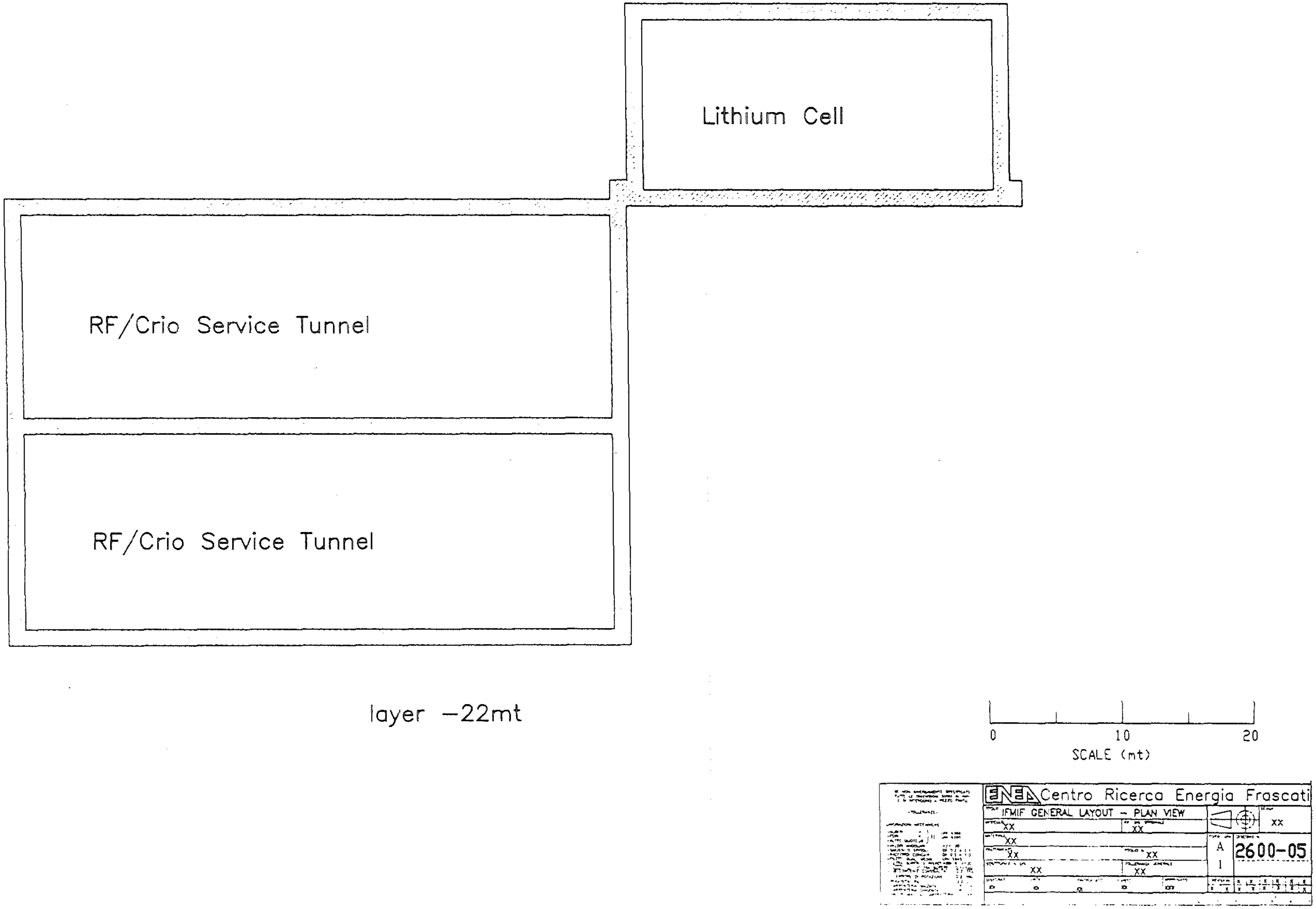
Lithium Cell
RF/Crio Service Tunnel
RF/Crio Service Tunnel
layer –22mt
0
10
20
SCALE (mt)
ENEA Centro Ricerca Energia Frascati
IFMIF GENERAL LAYOUT – PLAN VIEW
2600-05

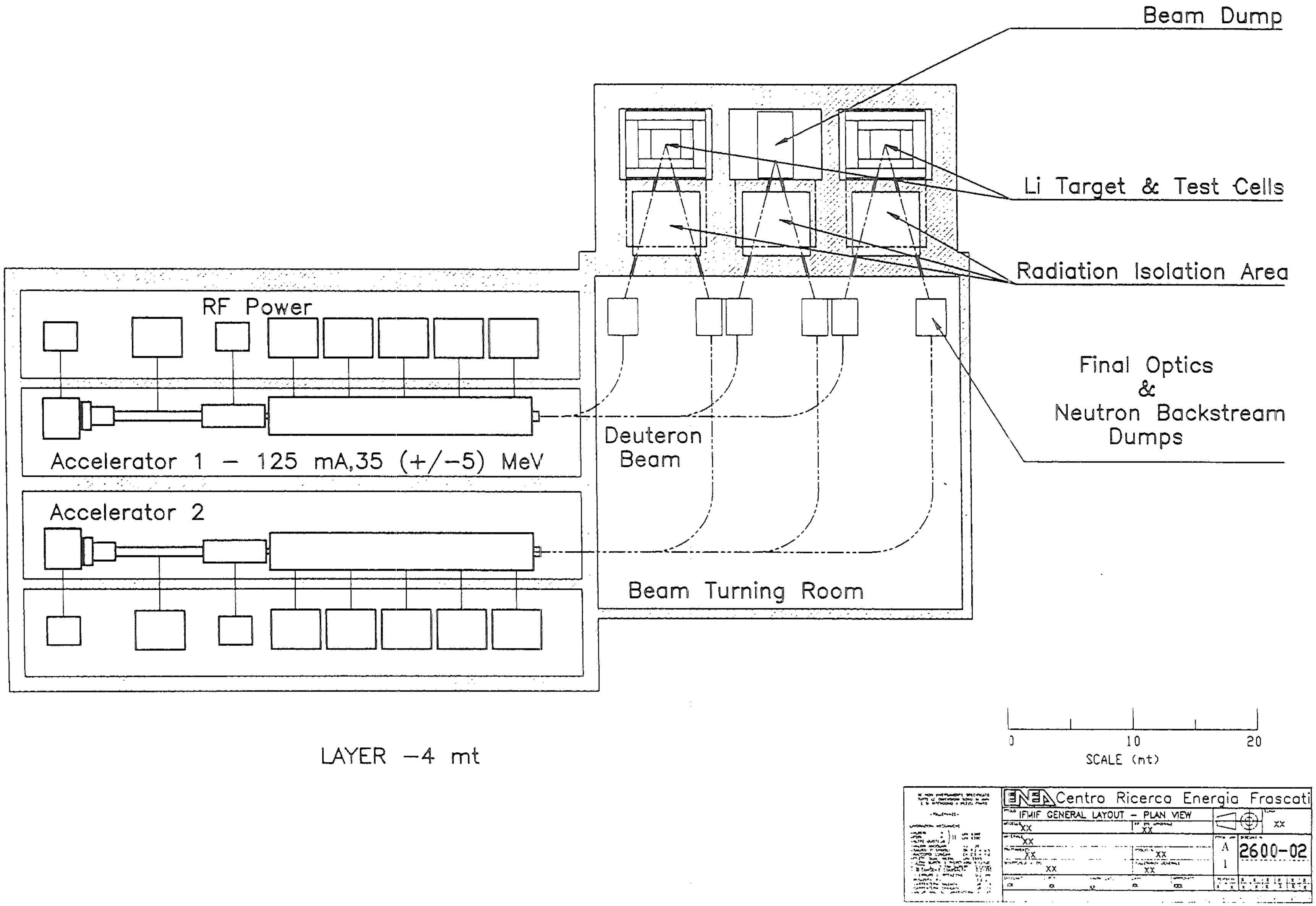
Beam Dump
Li Target & Test Cells
Radiation Isolation Area
RF Power
Final Optics
&
Neutron Backstream
Dumps
Deuteron
Beam
Accelerator 1 – 125 mA,35 (+/–5) MeV
Accelerator 2
Beam Turning Room
0
10
20
SCALE (mt)
LAYER –4 mt
Centro Ricerca Energia Frascati
IFMIF GENERAL LAYOUT – PLAN VIEW
2600-02

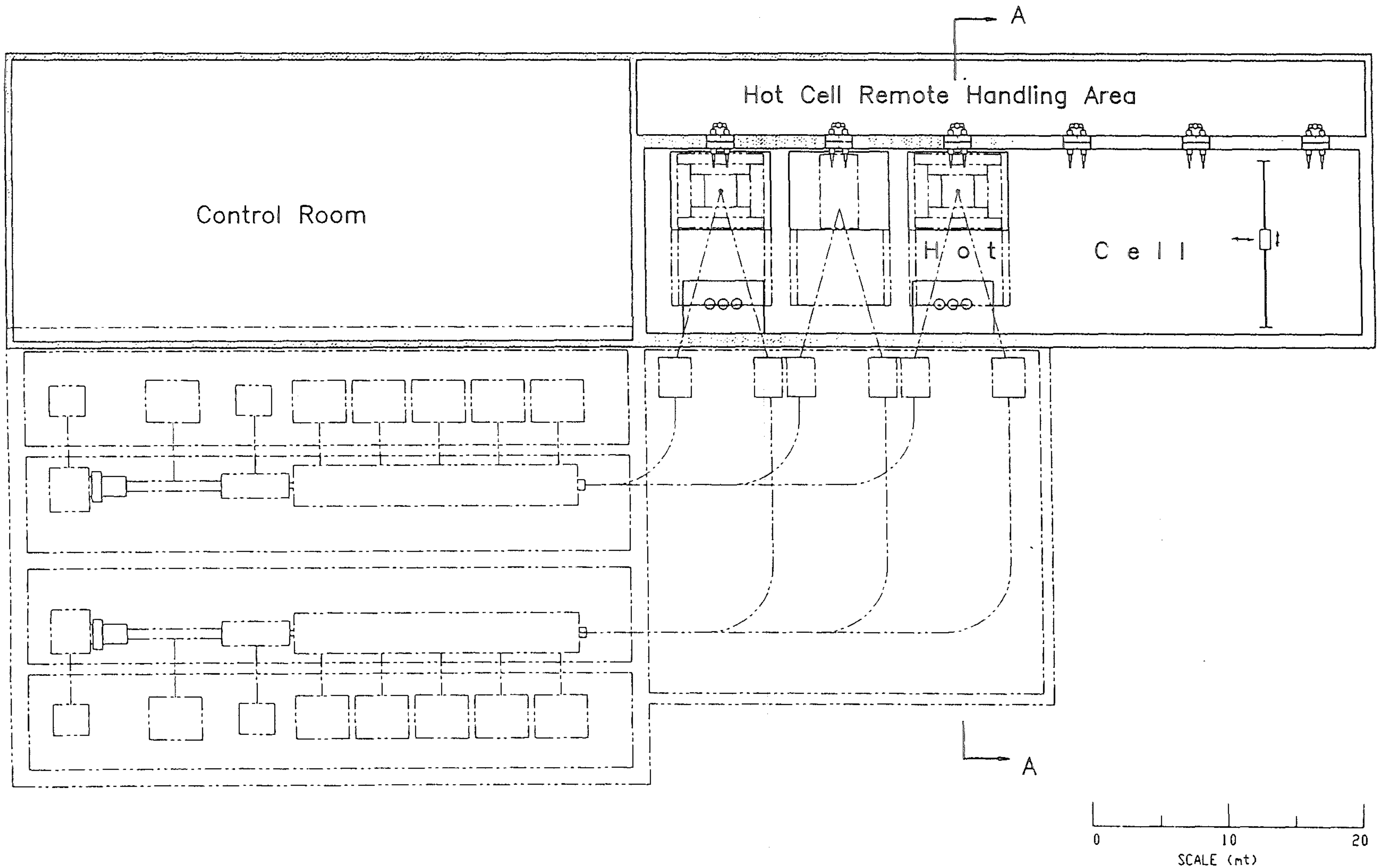

LAYER 0

Centro Ricerca Energia Frascati
IFMIF GENERAL LAYOUT – PLAN VIEW
2600-04